Universidad Autónoma de Madrid

PROGRAMA DE DOCTORADO EN

BIOCIENCIAS MOLECULARES

FACTORES DE INICIACIÓN IMPLICADOS EN LA TRADUCCIÓN DE mRNAS VIRALES. IMPORTANCIA DE LOS MOTIVOS ESTRUCTURALES EN EL RNA

ESTHER MARÍA GONZÁLEZ ALMELA

MADRID, 2019

DEPARTAMENTO DE BIOLOGÍA MOLECULAR
FACULTAD DE CIENCIAS
UNIVERSIDAD AUTÓNOMA DE MADRID

FACTORES DE INICIACIÓN IMPLICADOS EN LA TRADUCCIÓN DE mRNAS VIRALES. IMPORTANCIA DE LOS MOTIVOS ESTRUCTURALES EN EL RNA

TESIS DOCTORAL

Esther María González Almela

Grado en Biología por la Universidad Autónoma de Madrid

Directores: Dres. Luis Carrasco Llamas y Miguel Ángel Sanz Fernández

Madrid, 2019

"No hay nada que temer en la vida, únicamente se debe entender. Ahora es tiempo de entender más, para temer menos."

Marie Curie.

Departamento de Biología Molecular

Facultad de Ciencias

Universidad Autónoma de Madrid

Dr. LUIS CARRASCO LLAMAS, catedrático de la Universidad Autónoma de Madrid, y **Dr. MIGUEL ÁNGEL SANZ FERNÁNDEZ**, titulado superior especializado del CSIC

INFORMAN:

Que Dña. **Esther María González Almela**, graduada en Biología y máster en Biología Celular y Molecular por la Universidad Autónoma de Madrid, ha realizado su tesis doctoral en el grupo de investigación del Dr. Luis Carrasco Llamas en el Centro de Biología Molecular "Severo Ochoa" en Madrid. Su formación ha sido supervisada por los Dres. Carrasco y Sanz y está avalada por la presentación de los resultados obtenidos en 5 artículos científicos en revistas internacionales especializadas.

Artículos

GONZALEZ-ALMELA, E., WILLIAMS, H., SANZ, M. A. & CARRASCO, L. 2018. The Initiation Factors eIF2, eIF2A, eIF2D, eIF4A, and eIF4G Are Not Involved in Translation Driven by Hepatitis C Virus IRES in Human Cells. *Front Microbiol,* 9**,** 207.

SANZ, M. A., **GONZALEZ ALMELA, E.** & CARRASCO, L. 2017. Translation of Sindbis Subgenomic mRNA is Independent of eIF2, eIF2A and eIF2D. *Sci Rep,* 7**,** 43876.

GONZALEZ-ALMELA, E., SANZ, M. A., GARCIA-MORENO, M., NORTHCOTE, P., PELLETIER, J. & CARRASCO, L. 2015. Differential action of pateamine A on translation of genomic and subgenomic mRNAs from Sindbis virus. *Virology,* 484**,** 41-50.

CARRASCO, L., SANZ, M. A. & **GONZALEZ-ALMELA, E**. 2018. The Regulation of Translation in Alphavirus-Infected Cells. *Viruses*, 10.

SANZ, M. A., **GONZALEZ-ALMELA, E.**, GARCIA MORENO, M., MARINA, A. I. & CARRASCO, L. 2019. A Viral Rna Motif Involved in Signalling the Initiation of Translation on Non-Aug Codons. *RNA,* 25**,** 431-452.

GARCIA-MORENO, M., NOERENBERG, M., NI, S., JARVELIN, A. I., **GONZALEZ-ALMELA, E.**, LENZ, C. E., BACH-PAGES, M., COX, V., AVOLIO, R., DAVIS, T., HESTER, S., SOHIER, T. J. M., LI, B., HEIKEL, G., MICHLEWSKI, G., SANZ, M. A., CARRASCO, L., RICCI, E. P., PELECHANO, V., DAVIS, I., FISCHER, B., MOHAMMED, S. & CASTELLO, A. 2019. System-wide Profiling of RNA-Binding Proteins Uncovers Key Regulators of Virus Infection. *Mol Cell,* 74**,** 196-211.

El trabajo presentado en esta tesis doctoral ha sido realizado en el Centro de Biología Molecular "Severo Ochoa", bajo la dirección del Dr. Luis Carrasco Llamas y el Dr. Miguel Ángel Sanz Fernández, mediante la concesión de una beca FPU15/05709 del Ministerio de Educación, Cultura y Deporte. El trabajo presentado ha sido financiado por los proyectos SAF2015-66170-R y BFU2012-31861 otorgados por la Dirección General de Investigación Científica y Técnica, Ministerio de Economía y Competitividad.

AGRADECIMIENTOS

Me gustaría empezar por agradecer enormemente a Luis la oportunidad de unirme a su grupo de investigación y poder desarrollarme como científica bajo su dirección, confianza e inspirador ejemplo. También quiero darle las gracias a Miguel Ángel por su grandísima contribución al desarrollo de este trabajo, su apoyo continuo y su guía. Igualmente, quiero agradecer a Alfredo la oportunidad de realizar una colaboración tan enriquecedora y su gran ayuda durante estos años. Por supuesto también tengo que agradecer muchísimo a mis compañeras Ruth y Diana, que se convirtieron en una segunda familia y me ayudaron a crecer como profesional, pero sobre todo como persona. También a todos los compañeros que ya no están en el laboratorio: a Manuel, por su inestimable ayuda desde la distancia y sus buenos consejos; a Natalia, por ser la primera mentora que tuve en este laboratorio cuando aún era una estudiante de segundo de carrera; a Ana, por las ganas que le echa a todo lo que hace y a Pablo por su optimismo y su forma de quitarle peso a los problemas. Igualmente quiero agradecer a todas las personas de este centro que me han ayudado durante estos años, y no ha sido poca la ayuda, especialmente al personal que conforma los servicios científicos.

Especialmente quería darle las gracias a mi familia, no podría haber hecho nada de esto sin vosotros. A mi madre, que me ha apoyado y ayudado enormemente en todas mis decisiones y en mi día a día, tú me inspiraste a aportar lo mejor de mi misma a este mundo y a no tirar nunca la toalla. Fuiste mi primer contacto con la ciencia y aquí estamos ahora. A mi padre, con el que siempre puedo contar y me aporta otra perspectiva, muy necesaria, de las cosas. A mi abuelo Juan, que me anima todos los días y sigue todos mis pequeños pasos con ilusión, no podría ser mejor abuelo. A mi abuela Mercedes, aunque no esté, sé que sigue cuidando de mí. A mi abuela Pepa, que es una luchadora inagotable. A toda mi familia, incluso aunque no os vea todo lo que quiero, sé estáis ahí.

No puedo olvidarme de mis amigas, Cris, Silvia y Saioa, que aguantan todas mis penas y alegrías y me sacan sonrisas pase lo que pase. Habéis sido más importantes de lo que creéis. A Iyara, que con tantos años compartidos no me imagino sin ella. A Fer, Elsa, Julia, Arturo y Chagua que fueron los mejores amigos que podía conocer en la carrera. A Isa, que aún sigue desde la distancia. A todos los que me han apoyado en algún momento y han creído en mí cuando más lo necesitaba.

A Álvaro, que no puedo agradecerle lo suficiente toda su ayuda y apoyo incondicional, su enorme paciencia y comprensión, y su capacidad de ponerme de buen humor pase lo que pase y sus buenos consejos científicos.

Gracias a todos.

ÍNDICE

ÍNDICE

SUMMARY

RESUMEN EN INGLÉS - SUMMARY

Alphaviruses are positive polarity single-stranded RNA viruses responsible for several human and other animal diseases, causing usually arthrosis or encephalitis that continue to be a worldwide health threat. They are usually transmitted by blood-sucking arthropods to vertebrate hosts. Sindbis virus (SINV) is a well-characterized member of this group and is usually employed as a model system in molecular virology. SINV RNA genome contains two open reading frames (ORFs) that correspond to the translation of the genomic RNA (gRNA) and subgenomic RNA (sgRNA), translated at early or late times post-infection, respectively. SINV infection profoundly blocks cellular protein synthesis while sgRNA translation occurs, which follows a non-canonical mechanism, independent of several eukaryotic initiation factors (eIFs), which involves the scanning of 5'-UTR.

In this work, we have studied the requirement of different eIFs for SINV mRNAs translation. We have examined the role of the RNA helicase eIF4A using the selective inhibitor pateamine A. Translation of SINV gRNA involves the participation of eIF4A, while translation of sgRNA is independent of this factor in infected cells but dependent in transfected cells or in cell-free systems, indicating a dual mechanism of translation. Moreover, sgRNA translation does not require eIF2, and the identification of substitute factors has been the object of intensive research in the past few years. eIF2A and eIF2D were proposed as candidates by several studies. However, we have demonstrated that eIF2A and eIF2D are not required for the translation of SINV mRNAs, even when eIF2α is phosphorylated. In addition, eIF2A and eIF2D do not participate in the translation of SINV sgRNA bearing non-AUG codons. The initiation on non-AUG codons for sgRNA translation is highly dependent on the integrity of a downstream stable hairpin (DSH) structure located in the coding region of capsid protein.

Furthermore, in collaboration with Dr. A. Castelló (University of Oxford), we have demonstrated that the loss of cellular mRNAs and the emergence of viral RNA induced by SINV infection alters the dynamics and activity of the compendium of RNA-biding proteins (RBPs) of the host cell. Many of the RBPs whose activity is stimulated by SINV redistribute to viral replication factories and regulate the capacity of the virus to infect.

Finally, we examined the involvement of several eIFs in hepatitis C virus (HCV) IRES-driven translation in human cells in a comparative analysis with mRNAs bearing the encephalomyocarditis virus or the Cricket paralysis virus IRES elements. We concluded that eIF2, eIF2A, eIF2D, eIF4A and eIF4G are not involved in the initiation of translation driven by HCV IRES.

RESUMEN

RESUMEN

Los alfavirus se caracterizan por presentar un genoma constituido por una cadena de RNA de polaridad positiva. Estos virus suponen una amenaza para la salud a nivel mundial ya que pueden causar enfermedades fatales en humanos y otros animales. El virus Sindbis (SINV) es uno de los alfavirus mejor estudiado y suele emplearse como sistema modelo en virología molecular. El genoma de SINV contiene dos marcos de lectura abiertos (ORFs) que dirigen la traducción del RNA genómico (gRNA) y subgenómico (sgRNA), a tiempo temprano o tardío después de la infección, respectivamente. La infección por SINV bloquea la síntesis de proteínas celulares al tiempo que se produce la traducción del sgRNA, que sigue un mecanismo no canónico, independiente de varios factores de iniciación eucarióticos (eIFs), que incluye el *scanning* de la 5'-UTR.

En este trabajo, hemos estudiado el requerimiento de diferentes eIFs para la traducción de los mRNAs de SINV. Empleando el inhibidor selectivo pateamina A, se determinó que la traducción del gRNA de SINV implica la participación de eIF4A. En cambio, la traducción del sgRNA es independiente de este factor en células infectadas, pero dependiente de eIF4A en células transfectadas o en sistemas de traducción *in vitro*, lo que indica un mecanismo dual de traducción. Además, la traducción del sgRNA no requiere eIF2, por lo que varios estudios propusieron como sustitutos de este factor al eIF2A o al eIF2D. En este trabajo, demostramos que eIF2A y eIF2D no son necesarios para la traducción de los mRNAs de SINV, incluso cuando eIF2α está fosforilado. Asimismo, eIF2A y eIF2D no participan en la traducción de variantes del sgRNA de SINV que inician en codones no-AUG. La iniciación de la traducción del sgRNA en codones no-AUG depende en gran medida de la integridad del *downstream stable hairpin* (DSH) situado en la región codificante de la proteína de la cápsida.

En colaboración con el Dr. A. Castelló (Universidad de Oxford), hemos demostrado que la pérdida de los mRNAs celulares y la aparición del RNA viral tras la infección por SINV altera la dinámica y la actividad de las proteínas de unión al RNA (RBPs). Muchas de estas RBPs cuya actividad es estimulada por SINV se redistribuyen a las fábricas de replicación viral y regulan la capacidad del virus para infectar.

Finalmente, examinamos en células humanas la participación de varios eIFs en la traducción dirigida por el IRES del virus de la hepatitis C (HCV) concluyendo que eIF2, eIF2A, eIF2D, eIF4A y eIF4G no participan en el inicio de la traducción dirigida por IRES de HCV.

ABREVIATURAS

ABREVIATURAS

AUG_i	AUG iniciador
BHK	Célula de riñón de hámster neonato
C	Proteína de la cápsida
C6/36	Célula de larva del mosquito *Aedes albopictus*
CITE	Potenciador de la traducción cap-independiente
cRIC	Captura comparativa del RNA interactoma
CrPV	Virus de la Parálisis del grillo
DLP / DSH	*Downstream loop* / *Downstream stable hairpin*
eEF	Factor de elongación de traducción eucariótico
eIF	Factor de iniciación de la traducción eucariótico
EMCV	Virus de la encefalomiocarditis
G3BP	Proteína de unión al dominio SH3 de Ras-GAP
GDP	Guanosina difosfato
GTP	Guanosina trifosfato
gRNA / gmRNA	RNA genómico 49S
HAP1	Célula semi-haploide humana derivada de leucemia mielógena crónica
HEK293	Célula embrionaria de riñón humano
Huh-7	Célula derivada de hepatocarcinoma humano
hipp	Hippuristanol
hpi	Hora post-infección
hpt	Hora post-transfección
IGR	Región intergénica
IRES	Sitio de entrada interna del ribosoma
KO	*Knock out*
L26S	Secuencia *leader* del sgRNA o mRNA 26S
Leu	Leucina
Luc	Luciferasa
MEF	Fibroblasto de ratón

Abreviaturas

Met	Metionina
Met-Cis	Metionina-Cisteína
Met-tRNA$_i^{Met}$	tRNA iniciador unido a metionina
mRNA	RNA mensajero
nsP	Proteína no estructural
nt	nucleótidos
ORF	Fase abierta de lectura
PABP	Proteína de unión a la cola poli(A)
PKR	Proteína quinasa R
PTB	Proteína de unión al tracto de polipirimidina
RBP	Proteína de unión al RNA
rep	Replicón
RE	Retículo endoplasmático
RLU	Unidades relativas de luz
RRL	Lisado de reticulocitos de conejo
rRNA	RNA ribosómico
sfRNA	RNA subgenómico de flavivirus
SG	Gránulo de estrés
sgRNA / sgmRNA	RNA subgenómico 26S
SINV	Virus Sindbis
siRNA	RNA pequeño de interferencia
sP	Proteína estructural
TIA-1	Antígeno intracelular 1 restringido a linfocitos T
tRNA	RNA de transferencia
UTR	Región no traducida
Val	Valina
wt	Tipo salvaje o estándar (“*wild type*“)

INTRODUCCIÓN

INTRODUCCIÓN

Una característica general de todos los virus es su completa dependencia de la maquinaria celular de síntesis de proteínas para la traducción de los RNAs mensajeros (mRNAs) virales. Pese a que la complejidad de los virus es extremadamente variable, ninguno de ellos codifica en su genoma los componentes necesarios para la traducción de mensajeros virales, por lo que han evolucionado sofisticados mecanismos para secuestrar la maquinaria celular de síntesis de proteínas. Estos mecanismos pueden ser muy complejos y tienen como finalidad dirigir la maquinaria celular a la traducción de proteínas virales y, a su vez, bloquear la respuesta antiviral innata evitando el acceso de los mRNAs celulares a los ribosomas (Gale et al., 2000). Curiosamente, existen ciertas similitudes entre estos mecanismos y los empleados por las células en respuesta a estrés fisiológico (Jan et al., 2016). Generalmente, el control de la traducción para sintetizar proteínas virales implica subvertir los factores de traducción celular y las vías de señalización que controlan el aparato de síntesis de proteínas en la célula. Los virus, debido a la rápida evolución de sus mecanismos de control de la traducción y a la alta densidad de secuencias reguladoras localizadas en sus genomas, constituyen excelentes modelos para el estudio de mecanismos de expresión, como la transcripción, el procesamiento del RNA, el transporte y la traducción. De hecho, fue en sistemas virales donde se describieron los principios esenciales de varios procesos como la regulación de la expresión génica por RNAs de interferencia (Haasnoot and Berkhout, 2011, Pager et al., 2009), la compactación de la traducción de mRNAs virales y celulares (Martin and Ephrussi, 2009, Besse and Ephrussi, 2008), los mecanismos de iniciación de la traducción como el *leaky scanning*, el *shunting*, la traducción mediada por IRES (*Internal Ribosome Entry Site*) o CITEs (*Cap-Independent Translation Enhancer*) (Firth and Brierley, 2012), el descubrimiento de nuevos factores eucarióticos de iniciación de la traducción (eIFs) y los diferentes requisitos de participación de estos factores (Kim et al., 2011, Redondo et al., 2011, Sanz et al., 2009, Skabkin et al., 2010, Dmitriev et al., 2010, Parsyan et al., 2011), la regulación de la traducción mediada por gránulos de RNA (Thomas et al., 2011), la iniciación desde codones no-AUG (Zu et al., 2011, Pearson, 2011) y la regulación de la expresión génica por uORFs (*Upstream Open Reading Frame*) localizados antes del AUG iniciador (AUG_i) (Wethmar et al., 2010). Por lo tanto, la investigación sobre el control de la traducción en células infectadas por virus ha

descubierto mecanismos claves en la patogénesis viral, y ha definido paradigmas del control de la traducción celular en células no infectadas.

Nuestro grupo de investigación ha realizado diversas aportaciones en el campo de la regulación de la iniciación de la traducción como la demostración de que los factores eIF4G y eIF2 no eran necesarios para la traducción del RNA subgenómico (sgRNA) del virus Sindbis (SINV) y que además presenta un mecanismo dual de traducción dependiente del contexto celular (Sanz et al., 2009, Castello et al., 2006, Ventoso et al., 2006). También hemos mostrado que la proteasa 2A de poliovirus es capaz de conferir traducibilidad a los mRNAs virales cuando el factor eIF2 está inactivo (Redondo et al., 2011). Esta tesis doctoral está enfocada en el estudio de los mecanismos de iniciación de la traducción de los RNAs virales, con especial interés en el requerimiento de factores y en la relación entre estructura y función de estos RNAs. Se desconocen aún muchos aspectos de la dinámica de los RNAs virales que pudieran estar implicados en provocar efectos citopatogénicos, por lo que el estudio de la interacción de estos RNAs con proteínas constituirá un nuevo campo de investigación para desentrañar la patología viral a nivel molecular. Para poder determinar los mecanismos implicados en la infección viral resulta necesario identificar las proteínas celulares que se unen a los RNAs virales, y también aquellas que interfieren con los mRNAs celulares bloqueando su traducción. La importancia del estudio de estas cuestiones crece con la aparición de nuevas epidemias de gran relevancia médica y veterinaria donde el diseño de estrategias selectivas para inhibir la traducción viral podría derivar en potentes terapias antivirales.

1. EL VIRUS SINDBIS

El virus Sindbis (SINV) pertenece al género *Alfavirus* dentro de la familia *Togaviridae* (Griffin, 2007). Este género comprende unas 30 especies de virus que se transmiten en su mayoría por vectores artrópodos hematófagos, generalmente mosquitos, a gran variedad de hospedadores vertebrados tales como aves, roedores, cerdos, caballos y primates, incluyendo humanos (Forrester et al., 2012, Nasar et al., 2012). Existen excepciones respecto al vector de trasmisión, como es el caso de los alfavirus acuáticos que afectan a especies de salmónidos o al elefante marino del sur (Strauss and Strauss, 1994, Brown and Hernandez, 2012, Weaver et al., 2012). También se ha descrito el caso de un alfavirus que sólo replica en insectos y no en vertebrados, el virus Eilat (Nasar et al., 2012). Los alfavirus presentan una amplia distribución

geográfica, lo cual apunta a un origen antiguo y a una gran diversificación posterior (Novella et al., 2011, Weaver et al., 2012). Los alfavirus se pueden dividir en dos grupos según su origen geográfico: virus del Viejo Mundo y virus del Nuevo Mundo. Algunos ejemplos de los alfavirus del Viejo Mundo son el virus del Bosque Semliki (SFV), el virus Chikungunya (CHIKV), el virus del Río Ross (RRV) y el virus o'nyong'nyong (ONNV). El grupo del Nuevo Mundo incluye a SINV, y a los virus de encefalitis equinas occidental, oriental y venezolana (WEEV, EEEV y VEEV) (Forrester et al., 2012, Carrasco et al., 2018). Los alfavirus son responsables de numerosas enfermedades humanas y veterinarias en todo el mundo y su estudio tiene gran relevancia sanitaria y económica. En mamíferos, los alfavirus producen enfermedades que se desarrollan generalmente mediante una infección aguda, de corta duración, que cursa con variedad de síntomas dependiendo del virus y su hospedador. Estos síntomas pueden ser: encefalitis, poliartritis, mialgia, artritis, artralgia, sarpullidos y fiebre (Griffin, 2007). En concreto, los virus de las encefalitis equinas pueden causar enfermedades neurológicas fatales en humanos y animales domésticos. A su vez, el virus Chikungunya, que produce una artralgia intensa, ha resurgido como una seria amenaza para la salud humana causando grandes pandemias principalmente en África, Asia y América (Brown and Hernandez, 2012). Al contrario de lo que ocurre en vertebrados, los insectos superan la fase aguda de la infección y quedan persistentemente infectados sin consecuencias patológicas aparentes (Karpf et al., 1997, Mudiganti et al., 2006), aunque también se ha observado apoptosis en células de mosquito en cultivo infectadas con SINV (Mudiganti et al., 2006).

SINV ha sido utilizado ampliamente en investigación como modelo en estudios de síntesis de proteínas, transcripción y replicación viral, y para comprender la patogénesis viral y la interacción entre virus y hospedador. Estos estudios han revelado aspectos fundamentales de la regulación de la traducción en células infectadas por virus (Carrasco et al., 2018). Por ejemplo, los mRNAs de SINV han ayudado a comprender la relación existente entre la estructura y la función de los mRNAs virales. Por otra parte, SINV ha sido utilizado en la investigación de campos tan diversos como la terapia oncológica o la inmunidad adaptativa antiviral (Suzme et al., 2012, Tassetto et al., 2017).

1.1 Ciclo viral de SINV

El virión de SINV tiene aproximadamente 70 nm de diámetro y está formado por una nucleocápsida de estructura icosaédrica compuesta por 240 copias de la proteína de la cápsida (proteína C). Esta estructura contiene en su interior el RNA genómico (gRNA) también conocido como 49S, que es un RNA monocatenario de polaridad

positiva y de 11,7 Kb de longitud (Figura 1) (Fuller, 1987, Strauss and Strauss, 1994). La nucleocápsida está envuelta por una bicapa lipídica derivada de la membrana plasmática de la célula hospedadora, que tiene ancladas las glicoproteínas virales E1 y E2 (Chen et al., 2018). Estas glicoproteínas interaccionan con receptores de la membrana de las células diana y propician la fusión de las membranas celular y viral. Las partículas virales de SINV pueden llegar al citoplasma por diferentes vías, siendo la más común la endocitosis mediada por clatrina. Tras la endocitosis, los viriones acaban en endosomas (Perez and Carrasco, 1994, Mayor and Pagano, 2007, Leung et al., 2011). Alternativamente los viriones también pueden fusionar su membrana con la membrana plasmática celular liberando el gRNA directamente al citosol (Vancini et al., 2013). En cualquier caso, para que la infección sea eficaz, el gRNA debe mantener el contacto con la proteína C tras su liberación al citoplasma (Sokoloski et al., 2017).

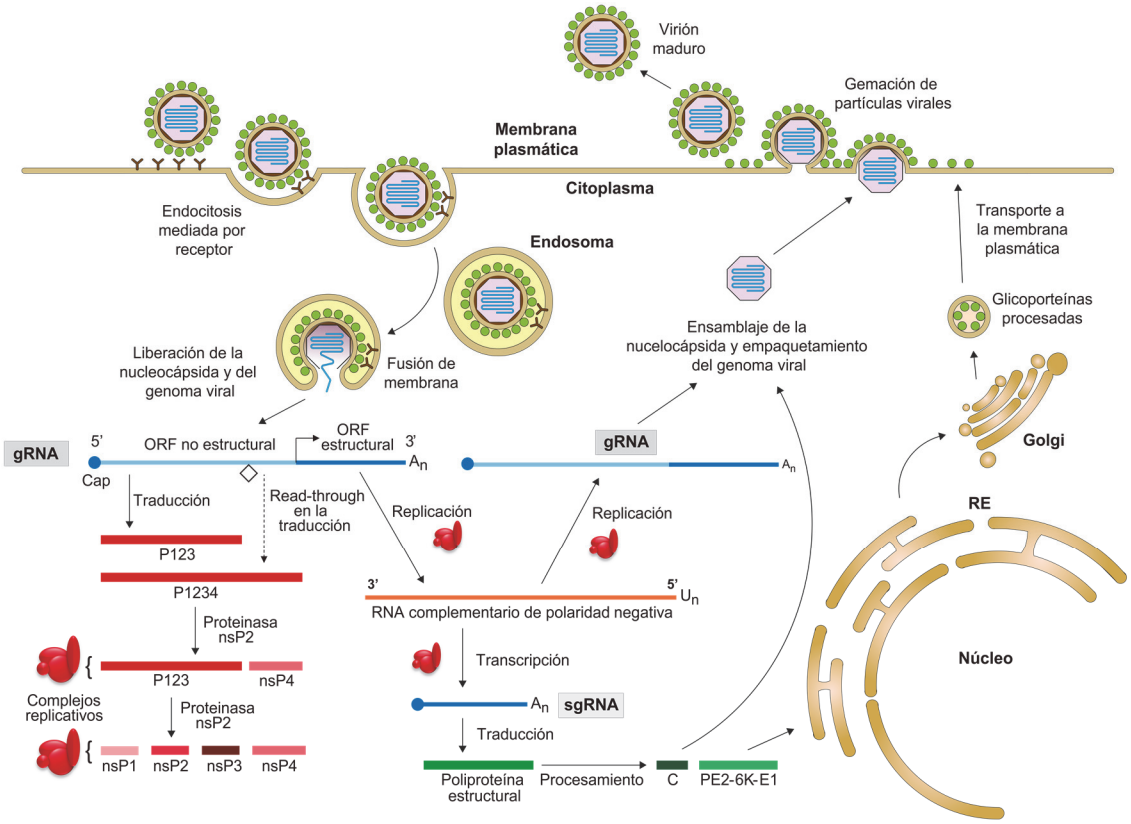

Figura 1. Ciclo infectivo y organización del genoma de SINV. Abreviaturas: *gRNA*, RNA genómico; *sgRNA*, RNA subgenómico; *C*, proteína de la cápsida; *nsP*, proteína no estructural; *ORF*, fase abierta de lectura; *RE*, retículo endoplasmático; ◊, codón de terminación opal 1897.

Cuando el genoma viral alcanza el citoplasma, comienza su traducción. El genoma de SINV contiene dos marcos de lectura abierta u ORFs (*Open Reading Frame*) que se expresan en dos mRNAs distintos: el gRNA y el sgRNA. El gRNA se traduce en las

proteínas no estructurales (nsPs), y el sgRNA codifica para las proteínas estructurales (sPs) (Figura 1). Mientras el gRNA es traducido preferentemente tras la liberación del genoma viral al citosol (fase temprana de la infección), el sgRNA se traduce preferencialmente durante la fase tardía (Shin et al., 2012). Ambos RNAs presentan una estructura cap en el extremo 5' y una cola poli(A) en su extremo 3'. Como excepción a esto, se ha encontrado una pequeña porción de gRNA que no presenta la estructura cap en su extremo 5' (Sokoloski et al., 2015).

El primer paso en la replicación del virus SINV es la síntesis de las proteínas no estructurales nsP1-4 codificadas en el gRNA, que participan en la replicación y transcripción viral (Strauss and Strauss, 1994). Las nsPs se traducen desde un único codón iniciador AUG (AUG_i) generándose dos tipos de poliproteínas precursoras: P123 y P1234, que serán posteriormente procesados mediante la proteólisis llevada a cabo por la nsP2 (Figura 1) (de Groot et al., 1990, Ahola et al., 2000). En la traducción de estos precursores, la mayoría de los ribosomas (90-95%) se detienen en el primer codón de parada que encuentran (UGA) – un codón opal, lo que genera el precursor P123 (Li and Rice, 1993). Sin embargo, y con escasa frecuencia, ocurre un fenómeno *read-through* de este codón de parada y se produce el precursor P1234. La función de cada una de las nsPs derivadas de estos precursores ha sido intensamente investigada (Laakkonen et al., 1996, Ahola et al., 1999, Ahola et al., 2000, Rupp et al., 2015). nsP1 es una proteína palmitoilada capaz de interaccionar con las membranas celulares a través de una hélice anfipática localizada en su región central (Peranen et al., 1995). De este modo, sirve de anclaje a la membrana para los complejos replicativos virales de los que forma parte (Salonen et al., 2003). nsP1 participa junto a nsP4, la RNA polimerasa viral, en la iniciación y elongación de la cadena de RNA de polaridad negativa complementario al RNA genómico de SINV (Shirako et al., 2000, Fata et al., 2002). El motivo N-terminal de nsP1 tiene actividad metiltransferasa y guanililtransferasa, que están implicadas en el proceso de "*capping*" (Mi et al., 1989, Ahola et al., 1997, Peranen et al., 1995). La proteína nsP2 también presenta varios dominios: (1) la región amino-terminal, con actividad RNA helicasa, (2) la región central, con actividad proteasa que cataliza todas las reacciones de escisión que darán lugar a las diferentes nsPs, y (3) un motivo inactivo tipo RNA metiltransferasa (Russo et al., 2006, Gomez de Cedron et al., 1999). nsP2 también participa en el bloqueo de las actividades de síntesis de macromoléculas celulares, tales como la transcripción y la traducción, antagonizando de esta forma la respuesta antiviral celular (Garmashova et al., 2006, Breakwell et al., 2007). Se ha observado que una fracción de la proteína nsP2 se localiza en el núcleo celular donde bloquea la exportación de RNAs al citoplasma (Breakwell et

al., 2007, Rikkonen et al., 1994). Además, nsP2 induce la degradación mediante ubiquitinación de Rpb1, que es una subunidad catalítica esencial de la RNA polimerasa II (Akhrymuk et al., 2012). La nsP3 presenta tres dominios: (1) un macrodominio amino-terminal, (2) una región central específica de alfavirus, y (3) una región de secuencia hipervariable en el extremo carboxilo con multitud de sitios susceptibles de fosforilación (Lark et al., 2017, Lulla et al., 2012). nsP3 bloquea la formación de gránulos de estrés (SGs) en la célula hospedadora, ya que estos participan en los mecanismos de respuesta antiviral innata, mediante la interacción de su dominio carboxi-terminal con G3BP (proteína de unión al dominio SH3 de Ras-GAP). De esta forma, nsP3 impide la función nucleadora de G3BP en la formación de SGs (Panas et al., 2012, Fros et al., 2012). Finalmente, nsP4 es una RNA polimerasa RNA-dependiente que lleva a cabo la síntesis de los diferentes RNAs virales – gRNA, sgRNA y el RNA monocatenario de polaridad negativa complementario al genoma (Rubach et al., 2009, Pietila et al., 2017). Cabe señalar que el complejo P123 + nsP4 sintetiza preferencialmente la cadena de RNA de polaridad negativa, mientras que el complejo nsP1 + P23 + nsP4 sintetiza tanto la cadena de polaridad positiva como la de polaridad negativa (Shirako and Strauss, 1994, Lemm et al., 1994). La escisión final de P23 en P2+P3 supone la maduración completa de todas las nsPs, que a partir ese momento priorizarán su función hacia la síntesis de los gRNAs y sgRNAs.

Las moléculas de gRNA de SINV participan en tres funciones: (1) síntesis de nsPs; (2) síntesis de la cadena de RNA de polaridad negativa; y (3) formación de la nucleocápsida durante el ensamblaje y la generación de nuevas partículas virales. Por otro lado, la cadena de RNA de polaridad negativa sirve como molde para que la maquinaria replicativa viral sintetice los dos mRNAs virales – gRNA y sgRNA (Lemm et al., 1994, LaStarza et al., 1994). En el caso de virus RNA citoplasmáticos, como SINV, la síntesis de RNA viral ocurre en estrecha asociación con las membranas celulares (Perez et al., 1994, Carrasco, 2002, Hellstrom et al., 2017). Los complejos replicativos de SINV se encuentran concentrados en regiones específicas del citoplasma formando las factorías de replicación viral. Estas factorías están asociadas a unas estructuradas denominadas esférulas, que son invaginaciones de la membrana de las vacuolas citopáticas, que a su vez se forman a partir de endosomas celulares modificados por la infección viral (Harak and Lohmann, 2015). El análisis del proteoma de los complejos replicativos ha conseguido la identificación de varias proteínas celulares cuya actividad puede estimular o inhibir la síntesis de RNA viral (Varjak et al., 2013). Varios factores

celulares pueden interaccionar con las nsPs, como se ha visto para nsP2 y nsP3, y así modular la replicación del RNA de SINV (Cristea et al., 2010).

Para iniciar la síntesis del sgRNA (también conocido como 26S) es necesario el reconocimiento de un promotor interno en la cadena de RNA de polaridad negativa. Este sgRNA es el mRNA más abundante durante la fase tardía de la infección y dirige la síntesis de la poliproteína C-E3-E2-6K-E1, que dará lugar a las sPs. La traducción de este sgRNA coincide con una drástica inhibición de la traducción de los mRNAs celulares. La secuencia codificante del sgRNA está flanqueada por dos regiones no traducibles, UTRs (*UnTranslated Regions*): la 5'-UTR contiene la estructura cap en su extremo 5', y la 3'-UTR termina en una cola poli(A). Cuando los ribosomas interaccionan con el sgRNA, avanzan sobre él mediante un proceso de *scanning* hasta alcanzar el primer codón AUG, donde inician la traducción. Primero se sintetiza la proteína de la cápsida (C), que se libera de la poliproteína naciente mediante autoproteólisis (Figura 2) (Strauss and Strauss, 1994). Tras este evento, la proteína C se une al gRNA para formar las nucleocápsidas. El nuevo extremo N-terminal de la poliproteína, que se corresponde con la proteína E3, tiene un péptido señal que dirige la traducción al retículo endoplasmático (RE). Una vez en el RE, la traducción continúa asociada a su membrana generándose el precursor de las tres glicoproteínas E3, E2 y E1, y la viroporina 6K. La translocación de las glicoproteínas virales a través de la membrana del RE está regulada por varias secuencias señal. Las glicoproteínas y la viroporina 6K son procesadas y cortadas por proteasas celulares, como la furina y la signalasa, del sistema vesicular celular (Sariola et al., 1995). Hace algunos años, fue descubierto un sitio de deslizamiento (*slip site*) de siete nucleótidos (UUUUUUA) dentro del gen que codifica para la proteína 6K, y se observó que, en aproximadamente el 10% de los casos, produce un desplazamiento del ribosoma a una posición -1 en el marco de lectura. En estos casos, se produce una forma *transframe* (TF) de 6K que acaba en un codón de parada próximo y, por tanto, no continúa con la traducción de E1 (Firth et al., 2008, Chung et al., 2010). La proteína 6K, con sólo 55 aminoácidos, pertenece a la familia de las viroporinas y se encuentra generalmente en forma palmitoilada, lo cual le permite interaccionar con las membranas (Gaedigk-Nitschko and Schlesinger, 1990, Sanz et al., 1994, Sanz et al., 2003, Nieva et al., 2012, Ramsey and Mukhopadhyay, 2017). 6K está implicada en el transporte de las glicoproteínas virales a través del sistema vesicular hacia la membrana plasmática (Sanz and Carrasco, 2001, Sanz, 2005), y en el ensamblaje de las partículas virales, aunque no se incorpora en los viriones, salvo en pequeñas proporciones (Nieva et al., 2012, Melton et al., 2002). Por el contrario, la proteína TF es preferencialmente incorporada

dentro de los viriones liberados (Snyder et al., 2013). pE2 y E1 interaccionan entre sí formando heterodímeros que migran hacia la membrana plasmática de tal forma que su extremo carboxi-terminal queda orientado hacia la cara citoplasmática de la membrana. Cuando el complejo pE2-E1 alcanza el *trans*-Golgi, pE2 es procesada para formar E3 y E2 mediante la acción de furinas. Este procesamiento de pE2 es necesario para generar partículas virales activas que inicien un nuevo ciclo infectivo (Jose et al., 2009, Weaver et al., 2012).

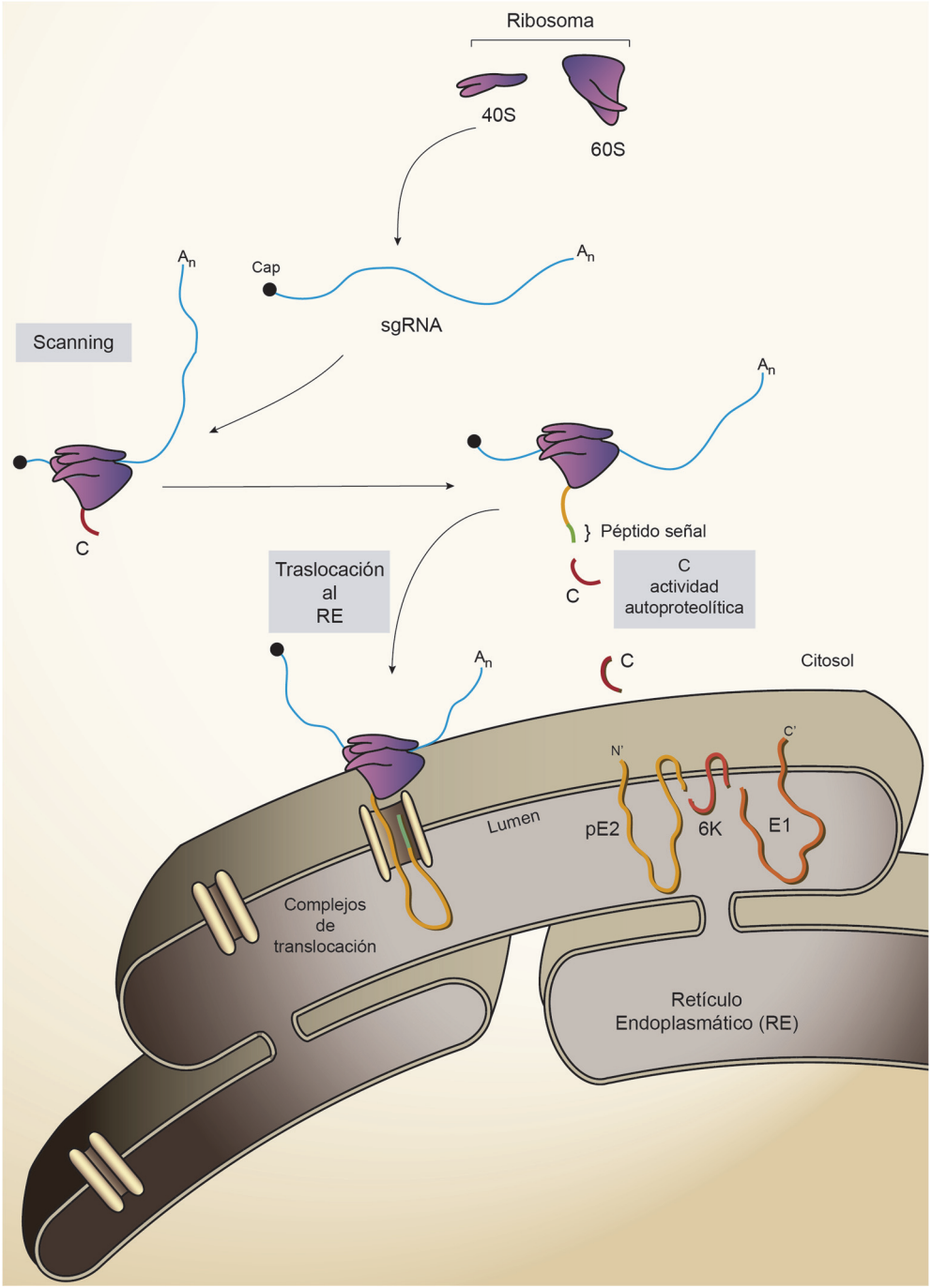

Figura 2. Representación esquemática de la traducción del sgRNA de SINV para producir las proteínas de la cápsida (C), pE2, 6K y E1.

2. MECANISMOS DE INICIACION DE LA TRADUCCIÓN EN EUCARIOTAS

La expresión de los genes está regulada a múltiples niveles, incluyendo la traducción de los mRNAs. El control a nivel de traducción permite cambios rápidos en la concentración de proteínas y, por eso, se emplea para regular la homeostasis y los cambios fisiológicos de la célula. El proceso de traducción se divide en las fases de iniciación, elongación, terminación y reciclado de ribosomas (Hinnebusch, 2014). La fase más regulada es la iniciación, durante la cual el codón de iniciación es identificado y decodificado por el RNA transferente especializado en iniciación: Met-tRNA$_i$. Existen gran variedad de mecanismos de iniciación de la traducción (Jackson et al., 2010).

2.1 Mecanismo canónico de iniciación de la traducción

En eucariotas, el mecanismo canónico de iniciación comienza con el reconocimiento de la estructura cap metilada m^{7}GpppN en el extremo 5' de los mRNAs por el factor eIF4E (Figura 3) (Gingras et al., 1999). eIF4E, junto con la helicasa tipo DEAD-box eIF4A y la proteína de andamiaje eIF4G, forma el complejo multiproteico eIF4F (Jackson et al., 2010, Sonenberg and Hinnebusch, 2009). La proteína PABP (*Poly(A) Binding Protein*) se asocia con el complejo eIF4F, a través del factor eIF4G, a la vez que une la cola poli(A) del mensajero promoviendo su circularización y facilitando el reciclado de los ribosomas (Gingras et al., 1999, Derry et al., 2006, Wells et al., 1998). Por otro lado, el factor eIF2 unido a GTP interacciona con el tRNA$_i$ asociado con metionina formando el complejo ternario Met-tRNA$_i^{Met}$-eIF2-GTP. La subunidad pequeña ribosómica 40S es precargada con el complejo ternario y, junto con los factores eIF1, eIF1A, eIF3, y eIF5, forma el complejo de preiniciación 43S (43S PIC) (Lorsch and Dever, 2010). El complejo eIF4F, unido al mRNA, recluta al 43S PIC mediante la interacción de eIF3 con el dominio central de eIF4G. De esta forma, el 43S PIC, que se encuentra en conformación "abierta", se desplazará desde el cap sobre el 5'-UTR del mRNA en dirección 5' →3', en un proceso de *scanning*, hasta reconocer el codón iniciador AUG en un contexto de secuencia adecuado. Desde hace muchos años, el contexto de Kozak RCCAUGG se ha considerado el óptimo para señalar el sitio de iniciación de los mRNAs en mamíferos (Kozak, 1991, Hinnebusch, 2011, Asano and Sachs, 2007, Pestova and Kolupaeva, 2002, Kozak, 1999). Para que el mecanismo de *scanning* sea eficiente es necesario que eIF4A, mediante su actividad helicasa y ATPasa, deshaga la estructura secundaria de la secuencia *leader* del mRNA (Parsyan et al., 2011). Otras helicasas como DHX29 y Ded1/DDX3 también pueden participar en este proceso (Parsyan et al., 2011,

Abaeva et al., 2011, Pisareva et al., 2008). El proceso de *scanning* finaliza con el reconocimiento del AUG_i, que se lleva a cabo mediante el apareamiento de bases entre el anticodón del Met-$tRNA_i^{Met}$ y el codón AUG_i en el sitio P ribosómico, y desencadena la hidrólisis de GTP liberándose eIF2-GDP y otros factores unidos a la subunidad 40S (Figura 3). Estas reestructuraciones moleculares y conformacionales conducen a la formación "cerrada" de la subunidad 40S del ribosoma, quedando ésta ya comprometida a continuar la traducción del mRNA (Pisareva et al., 2008, Shatsky et al., 2010). El papel de la proteína eIF5 es central en la regulación de estos eventos. eIF5 participa en la formación del complejo de preiniciación mediante la interacción de su extremo carboxilo-terminal con el eIF1 y el eIF2β (Asano et al., 2001, Yamamoto et al., 2005). También induce la disociación del eIF1 tras el reconocimiento codón-anticodón, lo cual permite que eIF5 catalice la hidrolisis de GTP a GDP del complejo ternario (Luna et al., 2012, Cheung et al., 2007). La salida de eIF1 despeja el sitio P, permitiendo que el

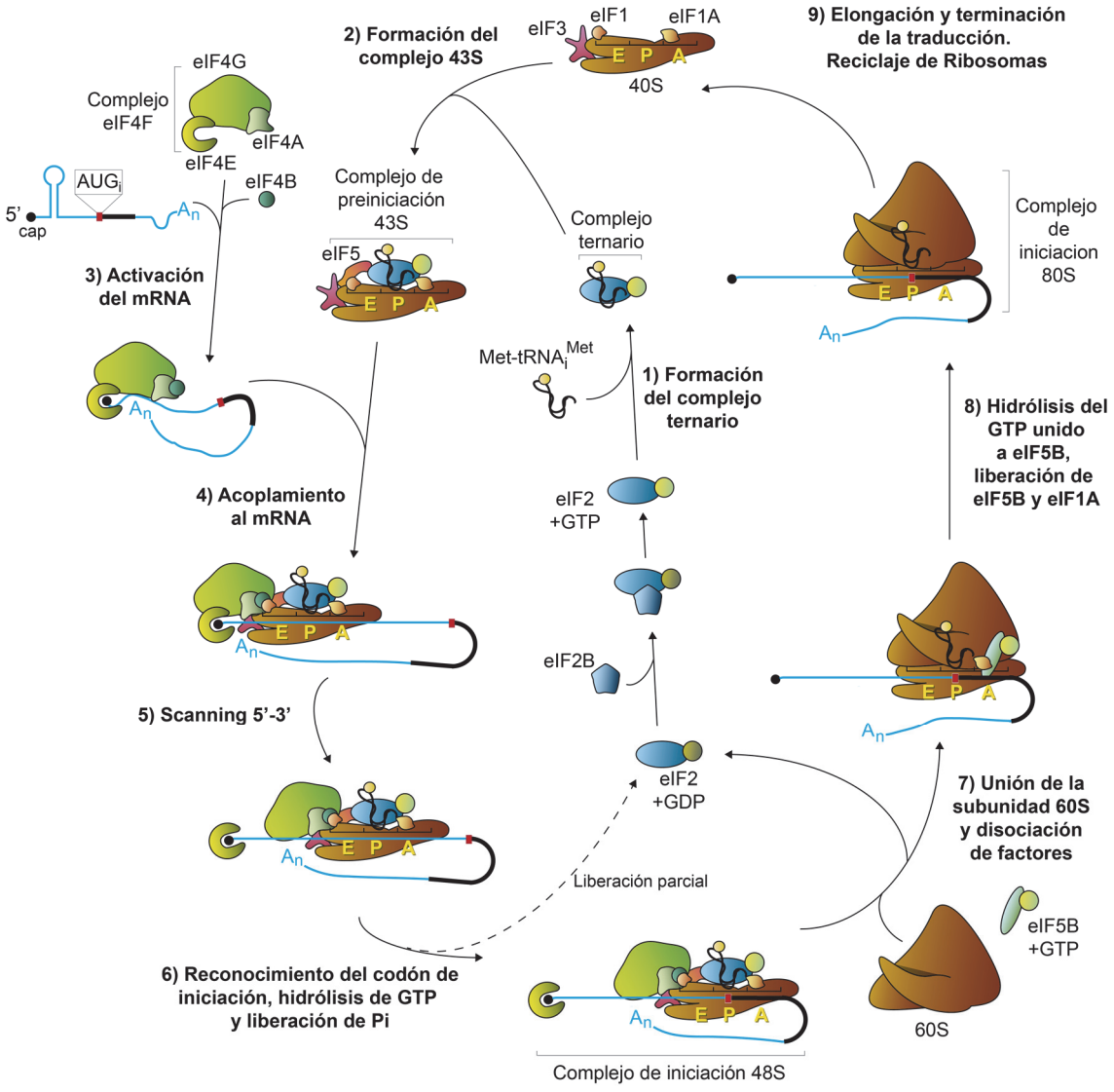

Figura 3. Esquema del mecanismo canónico de iniciación de la traducción en eucariotas.

Met-tRNA$_i^{Met}$ se una con más fuerza a este sitio (Lomakin et al., 2003). Simultáneamente, eIF5B-GTP interacciona con la subunidad 40S promoviendo la salida de eIF2-GDP y los demás factores, excepto eIF1A y eIF5B, y a su vez, estimula la unión de la subunidad 60S con la 40S (Pestova et al., 2000). eIF2-GDP debe reciclarse a eIF2-GTP mediante la acción del eIF2B para poder participar en el siguiente proceso de iniciación. Por último, eIF5B hidroliza GTP liberando eIF1A y eIF5B-GDP de los ribosomas 80S ensamblados y competentes para la elongación. Cuando el Met-tRNA$_i^{Met}$ queda anclado al sitio P, dejando libre el sitio A, finaliza la fase de iniciación de la traducción dando paso a la fase de elongación, que comienza en el momento en el que el primer aminoacil-tRNA$_e$-eEF1-GTP se une al sitio A ribosómico.

2.2 Otros mecanismos de iniciación dependientes de cap

Aunque la mayoría de los mRNAs eucarióticos inician su traducción por el mecanismo canónico, hay otros mecanismos dependientes de cap que siguen un proceso de *scanning* diferente al canónico. Estos mecanismos alternativos suelen estar implicados en la traducción de mensajeros con regiones 5'-UTR extremadamente cortas o de gran complejidad estructural, y son ventajosos bajo determinadas condiciones fisiológicas, por lo que han sido descritos principalmente para mRNAs virales.

- *Leaky scanning*: mecanismo por el cual la subunidad ribosómica 40S escanea la región 5'-UTR, pero no reconoce el primer AUG que encuentra, por estar éste en un contexto de secuencia subóptimo. Por tanto, la iniciación se produce en un codón AUG posterior (Lopez-Lastra et al., 2010).
- Mecanismo de salto o *shunting*: los ribosomas inician el *scanning* desde el cap en la 5'-UTR, pero al encontrar determinadas secuencias son traslocados directamente a una región posterior, saltando segmentos amplios de la 5'-UTR que pueden contener AUGs y estructuras secundarias fuertes (Yueh and Schneider, 1996, Yueh and Schneider, 2000).
- Mecanismo de terminación-reiniciación: tras alcanzar el codón de parada de traducción, la subunidad 40S no se separa del mRNA y reanuda el proceso de *scanning* en un segundo ORF (Lopez-Lastra et al., 2010).

2.3 Mecanismo de iniciación de la traducción dependiente de IRES

Este mecanismo no canónico independiente de cap dirige la iniciación de la traducción de muchos mRNAs virales y celulares que presentan elementos internos de entrada al ribosoma o IRES en sus regiones 5'-UTR (Kieft, 2008, Balvay et al., 2009,

Lozano and Martinez-Salas, 2015, Komar et al., 2012). Estos elementos presentan estructuras terciarias o secundarias particulares, ricas en "*stem-loops*", y son capaces de reclutar los ribosomas a posiciones internas del mRNA cercanas al AUG_i o directamente sobre él (Jackson et al., 2010). El requerimiento de eIFs varía según el IRES que dirige la traducción.

Los IRES se clasifican según su origen, estructura secundaria y funcionalidad (Belsham, 2009, Fitzgerald and Semler, 2009). Existen IRES celulares e IRES virales. Estos últimos aparecen en todos los picornavirus y en otros virus RNA como flavivirus, retrovirus, pestivirus y dicistrovirus (Balvay et al., 2009, Khawaja et al., 2015, Jang, 2006, Nakashima and Uchiumi, 2009, Lee et al., 2017). Los IRES de picornavirus se clasifican en cuatro tipos: tipo I (virus de la polio, rinovirus) requiere de todos los eIFs salvo de eIF4E y, tras posicionar el RNA en el ribosoma, encuentra el AUG_i mediante *scanning*; tipo II (virus de la fiebre aftosa, virus de la encefalomiocarditis) difiere del tipo I en que sitúa al ribosoma directamente sobre el AUG_i; tipo III (virus de la hepatitis A) el IRES se une directamente a la subunidad 40S y sólo requiere de eIF2 y eIF3; y tipo IV (teschovirus porcino) tras la unión a la 40S, la pseudotranslocación por eEF2 es necesaria para posicionar el codón de iniciación en el sitio A; sólo requiere de eIF2 (Balvay et al., 2009, Hertz and Thompson, 2011, Yamamoto et al., 2017).

El mecanismo de iniciación de la traducción dependiente de IRES es empleado también por el virus de la hepatitis C (HCV). HCV es responsable de la mayoría de las hepatitis crónicas de origen viral e induce hepatocarcinomas en humanos (Hajarizadeh et al., 2013, Khullar and Firpi, 2015). HCV pertenece a la familia *Flaviridae* y contiene un genoma compuesto por RNA monocatenario de polaridad positiva de unos 9,6 Kb. Este genoma constituye su único mensajero conocido y presenta una sola ORF que dirige la traducción de la poliproteína que, tras el procesamiento proteolítico, genera las proteínas virales maduras (Paul et al., 2014). La traducción del mRNA de HCV está promovida y regulada por un elemento IRES que media la interacción de los componentes que participan en la síntesis de proteínas (Hellen and Pestova, 1999, Khawaja et al., 2015). Varios trabajos realizados en sistemas *in vitro* sugieren que el factor eIF2 es necesario para la iniciación de la traducción de este mRNA viral (Pestova et al., 1998, Otto and Puglisi, 2004). Aunque se ha postulado que la traducción de HCV puede emplear eIF2 cuando este factor está activo en condiciones normales, su traducción, dirigida por IRES, ocurre tras la inactivación de este factor por fosforilación. Además, la interacción de este IRES viral con los complejos de preiniciación parece desplazar al eIF2 fuera de ellos (Jaafar et al., 2016). Esto ha suscitado que varios factores se hayan

propuesto como candidatos para reemplazar eIF2 en la traducción de HCV: eIF5B (Terenin et al., 2008), eIF2D (Dmitriev et al., 2010, Skabkin et al., 2010), y eIF2A (Kim et al., 2011). A pesar de que eIF2A y eIF2D pueden formar un complejo con el Met-tRNA$_i^{Met}$ e interaccionar con la subunidad 40S o con la 80S, resultados recientes parecen indicar que el silenciamiento de eIF2A, eIF2D o ambos no tiene efecto en la traducción de HCV (Jaafar et al., 2016). Se ha especulado que bajo condiciones en las que eIF2 no es funcional, el Met-tRNA$_i^{Met}$ puede unirse directamente con el ribosoma mediante un mecanismo que no requiere el complejo ternario, pero que es dirigido por el IRES de HCV (Jaafar et al., 2016).

2.4 Otros mecanismos de iniciación de la traducción independientes de cap

Existen otros mecanismos independientes de cap que utilizan secuencias conocidas como CITEs (*Cap-Independent Translation Enhancer*) que se encuentran en diversas regiones del genoma RNA de algunos virus de plantas, aunque preferentemente en la 3'-UTR (Simon and Miller, 2013). Estas secuencias parecen ser necesarias para reclutar diversos componentes de la maquinaria de traducción, que serán posteriormente transferidos a la secuencia 5' *leader* mediante la interacción de las 5'- y 3'-UTR, antes de iniciarse el proceso de *scanning* (Shatsky et al., 2010, Kraft et al., 2013, Kneller et al., 2006). Otros virus emplean mecanismos donde el RNA viral se une covalentemente a una proteína viral que recluta diferentes factores de iniciación de la traducción actuando de manera parecida a la estructura cap del mecanismo canónico (Lopez-Lastra et al., 2010, Kneller et al., 2006).

3. INICIACIÓN DE LA TRADUCCIÓN EN SINV

3.1 Iniciación de la traducción del sgRNA de SINV

Numerosos elementos estructurales han sido identificados en el sgRNA de SINV que lo hacen particularmente eficiente para la traducción durante la infección en dos hospedadores distintos: células de mamífero y de insecto. Este sgRNA está formado por 4105 nucleótidos (nt), sin incluir la secuencia de la cola poli(A), y dedica la mayor parte de su secuencia (3738 nt) a codificar la poliproteína estructural C-E3-E2-6K-E1. La secuencia codificante está flanqueada por dos UTRs (Hyde et al., 2015). La región 5'-UTR (49 nt) representa la secuencia *leader* y contiene una estructura cap de tipo 0 (N7mGppp) en su extremo 5' (Hyde et al., 2015). La región 3'-UTR (323 nt) está organizada en tres dominios diferentes: una secuencia conservada de 19 nt cerca de la cola poli(A), una

secuencia rica en AU de unos 60 nt, y tres estructuras repetidas *stem-loop* que están presentes no sólo en los alfavirus, sino también en otros virus transmitidos por artrópodos y que parecen conferir traducibilidad a los mRNAs de manera específica de huésped (Dickson et al., 2012, Sokoloski et al., 2010, Barnhart et al., 2013, Hardy, 2006, Ou et al., 1982, Pfeffer et al., 1998, Gritsun and Gould, 2006, Garneau et al., 2008, Garcia-Moreno et al., 2016).

Además de las 5'- y 3'-UTRs, otra estructura en forma de horquilla (*hairpin*) presente en la secuencia codificante desde la posición 77 a la 139 resulta fundamental para la traducción del sgRNA en células infectadas. Esta estructura *hairpin*, previamente denominada *downstream loop* (DLP) y actualmente renombrada como *downstream stable hairpin* (DSH), parece estar implicada en:

- La independencia de eIF2 en la traducción del sgRNA en células de mamífero infectadas (McInerney et al., 2005, Ventoso et al., 2006, Sanz et al., 2017).
- La colonización de hospedadores vertebrados y la consecuente expansión geográfica de los alfavirus por todo el mundo (Sokoloski et al., 2010, Ventoso, 2012).
- La señalización del codón exacto de iniciación para la traducción (Sanz et al., 2009, Frolov and Schlesinger, 1996, Sanz et al., 2019).

El mecanismo de iniciación de la traducción del sgRNA y la selección del codón AUG_i han sido estudiados en profundidad. En común con los mRNAs celulares, la iniciación de la traducción del sgRNA de SINV también ocurre siguiendo el mecanismo de *scanning* (Garcia-Moreno et al., 2013, Garcia-Moreno et al., 2015). Se ha sugerido que el primer evento en esta iniciación podría ser la interacción del eIF3, mediante su subunidad eIF3D, con la estructura cap en el extremo 5', sin la participación del eIF4E ni del complejo eIF4F (Skabkin et al., 2010, Lee et al., 2016, Castello et al., 2006). Después del reconocimiento de la estructura cap, la subunidad ribosómica 40S puede interaccionar con el mRNA. A pesar de que no se conoce exactamente que eIFs se unen con la subunidad ribosómica 40S, el complejo ternario conteniendo eIF2 activo no se requiere para esta interacción, ni tampoco para el *scanning* de la secuencia *leader* (Garcia-Moreno et al., 2016). Igualmente, la potente inhibición del eIF4A mediante inhibidores específicos, como el hippuristanol (hipp), no afecta a la traducción del sgRNA, reforzando la idea de que el complejo eIF4F no está implicado en ella durante la fase tardía de la infección (Cencic et al., 2012, Castello et al., 2006, Garcia-Moreno et al., 2013, Sanz et al., 2013).

3.2 Inhibición de la traducción celular por SINV

La mayoría de los virus animales con ciclo citolítico inducen una profunda inhibición de la síntesis de proteínas celulares en las células infectadas, especialmente durante la fase tardía de la infección, que podría interferir con la respuesta antiviral innata y facilitar que la maquinaria de síntesis de proteínas se dedique preferencialmente a traducir RNAs virales (Bushell and Sarnow, 2002, Fros and Pijlman, 2016). En el caso de SINV, se ha observado que esta inhibición puede comenzar aproximadamente a partir de las 3 horas post-infección (hpi), aunque este punto depende de la línea celular y puede variar entre 3-8 hpi. Curiosamente, la inhibición de la síntesis de proteínas celulares es más fuerte en células de vertebrado que en células de mosquito (Garcia-Moreno et al., 2013, Sanz et al., 2015). La inhibición de la traducción de los mensajeros celulares y del gRNA viral ocurre en fases tardías de la infección, cuando el sgRNA dirige la síntesis de proteínas estructurales (Strauss and Strauss, 1994).

Distintos mecanismos han sido sugeridos para explicar la inhibición de la síntesis de proteínas celulares mediada por SINV: (1) la fosforilación de la subunidad α del factor eIF2; (2) la competición de los mRNAs virales por la maquinaria de traducción celular; y (3) las modificaciones del entorno iónico. Atendiendo a la primera, eIF2 tiene un papel central en la traducción y su reciclaje de eIF2-GDP a eIF2-GTP se realiza por la acción de eIF2B. La actividad de eIF2 está altamente regulada por cuatro quinasas que responden a diferentes estímulos de estrés: (1) PKR (*Protein Kinase R*) se activa por la presencia del RNA de doble cadena en el citoplasma; (2) PERK (*PKR-like ER Kinase*) detecta proteínas no plegadas en el RE; y (3) GCN2 y (4) HRI (*Heme-Regulated Inhibitor*) se activan por falta de nutrientes o deficiencia en iones hemo, respectivamente (Koromilas, 2015). La fosforilación de la serina 51 de la subunidad α de eIF2 provoca la inactivación de este factor, ya que forma un complejo estable con eIF2B impidiendo el reciclado de eIF2-GDP a eIF2-GTP (Proud, 2005, Donnelly et al., 2013). Debido a que la cantidad de eIF2B en la célula es unas 10 ó 20 veces menor que la de eIF2, un pequeño porcentaje de eIF2 fosforilado basta para secuestrar todo el eIF2B, bloqueando el reciclaje de eIF2 y, por tanto, la iniciación de la traducción (Hershey, 1989). La moléculas de RNA de doble cadena viral de SINV en el citoplasma se unen a PKR provocando cambios conformacionales que inducen su actividad quinasa y autofosforilación (Berglund et al., 2007). En células de mamífero, PKR, una vez activada, fosforila también a eIF2α, bloqueando la traducción de los mRNAs celulares (McInerney et al., 2005, Ventoso et al., 2006, Sanz et al., 2009, Sanz et al., 2013). Sin embargo, en células deficientes en PKR, como en fibroblastos embrionarios de ratón (MEFs) $PKR^{-/-}$, la infección por SINV también

produce este bloqueo a pesar de no observarse un aumento de la fosforilación de eIF2α, lo que sugiere que podría estar activándose otro mecanismo de inhibición (Gorchakov et al., 2004, Ventoso et al., 2006).

La competición directa del sgRNA por la maquinaria de traducción celular no parece ser realmente necesaria para la inhibición de síntesis de proteínas celulares, ya que replicones de SINV que codifican sólo para nsPs y carecen de la secuencia correspondiente al sgRNA también logran inducir una profunda inhibición de la síntesis de proteínas celulares comparable a la observada en células infectadas con el virus *wild-type* (wt) (Frolov and Schlesinger, 1994, Sanz et al., 2007, Patel et al., 2013). Por otra parte, como se ha descrito para varios virus, el desequilibrio de las concentraciones iónicas en el citoplasma de células infectadas por SINV podría estar implicado en el *shut-off* de la traducción celular (Garry, 1994, Garry et al., 1979, Carrasco, 1978, Contreras and Carrasco, 1979, Nieva et al., 2012, Sanz et al., 2009, Sanz et al., 2007).

Varios trabajos apuntan a que el proceso de replicación de RNAs virales en el citoplasma podría ser el responsable de inducir esta inhibición. De hecho, el *shut-off* celular disminuye en presencia de inhibidores que reducen la replicación de RNA viral o en infecciones con virus mutantes defectivos en replicación (Sanz et al., 2015). La replicación de RNA viral genera altos niveles de secuencias virales en el citoplasma que inducen una redistribución de las proteínas nucleares, especialmente de proteínas que se unen al RNA (Sanz et al., 2015, Patel et al., 2013, Barnhart et al., 2013). La salida de proteínas nucleares, como TIA-1 (*T-cell restricted intracelular antigen-1*) o PTB (*polypyrimidine tract binding protein*), claramente puede detectarse en células infectadas por SINV, pero no en contextos de replicación viral reducida (Sanz et al., 2015). Por tanto, una alta tasa de replicación viral es necesaria para que se induzca la inhibición de la síntesis de proteínas celulares, y es probable que uno de los factores con mayor relevancia en este evento sea la relocalización de las proteínas nucleares. Esta relocalización puede implicar tanto la salida de proteínas nucleares que activen rutas para el bloqueo de la síntesis de proteínas celulares, como el secuestro de componentes nucleares necesarios para la expresión de proteínas celulares, debido a la actividad tipo esponja de los mRNAs virales (Barnhart et al., 2013). La futura caracterización de las proteínas que interaccionan específicamente con los mRNAs virales o celulares a tiempos tardíos de la infección por SINV podría esclarecer este tipo de inhibición. Recientemente se ha caracterizado mediante la técnica de *comparative RNA-interactome capture* (cRIC) el compendio de proteínas de unión al RNA (RBPs) cuya actividad de unión al RNA se ve estimulada o disminuida en respuesta a la infección por

SINV. Esta infección parece alterar la actividad de 245 RBPs mediante cambios en la localización subcelular de estas proteínas o en la disponibilidad de los mRNAs. Esta remodelación de las RBPs resulta esencial para que la infección viral sea efectiva (Garcia-Moreno et al., 2019).

3.3 La traducción sin eIF2

Como se ha mencionado anteriormente, la infección por SINV induce la inactivación del factor eIF2 mediante la fosforilación de su subunidad α por la quinasa PKR, sin embargo, la traducción del sgRNA no depende de eIF2. Varios trabajos apuntan a que el DSH, localizado entre 27 y 89 nt *downstream* del AUG_i, es crucial para traducir este mRNA cuando eIF2 está inactivado (Garcia-Moreno et al., 2013, McInerney et al., 2005, Ventoso et al., 2006, Sanz et al., 2013). También se ha especulado que, a pesar de que la mayoría del eIF2α está fosforilado en las células infectadas por SINV, una pequeña porción de eIF2 permanece activo en cercana proximidad a la maquinaria de traducción asociada a los sgRNA. En discordancia con esta hipótesis, se confirmó que en variantes del sgRNA de SINV con dos codones de iniciación AUG seguidos y en correcto marco de lectura, tras la fosforilación de eIF2 sólo la traducción dirigida por el AUG más cercano al DSH fue resistente (Garcia-Moreno et al., 2015).

En trabajos anteriores se propuso que la función del eIF2 en células infectadas por SINV podría ser reemplazada por otros factores celulares como el eIF2A (Ventoso et al., 2006). A pesar de que el eIF2A se descubrió hace varios años, su actividad en células de mamífero continúa siendo desconocida, y en levaduras la deleción de su ortólogo no tiene efecto en la viabilidad celular (Zoll et al., 2002). Inicialmente se demostró que eIF2A puede interaccionar con el Met-$tRNA_i^{Met}$ y transportarlo al ribosoma (Merrick and Anderson, 1975). Sin embargo, empleando sistemas artificiales se comprobó que esta unión con el tRNA era independiente de GTP y mucho menos eficiente que la observada con eIF2 (Golovko 2016). Por otra parte, se observó que eIF2A tampoco consigue promover la unión del Met-$tRNA_i^{Met}$ al mRNA de globina (Adams et al., 1975). Descubrimientos recientes sugieren que eIF2A está implicado en la traducción de algunos mRNAs celulares especializados que inician su traducción en codones no-AUG, como UUG y CUG (Liang et al., 2014, Starck et al., 2016). Resulta de interés que la participación de eIF2A en la iniciación de la traducción en ORFs *upstream* (uORFs) no-convencionales ha hecho que se relacione este factor con la progresión de algunos procesos cancerosos (Sendoel et al., 2017). Sorprendentemente, el desarrollo de ratones con el gen *eIF2A* delecionado es completamente normal, lo cual indica que eIF2A no es

requerido para la traducción de mRNAs normales ni especializados en ratones (Golovko et al., 2016).

Otro posible factor sustitutivo del eIF2 en la iniciación de la traducción del sgRNA de SINV es el eIF2D (Skabkin et al., 2010). Inicialmente se asoció este factor con el desplazamiento del tRNA deacetilado y del mRNA de la subunidad ribosómica 40S para su reciclaje. Además, eIF2D podría interferir con la formación del complejo de iniciación 48S promovida por eIF2 (Skabkin et al., 2010). eIF2D puede formar un complejo con el Met-tRNA$_i^{Met}$ de forma independiente de GTP, y después interaccionar con la subunidad 40S ribosómica para llevar el tRNA$_i$ al sitio P ribosómico (Dmitriev et al., 2010). Tras determinarse la estructura cristalográfica de este factor, se observaron dos dominios diferentes: el dominio SUI1 que presenta una estructura similar a un dominio del eIF1 (factor crucial para el *scanning* y la selección del codón iniciador), y el dominio SWIB/MDM2 (Vaidya et al., 2017). A pesar de estos esfuerzos, aún existe mucha controversia en cuanto al papel de estos factores en la traducción.

OBJETIVOS

OBJETIVOS

Los objetivos desarrollados en esta tesis doctoral han sido:

1. Estudio del efecto de inhibidores selectivos de eIFs, en concreto del eIF4A y del eIF2, sobre el requerimiento de factores para la traducción de SINV en células de mamífero en diferentes fases del ciclo infectivo.

2. Caracterización de la implicación de la estructura y la secuencia del mRNA en la traducción viral y el requerimiento de factores celulares. Determinar especialmente la estructura y función del DSH del sgRNA de SINV.

3. Descripción del papel de los factores eIF2A y eIF2D como posibles sustitutos del eIF2 para la traducción de los mRNAs virales de SINV.

4. Caracterización de los requerimientos de estructura del RNA y factores para la iniciación de la traducción en codones no-AUG, empleando como modelo el sgRNA de SINV.

5. Determinación del requerimiento de factores eucarióticos para la traducción del mRNA de HCV en células de origen humano.

6. Identificación de las proteínas que interaccionan con los mRNAs virales y celulares en células de mamífero infectadas por SINV y su dinámica durante el ciclo infectivo.

MATERIALES Y MÉTODOS Y RESULTADOS

ARTÍCULO 1:

Differential action of pateamine A on translation of genomic and subgenomic mRNAs from Sindbis virus

El estudio de los eIFs implicados en la traducción de RNAs virales es clave en la identificación de dianas potenciales para bloquear la infección viral. En células de mamífero, SINV inhibe la traducción de los mRNAs celulares para favorecer la expresión de sus mRNAs, especialmente del sgRNA, y esta inhibición está estrechamente relacionada con la replicación viral (Sanz, Garcia-Moreno et al. 2015). En este trabajo se estudió en profundidad el papel del factor eIF4A y su implicación en la traducción tanto del gRNA como del sgRNA, con especial interés en el cambio de requerimiento de factores de iniciación para la traducción del sgRNA, que sucede a la par que el *shut-off* de la expresión de los mRNAs celulares. Con este objetivo, se empleó un compuesto inhibidor del eIF4A, la pateamina A (Pat A).

En este artículo, se determinó el efecto de la Pat A en la traducción del gRNA, a tiempos tempranos de la infección por SINV, en células de riñón de hámster BHK (*Baby Hamster Kidney*). Además, se estudió el efecto de este inhibidor sobre la traducción del gRNA viral fuera del contexto de infección. Para ello, se transfectaron células BHK con construcciones de RNA no replicativas, obtenidas mediante transcripción *in vitro*, que contenían luciferasa como gen reportero. En ambos casos, la Pat A induce una fuerte supresión de la traducción del gRNA de SINV. Por otra parte, la traducción del sgRNA de SINV se analizó en dos condiciones diferentes: (1) cuando deriva de la replicación viral - en células infectadas y en células transfectadas con replicones, y (2) fuera del contexto de replicación - en sistemas de traducción *in vitro* (lisado de reticulocitos de conejo, RRL) y en células transfectadas con sgRNAs obtenidos mediante transcripción *in vitro*. En el contexto replicativo, la traducción del sgRNA se vio escasamente inhibida tras el tratamiento con Pat A. Por el contrario, fuera del contexto de replicación viral, la Pat A sí inhibe la traducción del sgRNA.

Finalmente, se comprobó que, al inicio de la fase tardía, el sgRNA necesita eIF4A para su traducción, pero a medida que avanza esta fase, se va volviendo más independiente de este factor. Esta independencia sólo ocurre en contextos donde el RNA de SINV está siendo replicado. Para examinar en qué momento ocurre este cambio, células BHK infectadas con SINV fueron tratadas con Pat A y la síntesis de proteínas fue determinada a diferentes hpi mediante la incorporación de metionina

marcada radiactivamente. A partir de las 4 hpi, se observó una mayor resistencia de la traducción del sgRNA de SINV a la Pat A.

En este artículo, se demostró que la Pat A inhibe potentemente la traducción del gRNA de SINV, como se observa en la reducción de la síntesis de nsP1 y nsP2. Por otro lado, la síntesis de proteínas dirigida por el sgRNA es resistente a la acción de la Pat A a tiempos tardíos del ciclo infectivo. Curiosamente, el sgRNA es sensible a Pat A fuera del contexto de infección, como se ha observado en células transfectadas o sistemas *in vitro*, lo cual parece indicar que el sgRNA de SINV presenta un mecanismo dual de traducción.

GONZALEZ-ALMELA, E., SANZ, M. A., GARCIA-MORENO, M., NORTHCOTE, P., PELLETIER, J. AND CARRASCO, L. 2015. Differential action of pateamine A on translation of genomic and subgenomic mRNAs from Sindbis virus. *Virology*, 484: 41-50.

Virology 484 (2015) 41–50

Contents lists available at ScienceDirect

Virology

journal homepage: www.elsevier.com/locate/yviro

Differential action of pateamine A on translation of genomic and subgenomic mRNAs from Sindbis virus

Esther González-Almela [a], Miguel Angel Sanz [a], Manuel García-Moreno [a], Peter Northcote [b], Jerry Pelletier [c], Luis Carrasco [a,*]

[a] Centro de Biología Molecular Severo Ochoa (CSIC-UAM), C/Nicolás Cabrera, 1, Universidad Autónoma de Madrid, Cantoblanco, 28049 Madrid, Spain
[b] School of Chemical and Physical Sciences, Victoria University of Wellington, Wellington 6140, New Zealand
[c] Department of Biochemistry and Goodman Cancer Center, McIntyre Medical Sciences Building, 3655 Promenade Sir William Osler, McGill University, Montreal, Quebec, Canada H3G 1Y6

ARTICLE INFO

Article history:
Received 18 March 2015
Returned to author for revisions
28 April 2015
Accepted 3 May 2015
Available online 5 June 2015

Keywords:
Translation inhibitors
eIF4A
Sindbis virus
Alphavirus protein synthesis
Helicase inhibitor

ABSTRACT

Pateamine A (Pat A) is a natural marine product that interacts specifically with the translation initiation factor eIF4A leading to the disruption of the eIF4F complex. In the present study, we have examined the activity of Pat A on the translation of Sindbis virus (SINV) mRNAs. Translation of genomic mRNA is strongly suppressed by Pat A, as shown by the reduction of nsP1 or nsP2 synthesis. Notably, protein synthesis directed by subgenomic mRNA is resistant to Pat A inhibition when the compound is added at late times following infection; however, subgenomic mRNA is sensitive to Pat A in transfected cells or in cell free systems, indicating that this viral mRNA exhibits a dual mechanism of translation. A detailed kinetic analysis of Pat A inhibition in SINV-infected cells demonstrates that a switch occurs approximately 4 h after infection, rendering subgenomic mRNA translation more resistant to Pat A inhibition.

Introduction

Translation of cellular and viral mRNAs can take place by a number of mechanisms depending on the mRNA and the context of its translation. The vast majority of cellular mRNAs contain a cap structure at their 5′ end and are translated following the canonical mechanism that involves the recognition of the cap structure by the heterotrimeric factor eIF4F followed by the interaction of the preinitiation 43S complex with the mRNA (Sonenberg and Hinnebusch, 2009). The eIF4F complex is composed of the cap-binding factor eIF4E, the helicase and ATPase enzyme eIF4A and the scaffolding protein eIF4G (Gingras et al., 1999). Unwinding of the secondary structure present in the mRNA leader sequence is accomplished by eIF4AI or eIF4AII, which are functionally interchangeable isoforms with 90% similarity (Parsyan et al., 2011). After RNA unwinding, the 40S ribosomal subunit containing several initiation factors linearly scans the leader sequence until an AUG codon is encountered in a good sequence context (Kozak, 1991). Initiation of translation can also occur by a mechanism which is independent of the cap structure whereby initiation takes place at an internal sequence located at the 5′ untranslated region (5′-UTR) of the mRNA, known as the Internal Ribosome Entry Site (IRES) (Au and Jan, 2014; Komar et al., 2012; Niepmann, 2009). This element promotes the direct interaction of preinitiation complexes, or even 40S ribosomal subunits, to an internal region of the mRNA leader sequence that can be followed by scanning until the initiation codon is reached (Au and Jan, 2014; Chamond et al., 2014). The number of eIFs that participate in this initiation mechanism, as well as the molecular events that occur to build up the 80S initiation complex, depends on the particular IRES analyzed. Yet another mechanism of translation has been observed with Sindbis virus (SINV) subgenomic mRNA (sgmRNA), which contains a cap structure and is translated by a scanning mechanism of its leader sequence, where cap recognition and linear scanning are accomplished without the participation of crucial eIFs, such as eIF2 or eIF4A (Garcia-Moreno et al., 2014). SINV belongs to the alphavirus genus in the *Togaviridae* family and contains a positive-stranded RNA as genome, which is delivered to the cytoplasm after virus entry (Brown and Hernandez, 2012; Schlesinger and Schlesinger, 1996; Strauss and Strauss, 1994). This genomic mRNA (gmRNA) directs the synthesis of early nonstructural proteins (nsP1-4), which are involved in RNA replication and transcription. In contrast, the sgmRNA is transcribed and translated in the late phase of the virus life cycle and gives rise to the production of structural proteins concomitant with the inhibition of cellular mRNA translation (Sanz et al., 2014). Interestingly, SINV sgmRNA exhibits a dual mechanism of translation depending on the context in which it is translated. Thus, translation of this mRNA

* Corresponding author. Tel.: +34 1 497 84 50.
E-mail address: lcarrasco@cbm.csic.es (L. Carrasco).

http://dx.doi.org/10.1016/j.virol.2015.05.002
0042-6822/

does not require eIF2, eIF4G nor eIF4A in infected cells (Castelló et al., 2006; Garcia-Moreno et al., 2013; Sanz et al., 2009; Ventoso et al., 2006). In contrast, these factors are necessary to initiate protein synthesis on sgmRNA in cell free systems or in transfected cells.

Inhibitors of cellular functions are very valuable as therapeutic agents, but they also represent important tools to help unravel the molecular events involved in a given cellular or viral process. This is the case for translation inhibitors, which have been widely employed to explore the processes of mRNA translation (Lindqvist and Pelletier, 2009; Vázquez, 1979). More recently, high throughput screening methods have led to the discovery of a number of new translation inhibitors with promising applications in molecular biology (Cencic et al., 2011, 2012). One such molecule is pateamine A (Pat A), a natural marine compound synthesized by the sponge *Mycale* sp. (Hood et al., 2001; Low et al., 2007). Pat A targets eIF4A and enhancing its helicase and ATPase activities disrupts its interaction with eIF4G while promoting the formation of a stable complex between eIF4A and eIF4B (Bordeleau et al., 2005, 2006; Low et al., 2005). This disruption may lead to an inhibition of the interaction of the preinitiation complexes with mRNA (Bordeleau et al., 2006), or to the stalling of initiation complexes at the leader region of mRNA *in vitro* (Low et al., 2005). Thus, translation of capped mRNAs that require the eIF4F complex is blocked. In contrast, hepatitis C virus (HCV) mRNA is not inhibited by Pat A, although other mRNAs bearing picornavirus IRES elements are blocked by this compound (Bordeleau et al., 2006; Low et al., 2005). Additionally, Pat A induces the formation of stress granules (SG) by a pathway independent of eIF2α phosphorylation (Dang et al., 2006). In the present work, we have tested the activity of Pat A on the translation of SINV gmRNA and sgmRNA, both of which contain a cap-structure at the 5′ end. Our results show that protein synthesis directed by sgmRNA is resistant to Pat A inhibition, whereas gmRNA translation is blocked. Moreover, resistance of sgmRNA to Pat A is only observed in SINV-infected cells, but not when this mRNA is translated out of the infection context. This represents the first example of a capped mRNA that is resistant to Pat A.

Results

Early translation of SINV gmRNA. Inhibition of nsP synthesis by Pat A

The first step in the SINV replication cycle after virus entry is the translation of the input gmRNA that has been delivered to the cytoplasm (Hernandez et al., 2014). The schematic representation of gmRNA, sgmRNA and the different constructs used in this work are shown in Fig. 1a. To analyze the action of Pat A on translation, BHK cells were initially infected with SINV for 1 h to allow virus entry. Then, increasing amounts of the inhibitor were added and cells were incubated for one additional hour. Synthesis of nsP1and nsP2 was analyzed by immunoblotting using specific polyclonal antibodies. Used at a concentration of 100 nM, Pat A markedly inhibited the synthesis of nsP1 and nsP2 (Fig. 1b and c). Next, translation of gmRNA was assayed by transfection of a non-replicative RNA lacking most of the coding region of nsP4 and bearing the luciferase gene embedded within the nsP3 sequence (see SV-Luc ΔnsP4 scheme in Fig. 1a). Synthesis of luciferase directed by this mRNA was strongly inhibited by Pat A in transfected BHK cells (Fig. 1d). The extent of inhibition was similar to that observed with a control cap-Luc mRNA, whereas synthesis of luciferase directed by CrPV IGR-Luc mRNA was moderately stimulated by Pat A. The cap-Luc contains the cellular leader sequence of luciferase mRNA, while CrPV IGR IRES has the intergenic region (IGR) from cricket paralysis virus (CrPV) genome that confers translatability in the absence of any eIFs (Jan and Sarnow, 2002). This finding indicated that Pat A has no effect on the elongation or termination steps of translation and is consistent with the idea that Pat A is a selective inhibitor of eIF4A. Therefore, SINV gmRNA requires this initiation factor for its translation early during infection.

To further analyze the synthesis of nsPs and to test the formation of SG by Pat A, BHK cells were treated with Pat A or sodium arsenite, an inducer of oxidative stress, and immunocytochemistry was used to analyze SG formation. Treatment of control uninfected BHK cells with Pat A (400 nM) resulted in TIA-1 release from the nucleus to the cytoplasm and stimulated formation of SGs at a level similar to that observed with sodium arsenite (Fig. 2). As expected, the synthesis of nsP2 was diminished by Pat A in SINV infected cells, as assessed by reduced staining with an antibody against nsP2 (Fig. 2). The amount of nsP2 observed in presence of 200 μM sodium arsenite may correspond to partial inhibition by this compound. Formation of SG was abrogated in SINV-infected cells at 3 h post infection (hpi), perhaps due to the production of nsP3 before treatment with the inhibitors (Panas et al., 2012).

Previous observations indicated that Pat A blocks eIF4A in an irreversible manner (Bordeleau et al., 2005; Low et al., 2005). Thus, we tested the potential irreversibility of Pat A inhibition directly on protein synthesis in SINV infected cells in order to assess the blockade of other steps of SINV replication, such as the synthesis of late viral proteins. To this end, BHK cells were infected with SINV (10 pfu/cell) and cells were treated from 2 to 3 hpi with 200 nM Pat A. Subsequently, the inhibitor was extensively washed out and cells were replenished with fresh medium and protein synthesis monitored for several hours after washing. As shown in Fig. 3, the application of Pat A in uninfected cells for only 1 h potently blocked cellular mRNA translation even several hours after washing off the inhibitor. On the other hand, Pat A strongly blocked the remaining cellular mRNA translation, and also late viral proteins in SINV-infected BHK cells treated from 2–3 hpi. This blockade extended over the ensuing hours even in the absence of Pat A, demonstrating that this compound exerts an irreversible inhibition of translation.

Translation of SINV sgmRNA to produce late viral proteins. Action of Pat A

Viral RNA replication gives rise to the negative-stranded RNA, which contains two promoters: one located at the 3′-end and one located internally. Viral transcription using this internal promoter on negative RNA generates sgmRNA. Translation of this messenger gives rise to the structural viral proteins, which are synthesized as a large precursor that is proteolytically cleaved to render the mature viral proteins. The initiation of translation of sgmRNA at late stages of infection is carried out by a mechanism that does not require certain eIFs (Garcia-Moreno et al., 2013, 2014; Sanz et al., 2009, 2013). The inhibition of the synthesis of SINV structural proteins was examined by radioactive labeling from 5 to 6 hpi using different concentrations of Pat A. Translation of cellular mRNAs was blocked by 32.5% with 100 nM Pat A and this inhibition increased to 70% with 200 nM Pat A (Fig. 4a and b). At these concentrations, the translation of SINV sgmRNA was only marginally affected and a concentration of 400 nM Pat A was required to provoke a reduction of viral protein synthesis of 50%. However, this inhibition may not have been due solely to the blockade of eIF4A activity, but perhaps also to side-effects of the inhibitor on other cellular functions. Nevertheless, it can be concluded that a concentration of Pat A that reduced cellular protein synthesis by approximately 70% inhibited SINV sgmRNA translation by only ~20%, suggesting that initiation of translation

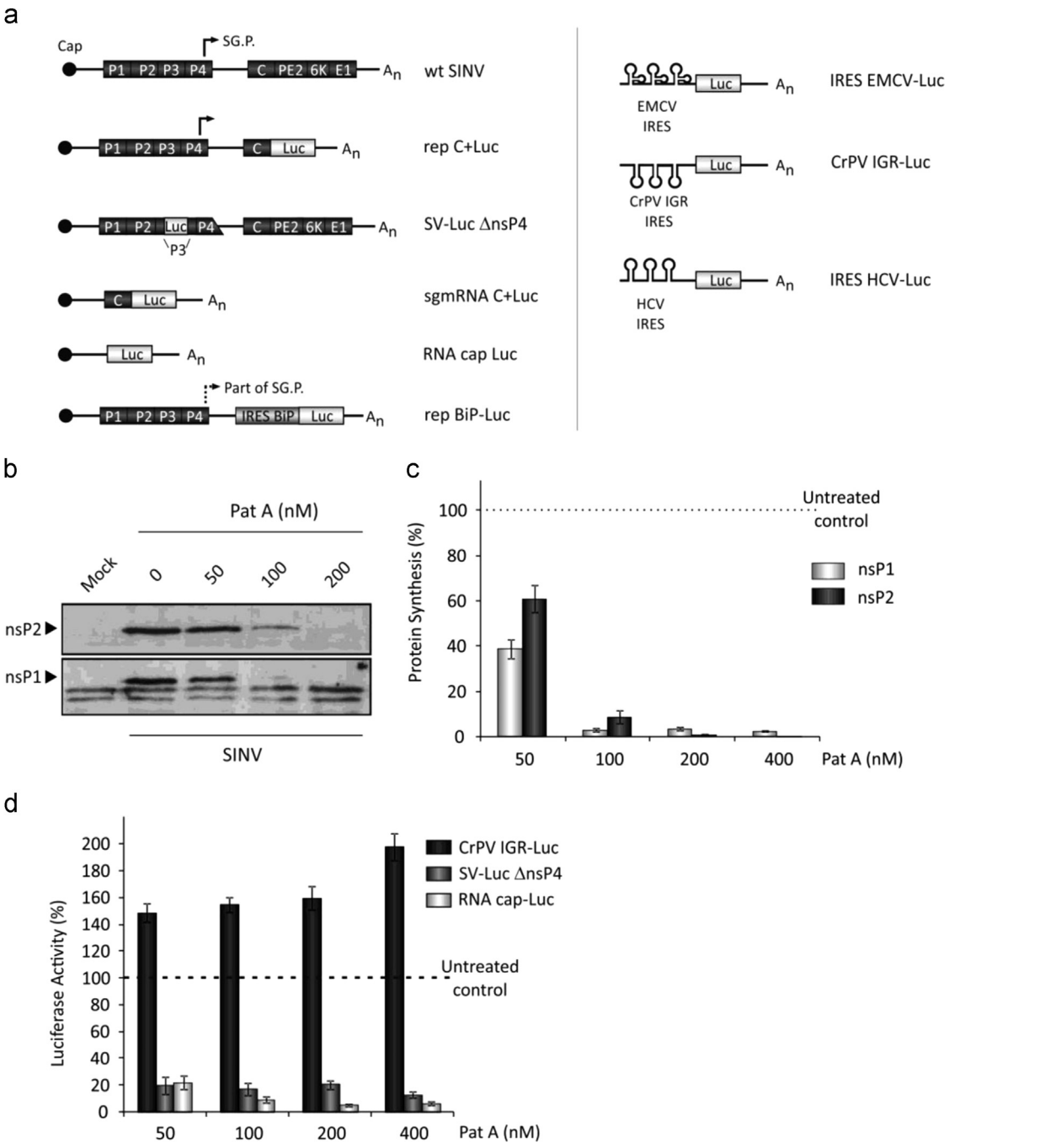

Fig. 1. Translation of SINV gmRNA. Effect of Pat A. **(a)** Schematic representation of the RNAs employed in this work. **(b)** BHK cells were mock-infected or infected with SINV at a multiplicity of infection (MOI) of 10 pfu/cell. At 1 hpi, cells were treated with vehicle or Pat A for 1 h at the indicated concentrations. SINV proteins nsP2 (upper panel) and nsP1 (lower panel) were analyzed by western blot. The results shown are representative of three independent experiments. **(c)** Densitometric values of western blots of the viral proteins nsP1 and nsP2 are expressed as the percentage of untreated samples. The results represent the mean ± SD of three independent experiments. **(d)** *In vitro* synthesized RNAs gmRNA SV-Luc ΔnsP4, RNA cap-Luc and CrPV IGR-Luc were transfected into BHK cells with Lipofectamine 2000. Different concentrations of Pat A (50, 100, 200 and 400 nM) or cycloheximide (100 mg ml^{-1}) were added at 1 hpt and cells were incubated for 1 h before analysis of luciferase activity. Values obtained from cycloheximide-treated cells were used to subtract the amount of luciferase synthesized prior to Pat A addition. Luciferase activity values of Pat A-treated cells are expressed as percentage of untreated samples. The results represent the mean ± SD of three independent experiments.

of this viral messenger does not require eIF4A or intact eIF4F complex at later times of the viral life cycle. Of note, the inhibition of endogenous translation was less efficient when compared with transfected cap-Luc mRNA (Fig. 1c). This result is consistent with the idea that disruption of the eIF4F complex has a greater impact on *de novo* translation of mRNAs as compared to protein synthesis directed by preexisting mRNAs already engaged in the polysome (Novoa and Carrasco, 1999).

As with most alphaviruses, SINV is an arthropod borne virus (arbovirus) that has two natural hosts for its transmission. Thus, aside from vertebrate cells, SINV also infects insect cells, giving rise to a productive infection without apparent inhibition of host protein synthesis. Therefore, we next explored the action of Pat A on translation in mosquito C6/36 cells infected of SINV (10 pfu/cell) and treated with different concentrations of the compound. As a control, the activity of Pat A was also examined in uninfected

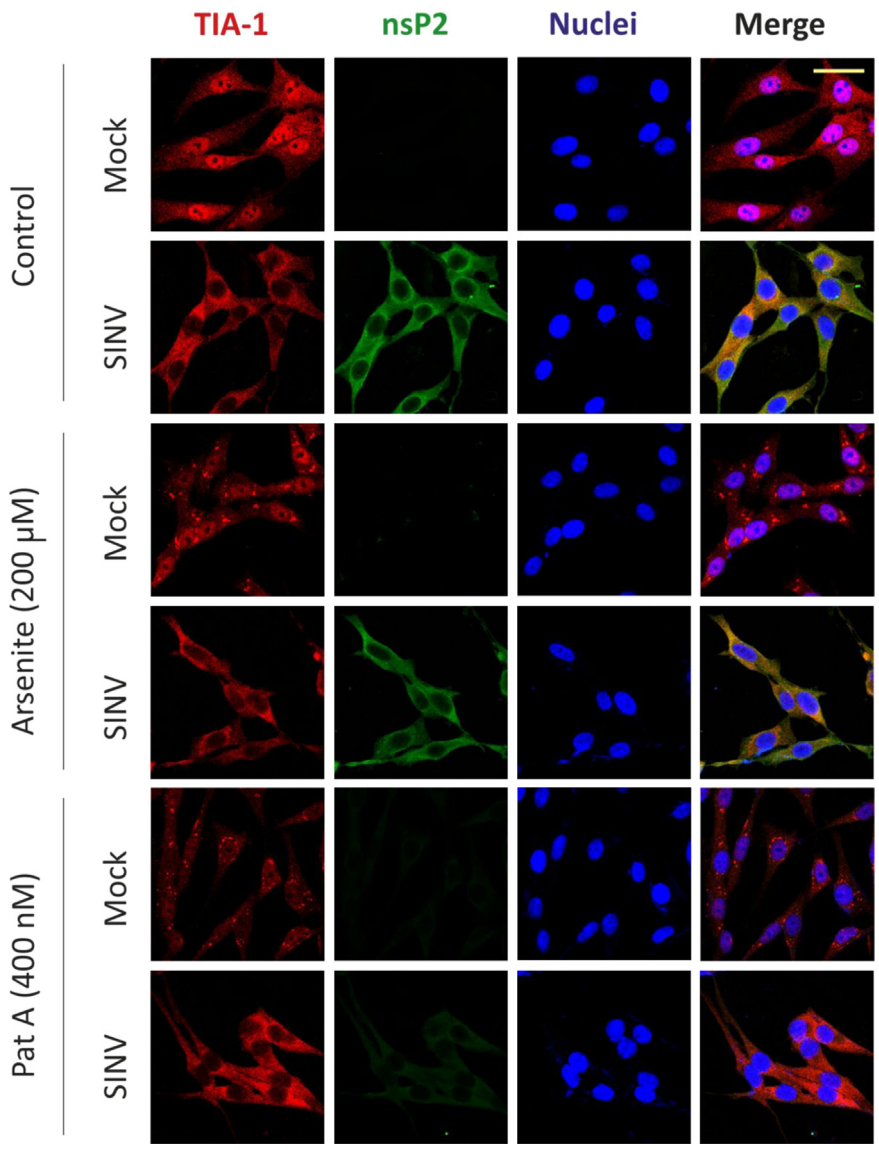

Fig. 2. Pat A-induced formation of stress granules. Blockade by SINV infection. BHK cells seeded on glass coverslips were mock-infected or infected with SINV (MOI of 10 pfu/cell). At 2 hpi, cells were treated or not with Pat A (400 nM) or sodium arsenite (200 μM) for 1 h. At 3 hpi, cells were fixed, permeabilized and processed for immunofluorescence using anti-TIA-1 (red), anti-nsP2 (green) and DAPI (blue). Images were acquired with a confocal microscope and subsequently processed with Zeiss Zen 2010B sp1 and Zen 2008 software (Zeiss). Merged images show the simultaneous visualization of TIA-1, nsP2 and nucleic acids. Scale bar represents 30 μm. The results shown are representative of three independent experiments.

mosquito cells. Analogous to vertebrate cells, protein synthesis was also inhibited by Pat A in insect cells (Fig. S1). In contrast, sgmRNA translation at 7 hpi was more resistant to inhibition by Pat A than cellular protein synthesis, even though the shut-off of host translation does not occur in mosquito cells. Therefore, the translation of sgmRNA appears to be more eIF4A/eIF4F-dependent in insect cells than in vertebrate settings. This result indicates that the resistance to Pat A in infected cells is specific for sgmRNA translation and does not occur with other mRNAs that are translated in the same cell.

It should be possible that Pat A resistance of SINV sgmRNA was due to the fact that it is synthesized in large amounts from SINV replicons and that these newly-synthesized mRNAs are located in specific foci in close proximity to components of the protein synthesizing machinery (Sanz et al., 2009). To test this possibility, the sequence of luciferase gene preceded by a cellular IRES element was cloned in place of SINV sgmRNA (see rep BiP-Luc scheme Fig. 1a). The sgmRNA that is rendered after transfection of rep BiP-Luc bears the IRES from the cellular mRNA that encodes for the chaperone BiP (binding immunoglobulin protein). Translation of this mRNA is independent of eIF2α phosphorylation (Fernandez et al., 2002) and therefore can be translated in BHK cells that replicate SINV RNA. Interestingly, Pat A strongly blocked luciferase synthesis directed by this mRNA, indicating that it requires eIF4A for translation under these conditions (Fig. 5). As a control SINV rep C+luc was tested. In this case, the inhibition of sgmRNA translation by Pat A was lower as compared to rep BiP-Luc. Luciferase synthesis was assayed by measuring its activity (Fig. 5). In conclusion, only protein synthesis directed by SINV sgmRNA was resistant to Pat A, whereas under the same conditions translation driven by a cellular IRES was sensitive to this inhibitor.

Pat A inhibits sgmRNA translation out of the viral infection context

We next questioned whether the resistance of sgmRNA translation to Pat A was an intrinsic property of the RNA structure or whether such a resistance was due to conditions existing in cells

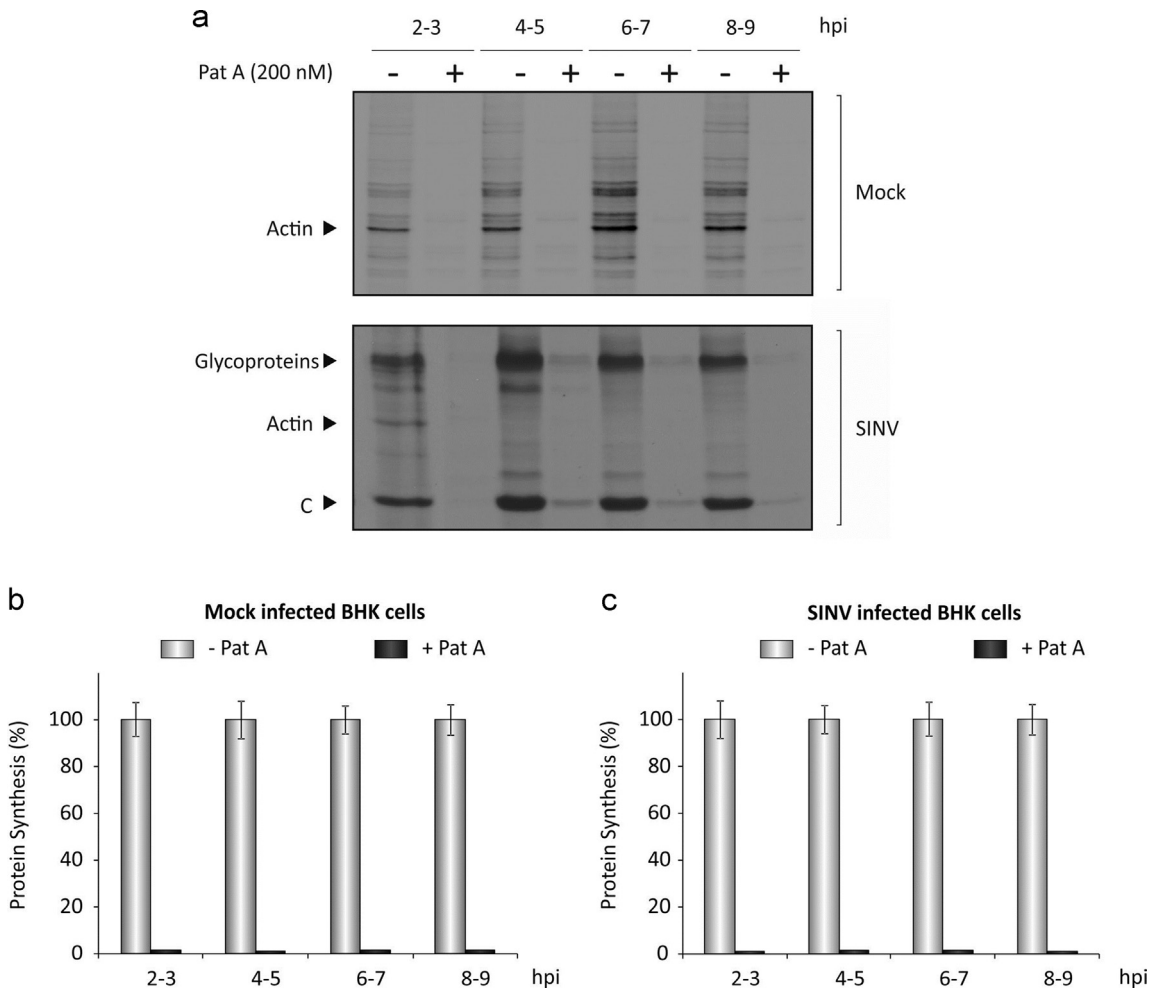

Fig. 3. Pat A blocks protein synthesis in an irreversible manner. **(a)** BHK cells were infected with SINV at a MOI of 10 pfu/cell for 1 h. Cells were then treated or not with Pat A (200 nM) from 1 to 2 hpi. Subsequently, Pat A was washed out and replaced by fresh medium. At the indicated times, cells were labeled with [^{35}S]Met−Cys for 1 h. Radiolabeled proteins were separated by SDS-PAGE, followed by autoradiography. The results shown are representative of three independent experiments. **(b)** The percentage of cellular (actin) and **(c)** viral C protein synthesis in cells treated or not with Pat A (200 nM) were calculated from values obtained by densitometric scanning of the corresponding bands. The results are mean ± SD of three independent experiments.

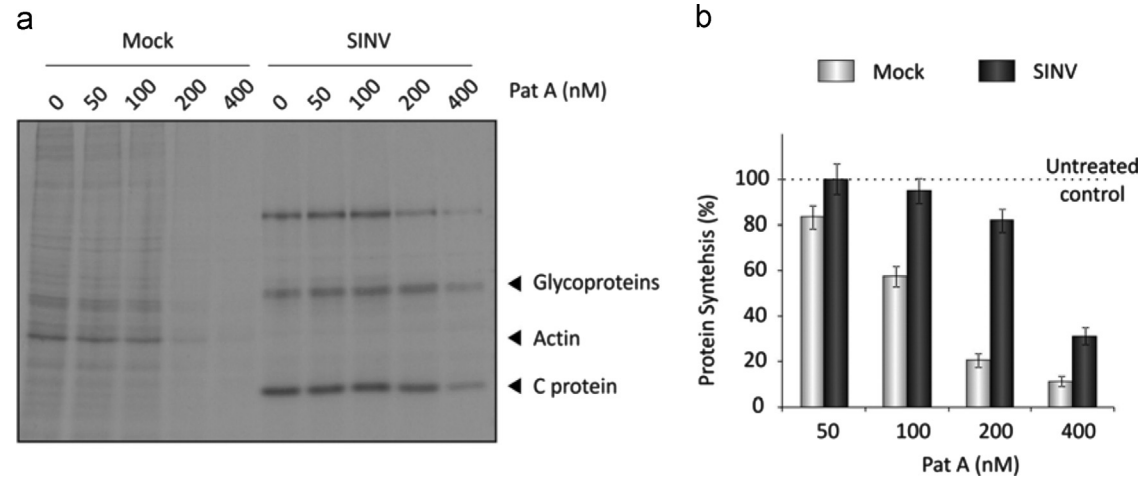

Fig. 4. Action of Pat A on the translation of SINV sgmRNA. **(a)** BHK cells were either mock-infected or infected with SINV (MOI of 10 pfu/cell). From 5 to 6 hpi, cells were treated or not with the indicated concentrations of Pat A while they were labeled with [^{35}S]Met−Cys. Radiolabeled proteins were separated by SDS-PAGE, followed by autoradiography. The results shown are representative of three independent experiments. **(b)** Values of cellular and viral protein synthesis were obtained by densitometric scanning of the radioactive signal and are expressed as the percentage of untreated samples. The results represent the mean ± SD of three independent experiments.

replicating SINV RNA. Initially, different mRNAs, including sgmRNA, were transfected into BHK cells and luciferase synthesis was measured after addition of increasing concentrations of Pat A. Cycloheximide was added at the same time and served to establish the amount of luciferase synthesized before the addition of Pat A, and this was subtracted from these samples. As positive controls of

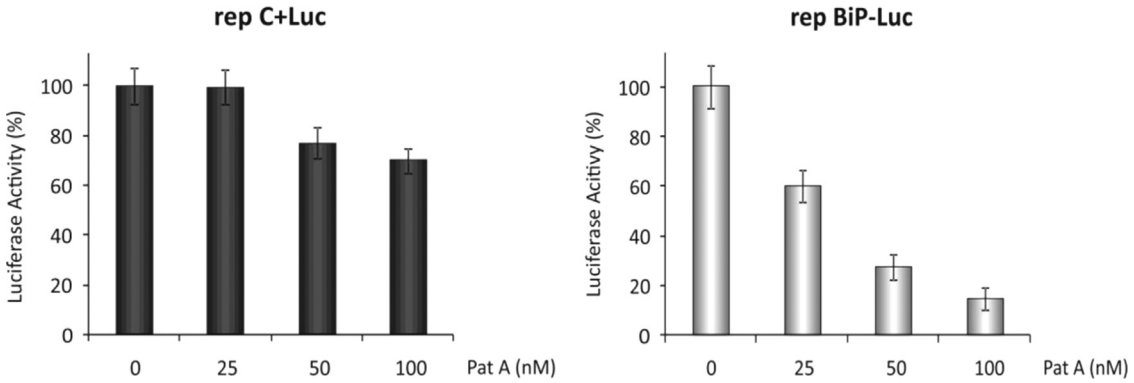

Fig. 5. Luciferase synthesis from rep C+Luc and rep BiP-Luc. Action of Pat A. BHK cells were transfected with *in vitro* synthesized RNAs rep C+Luc and rep BiP-Luc with Lipofectamine 2000. Different concentrations of Pat A (25, 50 and 100 nM) or cycloheximide (100 μg ml^{-1}) were added at 5 hpt and cells were incubated for 2 h before analysis of luciferase activity. Values obtained from cycloheximide-treated cells were used to subtract the amount of luciferase synthesized prior to Pat A addition. Luciferase activity values of Pat A-treated cells are expressed as percentage of untreated samples. The RLU values obtained once the luciferase obtained in presence of cycloheximide was subtracted were rep C+Luc: 4864404 ± 359965.9; rep BiP+Luc: 1591818 ± 135304.5. These luciferase values were taken as 100% of control. The results represent the mean ± SD of three independent experiments.

mRNAs that utilize eIF4A, we employed the eIF4A-dependent cap-Luc and IRES EMC-Luc mRNAs. CrPV IGR-Luc and IRES HCV-Luc mRNAs served as negative controls as these are not dependent on eIF4A for initiation. As shown in Fig. 6a, SINV sgmRNA was blocked by Pat A in transfected BHK cells to an extent similar to that observed with cap-Luc mRNA, while CrPV IGR-Luc and IRES HCV-Luc mRNAs were in fact stimulated by Pat A. This stimulation was presumably due to the fact that the inhibition of cellular mRNA translation avoids the competition with translation driven by CrPV or HCV IRES. In contrast, IRES EMC-Luc mRNA was partially inhibited by Pat A, in agreement with *in vitro* results (Bordeleau et al., 2005; Low et al., 2005). Further evidence that Pat A could inhibit sgmRNA translation out of the context of active infection was obtained through *in vitro* translation assays using rabbit reticulocyte lysates (RRL). Increasing concentrations of Pat A inhibited *in vitro* translation directed by sgmRNA C+Luc as well as by cap-Luc or IRES EMC-Luc mRNAs (Fig. 6b). Interestingly, the optimal translation of sgmRNA C+Luc required high concentrations of KCl (Fig. 6c), as occurs with a variety of viral mRNAs which are translated late during infection (Koch et al., 1980). Moreover, the inhibition of sgmRNA C+Luc translation by Pat A was higher at the optimal concentration of KCl (Fig. 6c). Collectively, these findings indicate that the structure of sgmRNA is not responsible for its resistance to inhibition by Pat A in infected cells; instead, this viral messenger requires eIF4A for initiation of protein synthesis in uninfected cells.

Determination of the stage during SINV infection when translation becomes resistant to eIF4A

To further assess the activity of Pat A on sgmRNA translation in BHK cells that replicate SINV RNA, we made use of rep C+Luc (see scheme, Fig. 1a). This SINV replicon was firstly synthesized by *in vitro* transcription from the corresponding plasmid. After transfection of rep C+Luc, C protein was analyzed at two distinct time points in order to assess viral C production early during the late phase or at later times. The activity of Pat A on the production of C protein from 3 to 5 or from 6 to 8 h post transfection (hpt) was estimated by western blotting using specific rabbit polyclonal antibodies (Fig. S2). As a control, we measured in parallel the amount of protein C synthesized prior to Pat A treatment by adding cycloheximide. Surprisingly, 100 nM Pat A was strongly inhibitory (91%) for C production at early times of the late phase, whereas this inhibition was lower (20%) as replication progressed (Fig. S2). These findings suggested that sgmRNA translation requires eIF4A at early times and becomes less dependent on this factor at later infection times.

Additionally, the above results indicated that gmRNA translation was sensitive to inhibition by Pat A very early during SINV infection (Fig. 1), whereas at late times sgmRNA translation was more resistant to the inhibition of eIF4A (Fig. 4). This behavior of sgmRNA to Pat A only occurs in SINV-infected cells or in cells replicating SINV RNA (Fig. S2), suggesting that when viral infection progresses there is a switch from a mechanism of initiation of protein synthesis dependent on eIF4A to a mode of translation that is less dependent of this factor. To determine more accurately when this switch takes place, SINV-infected cells were treated with 200 nM Pat A at different hpi and protein synthesis was analyzed by radioactive labeling followed by SDS PAGE and fluorography. During the initial hours of infection, cellular translation was potently blocked by Pat A (Fig. 7a and b). Conversely, the synthesis of viral C protein was observed from 2 hpi and was concomitant with the increased shut-off of cellular protein synthesis. Notably, from 2–3 and 3–4 hpi, the synthesis of C protein was drastically reduced by Pat A, whereas from 4 hpi sgmRNA translation became more resistant to the inhibitor (Fig. 7a–c). Therefore, at early periods during the late phase sgmRNA translation was sensitive to Pat A, suggesting that a change occurs after that time which confers less dependency on eIF4A for the initiation of translation of sgmRNA in infected cells (Fig. 7c). Thus, Pat A constitutes a good tool for future studies to investigate the molecular nature of this switch. Further support to the concept that sgmRNA translation is more dependent on eIF4A at early times of the late phase was obtained by hippuristanol, the other selective inhibitor of eIF4A (Garcia-Moreno et al., 2013). Indeed, analysis of the inhibition of sgmRNA translation at different times p.i. by hippuristanol clearly indicates that this inhibition varies and becomes more resistant as infection progresses (Fig. S3).

Discussion

From the perspective of therapeutic agents and molecular tools, marine organisms are providing a very interesting number of natural compounds for investigation (Singh and Pelaez, 2008; Stonik and Fedorov, 2014; Vera and Joullié, 2002). Since the discovery of didemnins, the first marine natural products administered to humans (Lee et al., 2012), the number of new inhibitors of cellular functions from marine sources continues to rise (Skropeta and Wei, 2014). This is the case for hippuristanol and Pat A, two natural compounds produced by invertebrate marine organisms (Lindqvist and Pelletier, 2009). These

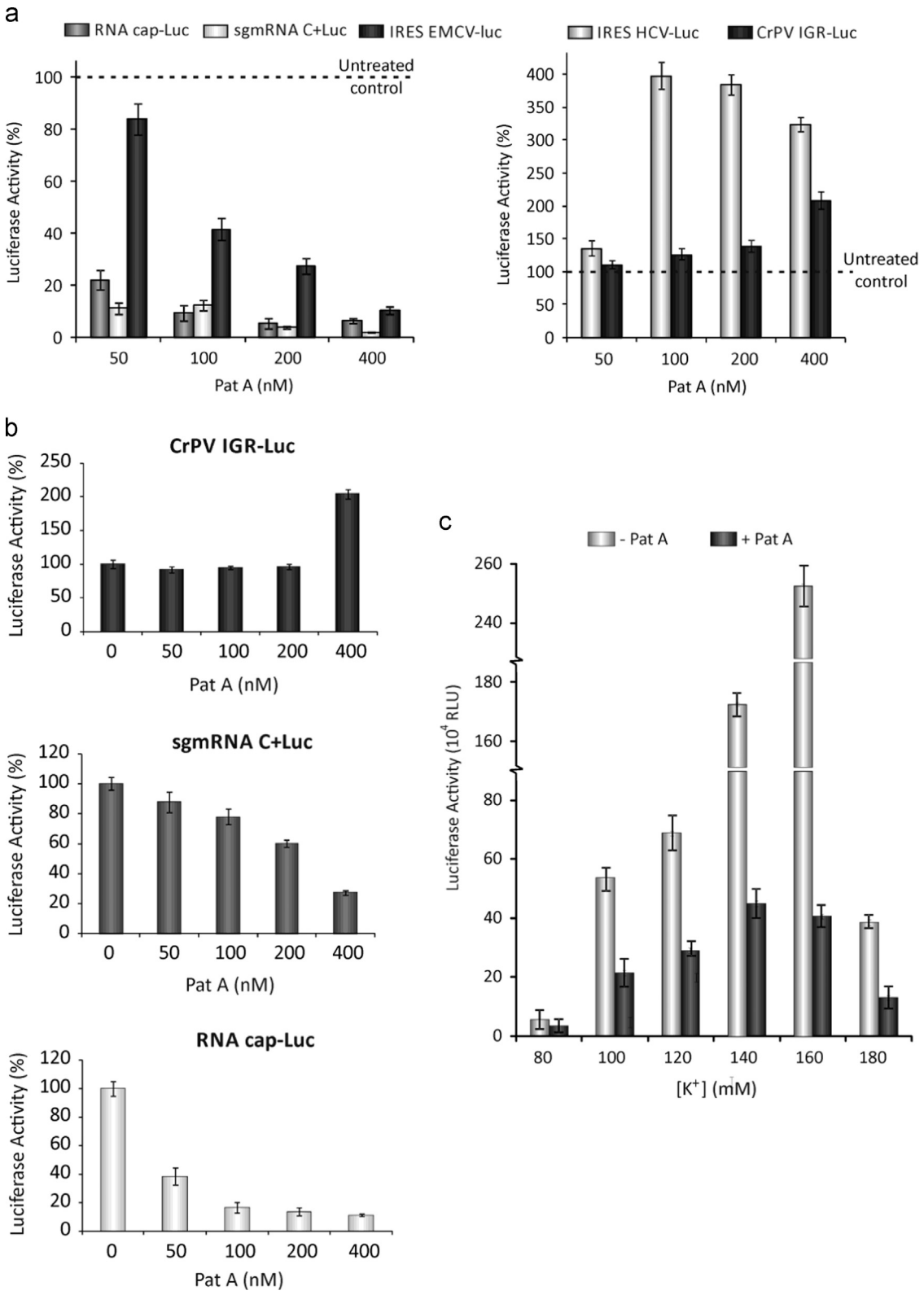

Fig. 6. Translation of sgmRNA outside the viral infection context. Activity of Pat A. **(a)** *In vitro* synthesized sgmRNA C+Luc and control RNAs eIF4A-dependent (RNA cap-Luc and IRES EMCV-Luc (left panel)) and eIF4A-independent (IRES HCV-Luc and CrPV IGR-Luc (right panel)) were transfected into BHK cells with Lipofectamine 2000. Cells were then incubated with different concentrations of Pat A (50, 100, 200 and 400 nM) or cycloheximide (100 μg ml^{-1}) for 1 h before analysis of luciferase activity. Values obtained from cycloheximide-treated cells were used to subtract the amount of luciferase synthesized prior to Pat A addition. Luciferase activity values of Pat A-treated cells are expressed as percentage of untreated samples. The results are mean ± SD of three independent experiments. **(b)** CrPV IGR-Luc (upper panel), sgmRNA C+Luc (medium panel) and RNA cap-Luc (lower panel) were generated by *in vitro* transcription using T7 RNA polymerase and then, *in vitro* translated using nuclease-treated rabbit reticulocyte lysate (RRL), programmed with 200 ng of the different mRNAs. Luciferase activity values of Pat A-treated cells are expressed as percentage of untreated samples. The results are mean ± SD of three independent experiments. **(c)** Effect of potassium [K^+] on *in vitro* translation of sgmRNA C+Luc and its inhibition by Pat A. *In vitro* transcribed sgmRNA C+Luc (200 ng) was translated in RRL at different concentrations of [K^+] (80, 100, 120, 140, 160 and 180 mM) and treated or not with 200 nM of Pat A. Luciferase activity results are mean ± SD of three independent experiments. The percentage values of Pat A-treated cells relative to their respective untreated cells are indicated in the figure.

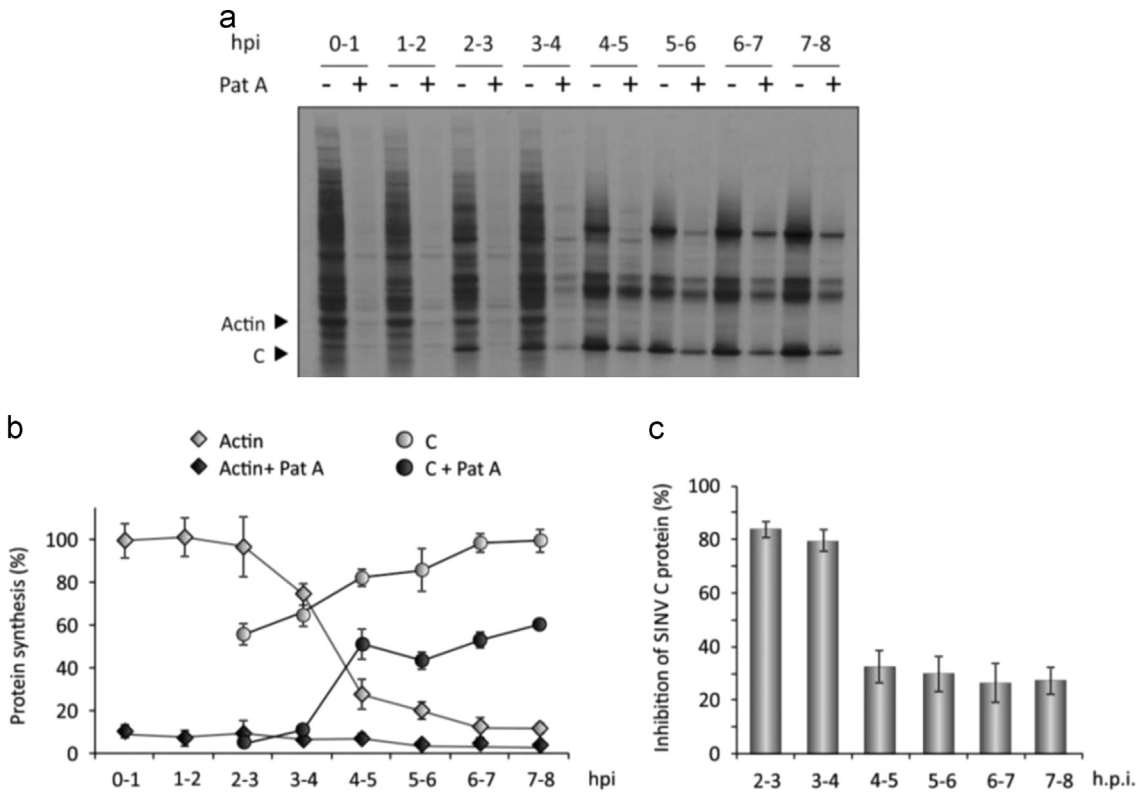

Fig. 7. Time-course of Pat A resistance of sgmRNA translation. **(a)** BHK cells were infected with SINV (MOI of 10 pfu/cell). At the indicated times post infection, cells were treated with vehicle or Pat A for 1 h at a concentration of 200 nM while they were labeled with [^{35}S]Met – Cys. Radiolabeled proteins were separated by SDS-PAGE, followed by autoradiography. The results shown are representative of three independent experiments. **(b)** The percentage of cellular (actin) and viral C protein synthesis in cells treated or not with Pat A (200 nM) were calculated from values obtained by densitometric scanning of the corresponding bands. The results are mean ± SD of three independent experiments. **(c)** Inhibition of Pat A on viral C protein is represented as the percentage of corresponding untreated samples. These results represent the mean ± SD of three independent experiments.

agents selectively inhibit the initiation of protein synthesis by targeting eIF4A, thus blocking the activity of the eIF4F complex. These inhibitors can be useful to ascertain the participation of eIF4A in the translation of some cellular and viral mRNAs. As reported in this work, Pat A strongly blocks the synthesis of SINV nsPs when used at early times post infection. This inhibition of viral translation is irreversible such that treatment for only 1 h is sufficient to block the synthesis of viral proteins at late times, as well as the inhibition of cellular translation. The arrest of late viral protein synthesis is most likely due to the inhibition of viral RNA replication and transcription that is accomplished by nsPs. Therefore, we can conclude that SINV gmRNA requires eIF4A for translation and the blockade of nsP synthesis abrogates the production of sgmRNA. The possibility that Pat A may affect other steps different to initiation is not supported by the finding that translation driven by the CrPV IRES is not only resistant, but is actually stimulated by Pat A, indicating that the elongation or termination processes of mRNA translation are not affected by this compound. The stimulation of CrPV IRES translation by Pat A may be a consequence of the inhibition of cellular protein synthesis and the concomitant release from mRNA competition. However, it is formally possible that Pat A affects other cellular functions, such as the redistribution of nuclear proteins, and that these reactions may affect sgmRNA translation at high concentrations of Pat A. The potential repercussions of these alterations for protein synthesis remains to be investigated, but we believe that the most important activity of Pat A on mRNA translation is its selective interaction with eIF4A, leading to the disruption of the eIF4F complex (Bordeleau et al., 2005; Low et al., 2005).

The results obtained with Pat A on the translation of SINV sgmRNA reinforce the view that eIF4A and the eIF4F complex are dispensable in infected cells (Castelló et al., 2006; Garcia-Moreno et al., 2013; Sanz et al., 2009). Thus, at concentrations of 200 nM Pat A there is a profound inhibition of cellular translation, while sgmRNA is only slightly blocked. Curiously, as observed with other translation inhibitors, protein synthesis directed by sgmRNA is negatively affected out of the replication complex (Garcia-Moreno et al., 2013). Therefore, our present results with Pat A are consistent with the concept that this messenger exhibits a dual mechanism for its translation and consequently the structure of sgmRNA does not confer independence for several eIFs (Sanz et al., 2009). This has been also clearly established for the requirement of eIF2. In this case, there is a stem-loop structure downstream of the AUG initiation codon (DLP) that confers eIF2 independence, but only in infected cells (Garcia-Moreno et al., 2013, 2014; McInerney et al., 2005; Ventoso et al., 2006). However, this DLP structure is not involved in providing independence for eIF4A (Garcia-Moreno et al., 2013). The structural requirements necessary for eIF4A-independent translation of sgmRNA remain to be investigated.

SINV infected cells undergo a drastic modification during infection, from a Pat A-sensitive status at early times to a more resistant status during the late phase of the viral cycle. Our kinetic analyses indicate that this change occurs at about 4 hpi. From this time onwards, translation of sgmRNA becomes independent of several eIFs, including the eIF4F complex. Future studies will be needed to determine the precise modifications that take place in SINV-infected cells to alter the mechanism of initiation of translation.

Methods

Cell lines and viruses

The cell lines used in this work were Baby hamster kidney (BHK-21) cells and *Aedes albopictus* C6/36 cells, both obtained from

ATCC. BHK-21 cells were grown at 37 °C, 5% CO_2 in Dulbecco's modified Eagle's medium (DMEM) supplemented with 5% fetal calf serum (FCS). C6/36 cells were cultured at 28 °C without CO_2 in M3 medium supplemented with 10% FCS. SINV derived from the pT7SVwt infective clone was used (Sanz and Carrasco, 2001). Viral infections of BHK-21 cells were carried out in DMEM without serum for 1 h at 37 °C, whereas infections of C6/36 cells were performed at 28 °C. Subsequently, medium was removed and infection was continued in DMEM with 5% FCS or M3 medium with 10% FCS, respectively, at the temperatures indicated. Infections with SINV were carried out at a multiplicity of 10 pfu per cell.

Plasmids and recombinant DNA procedures

The plasmids employed in this work are listed and described in Table S1. Plasmids were used as DNA templates for *in vitro* transcription with T7 or Sp6 RNA polymerases. pT7 SVwt (Sanz and Carrasco, 2001) was used as the parental plasmid for all of the constructs. The luciferase gene was derived from the plasmid pKS-Luc (Sanz et al., 2007).

Plasmid rep Bip-Luc was prepared with a product obtained after two consecutive PCRs between HpaI and SphI sites in rep C+luc. In the first PCR, oligonucleotides 5′ HpaI (5′-GCTATGGCGTTAACCGGTCTG-3′) and 3′ Nexo SV-Bip (5′-GGCCGGCGTCGACCTGCTGACTATTTAGG-3′) were used plus rep C+luc as DNA template. The other PCR product was obtained using 5′ Nexo SV-Bip (5′-CCTAAATAGTCAGCAGGTC-GACGCCGGCC-3′) and 3′ Luc SphI (5′-CCCGGGGCATGCGAGAATCT-GACGCAG-3′) oligonucleotides plus pBS-BIP-IRES-FFL-pA as DNA template, kindly provided from Dr. M. Hentze (EMBL Heidelberg, Germany). Oligonucleotides 5′ HpaI and 3′ Luc SphI with a mixture of the above products as DNA template were employed in the next PCR.

Antibodies

Rabbit polyclonal antibodies raised against SINV C protein and rat polyclonal antibodies raised against bacterially produced nsP1 were produced in our laboratory. Rabbit polyclonal anti-nsP2 was a kind gift from Dr. Richard W Hardy (Indiana University, USA). Goat polyclonal anti-TIA-1 was purchased from Invitrogen and Santa Cruz Biotechnology. Anti-rabbit and anti-rat immunoglobulin G antibodies coupled to peroxidase were purchased from Amersham. Specific antibodies conjugated to Alexa 488 or Alexa 555 (A-21202 and A-21432 respectively) were obtained from Invitrogen.

Inhibitors

The following chemical inhibitors were used: pateamine A was purified as previously described (Bordeleau et al., 2005), hippuristanol (Bordeleau et al., 2006), sodium arsenite (Riedel-de Haën) and cycloheximide (Sigma).

In vitro RNA transcription and translation

Linearized plasmids were used as templates for *in vitro* RNA transcription using T7 or SP6 RNA polymerases (New England Biolabs), as previously described (Garcia-Moreno et al., 2013). *In vitro* translation was carried out in nuclease-treated rabbit reticulocyte lysate (RRL) (Promega). One hundred nanograms of *in vitro* transcribed mRNAs were added to the translation mixture. Protein synthesis was estimated by measuring luciferase activity.

RNA transfection

In vitro transcribed RNAs were transfected using Lipofectamine 2000 (Invitrogen) according to the supplier's recommendations.

Measurement of luciferase activity

Luciferase activity was determined as described by Sanz et al. (2014).

Analysis of protein synthesis and western blotting

Protein synthesis was analyzed at the indicated times by replacing growth media for 1 h with 0.2 ml of methionine/cysteine-free DMEM supplemented with 1 μl of EasyTagTM EXPRESS ^{35}S Protein Labeling, [^{35}S]Met – Cys (11 mCi ml^{-1}, Perkin Elmer) per well of an L-24 plate. Labeling medium also included inhibitors when the action of these compounds was assayed. Radioactive proteins and samples for western blotting were analyzed as described (Garcia-Moreno et al., 2013). Protein synthesis was quantified by densitometry using a GS-800 Calibrated Densitometer (Bio-Rad).

Immunofluorescence assays

Fixation, permeabilization and confocal microscopy were performed as described (Madan et al., 2008) using a confocal laser scanning and multiphoton microscope LSM 710 coupled to an inverted microscope (Axio Observer, Zeiss). Primary antibodies used were: rabbit polyclonal anti SINV nsP2, and goat polyclonal anti-TIA-1 at a 1:500 dilution. Specific antibodies conjugated to Alexa 488 and Alexa 555 were employed as secondary antibodies at a 1:1000 dilution. DAPI (4′-6-diamidino-2-phenylindole) was used to stain the nuclei.

Acknowledgements

This study was supported by a DGICYT (Dirección General de Investigación Científica y Técnica. Ministerio de Economía y Competitividad, Spain) grant (BFU2012-31861). The Institutional Grant awarded to the Centro de Biología Molecular “Severo Ochoa” (CSIC-UAM) by the Fundación Ramón Areces is acknowledged.

Appendix. Supporting information

Supplementary data associated with this article can be found in the online version at http://dx.doi.org/10.1016/j.virol.2015.05.002.

References

Au, H.H., Jan, E., 2014. Novel viral translation strategies. Wiley Interdiscip. Rev. RNA 5, 779–801.
Bordeleau, M.-E., Matthews, J., Wojnar, J.M., Lindqvist, L., Novac, O., Jankowsky, E., Sonenberg, N., Northcote, P., Teesdale-Spittle, P., Pelletier, J., 2005. Stimulation of mammalian translation initiation factor eIF4A activity by a small molecule inhibitor of eukaryotic translation. Proc. Natl. Acad. Sci. USA 102, 10460–10465.
Bordeleau, M.-E., Cencic, R., Lindqvist, L., Oberer, M., Northcote, P., Wagner, G., Pelletier, J., 2006. RNA-mediated sequestration of the RNA helicase eIF4A by Pateamine A inhibits translation initiation. Chem. Biol. 13, 1287–1295.
Brown, D.T., Hernandez, R., 2012. Infection of cells by alphaviruses. Adv. Exp. Med. Biol. 726, 181–199.
Castelló, A., Sanz, M.A., Molina, S., Carrasco, L., 2006. Translation of Sindbis virus 26S mRNA does not require intact eukariotic initiation factor 4G. J. Mol. Biol. 355, 942–956.
Cencic, R., Hall, D.R., Robert, F., Du, Y., Min, J., Li, L., Qui, M., Lewis, I., Kurtkaya, S., Dingledine, R., et al., 2011. Reversing chemoresistance by small molecule inhibition of the translation initiation complex eIF4F. Proc. Natl. Acad. Sci. USA 108, 1046–1051.

Cencic, R., Galicia-Vázquez, G., Pelletier, J., 2012. Chapter twenty – inhibitors of translation targeting eukaryotic translation initiation factor 4A. In: Eckhard Jankowsky (Ed.), Methods in EnzymologyAcademic Press, pp. 437–461.
Chamond, N., Deforges, J., Ulryck, N., Sargueil, B., 2014. 40S recruitment in the absence of eIF4G/4A by EMCV IRES refines the model for translation initiation on the archetype of Type II IRESs. Nucleic Acids Res. 42, 10373–10384.
Dang, Y., Kedersha, N., Low, W.-K., Romo, D., Gorospe, M., Kaufman, R., Anderson, P., Liu, J.O., 2006. Eukaryotic initiation factor 2alpha-independent pathway of stress granule induction by the natural product pateamine A. J. Biol. Chem. 281, 32870–32878.
Fernandez, J., Yaman, I., Merrick, W.C., Koromilas, A., Wek, R.C., Sood, R., Hensold, J., Hatzoglou, M., 2002. Regulation of internal ribosome entry site-mediated translation by eukaryotic initiation factor-2alpha phosphorylation and translation of a small upstream open reading frame. J. Biol. Chem. 277, 2050–2058.
Garcia-Moreno, M., Sanz, M.A., Pelletier, J., Carrasco, L., 2013. Requirements for eIF4A and eIF2 during translation of Sindbis virus subgenomic mRNA in vertebrate and invertebrate host cells. Cell. Microbiol. 15, 823–840.
Garcia-Moreno, M., Sanz, M.A., Carrasco, L., 2014. Initiation codon selection is accomplished by a scanning mechanism without crucial initiation factors in Sindbis virus subgenomic mRNA. RNA 21, 93–112.
Gingras, A.C., Raught, B., Sonenberg, N., 1999. eIF4 initiation factors: effectors of mRNA recruitment to ribosomes and regulators of translation. Annu. Rev. Biochem. 68, 913–963.
Hernandez, R., Brown, D.T., Paredes, A., 2014. Structural differences observed in arboviruses of the alphavirus and flavivirus genera. Adv. Virol. *2014*, 259382.
Hood, K.A., West, L.M., Northcote, P.T., Berridge, M.V., Miller, J.H., 2001. Induction of apoptosis by the marine sponge (Mycale) metabolites, mycalamide A and pateamine. Apoptosis Int. J. Program. Cell Death 6, 207–219.
Jan, E., Sarnow, P., 2002. Factorless ribosome assembly on the internal ribosome entry site of cricket paralysis virus. J. Mol. Biol. 324, 889–902.
Koch, G., Bilello, J.A., Kruppa, J., Koch, F., Oppermann, H., 1980. Amplification of translational control by membrane-mediated events: a pleiotropic effect on cellular and viral gene expression. Annu. N. Y. Acad. Sci. 339, 280–306.
Komar, A.A., Mazumder, B., Merrick, W.C., 2012. A new framework for understanding IRES-mediated translation. Gene 502, 75–86.
Kozak, M., 1991. Structural features in eukaryotic mRNAs that modulate the initiation of translation. J. Biol. Chem. 266, 19867–19870.
Lee, J., Currano, J.N., Carroll, P.J., Joullié, M.M., 2012. Didemnins, tamandarins and related natural products. Nat. Prod. Rep. 29, 404–424.
Lindqvist, L., Pelletier, J., 2009. Inhibitors of translation initiation as cancer therapeutics. Future Med. Chem. 1, 1709–1722.
Low, W.-K., Dang, Y., Schneider-Poetsch, T., Shi, Z., Choi, N.S., Merrick, W.C., Romo, D., Liu, J.O., 2005. Inhibition of eukaryotic translation initiation by the marine natural product pateamine A. Mol. Cell 20, 709–722.
Low, W.-K., Dang, Y., Schneider-Poetsch, T., Shi, Z., Choi, N.S., Rzasa, R.M., Shea, H.A., Li, S., Park, K., Ma, G., et al., 2007. Isolation and identification of eukaryotic initiation factor 4A as a molecular target for the marine natural product Pateamine A. Methods Enzymol. 431, 303–324.
Madan, V., Castelló, A., Carrasco, L., 2008. Viroporins from RNA viruses induce caspase-dependent apoptosis. Cell. Microbiol. 10, 437–451.
McInerney, G.M., Kedersha, N.L., Kaufman, R.J., Anderson, P., Liljeström, P., 2005. Importance of eIF2alpha phosphorylation and stress granule assembly in alphavirus translation regulation. Mol. Biol. Cell 16, 3753–3763.
Niepmann, M., 2009. Internal translation initiation of picornaviruses and hepatitis C virus. Biochim. Biophys. Acta 1789, 529–541.
Novoa, I., Carrasco, L., 1999. Cleavage of eukaryotic translation initiation factor 4G by exogenously added hybrid proteins containing poliovirus 2Apro in HeLa cells: effects on gene expression. Mol. Cell. Biol. 19, 2445–2454.
Panas, M.D., Varjak, M., Lulla, A., Eng, K.E., Merits, A., Karlsson Hedestam, G.B., McInerney, G.M., 2012. Sequestration of G3BP coupled with efficient translation inhibits stress granules in Semliki Forest virus infection. Mol. Biol. Cell 23, 4701–4712.
Parsyan, A., Svitkin, Y., Shahbazian, D., Gkogkas, C., Lasko, P., Merrick, W.C., Sonenberg, N., 2011. mRNA helicases: the tacticians of translational control. Nat. Rev. Mol. Cell Biol. 12, 235–245.
Sanz, M.A., Carrasco, L., 2001. Sindbis virus variant with a deletion in the 6K gene shows defects in glycoprotein processing and trafficking: lack of complementation by a wild-type 6K gene in *trans*. J. Virol. 75, 7778–7784.
Sanz, M.A., Castelló, A., Carrasco, L., 2007. Viral translation is coupled to transcription in Sindbis virus-infected cells. J. Virol. 81, 7061–7068.
Sanz, M.A., Castelló, A., Ventoso, I., Berlanga, J.J., Carrasco, L., 2009. Dual mechanism for the translation of subgenomic mRNA from Sindbis virus in infected and uninfected cells. PloS One 4, e4772.
Sanz, M.A., Redondo, N., García-Moreno, M., Carrasco, L., 2013. Phosphorylation of eIF2α is responsible for the failure of the picornavirus internal ribosome entry site to direct translation from Sindbis virus replicons. J. Gen. Virol. 94, 796–806.
Sanz, M.A., García-Moreno, M., and Carrasco, L. (2014). Inhibition of host protein synthesis by Sindbis virus: correlation with viral RNA replication and release of nuclear proteins to the cytoplasm. Cell. Microbiol.
Schlesinger, M.J., Schlesinger, S., 1996. Togaviridae and their replication. Field's Virol. Ed BN Fields Al pp, 825–843.
Singh, S.B., Pelaez, F., 2008. Biodiversity, chemical diversity and drug discovery. Prog. Drug Res. Fortschritte Arzneimittelforschung Prog. Rech. Pharm 65 (141), 143–174.
Skropeta, D., Wei, L., 2014. Recent advances in deep-sea natural products. Nat. Prod. Rep. 31, 999–1025.
Sonenberg, N., Hinnebusch, A.G., 2009. Regulation of translation initiation in eukaryotes: mechanisms and biological targets. Cell 136, 731–745.
Stonik, V.A., Fedorov, S.N., 2014. Marine low molecular weight natural products as potential cancer preventive compounds. Mar. Drugs 12, 636–671.
Strauss, J.H., Strauss, E.G., 1994. The alphaviruses: gene expression, replication, and evolution. Microbiol. Rev. 58, 491–562.
Vázquez D., 1979. Inhibitors of protein biosynthesis (Molecular Biology Biochemistry and Biophysics).
Ventoso, I., Sanz, M.A., Molina, S., Berlanga, J.J., Carrasco, L., Esteban, M., 2006. Translational resistance of late alphavirus mRNA to eIF2alpha phosphorylation: a strategy to overcome the antiviral effect of protein kinase PKR. Genes Dev. 20, 87–100.
Vera, M.D., Joullié, M.M., 2002. Natural products as probes of cell biology: 20 years of didemnin research. Med. Res. Rev. 22, 102–145.

ARTÍCULO 2:

Translation of Sindbis subgenomic mRNA is independent of eIF2, eIF2A and eIF2D

En células de mamífero, la traducción del sgRNA de SINV no parece verse afectada por la inactivación del eIF2. Varios estudios han sugerido que la función del eIF2, suministrar Met-tRNA$_i^{Met}$, podría ser reemplazada, cuando está inactivado, por los factores eIF2A o eIF2D (Ventoso, Sanz et al. 2006, Kim, Park et al. 2011). Para determinar si eIF2A y eIF2D son requeridos en la traducción de mRNAs virales, se utilizaron líneas humanas semihaploides *knock out* (KO) estables (HAP1) para los factores eIF2A, eIF2D o ambos (Horizon Discovery Group plc). Inicialmente se comprobó que la viabilidad, la morfología y el crecimiento de estas líneas KO eran semejante al de la línea parental, HAP1 wt. Después, estas cuatro líneas fueron infectadas con SINV y se analizó la inhibición de la traducción celular y de la producción de proteínas virales en la fase tardía de la infección sin apreciar diferencias significativas entre las líneas HAP1 mencionadas. Adicionalmente, se confirmó que la producción de proteína viral en estas líneas celulares tampoco se veía afectada por la fosforilación del eIF2α, mediada por arsenito sódico. De forma paralela, se estudió la síntesis de proteínas tras el silenciamiento mediado por RNAs pequeños de interferencia (siRNAs) para eIF2A o el eIF2D en células HAP1 wt, HAP1 eIF2A$^-$ y HAP1 eIF2D$^-$. Estos resultados reafirmaron los obtenidos anteriormente y descartaron que los pequeños péptidos amino-terminales de eIF2A o eIF2D que aún pudieran producirse en las líneas KO intervengan en la traducción del sgRNA. De esta forma, se pudo concluir que eIF2, eIF2A y eIF2D no son necesarios para la traducción del sgRNA de SINV durante la fase tardía de la infección.

Por otra parte, se estudió la posible implicación de eIF2A y eIF2D en la iniciación de la traducción en codones no-AUG. Se mutó el AUG$_i$ del sgRNA de SINV a otros codones (CUG para leucina y GCG para alanina) en replicones de SINV con luciferasa como gen reportero. Las variantes mutadas mostraron una menor eficiencia en la producción de luciferasa en comparación con el replicón wt con AUG$_i$. Sin embargo, no se encontraron diferencias en la síntesis de proteínas de cada uno de estos replicones entre las líneas HAP1, lo que descarta que eIF2A o eIF2D sean necesarios para iniciar en codones no-AUG.

Los virus animales han evolucionado desarrollando una gran variedad de elementos estructurales en sus mRNAs que maximizan su expresión bajo las condiciones de estrés generadas durante la infección. El sgRNA de SINV contiene varios motivos

estructurales que promueven su traducción durante la fase tardía de la infección. Uno de estos motivos es el *hairpin* denominado DSH, que se localiza a 27 nt *downstream* del AUG_i del sgRNA de SINV (considerando A como la posición +1) (Frolov and Schlesinger 1996, Carrasco, Sanz et al. 2018). El DSH participa en la señalización correcta del codón de iniciación de la traducción del sgRNA y, por tanto, la alteración de su estructura conduce a una traducción con *leaky scanning* que inicia en otros codones AUG situados *downstream* (Frolov and Schlesinger 1996, Sanz, Castello et al. 2009, Garcia-Moreno, Sanz et al. 2015). En este trabajo, se analizó el papel del DSH en la señalización de CUG como codón de iniciación en la traducción del sgRNA. Para ello se transfectaron las líneas HAP1 wt, HAP1 eIF2A$^-$ y HAP1 eIF2D$^-$ con replicones que portaban el DSH desestructurado y AUG o CUG como codones de inicio. Los experimentos en las líneas HAP1 determinaron que eIF2A y eIF2D no estaban implicados en el reconocimiento del codón de iniciación y tampoco afectan a la función del DSH. Estos resultados apoyan la propuesta de que el eIF2 podría no ser reemplazado por ninguna proteína celular durante la traducción del sgRNA de SINV, sino que este mRNA viral podría haber evolucionado una estructura especializada que lo hace independiente de eIF2.

SANZ, M. A., **GONZALEZ ALMELA, E.** AND CARRASCO, L. 2017. Translation of Sindbis Subgenomic mRNA is Independent of eIF2, eIF2A and eIF2D. *Sci Rep* 7: 43876.

SCIENTIFIC REPORTS

OPEN

Translation of Sindbis Subgenomic mRNA is Independent of eIF2, eIF2A and eIF2D

Received: 19 October 2016
Accepted: 01 February 2017
Published: 27 February 2017

Miguel Angel Sanz, Esther González Almela & Luis Carrasco

Translation of Sindbis virus subgenomic mRNA (sgmRNA) can occur after inactivation of eIF2 by phosphorylation in mammalian cells. Several studies have suggested that eIF2 can be replaced by eIF2A or eIF2D. HAP1 human cell lines knocked-out for eIF2A, eIF2D or both by CRISPR/Cas9 genome engineering were compared with wild-type (WT) cells to test the potential role of eIF2A and eIF2D in translation. Sindbis virus infection was comparable between the four cell lines. Moreover, synthesis of viral proteins during late stage infection was similar in all four cell lines despite the fact that eIF2α became phosphorylated. These findings demonstrate that eIF2A and eIF2D are not required for the translation of sgmRNA when eIF2α is phosphorylated. Moreover, silencing of eIF2A or eIF2D by transfection of the corresponding siRNAs in HAP1 WT, HAP1-eIF2A$^-$ and HAP1-eIF2D$^-$ cells had little effect on the synthesis of viral proteins late in infection. Modification of AUG$_i$ to other codons in sgmRNA failed to abrogate translation. Sindbis virus replicons containing these sgmRNA variants could still direct the synthesis of viral proteins. No significant differences were found between the cell lines assayed, suggesting that neither eIF2A nor eIF2D are involved in the translation of this sgmRNA bearing non-AUG codons.

Upon infection of susceptible cells, animal viruses express their genomes to synthesize a number of viral proteins involved in genome replication and in the modulation of many cellular functions. Viral proteins are produced by translation of mRNAs that have evolved several structural characteristics to compete with cellular mRNAs. Accordingly, translation of some viral mRNAs follows a variety of virus-dependent non-canonical mechanisms. Sindbis virus (SINV), an alphavirus, has two different mRNAs that are translated at different times during infection. SINV genomic RNA is of positive polarity and is immediately translated early during infection to produce non-structural proteins (nsP1–4) that participate in genome replication and transcription[1,2]. The recognition of an internal promoter in the negative strand RNA that is complementary to the genomic RNA is necessary to initiate synthesis of subgenomic mRNA (sgmRNA), the most abundant viral mRNA during the late phase of infection that directs the synthesis of structural proteins when cellular translation is drastically inhibited. SINV sgmRNA (4,105 nt without the poly(A) tail) devotes the bulk of its sequence (3,738 nt) to encode the structural proteins C-E3-E2-6K-E1, initially synthesized as a polyprotein. The coding sequence is flanked by two untranslated regions (UTR). The 5′-UTR (49 nt) represents the leader sequence and contains a cap structure at its 5′ end. This leader sequence confers eukaryotic initiation factor complex, eIF4F, independence and is implicated in the shut-off of host translation[3,4]. It has been suggested that 80S ribosomes could directly interact with the AUG initiation codon without scanning by the preinitiation complex[5]; however, it has been demonstrated that scanning of the leader sequence is obligatory for sgmRNA translation[6]. For this scanning to occur, recognition of the cap-structure by eIF4E is likely not necessary since cleavage of eIF4G by poliovirus 2A^{pro} or human immunodeficiency virus protease does not impede sgmRNA translation in SINV-infected cells[3,7]. The 3′-UTR (323 nt) can be divided into three different domains. One region of 19 nt near to the poly-(A) tail is involved in RNA replication[8,9], while an A/U-rich domain of about 60 nt interacts with the host protein HuR, participating in mRNA stability[10–12]. The 240-nt-region located between the end of the coding region and the A/U-rich domain contains three repeated sequences[13] and is involved in the stimulation of translation in insect cells[14]. This structure at the 3′-UTR therefore constitutes a translational enhancer that functions in a cell-specific manner. Besides the aforementioned structures present at the 5′-and 3′-UTR, a hairpin in the coding sequence can be found located 77–139 nt from the 5′ end[15]. This downstream hairpin (DLP) is not a true enhancer of protein synthesis, but instead is involved in

Centro de Biología Molecular Severo Ochoa (CSIC-UAM) Universidad Autónoma de Madrid, 28049, Madrid, Spain. Correspondence and requests for materials should be addressed to M.A.S. (email: masanz@cbm.csic.es)

conferring eIF2-independent translation of sgmRNA in infected mammalian cells[16–18]. A second important function of the DLP is to signal the precise codon at which to start translation[7]. Thus, DLP disorganization does not diminish translation in PKR-deficient mouse embryonic fibroblasts, but its translation is obstructed when eIF2 is phosphorylated[17,18]. It is therefore interesting to note that sgmRNA translation can take place without an intact eIF4F complex and after eIF2 inactivation by eIF2α phosphorylation in SINV-infected cells, despite the fact that this mRNA does not contain an IRES motif[19] and is translated by a scanning mechanism[6].

The possibility that eIF2 function is replaced by other cellular factors has been proposed[5,17]. One such possibility is that eIF2A substitutes for eIF2 in SINV-infected cells. eIF2A is a 65 kDa protein that was described several years ago, but its precise function in mammalian cells remains unclear and deletion of the yeast orthologue has no effect on cell viability, although sporulation is affected[20]. Early results demonstrated that eIF2A can interact with Met-tRNA$_i^{Met}$ to bind it to the ribosome[21]; however, this binding was much less efficient than that observed using genuine eIF2 on artificial templates and eIF2A was unable to promote the binding of Met-tRNA$_i^{Met}$ to globin mRNA[22]. More recent results from mammalian cells suggest that eIF2A is involved in the translation of some specialized cellular mRNAs that initiate translation with non-AUG codons[23,24]. The finding that yeast eIF2A is found in 40S and 80S ribosomes suggests its involvement in the initiation of at least some mRNAs[25]. Indeed, eIF2A represses the translation of several yeast mRNAs bearing IRES structures[26,27]. Accordingly, the functioning of eIF2A in yeast and mammalian cells may differ.

A second possibility is that eIF2D initiates sgmRNA translation in place of eIF2[5]. eIF2D has two functional domains: PUA and SUI1[28]. The PUA domain is an RNA-binding domain found in several enzyme families, such as those that modify tRNA. The SUI1 domain, which is also found in eIF1, is involved in the recognition of the translation initiation codon. eIF2D is an initiation factor that was erroneously named ligatin[5], but further studies demonstrated that eIF2D and ligatin were two different proteins[29]. Initially, eIF2D was purified from rabbit reticulocyte lysates as a 65 kDa protein that could displace deacylated tRNA and mRNA from recycled 40S ribosomal subunits, and was also able to interfere with the formation of the 48S initiation complex promoted by eIF2[5]. A complex between Met-tRNA$_i^{Met}$ and eIF2D is formed in a GTP-independent fashion. This complex can interact with the 40S ribosomal subunit to deliver the initiator to the P site[29]. Accordingly, eIF2D has been considered as a true initiation factor, though the exact function of this protein in mammalian cells remains enigmatic. Akin to eIF2A, the orthologue of eIF2D is dispensable in yeast[20,29], but comparable studies have not been performed in mammalian cells. Our present results show that human cells with a knock-out for eIF2A or eIF2D are viable and synthesize proteins in a manner similar to wild-type cells. In addition, by investigating the potential involvement of these two proteins for the translation of SINV sgmRNA, we demonstrate that these factors are not required for sgmRNA translation, even when eIF2α is phosphorylated. These findings support the novel proposal that eIF2 is not replaced by a cellular protein during the translation of SINV sgmRNA, instead this viral mRNA has evolved a specialized structure that makes it independent for eIF2. The consequences for the virus life cycle are that significant amounts of structural proteins can be produced upon the translation of sgmRNA even under stress conditions that appear after viral infection.

Results

Characterization of cell lines and translation of cellular mRNAs. We first assessed the viability and cellular translation of WT and KO cell lines. No differences were found in these parameters between HAP1 parental (HAP1 WT) and the two KO cell lines, HAP1-eIF2A$^-$ and HAP1-eIF2D$^-$, and all cell lines display the same fibroblast-like morphology and grew equally well (results not shown). We next examined the expression of eIF2A and eIF2D by immunocytochemistry using specific antibodies. Double staining of HAP1 WT cells with Topro-3 revealed that eIF2A was clearly expressed in the cytoplasm and a proportion was also found in the nucleus, whereas eIF2D was mainly expressed in the cytoplasm (Fig. 1A). As anticipated, eIF2A was detected both in WT and HAP1-eIF2D$^-$ cells, but not in HAP1-eIF2A$^-$ cells (Fig. 1A). A similar result was found for eIF2D expression (Fig. 1A). Loss of eIF expression in the respective KO cell lines was verified by western blotting (Fig. 1B). This is the first time that KO cell lines for eIF2A or eIF2D have been obtained in mammalian cells.

We next examined the cellular response to sodium arsenite treatment, which induces endoplasmic reticulum stress response and phosphorylation of eIF2α, resulting in global translation inhibition[30]. As shown in Fig. 2, arsenite treatment of HAP1 WT cells induced the formation of stress granules containing TIA-1 protein, which redistributed from the nucleus to the cytoplasm. Analysis of eIF2A and eIF2D expression in WT cells following arsenite exposure revealed that eIF2D but not eIF2A clearly co-localized with TIA-1 in cytoplasmic stress granules (Fig. 2). Subsequently, the action of arsenite on cellular translation in WT and KO cell lines was measured by radioactive labeling of cellular proteins followed by their detection using SDS-PAGE and fluorography. No differences were found in protein synthesis between the three cell lines (Supplementary Figure 1). Accordingly, arsenite induced a similar concentration-dependent inhibition of cellular translation in all three cell lines, which was particularly profound at 50–100 μM and almost complete at 200 μM (Supplementary Figure 1A). This finding suggests that eIF2A or eIF2D do not substitute, even partially, the action of eIF2 during the initiation of global mRNA translation. Furthermore, the total amount of eIF2α and the degree of eIF2α phosphorylation was comparable between the three cell lines and increased in parallel with the blockade of cellular protein synthesis (Supplementary Figure 1B). In summary, HAP1-eIF2A$^-$ and HAP1-eIF2D$^-$ cell lines are viable and protein synthesis is blocked by eIF2α phosphorylation to an extent similar to that found in HAP1 WT cells.

Viral protein synthesis in HAP1 eIF2A and eIF2D KO cells. Previous studies testing the involvement of eIF2A on viral mRNA translation have used RNA interference approaches (siRNA) to reduce the amount of eIF2A in cultured cells[17,31]. Although instructive, this approach has two major weaknesses: often, residual amounts of eIF2A could partially maintain viral translation and siRNA treatment may have some side-effects on viral replication and/or translation steps. The use of KO cells overcomes these problems, constituting a more

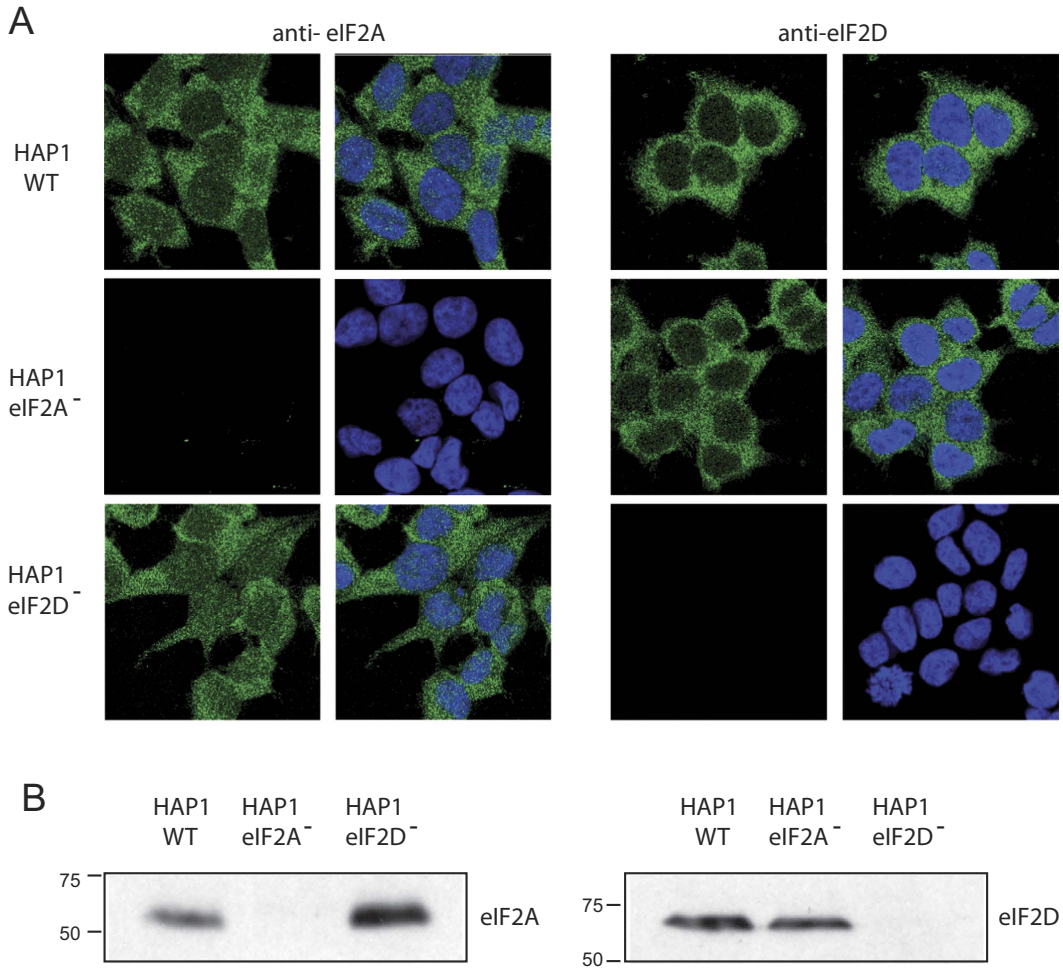

Figure 1. Characterization of the different HAP1 cell lines by immunocytochemistry and western blotting. (**A**) HAP1 WT, HAP1-eIF2A$^-$ and HAP1-eIF2D$^-$ cells were seeded on coverslips in wells of an L-4 plate, fixed and stained with anti-eIF2A or anti-eIF2D rabbit polyclonal antibodies. The presence and localization of eIF2A and eIF2D (green) were observed by confocal microscopy using secondary anti-rabbit antibodies conjugated to Alexa 488. Nuclei (blue) were stained with Topro-3. (**B**) The presence of eIF2A or eIF2D in HAP1 WT, HAP1-eIF2A$^-$ or HAP1-eIF2D$^-$ cells was also determined by western blotting with anti-eIF2A and anti-eIF2D antibodies.

robust approach to test the functionality of eIF2A or eIF2D in SINV-infected cells. Thus, WT and KO cell lines were infected with SINV and protein synthesis was analyzed by radioactive labeling at different periods post infection. No differences were found between the three cell lines in the amount or in the kinetics of viral proteins synthesized (Fig. 3A and B), supporting the view that neither eIF2A nor eIF2D are required for SINV sgmRNA translation. Additionally, the absence of these factors did not affect earlier steps of viral replication that are necessary for sgmRNA translation.

It is well established that SINV replication stimulates PKR, leading to eIF2α phosphorylation[7,16,17]. We therefore analyzed the induction of eIF2α phosphorylation in the three cell lines during SINV infection. The kinetics and the degree of eIF2α phosphorylation were similar in the three cell lines upon infection with SINV (Fig. 3C). Phosphorylation of eIF2α increased at 3 hours post infection (hpi) and reached a maximum after 5–7 h. To further question whether eIF2A or eIF2D could replace eIF2 for the translation of SINV sgmRNA, cells were treated with arsenite, which induces almost 100% phosphorylation of eIF2 in SINV-infected cells (7). At 7 hpi, mock-infected or SINV-infected HAP1 cells were treated with 200 μM arsenite and 15 min later protein synthesis was estimated by radioactive labeling over the next hour. Cellular translation was blocked by arsenite treatment, whereas almost no inhibition was detected in SINV-infected cells (Fig. 4A and B). Viral protein synthesis occurred at similar levels in all three cell lines and was equally resistant to arsenite. Although viral translation was not diminished by arsenite, polyprotein processing was affected leading to an accumulation of the glycoprotein precursor, which is in agreement with previous observations[7]. Consistent with our earlier results (Fig. 3), eIF2α was clearly phosphorylated in all three cell lines infected with SINV (Fig. 4C). eIF2α phosphorylation was maintained upon addition of arsenite, suggesting that virtually all eIF2α was phosphorylated under these conditions. As expected, eIF2A and eIF2D expression was absent in the respective HAP1 KO cell lines (Fig. 4D). Collectively, these results show that neither eIF2A nor eIF2D are necessary for SINV sgmRNA translation, even when eIF2α is phosphorylated.

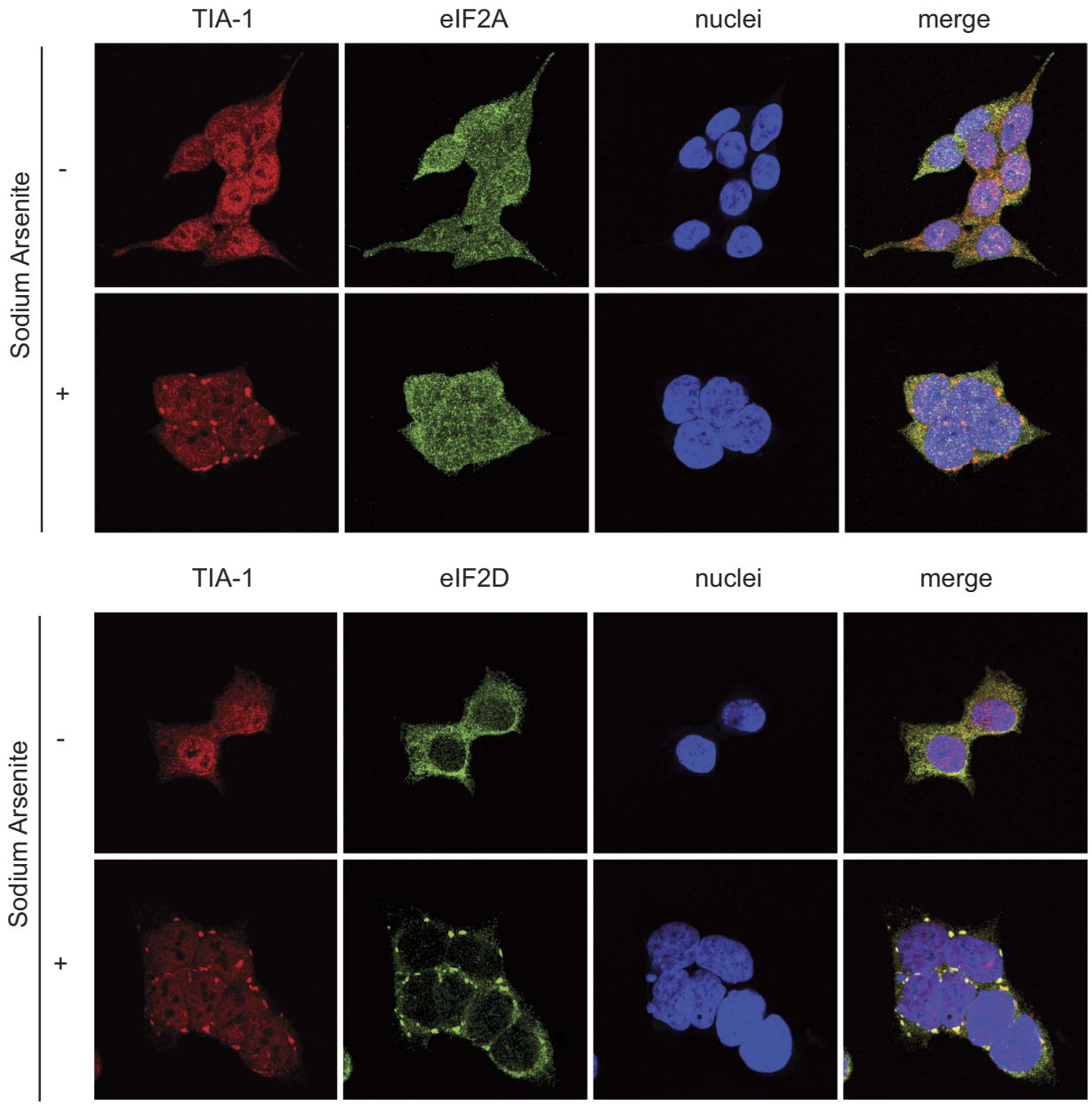

Figure 2. Induction of stress granules by sodium arsenite treatment in HAP1 cell lines. HAP1 WT, HAP1-eIF2A^{-} and HAP1-eIF2D^{-} cells previously seeded on coverslips in wells of an L-4 plate were treated or not with 200 μM arsenite for 1 h and then fixed and permeabilized. Immunodetection was carried out using primary goat anti-TIA-1, rabbit anti-eIF2A or rabbit anti-eIF2D antibodies. An anti-goat antibody conjugated to Alexa 555 was used to detect TIA-1 (red) and anti-rabbit antibodies conjugated to Alexa 448 were employed to detect eIF2A (green) or eIF2D (green). DAPI (4′-6-diamidino-2-phenylindole) was used to stain the nuclei (blue).

Translation of SINV sgmRNA in cells devoid of eIF2A and eIF2D. The possibility that eIF2A could be replaced by eIF2D and vice versa, although unlikely, in the single KO cell lines studied above was next evaluated. To do this, we used a double KO HAP1 cell line deficient for both eIF2A and eIF2D. Viability and morphology of this cell line was similar to that of wild-type HAP1 cells. As expected, HAP1 eIF2A^{-}/2D^{-} cells did not express eIF2A or eIF2D as revealed by immunocytochemistry and by western blotting using specific antibodies against these proteins (Fig. 5A and B). Next, translation of sgmRNA in these cells was assayed at different times after SINV infection by radioactive labeling and SDS PAGE. As shown in Fig. 5C and D, SINV infection of HAP1 eIF2A^{-}/2D^{-} resulted in a rapid inhibition of cellular translation and the synthesis of late viral proteins directed by sgmRNA to levels comparable to those observed with HAP1 WT cells. These findings are conclusive and are consistent with the notion that neither eIF2A nor eIF2D participate in the initiation of sgmRNA translation. As a complementary test to determine whether eIF2A or eIF2D participate in SINV sgmRNA translation, we used a gene silencing approach to knock-down these proteins. As stated earlier, a potential pitfall of this approach is that residual amounts of initiation factor remain after silencing. Nevertheless, it serves to bolster the experiments

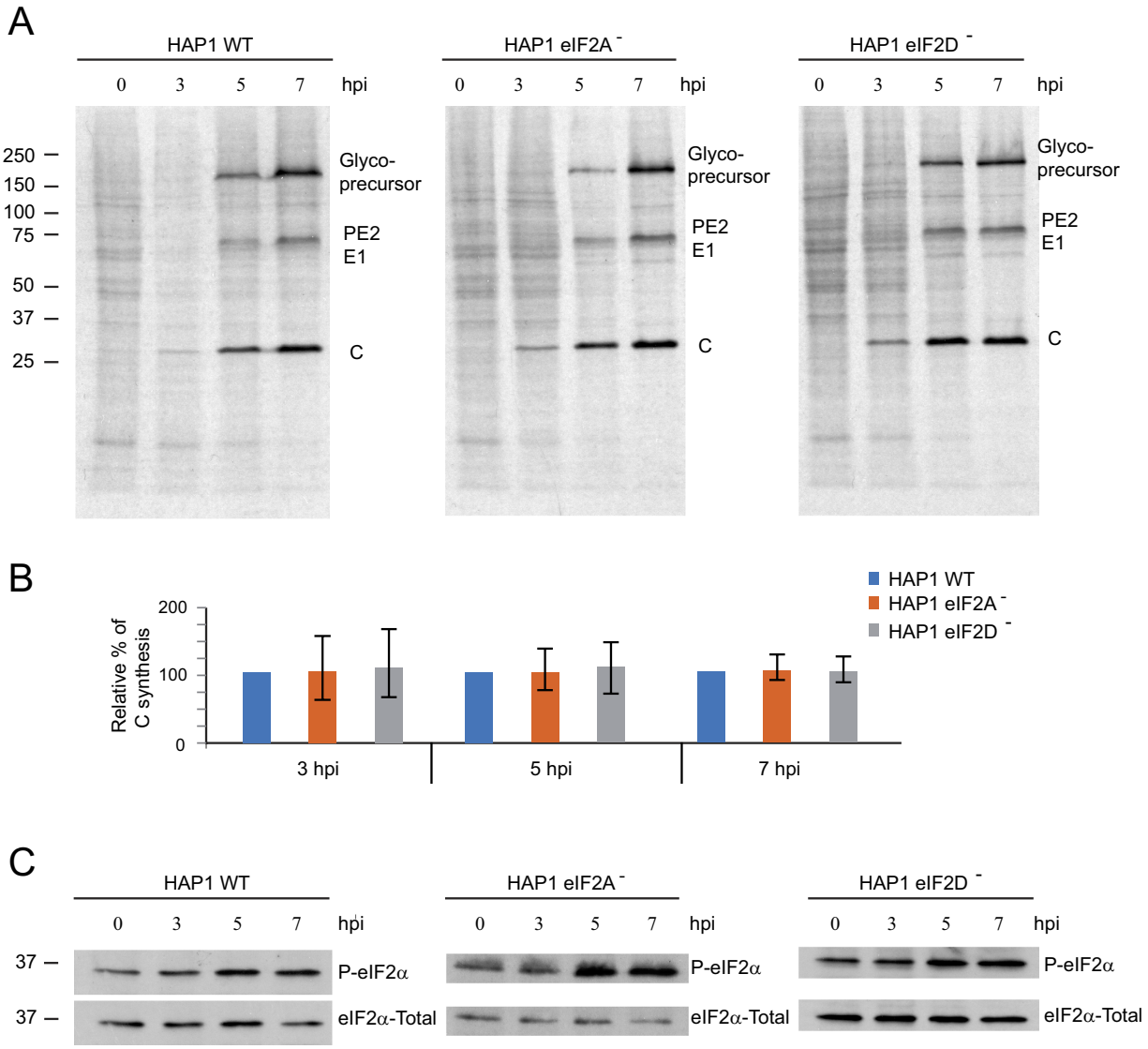

Figure 3. Effect of SINV infection on protein synthesis and eIF2α phosphorylation in HAP1 cell lines. Equal numbers of HAP1 WT, HAP1-eIF2A$^-$ and HAP1-eIF2D$^-$ cells were infected or not with 10 pfu/cell SINV and labeled with ^{35}S-Met/Cys from 3 to 4, 5 to 6 or 7 to 8 hpi. (**A**) After labeling, cells were collected in loading buffer and analyzed by SDS-PAGE and autoradiography to detect protein synthesis. (**B**) Densitometric analysis of C production in WT and KO cells. The graph shows the percentage values in relation to the amount of C synthesized in HAP1 WT cells at different hpi. The results are displayed as mean ± SD of three representative experiments. (**C**) The amount of phospho-eIF2α and total eIF2α was analyzed in parallel by western blotting.

using KO cell lines since siRNAs block translation of the corresponding mRNA and, in principle, no truncated initiation factors are synthesized. Cell lines were mock- or SINV-infected 42 h after transfection of the corresponding HAP1 cell lines with siRNAs. Protein synthesis was measured by radioactive labeling at 6–7 hpi and analyzed by SDS PAGE (Fig. 6A and B). Once again, translation of SINV sgmRNA was clearly apparent under all the conditions tested. siRNAs depleting eIF2A or eIF2D in HAP1 WT cells failed to block SINV protein synthesis. Furthermore, HAP1 eIF2A$^-$ cells transfected with siRNA for eIF2D also synthesized viral proteins at control levels. A similar situation was found when HAP1 eIF2D$^-$ cells were transfected with siRNA to deplete eIF2A. Therefore, the depletion of eIF2A or eIF2D in HAP1 WT or in the KO cell lines has no detrimental effects on sgmRNA translation. The amount of eIF2A or eIF2D present 48 h after siRNA transfection in the three cell lines was analyzed by western blotting. Densitometric analysis indicated that eIF2A was silenced by 83% in HAP1 WT and 99% in HAP1 eIF2D$^-$, whereas eIF2D was silenced by 81% in HAP1 WT and 85% in HAP1 eIF2A$^-$ (Fig. 6C). These results clearly indicate that depletion of eIF2A or eIF2D does not abrogate the synthesis of viral proteins directed by sgmRNA and are consistent with the findings described using KO cell lines.

Protein synthesis directed by SINV sgmRNA lacking the initiator AUG codón. In eukaryotes, a number of proteins are synthesized starting at non-AUG codons[32,33]. Recent evidence has implicated eIF2A in

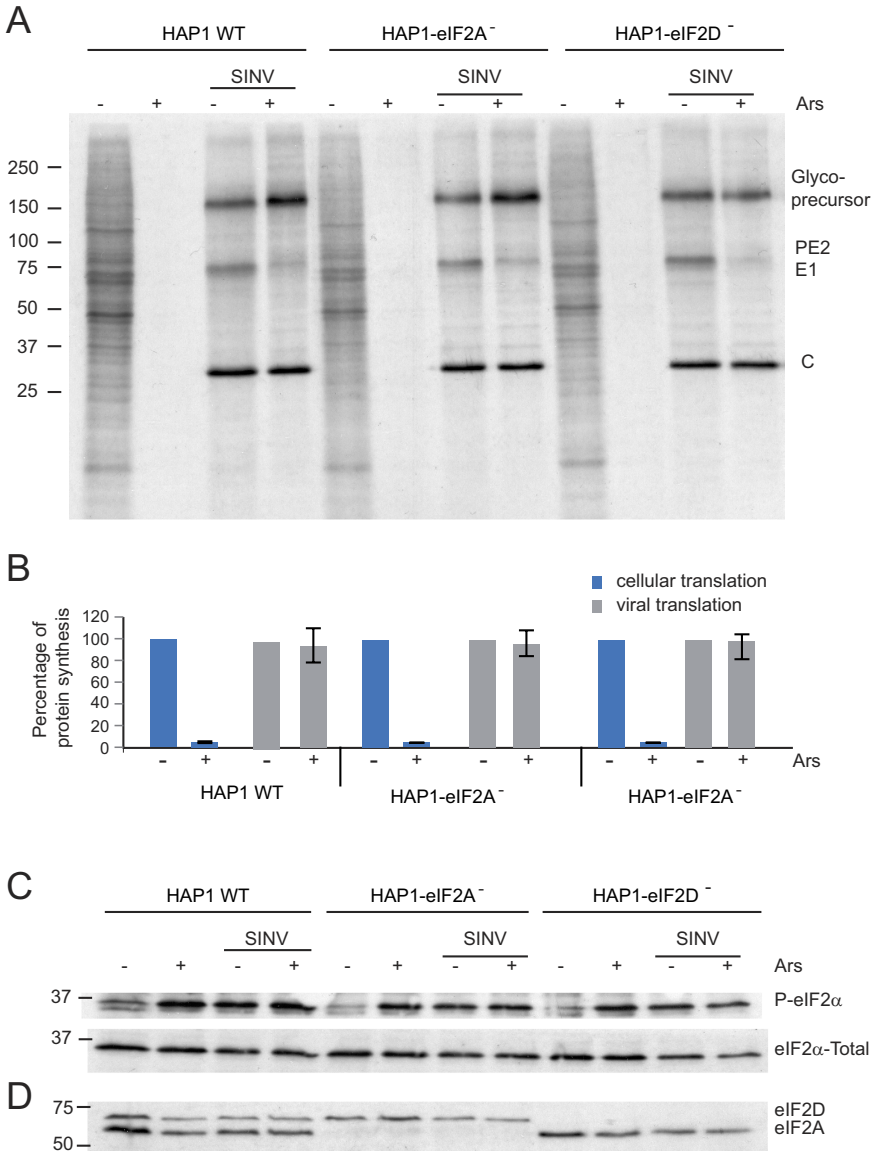

Figure 4. Effect of SINV infection and sodium arsenite treatment on protein synthesis and eIF2α phosphorylation in HAP1 cell lines. Mock-infected or SINV- infected cells from each HAP1 line were treated or not with 200 μM arsenite at 7 hpi during 1 h and 15 min and labeled with ^{35}S-Met/Cys during the last hour of treatment. (**A**) Cells were collected in loading buffer and analyzed by SDS-PAGE and autoradiography to detect the protein synthesis. (**B**) Densitometric analysis of cellular and viral proteins synthesized in the absence or presence of arsenite in the different cell lines. The graph shows the percentage values obtained from untreated versus their counterpart cells treated with arsenite. The results are displayed as mean ± SD of three representative experiments. (**C**) The amount of phospho-eIF2α and total eIF2α was analyzed in parallel by western blotting. (**D**) As a control for the presence of eIF2A and eIF2D, the amount of these proteins was also analyzed by western blotting using a mixture of rabbit polyclonal anti-eIF2A and rabbit polyclonal anti-eIF2D as primary antibodies.

the initiation of translation on non-AUG codons in mammalian cells[23,24]. Because SINV sgmRNA can still direct translation even when the initiator AUG codon has been changed to other codons[7], we questioned whether this initiation was mediated by a mechanism involving eIF2A or eIF2D. To do this, we examined SINV replicons bearing sgmRNAs with altered AUG_i codons (see scheme in Fig. 7A and B). Thus, AUG_i was modified to CUG (encoding Leu) or GCG (encoding Ala), rendering rep C + luc (Met-Leu) or rep C + luc (Met-Ala), respectively. These replicons were obtained by *in vitro* transcription of the corresponding plasmids and were transfected into the three HAP1 cell lines. We initially tested the kinetics of luciferase production and found that its synthesis from each replicon was very similar in the three cell lines; however, luciferase production was 50–60% (Met-Leu) and 20–25% (Met-Ala) relative to control (wt) values (Fig. 7C). Remarkably, this inhibition was similar in the three cell lines. Thus, the absence of eIF2A or eIF2D did not affect sgmRNA translation with the replicons when the AUG_i was changed to CUG or GCG. Previously, we found that the initiation of translation in SINV sgmRNA

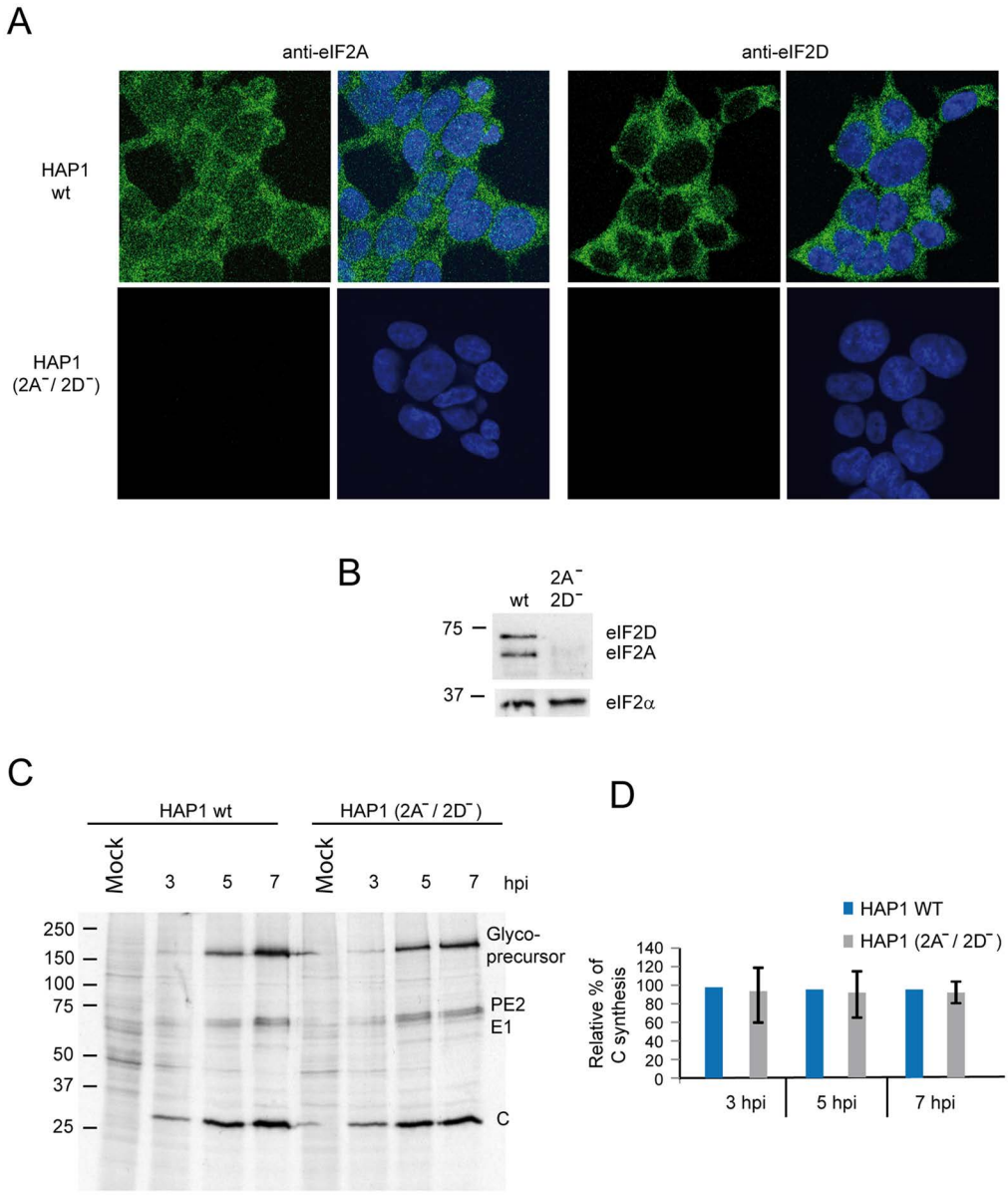

Figure 5. SINV protein synthesis of the double KO cell line HAP1 eIF2A^{-}/2D^{-}. (**A**) HAP1 WT, and HAP1 (eIF2A^{-}/eIF2D^{-}) cells were seeded on coverslips in wells of an L-4 plate, fixed and stained with anti-eIF2A or anti-eIF2D rabbit polyclonal antibodies. The presence and localization of eIF2A and eIF2D (green) were observed by confocal microscopy using secondary anti-rabbit antibodies conjugated to Alexa 488. Nuclei (blue) were stained with Topro-3. (**B**) Western blotting analysis using a mixture of rabbit polyclonal anti-eIF2A and rabbit polyclonal anti-eIF2D as primary antibodies and anti-rabbit immunoglobulin G antibody coupled to peroxidase as secondary antibodies in lysates of HAP1 WT and HAP1 (eIF2A^{-}/eIF2D^{-}) cells. (**C**) Equal numbers of HAP1 WT and HAP1 (eIF2A^{-}/eIF2D^{-}) cells were infected or not with 10 pfu/cell of SINV and labeled with ^{35}S-Met/Cys from 3 to 4, 5 to 6 or 7 to 8 hpi. Then, cells were collected in loading buffer and analyzed by SDS-PAGE and autoradiography to detect protein synthesis. (**D**) Densitometric analysis of C production in WT and double KO cells. The graph shows the percentage values in relation to the amount of C synthesized in HAP1 WT cells at different hpi. The results are displayed as mean ± SD of three representative experiments.

variants that do not contain AUG$_i$ takes place at the mutated AUG$_i$ and at the following AUG that appears in the C coding sequence[7]. To assess the start site of C synthesis, the different forms of this protein were analyzed by western blotting. The second AUG of the open reading frame of C from these variants was also mutated to distinguish easily by electrophoretic separation the products derived from initiation at the alternative codons because the protein derived from the translation at the AUG (3° in the wt sequence) yields a product with 20 amino acids less as compared to genuine C. As shown in Fig. 8A and B, rep C + luc synthesized genuine C protein, whereas rep C + luc (Met-Ala) synthesized similar amounts of two C products of different mobility. These two different forms of C differ in about 20 aminoacids, according to the expected products derived from the initiation at the

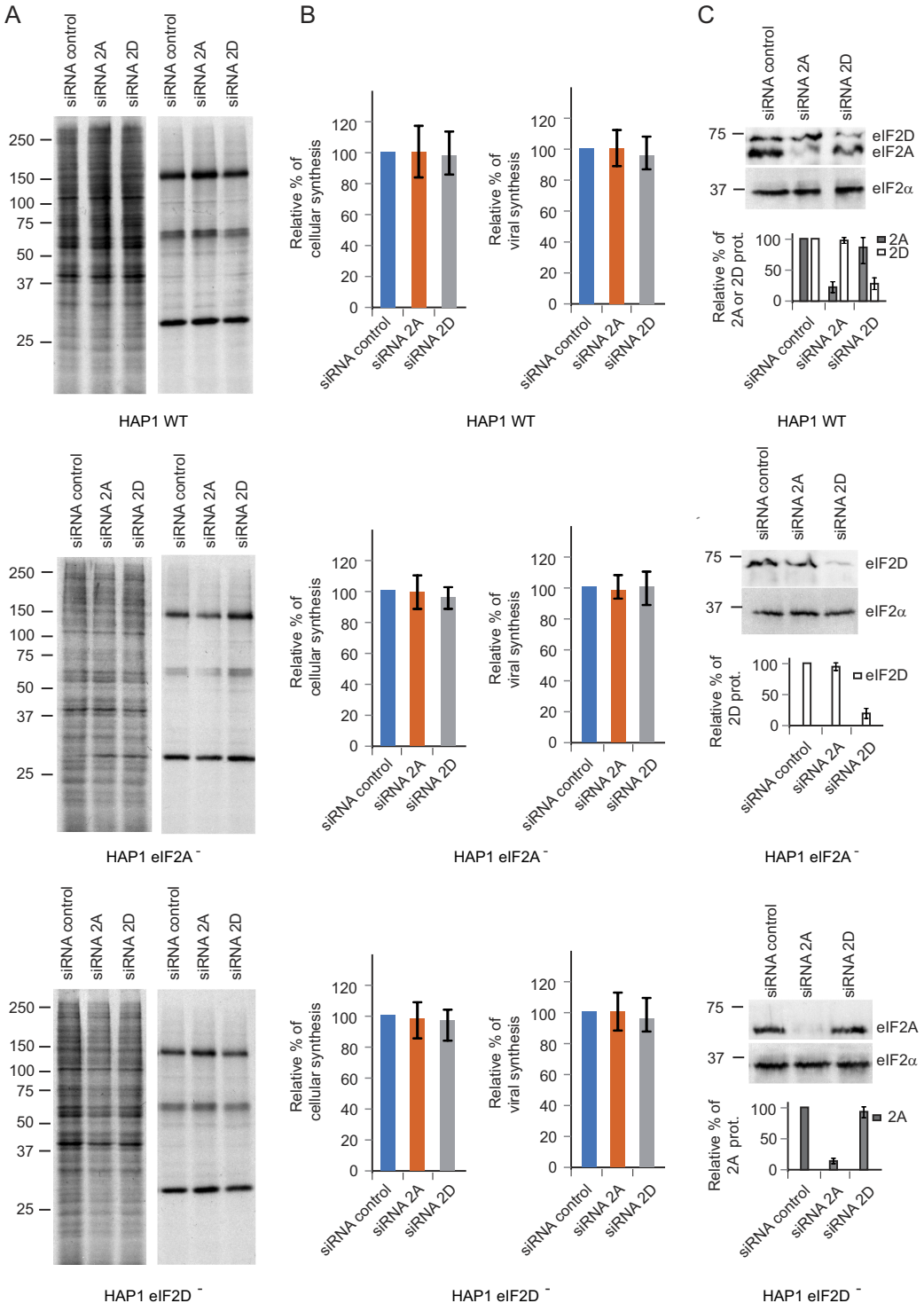

Figure 6. Effect of silencing eIF2A or eIF2D on SINV sgmRNA translation. HAP1 WT, HAP1-eIF2A^{-} and HAP1-eIF2D^{-} cells were treated with a mixture of siRNAs against eIF2A, eIF2D or control siRNAs and at 42 hpt cells were infected or not with SINV (10 pfu/cell). (**A**) Protein synthesis was analyzed from 6 to 7 hpi by radioactive labeling and SDS-PAGE. (**B**) Densitometric analysis of cellular and viral proteins synthesized in the siRNA-treated cells. The graphs show the percentage values obtained from cells treated with siRNAs against eIF2A or eIF2D versus their counterpart cells treated with control siRNAs. The results are displayed as mean ± SD of three representative experiments. (**C**) The degree of depletion of eIF2A or eIF2D was analyzed in parallel by western blotting using a mixture of rabbit polyclonal anti-eIF2A and rabbit polyclonal anti-eIF2D as primary antibodies. As a loading control, the amount of eIF2α was also determined (upper panel). Densitometric analysis of the amount of eIF2A or eIF2D in the siRNA-treated cells. The graph shows the percentage values obtained from cells treated with siRNAs against eIF2A or eIF2D versus their counterpart cells treated with control siRNAs. The results are displayed as mean ± SD of three representative experiments (lower panel).

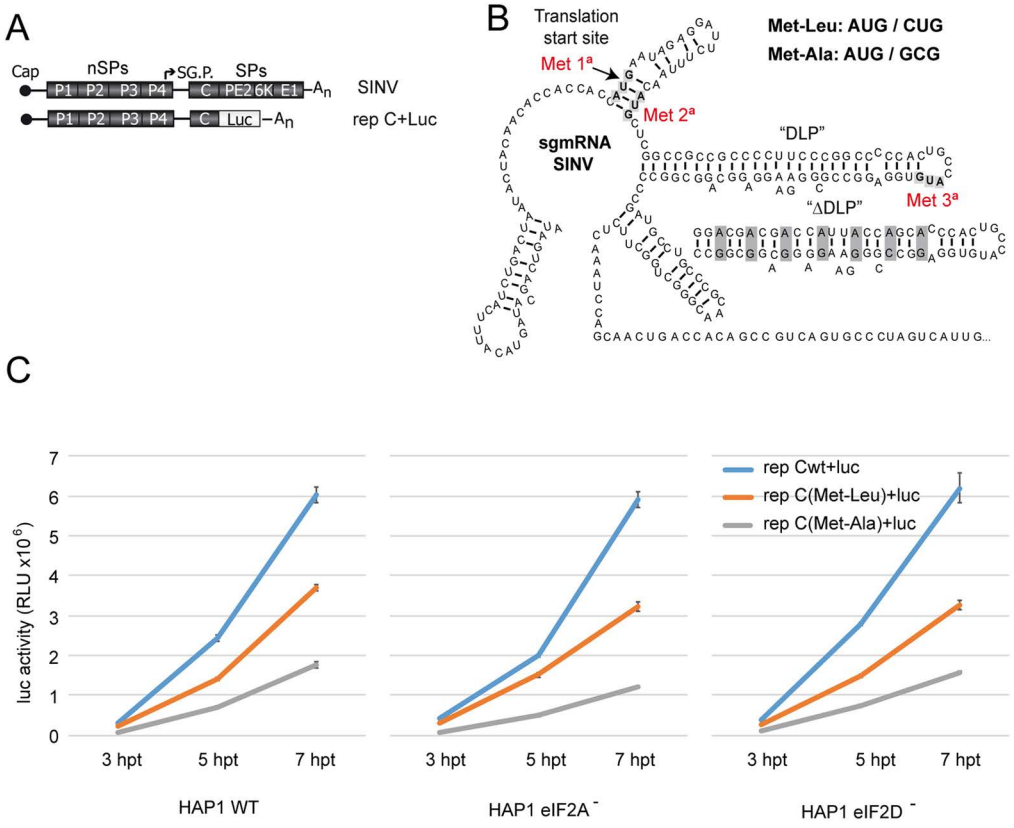

Figure 7. Translation of sgmRNA WT or mutated at the initiation codon in HAP1 cell lines transfected with SINV replicons. (**A**) Schematic representation of the SINV genome and the replicon wt used to make the different variants tested. (**B**) Schematic representation of the secondary structure of SINV sgmRNA. The AUGs mutated in the variants Met-Leu or Met-Ala are highlighted as well as the third in-frame AUG (the first and the second AUGs were mutated to CUG or GCG, respectively). Modified DLP structure, ΔDLP is also illustrated. (**C**) HAP1 WT, HAP1-eIF2A$^-$ and HAP1-eIF2D$^-$ cells were transfected with *in vitro* synthesized replicons rep C + luc, rep C + luc (Met-Leu) or rep C + luc (Met-Ala), and cells were recovered to measure luciferase activity at different periods post transfection. Luciferase activity results are displayed as mean ± SD of three representative experiments performed in triplicate.

alternative codon GCG (first AUG mutation) or third AUG. Moreover, rep C + luc (Met-Leu) rendered two C products, but the amount of genuine C, which presumably initiates at CUG, was more than 90% of the total. Again, no differences were observed regarding the different C products synthesized in WT and the different KO cell lines tested. These results indicate that neither eIF2A nor eIF2D are involved in the initiation of sgmRNA translation when CUG or GCG replaces AUG_i. Previous observations from our laboratory have demonstrated that SINV replicons induce the phosphorylation of eIF2α in a way akin to SINV infection [15]. We therefore used western blotting to assess whether the replicons described above also induce eIF2α phosphorylation in the HAP1 cell lines. Indeed, transfection of the SINV replicons induced the phosphorylation of eIF2α in a similar manner in the three cell lines (Fig. 8C).

The finding that rep C + luc (Met-Leu) used CUG in place of AUG_i quite efficiently while the third AUG of sgmRNA was practically ignored was striking. Since one of the functions of the DLP is to signal the precise codon to start translation, we decided to analyze the functioning of the DLP in the sgmRNA variant encoding Leu in place of Met. We generated a new construct bearing CUG as the initiation codon, followed by an unstructured DLP: rep C + luc (Met-Leu-ΔDLP) (see Fig. 7A and B). The corresponding replicative RNA was transfected into HAP1 cells and C protein production was analyzed by western blotting. As controls, we used rep C + luc, which renders a genuine C protein, and an unstructured DLP in rep C + luc (ΔDLP), which leads to a loss of fidelity in the election of the AUG_i. Thus, several C products are produced that initiate at different codons as a result of leaky scanning[7,17]. We found that rep C + luc (Met-Leu) almost entirely initiated at CUG, giving rise to a C protein of the same mobility as the control (Fig. 9). Notably, the presence of the unstructured DLP in the rep C + luc (Met-Leu-ΔDLP) construct abrogated the initiation at CUG and almost all of the C generated initiated at the third AUG codon (Fig. 9). Nonetheless, the recognition of CUG and the initiation at the third AUG codon when DLP was unstructured, were similar in all three HAP1 cell lines tested, further demonstrating that neither eIF2A nor eIF2D are involved in the recognition of the initiation codon in sgmRNA and in the functioning of the DLP.

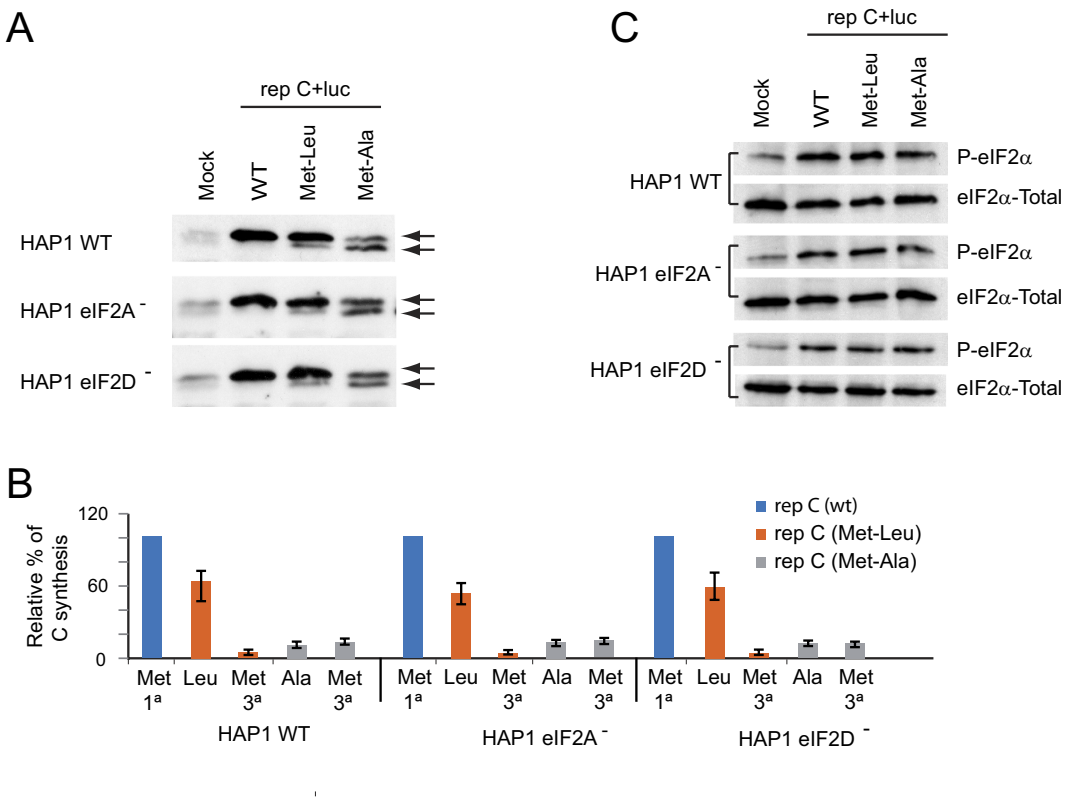

Figure 8. Western blot analysis of SINV protein C and phosphorylation of eIF2α. (**A**) HAP1 WT, HAP1-eIF2A$^-$ and HAP1-eIF2D$^-$ cells were transfected with *in vitro* synthesized replicons rep C + luc, rep C + luc (Met-Leu) or rep C + luc (Met-Ala). At 7 hpt, cells were collected in loading buffer and analyzed by western blotting with an anti-C antibody. The mobilities of the C products derived from the different replicons are indicated by arrows. (**B**) Densitometric analysis of the different C proteins synthesized from rep C + luc (Met-Leu) or rep C + luc (Met-Ala). The graph shows the percentage values in relation to the amount of C synthesized by rep C + luc in each cell line. The results are displayed as mean ± SD of three representative experiments. (**C**) Analysis of eIF2α phosphorylation and total eIF2α by western blotting using specific antibodies as described in Materials and Methods.

Discussion

Several mRNAs from animal viruses are able to direct translation even after phosphorylation of eIF2α[34–36]. In most cases, however, the precise mechanism by which the initiation event occurs when eIF2 is inactivated is unclear. An extreme case of initiation of mRNA translation in the absence of eIFs, including eIF2, is represented by mRNAs bearing an IRES in the intergenic region in Cricket paralysis virus (CrPV)[37]. In this setting, the IRES is a folded structure that mimics tRNA and can interact with the decoding A site of the ribosome[38,39]. The IRES is translocated to the P site by eEF2, leaving the A site free and the first codon ready to start translation. Other animal viruses including picornaviruses that contain an IRES element can initiate translation by a dual mechanism. Early during infection, intact eIF2 is necessary to initiate viral protein synthesis, whereas at late periods mRNA translation occurs even when eIF2 is phosphorylated[40–42]. In this case, picornavirus proteases confer eIF2 independence for IRES-driven translation[41,43,44]. However, the precise mechanism by which picornaviruses initiate translation without eIF2 remains to be elucidated. Hepatitis C virus provides another example of eIF2-independent translation driven by an IRES element[35,45]. In this context, several factors have been suggested to replace eIF2, including eIF5B, eIF2D or eIF2A[5,29,31,46]. A different example of eIF2-independent translation is provided by the capped sgmRNA from alphaviruses[7,16,17]. In this case, the hairpin located 24 nt downstream of the AUG_i is required to initiate translation without active eIF2. The precise functioning of this hairpin during initiation remains enigmatic. Initially, a stable hairpin structure was noticed in the coding region of sgmRNA, that enhaced its translation[15]. It was speculated that this hairpin stalled ribosomes leaving the AUG_i at the P site. However, this possibility seems unlikely because for this to occur the hairpin should be located at 14 nt downstream the initiation codon[47]. It was later observed that when eIF2α does not become phosphorylated, translation of the sgmRNA takes place without the integrity of this hairpin[16,17]. Another model for the function of DLP is that it interacts with the ribosomal P site in a manner similar to that described for CrPV[6]. The possibility that eIF2 is replaced by eIF2A has also been proposed based on gene silencing[17]. However, this possibility seems unlikely in view of our present findings since we demonstrate that sgmRNA is efficiently translated in HAP1 cells lacking eIF2A, even when eIF2α is phosphorylated. Moreover, our present observations on the effect of silencing eIF2A on sgmRNA translation clearly indicate that this factor is not necessary in the human cell line analyzed. Also, the suggestion that eIF2D (previously known as ligatin) participates in protein synthesis directed by SINV sgmRNA

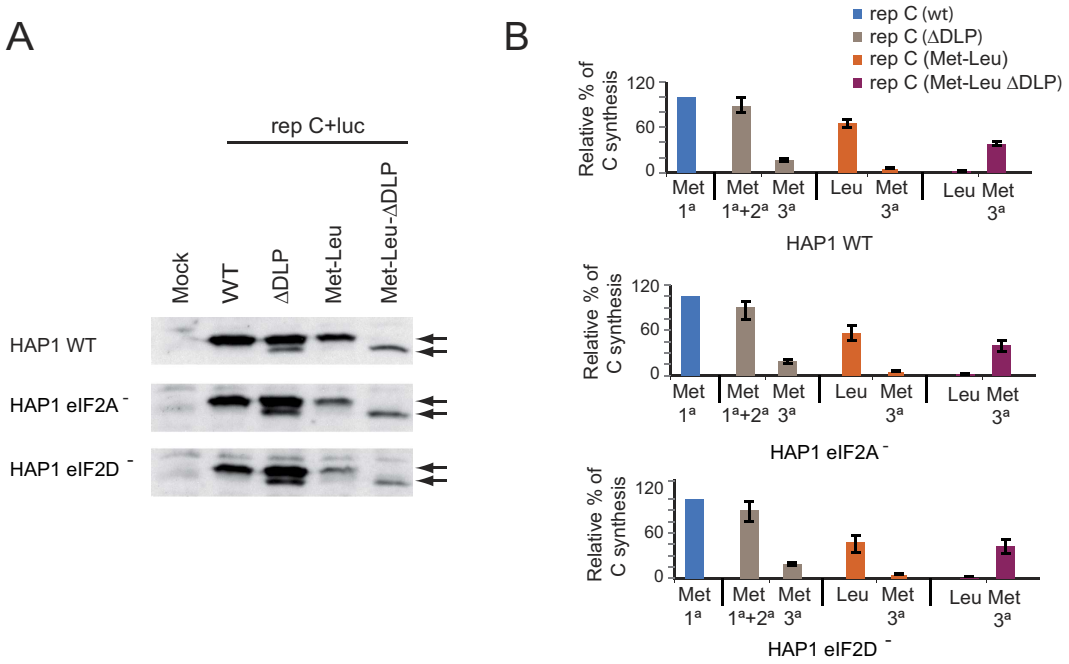

Figure 9. Involvement of the DLP hairpin in signaling the initiation codon. (**A**) HAP1 WT, HAP1-eIF2A$^-$ and HAP1-eIF2D$^-$ cells were transfected with *in vitro* synthesized replicons rep C + luc, rep C + luc (ΔDLP), rep C + luc (Met-Leu) or rep C + luc (Met-Leu-ΔDLP). The DLP structure and the mutations introduced to generate the variant ΔDLP are indicated in Fig. 7B. At 7 hpt, cells were collected in loading buffer and analyzed by western blotting with an anti-C antibody. The mobilities of the C products derived from the different replicons are indicated by arrows. (**B**) Densitometric analysis of the different C proteins synthesized by the replicons in relation to the canonical product of C synthesized by rep C + luc in each cell line. The results are displayed as mean ± SD of three representative experiments.

is not supported by our present results. It seems clear from our findings that cells lacking eIF2D and active eIF2 are infected with SINV and synthesize viral late proteins at levels similar to those of controls. Therefore, whereas the precise mechanism of protein synthesis directed by sgmRNA in the absence of active eIF2 remains to be resolved, we are confident that eIF2A or eIF2D are dispensable for this process.

An additional function of the hairpin DLP is to signal the start codon of sgmRNA in such a manner that the change of AUG_i to other codons engenders sgmRNA functional, albeit to a lower extent[7]. We show here that the substitution of CUG (leucine) for AUG_i has a moderate effect on viral protein synthesis directed by this mRNA variant. Indeed, only 40–50% inhibition of C synthesis was observed. Since binding of the ternary complex GTP-eIF2-Met-$tRNA_i^{Met}$ is only promoted by AUG codons, the synthesis of C protein initiating at Leu will take place without eIF2. Interestingly, even in this case neither eIF2A nor eIF2D were required for this non-AUG initiation of translation since the level of the production of C protein was similar in the three cell lines transfected with the rep C + luc (Met-Leu). However, the disorganization of the DLP has profound effects with regards to the initiation codon used. In rep C + luc (ΔDLP), initiation was observed at the first AUG_i and also at the second and third AUGs, indicating that the genuine DLP structure is important to signal the correct initiation codon. Notably, initiation at CUG in cells transfected with rep C + luc (Met-Leu-ΔDLP) was abrogated when the DLP was unstructured. In this case, a truncated C protein was synthesized that mainly starts at the third AUG, and a similar pattern was found in the three cell lines assayed. Therefore, we can conclude that the structure of the DLP hairpin is more important for initiation codon selection than the presence of eIF2A or eIF2D. In sharp contrast to previous reports, the possibility that now arises is that eIF2 is not substituted by any other factor to translate sgmRNA in SINV infected cells. It could even be possible that the DLP itself could carry out this function. We have previously proposed that the DLP directly interacts with the 40S ribosomal subunit or the 80S ribosome at either the A- or P-site, resembling in this regard the initiation event followed by the IGR IRES of CrPV[6,37,38]. The suggestion that Semliki Forest virus DLP can interact with a sequence present in 18S rRNA to signal the initiation start codon is interesting[48]; however, the speculation that eIF4A participates in the unwinding of DLP after this interaction is not supported by the evidence that selective inhibitors of eIF4A, such as hippuristanol or pateamine A, do not influence initiation of SINV sgmRNA[18,49]. Our current observations support the concept that eIF2 is not replaced by cellular proteins, instead the acquisition of the DLP structure during alphavirus evolution led to eIF2 independent translation. It is known that the presence of DLP structure allows the translation of sgmRNA when eIF2 is phosphorylated[16–18]. This is important for the virus biology because large amounts of structural proteins have to be synthesized under stress conditions. It is well established that alphavirus infection induces the phosphorylation of eIF2α upon infection of mammalian cells. Therefore, the virus has evolved the DLP within the coding region of sgmRNA to be translated under stress conditions that appear after infection. Curiously, the DLP

structure also allows the initiation of the translation using alternative codons as GCG or CUG. This represents a unique example of a viral mRNA that is capped, is translated following the scanning mechanism and still does not utilize eIF2 during the initiation process[6]. Thus, the functional replacement of eIF2 and the ternary complex by a viral RNA structure may be a common mechanism employed by a variety of animal viruses including those that contain an IRES in their mRNAs. Further experiments aimed to elucidate this step during the initiation of SINV sgmRNA are needed. Nonetheless, the important conclusion of our present observations is that neither eIF2A nor eIF2D substitute for eIF2 and are not required to initiate translation of this viral mRNA.

Methods

Cell lines and viruses. Wild-type (WT) HAP1 human haploid cells and HAP1 cells knocked-out for eIF2A (cat# HZGHC002650c001), eIF2D (cat# HZGHC002652c005) or double knock-out for eIF2A and eIF2D (HZGHC005122c010) were purchased from Horizon Discovery Group plc. The eIF2A knock-out (KO) cell line (gi|977380191|ref|NM_032025.4|) has a 16 bp deletion in exon 4 resulting in a frameshift that generates a protein of 108 aa rather than 585 aa of the WT protein. The eIF2D KO cell line (gi|56699484|ref|NM_006893.2|) has a 10 bp deletion in exon 3 resulting in a frameshift that generates a protein of 103 aa rather than 584 aa of the WT protein. The double KO line has the same 16 bp deletion in exon 4 of the single eIF2A KO cell line and a 22 bp deletion in exon 3 of eIF2D that generates a protein of 99 aa rather than 584 aa of the WT protein. Cells were cultured in IMDM (Invitrogen) supplemented with 10% fetal calf serum. SINV stock was obtained from a pT7 SV WT infective cDNA clone[50]. Titers of viruses were determined by plaque assay.

Plasmids and constructs. SINV replicons expressing C and luciferase were obtained by *in vitro* transcription from plasmids derived from pT7 SV wt[50]. pT7 rep C + luc[51] and pT7 rep C + luc ΔDLP[18] have been described previously. pT7 rep C + luc (Met-Ala), pT7 rep C + luc (Met-Leu) and pT7 rep C + luc (Met-Leu-ΔDLP) were constructed for the present study. To generate pT7 rep C + luc (Met-Ala), the Hpa I/Aat II digestion fragment from pT7 rep C (Met-Ala)[7] was cloned into the corresponding sites of pT7 rep C + luc. pT7 rep C + luc (Met-Leu) was designed as the variant Met-Ala, but in this case both the first and second ATGs of the 26S sequence were mutated to GTGs. pT7 rep C + luc (Met-Leu-ΔDLP) has an altered DLP sequence (ΔDLP) in addition to the GTG mutations.

***In vitro* RNA transcription and transfection.** Plasmids digested with Xho I were used as templates for *in vitro* RNA transcription with T7 RNA polymerase (New England Biolabs) in reactions containing the $m^7G(5')ppp(5')G$ cap analog (New England Biolabs). *In vitro*-synthesized RNAs were treated with DNase I and then transfected in cells using Lipofectamine 2000 reagent (Invitrogen).

Analysis of protein synthesis by radioactive labeling. Protein synthesis was measured by incubating cells in 0.2 ml DMEM without methionine and cysteine, supplemented with 1 μl EasyTag™ EXPRESS ^{35}S protein labeling mix, [^{35}S]Met/Cys (11 mCi ml^{-1}, 37.0 Tbq $mmol^{-1}$; Perkin Elmer) per well of a 24-well plate for 60 min. Cells were collected in loading buffer (62.5 mM Tris-HCl pH 6.8, 2% SDS, 0.1 M dithiothreitol, 17% glycerol and 0.024% bromophenol blue) and autoradiographic analysis was performed following SDS-polyacrylamide gel electrophoresis.

Measurement of luciferase activity. Cells were lysed in a buffer containing 0.5% Triton X-100, 25 mM glycylglycine pH 7.8, 1 mM dithiothreitol and complete, EDTA-free, protease inhibitor cocktail (Roche). Luciferase activity was detected using the Luciferase Assay System (Promega) in a Monolight 2010 luminometer (Analytical Luminescence Laboratory).

Antibodies. Primary antibodies used in this work included a rabbit polyclonal antibody raised against purified SINV C protein generated in our laboratory. Rabbit polyclonal anti-TIA-1 (C-20): sc-1751 and rabbit polyclonal anti-eIF2α antibodies were purchased from Santa Cruz Biotechnology. Rabbit polyclonal anti-eIF2D antibody was purchased from Proteintech, rabbit polyclonal anti-eIF2A antibody was purchased from Bethyl Laboratories Inc., and a rabbit polyclonal antibody raised against phospho-eIF2α (serine 51) was purchased from Cell Signaling Technology.

Immunocytochemistry and confocal microscopy. Fixation, permeabilization and confocal microscopy were performed as described[52] using the LSM 710 confocal laser scanning and multiphoton microscope coupled to an inverted microscope (Axio Observer, Zeiss). Primary antibodies were detected by secondary antibodies coupled to Alexa 488 or Alexa 555. Nuclei were stained with Topro-3 or DAPI (4′-6-diamidino-2-phenylindole). All images were collected and analyzed using Zeiss ZEN 2010 software.

Western blotting. Cells were collected in sample buffer, boiled for 5 min and processed by SDS-PAGE. After electrophoresis, proteins were transferred to a nitrocellulose membrane. Specific rabbit polyclonal antibodies raised against phospho-eIF2α (Ser 51), total eIF2α, SINV Capsid, eIF2A and eIF2D were used at 1:1000 dilution in PBS with 3% BSA and 0.1% Tween 20, except when phospho-eIF2α was analyzed we instead used TTBS (Tris-buffered saline, 0.1% Tween 20). Anti-rabbit immunoglobulin G antibody coupled to peroxidase (Amersham) was used at a 1:5000 dilution. Protein bands were visualized with the ECL detection system (Amersham).

siRNA transfection. For transient transfections, siRNAs targeting specifically eIF2A (L-014766-01-0005, Dharmacon), eIF2D (L-003680-01-0005, Dharmacon) or a control siRNA (D-001810-01-05, Dharmacon) were transfected with Lipofectamine 2000 reagent (Invitrogen) according to the manufacturer's instructions. At

42 hours post-transfection, cells were infected or not with SINV (multiplicity of infection, 10). Protein synthesis was analyzed from 6 to 7 hours post infection by radiactive labeling and SDS-PAGE and the degree of depletion of eIF2A and eIF2D was assessed by western-bloting.

References

1. Strauss, J. H. & Strauss, E. G. The alphaviruses: gene expression, replication, and evolution. *Microbiol Rev* **58,** 491–562 (1994).
2. Griffin, D. E. In *Fields Virology* (ed. Knipe, D.) 1023–1067 (Lippincott Williams & Wilkins, 2007).
3. Castello, A., Sanz, M. A., Molina, S. & Carrasco, L. Translation of Sindbis virus 26S mRNA does not require intact eukariotic initiation factor 4G. *J Mol Biol* **355,** 942–956, doi: 10.1016/j.jmb.2005.11.024 (2006).
4. Patel, R. K., Burnham, A. J., Gebhart, N. N., Sokoloski, K. J. & Hardy, R. W. Role for subgenomic mRNA in host translation inhibition during Sindbis virus infection of mammalian cells. *Virology* **441,** 171–181, doi: 10.1016/j.virol.2013.03.022 (2013).
5. Skabkin, M. A. *et al.* Activities of Ligatin and MCT-1/DENR in eukaryotic translation initiation and ribosomal recycling. *Genes Dev* **24,** 1787–1801, doi: 10.1101/gad.1957510 (2010).
6. Garcia-Moreno, M., Sanz, M. A. & Carrasco, L. Initiation codon selection is accomplished by a scanning mechanism without crucial initiation factors in Sindbis virus subgenomic mRNA. *RNA* **21,** 93–112, doi: 10.1261/rna.047084.114 (2015).
7. Sanz, M. A., Castello, A., Ventoso, I., Berlanga, J. J. & Carrasco, L. Dual mechanism for the translation of subgenomic mRNA from Sindbis virus in infected and uninfected cells. *PLoS One* **4,** e4772, doi: 10.1371/journal.pone.0004772 (2009).
8. Ou, J. H., Trent, D. W. & Strauss, J. H. The 3′-non-coding regions of alphavirus RNAs contain repeating sequences. *J Mol Biol* **156,** 719–730 (1982).
9. Hardy, R. W. The role of the 3′ terminus of the Sindbis virus genome in minus-strand initiation site selection. *Virology* **345,** 520–531, doi: 10.1016/j.virol.2005.10.018 (2006).
10. Sokoloski, K. J. *et al.* Sindbis virus usurps the cellular HuR protein to stabilize its transcripts and promote productive infections in mammalian and mosquito cells. *Cell Host Microbe* **8,** 196–207, doi: 10.1016/j.chom.2010.07.003 (2010).
11. Dickson, A. M. *et al.* Dephosphorylation of HuR protein during alphavirus infection is associated with HuR relocalization to the cytoplasm. *J Biol Chem* **287,** 36229–36238, doi: 10.1074/jbc.M112.371203 (2012).
12. Barnhart, M. D., Moon, S. L., Emch, A. W., Wilusz, C. J. & Wilusz, J. Changes in cellular mRNA stability, splicing, and polyadenylation through HuR protein sequestration by a cytoplasmic RNA virus. *Cell Rep* **5,** 909–917, doi: 10.1016/j.celrep.2013.10.012 (2013).
13. Pfeffer, M., Kinney, R. M. & Kaaden, O. R. The alphavirus 3′-nontranslated region: size heterogeneity and arrangement of repeated sequence elements. *Virology* **240,** 100–108, doi: 10.1006/viro.1997.8907 (1998).
14. Garcia-Moreno, M., Sanz, M. A. & Carrasco, L. A Viral mRNA Motif at the 3′-Untranslated Region that Confers Translatability in a Cell-Specific Manner. Implications for Virus Evolution. *Sci Rep* **6,** 19217, doi: 10.1038/srep19217 (2016).
15. Frolov, I. & Schlesinger, S. Translation of Sindbis virus mRNA: analysis of sequences downstream of the initiating AUG codon that enhance translation. *J Virol* **70,** 1182–1190 (1996).
16. McInerney, G. M., Kedersha, N. L., Kaufman, R. J., Anderson, P. & Liljestrom, P. Importance of eIF2alpha phosphorylation and stress granule assembly in alphavirus translation regulation. *Mol Biol Cell* **16,** 3753–3763, doi: 10.1091/mbc.E05-02-0124 (2005).
17. Ventoso, I. *et al.* Translational resistance of late alphavirus mRNA to eIF2alpha phosphorylation: a strategy to overcome the antiviral effect of protein kinase PKR. *Genes Dev* **20,** 87–100, doi: 10.1101/gad.357006 (2006).
18. Garcia-Moreno, M., Sanz, M. A., Pelletier, J. & Carrasco, L. Requirements for eIF4A and eIF2 during translation of Sindbis virus subgenomic mRNA in vertebrate and invertebrate host cells. *Cell Microbiol* **15,** 823–840, doi: 10.1111/cmi.12079 (2013).
19. Sanz, M. A., Welnowska, E., Redondo, N. & Carrasco, L. Translation driven by picornavirus IRES is hampered from Sindbis virus replicons: rescue by poliovirus 2A protease. *J Mol Biol* **402,** 101–117, doi: 10.1016/j.jmb.2010.07.014 (2010).
20. Zoll, W. L., Horton, L. E., Komar, A. A., Hensold, J. O. & Merrick, W. C. Characterization of mammalian eIF2A and identification of the yeast homolog. *J Biol Chem* **277,** 37079–37087, doi: 10.1074/jbc.M207109200 (2002).
21. Merrick, W. C. & Anderson, W. F. Purification and characterization of homogeneous protein synthesis initiation factor M1 from rabbit reticulocytes. *J Biol Chem* **250,** 1197–1206 (1975).
22. Adams, S. L., Safer, B., Anderson, W. F. & Merrick, W. C. Eukaryotic initiation complex formation. Evidence for two distinct pathways. *J Biol Chem* **250,** 9083–9089 (1975).
23. Liang, H. *et al.* PTENalpha, a PTEN isoform translated through alternative initiation, regulates mitochondrial function and energy metabolism. *Cell Metab* **19,** 836–848, doi: 10.1016/j.cmet.2014.03.023 (2014).
24. Starck, S. R. *et al.* Translation from the 5′ untranslated region shapes the integrated stress response. *Science* **351,** aad3867, doi: 10.1126/science.aad3867 (2016).
25. Komar, A. A. *et al.* Novel characteristics of the biological properties of the yeast Saccharomyces cerevisiae eukaryotic initiation factor 2A. *J Biol Chem* **280,** 15601–15611, doi: 10.1074/jbc.M413728200 (2005).
26. Reineke, L. C., Cao, Y., Baus, D., Hossain, N. M. & Merrick, W. C. Insights into the role of yeast eIF2A in IRES-mediated translation. *PLoS One* **6,** e24492, doi: 10.1371/journal.pone.0024492 (2011).
27. Reineke, L. C. & Merrick, W. C. Characterization of the functional role of nucleotides within the URE2 IRES element and the requirements for eIF2A-mediated repression. *RNA* **15,** 2264–2277, doi: 10.1261/rna.1722809 (2009).
28. Cerrudo, C. S., Ghiringhelli, P. D. & Gomez, D. E. Protein universe containing a PUA RNA-binding domain. *FEBS J* **281,** 74–87, doi: 10.1111/febs.12602 (2014).
29. Dmitriev, S. E. *et al.* GTP-independent tRNA delivery to the ribosomal P-site by a novel eukaryotic translation factor. *J Biol Chem* **285,** 26779–26787, doi: 10.1074/jbc.M110.119693 (2010).
30. McEwen, E. *et al.* Heme-regulated inhibitor kinase-mediated phosphorylation of eukaryotic translation initiation factor 2 inhibits translation, induces stress granule formation, and mediates survival upon arsenite exposure. *J Biol Chem* **280,** 16925–16933, doi: 10.1074/jbc.M412882200 (2005).
31. Kim, J. H., Park, S. M., Park, J. H., Keum, S. J. & Jang, S. K. eIF2A mediates translation of hepatitis C viral mRNA under stress conditions. *EMBO J* **30,** 2454–2464, doi: 10.1038/emboj.2011.146 (2011).
32. Touriol, C. *et al.* Generation of protein isoform diversity by alternative initiation of translation at non-AUG codons. *Biol Cell* **95,** 169–178 (2003).
33. Wethmar, K. The regulatory potential of upstream open reading frames in eukaryotic gene expression. *Wiley Interdiscip Rev RNA* **5,** 765–778, doi: 10.1002/wrna.1245 (2014).
34. Clemens, M. J. Translational control in virus-infected cells: models for cellular stress responses. *Semin Cell Dev Biol* **16,** 13–20, doi: 10.1016/j.semcdb.2004.11.011 (2005).
35. Dabo, S. & Meurs, E. F. dsRNA-dependent protein kinase PKR and its role in stress, signaling and HCV infection. *Viruses* **4,** 2598–2635, doi: 10.3390/v4112598 (2012).
36. Roberts, L. O., Jopling, C. L., Jackson, R. J. & Willis, A. E. Viral strategies to subvert the mammalian translation machinery. *Prog Mol Biol Transl Sci* **90,** 313–367, doi: 10.1016/S1877-1173(09)90009-6 (2009).
37. Hellen, C. U. IRES-induced conformational changes in the ribosome and the mechanism of translation initiation by internal ribosomal entry. *Biochim Biophys Acta* **1789,** 558–570, doi: 10.1016/j.bbagrm.2009.06.001 (2009).

38. Fernandez, I. S., Bai, X. C., Murshudov, G., Scheres, S. H. & Ramakrishnan, V. Initiation of translation by cricket paralysis virus IRES requires its translocation in the ribosome. *Cell* **157,** 823–831, doi: 10.1016/j.cell.2014.04.015 (2014).
39. Muhs, M. *et al.* Cryo-EM of ribosomal 80S complexes with termination factors reveals the translocated cricket paralysis virus IRES. *Mol Cell* **57,** 422–432, doi: 10.1016/j.molcel.2014.12.016 (2015).
40. Redondo, N. *et al.* Translation directed by hepatitis A virus IRES in the absence of active eIF4F complex and eIF2. *PLoS One* **7,** e52065, doi: 10.1371/journal.pone.0052065 (2012).
41. Redondo, N., Sanz, M. A., Welnowska, E. & Carrasco, L. Translation without eIF2 promoted by poliovirus 2A protease. *PLoS One* **6,** e25699, doi: 10.1371/journal.pone.0025699 (2011).
42. Welnowska, E., Sanz, M. A., Redondo, N. & Carrasco, L. Translation of viral mRNA without active eIF2: the case of picornaviruses. *PLoS One* **6,** e22230, doi: 10.1371/journal.pone.0022230 (2011).
43. Moral-Lopez, P., Alvarez, E., Redondo, N., Skern, T. & Carrasco, L. L protease from foot and mouth disease virus confers eIF2-independent translation for mRNAs bearing picornavirus IRES. *FEBS Lett* **588,** 4053–4059, doi: 10.1016/j.febslet.2014.09.030 (2014).
44. Sanz, M. A., Redondo, N., Garcia-Moreno, M. & Carrasco, L. Phosphorylation of eIF2alpha is responsible for the failure of the picornavirus internal ribosome entry site to direct translation from Sindbis virus replicons. *J Gen Virol* **94,** 796–806, doi: 10.1099/vir.0.049064-0 (2013).
45. Niepmann, M. Internal translation initiation of picornaviruses and hepatitis C virus. *Biochim Biophys Acta* **1789,** 529–541, doi: 10.1016/j.bbagrm.2009.05.002 (2009).
46. Terenin, I. M., Dmitriev, S. E., Andreev, D. E. & Shatsky, I. N. Eukaryotic translation initiation machinery can operate in a bacterial-like mode without eIF2. *Nat Struct Mol Biol* **15,** 836–841, doi: 10.1038/nsmb.1445 (2008).
47. Kozak, M. Downstream secondary structure facilitates recognition of initiator codons by eukaryotic ribosomes. *Proc Natl Acad Sci USA* **87,** 8301–8305 (1990).
48. Toribio, R., Diaz-Lopez, I., Boskovic, J. & Ventoso, I. An RNA trapping mechanism in Alphavirus mRNA promotes ribosome stalling and translation initiation. *Nucleic Acids Res*, doi: 10.1093/nar/gkw172 (2016).
49. Gonzalez-Almela, E. *et al.* Differential action of pateamine A on translation of genomic and subgenomic mRNAs from Sindbis virus. *Virology* **484,** 41–50, doi: 10.1016/j.virol.2015.05.002 (2015).
50. Sanz, M. A. & Carrasco, L. Sindbis virus variant with a deletion in the 6K gene shows defects in glycoprotein processing and trafficking: lack of complementation by a wild-type 6K gene in trans. *J Virol* **75,** 7778–7784, doi: 10.1128/JVI.75.16.7778-7784.2001 (2001).
51. Sanz, M. A., Castello, A. & Carrasco, L. Viral translation is coupled to transcription in Sindbis virus-infected cells. *J Virol* **81,** 7061–7068, doi: 10.1128/JVI.02529-06 (2007).
52. Madan, V., Castello, A. & Carrasco, L. Viroporins from RNA viruses induce caspase-dependent apoptosis. *Cell Microbiol* **10,** 437–451, doi: 10.1111/j.1462-5822.2007.01057.x (2008).

Acknowledgements

This study was supported by a DGICYT (Dirección General de Investigación Científica y Técnica, Ministerio de Economía y Competitividad, Spain) grant (SAF2015-66170-R (MINECO/FEDER). The Institutional Grant awarded to the Centro de Biología Molecular "Severo Ochoa" (CSIC-UAM) by the Fundación Ramón Areces is acknowledged.

Author Contributions

Experiments were performed by M.A.S. and E.G.-A. L.C. wrote the manuscript. All these authors conceived and designed the experiments.

Additional Information

Supplementary information accompanies this paper at http://www.nature.com/srep

Competing Interests: The authors declare no competing financial interests.

How to cite this article: Sanz, M. A. *et al.* Translation of Sindbis Subgenomic mRNA is Independent of eIF2, eIF2A and eIF2D. *Sci. Rep.* **7**, 43876; doi: 10.1038/srep43876 (2017).

Publisher's note: Springer Nature remains neutral with regard to jurisdictional claims in published maps and institutional affiliations.

ARTÍCULO 3:

A viral RNA motif involved in signaling the initiation of translation on non-AUG codons.

La iniciación en codones no-AUG es una estrategia de traducción empleada tanto por mRNAs virales como celulares. El sgRNA de SINV constituye un excepcional sistema modelo para analizar esta traducción, ya que se trata de un mRNA capeado que inicia su traducción mediante *scanning* y sin la participación de ciertos factores de iniciación. Partiendo de los resultados del anterior artículo, en este trabajo se investigó el mecanismo de iniciación de la traducción del sgRNA con CUG en lugar de AUG_i, así como los requerimientos estructurales del DSH para señalizar correctamente el codón de inicio. Investigaciones previas habían determinado que la traducción del sgRNA podía iniciar, aunque ineficientemente, en diferentes codones no-AUG. Por este motivo, se estudió (1) qué aminoácido se incorpora en la proteína C de SINV cuando la traducción inicia en un codón CUG o GUG, (2) los requerimientos de la estructura DSH situada en la secuencia codificante para señalizar correctamente la iniciación en CUG, y (3) la posible participación en esa iniciación de eIF2, eIF2A o eIF2D.

Inicialmente se estudió la participación del eIF2 en la iniciación cuando el AUG_i es reemplazado por CUG. Como era de esperar, eIF2 no participa en la iniciación sobre codones CUG. Se analizó la plasticidad del sgRNA de SINV para iniciar en codones no-AUG mediante la transfección de una batería de replicones con CUG, CUC, GUG o AUU en lugar del AUG_i en células BHK y C6/36. CUG, seguido de GUG, fueron los codones más eficientes en dirigir la iniciación, por lo que la investigación se enfocó en ellos. La siguiente cuestión de interés era averiguar cuál tRNA reconocía el codón CUG como codón de iniciación, puesto que trabajos anteriores han sugerido que CUG podría reconocerse tanto por el Met-$tRNA_i$ (Kearse and Wilusz 2017, Liang, Chen et al. 2017, Na, Barbhuiya et al. 2018) como por el Leu-tRNA (Starck, Jiang et al. 2012). Estos tRNAs incorporarían metionina o leucina, respectivamente. En este trabajo, se analizaron por espectrometría de masas (LC-MS/MS) los péptidos derivados de la proteína C producida por virus o replicones con el AUG_i mutado a CUG o GUG para determinar el primer aminoácido incorporado. De este modo, se pudo detectar que para CUG tanto leucina como metionina fueron incorporados como primer aminoácido, mientras que para GUG fueron metionina o valina. Sin embargo, la proporción exacta entre los péptidos iniciados con metionina o con leucina o valina no pudo ser determinada con esta metodología. Posteriormente, se realizó una estimación cuantitativa de la proporción de

estos péptidos a través del análisis de la síntesis de proteínas dirigido por diferentes construcciones con mutaciones puntuales sobre los codones AUG.

En este trabajo también se analizó la importancia de la secuencia *leader* y de la estructura y secuencia del DSH en la señalización del codón de iniciación. Se examinó la producción de la proteína C a partir de distintos replicones con variaciones tanto en estructura como en secuencia para el DSH, en paralelo con variantes que tenían AUG o CUG como codón de iniciación del sgRNA. Este estudio se realizó comparativamente en células de mamífero (BHK) y de mosquito (C6/36). Por otra parte, el papel de la estructura del DSH en la traducción del sgRNA fue examinado fuera del contexto replicativo. Para ello, se emplearon sgRNAs obtenidos *in vitro* que presentaban el DSH wt o el DSH desestabilizado, y AUG o CUG como codón de iniciación. Este ensayo se realizó con variantes del sgRNA de SINV obtenidas *in vitro* transfectadas tanto en células (BHK y C6/36) como en los sistemas de traducción *in vitro* (lisado de reticulocitos de conejo y extractos de *Drosophila melanogaster*).

Para conocer el proceso de iniciación con codones alternativos resulta fundamental determinar en qué sitio ribosómico entra el primer tRNA. Se utilizó bruceantina para bloquear la iniciación en el sitio P ribosómico y averiguar si el sgRNA de SINV inicia la traducción en el sitio A. Finalmente, se examinó la posible participación de eIF2A y eIF2D en la iniciación en CUG para el sgRNA de SINV. Células HAP1 wt y doble KO para los mencionados factores fueron infectadas por SINV (wt y variante CUG) y la síntesis de proteínas fue analizada mediante marcaje radioactivo.

Nuestros resultados mostraron que tanto el Leu-tRNA como el Val-tRNA pueden participar en la iniciación de la traducción del sgRNA mediante un mecanismo dependiente del DSH e independiente de los factores eIF2, eIF2A y eIF2D. Además, se demostró que la estructura del DSH en el mRNA controla su habilidad de señalar la iniciación de la traducción en codones no-AUG.

SANZ, M. A., **GONZALEZ-ALMELA, E.**, GARCIA MORENO, M., MARINA, A.I. AND CARRASCO, L. 2019. A Viral RNA Motif Involved in Signalling the Initiation of Translation on Non-AUG Codons. *RNA,* 25: 431-452

A viral RNA motif involved in signaling the initiation of translation on non-AUG codons

MIGUEL ANGEL SANZ, ESTHER GONZÁLEZ ALMELA, MANUEL GARCÍA-MORENO,[1] ANA ISABEL MARINA, and LUIS CARRASCO

Centro de Biología Molecular Severo Ochoa (CSIC-UAM), Universidad Autónoma de Madrid, Cantoblanco 28049 Madrid, Spain

ABSTRACT

Noncanonical translation, and particularly initiation on non-AUG codons, are frequently used by viral and cellular mRNAs during virus infection and disease. The Sindbis virus (SINV) subgenomic mRNA (sgRNA) constitutes a unique model system to analyze the translation of a capped viral mRNA without the participation of several initiation factors. Moreover, sgRNA can initiate translation even when the AUG initiation codon is replaced by other codons. Using SINV replicons, we examined the efficacy of different codons in place of AUG to direct the synthesis of the SINV capsid protein. The substitution of AUG by CUG was particularly efficient in promoting the incorporation of leucine or methionine in similar percentages at the amino terminus of the capsid protein. Additionally, valine could initiate translation when the AUG is replaced by GUG. The ability of sgRNA to initiate translation on non-AUG codons was dependent on the integrity of a downstream stable hairpin (DSH) structure located in the coding region. The structural requirements of this hairpin to signal the initiation site on the sgRNA were examined in detail. Of interest, a virus bearing CUG in place of AUG in the sgRNA was able to infect cells and synthesize significant amounts of capsid protein. This virus infects the human haploid cell line HAP1 and the double knockout variant that lacks eIF2A and eIF2D. Collectively, these findings indicate that leucine-tRNA or valine-tRNA can participate in the initiation of translation of sgRNA by a mechanism dependent on the DSH. This mechanism does not involve the action of eIF2, eIF2A, or eIF2D.

Keywords: initiation of translation; Sindbis virus translation; noncanonical translation; non-AUG codon; RNA motif

INTRODUCTION

Animal viruses have evolved a variety of elements in their mRNAs to maximize their translatability under stress conditions generated after infection. Accordingly, some viruses contain elements that promote the interaction of preinitiation complexes or even ribosomes to internal structures known as internal ribosome entry sites (IRESs) (Lee et al. 2017; Martinez-Salas et al. 2017). Viral mRNAs bearing IRES elements can be translated under conditions that could be antagonistic to the activity of cellular mRNAs. Another interesting example is provided by the subgenomic mRNA (sgRNA) of Sindbis virus (SINV), which contains motifs that promote its translatability during the late phase of the virus life cycle (Carrasco et al. 2018). SINV belongs to the alphavirus genus and contains a single stranded RNA of positive polarity as genome, which encodes two open reading frames (ORFs). The first ORF is expressed from the genomic mRNA (gRNA), which synthesizes the nonstructural proteins (nsP1–4) involved in RNA replication (Rupp et al. 2015). The second ORF is expressed from the sgRNA and directs the synthesis of viral structural proteins, initially translated as a polyprotein that is subsequently cleaved to the mature products: capsid protein, glycoproteins E1, E2, and E3 and viroporin 6K and its truncated product TF (Griffin 2013; Ramsey and Mukhopadhyay 2017). Synthesis of sgRNA requires the recognition of an internal promoter located on the negative stranded RNA that promotes transcription of multiple copies of this subgenomic messenger. This negative stranded RNA is complementary to the genome and is produced by viral RNA replication in close association with spherules protruding from cytoplasmic vacuoles (Pietila et al. 2017a,b). Most alphaviruses, exemplified by SINV, replicate in two quite different hosts, insects and mammals and, accordingly, viral mRNA structures have adapted to these diverse host species. One adaptation is an RNA motif found at the 3′

[1]**Present address:** Department of Biochemistry, University of Oxford, OX1 3QU Oxford, United Kingdom

Corresponding author: lcarrasco@cbm.csic.es

Article is online at http://www.rnajournal.org/cgi/doi/10.1261/rna.068858.118.

untranslated region (3′-UTR), which contains three repeated sequences forming three stem–loop hairpins. This motif is involved in enhancing translation specifically in insect cells, whereas the absence of this structure is not important for sgRNA translation in mammalian cells (Garcia-Moreno et al. 2016). This element thus confers translatability in a cell-specific manner. A second RNA structure involved in translation is found in the coding region of the sgRNA, in the form of a hairpin located 27–84 nt downstream from the AUG initiation codon (with A at the +1 position) (Carrasco et al. 2018). This downstream stable hairpin (DSH) provides eIF2-independence after the inactivation of this factor by its phosphorylation at serine 51 (Ventoso et al. 2006; Garcia-Moreno et al. 2013). This phosphorylation event is mediated by protein kinase R (PKR), which is activated by viral dsRNA synthesis. eIF2 inactivation is observed in mammalian, but not in insect cells, which lack PKR (Ventoso 2012). Thus, the repeated stem–loop motif at the 3′-UTR is necessary for alphavirus translation in insect cells, whereas the DSH is required for efficient synthesis of structural proteins in mammalian cells.

Another important function of the DSH is its participation in the correct signaling of the initiation codon of sgRNA. Interestingly, alterations in the DSH structure result in leaky scanning, such that initiation of capsid (C) protein synthesis is observed at downstream AUG codons (Frolov and Schlesinger 1996; Sanz et al. 2009). It was recently demonstrated that the initiation of protein synthesis directed by sgRNA occurs following the classical scanning model (Garcia-Moreno et al. 2015); however, scanning can occur in the absence of some crucial eIFs, such as eIF4G, eIF4A, and eIF2 (Castello et al. 2006; Garcia-Moreno et al. 2013; Gonzalez-Almela et al. 2015). The current model for translation initiation on sgRNA is that preinitiation complexes interact with the cap structure present at the 5′-end, perhaps promoted by eIF3D, and without the participation of the eIF4F complex (Lee et al. 2016). After binding, the preinitiation complex scans the leader sequence of sgRNA base-by-base until the initiation codon is encountered. Subsequently, the correct functioning of the DSH element is required to build up the 80S ribosome, which will start the elongation phase (Carrasco et al. 2018). We previously found that the AUG initiation codon could be replaced by other codons, although protein synthesis directed by these variant sgRNAs was reduced (Sanz et al. 2009, 2017). Nevertheless, replacement of AUG by CUG was particularly efficient and the synthesis of the C protein by this sgRNA variant was ∼60% of that from the control AUG. Thus, the precise mechanism of sgRNA translation in the absence of the AUG initiation codon, as well as the functioning of DSH in this process, remains unknown. In the present study, we investigated the mechanism of initiation on sgRNA containing CUG in place of AUG, and also the structural requirements of DSH for its proper functioning in signaling the initiation codon. These events occur in cells more frequently than previously anticipated and have a profound impact on cell functioning, especially during stress conditions and disease, as revealed recently using ribosome profiling (Kearse and Wilusz 2017). For instance, a variety of aberrant peptides are synthesized on non-AUG codons, that play a part in the pathology of several neurodegenerative diseases (Kumar et al. 2017; Tabet et al. 2018). Our current findings are further insight into the mechanism of the initiation of translation on non-AUG codons. We found that leucine or methionine is incorporated at the amino terminus of the SINV C protein directed by the CUG codon. Notably, translation initiation on sgRNA bearing CUG does not require eIF2 and this factor is not replaced by eIF2A or eIF2D. Overall, these observations add new insight into the mechanism of initiation of this viral mRNA and highlight the functioning of the DSH structural motif.

RESULTS

Replacement of the AUG initiation codon with other codons in sgRNA: synthesis of capsid protein by SINV replicons

We recently demonstrated that sgRNA is able to direct protein synthesis in human cells transfected with SINV replicons when the AUG initiation codon is replaced with CUG (Sanz et al. 2017). To gain further insight into the mechanism of this phenomenon, we initially studied the participation of eIF2 in this process. We used two replicons that produce sgRNA encoding the C protein upstream of the luciferase gene: one containing AUG as the intiation codon, rep C + luc (AUG), and the other containing CUG as the initiation codon, rep C + luc (CUG) (see scheme Fig. 1A). We first analyzed the synthesis of C and luciferase in mammalian baby hamster kidney (BHK) cells transfected with the two replicons. It is well established that replication of SINV in BHK cells induces eIF2α phosphorylation (Sanz et al. 2009; Garcia-Moreno et al. 2013). To ensure that eIF2 was phosphorylated at high levels, some cultures were treated with thapsigargin (TG), which inactivates eIF2 by inducing the phosphorylation of the α subunit. Thus, 3 h after transfection cells were treated with 2 or 5 μM TG for a further 2 h. The synthesis of C and luciferase was examined in cell extracts by western blotting and measurement of luciferase was also analyzed by measuring its activity. Results showed robust levels of C and luciferase synthesis by the two replicons, indicating that CUG can also initiate protein synthesis directed by sgRNA in BHK cells (Fig. 1B–D). eIF2α phosphorylation was induced by both SINV replicons and was modestly increased by TG treatment (Fig. 1B). Consistent with previous results (McInerney et al. 2005; Ventoso et al. 2006; Sanz et al. 2009), the phosphorylation of eIF2α had no inhibitory effects on sgRNA translation from rep C + luc (AUG). Further, almost no

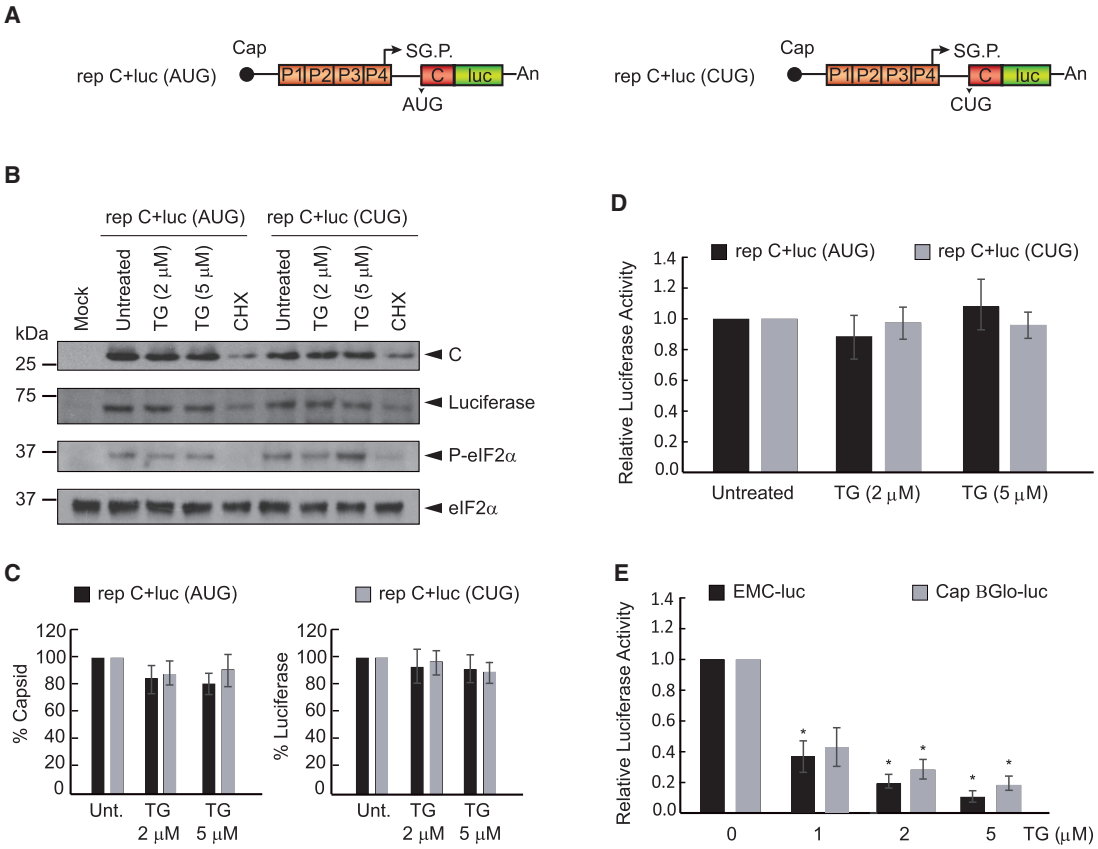

FIGURE 1. Analysis of C protein synthesis by SINV replicons bearing AUG or CUG as the initiation codon. (*A*) Schematic representation of rep C + luc (AUG) and rep C + luc (CUG). (*B*) BHK cells were transfected with in vitro transcribed replicons. After 3 h, cells were treated or not with thapsigargin (TG; 2 or 5 μM) or cyclohexamide (CHX; 50 μg/mL) for 2 h. Cells were collected in loading buffer and analyzed by western blotting using anti-C, anti-luciferase and anti-P-eIF2α antibodies. Additionally, eIF2α was analyzed as a loading control. (*C*) Densitometric analysis of C and luciferase are shown in the graphs as the relative percentage of their corresponding untreated controls. The values from CHX treatments were subtracted from all as a baseline. Error bars represent the standard error of the mean, $n = 3$. (*D*) Luciferase activity is represented as the percentage relative to the untreated controls. The readings from CHX treatments were subtracted from all as a baseline. Error bars represent the standard error of the mean, $n = 3$. (*E*) BHK cells were transfected with in vitro transcribed RNAs EMCV-luc or Cap.BGlo-luc. One hpt, cells were treated or not with TG (1, 2, or 5 μM) or CHX (50 μg/mL) for 2 h. Then, luciferase activity was measured and is represented in the graph as percentage relative to the untreated control. The readings from CHX treatments were subtracted from all as a baseline. Error bars represent the standard error of the mean, $n = 3$. Statistical significance in panels *C–E* was calculated compared to control using Student's *t*-test unpaired two-tails *t*-test, and is shown as: (*) $P < 0.05$

inhibition of sgRNA translation occured with or without TG treatment in cells transfected with rep C + luc (CUG), indicating that eIF2 does not participate in the initiation event directed by the CUG codon. As a control of the inhibitory action of TG, the translation of mRNAs bearing the EMCV IRES or the Globin leader sequence was strongly blocked by treatment with TG in BHK cells (Fig. 1E). We also assessed the production of C protein in transfected BHK cells by immunocytochemistry with an anti-C polyclonal rabbit antibody. Abundant amounts of C were detected in cells transfected with either rep C + luc (CUG) or rep C + luc (AUG) (Supplemental Fig. 1), and levels did not noticeably decrease after TG treatment. Of note, the replication of the SINV replicons induced the release of TIA1 protein from the nucleus to the cytoplasm, but no stress granules were formed, contrary to what happens in untransfected cells after TG treatment. Indeed, stress granules were not apparent in transfected cells even with TG treatment.

The extent of translation initiation on non-AUG codons in cellular mRNAs depends on the codon used (Kearse and Wilusz 2017). After AUG, CUG is usually the most efficient codon to promote initiation, followed by GUG or AUU (Kearse and Wilusz 2017). We compared the efficacy of different codons to direct C protein synthesis using a battery of SINV replicons bearing CUG, CUC, GUG, or AUU in place of the initiator AUG codon in sgRNA. A second and third AUG codon in the C sequence are located 7 and 19 codons, respectively, downstream from the first AUG (Fig. 2A). All variants with mutations in the initiator AUG codon were also modified at the second AUG codon (to

CUG), to facilitate the electrophoretic separation of the C proteins produced by leaky scanning. The synthesis of C protein was evaluated by western blotting of cell extracts after transfection of the replicons in BHK cells, and densitometry of the corresponding band was performed to give an estimation of the efficacy of the codons to initiate translation. Results showed that AUG was the best codon to initiate C synthesis on sgRNA, but substantial levels of C were also produced from rep C + luc (CUG) (Fig. 2B,C). In this case, the anti-C antibody recognized two products: one, named C1, migrated as authentic C and was produced with an efficiency of 64% as compared with the

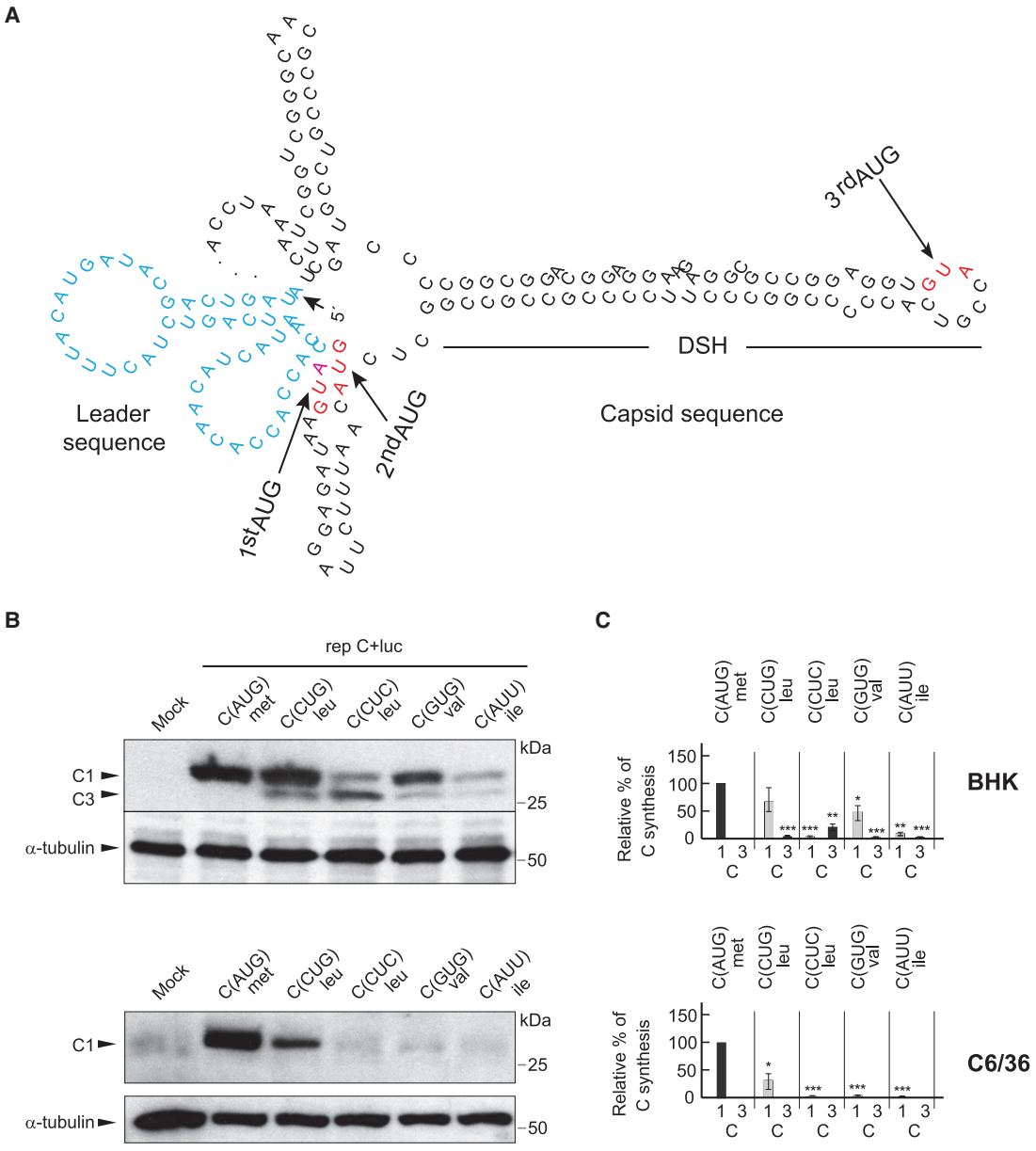

FIGURE 2. Translation initiation by SINV replicons using different non-AUG codons. (*A*) Representation of the secondary structure of the first 180 nt of sgRNA. The leader sequence is colored in blue. First, second and third AUGs in wt sequence of C are highlighted in red. (*B*) BHK or C6/36 cells were transfected with the different replicons produced by in vitro transcription. After 7 h, cells were collected in loading buffer and analyzed by western blotting with an anti-C antibody. The mobilities of the C products from the different replicons are indicated as C1 (initiation in the first AUG or in the same codon mutated to CUG, CUC, GUG, or AUU), and C3 (initiation in the third AUG codon relative to the wt sequence). α-tubulin was analyzed as a loading control. (*C*) Densitometric analysis of the different C proteins synthesized from the replicons. Graphs show the percentage values relative to the amount of C synthesized by rep C + luc (AUG) in each cell line. The black bars correspond to translation initiation at AUG and the gray bars at non-AUGs. The results are shown as mean ± SD of three experiments. Statistical significance in panel *C* was calculated compared to control using Student's *t*-test, (*) $P < 0.05$, (**) $P < 0.01$, (***) $P < 0.001$.

only one produced by rep C + luc (AUG); the second product, named C3, represented only 1% and migrated faster (Fig. 2B,C). The product C1 derives from translation initiation at the first CUG whereas C3 corresponds to initiation at the first nonmutated AUG codon by leaky scanning, which matches the third AUG in the wild-type (wt) sequence (Fig. 2A). The second most efficient codon after CUG was GUG (46%), which encodes for valine, whereas practically no C synthesis was found with CUC (leucine) or AUU (isoleucine). Nevertheless, a small production of C3, <6%, could be observed in all these variants (Fig. 2B). These findings indicate that, following AUG, the $tRNA^{leu}$ isoform containing the anti-codon corresponding to CUG is presumably the best to initiate translation on sgRNA, followed by GUG, whereas the $tRNA^{leu}$ (CUC) and the $tRNA^{ile}$ (AUU) isoforms are devoid of this activity.

Since SINV has two different natural hosts (mammals and insects), it was of interest to analyze the replicons containing the different codons in insect cells. Accordingly, *Aedes albopictus* C6/36 cells were transfected with the same replicons and C synthesis was estimated as before. Curiously, the activity of these codons was much lower in C6/36 cells and only C produced by initiation on CUG could be detected with any certainty, yielding ~30% of the control levels (Fig. 2B,C). This observation suggests that the mechanism followed by mammals and insects to select the start codon has a different stringency. Indeed, no leaky scanning was apparent in mosquito cells with the sgRNAs analyzed.

Leucine or methionine can be incorporated at the amino terminus of C when AUG is replaced by CUG

It is thought that in the majority of cases, translation initiation with CUG involves the misincorporation of methionine, mediated by the ternary complex Met-$tRNA_i^{Met}$-eIF2-GTP, which should be capable of recognizing CUG instead of AUG (Kearse and Wilusz 2017; Liang et al. 2017; Sellier et al. 2017; Na et al. 2018). Leucyl-tRNA has also been shown to participate in the initiation event mediated by CUG (Starck et al. 2012). To distinguish which aminoacyl tRNA is involved in the initiation directed by CUG or GUG, the corresponding SINV replicons (and control AUG) were transfected into BHK cells, cell extracts were separated by SDS-PAGE, and the band corresponding to C protein was excised and digested for mass spectrometry (LC–MS/MS) analysis. For this purpose, the arginine residue at the third position of the C protein sequence was mutated to valine in order to obtain a tryptic peptide of an adequate size (see scheme in Fig. 3A). Following transfection of rep C + luc (AUG), a peptide of 11 amino acids was detected that was consistent with the amino-terminal sequence of C, which has the initial methionine modified by acetylation (Fig. 3B, upper panel). Notably, the corresponding peptide containing leucine at the amino terminus was also identified in cells transfected with rep C + luc (CUG) (Fig. 3B, middle panel). In this case, a peptide starting with methionine was also detected (Supplemental Fig. 2A). The precise proportion of each peptide bearing leucine or methionine cannot be determined by this analysis, since it is qualitative and not quantitative. Similarly, the corresponding peptides bearing valine (Fig. 3B, lower panel) or methionine (Supplemental Fig. 2B) at the amino terminus were found in cells transfected with rep C + luc (GUG). Therefore, we conclude that in addition to methionine, leucyl-tRNA, or valyl-tRNA can recognize CUG or GUG, respectively, during the initiation of C synthesis.

To obtain a quantitative estimation of the percentage of incorporation of methionine or leucine at the amino terminus, we constructed replicons in which all the AUG codons present in the C protein, except for the first AUG, were mutated to CUG (termed rep C [one AUG]), or in which no AUGs were present in the entire C sequence (termed rep C [no AUGs]). These two replicons differ from rep C + luc by the presence of a stop codon at the end of the C sequence and also the absence of the luciferase gene. These modifications were designed to obtain only the C protein, since the mutations introduced into the C sequence to suppress the ten AUGs may affect its proteolytic activity when C plus luciferase are synthesized. BHK cells transfected with these replicons were radioactively labeled with translabel [^{35}S] methionine/cysteine from 6–7 hpt. It must also be remembered that the C sequence contains no cysteine residues. Since only a proportion of cells are transfected with these replicons, most of the radiolabeled proteins are cellular. Thus, cells were treated or not with 200 µM sodium arsenite (Ars) during labeling to block cellular protein synthesis (SINV sgRNA translation is resistant to this inhibitor). Results from western blotting showed a band corresponding to the size of authentic C protein from both replicons (Fig. 3C), suggesting that translation begins at the corresponding initiation codons, AUG or CUG. We next inactivated the peroxidase activity of the membrane and exposed it to X-ray film to detect the radioactively labeled C protein. Radioactive methionine was clearly incorporated into C protein produced by rep C (one AUG) and, albeit in a lower proportion, also in C derived from rep C (no AUGs) (Fig. 3C), which agrees with the data obtained by LC–MS/MS. We then calculated the proportion of C obtained by immunoblotting versus radioactive labeling in cells transfected with either replicon. Densitometric analysis indicated that leucine was incorporated at the CUG codon in ~65% of cases, whereas methionine was incorporated in 35% of the initiation events (Fig. 3D).

Analysis of the role of sgRNA leader sequence in signaling the initiation codon of translation

The leader sequence of mRNAs plays an important role in signaling the correct initiation codon to start translation

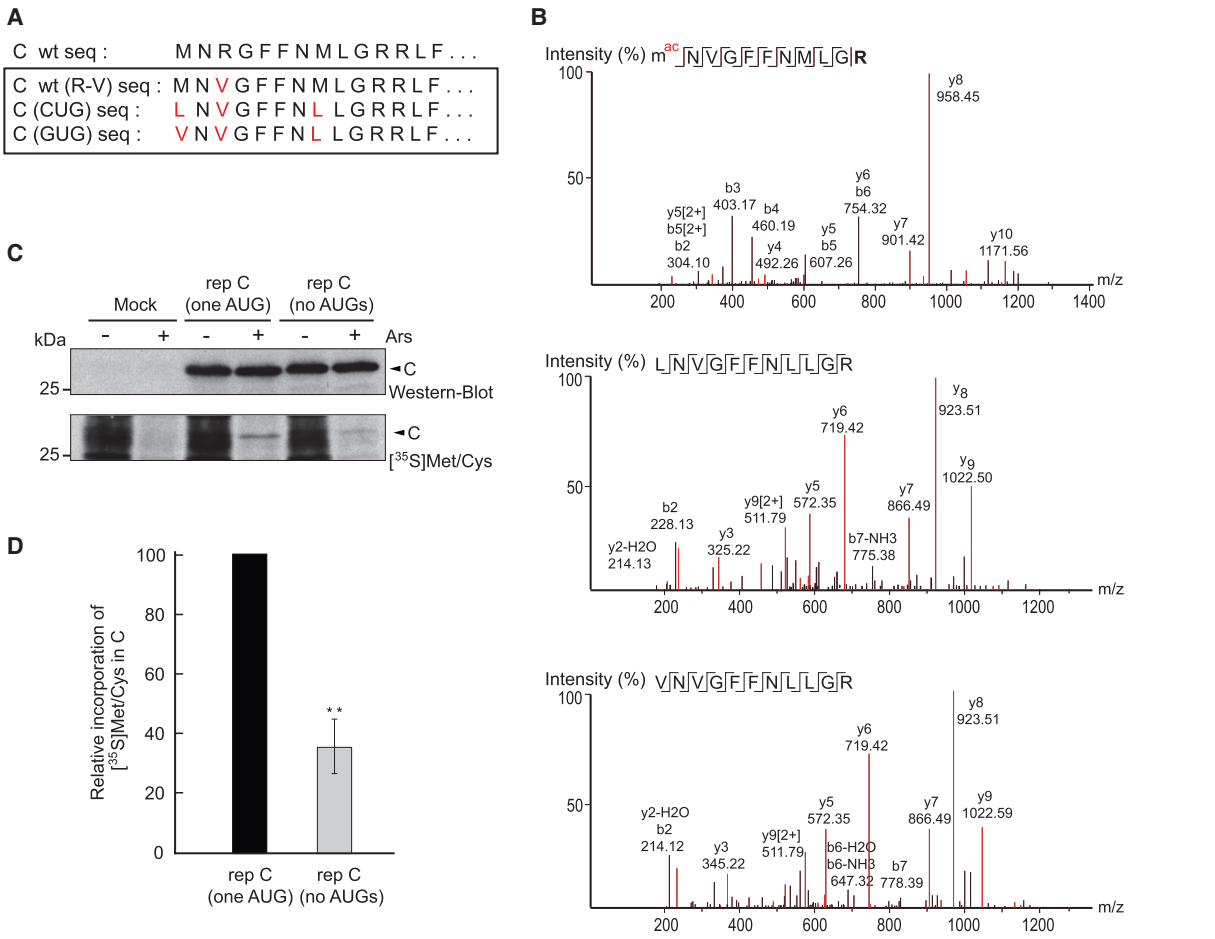

FIGURE 3. Leucine or methionine can be incorporated at the amino terminus when AUG is replaced by CUG. (*A*) Amino-terminal amino acid sequences of wt C protein and corresponding mutants, marked in red. (*B*) BHK cells were transfected with in vitro synthesized replicons rep C + luc (AUG), rep C + luc (CUG), or rep C + luc (GUG), all containing the R to V mutation in C. After 8 h, cultures were collected and extracted proteins were separated by SDS-PAGE, visualized by Coomassie blue staining, and then protein bands from the different samples were excised, trypsin-digested and analyzed by LC–MS/MS. The MS/MS spectra of amino-terminal peptides of C detected are displayed. (*C*) BHK cells were mock-transfected or transfected with in vitro synthesized replicons rep C (one AUG) or rep C (no AUGs). After 7 h, cells were treated or not with sodium arsenite (Ars) for 15 min and then protein synthesis was detected with [^{35}S] Met/Cys labeling for 45 min. Samples were immunoblotted with anti-C antibodies (western blot). Then, peroxidase activity was inactivated by heating the membrane at 120°C for 15 min before exposure to an X-ray film to detect radioactive signals ([^{35}S] Met/Cys.) (*D*) The proportion obtained by immunoblotting or radioactive labeling of C protein in cells transfected with both replicons was calculated and the radioactive signal was normalized to the amount of C by immunoblotting; the graph shows the percentage incorporation of [^{35}S] Met/Cys in C protein by rep C (no AUGs) relative to rep C (one AUG). The results are shown as mean ± SD of three experiments. Statistical significance in panel *D* was calculated compared to control using Student's *t*-test, (*) $P < 0.05$, (**) $P < 0.01$, (***) $P < 0.001$.

and, in particular, the sequence context around the AUG is critical in this respect (Kozak 1991; Kearse and Wilusz 2017). For optimal signaling of the AUG codon, positions located at −6, −3 and +4 (with the A at position +1) should contain a purine residue. Initially, we assayed the importance of the AUG in the luciferase gene expressed from a SINV replicon. To this end, we made use of the replicon rep Lluc-luc (AUG) (see scheme Fig. 4A; Sanz et al. 2010), which has the last 38 nt of the leader sequence of sgRNA (L26S) substituted for the last 42 nt of the leader sequence of luciferase, followed by the complete sequence of this gene. We also constructed a variant, rep Lluc-luc (CUG), bearing CUG in place of AUG. The synthesis of luciferase was then assayed by western blotting in BHK cells. Results showed that the expression of luciferase was rather inefficient as compared with luciferase produced by rep C + luc even when the initiation codon is AUG, <25%, because it does not contain the genuine sgRNA leader sequence and the DSH structure (Fig. 4B,E). Replacement of the AUG for CUG led to barely detectable levels of luciferase, indicating poor initiation (Fig. 4B,E). Two additional SINV replicons were constructed bearing the luciferase

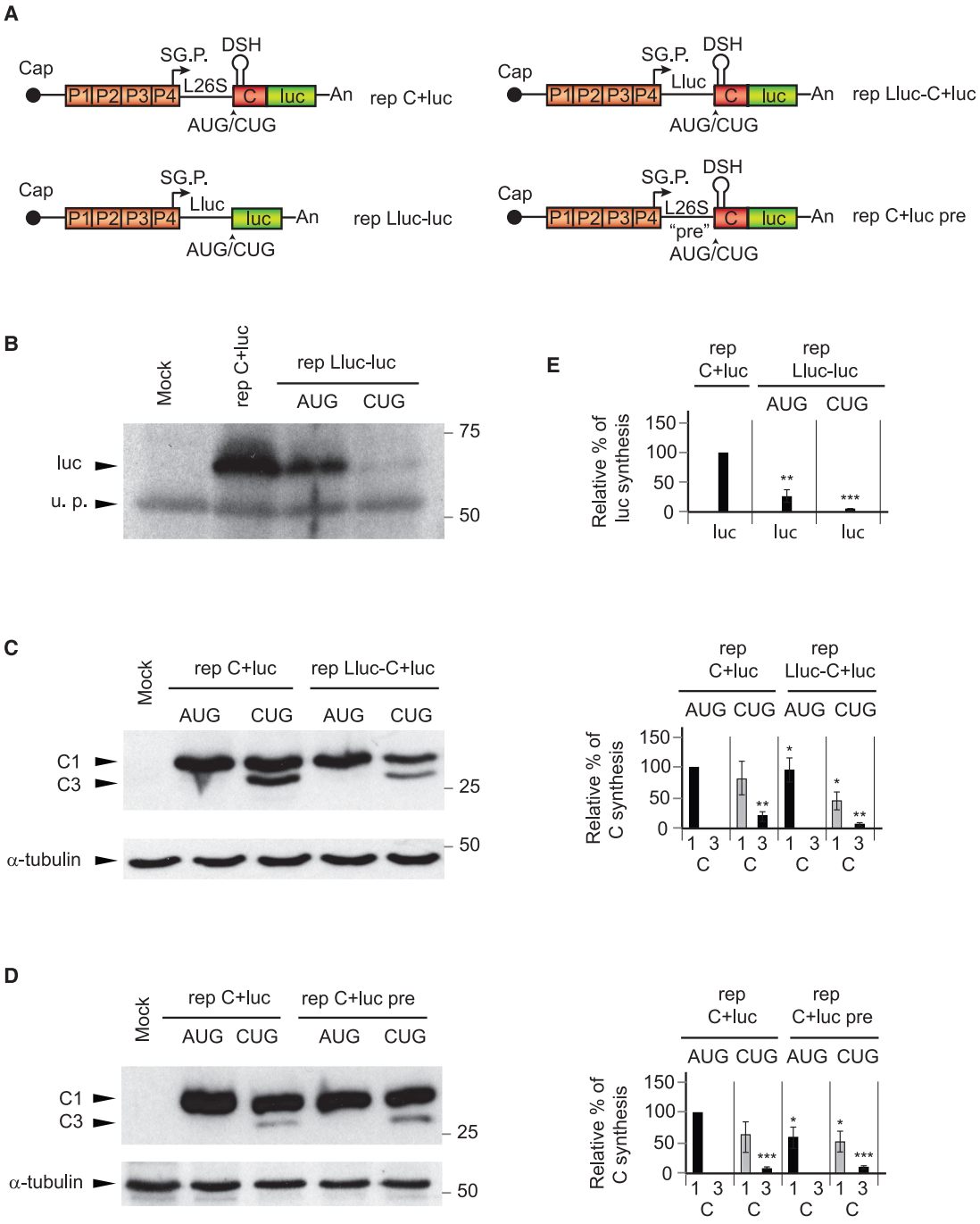

FIGURE 4. The DSH structure, by itself, specifies the translation initiation site. (*A*) Schematic representation of the replicons: rep C + luc, rep Lluc-luc, rep Lluc C + luc, and rep C + luc pre. L26S is equivalent to the wt leader sequence of sgRNA, Lluc indicates that the leader sequence of luciferase is replacing the wt leader sequence and the indication pre refers to six nucleotides mutated in the leader sequence before the initiator AUG/CUG codon. (*B*) BHK cells were transfected with rep C + luc (AUG) as a control, rep Lluc-luc (AUG), or rep Lluc-luc (CUG). After 7 h, cells were collected in loading buffer and extracted proteins were analyzed by western blotting with an anti-luciferase antibody. A protein that is recognized nonspecifically by antibodies is also shown as a loading control (u.p.). (*C*) BHK cells were transfected with rep C + luc (AUG), rep C + luc (CUG), rep Lluc-C + luc (AUG), or rep Lluc-C + luc (CUG). After 7 h, cells were collected in loading buffer and extracted proteins were analyzed by western blotting with an anti-C antibody. The mobilities of the C products are indicated as C1 (initiation in the first AUG or in the same codon mutated to CUG) and C3 (initiation in the third AUG codon relative to the wt sequence). α-tubulin was analyzed as a loading control. (*D*) BHK cells were transfected with rep C + luc (AUG), rep C + luc (CUG), rep C + luc pre (AUG), or rep C + luc pre (CUG). After 7 h, cells were collected in loading buffer and extracted proteins were analyzed by western blotting with an anti-C antibody. The mobilities of the C products are indicated as in panel *C*. α-tubulin was analyzed as a loading control. (*E*) Densitometric analysis of luciferase or C proteins synthesized from the respective replicons. The graphs show the percentage values in relation to the amount of luciferase or C synthesized by rep C + luc (AUG). The black bars correspond to translation initiation at AUG and gray at CUG. The results are displayed as mean ± SD of three experiments. Statistical significance in panel *E* was calculated compared to control using Student's *t*-test, (*) $P < 0.05$, (**) $P < 0.01$, (***) $P < 0.001$.

leader sequence followed by the sequence encoding C plus luciferase: rep Lluc-C + luc (AUG) and rep Lluc-C + luc (CUG) (see scheme Fig. 4A). The first replicon containing the AUG initiation codon synthesized C protein to a level similar (92%) to that of BHK cells transfected with control rep C + luc (AUG). Interestingly, rep Lluc-C + luc (CUG) also synthesized C protein, although with a lower efficiency than rep C + luc (CUG): 45% versus 80%, with 100% as the control rep C + luc (AUG) (Fig. 4C,E). This result indicates that CUG can still be partially recognized as an initiation codon when the DSH structure is present in the C protein sequence, but replacement of the genuine leader 26S sequence of sgRNA by the luciferase counterpart affects this recognition.

Finally, we wished to analyze the sequence prior to the initiation codon without altering the composition of purines and pyrimidines. Thus, the six nucleotides upstream of the initiation codon were mutated from ACCACC to GUUGUU, rendering the replicons rep C + luc pre (AUG) and rep C + luc pre (CUG). Transfection of these SINV replicons in BHK cells led to the production of C protein to levels comparable with the corresponding rep C + luc counterparts (Fig. 4D,E). Therefore, the exact sequence ACCACC upstream of the initiation codon is not crucial to initiate at the correct position.

Involvement of the DSH structure in signaling the initiation of sgRNA translation in transfected cells and in cell-free systems

To evaluate the participation of the DSH structure in sgRNA translation out of the replication context, we compared C production in cells transfected with replicons C + luc or their respective sgRNAs made by in vitro transcription. We tested sgRNAs containing wild-type DSH (DSH-wt) or a destabilized DSH (DSH-destab), previously designated as ΔDLP. (Ventoso et al. 2006; Garcia-Moreno et al. 2013). No base-pairing occurs in the stem of the variant DSH-destab and the hairpin structure fails to form. Analysis of DSH function was performed both in BHK and insect cells. Consistent with the results described above, transfection of replicons bearing AUG or CUG as sgRNA initiation codons gave rise to considerable C protein production in BHK cells (Fig. 5A, upper panel). In contrast, the initiation of translation on CUG in C6/36 cells was very inefficient (Fig. 5A, lower panel). Destablization of the DSH in rep C + luc (AUG) led to leaky scanning in BHK transfected cells, resulting in the synthesis of smaller forms of C protein that initiate at downstream AUGs (Fig. 5A, upper panel), which agrees with previous results (Frolov and Schlesinger 1996; Ventoso et al. 2006; Sanz et al. 2009).

This leaky scanning was not observed in rep C + luc (AUG) DSH-destab-transfected insect cells (Fig. 5A, lower panel). Of note, the integrity of the DSH was crucial to initiate translation on CUG, since no C production initiating at this codon was detected either in BHK or in mosquito cells transfected with rep C + luc (CUG) DSH-destab (Fig. 5A,D). We next studied translation of sgRNA in the absence of viral replication by transfection of sgRNAs produced by in vitro transcription from their respective plasmids. As shown in Figure 5B, sgRNA C + luc (AUG) DSH-wt was efficiently translated both in BHK and insect cells, whereas the variant sgRNA C + luc (AUG) DSH-destab exhibited leaky scanning only in BHK cells, as occurred with the replicons. Also consistent with the findings using replicons, transfection of the sgRNA C + luc (CUG) DSH-wt synthesized appreciable amounts of C protein only in BHK cells (Fig. 5B). Strikingly, the sgRNA C + luc (CUG) DSH-destab was unable to initiate translation at the CUG codon, both in BHK and insect cells (Fig. 5B,D).

Finally, to analyze the behavior of the RNA variants, they were in vitro translated in rabbit reticulocyte lysates (RRL) and in *Drosophila melanogaster* extracts (DME). Figure 5C shows that C synthesis was efficiently synthesized in both extracts by sgRNA C + luc (AUG) DSH-wt. Notably, the sgRNA bearing CUG as the initiation codon was translated less efficiently than the AUG counterpart in both cell-free systems. In addition, the sgRNA bearing the destabilized DSH was devoid of any activity to generate C proteins using CUG as initiation codon (Fig. 5C,D). Collectively, these findings reveal that CUG can initiate translation on sgRNA outside the viral replication context. More importantly, the integrity of the DSH is necessary to initiate translation on CUG.

Structure-activity relationship of DSH in signaling the initiation on CUG

We next sought to analyze in more detail the structural requirements of DSH to participate in the initiation of C synthesis using the CUG codon, in particular to know whether the structure or the sequence, or both, were important for DSH functioning. We thus designed a number of DSH variants with modifications in the stem or the loop and analyzed in parallel DSH variants bearing AUG or CUG as initiation codons in SINV replicons. The replicons were transfected both into BHK and mosquito cells and the level of C protein was estimated by western blotting as described above.

The computer predictions of the structures, including the DSH-wt and DSH-destab, and the free energy required for their melting are shown in Figure 6. The first variant tested had the entire DSH structure replaced by a new sequence (DSH-new), with a free energy similar to genuine DSH. The replicon bearing DSH-new produces a C protein nine amino acids shorter than authentic C protein and has 16 residues different. When compared with DSH-wt, the production of C with DSH-new was 75% in BHK cells and 40% in C6/36 cells (Fig. 7A,C,E). Curiously, the replicon bearing DSH-new and containing CUG in place of AUG

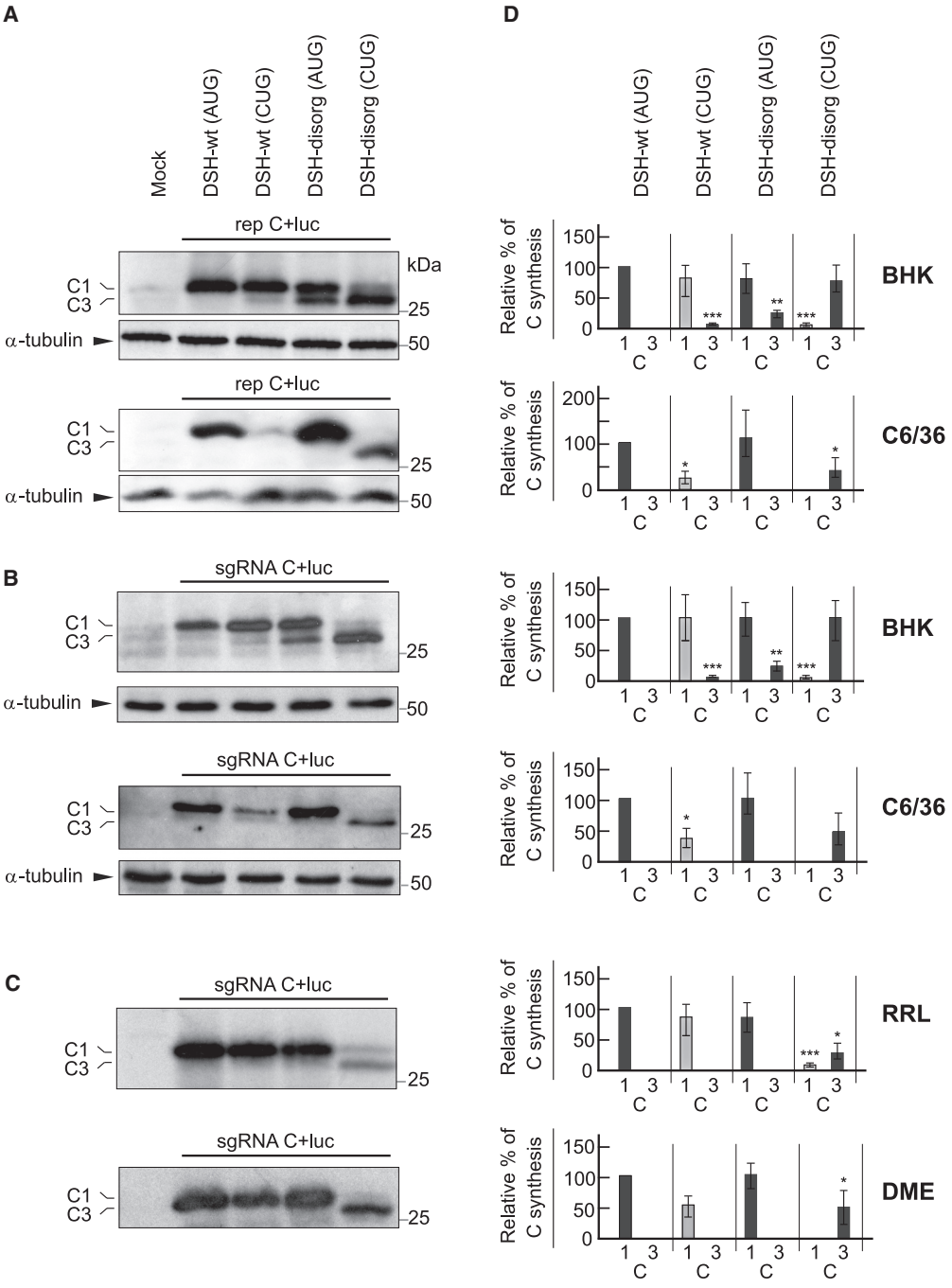

FIGURE 5. Translation of sgRNA with wild-type or destabilized DSH and AUG or CUG initiation codons in different systems. (*A*) BHK (*top*) or C6/36 (*bottom*) cells were transfected with the following rep C + luc replicons: DSH-wt (AUG), DSH-wt (CUG), DSH-destab (AUG), or DSH-destab (CUG). After 7 h, cells were collected in loading buffer and extracted proteins were analyzed by western blotting with an anti-C antibody. The mobilities of the C products are indicated as C1 (initiation in the first AUG or in the same codon mutated to CUG) and C3 (initiation in the third AUG codon relative to the wt sequence). α-tubulin was analyzed as a loading control. (*B*) BHK (*top*) or C6/36 (*bottom*) cells were transfected with the different sgRNAs synthesized by in vitro transcription and, 3 h later, cells were collected and extracted proteins were analyzed by western blotting as in panel *A*. (*C*) The different sgRNAs were in vitro translated using rabbit reticulocyte lysates (RRL) or *Drosophila melanogaster* extracts (DME). After 2 h, protein production was analyzed by western blotting with an anti-C antibody, as in *A* or *B*. (*D*) Densitometric analysis of the different C proteins synthesized in relation to the amount of C of their respective DSH-WT (AUG) controls. Black bars correspond to translation initiation at AUG and gray at CUG. The results are displayed as mean ± SD of three representative experiments. Statistical significance in panel *D* was calculated compared to control using Student's *t*-test; (*) $P < 0.05$, (**) $P < 0.01$, (***) $P < 0.001$.

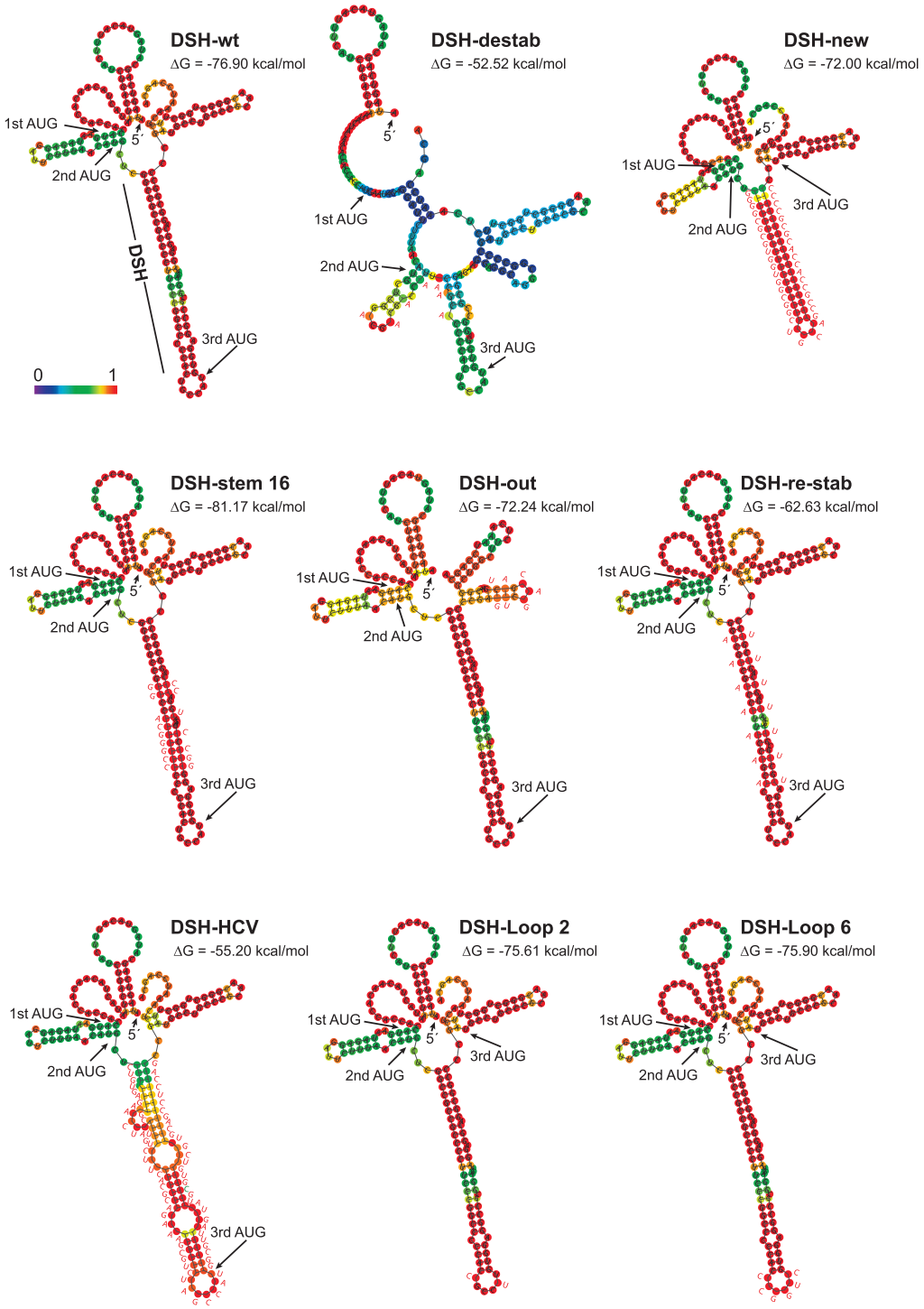

FIGURE 6. Secondary structure prediction of wild-type sgRNA and the variants mutated in the DSH structure. The secondary structures of the first 180 nt of the different sgRNAs (except for DSH-new and DSH-HCV, whose secondary structures comprise only the first 156 or 189 nt, respectively) were obtained using the Vienna RNA Website (http://rna.tbi.univie.ac.at/cgi-bin/RNAWebSuite/RNAfold.cgi) and are colored by base-pairing probability. The free energy of the thermodynamic assembly (ΔG) is shown in each case. The three first AUG codons in phase are marked. In each case the mutated bases are indicated in red font next to the structure. The mutation A to C introduced to avoid a STOP codon in DSH-HCV is highlighted in green. DSH-destab: mutations were made to destabilize the DSH. DSH-new: to replace the DSH with a new hairpin. DSH-stem 16: to modify the sequence reinforcing DSH hairpin stability. DSH-out: to modify the sequence and the structure downstream from DSH. DSH-re-stab: to reconstitute the structure previously destabilized in DSH-destab. DSH-HCV: to replace the DSH by the domain II of HCV IRES. DSH-Loop 2 and DSH-Loop 6: to modify the sequence of DSH loop.

failed to produce C protein in either of the cell lines. Thus, DSH-new cannot replace the genuine DSH structure in signaling the translation initiation site on CUG, even though they both have a similar free energy. This finding demonstrates that the function of the DSH is not to stall the initiation complex, as previously speculated (Frolov and Schlesinger 1996). The next variant tested has 16 modified nucleotides in the sequence, but these changes do not alter the structure of the stem (DSH-stem 16), although it slightly increases its free energy and modifies seven amino acids in the sequence of C (Fig. 6). The production of C with this variant was similar to the control in transfected BHK cells, even when CUG was present (Fig. 7A,E). Of note, there was a substantial inhibition in the synthesis of C protein in insect cells (~70%) with replicons bearing AUG or CUG (Fig. 7C,E), likely because melting of this DSH variant is hampered by insect ribosomes as was described previously (Garcia-Moreno et al. 2015).

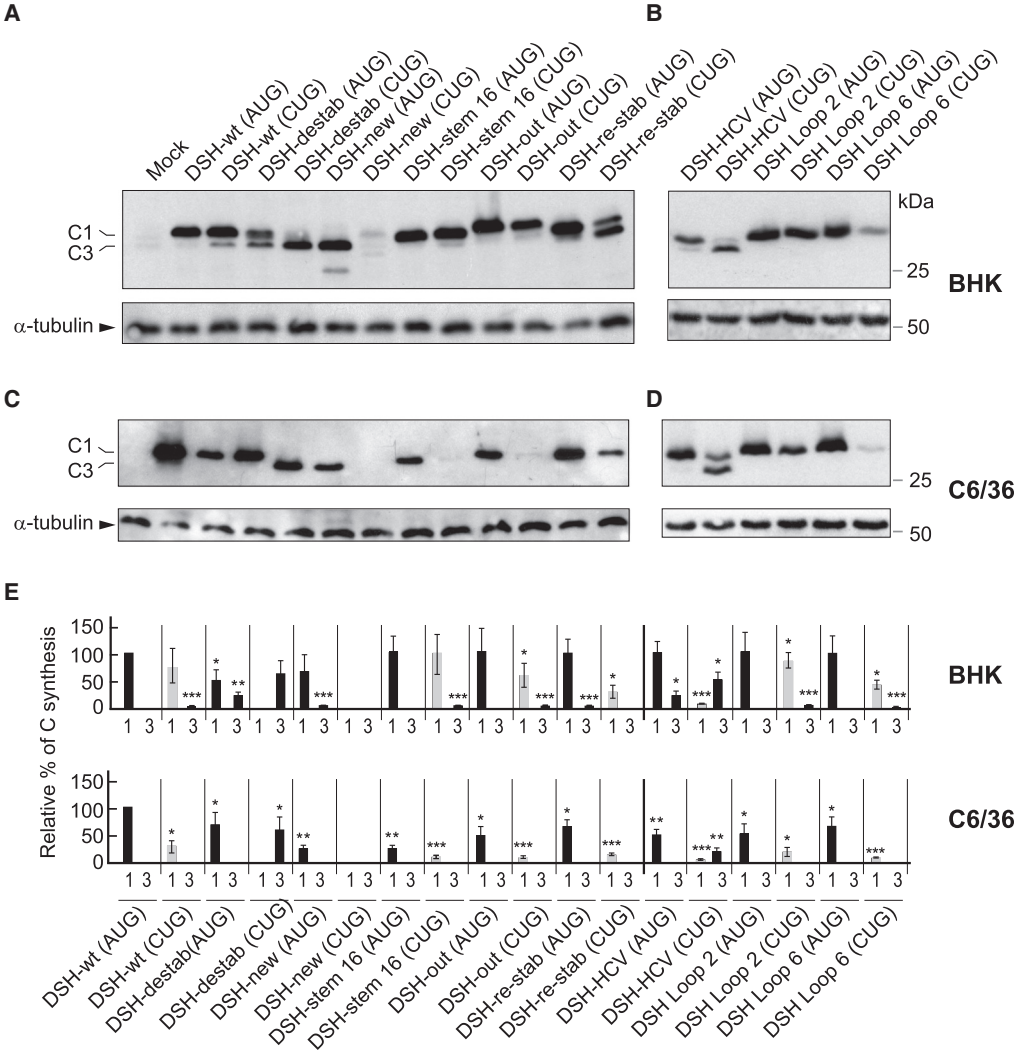

FIGURE 7. Participation of stem and loop regions of DSH in the initiation of translation. (*A*,*B*) BHK cells were transfected with the in vitro transcribed replicons indicated in the figure. After 7 h, cells were collected in loading buffer and extracted proteins were analyzed by western blotting with an anti-C antibody. The mobilities of the C products are indicated as C1 (initiation in the first AUG or in the same codon mutated to CUG) and C3 (initiation in the third AUG codon relative to the wt sequence). α-tubulin was analyzed as a loading control. (*C*,*D*) C6/36 cells were transfected with the in vitro transcribed replicons indicated in the figure. After 16 h, cells were collected in loading buffer and extracted proteins were analyzed by western blotting with an anti-C antibody. The mobilities of the C products are indicated as C1 (initiation in the first AUG or in the same codon mutated to CUG) and C3 (initiation in the third AUG codon relative to the wt sequence). α-tubulin was analyzed as a loading control. (*E*) Densitometric analysis of the C protein synthesized from the respective replicons. The graphs show the percentage values in relation to the amount of C synthesized by rep C + luc (AUG) in each cell line. The black bars correspond to translation initiation at AUG and gray at CUG. The results are displayed as mean ± SD of three representative experiments. Statistical significance in panel *E* was calculated compared to control using Student's *t*-test, (*) $P < 0.05$, (**) $P < 0.01$, (***) $P < 0.001$.

A sequence close to the DSH that has the ability to form another shorter hairpin was also mutated (DSH-out). In this variant, seven conservative mutations were introduced maintaining the amino acid sequence. This alteration modifies the secondary structure of the RNA after the DSH sequence generating even shorter hairpins (Fig. 6). The behavior of this variant was quite similar to that of the control with regard to the production of C and the signaling of the initiation codon, even when CUG was present (Fig. 7A, E). Moreover, in mosquito cells this variant was more effective than DSH-stem 16, perhaps due to the differences in the free energy of both variants (Fig. 7C,E). Using DSH-destab, we also designed a construct to restabilize the stem by mutating the corresponding bases to hybridize with the formerly mutated bases (DSH-re-stab). This variant shows a similar structure to DSH-wt by computer prediction, but exhibited a lower free energy and the mutations modified the composition of C protein in six amino acids (Fig. 6). Transfection of the replicon containing DSH-re-stab (AUG) recovered its ability to produce C protein similar to that of DSH-wt (AUG) in BHK cells (Fig. 7A,E). However, the DSH-re-stab (CUG) variant only partially recovered its activity to use CUG as the initiation codon, as the synthesis of authentic C was only 15% as compared with 80% using DSH-wt (CUG). Moreover, we observed high leaky scanning of the DSH-re-stab (CUG) variant since part of the C protein synthesized started at the third AUG codon, rendering a smaller product (C3). In C6/36 cells, DSH-re-stab (CUG) partially recovered its functioning to signal CUG as the initiation codon as compared with DSH-destab (CUG) (15% versus 0%) (Fig. 7C,E). Thus, restabilization of the DSH results in substantial synthesis of C protein from the CUG initiation codon, suggesting that the structure of the stem is important, but also that the sequence plays a part in the DSH activity. A similar conclusion could be drawn with the DSH-stem 16, in which substantial levels of C proteins were observed. However, the free energy of the hairpin seems also to be important for its correct functioning, since a more stable DSH is better than that with lower stability. Nevertheless, if the DSH is very stable, then insect ribosomes are hampered in their ability to melt the structure. Regarding the DSH-out variant, practically no influence in the synthesis of C protein was found, indicating that this sequence does not contribute to signal the start codon.

We recently reported that the DSH bears a resemblance to the domain II of the IRES sequence of hepatitis C virus (HCV) (Carrasco et al. 2018). Not only was the structural organization of DSH and HCV domain II similar, but the sequences of the loop of DSH and the apical loop of HCV domain II were almost the same: CUAGCCAUG in HCV and CUGCCAUG in SINV DSH. This observation prompted us to analyze whether there is functional convergence between the two structures and to what extent the DSH could be replaced by HCV domain II in SINV replicons. Our attention was also directed to know whether the IRES domain from HCV could be involved in the signaling of the start codon. It is well established that the mechanism of action of HCV domain II involves its interaction with the E and P ribosomal sites to replace the initiator Met-tRNA$_i^{Met}$ (Spahn et al. 2001; Lukavsky et al. 2003; Locker et al. 2007). Notably, domain II can even displace the ternary complex from preloaded ribosomes (Jaafar et al. 2016). Moreover, as occurs with SINV, the AUG initiation codon of HCV RNA can be replaced by other codons to initiate translation (Reynolds et al. 1995). The replacement of the DSH by domain II involves an increase in three amino acids of C protein. Also, the inserted sequence contains 25 different codons. To avoid a stop codon, a point mutation was made without affecting the base-pairing in the stem. The secondary structure of this DSH–HCV construct is shown in Figure 6. Production of C from DSH–HCV (AUG) in BHK cells reached 55% of control DSH-wt (AUG) levels, and only a small production of C3 (3%) was observed (Fig. 7B,E). A similar proportion was detected in C6/36 cells, but no leaky scanning was detected (Fig. 7D,E). The initiation on CUG in DSH–HCV (CUG) was very inefficient as compared with the control, with about 5% of initiation on CUG in BHK cells (Fig. 7B,E) and slightly more (7%) in insect cells (Fig. 7D,E). In addition, leaky scanning was evident in both cell lines (20% in BHK cells and 10% in C6/36 cells).

In the case of HCV, the sequence of the apical loop in domain II is important for IRES function (Kalliampakou et al. 2002). Thus, we next tested whether the sequence of the DSH loop from SINV was important for the functioning of this structure. Accordingly, two additional variants were made: one containing two point mutations in this loop (DSH-Loop2), and the other with 6 nt modified (DSH-Loop6) (Fig. 6). Both variants were tested with AUG or CUG as the initiation codon of C protein. The replicons DSH-Loop2 bearing AUG or CUG behaved similar to their controls in both cell lines (Fig. 7B,D,E). In contrast, initiation at CUG in DSH-Loop6 resulted in a very poor production of C, representing only 10% as compared with the control in BHK cells and even less (2%) in insect cells. This finding is paramount in understanding the functioning of DSH, since in this case the structure and the free energy of DSH were not modified, but it was unable to signal CUG as the initiation codon in both cell lines. Also, this finding is consistent with the potential functional convergence between domain II of HCV and SINV DSH, since the exact sequence in the loop plays an important part in their activity.

Construction of a SINV variant bearing CUG in place of AUG in sgRNA

We reasoned that since substantial levels of C protein are produced with the sgRNA variant bearing CUG, it might be possible to obtain a viable virus containing this initiation

codon for further analyses under infection conditions. Accordingly, the plasmid containing the genomic RNA clone was mutated at the AUG to CUG in the sgRNA sequence. Also, the third arginine of C was mutated to a valine to facilitate proteomic analysis. The transcribed genomic RNA (gRNA [CUG]) was transfected into BHK cells and the virus was collected after four passages. We initially confirmed the presence of CUG in this gRNA using RT-PCR and sequence analysis of the corresponding band, which indicated that the CUG was present in SINV-CUG. Once it was assured that the CUG remained in the virus after these passages, BHK cells were infected with wt SINV or the variant SINV-CUG. Cells were then radioactively labeled at different stages post-infection, and the proteins synthesized were analyzed by SDS-PAGE followed by autoradiography. Figure 8A shows that the kinetics of viral protein synthesis were similar between wt SINV and SINV-CUG, albeit in the latter case the level of the structural proteins synthesized was lower than in the control. Nevertheless, both viruses were able to interfere with cellular translation.

It was of interest to test whether the initiation of C protein was with leucine or with methionine in BHK cells infected with SINV-CUG. Cells were thus infected and extracted proteins were separated by SDS-PAGE at 7 h post-infection (hpi). As before, the band corresponding to C protein was excised from the gel and subjected to proteomic analysis. Notably, a variety of amino-terminal peptides were obtained, some of them starting with leucine, and others with methionine (Supplemental Table 1). This finding demonstrates that the initiation of sgRNA (CUG) can occur with leucine or methionine under the intracellular conditions generated in SINV infected cells. The finding that other peptides were also identified was striking. For instance, threonine was incorporated before leucine, indicating that the ACC codon located before CUG was recognized by the initiation complex. This ACC codon is in a good genomic context since there are purines at −6, −3, and +4 positions. Indeed, initiation of cellular mRNA translation with threonine has been recently reported (Na et al. 2018). Curiously, leaky scanning occurred in some instances, since phenylalanine, glycine or valine were also found at the amino terminus. Moreover, a peptide starting with asparagine was detected, suggesting that initiation can also occur at this AAU codon. Another possibility, however, is that these peptides are generated after the removal of the initial amino acids present at the amino terminus. In conclusion, the initiation event on sgRNA exhibits great plasticity for translation initiation on non-AUG codons in virus-infected cells.

Action of bruceantin on the translation of sgRNA

The inhibitor bruceantin has been previously used to selectively block the initiation of protein synthesis; specifically, it is thought that bruceantin at low concentrations blocks the initiation at the P ribosomal site, whereas at higher concentrations it can interfere with the elongation steps (Liao et al. 1976; Starck et al. 2008; Gürel et al. 2009). To test the action of bruceantin on the initiation of translation mediated by AUG or CUG, sgRNA was translated in RRL. As control mRNAs, we used SINV gRNA-luc, which is translated by a canonical mechanism (Carrasco et al. 2018), and an mRNA bearing the intergenic region (IGR) of Cricket paralysis virus (CrPV) followed by the luciferase gene: IGR CrPV-luc mRNA (see scheme in Fig. 8B). This latter messenger contains an IRES that initiates translation at the A site. We found that concentrations of bruceantin >10 nM inhibited protein synthesis directed by SINV gRNA-luc, whereas under the same conditions translation directed by IGR CrPV-luc mRNA was stimulated (Fig. 8C). Of note, translation of sgRNA C + luc (CUG) was also stimulated by bruceantin under the same conditions, whereas protein synthesis directed by sgRNA C + luc (AUG) was partially inhibited. These findings indicate that sgRNA C + luc (CUG) translation is not blocked by bruceantin, but rather stimulated. In this regard, the behavior of sgRNA C + luc (CUG) may be similar to that of IGR CrPV-luc mRNA, suggesting that it might start translation at the A site.

We also wished to analyze the action of bruceantin on viral protein synthesis in infected cells. Thus, BHK cells were infected with wt SINV or SINV-CUG and 7 h later the cultures were preincubated for 15 min with different concentrations of bruceantin. Subsequently, the cell cultures were radioactively labeled during 1 h in the presence of the inhibitor and extracted proteins were separated by SDS-PAGE. Results showed that in control BHK cells, bruceantin blocked cellular translation by 80% at 100 nM and >90% at higher concentrations (Fig. 8D,E). We noted that the sensitivity of protein synthesis to bruceantin in intact cells was lower than in cell-free systems, as higher concentrations were necessary to interfere with translation in intact cells. In cells infected with wt SINV, the inhibition of sgRNA translation was less affected than for cellular mRNAs after bruceantin treatment. Accordingly, an inhibition of only 30% was observed at 100 nM bruceantin, although higher concentrations (400 nM) resulted in a profound blockade of translation (Fig. 8D,E). sgRNA translation was even less affected in SINV-CUG-infected cells and 100 nM bruceantin inhibited viral protein synthesis by only 22%. It is likely that high concentrations of this inhibitor interfere with the elongation steps, as previously reported (Liao et al. 1976; Fresno et al. 1978). Therefore, bruceantin selectively inhibits the initiation steps only at low concentrations, such as those used in cell-free systems, whereas higher concentrations might block the ribosomal A-site and, consequently, the elongation phase of translation (Liao et al. 1976; Starck et al. 2008; Gürel et al. 2009).

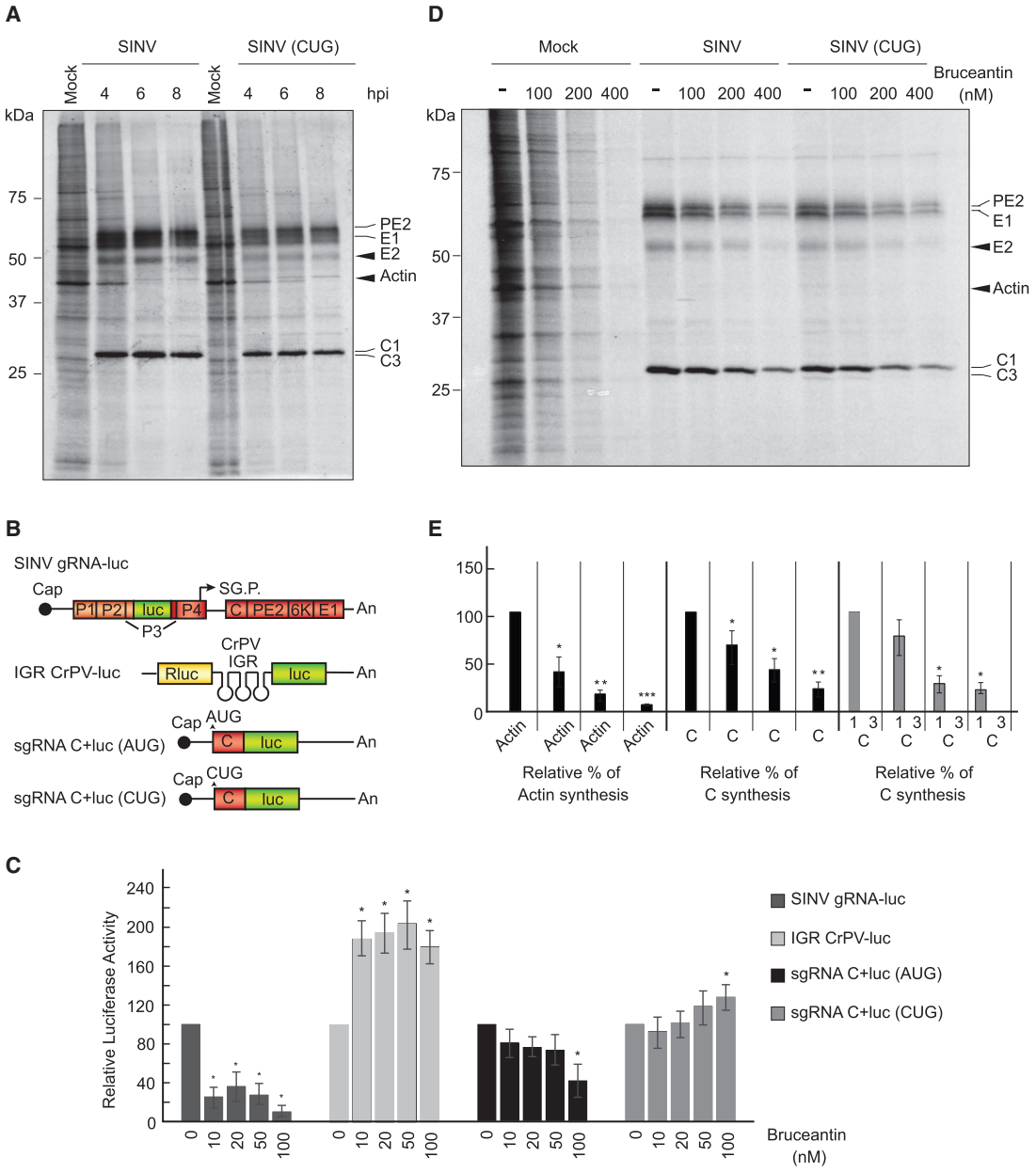

FIGURE 8. Bruceantin differentially affects cellular and viral protein synthesis. (*A*) BHK cells were mock infected or infected with 10 plaque-forming units/cell wt SINV or SINV (CUG). Then, the medium was changed to a labeling medium with [^{35}S] Met/Cys to detect the proteins synthesized during the next hour at the indicated times post-infection. Proteins were separated by SDS-PAGE and fixed and labeled proteins were visualized by autoradiography. Synthesized viral proteins C, PE2, E1 and E2 are indicated in the gel as well as cellular actin. (*B*) Schematic representation of the in vitro transcribed mRNAs: SINV gRNA-luc, IGR CrPV-luc, sgRNA C + luc (AUG), and sgRNA C + luc (CUG). (*C*) RRL were pretreated or not with the indicated concentrations of bruceantin for 20 min. Subsequently, 100 ng SINV gRNA-luc, IGR CrPV-luc, as controls, and sgRNA C + luc (AUG) and sgRNA C + luc (CUG) mRNAs were added and incubated for 90 min at 30°C. Luciferase synthesis was estimated by measuring luciferase activity. The values shown are percentages of the value of their respective nontreated counterparts and are the mean ± SD of three independent experiments. Statistical significance was calculated compared to each respective control using Student's *t*-test, and is shown as (*) $P < 0.05$. (*D*) BHK cells mock infected or infected with 10 plaque-forming units/cell wt SINV or SINV (CUG) were maintained in growth medium for 7 h. The medium was then changed to a labeling medium and cells were nontreated or treated with different amounts of bruceantin for 15 min before addition of [^{35}S] Met/Cys to detect the proteins synthesized during the next hour. Proteins were separated by SDS-PAGE and fixed and labeled proteins were visualized by autoradiography. The viral proteins C, PE2, E1, and E2 are indicated in the gel and also the cellular actin. (*E*) Densitometric analysis of protein synthesis. In mock-infected cells, the level of actin was used to determine the effect of bruceantin in treated versus untreated cells. In cells infected with wt SINV or SINV (CUG), protein C was used to determine the inhibitory effect of the compound by comparing the amounts present in treated cells versus their nontreated counterparts. The results are displayed as mean ± SD of three representative experiments.

Infection of wild-type and double knockout (*eIF2A*$^{-}$/*eIF2D*$^{-}$) HAP1 cells by SINV

It is generally considered that translation initiation on non-AUG codons can occur with the ternary complex of active eIF2 incorporating a methionine, whereas when leucine is at the amino terminus, this role is fulfilled by eIF2A, that could deliver leucyl-tRNA to the ribosome, for a review see (Kearse and Wilusz 2017). However, the exact functioning of eIF2A remains a mystery, since KO mice for *eIF2A* gene do not show any alteration (Golovko et al. 2016). In some viral RNAs such as HCV or SINV, the possibility that eIF2A or eIF2D are involved in the initiation event on AUG codons has been suggested (Ventoso et al. 2006; Dmitriev et al. 2010; Skabkin et al. 2010). However, using a human haploid cell line (HAP1) with a double knockout (KO) for *eIF2A* and *eIF2D* (*eIF2A*$^{-}$/*eIF2D*$^{-}$), we recently demonstrated that these factors were not required to initiate translation on HCV or SINV mRNAs (Sanz et al. 2017; Gonzalez-Almela et al. 2018). Nevertheless, it might still be possible that initiation on CUG in sgRNA could be mediated by eIF2A or eIF2D, as proposed for other cellular mRNAs (Starck et al. 2012, 2016). To address this, we analyzed SINV infection in wt HAP1 and HAP1-double KO cells. Results showed that the kinetics and the level of SINV protein synthesis were similar between the two cell lines infected with wt SINV or SINV-CUG (Supplemental Fig. 3A). Moreover, the shut-off of host translation was also extremely potent in both cell lines. This finding clearly indicates that eIF2A and eIF2D are not necessary to initiate translation on CUG in SINV-infected cells.

As it was possible that active eIF2 may participate in this initiation event when eIF2A and eIF2D are absent, as in double KO cell line, we treated cells with different concentrations of TG or Ars to inhibit the activity of eIF2. Both compounds potently blocked protein synthesis in the two cell lines examined (Supplemental Fig. 3B). Western blotting confirmed that TG and Ars induced the phosphorylation of eIF2α (Supplemental Fig. 3C). Finally, the action of 5 μM TG or 200 μM Ars, was assayed in both cell lines infected with wt SINV or SINV-CUG. As shown in Figure 9, TG or Ars treatment exhibited a similar action on protein synthesis in cells infected with these viruses. Consistent with the observation that sgRNA translation is resistant to the inactivation of eIF2 in infected

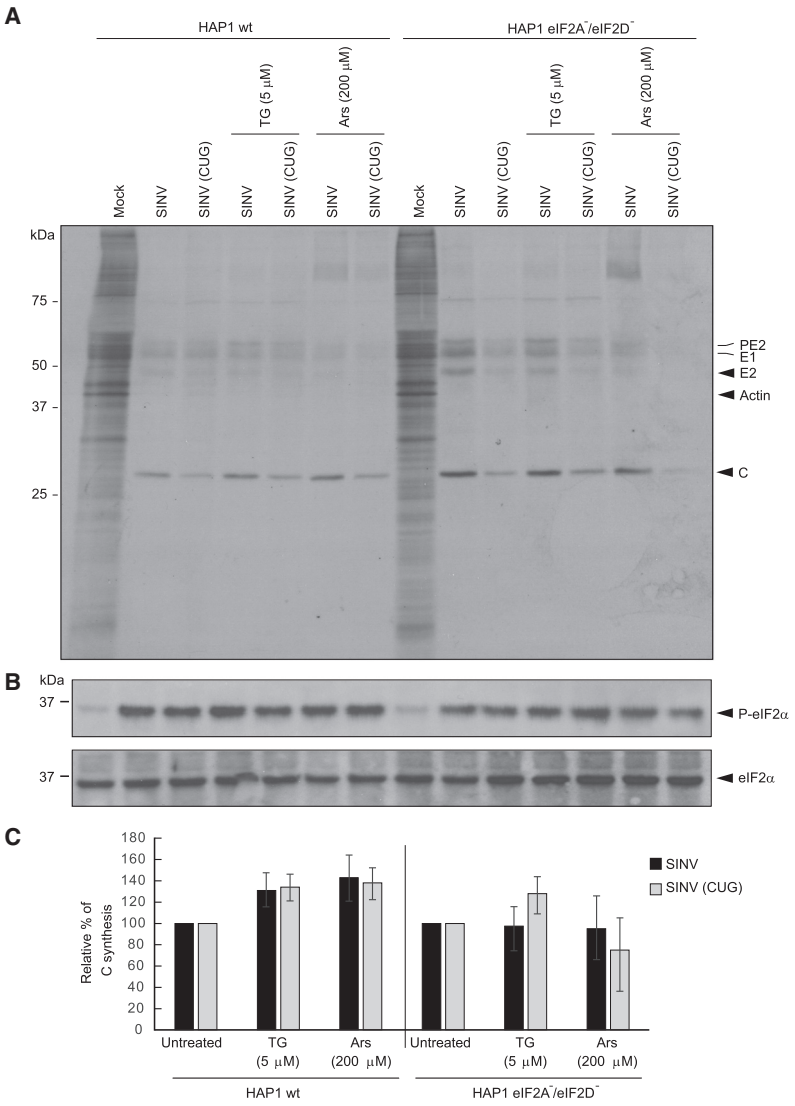

FIGURE 9. Infection of HAP1 wild-type (wt) and the double KO cell line HAP1 *eIF2A*$^{-}$/*eIF2D*$^{-}$ by wt SINV or SINV CUG. (*A*) HAP1 wt and HAP1 double KO cells were mock infected or infected with 10 plaque-forming units/cell wt SINV or SINV (CUG) for 1 h. Then, the infective medium was replaced by fresh growth medium. At 7 h post-transfection, cells were incubated in radioactive labeling medium with [^{35}S] Met/Cys and treated or not with thapsigargin (TG; 5 μM) or sodium arsenite (Ars; 200 μM) for 1 h. Then, cells were collected in loading buffer and analyzed by SDS-PAGE, fluorography and autoradiography. (*B*) In parallel, the state of phosphorylation of eIF2 was analyzed by western blotting with anti-P-eIF2α and anti-eIF2α antibodies. (*C*) Densitometric analysis of C synthesis is shown in the graphs as relative to their corresponding untreated samples. The results are displayed as mean ± SD of three representative experiments. The black bars correspond to translation initiation at AUG and gray at CUG.

cells, there was very little inhibition of viral protein synthesis in the human cell lines. Analysis of eIF2α phosphorylation in the infected cells, with or without TG or Ars treatment, showed that SINV infection resulted in increased phosphorylation of eIF2α, which was very clear after TG or Ars treatment, both in wt HAP1 and HAP1-double KO cells (Fig. 9B). These observations demonstrate that eIF2, eIF2A and eIF2D are not required to initiate translation of sgRNA using CUG as the initiation codon.

DISCUSSION

All living organisms, including viruses, need to synthesize the correct proteome in order to replicate and survive. Accordingly, the adequate selection of the initiation codon is very important for the synthesis of authentic proteins, since initiation at other sites would lead to aberrant polypeptides (Drummond and Wilke 2009; Rozov et al. 2016). Whereas the vast majority of both cellular and viral mRNAs initiate translation at AUG codons (Haimov et al. 2015; Kearse and Wilusz 2017), some can initiate their protein synthesis on codons other than AUG, particularly upstream ORFs (Starck et al. 2016; Kearse and Wilusz 2017). On these occasions, initiation can take place at codons such as CUG, GUG, AUU, among others (Peabody 1989; Van Damme et al. 2014). To what extent methionine is also incorporated at these non-AUG codons or whether the initiation of translation can take place with other amino acids remains contentious (Starck et al. 2012; Liang et al. 2017; Sellier et al. 2017; Na et al. 2018). In this regard, it has been shown that in mammalian cells leucine is incorporated as the first amino acid during translation of some mRNAs that contain CUG instead of AUG (Starck et al. 2012). However, few studies have analyzed the initiation with amino acids other than methionine in near-AUG codons, perhaps because the initiation in near-AUGs codons is little efficient (Liang et al. 2017). In this sense, the viral system we used allows to obtain relatively high amounts of protein C initiating in near-AUG codons, particularly in CUG, which facilitates this type of study. It is thought that in those cases where methionine incorporation is directed by non-AUG codons, the ternary complex Met-tRNA$_i^{Met}$-eIF2-GTP is misincorporated at the amino terminus at the ribosomal P site. In other instances, as occurs when the initiator is leucyl-tRNA^{leu}, it has been suggested that the monomeric protein eIF2A replaces the trimeric eIF2 (Starck et al. 2012, 2016). However, only partial inhibition of this initiation event was found after knockdown of eIF2A. Thus, the exact mechanism by which initiation takes place using non-AUG codons is still a matter of research. In this sense, the use of KO cell lines similar to the one used in the present work will be important to uncover the proteins involved in this process.

The best understood mechanism of initiation at non-AUG codons is on the second cistron of CrPV RNA. In this case, initiation is mediated by an IRES present in the IGR of CrPV in such a way that a pseudoknot structure in the region 3 of the IGR IRES interacts with the ribosomal A site and is then translocated to the P site (Johnson et al. 2017; Pisareva et al. 2018). The initiation codon used is GCU, which directs the incorporation of alanine at the amino terminus when the second cistron is translated. None of the eIFs participate in this initiation event and alanyl-tRNA is bound to the A ribosomal site mediated by translation elongation factor 1A (eEF1A) (Jan and Sarnow 2002; Fernandez et al. 2014). This aminoacyl-tRNA is then translocated to the P site mediated by eEF2 in a GTP-dependent process. We have previously advanced the idea that some similarities exist between the mechanism of initiation directed by IGR CrPV and the alphavirus sgRNA (Garcia-Moreno et al. 2015; Sanz et al. 2017; Carrasco et al. 2018).

SINV provides a unique model to study the initiation of translation on non-AUG codons and the mRNA requirements to accomplish this task. In principle, several possibilities might account for translation initiation on non-AUG codons. One is that methionine can be incorporated even when CUG was present. Alternatively, it is possible that leucine is the first amino acid at the amino terminus. Our present findings demonstrate that both possibilities can occur, although leucine is preferentially incorporated at the amino terminus. Therefore, methionyl-tRNA or leucyl-tRNA act as initiators on this CUG codon. However, we do not yet know which isoform of Met-tRNA participates in this process: the initiator, Met-tRNA$_i^{Met}$, or the isoform that participates during the elongation phase Met-tRNA$_e^{Met}$. Met-tRNA$_i^{Met}$ forms the ternary complex with eIF2 and GTP, whereas Met-tRNA$_e^{Met}$ interacts with eEF1A and GTP. Two models can thus be envisaged. Either leucyl-tRNA or methionyl-tRNA forms a ternary complex with eIF2, or they both interact with eEF1A. The fact that eIF2 is very selective for the initiator Met-tRNA$_i^{Met}$ and that this initiation factor forms ternary complexes with other aminoacyl-tRNAs very inefficiently (Kolitz and Lorsch 2010), does not support the participation of eIF2 in this process. Moreover, the demonstration that eIF2 becomes inactive after its phosphorylation in SINV-infected cells is also consistent with the idea that eIF2 is not involved in this initiation event. The replacement of eIF2 by other factors such as eIF2A or eIF2D can also be discarded, because the synthesis of SINV capsid protein can occur on double KO cell lines for these factors, even when AUG has been replaced by CUG. Yet another mechanism could involve the participation of a putative cellular factor that interacts with some aminoacyl-tRNAs and is able to bind them to ribosomes (Schleich et al. 2017; Hellen 2018). For instance, the heterodimer DENR-MCT-1 can interact with tRNA to recruit it to ribosomes during the reinitiation of translation (Schleich et al. 2014; Lomakin et al. 2017; Ahmed et al. 2018). There is still the possibility that low amounts of unphosphorylated eIF2 may participate in

sgRNA translation. Also, the presence of phosphatases in the foci where sgRNA translation takes place could provide small amounts of unphosphorylated eIF2. We believe that these speculations are unlikely because eIF2 and ribosomes do not colocalize in SINV-infected cells (Sanz et al. 2009). Moreover, even low amounts of phosphorylated eIF2 strongly decrease translation since GDP-GTP exchange is blocked (Donnelly et al. 2013). It could also be possible that eEF1A or another cellular protein with the ability to interact with aminoacyl-tRNA participates in this initiation event. In the case of the ternary complex aminoacyl-tRNA-eEF1A-GTP, it has to interact with the A site on the 80S ribosomes, since elongation factors have to bind to the GTPase center located at the major ribosomal subunit. We have previously suggested that this A site should be open if the P site is occupied by the DSH element (Garcia-Moreno et al. 2015; Carrasco et al. 2018). Our present findings are in good agreement with this idea since bruceantin had no effect on sgRNA C + luc (CUG) translation in RRL, and the blockade of viral translation by bruceantin was poorer than that for cellular protein synthesis in BHK cells infected with SINV-CUG. Interestingly, the DSH element can directly interact with the 18S rRNA (Toribio et al. 2016) and, in this manner, could promote the formation of the 80S ribosome on the initiation codon, as we have previously suggested (Fig. 10; Carrasco et al. 2018). In addition, DSH exhibits structural similarities to the domain II of the HCV IRES (Carrasco et al. 2018), and there are similarities between this domain and the CrPV IRES (Pisareva et al. 2018). Hence, it is likely that both DSH and the HCV domain II share functional properties. Also, consistent with this model is the finding that threonine or valine, among others, can be found at the amino terminus of C protein, indicating that other amino acids can also participate in the initiation event depending on the codon present at the A site.

The finding that CUG can replace the AUG initiation codon in SINV sgRNA and that this is dependent on the integrity of DSH opened the possibility to analyze the structural requirements of DSH in this process. Our present findings provide further insight into the structural requirements of DSH to participate in signaling the initiation codon. Overall, our observations lend support to the model in which DSH interacts with the 40S subunit, promoting the recruitment of the 60S to form the 80S ribosome (Fig. 10; Carrasco et al. 2018). For this interaction, the structure, but not the sequence of the stem region, seems to be important. However, the loop sequence is crucial because the mutation of the six nucleotides of this loop decreases the initiation on CUG codons, particularly in insect cells. Indeed, this DSH variant demonstrates that the functioning of DSH is not to stall the preinitiation complexes at the correct codon. According to Kozak's model, the optimal position for a hairpin to stall ribosomes at the initiation codon is at 14 nt (Kozak 1990, 1991). However, positioning DSH from 24 to 15 nt downstream from the AUG is highly detrimental for its activity (Frolov and Schlesinger 1996). DSH structure is very important for sgRNA translation (for review, see Carrasco et al. 2018). However, DSH structure can be modified to some extent maintaining its function, although it cannot be replaced by any hairpin, even if it has a similar free energy (Garcia-Moreno et al. 2015). Our current results lead to the following conclusions about the structure-activity relationship of DSH: (i) The structure of the stem is crucial, but not its sequence, (ii) the sequence of the loop plays an important part in the function of DSH, and (iii) the DSH can be replaced to some extent by domain II of the HCV IRES.

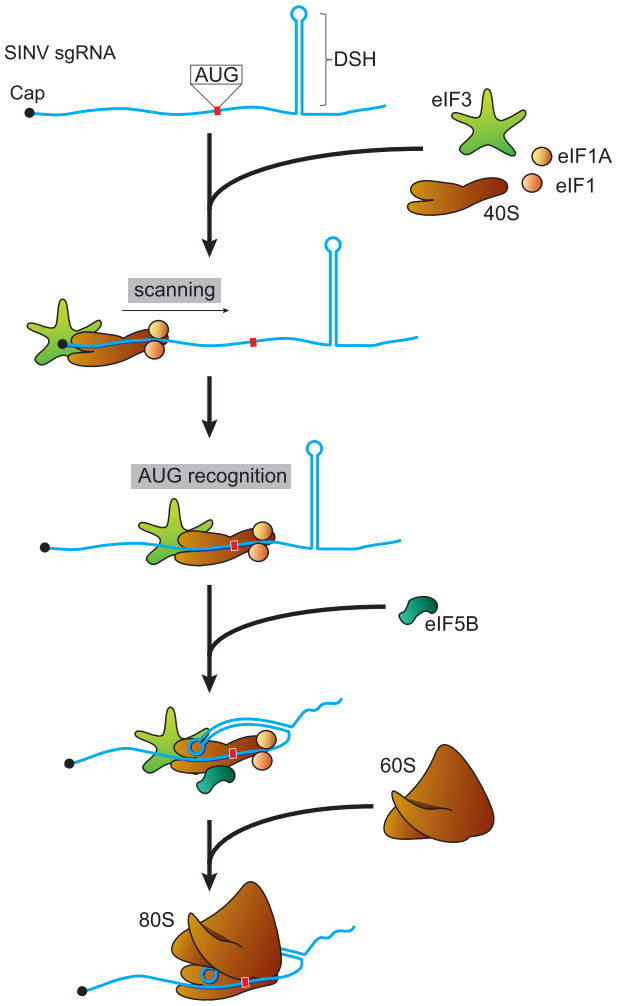

FIGURE 10. Schematic representation of the initiation events of SINV sgRNA. Initially, the 40S ribosomal subunit together with eIF1, eIF1A, and eIF3 interact with the cap structure at the 5′ end of sgRNA. Then, scanning of the leader sequence takes place until the AUG initiation codon is recognized. The DSH structure interacts with the 40S to stop scanning and to promote the binding of the 60S ribosomal subunit, after the dissociation of eIFs promoted by eIF5B. Once the 80S ribosome is formed, the elongation phase proceeds.

MATERIALS AND METHODS

Cell cultures and viruses

BHK-21 cells (ATCC: CCL-10) were cultured at 37°C in Dulbecco's modified Eagle's medium (DMEM) supplemented with 10% fetal calf serum (FCS) at 5% CO_2. Wild-type HAP1 human haploid cells and cells double knockout for eIF2A and eIF2D (cat# HZGHC005122c010) were purchased from Horizon Discovery Group plc. This line has a 16 bp deletion in exon 4 of the eIF2A gene and a 22 bp deletion in exon 3 of eIF2D gene. HAP1 cells were cultured in Iscove's modified Dulbecco's medium (Invitrogen) supplemented with 10% FCS at 5% CO_2. The *Aedes albopictus* cell line C6/36 (ATCC: CRL-1660) was grown at 28°C in M3 medium, containing 10% FCS and without CO_2. All media contained 100 µg/mL streptomycin and 100 IU/mL penicillin. Viral stocks were derived from the infective cDNA clones wt SINV, from pT7 SVwt (Sanz and Carrasco 2001), and the SINV CUG-variant, from the same plasmid but with the AUG initiation codon of C mutated to CUG. In vitro transcribed genomes were transfected into BHK cells and viruses were amplified in the same cell line.

Plasmids

Plasmids were used as DNA templates for in vitro RNA transcription with T7 or SP6 RNA polymerases. pToto1101/Luc (SINV gRNA-luc) was generously provided by Charles Rice (Rockefeller University) (Bick et al. 2003). Plasmid T7 Rluc ΔEMCV IGR-Fluc was used to obtain IGR CrPV luc mRNA (Wilson et al. 2000). The pTM1-Luc vector was constructed as described previously (Sanz et al. 2010). Cap.βGlobin-Luc transcripts were obtained by in vitro transcription using pKS-GL-FL as a template, as described previously (Castello et al. 2009)

pT7 SVwt (Sanz and Carrasco 2001) and pT7 rep C + luc (Sanz et al. 2007) were used as template plasmids to obtain variants of infective clones or replicons, respectively. The plasmids to produce sgRNAs derived from their respective replicons, which were modified to introduce the promotor sequence of T7 RNA polymerase directly upstream of the sgRNA sequences. To obtain each variant, we used four oligonucleotides: Two included HpaI or AatII restriction sites and two were designed specifically to introduce the mutations with complementary sequences. We carried out two PCR reactions using pT7SV wt or pT7 rep C + luc as template DNA and the oligonucleotides 5′HpaI and the 3′-specific oligonucleotide or 5′-specific oligonucleotide and 3′AatII. We then performed a second PCR with a mixture of these products as DNA template and the oligonucleotides with HpaI and AatII sites. The products of the second PCR were digested as appropriate and cloned into pT7 SV wt or pT7 rep C + luc. To introduce the CUG mutation into pT7 rep Lluc-luc (Sanz et al. 2010), we used the same protocol but used the oligonucleotide 3′SphI-luc in place of 3′AatII. To obtain the plasmids to produce sgRNAs, we used the oligonucleotides 5′SacI - T7prom and 3′AatII with the respective pT7 rep C + luc variant DNA templates. The PCR products are digested with SacI and AatII and cloned into pT7 rep C + luc. The sequence of C with all in frame AUG triplets mutated to CUG (or all but the first) was obtained by multiple PCR reactions using specific oligonucleotides. The sequences introduced into plasmids were then verified by sequencing. The list of oligonucleotides used is shown in Supplemental Table 1.

Antibodies

The following primary antibodies were used: rabbit polyclonal antibody against purified SINV C protein, generated in our laboratory; rabbit polyclonal anti-firefly luciferase (ab 21176, Abcam); goat polyclonal anti-TIA-1 (C-20) sc-1751 and rabbit polyclonal anti-eIF2α antibodies (Santa Cruz Biotechnology); mouse monoclonal anti-α-tubulin (T5168, Sigma-Aldrich); rabbit polyclonal anti-eIF2D antibody (Proteintech Group); rabbit polyclonal anti-eIF2A (Bethyl Laboratories Inc.); and rabbit polyclonal antibody anti-phospho-eIF2α (serine 51) (Cell Signaling Technology). Anti-rabbit or anti-mouse IgG secondary antibodies coupled to peroxidase (Amersham Biosciences) were used at a 1:5000 dilution.

In vitro transcription and transfection

Plasmids digested with XhoI were used as templates for in vitro RNA transcription with T7 or Sp6 RNA polymerases (New England Biolabs). With the exception of IGR CrPV luc, all in vitro produced RNAs were capped by adding the $m^7G(5')ppp(5')G$ cap analog to the transcription mixture. The transcription mixtures were treated with DNAse I and used directly for transfection. BHK or C6/36 subconfluent cells grown in 24-well plates were transfected (per well) with a mixture of 1 µg RNA and 2 µL Lipofectamine 2000 in 200 µL Opti-MEM I medium (both from Invitrogen). Experiments to analyze the translation of sgRNAs were performed in Opti-MEM I medium. For those experiments requiring a longer duration, the transfection medium was changed after 2 h to DMEM with 10% FCS for BHK cells or M3 with 10% FCS for C6/36 cells.

Immunofluorescence and confocal microscopy

Fixation, permeabilization, and confocal microscopy were performed as described previously (Madan et al. 2008) using an LSM 710 confocal laser scanning and multiphoton microscope coupled to an inverted microscope (Axio Observer). Primary antibodies were detected by secondary antibodies coupled to Alexa 488 or Alexa 555. Nuclei were stained with DAPI (4′-6-diamidino-2-phenylindole). All images were collected and analyzed using Zeiss ZEN 2010 software.

In vitro translation

A nuclease-treated rabbit reticulocyte lysate system (RRL, Promega) was used for in vitro translation. Reactions containing 100 ng of in vitro transcribed mRNAs were incubated for 90 min at 30°C. An in vitro translation assay in *Drosophila* embryo extracts was also carried out, as previously described (Gebauer et al. 1999). Reaction mixtures containing 1 µg of in vitro synthesized RNA, 40% embryo extract (a kind gift from Dr. F. Gebauer, Centre for Genomic Regulation, Barcelona, Spain), 0.1 mM spermidine, 60 µM amino acids, 16.8 mM creatine phosphate, 80 ng/µL creatine kinase, 24 mM HEPES pH 7.4, 1.4 mM

magnesium acetate, 100 mM potassium acetate and 100 ng/µL calf liver tRNA were incubated in a final volume of 50 µL at 25° C for 90 min. Protein synthesis was determined by measuring luciferase activity or by western blotting.

Luciferase activity measurement

BHK cells were lysed in a buffer containing 0.5% Triton X-100, 25 mM glycylglycine pH 7.8, 1 mM dithiothreitol and complete EDTA-free protease inhibitor cocktail (Roche Molecular Systems Inc.) at the concentration indicated by the supplier. Luciferase activity for cells and RRL assays was determined using the Luciferase Assay System (Promega) and a Sirius Luminometer (Titertek-Berthold).

As a control, cycloheximide was added to block translation, which allowed us to determine the luciferase synthesized in the absence of compounds during the first hour of transfection.

Analysis of protein synthesis by radioactive labeling

Protein synthesis was analyzed at the times indicated by replacing growth media with 0.2 mL DMEM without methionine-cysteine supplemented with 1 µL of EasyTag EXPRESS ^{35}S Protein Labeling mix, [^{35}S]Met-Cys (11 mCi mL^{-1}; PerkinElmer) per well of an L-24 plate. Cells were then collected in sample buffer, boiled for 5 min and analyzed by autoradiography on SDS-polyacrylamide gels. Protein synthesis was quantified by densitometry using a GS-800 calibrated imaging densitometer (Bio-Rad).

Western blotting

Cells were collected in sample buffer, boiled for 5 min and processed by SDS-PAGE. After electrophoresis, proteins were transferred to nitrocellulose membranes. Protein bands were visualized with the ECL detection system (Amersham). Quantification was made by densitometry, as above.

Mass spectrometry analysis of SINV capsid amino terminus

BHK cells (1 × 10^6) were transfected with 5 µg of in vitro synthesized replicons, rep C + luc (AUG), rep C + luc (CUG), or rep C + luc (GUG), all containing the R3 to V mutation in C, and 10 µL Lipofectamine 2000. After 8 h, cultures were collected and protein extracts were separated by SDS-PAGE and visualized by coomassie blue staining. Protein bands migrating at the molecular weight of C from each replicon were excised. A sample of cells infected with wt virus was used to determine C mobility. The same protocol was followed for the analysis of cells infected with SINV (CUG) at 10 plaque-forming units/cell and collected after 7 h.

In-gel digestion

After drying, gel bands were destained in acetonitrile:water (1:1), reduced and alkylated (disulfide bonds from cysteinyl residues were reduced with 10 mM DTT for 1 h at 56°C, and thiol groups were alkylated with 50 mM iodoacetamide for 1 h at room temperature in the dark), and then digested in situ with sequencing grade trypsin (Promega) as described previously (Perez et al. 2012). The gel pieces were dehydrated by removing all liquid using sufficient acetonitrile, which was then removed and the gel pieces dried in a speed vac. Gels were reswollen in 50 mM ammonium bicarbonate pH 8.8 with 12.5 ng/µL trypsin for 1 h in an ice-bath. The digestion buffer was then removed and gels were covered again with 50 mM ammonium bicarbonate and incubated at 37°C for 12 h. Digestion was stopped by the addition of 1% trifluoroacetic acid. Supernatants were dried down and then desalted onto ZipTip C18 Pipette tips (Millipore) for mass spectrometric analysis.

Reverse phase-liquid chromatography RP-LC–MS/MS analysis

The desalted protein digest was dried, resuspended in 10 µL of 0.1% formic acid and analyzed by RP-LC–MS/MS in an Easy-nLC II system coupled to an ion trap LTQ-Orbitrap-Velos-Pro hybrid mass spectrometer (Thermo Scientific). The peptides were concentrated (on-line) by reverse phase chromatography using a 0.1 mm × 20 mm C18 RP precolumn (Thermo Scientific), and then separated using a 0.075 mm × 250 mm C18 RP column (Thermo Scientific) operating at 0.3 µL/min. Peptides were eluted using a 100-min dual gradient from 5% to 25% solvent B in 68 min followed by gradient from 25% to 40% solvent B over 90 min (Solvent A: 0.1% formic acid in water, solvent B: 0.1% formic acid, 80% acetonitrile in water). ESI ionization was done using a stainless steel nano-bore emitter, ID 30 µm, interface (Proxeon Biosystems). The Orbitrap resolution was set at 30.000. Peptides were detected in survey scans from 400 to 1600 amu (1 µscan), followed by fifteen data-dependent MS/MS scans (Top 15), using an isolation width of 2 u (in mass-to-charge ratio units), normalized collision energy of 35%, and dynamic exclusion applied during 30 sec periods. Peptide identification from raw data was carried out using PEAKS Studio 8.5 software (Bioinformatics Solutions Inc.) (Han et al. 2004, 2011; Zhang et al. 2012). Database searching was performed against Local Data Base (SINV capsid sequence). The following constraints were used for the searches: tryptic cleavage after Arg and Lys, up to two missed cleavage sites, and tolerances of 20 ppm for precursor ions and 0.6 Da for MS/MS fragment ions, and the searches were performed allowing optional Met oxidation, amino-terminal acetylation and Cys carbamidomethylation. False discovery rates (FDRs) for peptide spectrum matches were limited to 0.01.

Secondary structure prediction

RNA optimal secondary structures were predicted using the RNAfold webServer: http://rna.tbi.univie.ac.at/cgi-bin/RNAfold.cgi.

Statistical analysis

Data analysis was performed using Excel (Microsoft). Data are shown as mean with standard error. Statistical validation was done using unpaired two tails Student's *t*-test with unequal variances. Statistical significance is shown as * $P < 0.05$, ** $P < 0.01$, *** $P < 0.001$.

SUPPLEMENTAL MATERIAL

Supplemental material is available for this article.

ACKNOWLEDGMENTS

This study was supported by a DGICYT (Dirección General de Investigación Científica y Técnica, Ministerio de Economía y Competitividad, Spain) grant (SAF2015-66170-R; MINECO/FEDER). E.G.A. has an FPU (Formación de Personal Universitario) Fellowship (Ministerio de Educación, Cultura y Deporte, FPU15/05709). We thank Dr. F. Gebauer (Universidad Pompeu Frabra, Barcelona, Spain) for kindly providing the *Drosophila melanogaster* extracts. The Institutional Grant awarded to the Centro de Biología Molecular "Severo Ochoa" (CSIC-UAM) by the Fundación Ramón Areces and Banco de Santander is acknowledged. The proteomic analysis (protein identification by LC-MS/MS) was carried out in the CBMSO protein chemistry facility, which is a member of ProteoRed, PRB3-ISCIII, supported by grant PT17/0019. Bruceantin was obtained from the NCI/DTP Open Chemical Repository http://dtp.nci.nih.gov; NSC165563.

Received September 12, 2018; accepted January 11, 2019.

REFERENCES

Ahmed YL, Schleich S, Bohlen J, Mandel N, Simon B, Sinning I, Teleman AA. 2018. DENR-MCTS1 heterodimerization and tRNA recruitment are required for translation reinitiation. *PLoS Biol* **16:** e2005160. doi:10.1371/journal.pbio.2005160

Bick MJ, Carroll JW, Gao G, Goff SP, Rice CM, MacDonald MR. 2003. Expression of the zinc-finger antiviral protein inhibits alphavirus replication. *J Virol* **77:** 11555–11562. doi:10.1128/JVI.77.21.11555-11562.2003

Carrasco L, Sanz MA, González-Almela E. 2018. The regulation of translation in alphavirus-infected cells. *Viruses* **10:** E70. doi:10.3390/v10020070

Castelló A, Sanz MÁ, Molina S, Carrasco L. 2006. Translation of Sindbis virus 26S mRNA does not require intact eukariotic initiation factor 4G. *J Mol Biol* **355:** 942–956. doi:10.1016/j.jmb.2005.11.024

Castelló A, Franco D, Moral-López P, Berlanga JJ, Álvarez E, Wimmer E, Carrasco L. 2009. HIV-1 protease inhibits Cap- and poly(A)-dependent translation upon eIF4GI and PABP cleavage. *PLoS One* **4:** e7997. doi:10.1371/journal.pone.0007997

Dmitriev SE, Terenin IM, Andreev DE, Ivanov PA, Dunaevsky JE, Merrick WC, Shatsky IN. 2010. GTP-independent tRNA delivery to the ribosomal P-site by a novel eukaryotic translation factor. *J Biol Chem* **285:** 26779–26787. doi:10.1074/jbc.M110.119693

Donnelly N, Gorman AM, Gupta S, Samali A. 2013. The eIF2α kinases: their structures and functions. *Cell Mol Life Sci* **70:** 3493–3511. doi:10.1007/s00018-012-1252-6

Drummond DA, Wilke CO. 2009. The evolutionary consequences of erroneous protein synthesis. *Nat Rev Genet* **10:** 715–724. doi:10.1038/nrg2662

Fernández IS, Bai XC, Murshudov G, Scheres SH, Ramakrishnan V. 2014. Initiation of translation by cricket paralysis virus IRES requires its translocation in the ribosome. *Cell* **157:** 823–831. doi:10.1016/j.cell.2014.04.015

Fresno M, Gonzales A, Vazquez D, Jiménez A. 1978. Bruceantin, a novel inhibitor of peptide bond formation. *Biochim Biophys Acta* **518:** 104–112. doi:10.1016/0005-2787(78)90120-X

Frolov I, Schlesinger S. 1996. Translation of Sindbis virus mRNA: analysis of sequences downstream of the initiating AUG codon that enhance translation. *J Virol* **70:** 1182–1190.

Garcia-Moreno M, Sanz MA, Pelletier J, Carrasco L. 2013. Requirements for eIF4A and eIF2 during translation of Sindbis virus subgenomic mRNA in vertebrate and invertebrate host cells. *Cell Microbiol* **15:** 823–840. doi:10.1111/cmi.12079

Garcia-Moreno M, Sanz MA, Carrasco L. 2015. Initiation codon selection is accomplished by a scanning mechanism without crucial initiation factors in Sindbis virus subgenomic mRNA. *RNA* **21:** 93–112. doi:10.1261/rna.047084.114

Garcia-Moreno M, Sanz MA, Carrasco L. 2016. A viral mRNA motif at the 3′-untranslated region that confers translatability in a cell-specific manner. Implications for virus evolution. *Sci Rep* **6:** 19217. doi:10.1038/srep19217

Gebauer F, Corona DF, Preiss T, Becker PB, Hentze MW. 1999. Translational control of dosage compensation in *Drosophila* by Sex-lethal: cooperative silencing via the 5′ and 3′ UTRs of msl-2 mRNA is independent of the poly(A) tail. *EMBO J* **18:** 6146–6154. doi:10.1093/emboj/18.21.6146

Golovko A, Kojukhov A, Guan BJ, Morpurgo B, Merrick WC, Mazumder B, Hatzoglou M, Komar AA. 2016. The eIF2A knockout mouse. *Cell Cycle* **15:** 3115–3120. doi:10.1080/15384101.2016.1237324

González-Almela E, Sanz MA, García-Moreno M, Northcote P, Pelletier J, Carrasco L. 2015. Differential action of pateamine A on translation of genomic and subgenomic mRNAs from Sindbis virus. *Virology* **484:** 41–50. doi:10.1016/j.virol.2015.05.002

González-Almela E, Williams H, Sanz MA, Carrasco L. 2018. The initiation factors eIF2, eIF2A, eIF2D, eIF4A, and eIF4G are not involved in translation driven by hepatitis C virus IRES in human cells. *Front Microbiol* **9:** 207. doi:10.3389/fmicb.2018.00207

Griffin D. 2013. Alphaviruses. In *Fields virology* (ed. Howley P, Knipe DM), pp. 2664. Lippincott Williams & Wilkins, Philadelphia.

Gürel G, Blaha G, Moore PB, Steitz TA. 2009. U2504 determines the species specificity of the A-site cleft antibiotics: the structures of tiamulin, homoharringtonine, and bruceantin bound to the ribosome. *J Mol Biol* **389:** 146–156. doi:10.1016/j.jmb.2009.04.005

Haimov O, Sinvani H, Dikstein R. 2015. Cap-dependent, scanning-free translation initiation mechanisms. *Biochim Biophys Acta* **1849:** 1313–1318. doi:10.1016/j.bbagrm.2015.09.006

Han Y, Ma B, Zhang K. 2004. SPIDER: software for protein identification from sequence tags with *de novo* sequencing error. *J Bioinform Comput Biol* **3:** 697–716. doi:10.1142/S0219720005001247

Han X, He L, Xin L, Shan B, Ma B. 2011. PeaksPTM: mass spectrometry-based identification of peptides with unspecified modifications. *J Proteome Res* **10:** 2930–2936. doi:10.1021/pr200153k

Hellen CUT. 2018. Translation termination and ribosome recycling in eukaryotes. *Cold Spring Harb Perspect Biol* **10:** a032656. doi:10.1101/cshperspect.a032656

Jaafar ZA, Oguro A, Nakamura Y, Kieft JS. 2016. Translation initiation by the hepatitis C virus IRES requires eIF1A and ribosomal complex remodeling. *Elife* **5:** e21198. doi:10.7554/eLife.21198

Jan E, Sarnow P. 2002. Factorless ribosome assembly on the internal ribosome entry site of cricket paralysis virus. *J Mol Biol* **324:** 889–902. doi:10.1016/S0022-2836(02)01099-9

Johnson AG, Grosely R, Petrov AN, Puglisi JD. 2017. Dynamics of IRES-mediated translation. *Philos Trans R Soc Lond B Biol Sci* **372:** 20160177. doi:10.1098/rstb.2016.0177

Kalliampakou KI, Psaridi-Linardaki L, Mavromara P. 2002. Mutational analysis of the apical region of domain II of the HCV IRES. *FEBS Lett* **511:** 79–84. doi:10.1016/S0014-5793(01)03300-2

Kearse MG, Wilusz JE. 2017. Non-AUG translation: a new start for protein synthesis in eukaryotes. *Genes Dev* **31:** 1717–1731. doi:10.1101/gad.305250.117

Kolitz SE, Lorsch JR. 2010. Eukaryotic initiator tRNA: finely tuned and ready for action. *FEBS Lett* **584:** 396–404. doi:10.1016/j.febslet.2009.11.047

Kozak M. 1990. Downstream secondary structure facilitates recognition of initiator codons by eukaryotic ribosomes. *Proc Natl Acad Sci* **87:** 8301–8305. doi:10.1073/pnas.87.21.8301

Kozak M. 1991. Structural features in eukaryotic mRNAs that modulate the initiation of translation. *J Biol Chem* **266:** 19867–19870.

Kumar V, Hasan GM, Hassan MI. 2017. Unraveling the role of RNA mediated toxicity of *C9orf72* repeats in C9-FTD/ALS. *Front Neurosci* **11**. doi:10.3389/fnins.2017.00711

Lee AS, Kranzusch PJ, Doudna JA, Cate JH. 2016. eIF3d is an mRNA cap-binding protein that is required for specialized translation initiation. *Nature* **536:** 96–99. doi:10.1038/nature18954

Lee KM, Chen CJ, Shih SR. 2017. Regulation mechanisms of viral IRES-driven translation. *Trends Microbiol* **25:** 546–561. doi:10.1016/j.tim.2017.01.010

Liang H, Chen X, Yin Q, Ruan D, Zhao X, Zhang C, McNutt MA, Yin Y. 2017. PTENβ is an alternatively translated isoform of PTEN that regulates rDNA transcription. *Nat Commun* **8:** 14771. doi:10.1038/ncomms14771

Liao LL, Kupchan SM, Horwitz SB. 1976. Mode of action of the antitumor compound bruceantin, an inhibitor of protein synthesis. *Mol Pharmacol* **12:** 167–176.

Locker N, Easton LE, Lukavsky PJ. 2007. HCV and CSFV IRES domain II mediate eIF2 release during 80S ribosome assembly. *EMBO J* **26:** 795–805. doi:10.1038/sj.emboj.7601549

Lomakin IB, Stolboushkina EA, Vaidya AT, Zhao C, Garber MB, Dmitriev SE, Steitz TA. 2017. Crystal structure of the human ribosome in complex with DENR-MCT-1. *Cell Rep* **20:** 521–528. doi:10.1016/j.celrep.2017.06.025

Lukavsky PJ, Kim I, Otto GA, Puglisi JD. 2003. Structure of HCV IRES domain II determined by NMR. *Nat Struct Biol* **10:** 1033–1038. doi:10.1038/nsb1004

Madan V, Castello A, Carrasco L. 2008. Viroporins from RNA viruses induce caspase-dependent apoptosis. *Cell Microbiol* **10:** 437–451.

Martinez-Salas E, Francisco-Velilla R, Fernandez-Chamorro J, Embarek AM. 2017. Insights into structural and mechanistic features of viral IRES elements. *Front Microbiol* **8:** 2629. doi:10.3389/fmicb.2017.02629

McInerney GM, Kedersha NL, Kaufman RJ, Anderson P, Liljeström P. 2005. Importance of eIF2α phosphorylation and stress granule assembly in alphavirus translation regulation. *Mol Biol Cell* **16:** 3753–3763. doi:10.1091/mbc.e05-02-0124

Na CH, Barbhuiya MA, Kim MS, Verbruggen S, Eacker SM, Pletnikova O, Troncoso JC, Halushka MK, Menschaert G, Overall CM, et al. 2018. Discovery of noncanonical translation initiation sites through mass spectrometric analysis of protein N termini. *Genome Res* **28:** 25–36. doi:10.1101/gr.226050.117

Peabody DS. 1989. Translation initiation at non-AUG triplets in mammalian cells. *J Biol Chem* **264:** 5031–5035.

Pérez M, García-Limones C, Zapico I, Marina A, Schmitz ML, Muñnoz E, Calzado MA. 2012. Mutual regulation between SIAH2 and DYRK2 controls hypoxic and genotoxic signaling pathways. *J Mol Cell Biol* **4:** 316–330. doi:10.1093/jmcb/mjs047

Pietilä MK, Albulescu IC, Hemert MJV, Ahola T. 2017a. Polyprotein processing as a determinant for in vitro activity of semliki forest virus replicase. *Viruses* **9:** E292. doi:10.3390/v9100292

Pietilä MK, Hellström K, Ahola T. 2017b. Alphavirus polymerase and RNA replication. *Virus Res* **234:** 44–57. doi:10.1016/j.virusres.2017.01.007

Pisareva VP, Pisarev AV, Fernández IS. 2018. Dual tRNA mimicry in the Cricket Paralysis Virus IRES uncovers an unexpected similarity with the Hepatitis C Virus IRES. *Elife* **7:** e34062. doi:10.7554/eLife.34062

Ramsey J, Mukhopadhyay S. 2017. Disentangling the frames, the state of research on the alphavirus 6K and TF proteins. *Viruses* **9:** E228. doi:10.3390/v9080228

Reynolds JE, Kaminski A, Kettinen HJ, Grace K, Clarke BE, Carroll AR, Rowlands DJ, Jackson RJ. 1995. Unique features of internal initiation of hepatitis C virus RNA translation. *EMBO J* **14:** 6010–6020. doi:10.1002/j.1460-2075.1995.tb00289.x

Rozov A, Demeshkina N, Westhof E, Yusupov M, Yusupova G. 2016. New structural insights into translational miscoding. *Trends Biochem Sci* **41:** 798–814. doi:10.1016/j.tibs.2016.06.001

Rupp JC, Sokoloski KJ, Gebhart NN, Hardy RW. 2015. Alphavirus RNA synthesis and non-structural protein functions. *J Gen Virol* **96:** 2483–2500. doi:10.1099/jgv.0.000249

Sanz MÁ, Carrasco L. 2001. Sindbis virus variant with a deletion in the 6K gene shows defects in glycoprotein processing and trafficking: lack of complementation by a wild-type 6K gene in trans. *J Virol* **75:** 7778–7784. doi:10.1128/JVI.75.16.7778-7784.2001

Sanz MÁ, Castello A, Carrasco L. 2007. Viral translation is coupled to transcription in Sindbis virus-infected cells. *J Virol* **81:** 7061–7068. doi:10.1128/JVI.02529-06

Sanz MÁ, Castelló A, Ventoso I, Berlanga JJ, Carrasco L. 2009. Dual mechanism for the translation of subgenomic mRNA from Sindbis virus in infected and uninfected cells. *PLoS One* **4:** e4772. doi:10.1371/journal.pone.0004772

Sanz MÁ, Welnowska E, Redondo N, Carrasco L. 2010. Translation driven by picornavirus IRES is hampered from Sindbis virus replicons: rescue by poliovirus 2A protease. *J Mol Biol* **402:** 101–117. doi:10.1016/j.jmb.2010.07.014

Sanz MÁ, González Almela E, Carrasco L. 2017. Translation of Sindbis subgenomic mRNA is independent of eIF2, eIF2A and eIF2D. *Sci Rep* **7:** 43876. doi:10.1038/srep43876

Schleich S, Strassburger K, Janiesch PC, Koledachkina T, Miller KK, Haneke K, Cheng YS, Küchler K, Stoecklin G, Duncan KE, et al. 2014. DENR-MCT-1 promotes translation re-initiation downstream of uORFs to control tissue growth. *Nature* **512:** 208–212. doi:10.1038/nature13401

Schleich S, Acevedo JM, Clemm von Hohenberg K, Teleman AA. 2017. Identification of transcripts with short stuORFs as targets for DENR*MCTS1-dependent translation in human cells. *Sci Rep* **7:** 3722. doi:10.1038/s41598-017-03949-6

Sellier C, Buijsen RAM, He F, Natla S, Jung L, Tropel P, Gaucherot A, Jacobs H, Meziane H, Vincent A, et al. 2017. Translation of expanded CGG repeats into FMRpolyG is pathogenic and may contribute to fragile X tremor ataxia syndrome. *Neuron* **93:** 331–347. doi:10.1016/j.neuron.2016.12.016

Skabkin MA, Skabkina OV, Dhote V, Komar AA, Hellen CU, Pestova TV. 2010. Activities of Ligatin and MCT-1/DENR in eukaryotic translation initiation and ribosomal recycling. *Genes Dev* **24:** 1787–1801. doi:10.1101/gad.1957510

Spahn CM, Kieft JS, Grassucci RA, Penczek PA, Zhou K, Doudna JA, Frank J. 2001. Hepatitis C virus IRES RNA-induced changes in the conformation of the 40s ribosomal subunit. *Science* **291:** 1959–1962. doi:10.1126/science.1058409

Starck SR, Ow Y, Jiang V, Tokuyama M, Rivera M, Qi X, Roberts RW, Shastri N. 2008. A distinct translation initiation mechanism generates cryptic peptides for immune surveillance. *PLoS One* **3:** e3460. doi:10.1371/journal.pone.0003460

Starck SR, Jiang V, Pavon-Eternod M, Prasad S, McCarthy B, Pan T, Shastri N. 2012. Leucine-tRNA initiates at CUG start codons for protein synthesis and presentation by MHC class I. *Science* **336:** 1719–1723. doi:10.1126/science.1220270

Starck SR, Tsai JC, Chen K, Shodiya M, Wang L, Yahiro K, Martins-Green M, Shastri N, Walter P. 2016. Translation from the 5′

untranslated region shapes the integrated stress response. *Science* **351:** aad3867. doi:10.1126/science.aad3867

Tabet R, Schaeffer L, Freyermuth F, Jambeau M, Workman M, Lee CZ, Lin CC, Jiang J, Jansen-West K, Abou-Hamdan H, et al. 2018. CUG initiation and frameshifting enable production of dipeptide repeat proteins from ALS/FTD C9ORF72 transcripts. *Nat Commun* **9:** 152. doi:10.1038/s41467-017-02643-5

Toribio R, Díaz-López I, Boskovic J, Ventoso I. 2016. An RNA trapping mechanism in Alphavirus mRNA promotes ribosome stalling and translation initiation. *Nucleic Acids Res* **44:** 4368–4380. doi:10.1093/nar/gkw172

Van Damme P, Gawron D, Van Criekinge W, Menschaert G. 2014. N-terminal proteomics and ribosome profiling provide a comprehensive view of the alternative translation initiation landscape in mice and men. *Mol Cell Proteomics* **13:** 1245–1261. doi:10.1074/mcp.M113.036442

Ventoso I. 2012. Adaptive changes in alphavirus mRNA translation allowed colonization of vertebrate hosts. *J Virol* **86:** 9484–9494. doi:10.1128/JVI.01114-12

Ventoso I, Sanz MA, Molina S, Berlanga JJ, Carrasco L, Esteban M. 2006. Translational resistance of late alphavirus mRNA to eIF2α phosphorylation: a strategy to overcome the antiviral effect of protein kinase PKR. *Genes Dev* **20:** 87–100. doi:10.1101/gad.357006

Wilson JE, Powell MJ, Hoover SE, Sarnow P. 2000. Naturally occurring dicistronic cricket paralysis virus RNA is regulated by two internal ribosome entry sites. *Mol Cell Biol* **20:** 4990–4999. doi:10.1128/MCB.20.14.4990-4999.2000

Zhang J, Xin L, Shan B, Chen W, Xie M, Yuen D, Zhang W, Zhang Z, Lajoie GA, Ma B. 2012. PEAKS DB: *de novo* sequencing assisted database search for sensitive and accurate peptide identification. *Mol Cell Proteomics* **11:** M111 010587. doi:10.1074/mcp.M111.010587

ARTÍCULO 4:

System-wide profiling of RNA-Binding Proteins uncovers key regulators of virus infection

Otro de los objetivos de esta tesis es determinar las proteínas que interaccionan con los mRNAs virales y celulares y que, por tanto, puedan estar implicadas en su ciclo replicativo, incluyendo la traducción. La identificación de estas proteínas es esencial para conocer en detalle el mecanismo de síntesis de proteínas virales y el proceso de inhibición de la expresión de mRNAs celulares. Los trabajos anteriores se enfocan en el estudio analítico de proteínas celulares específicas que previamente han sido sugeridas como factores potencialmente implicados en la traducción viral. Siguiendo otra aproximación, esta parte del proyecto de tesis pretende abordar el estudio exploratorio del total de proteínas, virales y celulares, que interaccionan con todos los mRNAs presentes en la célula durante la infección de SINV. Para llevar a cabo el aislamiento y clasificación de estas proteínas, se realizó una colaboración con el laboratorio del Dr. Alfredo Castelló (Universidad de Oxford), experto en la identificación de las proteínas que interaccionan con los mRNAs y autor el método de captura del interactoma (*RNA-interactome capture*, RIC) (Castello, Fischer et al. 2012). Esta colaboración comenzó con un periodo de tres meses de estancia en el laboratorio del Dr. Castelló durante el año 2015, y posteriormente siguió desarrollándose a distancia. En esta colaboración, se desarrolló y se empleó por primera vez la técnica de *comparative RNA-interactome capture* (cRIC) en células infectadas con SINV. Esta metodología permite analizar la respuesta del conjunto de proteínas de unión a RNA (*RNA-binding proteins*, RBPs) a cambios en las condiciones del ambiente celular, como los que ocurren durante la infección viral. Con esto, se pudo determinar la interacción diferencial de las RBPs con los RNAs tras la infección por SINV.

Durante mi estancia en Oxford realicé la captura del interactoma de células HEK293 infectadas con SINV, aplicando conjuntamente la técnica SILAC (*Stable Isotpe Labeling with Amino acids in Cell culture*). Esta última técnica está basada en detectar, mediante espectrometría de masas, cambios en la abundancia de proteínas entre distintas muestras que han sido marcadas con isotopos no radioactivos. Las células se cultivaron en medios que contenían aminoácidos marcados con diferentes isótopos estables para que fueran incorporados en las proteínas de nueva síntesis. Estas células se infectaron con SINV y se irradiaron con luz ultravioleta para unir covalentemente las proteínas al RNA. Posteriormente, las muestras obtenidas fueron procesadas

paralelamente por análisis transcriptómico y proteómico convencional. Después, se realizaron los análisis de proteómica cuantitativa, secuenciación del RNA y estadística.

En este trabajo se ha detectado un gran número de RBPs (247) cuya actividad de unión al RNA se ve alterada por la infección por SINV. Muchas de ellas carecen de dominios de unión al RNA clásicos. Asimismo, se ha determinado que estas alteraciones en su actividad están relacionadas con la degradación de RNAs celulares y el cambio en el patrón de distribución de numerosas proteínas celulares, que pueden encontrarse concentradas en lugares próximos a los centros de replicación viral. También se ha estudiado, mediante técnicas de silenciamiento génico, empleo de inhibidores y sobreexpresión de factores, el papel de algunas de estas RBPs en promover u obstaculizar la infección, obteniendo resultados muy interesantes para algunas RBPs, como la exonucleasa XRN1 o GEMIN5. La primera resultó ser vital para la progresión de la infección de SINV, ya que la línea KO para XRN1 resulta refractaria a la infección, mientras que GEMIN5 inhibe la traducción viral.

GARCIA-MORENO, M., NOERENBERG, M., NI, S., JARVELIN, A. I., **GONZALEZ-ALMELA, E.**, LENZ, C. E., BACH-PAGES, M., COX, V., AVOLIO, R., DAVIS, T., HESTER, S., SOHIER,T.J.M., LI,B., HEIKEL,G., MICHLEWSKI, G., SANZ, M.A., CARRASCO, L., RICCI, E.P., PELECHANO, V., DAVIS, I., FISCHER, B., MOHAMMED, S. AND CASTELLO, A. 2019. System-wide Profiling of RNA-Binding Proteins Uncovers Key Regulators of Virus Infection. *Mol Cell*, 74: 1–16

Resource

Molecular Cell

System-wide Profiling of RNA-Binding Proteins Uncovers Key Regulators of Virus Infection

Graphical Abstract

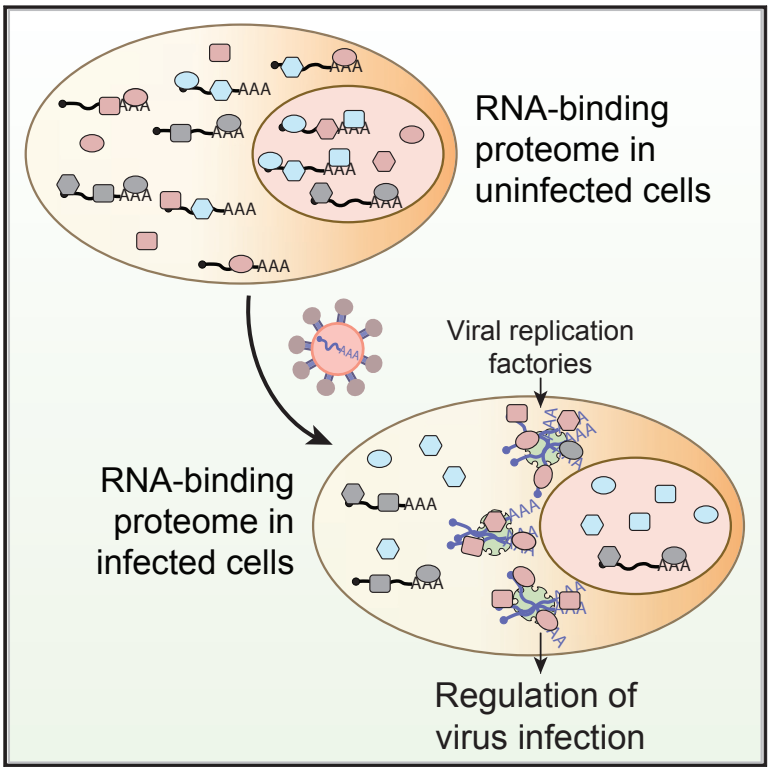

Highlights

- A quarter of the RBPome changes upon SINV infection
- Alterations in RBP activity are largely explained by changes in RNA availability
- Altered RBPs are crucial for viral infection efficacy
- GEMIN5 binds to the 5′ end of SINV RNAs and regulates viral gene expression

Authors

Manuel Garcia-Moreno, Marko Noerenberg, Shuai Ni, ..., Bernd Fischer, Shabaz Mohammed, Alfredo Castello

Correspondence

alfredo.castellopalomares@bioch.ox.ac.uk

In Brief

Garcia-Moreno, Noerenberg, Ni, and colleagues developed "comparative RNA-interactome capture" to analyze the RNA-bound proteome during virus infection. More than 200 cellular RNA-binding proteins change their binding activity in response to this challenge, mainly driven by transcript availability. Many of these RNA-binding proteins regulate viral replication and can be targeted to influence infection outcome.

Garcia-Moreno et al., 2019, Molecular Cell *74*, 1–16
April 4, 2019
https://doi.org/10.1016/j.molcel.2019.01.017

CellPress

Please cite this article in press as: Garcia-Moreno et al., System-wide Profiling of RNA-Binding Proteins Uncovers Key Regulators of Virus Infection, Molecular Cell (2019), https://doi.org/10.1016/j.molcel.2019.01.017

Molecular Cell
Resource

System-wide Profiling of RNA-Binding Proteins Uncovers Key Regulators of Virus Infection

Manuel Garcia-Moreno,[1,12] Marko Noerenberg,[1,12] Shuai Ni,[3,4,12] Aino I. Järvelin,[1] Esther González-Almela,[5] Caroline E. Lenz,[1] Marcel Bach-Pages,[1] Victoria Cox,[1] Rosario Avolio,[1,6] Thomas Davis,[1] Svenja Hester,[1] Thibault J.M. Sohier,[7] Bingnan Li,[8] Gregory Heikel,[9,10] Gracjan Michlewski,[9,10,11] Miguel A. Sanz,[5] Luis Carrasco,[5] Emiliano P. Ricci,[7] Vicent Pelechano,[8] Ilan Davis,[1] Bernd Fischer,[3,13] Shabaz Mohammed,[1,2] and Alfredo Castello[1,14,*]
[1]Department of Biochemistry, University of Oxford, OX1 3QU Oxford, UK
[2]Department of Chemistry, Chemistry Research Laboratory, University of Oxford, Mansfield Road, Oxford OX1 3TA, UK
[3]German Cancer Research Center (DKFZ), 69120 Heidelberg, Germany
[4]Faculty of Biosciences, Heidelberg University, Heidelberg, Germany
[5]Centro de Biologia Molecular "Severo Ochoa," Universidad Autonoma de Madrid, 28049 Madrid, Spain
[6]Department of Molecular Medicine and Medical Biotechnology, University of Naples Federico II, Naples, Italy
[7]Université de Lyon, ENSL, UCBL, CNRS, INSERM, LBMC, 46 Allée d'Italie, 69007 Lyon, France
[8]SciLifeLab, Department of Microbiology, Tumor, and Cell Biology, Karolinska Institutet, 17165 Solna, Sweden
[9]Wellcome Centre for Cell Biology, University of Edinburgh, Michael Swann Building, Edinburgh EH9 3BF, UK
[10]Division of Infection and Pathway Medicine, University of Edinburgh, The Chancellor's Building, 49 Little France Crescent, Edinburgh EH16 4SB, UK
[11]Zhejiang University-University of Edinburgh Institute, Zhejiang University, 718 East Haizhou Road, Haining, Zhejiang 314400, People's Republic of China
[12]These authors contributed equally
[13]Deceased
[14]Lead Contact
*Correspondence: alfredo.castellopalomares@bioch.ox.ac.uk
https://doi.org/10.1016/j.molcel.2019.01.017

SUMMARY

The compendium of RNA-binding proteins (RBPs) has been greatly expanded by the development of RNA-interactome capture (RIC). However, it remained unknown if the complement of RBPs changes in response to environmental perturbations and whether these rearrangements are important. To answer these questions, we developed "comparative RIC" and applied it to cells challenged with an RNA virus called sindbis (SINV). Over 200 RBPs display differential interaction with RNA upon SINV infection. These alterations are mainly driven by the loss of cellular mRNAs and the emergence of viral RNA. RBPs stimulated by the infection redistribute to viral replication factories and regulate the capacity of the virus to infect. For example, ablation of XRN1 causes cells to be refractory to SINV, while GEMIN5 moonlights as a regulator of SINV gene expression. In summary, RNA availability controls RBP localization and function in SINV-infected cells.

INTRODUCTION

RNA-binding proteins (RBPs) assemble with RNA forming ribonucleoproteins (RNPs) that dictate RNA fate (Glisovic et al., 2008). Historically, most of the known RBPs were characterized by the presence of well-established RNA-binding domains (RBDs), which include the RNA recognition motif, K-homology domain, and others (Lunde et al., 2007). However, stepwise identification of unconventional RBPs evoked the existence of a broader universe of protein-RNA interactions than previously anticipated (Castello et al., 2015). Recently, a system-wide approach termed RNA-interactome capture (RIC) has greatly expanded the compendium of RBPs (RBPome) (Hentze et al., 2018). RIC employs UV crosslinking, oligo(dT) capture under denaturing conditions, and quantitative proteomics to identify the complement of proteins interacting with polyadenylated (poly(A)) RNA in living cells (Baltz et al., 2012; Castello et al., 2012). RIC uncovered hundreds of unconventional RBPs, several of which are now known to play crucial roles in cell biology (Hentze et al., 2018). Recent work has suggested that cells can adapt to physiological cues through discrete alterations in the RBPome (Perez-Perri et al., 2018; Sysoev et al., 2016). However, it remains unknown to what extent the RBPome can be remodeled, how RBP responses are triggered, and what are the biological consequences of this plasticity. For example, RIC reported changes in the composition of the RBPome during fruit fly embryo development that could be explained by matching alterations in protein abundance (Sysoev et al., 2016). However, several RBPs did not follow this trend, displaying protein-level independent changes in RNA binding and raising the question of whether physiological perturbations can induce such responsive behavior more widely. To address this possibility, we developed a "comparative RIC" (cRIC) approach to profile with high accuracy RBP dynamics in cells infected with sindbis virus (SINV) (Figures 1A and 1B).

Viruses have been fundamental for the discovery and characterization of important steps of cellular RNA metabolism such as

Please cite this article in press as: Garcia-Moreno et al., System-wide Profiling of RNA-Binding Proteins Uncovers Key Regulators of Virus Infection, Molecular Cell (2019), https://doi.org/10.1016/j.molcel.2019.01.017

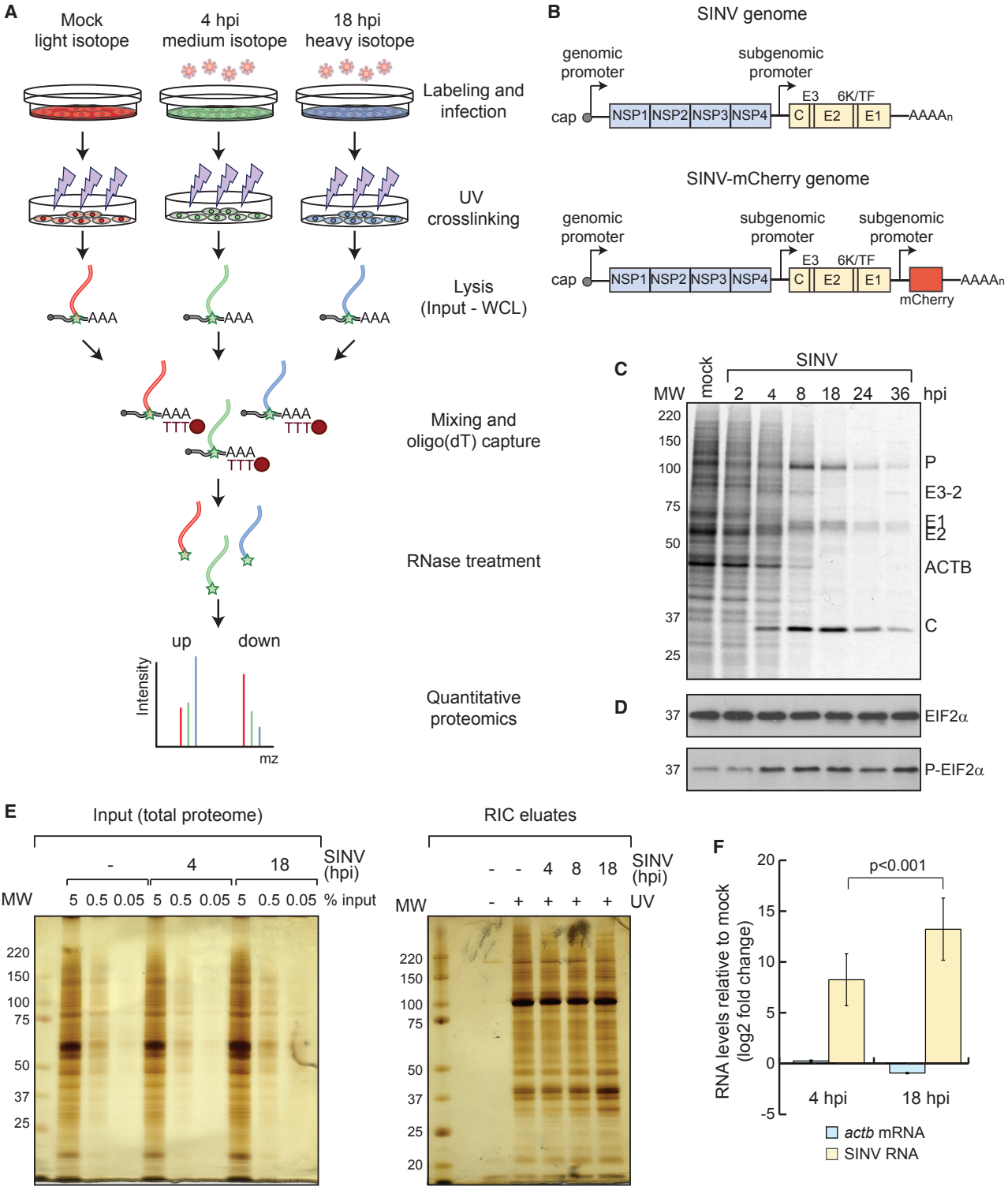

Figure 1. Application of RIC to HEK293 Cells Infected with SINV

(A) Schematic representation of cRIC.

(B) Schematic representation of SINV and chimeric SINV-mCherry genomes.

(C) Analysis of the proteins synthesized in uninfected and SINV-infected HEK293 cells by [^{35}S]-Met/Cys incorporation for 1 h followed by autoradiography.

(D) Analysis of total and phosphorylated eIF2α by western blotting.

(legend continued on next page)

RNA splicing, nuclear export, and translation initiation. This is due to their ability to hijack key cellular pathways by interfering with the activity of master regulatory proteins (Akusjarvi, 2008; Carrasco et al., 2018; Castelló et al., 2011; Garcia-Moreno et al., 2018; Lloyd, 2015). Furthermore, specialized RBPs are at the frontline of cellular antiviral defenses, detecting pathogen-associated molecular patterns (PAMPs) such as double-stranded RNA (dsRNA) or RNAs with 5′ triphosphate ends (Barbalat et al., 2011; Vladimer et al., 2014). Hence, virus infected cells represent an optimal scenario to assess the RBPome rearrangements.

Our data show that the complement of active cellular RBPs strongly changes in response to SINV infection, mainly due to deep variations in RNA availability. Importantly, "altered" RBPs are critical, as their perturbation affects viral fitness or/and the ability of the cell to counteract the infection. We envision that these RBPs represent novel targets for host-based antiviral therapies.

RESULTS AND DISCUSSION

Applying RIC to Cells Infected with SINV

To study the dynamics of cellular RBPs in response to physiological cues, we challenged cells with a cytoplasmic RNA virus and applied RIC. We chose SINV and HEK293 cells as viral and cellular models, respectively. SINV is a highly tractable virus that is transmitted from mosquito to vertebrates, causing high fever, arthralgia, malaise, and rash in humans. SINV replicates in the cytoplasm of the infected cell and produces three viral RNAs (Figures 1B and S1A): genomic RNA (gRNA), subgenomic RNA (sgRNA), and negative-stranded RNA. gRNA is packaged into the viral capsid and is translated to produce the nonstructural proteins (NSPs) that form the replication complex. The sgRNA is synthesized from an internal promoter and encodes the structural proteins (SPs), which are required to generate the viral particles. The negative strand serves as a template for replication. Both gRNA and sgRNA have cap and poly(A) tail.

HEK293 cells are an excellent cellular model to study SINV, as its infection exhibits all the expected molecular signatures, including (1) active viral replication (Figures 1C, S1B, and S1C), (2) host protein synthesis shutoff while viral proteins are massively produced (Figures 1C and S1B), (3) phosphorylation of the eukaryotic initiation factor 2 subunit alpha (EIF2α) (Figure 1D), and (4) formation of cytoplasmic foci enriched in viral RNA and proteins, commonly known as viral replication factories (Figures S1C and S1D). SINV infection causes a strong induction of the antiviral program, including β-interferon (β-IFN), which reflects the existence of active antiviral sensors and effectors (Figure S1E). Importantly, SINV achieves infection in a high proportion of cells (~85%) with relatively low number of viral particles (MOI) (Figure S1F), reducing cell-to-cell variability and biological noise.

Pilot RIC experiments in uninfected and SINV-infected cells revealed the isolation of a protein pool matching that previously observed for human RBPs (Castello et al., 2012), which strongly differed from the total proteome (Figure 1E). No proteins were detected in nonirradiated samples, demonstrating the UV dependency of RIC. Infection did not induce major alterations in the protein pattern observed by silver staining, which correspond to the most abundant housekeeping RBPs (Figure 1E). However, other less predominant bands displayed substantial differences, calling for in-depth proteomic analysis. Oligo(dT) capture led to the isolation of both host and SINV RNAs in infected cells (Figure 1F), which is expected as gRNA and sgRNA are polyadenylated.

SINV Infection Alters the Activity of Hundreds of RBPs

To allow accurate quantification of RBPs associated with poly(A) RNA under different physiological conditions, we developed a cRIC approach by combining the original protocol (Castello et al., 2013) with stable isotope labeling by amino acids in cell culture (SILAC) (Figure 1A). In brief, cells were grown in presence of light, medium, or heavy amino acids with incorporation efficiency >98%. Labeled cells were infected with SINV and irradiated with UV light at 4 and 18 h post-infection (hpi), using uninfected cells as a control (Figure 1A). These times correlate with key states in the SINV biological cycle; i.e., at 4 hpi, viral gene expression coexists with host protein synthesis, while the proteins synthesized at 18 hpi are almost exclusively viral (Figure 1C). SILAC labels were permutated among uninfected, 4 hpi, and 18 hpi in the three biological replicates to correct for possible isotope-dependent effects. After lysis, aliquots were stored for parallel transcriptomic and whole-proteome analyses. We combined equal amounts of the lysates from the three conditions prior to the oligo(dT) capture, and eluates were analyzed by quantitative proteomics (Figure 1A). Protein intensity ratios between condition pairs were computed, and the significance of each protein intensity change was estimated using a moderated t test (Figures 2A–2D, S2A, and S2B). We used a semiquantitative method for the cases in which an intensity value was missing ("zero") in one of the two conditions leading to "infinite" or zero ratios (Sysoev et al., 2016).

We identified a total of 794 proteins, 91% of which were already annotated by the Gene Ontology term "RNA-binding" or/and previously reported to be RBPs in eukaryotic cells by RIC (Hentze et al., 2018). Hence, the protein composition of our dataset largely resembles that of previously established RBPomes. Only 17 proteins displayed differential interaction with RNA at 4 hpi (Figures 2A, 2B, and S2A; Table S1). Fifteen of these were detected exclusively by the semiquantitative method due to the lack of intensity value in one condition, reflecting possible "on-off" and "off-on" states (Table S1). By contrast, 236 RBPs displayed altered RNA-binding activities at 18 hpi (Figures 2C, 2D, and S2B; Table S1). A total of 247 RBPs displayed

(E) Silver staining analysis of the "inputs" (i.e., total proteome, left) and eluates (i.e., RBPome, right) of a representative RIC experiment in SINV-infected cells.
(F) qRT-PCR analysis of the eluates of a representative RIC experiment using specific primers against SINV RNAs, *actb* and *gapdh* (for normalization) mRNAs. Error bars represent SE.
hpi, hours post-infection; MW, molecular weight.
See also Figure S1.

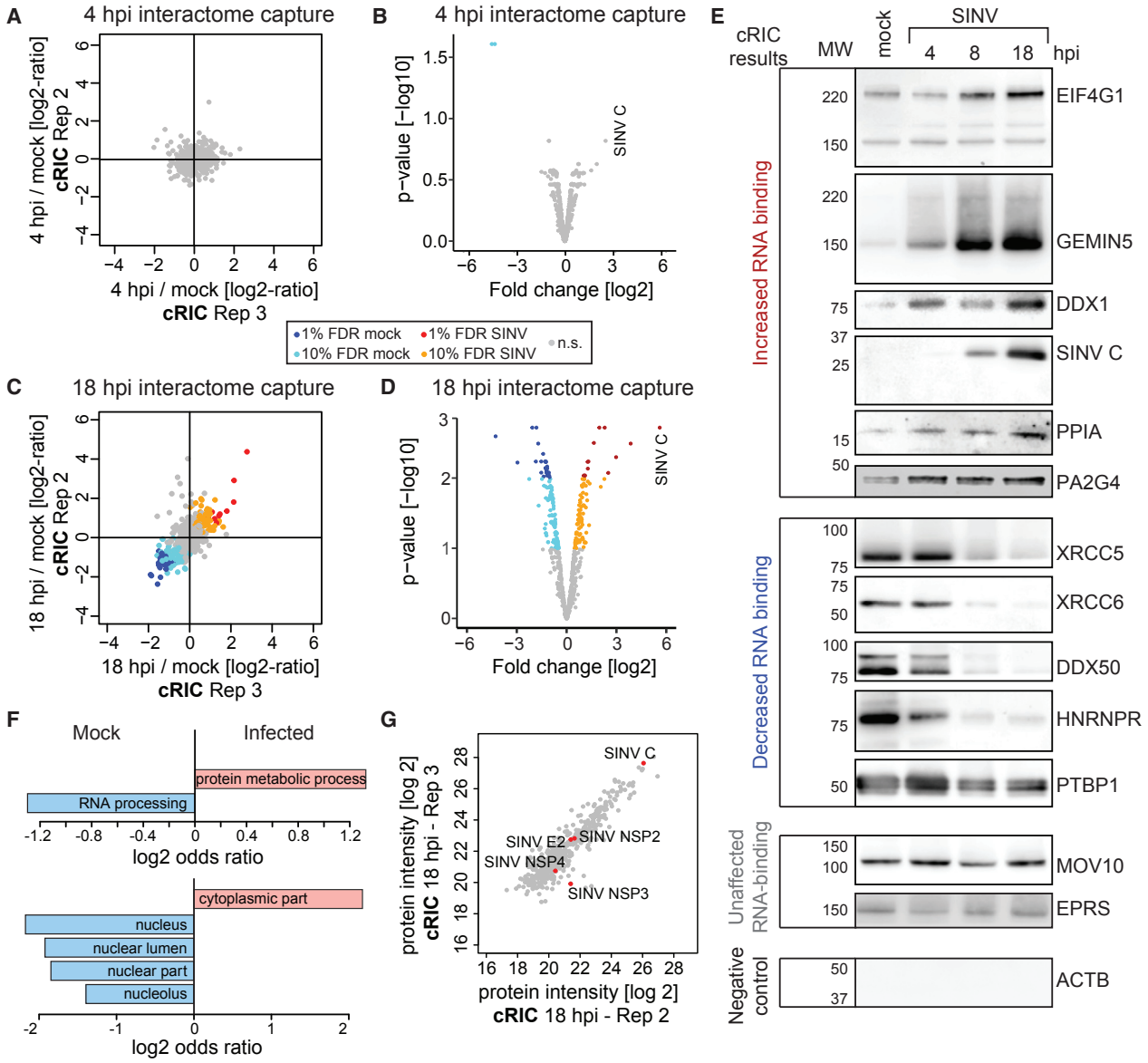

Figure 2. Analysis of the RNA-Bound Proteome in SINV-Infected HEK293 Cells by cRIC

(A) Scatterplot showing the intensity ratio between 4 hpi and uninfected conditions of each protein (dots) in the eluates of two biological replicates of cRIC.

(B) Volcano plot showing the log2 fold change and the significance (p value) of each protein between 4 hpi and uninfected conditions using data from three biological replicates.

(C) As in (A) but for 18 hpi.

(D) As in (B) but for 18 hpi.

(E) Western blotting analysis with specific antibodies of the eluates of a representative RIC experiment in SINV-infected HEK293 cells.

(F) Molecular function (top) and cellular component (bottom) Gene Ontology (GO) term enrichment analysis of the stimulated (salmon) against inhibited (blue) RBPs (18 hpi).

(G) Representative scatterplot comparing the raw intensity of each protein in the eluates of two cRIC replicates at 18 hpi.

FDR, false discovery rate; n.s., non-significant.

See also Figure S2 and Table S1.

differential binding in infected cells (4 and 18 hpi) and are referred to here as "altered RBPs." Interestingly, 181 of these lack classical RBDs, highlighting the importance of unconventional RBPs in virus infection.

To validate these results, we applied RIC to cells infected with SINV but, in this case, the eluates were analyzed by western blotting. We selected nine altered RBPs falling into three statistical categories; i.e., four with 1% false discovery rate (FDR), four

with 10% FDR, and one with nonsignificant changes. We included a positive control (the viral RBP SINV capsid [C]), two "non-altered" RBPs (MOV10 and EPRS), and a negative control (β-actin [ACTB]). Strikingly, the RNA-binding behavior of each protein fully matched the proteomic outcome, including those classified with 10% FDR (Figure 2E). Changes in RNA binding increased progressively throughout the infection. The proteomic data assigned a nonsignificant downregulation to HNRNPR (Table S1); however, the reduced activity of this protein was apparent by western blotting (Figure 2E), suggesting that our dataset may contain false negatives. Nonetheless, the excellent agreement between the proteomic and western blotting data supports the high quality of our results.

Determination of the RBP Networks Altered by SINV Infection

Among the 247 altered RBPs, 133 presented reduced and 114 increased association with RNA, and they are here referred to as "inhibited" and "stimulated" RBPs, respectively. Most of the inhibited RBPs were linked to nuclear processes such as RNA processing and export (Figures 2F and S2C). While cytoplasmic viruses are known to hamper nuclear RNA metabolism, the mechanisms by which this occurs remain poorly understood (Castelló et al., 2011; Gorchakov et al., 2005; Lloyd, 2015). Whether the inhibition of nuclear RBPs contributes to this phenomenon should be further investigated. Conversely, a large proportion of the stimulated RBPs are cytoplasmic and are linked to protein synthesis, 5′ to 3′ RNA degradation, RNA transport, protein metabolism, and antiviral response (Figures 2F and S2D).

Interestingly, several RBPs involved in translation were stimulated at 18 hpi despite the shutoff of host protein synthesis (Figure 1C), including 9 eukaryotic initiation factors, 3 elongation factors, and 12 ribosomal proteins. This enhancement is likely due to the high translational activity of SINV RNAs (Figure 1C) (Frolov and Schlesinger, 1996). The core components of the cap-binding complex EIF4A1 and EIF4E were not stimulated by the infection despite the activation of their protein partner, EIF4G1 (Table S1). In agreement, EIF4A1 and EIF4E do not participate in SINV sgRNA translation (Carrasco et al., 2018). A recent report showed that EIF3D is a cap-binding protein that controls the translation of specific mRNA pools (Lee et al., 2016). EIF3D is stimulated by SINV, and thus its potential contribution to SINV RNA translation deserves further consideration. Importantly, 88 altered RBPs associate with ribosomes in mouse cells (Table S2) (Simsek et al., 2017). The existence of "specialized ribosomes" has been proposed; however, experimental evidence is sparse (Au and Jan, 2014). Our results indicate that the composition of ribosomes and the scope of proteins associated with them may strongly differ between infected and uninfected cells, possibly resulting in differential translational properties.

cRIC uncovered 16 altered RNA helicases (Table S2), 13 of which were inhibited upon infection. RNA helicases are fundamental at virtually every stage of RNA metabolism (Chen and Shyu, 2014), and their inhibition is expected to have important consequences in RNA metabolism. Only 3 helicases were stimulated by SINV (DDX1, DHX57, and DHX29) (Figure 2E; Table S2). DHX29 enhances 48S complex formation on SINV sgRNA in reconstituted *in vitro* systems (Skabkin et al., 2010), and its stimulation supports its regulatory role in infected cells.

Notably, a defined subset of antiviral RBPs is stimulated upon SINV infection, including IFI16, IFIT5, TRIM25, TRIM56, and ZC3HAV1 (ZAP) (Table S1). IFI16 was previously described to bind dsDNA in cells infected with DNA viruses (Ni et al., 2016). Our data reveal that IFI16 also binds RNA, and it is activated early after SINV infection (4 hpi). This agrees with the recently described ability of IFI16 to restrict RNA virus infection (Thompson et al., 2014). These findings highlight the capacity of cRIC to identify antiviral factors responding virus infection.

Interestingly, cRIC also identified viral RBPs associated with poly(A) RNA, including the known viral RBPs (i.e., RNA helicase NSP2, the RNA polymerase NSP4, and capsid) and, unexpectedly, also NSP3 and E2 (Figures 2G and S2E). NSP3 was only quantified in two replicates (Figure S2E), and thus its interaction with RNA requires experimental confirmation. The identification of E2 in cRIC eluates was unexpected. In the viral particle of the related VEEV, E2 interacts with the capsid protein nearby cavities that communicate with the inner part of the virion where the gRNA density resides (Zhang et al., 2011), potentially enabling transitory or stochastic interactions with viral RNA.

RBP Responses to SINV Are Not Caused by Changes in Protein Abundance

Changes detected by cRIC can be a consequence of matching alterations in protein abundance (Sysoev et al., 2016). To assess this possibility globally, we analyzed the total proteome by quantitative proteomics (cRIC inputs; Figure 1A). Importantly, SINV infection did not cause noticeable changes in host RBP levels, including 129 RBPs with altered RNA-binding activity (Figures 3A–3C and S3A–S3C; Table S3). In agreement, silver and Coomassie staining did not show noticeable protein fluctuations except for the viral capsid (Figure 1E and 3D). The lack of changes in protein levels, even for altered RBPs, was confirmed by western blotting (Figure 3E; Table S3). It is not wholly unexpected that RBPs are unaffected in spite of the shutoff of cellular protein synthesis. Analogous to siRNA experiments, detectable decreases in protein abundance may require hours or even days after translational suppression, especially for relatively stable proteins.

The Transcriptome Undergoes Pervasive Changes in SINV-Infected Cells

Mechanistically, the activity of host RBPs can also be dictated by changes in the availability of their target RNAs. To test this possibility, we analyzed by RNA sequencing (RNA-seq) the total RNA isolated from cRIC input samples (Figure 1A). 4 h of SINV infection had a relatively minor impact on the host transcriptome (Figure 3F). By contrast, deep changes were observed at 18 hpi, with 12,372 differentially expressed RNAs ($p < 0.1$; Figures 3G and S3E–S3G). Only 1,448 RNAs were upregulated, and these were enriched in the Gene Ontology (GO) term "antiviral response." By contrast, 10,924 RNAs were downregulated, including many housekeeping genes (Table S4).

To validate these results by an orthogonal approach, we used qRT-PCR focusing on 20 mRNAs randomly chosen across the whole variation range. Importantly, data obtained

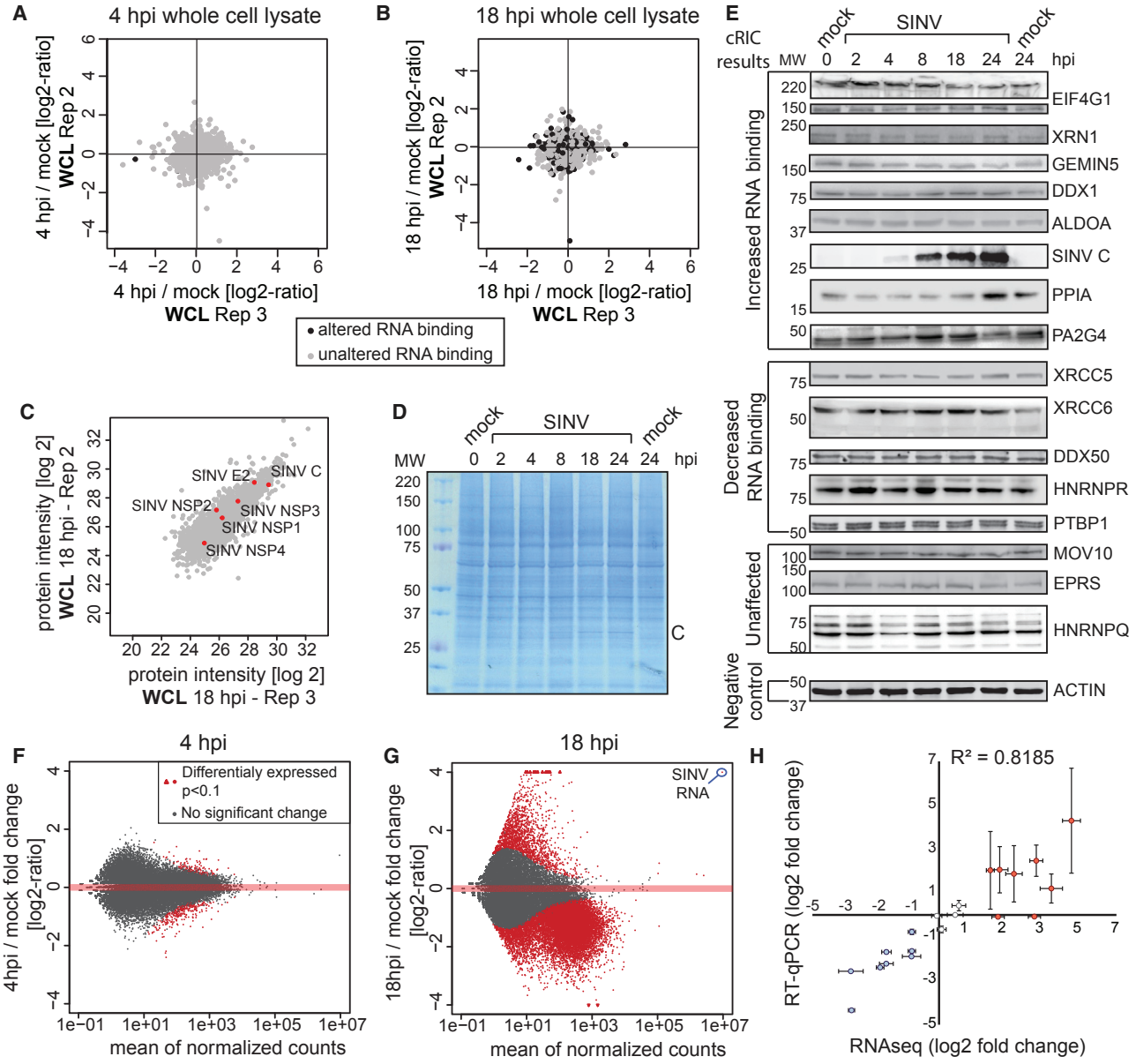

Figure 3. Proteomic and Transcriptomic Analyses of Whole SINV-Infected Cell Lysates

(A) Scatterplot comparing the intensity ratio between 4 hpi and uninfected conditions of each protein (dots) in the inputs (total proteome) of two biological replicates of cRIC. Black dots represent proteins significantly enriched in either 4 hpi or uninfected conditions in Figure 2A.

(B) As in (A) but for 18 hpi.

(C) Scatterplot comparing the intensity of each protein in the inputs of two cRIC replicates at 18 hpi.

(D) Representative Coomassie blue staining of cells infected with SINV.

(E) Western blotting analysis of lysates of cells infected with SINV (see Table S3 for quantification).

(F) MA plot comparing the read coverage and the log2 fold change between 4 hpi and uninfected cells of each gene detected in the RNA sequencing (RNA-seq) experiment. Red dots represent RNAs enriched with $p < 0.1$.

(G) As in (F) but for 18 hpi.

(H) Correlation of the RNA-seq and RT-qPCR data by plotting the log2 fold change for randomly selected transcripts by the two methods. Error bars represent SE of three independent experiments.

See also Figure S3 and Tables S3 and S4.

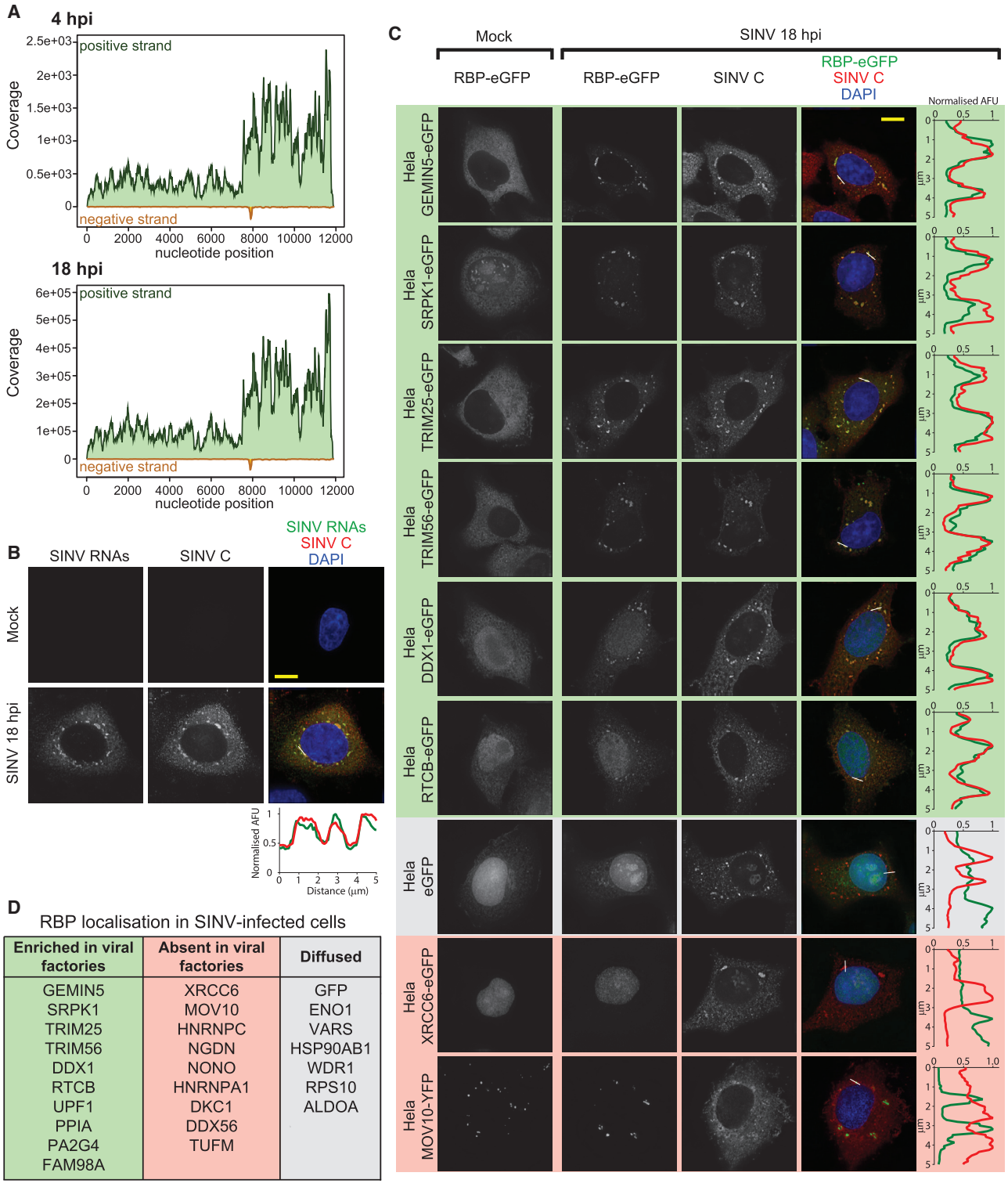

D

RBP localisation in SINV-infected cells

Enriched in viral factories	Absent in viral factories	Diffused
GEMIN5	XRCC6	GFP
SRPK1	MOV10	ENO1
TRIM25	HNRNPC	VARS
TRIM56	NGDN	HSP90AB1
DDX1	NONO	WDR1
RTCB	HNRNPA1	RPS10
UPF1	DKC1	ALDOA
PPIA	DDX56	
PA2G4	TUFM	
FAM98A		

Figure 4. Host RBP Localization in SINV-Infected Cells

(A) RNA-seq read coverage of the positive and negative RNA strand of SINV. Note that the y axes in both plots have different scales.

(B) Localization analysis of SINV RNA and capsid protein in infected HeLa cells at 18 hpi by combined *in situ* hybridization and immunofluorescence.

(legend continued on next page)

with both techniques strongly correlated (R^2 = 0.82) (Figure 3H), confirming the RNA-seq results. The decreased availability of cellular RNA could explain why 133 RBPs display reduced association with poly(A) RNA in infected cells (Table S1). In addition, inhibited RBPs could exchange poly(A) mRNA for non-poly(A) RNAs, which are not captured by the oligo(dT) beads.

Stimulated RBPs Are Relocated to the Viral Replication Factories

SINV produces two overlapping mRNAs, gRNA and sgRNA (Figures 1B and S1A), and, consequently, the read coverage was substantially higher in the last third of the gRNA, where both transcripts overlap (Figure 4A). Both sgRNA and gRNA have poly(A) and thus should contribute to the cRIC results (Figures 4A and S4A). Conversely, the negative strand has low abundance and lacks a poly(A) tail. Importantly, SINV RNAs become the most abundant RNA species, after rRNA, at 18 hpi (Figures 3G and S3G). The emergence of such abundant RNA substrates likely induces cellular RBPs to exchange the "declining" cellular mRNAs for "emerging" viral RNAs, driving the remodeling of the RBPome. Alternatively, "dormant" RBPs could be "awakened" by the recognition of signatures within the viral RNA, analogous to known antiviral RBPs (Vladimer et al., 2014). We thus hypothesized that RBPs displaying enhanced binding should co-localize with viral RNA.

SINV RNA and capsid accumulate in cytoplasmic foci that correspond to the viral factories (Figures S1D, 4B, and S4A). To test whether stimulated RBPs relocate to these foci, we generated 26 tetracycline-inducible cell lines expressing host RBPs fused to EGFP. These included 16 lines expressing stimulated RBPs and 8 expressing inhibited RBPs. The non-altered RBP, MOV10, and unfused EGFP were used as controls. Strikingly, 9 out of the 16 stimulated RBPs (56%) accumulated at viral factories demarcated by SINV C (Figures 4C, 4D, and S4B). Five additional stimulated RBPs (29%) showed diffuse localization in cytoplasm but were also present at the capsid-containing foci (Figure S4B). *In situ* hybridization analysis confirmed that SINV RNA co-localized with a representative stimulated RBP, GEMIN5, supporting the potential interplay between stimulated RBPs and viral RNA (Figure S4C). Among the stimulated RBPs, only NGDN, HNRNPA1 and the mitochondrial translation elongation factor TUFM (3 out of 16; 17%) were absent in the viral factories, which suggests that their function is restricted to host RNAs. HNRNPA1 was shown to bind SINV RNA (LaPointe et al., 2018; Lin et al., 2009), while in our analysis, it strictly displays nuclear localization (Figure S4B). We cannot rule out that a small pool of HNRNPA1 is present in the viral factories at undetectable levels or, alternatively, that the EGFP tag is affecting HNRNPA1 localization.

In contrast to stimulated RBPs, only one (out of 8; 12.5%) inhibited RBP was enriched in the viral factories (Figures 4D and S4B). This protein, called UPF1, is a helicase involved in the nonsense-mediated decay pathway and is known to inhibit infection of alphaviruses (Balistreri et al., 2014). Conversely, 5 out of 8 (62.5%) virus-inhibited RBPs are nuclear and remained nuclear after infection (Figures 4C, 4D, and S4B). These results indicate that, with exceptions, inhibited RBPs do not redistribute to the viral factories.

The Exonuclease XRN1 Is Essential for SINV Infection

The loss of cellular mRNAs is likely contributing to the remodeling of the RBPome by diminishing substrate availability. However, it is unclear how this phenomenon is triggered and whether it benefits or hampers viral infection. Changes in RNA levels can globally be a consequence of reduced transcription and/or increased RNA degradation. To explore which of these pathways contribute the most to RNA loss in SINV-infected cells, we compared the fold change of each mRNA in our dataset to the rate of synthesis, processing, and degradation of each individual transcript (Mukherjee et al., 2017). Transcription could explain most of the differences at 4 hpi, whereas RNA degradation accounted for more than 50% of the explained variance at 18 hpi (Figures 5A and S5A). We reasoned that this phenomenon can be a combined effect of the activation of the 5′ to 3′ RNA degradation machinery, as the exonuclease XRN1 and its interactor, PATL1, are stimulated at 18 hpi (Table S1), and a reduced transcriptional activity (Gorchakov et al., 2005).

XRN1 is broadly considered as an antiviral factor that erases viral RNA (Molleston and Cherry, 2017). RNA pseudoknots present in several viral RNAs are able to stall XRN1, leading to the production of sgRNAs (Chapman et al., 2014; Pijlman et al., 2008). In dengue virus (DENV), XRN1-derived sgRNAs can benefit infection by interfering with the antiviral response (Manokaran et al., 2015).

In SINV-infected cells, XRN1 and MOV10 foci (corresponding to P-bodies) are juxtaposed to the viral replication factories, suggesting that the exonuclease could attack viral RNA (Figures 4C, S4C, and 5B). To our surprise, XRN1 knockout (KO) cells were refractory to SINV infection, while partial KO led to an intermediate phenotype (Figure 5C). These results suggest that XRN1 activity is instead essential for SINV infection. XRN1 KO cells did not exhibit any defect in cell morphology, proliferation rate, or viability, and they supported efficiently the replication of HIV-1 (Figures 5D and S5C–S5F). These results indicate that XRN1 KO lines are not metabolically deficient or subjected to a heavy stress incompatible with virus infection.

To determine if XRN1 activity involves the generation of RNA degradation products, we analyzed our RNA-seq data. However, we did not found any increase in read coverage compatible with XRN1-derived degradation products, suggesting that XRN1 role in SINV infection differs from that described for DENV.

(C) Localization by immunofluorescence of the EGFP-fused RBPs and SINV C. Green and red fluorescence intensity profiles in a representative 5-μm section (white line) are plotted in (B) and (C).
(D) Summary of the observed localization of the 26 proteins tested in (C) and Figure S4B.
Scale bars represent 10 μm. AFU, arbitrary fluorescence units.
See also Figure S4.

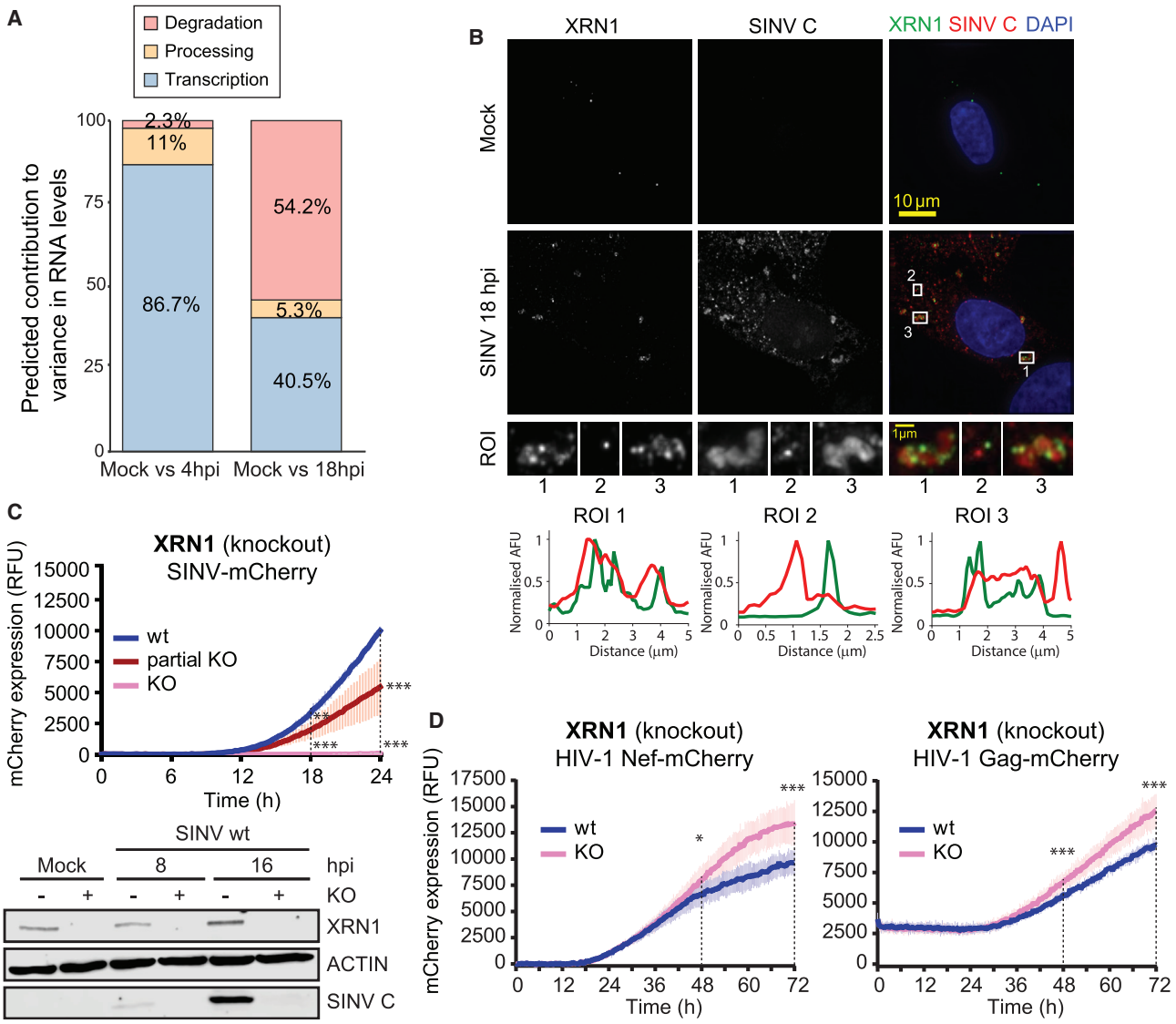

Figure 5. The Exonuclease XRN1 in Cells Infected with SINV

(A) Contribution of transcription, processing, and degradation to the transcriptomic changes induced by SINV. We compared our RNA-seq data to available data estimating these parameters (Mukherjee et al., 2017). ANOVA was used to predict the contribution of each RNA biological process to the variance in RNA levels.

(B) Immunolocalization of XRN1 and SINV C. Green and red fluorescence profiles for regions of interest (ROI) are displayed.

(C) Top: mCherry fluorescence in XRN1 KO and control cells infected with SINV-mCherry measured every 15 min in a plate reader with atmospheric control (5% CO2 and 37°C). RFU, relative fluorescence units. Western blot of XRN1 and SINV C (bottom).

(D) Infection fitness of HIV-$1_{Nef\text{-}mCherry}$ and HIV-$1_{Gag\text{-}mCherry}$ pseudotyped viruses in XRN1 KO cells. mCherry expression was measured as in (C).

mCherry fluorescence is represented as mean ± SD of three independent infections in each of the three biological replicates (n = 9). ***p < 0.001; **p < 0.01; *p < 0.05.

See also Figure S5.

RBPome Responses Are Biologically Important

To determine to a broader extent whether RBP responses are functionally important, we sought to study the impact of altered RBPs on virus infection. The ligase RTCB, together with DDX1, FAM98A, and other RBPs, forms the tRNA ligase complex (TRLC) (Popow et al., 2011). RTCB and DDX1 were stimulated by SINV (Table S1), and these and FAM98A accumulated in the viral factories (Figures 4C and S4B). TRLC mediates the unusual ligation of 3′-phosphate or 2′,3′-cyclic phosphate to a 5′-hydroxyl and these molecule ends are generated by a limited repertoire of cellular endonucleases, which include the endoplasmic reticulum resident protein IRE1α (Popow et al., 2011). SINV has been proposed to cause unfolded protein response (Rathore et al., 2013), which is compatible with the activation of IRE1α and TRLC in infected cells (Jurkin et al., 2014). Notably, inhibition of IRE1α with 4μ8C strongly reduced viral fitness in low,

non-cytotoxic concentrations (Figures 6A and S6A), suggesting that IRE1α and TRLC are positively contributing to SINV infection.

PPIA (also cyclophilin A) has also been classified as an RBP by RIC studies (Hentze et al., 2018). It switches proline conformation-modulating protein activity, which plays a crucial role in hepatitis C virus infection (Rupp and Bartenschlager, 2014). PPIA is also important for the infection of other viruses, such as HIV-1 (Li et al., 2007). PPIA RNA-binding activity is stimulated by SINV infection and is recruited to the viral factories (Figures 2E and S4B). Interestingly, SINV-mCherry infection is delayed by PPIA loss of function (KO and inhibition; Figures 6B, S6A, and S6B). Overexpression had no effect in SINV-mCherry fitness (Figure 6B, bottom).

The heat shock chaperone HSP90AB1 is stimulated by SINV (Table S1). HSP90AB1 has been classified as an RBP by RIC (Hentze et al., 2018), and its RBD has been located in a discrete region at its C-terminal domain (Figure S6C) (Castello et al., 2016). Chaperones from the HSP90 family are important in the remodeling of RNPs and are linked to virus infection (Geller et al., 2012; Iwasaki et al., 2010). Notably, SINV-mCherry infection was significantly delayed in HSP90AB1 KO cells, even though four homologs of this protein exist (Figures 6C and S6B). Moreover, the pro-viral activity of HSP90AB1 was confirmed by treatment with specific inhibitors (Figures 6C and S6A). Again, overexpression had no effect in SINV-mCherry fitness (Figure 6C). The implication of PPIA and HSP90 in the biological cycle of a variety of unrelated viruses highlights these proteins as master regulators of infection (Garcia-Moreno et al., 2018).

PA2G4 RNA-binding activity was also enhanced by SINV (Table S1). It associates with ribosomes (Table S2) (Simsek et al., 2017) and regulates the cap-independent translation of foot-and-mouth disease virus (FMDV) RNA (Monie et al., 2007). Treatment with its specific inhibitor WS6 hampered SINV-mCherry fitness (Figures 6D and S6A), suggesting that this protein promotes SINV infection. Overexpression did not cause any effect, as with previous examples (Figure 6D). The possibility that PA2G4 contributes to the non-canonical, cap-dependent translation of SINV RNAs should be further investigated.

SRPK1 is a kinase that phosphorylates the RS repeats present in SR proteins, which are involved in alternative splicing regulation, RNA export, and stability (Howard and Sanford, 2015). SINV infection stimulates SRPK1 RNA-binding activity (Table S1) and causes its relocation to viral replication factories (Figure 4C). Inhibition of SRPK1 hampers SINV and HIV-1 infection (Fukuhara et al., 2006), and we show here that overexpression of SRPK1 enhances SINV fitness (Figure 6E). This suggests that SRPK1 positively contributes to SINV infection. Future work should determine if SRPK1 kinase activity is involved in infection, and if so, which proteins it phosphorylates.

We tested the effects of overexpression of nine additional stimulated or inhibited RBPs fused to EGFP (Figures S6D and S6E). Phenotypes in viral fitness ranged from nonexistent (ALDOA, XRCC6, RPS10, MOV10, NGDN, and CSTF2) to mild (RPS27, NONO, and DKC1). The lack of phenotypic effects in overexpression experiments does not rule out that the protein actually participates in SINV infection (see above). Nevertheless, RBPs whose overexpression affects infection fitness have potential as regulatory proteins.

The family of tripartite-motif-containing (TRIM) proteins comprises more than 75 members endowed with E3 ubiquitin ligase activity, and few of them have been classified as RBPs by RIC (Hentze et al., 2018). Notably, SINV infection enhanced TRIM25 and TRIM56 interaction with RNA (Table S1), correlating with their redistribution to viral replication factories (Figure 4C). TRIM25 was proposed to interact with DENV RNA (Manokaran et al., 2015); however, this analysis employed native immunoprecipitation (IP) that cannot distinguish between direct and indirect protein-RNA interactions. To test if TRIM25 interacts directly with SINV RNA, we immunoprecipitated under stringent conditions TRIM25-EGFP from SINV-infected cells irradiated with UV light. Co-precipitated RNA was analyzed by RT-PCR using specific primers against SINV RNA. A band with the expected size was detected in TRIM25-EGFP IPs, but not in the negative controls (Figure 7A), confirming that TRIM25 interacts with SINV RNA directly. TRIM25 interaction with RNA enhances its E3 ubiquitin ligase activity (Choudhury et al., 2017). TRIM25-EGFP overexpression inhibited SINV-mCherry infection (Figure 7B), which agrees with its ability to activate the key antiviral factors RIG-I and ZC3HAV1 through ubiquitination (Gack et al., 2007; Li et al., 2017). It is known that TRIM56 binds double-stranded DNA. However, it enhances the antiviral response in cells infected with both DNA and RNA viruses (Seo et al., 2018; Tsuchida et al., 2010). cRIC thus complements these results, revealing that TRIM56 interacts directly with RNA (Table S1). As with TRIM25, overexpression of TRIM56-EGFP reduced SINV fitness (Figure 7B), confirming its capacity to restrict the infection of the RNA virus, SINV.

Importantly, 160 out of the 247 altered RBPs lack previous connections to virus infection (Garcia-Moreno et al., 2018). Hence, our dataset likely contains numerous pro- and antiviral RBPs yet to be uncovered.

GEMIN5 Binds to the 5′ UTR of SINV RNAs and Regulates Viral Protein Expression

GEMIN5 is a member of the survival motor neuron (SMN) complex, which mediates the assembly of the small nuclear RNPs (snRNPs) (Gubitz et al., 2002). It is strongly stimulated by SINV infection and redistributed to the viral factories co-localizing with SINV RNA (Figures 2E, 4C, and S4C). To our surprise, none of the known molecular partners of GEMIN5 (i.e., GEMIN and SMN proteins) were stimulated by SINV (Table S1), implying a GEMIN5-specific response that agrees with the existence of a free pool of GEMIN5 (Battle et al., 2007). In SINV-infected cells, overexpression of GEMIN5-EGFP caused a moderate but significant delay of mCherry production and strongly inhibited capsid synthesis (Figure 7B). These results align well with the described role of GEMIN5 in translational control (Francisco-Velilla et al., 2018; Piñeiro et al., 2015).

Protein-protein interaction analysis of GEMIN5-EGFP revealed that, in our experimental settings, it interacts with the ribosome, especially with the 60S subunit (Figure 7C, pink

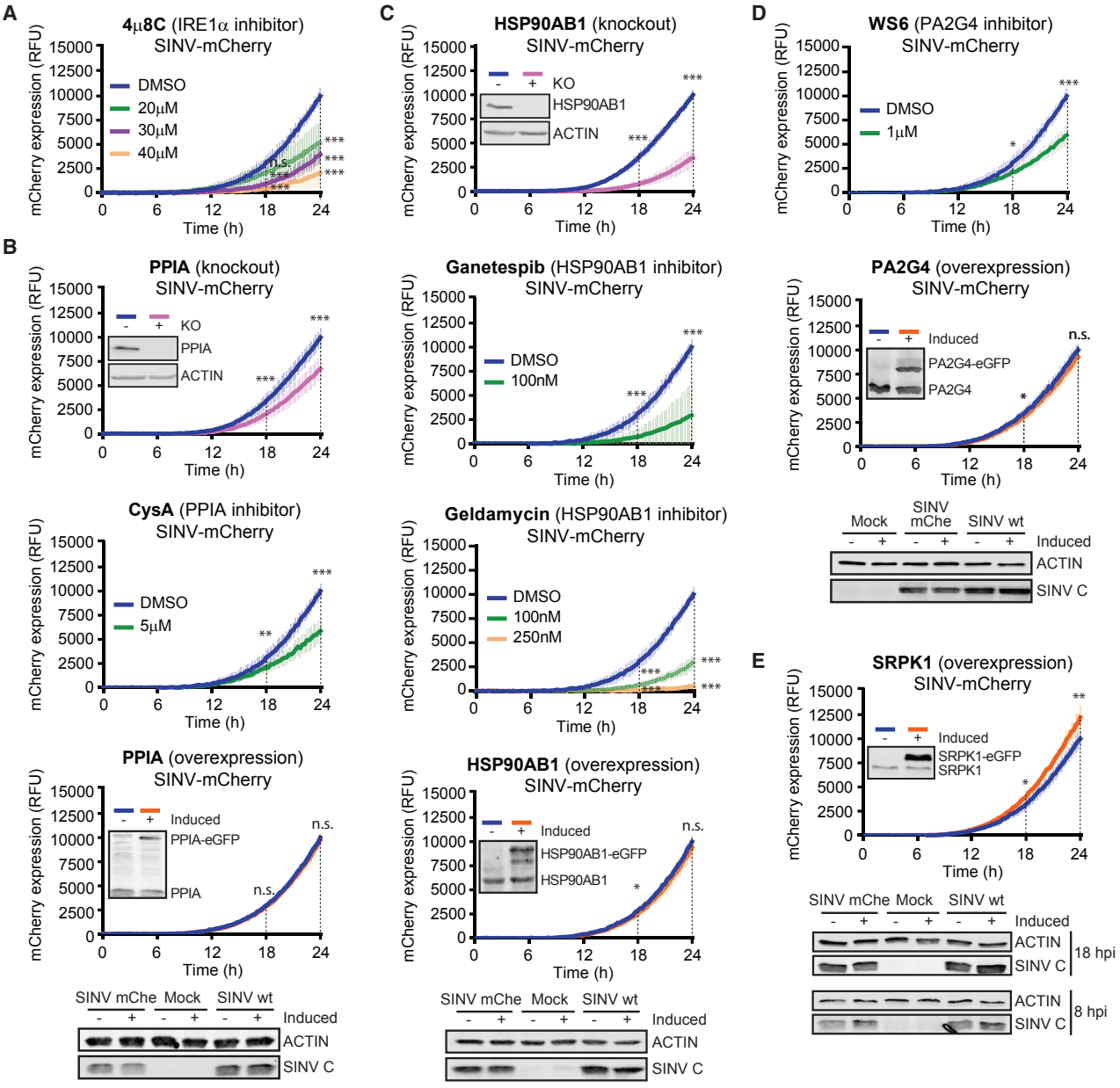

Figure 6. Impact of Stimulated RBPs in SINV Infection

(A) Expression of mCherry in HEK293 cells infected with SINV-mCherry and treated or not with the IRE1α inhibitor 4μ8C. Red fluorescence was measured as in Figure 5C.

(B) As in (A) but with PPIA KO cells (top), the PPIA inhibitor cyclosporine A (CysA) (middle), and cells overexpressing PPIA-EGFP (bottom). KO and overexpression of PPIA and SINV C accumulation (18 hpi) were assessed by western blotting.

(C) mCherry fluorescence in HSP90AB1 KO cells (top), cells treated with ganetespib or geldamycin (middle panels), or cells overexpressing HSP90AB1-EGFP (bottom) and infected with SINV-mCherry. KO and overexpression of HSP90AB1 and SINV C accumulation (18 hpi) were assessed by western blotting.

(D) As in (A) but using the PA2G4 inhibitor WS6 (top) and cells overexpressing PA2G4-eGFP (midde). Right: western blots against SINV C at 18 hpi.

(E) As in (A) but with cells overexpressing SRPK1 (top). Overexpression of SRPK1 was assessed by western blotting. Bottom: western blots of SINV C in these cells at 18 hpi.

mCherry fluorescence is shown as the mean ± SD of three independent infections in each of the three biological replicates (n = 9). ***$p < 0.001$; **$p < 0.01$; *$p < 0.05$. SINV-mChe, SINV-mCherry; n.s., non-significant.

See also Figure S6.

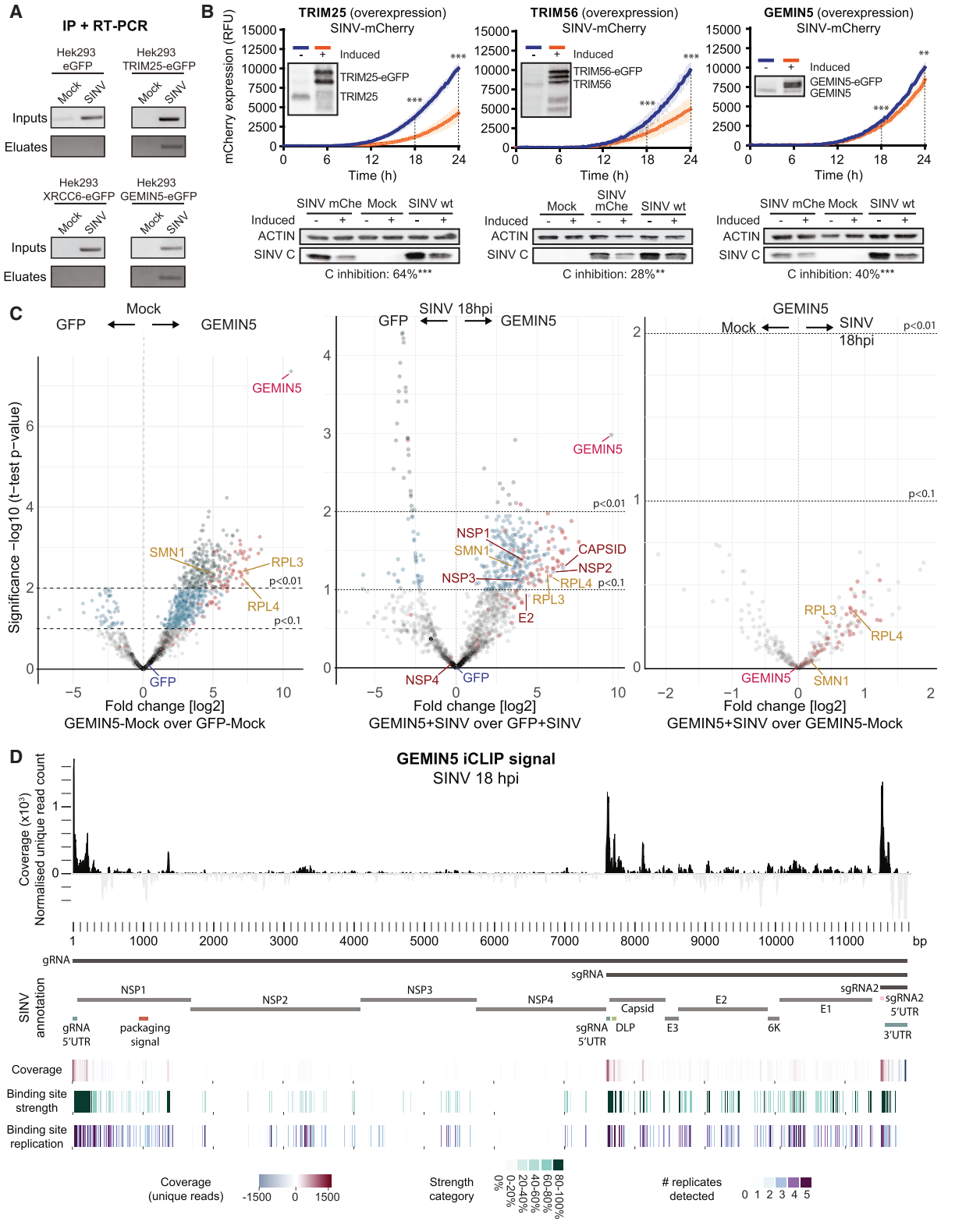

(legend on next page)

dots, left; Figures S7C and S7D; Table S5). This interaction is sustained in SINV-infected cells (Figure 7C, pink dots, middle and right). These results are in agreement with previous studies showing that GEMIN5 impacts protein synthesis at the translation elongation step through its direct interaction with the 60S ribosomal subunit and, in particular, with RPL3 and RPL4, which are also enriched in our IPs (Table S5) (Francisco-Velilla et al., 2016). We noticed that GEMIN5 is by far the most enriched protein in our IPs and that its Intensity Based Absolute Quantification (iBAQ) score is significantly higher than that of EGFP, suggesting that GEMIN5-EGFP interacts with the endogenous GEMIN5, likely forming oligomers, as previously described (Xu et al., 2016). Moreover, our data showed that GEMIN5 interacts with various viral proteins, chiefly with NSP1, NSP2, NSP3 and SINV C (Figure 7C, middle). The implications of these interactions in the modulation of GEMIN5 function deserve future considerations.

GEMIN5 is cleaved by the L protease of FMDV, and resulting C-terminal moiety enhances internal ribosome entry site (IRES)-driven translation (Piñeiro et al., 2013). However, GEMIN5 is not cleaved in SINV-infected cells (Figure 3E), and SINV RNAs lack an IRES and are capped (Carrasco et al., 2018). To test whether GEMIN5 binds SINV RNA, we performed an IP and RT-PCR analysis as outlined above. A PCR product was amplified in GEMIN5-EGFP eluates (Figure 7A), which agrees with the striking co-localization of SINV RNA and GEMIN5 (Figure S4C). To get insights into how GEMIN5 recognizes SINV RNAs, we employed single-nucleotide-resolution crosslinking and immunoprecipitation followed by sequencing (iCLIP) (König et al., 2010). Interestingly, the footprints with highest coverage mapped to the 5′ ends of the gRNA and sgRNA (Figures 7D and S7E–S7G). These reads often presented an additional guanosine at the 5′ end (Figure S7H), likely reflecting binding to the cap structure. These results support previous data showing that GEMIN5 is captured in cap-Sepharose beads (Bradrick and Gromeier, 2009). Additional peaks overlap with the downstream loop (DLP), which is a hairpin structure that stimulates the translation of the sgRNA (Frolov and Schlesinger, 1996). Interaction with the cap, 5′ UTR, and DLP of viral RNAs aligns well with the proposed role as translational regulator and the observed inhibition of capsid expression. Our data support the model in which GEMIN5 recognizes the 5′ end of the gRNA and sgRNA and prevents their translation by interfering with ribosomal function.

Outlook

We show here that SINV infection induces changes in the active RBPome that affects both well-established and unconventional RBPs. Mechanistically, the RBPome rearrangement can be explained by the loss of cellular RNA and the emergence of the highly abundant viral RNA. Supporting this conclusion, we observed that most of the RBPs with enhanced activity accumulate in the viral factories together with the viral RNA. However, this RNA-driven remodeling of the RBPome is not incompatible with complementary "fine-tuning" regulatory mechanisms affecting RBPs on an individual basis. For example, it is known that virus infection triggers signaling pathways involving kinases (Figure 1D), E3 ubiquitin ligases, prolyl *cis/trans* isomerases, and chaperones (Carrasco et al., 2018; Gack et al., 2007; Li et al., 2017). Here, we show that these protein families are represented among the stimulated RBPs, including SRPK1, TRIM25, TRIM56, PPIA, and HSP90AB1. Hence, it is plausible that post-translational control also contributes to RBP regulation in SINV-infected cells. Moreover, interactions with viral proteins can regulate RBP function (Fros et al., 2012). We show that GEMIN5 interacts with several viral proteins, suggesting that this regulatory mechanism may apply to altered RBPs more broadly (Figure 7C).

Importantly, changes in the RBPome are biologically important, as perturbation of the altered RBPs strongly affects SINV infection. Therefore, every protein reported here to respond to SINV infection has potential as anti- or pro-viral factor, highlighting cellular RBPs as promising targets for antiviral therapies.

Some of the outstanding questions derived from this work include whether the distinct composition of ribosomes in infected cells affects their translational properties, why the lack of the exonuclease XRN1 makes the cells refractory to SINV, what triggers the degradation of host RNA, and why the transcripts induced by the antiviral response are resistant to degradation. Moreover, GEMIN5 emerges as a highly responsive RBP that impairs SINV infection. The exact mechanisms underpinning GEMIN5 effects in translation require further investigation.

Figure 7. Effects of RBPs with Antiviral Potential in SINV Infection

(A) UV crosslinking and immunoprecipitation of TRIM25-EGFP, GEMIN5-EGFP, XRCC6-EGFP, or unfused EGFP in cells infected or not with SINV for 18 h. The presence of SINV RNA in eluates and inputs was detected by RT-PCR using specific primers against SINV RNAs.

(B) Relative mCherry fluorescence produced in cells overexpressing TRIM25-EGFP (top left), TRIM56-eGFP (top middle), GEMIN5-eGFP (top right), and infected with SINV-mCherry (measured as in Figure 5C). mCherry expression is represented as the mean ± SD of three independent infections in each of the three biological replicates (n = 9). Overexpression was assessed by western blotting. Bottom: western blots of SINV C at 18 hpi, indicating below the average inhibition of C relative to control cells. ***$p < 0.001$; **$p < 0.01$.

(C) Volcano plots comparing the intensity of proteins in GEMIN5-EGFP versus unfused EGFP IPs in uninfected (left) and infected cells (middle); every dot represents a protein. Dark green dots are proteins enriched with $p < 0.01$, blue dots are those enriched with $p < 0.1$, and gray dots represent nonenriched proteins. Pink dots represent ribosomal proteins. Right: a volcano plot comparing the intensity of proteins in GEMIN5 IPs in infected versus uninfected cells.

(D) iCLIP analysis of GEMIN5-binding sites on SINV RNA. Top: coverage pileup of 5′ first base of unique molecules mapping to the SINV genome, shown as 20-nt sliding mean of five replicates after GFP background subtraction. Each position is given relative to total SINV count (RPM). Middle: key features of SINV annotation. Bottom: the top track shows iCLIP coverage but as a heatmap representation. The middle heatmap shows GEMIN5 binding sites along SINV divided into five groups according to strength of binding. The bottom heatmap shows the number of replicates supporting each binding site when binding sites are called independently for each replicate.

See also Figure S7 and Table S5.

Finally, cRIC has been applied here to cells infected with SINV. However, it can now be extended to other viruses or physiological cues to improve our understanding of RBP regulation and its biological importance.

STAR★METHODS

Detailed methods are provided in the online version of this paper and include the following:

- KEY RESOURCES TABLE
- CONTACT FOR REAGENT AND RESOURCE SHARING
- EXPERIMENTAL MODEL AND SUBJECT DETAILS
  - Cell culture
  - Cell culture in SILAC media
  - Viruses
- METHOD DETAILS
  - RNA interactome capture
  - Conventional protein analyses
  - Reverse-transcription and quantitative PCR
  - Plasmids and recombinant DNA procedures
  - mCherry-based viral fitness assay
  - Drugs and cell viability assay
  - Protein-protein interactions analysis
  - RBP-RNA interaction analysis: CLIP/RT-PCR
  - Analysis of GEMIN5 binding sites by iCLIP
  - Immunofluorescence and RNA FISH assays
  - Determining the percentage of infected cells
  - Mass spectrometry
  - RNA sequencing
- QUANTIFICATION AND STATISTICAL ANALYSES
  - Proteomic quantitative analysis
  - RNA sequencing data analysis
  - Analysis of RNA synthesis, processing, and degradation
  - iCLIP-seq data processing
- DATA AND SOFTWARE AVAILABILITY

SUPPLEMENTAL INFORMATION

Supplemental Information can be found with this article online at https://doi.org/10.1016/j.molcel.2019.01.017.

ACKNOWLEDGMENTS

We dedicate this work to our colleagues and friends Bernd Fischer and Katrin Eichelbaum, who sadly passed away during the development of this work. We thank Matthias W. Hentze, Encarnacion Martinez-Salas, Javier Martinez, Kui Li, Quentin Sattentau, Ilan Davis, Richard Parton, and Jan Rehwinkel for reagents and advice. We thank the Oxford Micron Advanced Bioimaging Unit for support in microscopy experiments. A.C. is funded by MRC Career Development Award MR/L019434/1, MRC grant MR/R021562/1, and John Fell Funds from the University of Oxford. M.G.M. is funded by the European Union's Horizon 2020 research and innovation programme under Marie-Sklodowska-Curie grant agreement 700184. I.D. is funded by Wellcome Trust Investigator Award 209412/Z/17/Z. V.P. is funded by a SciLifeLab Fellowship, the Swedish Research Council (VR 2016-01842), a Wallenberg Academy Fellowship (KAW 2016.0123), and the Ragnar Söderberg Foundation. L.C. is funded by grant DGICYT SAF2015-66170-R (MINECO/FEDER). E.G.A. was awarded with a short-term EMBO fellowship (ASTF 358-2015) and an FPU fellowship FPU15/05709. G.M. was supported by the Wellcome Seed Award in Science (210144/Z/18/Z) and the Wellcome Trust Centre Core Grant (092076). G.H. was a recipient of a Wellcome Trust PhD studentship (105246/Z/14/Z).

AUTHOR CONTRIBUTIONS

Conceptualization, M.N., L.C., B.F., S.M., and A.C.; Methodology, M.G.-M., M.N., S.N., A.I.J., E.G.-A., C.E.L., I.D., B.F., S.M., and A.C.; Investigation, M.G.-M., M.N., S.N., A.I.J., E.G.-A., C.E.L., M.B.-P., V.C., R.A., T.D., S.H., T.J.M.S., B.L., M.A.S., E.P.R., V.P., B.F., S.M., and A.C.; Writing – Original Draft, M.G.-M., M.N., A.I.J., and A.C.; Writing – Editing, M.G.-M., M.N., S.N., A.I.J., C.E.L., S.M., and A.C.; Funding Acquisition, M.G.-M. and A.C.; Resources, G.H., G.M., L.C., E.P.R., V.P., I.D., B.F., S.M., and A.C.; Supervision, M.G.-M., M.N., A.I.J., B.F., S.M., and A.C.

DECLARATION OF INTERESTS

The authors declare no competing interests.

Received: June 18, 2018
Revised: December 18, 2018
Accepted: January 11, 2019
Published: February 21, 2019

REFERENCES

Akusjarvi, G. (2008). Temporal regulation of adenovirus major late alternative RNA splicing. Front. Biosci. *13*, 5006–5015.

Au, H.H., and Jan, E. (2014). Novel viral translation strategies. Wiley Interdiscip. Rev. RNA *5*, 779–801.

Balistreri, G., Horvath, P., Schweingruber, C., Zünd, D., McInerney, G., Merits, A., Mühlemann, O., Azzalin, C., and Helenius, A. (2014). The host nonsense-mediated mRNA decay pathway restricts mammalian RNA virus replication. Cell Host Microbe *16*, 403–411.

Baltz, A.G., Munschauer, M., Schwanhäusser, B., Vasile, A., Murakawa, Y., Schueler, M., Youngs, N., Penfold-Brown, D., Drew, K., Milek, M., et al. (2012). The mRNA-bound proteome and its global occupancy profile on protein-coding transcripts. Mol. Cell *46*, 674–690.

Barbalat, R., Ewald, S.E., Mouchess, M.L., and Barton, G.M. (2011). Nucleic acid recognition by the innate immune system. Annu. Rev. Immunol. *29*, 185–214.

Battle, D.J., Kasim, M., Wang, J., and Dreyfuss, G. (2007). SMN-independent subunits of the SMN complex. Identification of a small nuclear ribonucleoprotein assembly intermediate. J. Biol. Chem. *282*, 27953–27959.

Bradrick, S.S., and Gromeier, M. (2009). Identification of gemin5 as a novel 7-methylguanosine cap-binding protein. PLoS ONE *4*, e7030.

Carlson, M., and Pages, H. (2015). Homology information for Homo sapiens from Inparanoid. R package version 3.1.2 (Bioconductor).

Carrasco, L., Sanz, M.A., and González-Almela, E. (2018). The regulation of translation in alphavirus-infected cells. Viruses *10*, E70.

Castelló, A., Alvarez, E., and Carrasco, L. (2011). The multifaceted poliovirus 2A protease: regulation of gene expression by picornavirus proteases. J. Biomed. Biotechnol. *2011*, 369648.

Castello, A., Fischer, B., Eichelbaum, K., Horos, R., Beckmann, B.M., Strein, C., Davey, N.E., Humphreys, D.T., Preiss, T., Steinmetz, L.M., et al. (2012). Insights into RNA biology from an atlas of mammalian mRNA-binding proteins. Cell *149*, 1393–1406.

Castello, A., Horos, R., Strein, C., Fischer, B., Eichelbaum, K., Steinmetz, L.M., Krijgsveld, J., and Hentze, M.W. (2013). System-wide identification of RNA-binding proteins by interactome capture. Nat. Protoc. *8*, 491–500.

Castello, A., Hentze, M.W., and Preiss, T. (2015). Metabolic enzymes enjoying new partnerships as RNA-binding proteins. Trends Endocrinol. Metab. *26*, 746–757.

Castello, A., Fischer, B., Frese, C.K., Horos, R., Alleaume, A.M., Foehr, S., Curk, T., Krijgsveld, J., and Hentze, M.W. (2016). Comprehensive identification of RNA-binding domains in human cells. Mol. Cell *63*, 696–710.

Chapman, E.G., Costantino, D.A., Rabe, J.L., Moon, S.L., Wilusz, J., Nix, J.C., and Kieft, J.S. (2014). The structural basis of pathogenic subgenomic flavivirus RNA (sfRNA) production. Science *344*, 307–310.

Chen, C.Y., and Shyu, A.B. (2014). Emerging mechanisms of mRNP remodeling regulation. Wiley Interdiscip. Rev. RNA *5*, 713–722.

Choudhury, N.R., Heikel, G., Trubitsyna, M., Kubik, P., Nowak, J.S., Webb, S., Granneman, S., Spanos, C., Rappsilber, J., Castello, A., and Michlewski, G. (2017). RNA-binding activity of TRIM25 is mediated by its PRY/SPRY domain and is required for ubiquitination. BMC Biol. *15*, 105.

Cox, J., and Mann, M. (2008). MaxQuant enables high peptide identification rates, individualized p.p.b.-range mass accuracies and proteome-wide protein quantification. Nat. Biotechnol. *26*, 1367–1372.

Deutsch, E.W., Csordas, A., Sun, Z., Jarnuczak, A., Perez-Riverol, Y., Ternent, T., Campbell, D.S., Bernal-Llinares, M., Okuda, S., Kawano, S., et al. (2017). The ProteomeXchange consortium in 2017: supporting the cultural change in proteomics public data deposition. Nucleic Acids Res. *45* (D1), D1100–D1106.

Dobin, A., Davis, C.A., Schlesinger, F., Drenkow, J., Zaleski, C., Jha, S., Batut, P., Chaisson, M., and Gingeras, T.R. (2013). STAR: ultrafast universal RNA-seq aligner. Bioinformatics *29*, 15–21.

Durinck, S., Spellman, P.T., Birney, E., and Huber, W. (2009). Mapping identifiers for the integration of genomic datasets with the R/Bioconductor package biomaRt. Nat. Protoc. *4*, 1184–1191.

Francisco-Velilla, R., Fernandez-Chamorro, J., Ramajo, J., and Martinez-Salas, E. (2016). The RNA-binding protein Gemin5 binds directly to the ribosome and regulates global translation. Nucleic Acids Res. *44*, 8335–8351.

Francisco-Velilla, R., Fernandez-Chamorro, J., Dotu, I., and Martinez-Salas, E. (2018). The landscape of the non-canonical RNA-binding site of Gemin5 unveils a feedback loop counteracting the negative effect on translation. Nucleic Acids Res. *46*, 7339–7353.

Frolov, I., and Schlesinger, S. (1996). Translation of sindbis virus mRNA: analysis of sequences downstream of the initiating AUG codon that enhance translation. J. Virol. *70*, 1182–1190.

Fros, J.J., Domeradzka, N.E., Baggen, J., Geertsema, C., Flipse, J., Vlak, J.M., and Pijlman, G.P. (2012). Chikungunya virus nsP3 blocks stress granule assembly by recruitment of G3BP into cytoplasmic foci. J. Virol. *86*, 10873–10879.

Fukuhara, T., Hosoya, T., Shimizu, S., Sumi, K., Oshiro, T., Yoshinaka, Y., Suzuki, M., Yamamoto, N., Herzenberg, L.A., Herzenberg, L.A., and Hagiwara, M. (2006). Utilization of host SR protein kinases and RNA-splicing machinery during viral replication. Proc. Natl. Acad. Sci. USA *103*, 11329–11333.

Gack, M.U., Shin, Y.C., Joo, C.H., Urano, T., Liang, C., Sun, L., Takeuchi, O., Akira, S., Chen, Z., Inoue, S., and Jung, J.U. (2007). TRIM25 RING-finger E3 ubiquitin ligase is essential for RIG-I-mediated antiviral activity. Nature *446*, 916–920.

Garcia-Moreno, M., Järvelin, A.I., and Castello, A. (2018). Unconventional RNA-binding proteins step into the virus-host battlefront. Wiley Interdiscip. Rev. RNA *9*, e1498.

Geller, R., Taguwa, S., and Frydman, J. (2012). Broad action of Hsp90 as a host chaperone required for viral replication. Biochim. Biophys. Acta *1823*, 698–706.

Glisovic, T., Bachorik, J.L., Yong, J., and Dreyfuss, G. (2008). RNA-binding proteins and post-transcriptional gene regulation. FEBS Lett. *582*, 1977–1986.

Gorchakov, R., Frolova, E., and Frolov, I. (2005). Inhibition of transcription and translation in sindbis virus-infected cells. J. Virol. *79*, 9397–9409.

Gubitz, A.K., Mourelatos, Z., Abel, L., Rappsilber, J., Mann, M., and Dreyfuss, G. (2002). Gemin5, a novel WD repeat protein component of the SMN complex that binds Sm proteins. J. Biol. Chem. *277*, 5631–5636.

Hentze, M.W., Castello, A., Schwarzl, T., and Preiss, T. (2018). A brave new world of RNA-binding proteins. Nat. Rev. Mol. Cell Biol. *19*, 327–341.

Howard, J.M., and Sanford, J.R. (2015). The RNAissance family: SR proteins as multifaceted regulators of gene expression. Wiley Interdiscip. Rev. RNA *6*, 93–110.

Huppertz, I., Attig, J., D'Ambrogio, A., Easton, L.E., Sibley, C.R., Sugimoto, Y., Tajnik, M., König, J., and Ule, J. (2014). iCLIP: protein-RNA interactions at nucleotide resolution. Methods *65*, 274–287.

Iwasaki, S., Kobayashi, M., Yoda, M., Sakaguchi, Y., Katsuma, S., Suzuki, T., and Tomari, Y. (2010). Hsc70/Hsp90 chaperone machinery mediates ATP-dependent RISC loading of small RNA duplexes. Mol. Cell *39*, 292–299.

Jurkin, J., Henkel, T., Nielsen, A.F., Minnich, M., Popow, J., Kaufmann, T., Heindl, K., Hoffmann, T., Busslinger, M., and Martinez, J. (2014). The mammalian tRNA ligase complex mediates splicing of XBP1 mRNA and controls antibody secretion in plasma cells. EMBO J. *33*, 2922–2936.

Kolde, R. (2015). pheatmap: Pretty Heatmaps R package version 108.

König, J., Zarnack, K., Rot, G., Curk, T., Kayikci, M., Zupan, B., Turner, D.J., Luscombe, N.M., and Ule, J. (2010). iCLIP reveals the function of hnRNP particles in splicing at individual nucleotide resolution. Nat. Struct. Mol. Biol. *17*, 909–915.

LaPointe, A.T., Gebhart, N.N., Meller, M.E., Hardy, R.W., and Sokoloski, K.J. (2018). The identification and characterization of Sindbis virus RNA:host protein interactions. J. Virol. *92*, e02171-17.

Lee, A.S., Kranzusch, P.J., Doudna, J.A., and Cate, J.H. (2016). eIF3d is an mRNA cap-binding protein that is required for specialized translation initiation. Nature *536*, 96–99.

Li, J., Tang, S., Hewlett, I., and Yang, M. (2007). HIV-1 capsid protein and cyclophilin a as new targets for anti-AIDS therapeutic agents. Infect. Disord. Drug Targets *7*, 238–244.

Li, H., Handsaker, B., Wysoker, A., Fennell, T., Ruan, J., Homer, N., Marth, G., Abecasis, G., and Durbin, R.; 1000 Genome Project Data Processing Subgroup (2009). The Sequence Alignment/Map format and SAMtools. Bioinformatics *25*, 2078–2079.

Li, M.M., Lau, Z., Cheung, P., Aguilar, E.G., Schneider, W.M., Bozzacco, L., Molina, H., Buehler, E., Takaoka, A., Rice, C.M., et al. (2017). TRIM25 enhances the antiviral action of zinc-finger antiviral protein (ZAP). PLoS Pathog. *13*, e1006145.

Liao, Y., Smyth, G.K., and Shi, W. (2013). The Subread aligner: fast, accurate and scalable read mapping by seed-and-vote. Nucleic Acids Res. *41*, e108.

Lin, J.Y., Shih, S.R., Pan, M., Li, C., Lue, C.F., Stollar, V., and Li, M.L. (2009). hnRNP A1 interacts with the 5′ untranslated regions of enterovirus 71 and Sindbis virus RNA and is required for viral replication. J. Virol. *83*, 6106–6114.

Lloyd, R.E. (2015). Nuclear proteins hijacked by mammalian cytoplasmic plus strand RNA viruses. Virology *479-480*, 457–474.

Love, M.I., Huber, W., and Anders, S. (2014). Moderated estimation of fold change and dispersion for RNA-seq data with DESeq2. Genome Biol. *15*, 550.

Lunde, B.M., Moore, C., and Varani, G. (2007). RNA-binding proteins: modular design for efficient function. Nat. Rev. Mol. Cell Biol. *8*, 479–490.

Manokaran, G., Finol, E., Wang, C., Gunaratne, J., Bahl, J., Ong, E.Z., Tan, H.C., Sessions, O.M., Ward, A.M., Gubler, D.J., et al. (2015). Dengue subgenomic RNA binds TRIM25 to inhibit interferon expression for epidemiological fitness. Science *350*, 217–221.

Molleston, J.M., and Cherry, S. (2017). Attacked from all sides: RNA decay in antiviral defense. Viruses *9*, 2.

Monie, T.P., Perrin, A.J., Birtley, J.R., Sweeney, T.R., Karakasiliotis, I., Chaudhry, Y., Roberts, L.O., Matthews, S., Goodfellow, I.G., and Curry, S. (2007). Structural insights into the transcriptional and translational roles of Ebp1. EMBO J. *26*, 3936–3944.

Mukherjee, N., Calviello, L., Hirsekorn, A., de Pretis, S., Pelizzola, M., and Ohler, U. (2017). Integrative classification of human coding and noncoding genes through RNA metabolism profiles. Nat. Struct. Mol. Biol. *24*, 86–96.

Müller, B., Daecke, J., Fackler, O.T., Dittmar, M.T., Zentgraf, H., and Kräusslich, H.G. (2004). Construction and characterization of a fluorescently labeled infectious human immunodeficiency virus type 1 derivative. J. Virol. *78*, 10803–10813.

Ni, X., Ru, H., Ma, F., Zhao, L., Shaw, N., Feng, Y., Ding, W., Gong, W., Wang, Q., Ouyang, S., et al. (2016). New insights into the structural basis of DNA recognition by HINa and HINb domains of IFI16. J. Mol. Cell Biol. *8*, 51–61.

Perez-Perri, J.I., Rogell, B., Schwarzl, T., Stein, F., Zhou, Y., Rettel, M., Brosig, A., and Hentze, M.W. (2018). Discovery of RNA-binding proteins and characterization of their dynamic responses by enhanced RNA interactome capture. Nat. Commun. *9*, 4408.

Pfaffl, M.W. (2001). A new mathematical model for relative quantification in real-time RT-PCR. Nucleic Acids Res. *29*, e45.

Pijlman, G.P., Funk, A., Kondratieva, N., Leung, J., Torres, S., van der Aa, L., Liu, W.J., Palmenberg, A.C., Shi, P.Y., Hall, R.A., and Khromykh, A.A. (2008). A highly structured, nuclease-resistant, noncoding RNA produced by flaviviruses is required for pathogenicity. Cell Host Microbe *4*, 579–591.

Piñeiro, D., Fernández, N., Ramajo, J., and Martínez-Salas, E. (2013). Gemin5 promotes IRES interaction and translation control through its C-terminal region. Nucleic Acids Res. *41*, 1017–1028.

Piñeiro, D., Fernandez-Chamorro, J., Francisco-Velilla, R., and Martinez-Salas, E. (2015). Gemin5: a multitasking RNA-binding protein involved in translation control. Biomolecules *5*, 528–544.

Popow, J., Englert, M., Weitzer, S., Schleiffer, A., Mierzwa, B., Mechtler, K., Trowitzsch, S., Will, C.L., Lührmann, R., Söll, D., and Martinez, J. (2011). HSPC117 is the essential subunit of a human tRNA splicing ligase complex. Science *331*, 760–764.

Rathore, A.P., Ng, M.L., and Vasudevan, S.G. (2013). Differential unfolded protein response during Chikungunya and Sindbis virus infection: CHIKV nsP4 suppresses eIF2α phosphorylation. Virol. J. *10*, 36.

Rupp, D., and Bartenschlager, R. (2014). Targets for antiviral therapy of hepatitis C. Semin. Liver Dis. *34*, 9–21.

Sanz, M.A., and Carrasco, L. (2001). Sindbis virus variant with a deletion in the 6K gene shows defects in glycoprotein processing and trafficking: lack of complementation by a wild-type 6K gene in trans. J. Virol. *75*, 7778–7784.

Seo, G.J., Kim, C., Shin, W.J., Sklan, E.H., Eoh, H., and Jung, J.U. (2018). TRIM56-mediated monoubiquitination of cGAS for cytosolic DNA sensing. Nat. Commun. *9*, 613.

Sielaff, M., Kuharev, J., Bohn, T., Hahlbrock, J., Bopp, T., Tenzer, S., and Distler, U. (2017). Evaluation of FASP, SP3, and iST protocols for proteomic sample preparation in the low microgram range. J. Proteome Res. *16*, 4060–4072.

Simsek, D., Tiu, G.C., Flynn, R.A., Byeon, G.W., Leppek, K., Xu, A.F., Chang, H.Y., and Barna, M. (2017). The mammalian ribo-interactome reveals ribosome functional diversity and heterogeneity. Cell *169*, 1051–1065.e1018.

Skabkin, M.A., Skabkina, O.V., Dhote, V., Komar, A.A., Hellen, C.U., and Pestova, T.V. (2010). Activities of Ligatin and MCT-1/DENR in eukaryotic translation initiation and ribosomal recycling. Genes Dev. *24*, 1787–1801.

Smyth, G.K. (2004). Linear models and empirical Bayes methods for assessing differential expression in microarray experiments. Stat. Appl. Genet. Mol. Biol. *3*, Article3.

Sysoev, V.O., Fischer, B., Frese, C.K., Gupta, I., Krijgsveld, J., Hentze, M.W., Castello, A., and Ephrussi, A. (2016). Global changes of the RNA-bound proteome during the maternal-to-zygotic transition in Drosophila. Nat. Commun. *7*, 12128.

Szklarczyk, D., Morris, J.H., Cook, H., Kuhn, M., Wyder, S., Simonovic, M., Santos, A., Doncheva, N.T., Roth, A., Bork, P., et al. (2017). The STRING database in 2017: quality-controlled protein-protein association networks, made broadly accessible. Nucleic Acids Res. *45* (D1), D362–D368.

Thompson, M.R., Sharma, S., Atianand, M., Jensen, S.B., Carpenter, S., Knipe, D.M., Fitzgerald, K.A., and Kurt-Jones, E.A. (2014). Interferon γ-inducible protein (IFI) 16 transcriptionally regulates type i interferons and other interferon-stimulated genes and controls the interferon response to both DNA and RNA viruses. J. Biol. Chem. *289*, 23568–23581.

Tsuchida, T., Zou, J., Saitoh, T., Kumar, H., Abe, T., Matsuura, Y., Kawai, T., and Akira, S. (2010). The ubiquitin ligase TRIM56 regulates innate immune responses to intracellular double-stranded DNA. Immunity *33*, 765–776.

Tyanova, S., Temu, T., Sinitcyn, P., Carlson, A., Hein, M.Y., Geiger, T., Mann, M., and Cox, J. (2016). The Perseus computational platform for comprehensive analysis of (prote)omics data. Nat. Methods *13*, 731–740.

Vladimer, G.I., Górna, M.W., and Superti-Furga, G. (2014). IFITs: emerging roles as key anti-viral proteins. Front. Immunol. *5*, 94.

Wickham, H. (2009). ggplot2: Elegant Graphics for Data Analysis (Springer-Verlag).

Xu, C., Ishikawa, H., Izumikawa, K., Li, L., He, H., Nobe, Y., Yamauchi, Y., Shahjee, H.M., Wu, X.H., Yu, Y.T., et al. (2016). Structural insights into Gemin5-guided selection of pre-snRNAs for snRNP assembly. Genes Dev. *30*, 2376–2390.

Zhang, R., Hryc, C.F., Cong, Y., Liu, X., Jakana, J., Gorchakov, R., Baker, M.L., Weaver, S.C., and Chiu, W. (2011). 4.4 Å cryo-EM structure of an enveloped alphavirus Venezuelan equine encephalitis virus. EMBO J. *30*, 3854–3863.

Please cite this article in press as: Garcia-Moreno et al., System-wide Profiling of RNA-Binding Proteins Uncovers Key Regulators of Virus Infection, Molecular Cell (2019), https://doi.org/10.1016/j.molcel.2019.01.017

STAR★METHODS

KEY RESOURCES TABLE

REAGENT or RESOURCE	SOURCE	IDENTIFIER
Antibodies		
anti-SINV C (304 and 306)	Laboratory of L. Carrasco	N/A
β-ACTIN	Sigma	Cat# A1978; RRID: AB_476692
ALDOA	Cusabio	Cat# PA00015A0Rb
DDX1	Bethyl	Cat# A300-521Q; RRID: AB_451046; Cat# A300-520; RRID: AB_451045
DDX50	Cusabio	Cat# PA861080LA01HU
EIF2α	Santa Cruz Biotechnology	Cat# sc-11386; RRID: AB_640075
Phospho-EIF2α (serine 51)	Cell Signaling Technology	Cat# 9721; RRID: AB_330951
EIF3G	Cusabio	Cat# PA03099A0Rb
EIF4G1 Nt - 981	Laboratory of L. Carrasco	N/A
EIF4G1 Ct - 987	Laboratory of L. Carrasco	N/A
ENO1	Cusabio	Cat# PA02395A0Rb
EPRS	Abcam	Cat# ab31531; RRID: AB_880047
GEMIN5	Abcam	Cat# ab201691
GFP	ChromoTek GmbH	Cat# 3h9-100; RRID: AB_10773374
HNRNP A1	Cusabio	Cat# PA010600HA01HU
HNRNP Q/R	Cell Signaling	Cat# 8588; RRID: AB_10897511
HSP90AB1	Cusabio	Cat# PA00109A0Rb
IFIT5	Cusabio	Cat# PA011023LA01HU
IRE1	Abcam	Cat# ab37073; RRID: AB_775780
MOV10	Cusabio	Cat# PA862068LA01HU
NGDN	Cambridge Bioscience	Cat# 16524-1-AP; RRID: AB_2152270
PA2G4	Cusabio	Cat# PA891987LA01HU
PPIA	Cusabio	Cat# PA07814A0Rb
PTBP1	Sigma	Cat# WH0005725M1; RRID: AB_1843067
RTCB	Cusabio	Cat# PA897546LA01HU
RPS10	Cusabio	Cat# PA02565A0Rb
RPS27	Sigma Aldrich	Cat# SAB4300952
SRPK1	Sino Biological Inc	Cat# 12249-MM03
TRIM25	Abcam	Cat# ab167154; RRID: AB_2721902
TRIM56	Abcam	Cat# ab154862
XRCC5	Cusabio	Cat# PA026233LA01HU
XRCC6	Cusabio	Cat# PA01617A0Rb
XRN1	Santa Cruz	Cat# sc-165985; RRID: AB_2304774
Donkey anti-Mouse IgG (H+L) Highly Cross-Adsorbed Secondary Antibody, Alexa Fluor 488	ThermoFisher Scientific	Cat# A-21202; RRID: AB_141607
Donkey anti-Rabbit IgG (H+L) Highly Cross-Adsorbed Secondary Antibody, Alexa Fluor 488	ThermoFisher Scientific	Cat# A-21206; RRID: AB_141708
Donkey anti-Rabbit IgG (H+L) Highly Cross-Adsorbed Secondary Antibody, Alexa Fluor 594	ThermoFisher Scientific	Cat# A-21207; RRID: AB_141637
Bacterial and Virus Strains		
pT7-SVmCherry	This paper	N/A
pT7-SVwt	Laboratory of L. Carrasco (Sanz and Carrasco, 2001)	N/A

(*Continued on next page*)

Continued

REAGENT or RESOURCE	SOURCE	IDENTIFIER
pNL4-3.R-E- Nef-mCherry	This paper	N/A
pNL4-3.R-E- Gag-mCherry	This paper	N/A
Chemicals, Peptides, and Recombinant Proteins		
L-Arginine HCL 13C, 15N	SILANTES GmbH	Cat# 201604102
L-Arginine HCL 13C	SILANTES GmbH	Cat# 201204102
L-Lysine HCL 13C, 15N	SILANTES GmbH	Cat# 211604102
4.4.5.5-D4-L-Lysine	SILANTES GmbH	Cat# 211104113
Cyclosporin A (CAS N° 59865-13-3)	Insight Biotechnology Ltd	Cat# sc-3503
Ganetespib (CAS N° 888216-25-9)	Cambridge Bioscience Ltd	Cat# 19432
Geldanamycin (CAS N° 30562-34-6)	Cambridge Bioscience Ltd	Cat# SM55-2
IRE1 Inhibitor III, 4μ8C (CAS N° 14003-96-4)	Merck Chemicals Ltd	Cat# 412512
WS6 (CAS N° 1421227-53-3)	Cambridge Bioscience Ltd	Cat# 17672
Critical Commercial Assays		
CellTiter 96 AQ_{ueous} One Solution Cell Proliferation Assay (MTS)	Promega	Cat# G3580
Deposited Data		
Proteome Xchange via PRIDE	Deutsch et al., 2017	PXD009789
RNA-seq via GEO		GEO: GSE125182
iCLIP via GEO		GEO: GSE125182
Experimental Models: Cell Lines		
HEK293	ECACC	Cat# 85120602 RRID:CVCL_0045
HeLa Kyoto	ATCC	Cat# CCL-2 RRID:CVCL_1922
Flp-In-T-Rex-293	Thermo Fisher Scientific	Cat#R78007 RRID:CVCL_U427
Flp-In-T-Rex-HeLa	Laboratory of M. Gromeier	N/A
BHK-21	ECACC	Cat# 85011433 RRID:CVCL_1915
Oligonucleotides		
CRISPR guide RNA targeting XRN1: AAUGCGAAACA ACACCUCCGUUUUAGAGCUAUGCUGUUUUG	Sigma-Aldrich Co Ltd	HS0000076809
TRIM25 left sgRNA: CCACGTTGCACAGCACCGTGTTC	This paper	N/A
TRIM25 right sgRNA: CTGCGGTCGCGCCTGGTAGACGG	This paper	N/A
Primers for cloning, see Table S6	This paper	N/A
Primers for RT-PCR, see Table S6	This paper	N/A
Recombinant DNA		
CRISPR/CAS9 plasmid: PX459 HSP90AB1_out_of_frame_67 guide sequence: CTCACACCTTGACTGCCAAG	This paper	N/A
CRISPR/CAS9 plasmid: PX459 PPIA_out_of_frame_57 guide sequence: GCCCGACCTCAAAGGAGACG	This paper	N/A
pOG44	ThermoFisher Scientific	Cat# V600520
pcDNA5/FRT/TO	ThermoFisher Scientific	Cat# V652020
pNL4-3.Luc.R-E-	NIBSC – Centre for AIDS Reagents	Cat# 2128
pNL4-3	NIBSC – Centre for AIDS Reagents	Cat# 2006
pHEF-VSVG	NIH AIDS Reagent Program	Cat# 4693
Software and Algorithms		
REST	Pfaffl, 2001	
STRING	Szklarczyk et al., 2017	https://string-db.org/

(*Continued on next page*)

Continued

REAGENT or RESOURCE	SOURCE	IDENTIFIER
STAR	Dobin et al., 2013	https://github.com/alexdobin/STAR
Subread FeatureCount	Liao et al., 2013	http://bioinf.wehi.edu.au/subread-package/
SAMtools	Li et al., 2009	http://samtools.sourceforge.net/
RBDmap	Castello et al., 2016	https://www-huber.embl.de/users/befische/RBDmap/
DSseq2	Love et al., 2014	https://bioconductor.org/packages/release/bioc/html/DESeq2.html
Pheatmap	Kolde, 2015	https://cran.r-project.org/web/packages/pheatmap/index.html
iCount		https://github.com/tomazc/iCount
biomaRt	Durinck et al., 2009	https://bioconductor.org/packages/release/bioc/html/biomaRt.html
ggplot2	Wickham, 2009	https://cran.r-project.org/web/packages/ggplot2/index.html
MaxQuant (version 1.5.0.35)	Cox and Mann, 2008	https://www.maxquant.org/
Perseus	Tyanova et al., 2016	http://maxquant.net/perseus/
hom.Hs.inp.db	Carlson and Pages, 2015	http://bioconductor.org/packages/release/data/annotation/html/hom.Hs.inp.db.html
mRNAinteractomeHeLa	Castello et al., 2012	http://www.hentze.embl.de/public/RBDmap/
Semiquantitative test for protein differential analysis	This paper	N/A
limma (for moderated t test)	Smyth, 2004	https://bioconductor.org/packages/release/bioc/html/limma.html
ANOVA		https://www.itl.nist.gov/div898/handbook/eda/section3/eda355.htm

CONTACT FOR REAGENT AND RESOURCE SHARING

Further information and requests for resources and reagents should be directed to and will be fulfilled by the Lead Contact, Alfredo Castello (alfredo.castellopalomares@bioch.ox.ac.uk).

EXPERIMENTAL MODEL AND SUBJECT DETAILS

Cell culture

We used here human embryo kidney 293 cells (HEK293, ECACC #85120602), HeLa (ATCC cat. no. CCL-2) and baby hamster kidney cells (BHK-21, clone 13, ECACC #85011433); HEK293 Flp-In TREx are commercially available (Thermo Fisher Scientific, #R78007), while HeLa Flp-In TREx are a generous gift from Dr. Matthias Gromeier (Duke University Medical Center, Durham, NC, USA). All cells were cultured in DMEM with 10% FBS and 1x penicillin/streptomycin (Sigma Aldrich, #P4458) at 37°C with 5% CO_2. The media of Flp-In TREx (Tet-on) cells was supplemented with 15 μg/ml Blasticidin S and 100 μg/ml Zeocin. To generate RBP-eGFP-expressing cell lines, cells were transfected with pOG44 and the corresponding pcDNA5-FTR-TO plasmid (Table S6) using X-tremeGENE 9 DNA transfection reagent following manufacturer's recommendations (Sigma-Aldrich, #6365787001). For the selection of inducible cell lines, Zeocin was replaced by 150 μg/ml Hygromycin B as indicated in the manufacturer's manual (Thermo Fisher Scientific). Protein induction was achieved by supplementation of the medium with 1 μg/ml doxycycline. To generate KO cells, we transfected HEK293 using TRANSIT-CRISPR (Sigma-Aldrich) with SygRNAs assembled with Cas9 (Sigma-Aldrich, #CAS9PROT-50UG) and tracrRNA (Sigma-Aldrich, #TRACRRNA05N-5NMOL), followed by cell serial dilution and selection of KO cell clones. Alternatively, we generated px459 derived plasmids including sequences targeting the genes of interest (pX459 was a gift from Feng Zhang; Addgene plasmid #62988). These plasmids were transiently transfected into HEK293 cells using X-tremeGENE 9. Cells expressing the construct were selected with 1 μg/ml puromycine for 96 h, followed by cell serial dilution to obtain individual clones. To generate TRIM25 KO cells, HEK293 were transfected with 200 ng GeneArt CRISPR nuclease mRNA (Thermo Fisher Scientific, #A29378) along with 50 ng of two distinct, *in vitro* transcribed sgRNAs targeting sequences in exon 1 of the TRIM25 gene. Single cells were seeded, grown and checked for KO by western blotting.

Cell culture in SILAC media

Cells were grown in SILAC DMEM media (Thermo Scientific, #10107883) containing 10% dialysed FBS (Silantes GmbH, #281000900) and isotopic labeled arginine and lysine (Silantes GmbH amino acids: L-Arginine 13C,15N labeled #201604102; L-Arginine 13C labeled #201204102; L-Lysine 13C,15N labeled #211604102; 4.4.5.5.-D4-L-Lysine #211104113). Prior to experiments, we confirmed by mass spectrometry that the incorporation of isotopic labeled amino acids was superior to 98% using whole cell lysates.

Viruses

We used the SINV clone pT7-SVwt (Sanz and Carrasco, 2001) to generate the SINV suspension. The plasmid pT7-SVmCherry was generated by inserting mCherry after the duplicated subgenomic promoter in pT7-SVwt. To obtain SINV and SINV-mCherry viruses, pT7-SVwt and pT7-SVmCherry plasmids were first linearized with XhoI and used as a template for *in vitro* RNA transcription with HiScribe T7 ARCA mRNA kit (New England Biolabs, #E2065S). Transcribed genomic RNA was transfected into BHK-21 using Lipofectamine 2000 reagent (Invitrogen, #11668027). Viruses were collected from the supernatant 24 h later and cleared by centrifugation at 2000 rpm for 3 min followed by filtration with 0.45μm PVDF syringe filter units (Merck, #SLHV033RS). Cleared supernatants were titrated by plaque assay using BHK-21 cells.

Pseudotyped HIV-$1_{Nef\text{-}mCherry}$ and HIV-$1_{Gag\text{-}mCherry}$ were produced as follows. For HIV-$1_{Nef\text{-}mCherry}$, a sequence encoding the end of *env* followed by a linker, mCherry, T2A self-cleaving peptide and the beginning of Nef protein was synthesized using the GeneArt Gene synthesis service (Thermo Fisher Scientific), and cloned between the BamHI and XhoI restriction sites of pNL4-3.Luc.R-E- plasmid (NIBSC – Centre for AIDS Reagents, #2128), which is defective for Vpr and Env. For HIV-$1_{Gag\text{-}mCherry}$, a PSPXI restriction site flanked by flexible linker was introduced into *gag* of the pNL4-3 plasmid (NIBSC – Centre for AIDS Reagents, #2006) by overlapping PCR (primers in Table S6) as in (Müller et al., 2004). mCherry sequence was amplified by PCR flanked by PspXI restriction sites and cloned into pNL4-3 using the newly generated PspXI site. Finally, the fragment between SpeI and BamHI was replaced by that of pNL4-3.Luc.R-E-. Pseudotyped viral particles were produced by co-transfecting HEK293T cells (kindly provided by Prof. Jan Rehwinkel, University of Oxford, UK) with pNL4-3.R-E-$_{Nef\text{-}mCherry}$ or pNL4-3.R-E-$_{Gag\text{-}mCherry}$ plus pHEF-VSVG (NIH AIDS Reagent Program, #4693), which encodes for the glycoprotein of vesicular stomatitis virus (VSV).

METHOD DETAILS

RNA interactome capture

Comparative RNA interactome capture (cRIC) was performed based on the previously described protocol (Castello et al., 2012; Castello et al., 2013) with the following alterations: HEK293 cells, previously grown in media with isotopic labeled amino acids, were seeded in three sets of 3x15 cm dishes at 80% confluence, each set with a different SILAC label. One set of dishes remained uninfected and two sets were infected with SINV at a multiplicity of infection (MOI) of 10. One of these infected cell sets was incubated for 4 h and the other for 18 h. To correct for isotope-dependent effects, we permutated the SILAC labels between the three conditions in the three biological replicates. After incubation, cells were irradiated with 150 mJ/cm^2 of UV light at 254 nm, and lysed with 3 mL of lysis buffer (20 mM Tris-HCl pH 7.5, 500 mM LiCl, 0.5% LiDS wt/vol, 1 mM EDTA, 0.1% IGEPAL (NP-40) and 5 mM DTT). Lysates were homogenized by passing the lysate at high speed through a 5 mL syringe with a 27G needle, repeating this process until the lysate was fully homogeneous. 400 μl of lysate were taken for total proteome and transcriptome analysis (Figure 3; Tables S3 and S4). Protein content was measured using a kit compatible with ionic detergents (Thermo Fisher, Pierce 660nm Protein Assay Kit #22662 with IDC reagent #22663) and equal amounts of each of the three lysates were mixed. The final volume was adjusted to 9 mL and 1.5 mL of pre-equilibrated oligo$(dT)_{25}$ magnetic beads (New England Biolabs, #S1419S) were added and incubated for 1 h at 4°C with gentle rotation. Beads were collected in the magnet and the lysate was transferred to a new tube and stored at 4°C. Beads were washed once with 10 mL of lysis buffer, incubating for 5 min at 4°C with gentle rotation, followed by two washes with 10 mL of buffer 1 (20 mM Tris-HCl pH 7.5, 500 mM LiCl, 0.1% LiDS wt/vol, 1 mM EDTA, 0.1% IGEPAL and 5 mM DTT) for 5 min at 4°C with gentle rotation and two washes with buffer 2 (20 mM Tris-HCl pH 7.5, 500 mM LiCl, 1 mM EDTA, 0.01% IGEPAL and 5 mM DTT). Beads were then washed twice with 10 mL of buffer 3 (20 mM Tris-HCl pH 7.5, 200 mM LiCl, 1 mM EDTA and 5 mM DTT) at room temperature. Beads were resuspended in 900 μl of elution buffer and incubated for 3 min at 55°C with agitation. Eluates were stored at −80°C and beads were recycled as indicated in the manufacturer's manual, and re-used for two additional capture rounds. For RIC experiments followed by western blot analysis, we used the small scale RIC settings described in (Castello et al., 2013).

Conventional protein analyses

Samples were resolved on SDS-PAGE and analyzed by i) western blotting using specific antibodies, the Li-Cor Odyssey system for visualization and the Image Studio Lite software (Li-Cor) for quantification, ii) Coomassie blue staining with the InstantBlue Protein Stain reagent (Expedeon, #ISB1L) or iii) silver staining using SilverQuest kit (Invitrogen, #LC6070). Data shown in the manuscript are representative gels from at least three independent replicates. Details on antibodies can be found in the key resource table. Radioactive labeling of newly synthesized proteins was performed by replacing the growth media for 1 h with DMEM lacking methionine and cysteine and supplemented with Easytag EXPRESS^{35}S Protein Labeling Mix [^{35}S]Met-Cys (Perkin Elmer, #NEG772002MC). Samples were then analyzed by SDS-polyacrylamide gels (15%) followed by autoradiography.

Reverse-transcription and quantitative PCR

Total RNA was isolated using TRIzol (Invitrogen, #15596026). Reverse transcription was performed using Superscript III reverse transcriptase (Invitrogen, #18080044) with random hexamers priming (Invitrogen, #N8080127), following manufacturer's instructions. RT-qPCR analysis was performed with 2x qPCR SyGreen Mix Lo-ROX (PCRBiosystems, #PB20.11-01) and gene specific primers (Table S6) in a BioRad CFX96 Real-Time system, and analyzed with REST software (Pfaffl, 2001).

Plasmids and recombinant DNA procedures

Plasmids for generation of inducible cell lines were created by conventional cloning methods. Inserts were generally amplified from HEK293 cDNA or template plasmids using specific primers (Table S6). Inserts were cloned into the pcDNA5/FRT/TO with eGFP preceded or followed by a flexible linker encoding for GGSGGSGG (glycine and serine repeats) to facilitate the folding of the RBP of interest independently from the eGFP. For CRISPR/Cas9 expression plasmids, annealed oligos were inserted into the BbsI site of px459.

mCherry-based viral fitness assay

$5x10^4$ cells were seeded on each well of a 96-well microplate with flat μClear bottom (Greiner Bio-One, #655986) in DMEM lacking phenol-red and supplemented with 5% FBS and 1 mM sodium pyruvate. Cells (control, knock-out and Tet-on) were infected with SINV-mCherry at 0.1 MOI in complete DMEM (lacking phenol-red) with 2.5% FBS. Cells were incubated at 37°C and 5% CO_2 in a CLARIOstar fluorescence plate reader (BMG Labtech) for 24 h; eGFP and/or mCherry signal was monitored by measuring fluorescence (eGFP: excitation 470 nm, emission 515 nm; mCherry: excitation 570 nm, emission 620 nm) every 15 min. To monitor the shut off of protein synthesis with this method (Figure S1B), Tet-on HEK293 eGFP-control cells were induced with 1 μg/ml doxycycline for 4 h and then infected as indicated above. In experiments with HIV-1 mCherry replicons, $5x10^4$ cells were seeded on each well of a 96-well plate in clear DMEM supplemented with 2.5% FBS and 1 mM sodium pyruvate, and infected with pseudotyped HIV-$1_{Nef\text{-}mCherry}$ or HIV-$1_{Gag\text{-}mCherry}$. mCherry signal was monitored for 72 h in a fluorescence plate reader as indicated above. In overexpression experiments, Tet-on HEK293 cells expressing RBP-eGFP fusion proteins were either induced with 1 μg/ml doxycycline for 16 h or mock-induced and then infected with SINV-mCherry. In inhibitor assays, HEK293 cells were infected with SINV-mCherry as above and inhibitors or vehicle (DMSO) were added at 1 hpi at the concentrations indicated in the figures. Statistical significance of the difference in mCherry expression at 18 and 24 hpi was determined by t test (n = 9).

Drugs and cell viability assay

The following chemical inhibitors were used in this work: cyclosporin A (Insight Biotechnology Ltd, #sc-3503), Ganetespib (Cambridge Bioscience Ltd, #19432), Geldanamycin (Cambridge Bioscience Ltd, #SM55-2), 4μ8C (Merck Chemicals, #412512) and WS6 (Cambridge Bioscience Ltd, #17672). To test cell viability at the concentrations used, $5x10^4$ HEK293 cells were seeded on each well of a 96-well microplate with flat, transparent bottom and incubated with DMEM (no phenol red) supplemented with 5% FBS and 1 mM sodium pyruvate. 24 h later cells were treated with the compounds and incubated for another 24 h at 37°C and 5% CO_2. Cell viability was estimated by adding CellTiter 96 Aqueous One Solution (Promega, #G3580) and measuring 490 nm absorbance following the manufacturer's recommendations. To evaluate cell viability and proliferation in knockout cells, $2.5x10^4$ cells were seeded per well of a 96-well plate and incubated in DMEM (no phenol red, 5% FBS, 1mM sodium pyruvate) at 37°C and 5% CO_2. Cell viability was measured at the indicated times using CellTiter 96 Aqueous One Solution as described above. In parallel, the number of cells was counted using the Countess II FL Automated Cell Counter (Thermo Fisher Scientific).

Protein-protein interactions analysis

$4.2x10^6$ HEK293 Tet-on cells expressing eGFP or GEMIN5-eGFP proteins were seeded on a 10 cm dish and incubated with DMEM supplemented with 10% FBS and 1 μg/ml doxycycline. After 24 h, cells were infected with 10 MOI of SINV in DMEM lacking FBS and incubated for 1 h, followed by media exchange (DMEM with 1% FBS). Cells were harvested at 18 hpi and lysed in 1 mL of Triton-X-lysis buffer (10 mM Tris HCl pH 7.5, 150 mM NaCl, 1% Triton X-100, 5 mM $MgCl_2$, 5 mM DTT and 0.1 mM AEBSF serine protease inhibitor). For immunoprecipitation (IP), 40 μl GFP-Trap_A beads slurry (ChromoTek GmbH, #gta-20) were equilibrated in Triton-X-lysis buffer and then added to 500 μl of whole-cell lysate. Mixture was diluted with 4.5 mL of Triton-X-lysis buffer, and mixed with gentle rotation for 16 h at 4°C. GFP-Trap beads were washed once with Triton-X-lysis buffer, collecting the beads by gentle centrifugation after each wash (1000 g for 5 min at 4°C). In the second wash, the Triton-X-lysis buffer was supplemented with 1 μl/ml RNase A (Sigma Aldrich, #4642) and beads were incubated for 5 min at 37°C with gentle rotation. Beads were washed three additional times with Triton-X-lysis buffer. Proteins were released from the GFP-Trap beads via pH elution by resuspension in 50 μl 0.2 M glycine pH 2.5 for 30 s followed by collection of the beads through a quick spin. The supernatant was transferred to a new tube and neutralised with 5 μl of 1 M Tris base pH 10.4.

RBP-RNA interaction analysis: CLIP/RT-PCR

$6.5x10^5$ cells were seeded on each well of a 6-well plate and incubated in DMEM without phenol red and supplemented with 5% FBS and 1 μg/ml doxycycline. After 24 h, cells were either mock-infected or infected with SINV at a MOI of 10. At 18 hpi, culture media was removed and cells were irradiated with 150 mJ/cm^2 of UV light at 254 nm. Cells were lysed in 400 μl of lysis buffer (100 mM KCl,

5 mM $MgCl_2$, 10 mM Tris pH 7.5, 1% IGEPAL, 1 mM DTT, 100 U/ml Ribolock RNase inhibitor [ThermoFisher Scientific, #EO0381], 0.1 mM AEBSF, 200 μM ribonucleoside vanydil complex). Lysates were diluted with 5x high-salt buffer (1.25 M NaCl, 100 mM Tris pH 7.5, 0.1% SDS) and H_2O to reach 500 μl of 1x high-salt buffer. Lysates were then cleared by centrifugation (5000 rpm for 3 min at 4°C). Supernatants were transferred to a new tube and snap frozen in dry ice. An aliquot (50 μl) was taken as 'input'. Lysates were pre-cleared with 15 μl of pre-equilibrated control agarose beads (Pierce Control Agarose resin, Thermo Fisher Scientific, #26150) by incubation under gentle rotation for 30 min at 4°C followed by centrifugation at 1000 g for 2 min at 4°C. Supernatants were transferred to a new tube. 15 μl GFP-Trap_A bead slurry were equilibrated with 1x dilution buffer (500 mM NaCl, 1 mM $MgCl_2$, 0.05% SDS, 0.05% IGEPAL, 50 mM Tris pH 7.5, 100 U/ml Ribolock RNase inhibitor, 0.1 mM AEBSF), incubated with 1 mg/ml *E. coli* tRNA for 15 min and, after two washes with dilution buffer, they were added to the lysates. The mixture was incubated for 2 h at 4°C with gentle rotation and beads were recovered by centrifugation at 1000 g for 2 min at 4°C. Beads were washed twice with 100 μl of ice-cold high-salt buffer (500 mM NaCl, 20 mM Tris pH 7.5, 1 mM $MgCl_2$, 0.05% IGEPAL, 0.1% SDS, 100 U/ml Ribolock RNase inhibitor, 0.1 mM AEBSF), three times with 100 μl ice-cold low-salt wash buffer (150 mM NaCl, 20 mM Tris pH 7.5, 1 mM $MgCl_2$, 0.01% IGEPAL, 50 U/ml Ribolock RNase inhibitor) and resuspended in 50 μl of proteinase K buffer (100 mM NaCl, 10 mM Tris pH 7.5, 1 mM EDTA, 0.5% SDS). Protein digestion was carried out by incubation with 200 μg/ml of proteinase K (Invitrogen, #AM2546) for 30 min at 37°C with agitation (1100 rpm) and then raising temperature to 50°C for 1 h. After centrifugation at 1000 g and 4°C for 2 min, the supernatant containing the RNA was transferred to a low binding tube. RNA was then purified using RNeasy mini kit (QIAGEN, #74104) in parallel to the total RNA present in inputs. cDNA library was prepared with Superscript III reverse transcriptase and oligo$(dT)_{20}$ primer (Thermo Fisher Scientific, #18418020) following the manufacturer's recommendations. Finally, the presence of SINV sequences in cDNA libraries was detected by PCR using Phusion polymerase (New England Biolabs, #M0530S) and SINV C specific primers (Table S6).

Analysis of GEMIN5 binding sites by iCLIP

In order to identify GEMIN5 binding sites on SINV RNA at a high resolution, we employed iCLIP-seq (König et al., 2010). $10x10^6$ HEK293 Tet-on GEMIN5-eGFP cells were seeded in 5 sets of 3x15 cm dishes and induced for 24 h with doxycycline. Each cell set was then infected with 10 MOI of SINV. Similar procedure was carried out for 1 set 3x15 cm dishes of control HEK293 Tet-on eGFP cells with 8 h doxycycline induction. At 18 hpi, cells were washed with PBS 1x and UV irradiated with 150 mJ/cm^2 at 254 nm. Cells were then lysed with 1 mL of lysis buffer (NaCl 100 mM, $MgCl_2$ 5 mM, Tris pH 7.5 10 mM, IGEPAL 0.5%, SDS 0.1%, Na deoxycholate 0.5%, DTT 1 mM, 0.1 mM AEBSF) and the three plates of each condition set were pooled (3 mL of final volume). Lysates were then passed through a 27G needle three times and sonicated with three cycles of 10 s, with 15 s pause between pulses, using a Digenonde bioruptor at level M at 4°C. The homogenate was centrifuged 17900 g at 4°C for 10 min, and topped up to 3 mL with lysis buffer. To obtain RNA fragments of suitable length and to degrade DNA, 3 mL (replicates 1-2, control) or 1 mL (replicates 3-5) of thawed lysate was incubated with 20 U RNase I (Life Technologies, #AM2295) and 4 U Turbo DNase (Life Technologies, #AM2238) per ml of lysate for 3 min at 37°C, with 1100 rpm agitation. Subsequently, lysates were placed on ice and supplemented with 440 U RiboLock RNase Inhibitor. 40 μL of control agarose bead slurry per ml of lysate was pre-equilibrated in lysis buffer and resuspended in 50 μl of lysis buffer. Beads were added to the lysate and incubated for 30 min at 4°C with gentle rotation. The supernatants were then collected by centrifugation for 2 min at 4°C and 2500 g, and then incubated with 40 μL of pre-equilibrated GFP_trap_A beads per ml of lysate for 2 h at 4°C with gentle rotation. Next, the beads were collected by centrifugation (2 min, 4°C, 2500 g) and washed twice with 1 mL of high salt buffer (NaCl 500 mM, Tris HCl pH 7.5 20 mM, $MgCl_2$ 1 mM, IGEPAL 0.05%, SDS 0.1%, 0.1 mM AEBSF, 1 mM DTT), twice with 1 mL of medium salt buffer (NaCl 250 mM, Tris HCl pH 7.5 20 mM, $MgCl_2$ 1 mM, IGEPAL 0.05%, 0.1 mM AEBSF, 1 mM DTT), and twice with 1 mL of PNK wash buffer (20 mM Tris-HCl pH 7.4, 10 mM $MgCl_2$, 0.2% Tween-20) (replicates 1-2, GFP control) or low salt buffer (NaCl 150 mM, Tris HCl pH 7.5 20 mM, $MgCl_2$ 1 mM, IGEPAL 0.01%, 0.1 mM AEBSF, 1 mM DTT) (replicates 3-5). Beads were resuspended in 20 μL PNK mix [15 μL H_2O, 4 μL 5x PNK buffer pH6.5 (350 mM Tris-HCl pH 6.5, 50 mM $MgCl_2$, 25 mM DTT), 5 U of PNK enzyme (NEB, #M0201S), 20 U of Ribolock] and incubated for 20 min, at 37°C at 1100 rpm. Beads were then washed once with low salt buffer, once with high salt buffer, and twice with low salt or PNK wash buffer. Beads were then resuspended in 20 μL ligation mix [ligation buffer (50 mM Tris-HCl, 10 mM $MgCl_2$, 10 mM DTT), 10 U of RNA ligase (NEB, M0204S), 20 U of Ribolock, 1.5 μM pre-adenylated linker L3 (TriLink Biotechnologies, # T1-BGV01A), 4 μL PEG400 (Sigma-Aldrich, #202398-250G)] and incubated O/N at 16°C shaking at 1100 rpm. Subsequently, beads were washed with 500 μL of cold low salt or PNK wash buffer and three times with 1 mL of high salt buffer. Beads were transferred to a low binding tube during the third wash. The beads were further washed twice with 1 mL ice-cold low salt or PNK wash buffer and resuspended in 20 μL low salt or PNK wash buffer, 1x NuPAGE loading buffer (Invitrogen, #NP0007) and 100 mM DTT and denatured at 70°C (1200 rpm, 10 min). The supernatant was collected by centrifugation (1 min at 4°C and 2500 g), loaded on a 4%–12% Bis-Tris NuPage gel (Invitrogen, #NP0321) and run 90 min at 150 V in 1x MOPS running buffer (Life Technologies, #NP0001). Protein-RNA complexes were transferred to a membrane of nitrocellulose (30 V for 1 h). Region matching 190-280 kDa was then cut out, transferred to a fresh microfuge tube, topped up with 200 μL of proteinase K mix (80 mM Tris-Cl pH 7.4; 40 mM NaCl; 8 mM EDTA and 800 μg of proteinase K), and incubated for 20 min at 37°C and 1100 rpm. Subsequently, 200 μL of PKurea buffer (100 mM Tris-Cl pH 7.4; 50 mM NaCl; 10 mM EDTA; 7 M urea) was added and the sample then incubated for 20 min at 37°C at 1100 rpm. RNA was then phenol/chloroform extracted as in (Huppertz et al., 2014; König et al., 2010). Pellets were resuspended in 5 μL of nuclease free H_2O and stored at −20°C. Reverse transcription was carried out using Superscript III

(Life Technologies, #18080-044) and unique Rclip primers as in (Huppertz et al., 2014; König et al., 2010). The reaction was then transferred to a low DNA binding tube and precipitated with ethanol as in (König et al., 2010). The pellets were resuspended in 12 μL of 1x TBE-urea loading buffer, heated for 3 min at 80°C and separated on a 6% TBE-urea precast gel (Life Technologies, #EC6865BOX) for 40 min at 180 V. For replicates 1-2 and the control, the region of the gel corresponding to 85-200 nucleotides was cut off the gel and placed in a 0.5 mL microtube pierced with a needle inside a 1.5 mL microtube. Samples were spun at 16000 g for 1 min, and the flow-through topped up with 400 μl of diffusion buffer (0.5 M ammonium acetate, 10 mM magnesium acetate, 1 mM EDTA, 0.1% SDS) and incubated at 50°C for 30 min. For replicates 3-5, two regions of the gel containing cDNA fragments of 120-200 nucleotides and 85-120 nucleotides were cut off from the gel and crushed into small pieces using a pestle in 400 μL TE buffer. The samples were then incubated for 1 h at 37°C and 1100 rpm, placed on dry ice for 2 min, and incubated again for 1 h at 37°C and 1100 rpm. In all cases, the disrupted gel was then filtered by spinning through a Costar SpinX column (Sigma, #CLS8160-96EA) by centrifugation at 16000 g. The cDNA was then extracted using phenol/chloroform as in (König et al., 2010). Pellets were resuspended in 8 μL ligation mix [1x CircLigase Buffer II; 2.5 mM $MnCl_2$; 30 U of CircLigase II (Epicenter, #CL9025K)] and incubated for 1 h at 60°C. We next added 30 μL of oligo annealing mix [25 μL H_2O; 4 μL NEBuffer 4 (NEB, #B7004S); 0.3 μM cut_oligo (Sigma-Aldrich)] and the sample was heated for 1 min at 95°C followed by a temperature decrease of 1°C every 40 s until reaching 25°C. The samples were then digested with 2 μL of BamHI (Thermo Fisher, #FD0054) and incubated for 30 min at 37°C. After incubation at 80°C for 5 min, cDNA was ethanol precipitated (König et al., 2010). Pellets were resuspended in 20 μL H_2O and mixed with 1 μL of 10 μM primer mix P5/P3 Solexa and 20 μL Accuprime Supermix 1 (Life Technologies, #12342-010). The libraries were then amplified for 18 cycles (replicate 1), 23 cycles (replicate 2), 25 cycles (replicates 3-5) or 30 cycles (control GFP) and the products were then analyzed on a 6% TBE precast gel (Life Technologies, #EC6265BOX) in TBE buffer for 60 min at 140 V. The gel was stained with 1x TBE plus 1x SybrGold for 20 min (Life Technologies, #S11494) and bands of appropriate size cut out under blue light trans-illuminator. The gel slices were dissolved with a pestle in 100 μL diffusion buffer (0.5 M ammonium acetate; 10 mM magnesium acetate; 1 mM EDTA pH 8.0; 0.1% SDS), incubated for 30 min at 50°C at 1100 rpm and filtered in a Costar SpinX column as above. The library was purified using QIAquick Gel Extraction Kit (QIAGEN, #28704) and quantified on a Bioanalyser using a DNA high-sensitivity chip. Libraries were pooled for sequencing and processed using single-end sequencing mode with a NextSeq 500/550 High Output v2 kit (75 cycles, Illumina, #FC-404-2005).

Immunofluorescence and RNA FISH assays

High Precision Coverslips (Marienfeld, #0107052) were washed once in 1 M HCl for 30 min on a rocking machine, twice in double distilled water for 10 min and once in ethanol 70% for 10 min. 150,000 cells were seeded on the dried coverslips and incubated in DMEM with 10% FBS. In the case of the Tet-on cells, protein induction was performed with 1 μg/ml doxycycline. 16 h later cells were either mock-infected or infected for 1 h at 37°C with 10 MOI of SINV in DMEM without FBS, followed by the replacement of the medium with DMEM supplemented with 1% FBS. At the corresponding times post-infection, cells were rinsed once in PBS and fixed in 4% methanol-free formaldehyde for 10 min. After three 5 min washes in PBS, cells were permeabilised for 5 min with 1x PBS supplemented with 0.1% Triton X-100 (PBST). Next, cells were rinsed twice in PBST and once in PBST supplemented with 2% BSA, and blocked for 1 h with PBST supplemented with 2% BSA. Cells were later incubated for 1 h with primary antibodies (α-SINV C at 1:200 dilution or α-XRN1 at 1:50 dilution) in PBST + 2% BSA. Cells were subsequently rinsed in PBST + 2% BSA and washed three times with PBST + 2% BSA for 10 min. Cells were then incubated for 1 h in darkness with the secondary antibodies (α-rabbit Alexa488, α-rabbit Alexa594 or/and α-mouse Alexa488; Thermo Fisher Scientific, #A-21206, #A-21207, #A-21202 respectively) and/or GFP-Booster_Atto488 (ChromoTek GmbH, #gba488-100) at 1:500 dilution in PBST supplemented with 2% BSA. Cells were washed once with PBST supplemented with 2% BSA and three additional times with PBST supplemented with 2% BSA for 10 min. Cells were incubated with 2 μg/ml of DAPI in PBS for 5 min. Finally, cells were washed twice in PBST, once in PBS for 5 min, once in milliQ H_2O and mounted on glass slides using Vectashield Antifade mounting medium (Vector Laboratories, #H-1000).

For combined immunofluorescence and RNA FISH, cells were seeded in coverslips and fixed and permeabilised as described above. Then, cells were rinsed three times in PBST and incubated for 1 h with primary antibody (α-SINV C at 1:200 dilution) in PBST + 0.5 U/μl RiboLock RNase inhibitor. Next, cells were washed once in PBST and three additional times with PBST for 10 min. Cells were then incubated with secondary antibody (α-rabbit Alexa488 at 1:500 dilution) in PBST supplemented with 0.5 U/μl RiboLock RNase inhibitor for 1 h in darkness. Cells were washed once with PBST, and two additional times with PBST for 10 min, once in PBS for 10 min and fixed again in 4% methanol-free formaldehyde for 10 min. Cells were washed twice in PBS for 5 min, once in 1x PBS / 1x SSC for 5 min, once with 2x SSC for 5 min and twice with pre-hybridization buffer (2x SSC and 10% deionized formamide in DEPC water) at 37°C for 10 min. Next, cells were incubated with RNA probes [2 pmol/μl $oligo(dT)_{25}$ or $oligo(dA)_{25}$ coupled to Alexa 594 (Life technologies Ltd), or 125 nM SINV RNAs-specific Stellaris probes (LGC Biosearch Technologies)] in hybridization buffer (2x SSC, 10% deionized formamide and 10% dextran sulfate in DEPC water) for 16 h at 37°C in a wet chamber. In the case of Tet-on cells expressing GEMIN5-eGFP or MOV10-YFP proteins, GFP-Booster_Atto488 (1:500 dilution) was included at this step. Cells were subsequently washed twice with pre-hybridization buffer for 10 min at 37°C and incubated for 5 min at 37°C with 2 μg/ml DAPI in pre-hybridization buffer. Finally, cells were washed twice with 2x SSC for 5 min, twice with 1x PBS, once for 5 min with 1x PBS and once in milliQ H_2O. The coverslip was mounted immediately after on glass slides using Vectashield.

In both cases, images were acquired on an API DeltaVision Elite widefield fluorescence microscope using a 100X oil UPlanSApo objective (1.4 NA) and deconvolved with SoftWoRx v6.5.2 (GE Healthcare). Fluorescence intensity profiles were obtained using the

script "Multichannel Plot Profile" in the BAR collection for ImageJ (https://imagej.net/BAR). In Figures 4 and S4, RBPs were classified as 'enriched' when accumulating in viral factories co-localizing with SINV C; 'absent' when undetectable in viral factories; and 'diffused' RBPs when distributed across the cytoplasm and thus present but not enriched in viral factories.

Determining the percentage of infected cells

$9x10^5$ HEK293 cells were seeded on washed coverslips and incubated in DMEM minus phenol red + 5% FBS + 1 mM sodium pyruvate for 24 h. Cells were infected with different MOI of SINV-mCherry in complete DMEM (lacking phenol-red) with 2.5% FBS. At 18 hpi, cells were fixed and processed for immunofluorescence as indicated above using α-SINV C antibody and DAPI. Images were acquired on an API DeltaVision Elite widefield fluorescence microscope using a 60X oil PlanApo objective (1.42 NA). The percentage of infected cells was calculated by counting C-expressing cells and the total number of DAPI-stained cells using the "Cell Counter" plugin in ImageJ. To define the MOI of SINV used in cRIC experiments and fitness assays, different concentration of viruses were tested. We selected 10 MOI for cRIC experiments because it is the minimal dose promoting high percentage of infected cells in a reproducible manner. We selected 0.1 MOI for fitness experiments as it allows optimal measurement of the mCherry fluorescence in the CLARIOstar plate reader.

Mass spectrometry

cRIC inputs (whole cell lysates) and eluates were processed following the filter aided sample preparation (FASP) as in (Castello et al., 2013). GEMIN5-eGFP and eGFP IPs were processed with a single-pot solid-phase-enhanced sample preparation (SP3) protocol using 70% acetonitrile for protein binding (Sielaff et al., 2017). All samples were acidified with 5% formic acid prior to mass spectrometric analysis.

Peptides from the cRIC inputs, and GEMIN5-eGFP and eGFP IPs were analyzed on an Ultimate 3000 ultra-HPLC system (Thermo Fisher Scientific) and electrosprayed directly into a QExactive mass spectrometer (Thermo Fisher Scientific). They were initially trapped on a C18 PepMap100 pre-column (300 μm inner diameter x 5 mm, 100Å, Thermo Fisher Scientific) in solvent A (0.1% [vol/vol] formic acid in water). The peptides were then separated on an in-house packed analytical column (75 μm inner diameter x 50cm packed with ReproSil-Pur 120 C18-AQ, 1.9 μm, 120 Å, Dr. Maisch GmbH) using a linear 15%–35% [vol/vol] acetonitrile gradient (2 h for whole cell lysates and 1 h for protein-protein interaction samples) and a flow rate of 200 nl/min. Full-scan mass spectra were acquired in the Orbitrap (scan range 350-1500 m/z, resolution 70000, AGC target 3×10^6, maximum injection time 50 ms) in a data-dependent mode. After the mass spectrum scans, the 20 (for whole cell lysates) or 10 (GEMIN5 IPs) most intense peaks were selected for higher-energy collisional dissociation fragmentation at 30% of normalized collision energy. Higher-energy collisional dissociation fragmentation spectra were also acquired in the Orbitrap (resolution 17500, AGC target 5×10^4, maximum injection time 120 ms) with first fixed mass at 180 m/z.

For cRIC eluates, liquid chromatography (LC) was performed using an EASY-nano-LC 1000 system (Thermo Fisher Scientific) in which peptides were initially trapped on a 75 μm internal diameter guard column packed with Reprosil-Gold 120 C18, 3 μm, 120 Å pores (Dr. Maisch GmbH, #r13.9g) in solvent A using a constant pressure of 500 bar. Peptides were then separated on a 45°C heated EASY-Spray column (50 cm x 75 μm ID, PepMap RSLC C18, 2 μm, Thermo Fisher Scientific #164540) using a 3 h linear 8%–30% [vol/vol] acetonitrile gradient and constant 200 nl/min flow rate. Peptides were introduced via an EASY-Spray nano-electrospray ion source into an Orbitrap Elite mass spectrometer (Thermo Fisher Scientific). Spectra were acquired with resolution 30000, m/z range 350-1500, AGC target $1x10^6$, maximum injection time 250 ms. The 20 most abundant peaks were fragmented using CID (AGC target $5x10^3$, maximum injection time 100 ms, normalized collision energy 35%) in a data dependent decision tree method.

Peptide identification and quantitation of all proteomics experiments was then performed using MaxQuant (v1.5.0.35) (Cox and Mann, 2008). Data were searched against the Human Uniprot database (version, January 2016) alongside a custom database including all the known SINV polypeptides and a list of common contaminants provided by the software. eGFP protein sequence was included in the analysis of GEMIN5-eGFP and eGFP IPs (Uniprot ID C5MKY7). The search parameters for the Andromeda search engine were: full tryptic specificity, allowing two missed cleavage sites, fixed modification was set to carbamidomethyl (C) and the variable modification to acetylation (protein N terminus), oxidation (M). Match between runs was applied. All other settings were set to default, leading to a 1% FDR for protein identification. Raw and processed proteomic data have been deposited to the ProteomeXchange Consortium (Deutsch et al., 2017) via the PRIDE partner repository with the dataset identifier PXD009789.

RNA sequencing

RNA from the 'inputs' (whole cell lysate) of cRIC experiments was extracted using TRIzol. Strand-specific RNA-seq was performed with 100 ng of total RNA. Libraries were prepared using NEBNext Ultra Directional RNA library Prep Kit for Illumina (New England Biolabs, #E7420S) according to manufacturer instructions. In brief, RNA was fragmented for 15 min at 94°C and then reverse transcribed. cDNA and double-stranded cDNA was purified with AMPure XP beads (Beckman Coulter, #A63881). After end repair, NEBNext Adaptors for Illumina (New England Biolabs, #E7335S) were ligated onto the cDNA according to the kit manual. Libraries were amplified by 15 cycles of PCR. We used the following combination of barcodes for sample multiplexing: S1_Mock ATCACG, S1_SV4h CGATGT, S1_SV18h TTAGGC, S2_Mock ACAGTG, S2_SV4h CAGATC, S2_SV18h ACTTGA, S3_Mock GATCAG, S3_SV4h TAGCTT and S3_SV18h GGCTAC. Libraries with an average length of 320 nt were pooled and sequenced with an Illumina

NextSeq instrument, using 78 nt paired-end sequencing mode with a NextSeq 500/550 High Output v2 kit (150 cycles, Illumina #FC-404-2002). Raw and processed RNA-seq are available at GEO: GSE125182.

QUANTIFICATION AND STATISTICAL ANALYSES

Proteomic quantitative analysis

To compare the cRIC inputs and eluates under different conditions, peptide intensity ratios between two samples were computed and summarized. The log2-intensity ratio of each protein was tested to be different from zero in the three biological replicates using moderated t test, which is implemented in the R/Bioconductor package limma (Smyth, 2004). p values were corrected for multiple testing by controlling the false discovery rate with the method of Benjamini-Hochberg. For proteins for which the protein intensity was 'zero' in one of the two conditions, we applied a semiquantitative approach that assumes that proteins without quantitative information are below the detection limit (Sysoev et al., 2016). The approach compiles the number of replicates in each condition in which a given protein has an intensity value. When comparing 2 conditions and three biological replicates, this leads to a matrix with 16 different groups (detected 0, 1, 2 or 3 times in condition 1 versus detected 0, 1, 2 or 3 times in condition 2). A protein is classified as 'altered RBP' by the semiquantitative method if an intensity value is assigned to it in 3 or 2 of the replicates in one of the two conditions, while only 1 or 0 intensity values are detected in the other condition.

The fraction of RNA-bound RBPs was determined by computing the ratio between the protein intensity of each individual RBP in the cRIC eluates and that in the whole cell lysate (Figure S3D). Hence, this calculation reflects amount of protein crosslinked to RNA (cRIC eluates) divided by the total amount of protein (cRIC inputs).

Results were visualized using the R package ggplot2 (Wickham, 2009). To assess the scope of previously known RBPs within the RBPome of uninfected and SINV-infected HEK293 cells, proteins identified by cRIC here were compared to those compressing the superset of human RBPs reported in (Hentze et al., 2018). GO annotations were obtained from the R package mRNAinteractomeHeLa (http://www.hentze.embl.de/public/RBDmap/) (Castello et al., 2012) (Key Resources Table), and gene set enrichment analysis was performed by applying Fisher's exact test to categories of GO annotations with at least three annotated proteins.

We compared the repertoire of RBPs with differential RNA-binding activity at 18 hpi (Table S1) with the mouse ribo-interactome (Table S2) (Simsek et al., 2017). Specifically, we considered proteins in the Table S3 of (Simsek et al., 2017) with negative predictive values (NPV) $\geq$ 0.99 in puromycin and RNase samples as 'ribosome-associated proteins', as described in that study. To find mouse orthologs for RBPs responding to SINV infection, we used the R package biomaRt to identify ENSEMBL peptide IDs for our RBPome dataset and hom.Hs.inp.db (Carlson and Pages, 2015) to provide mapping between human and mouse proteins using these IDs (Key Resources Table). If a mouse ortholog of an altered RBP identified at 18 hpi was found in the 'ribo-interactome' (Simsek et al., 2017) or if the gene symbols between human and mouse matched directly, the human RBP was considered as 'ribosome-associated'. Results of this analysis are provided in Table S2.

For GEMIN5 protein-protein interaction analysis, protein quantification was performed by label free quantification using MaxQuant. Ratios were compiled and normalized to eGFP protein intensity in each sample, which is expected to be the same across samples. Significance of the fold changes was estimated by t test using the software Perseus (Tyanova et al., 2016). We performed three main comparisons with the data from the IPs: i) GEMIN5-eGFP versus eGFP both in uninfected cells; ii) GEMIN5-eGFP versus eGFP both in SINV-infected cells; and iii) GEMIN5-eGFP in uninfected cells versus GEMIN5-eGFP in SINV-infected cells (Figure 7C, left, middle and right, respectively). Resulting data are summarized in Table S5. Raw and processed proteomic data from GEMIN5-eGFP IPs have been deposited to the ProteomeXchange Consortium via the PRIDE partner repository with the dataset identifier PXD009789.

The R package ggplot2 was utilized to visualize GEMIN5-eGFP proteomics data in volcano plots (Figures 7C). Only proteins that were identified as high-confidence interactors of GEMIN5-eGFP (i.e., p value < 0.01 and positive log2 fold change) in the left panel of Figure 7C were displayed in the comparison between infected and uninfected cells in the right panel. Proteins with names starting with 'RPS' or 'RPL', were classified as 'ribosomal' and displayed in the volcano plots as pink dots.

STRING (Szklarczyk et al., 2017) was used to display the connectivity between altered RBPs in SINV-infected cells (Figures S2C and S2D) and between the proteins comprising the GEMIN5 interactome (Figure S7D). Protein networks were generated using the following parameters: display – confidence; Interaction sources – experiments and databases; interaction score – high-confidence (0.700). Disconnected nodes were hidden from display and nodes colored based on functional enrichment within the network as determined by STRING. GEMIN5 protein interactome (Figure S7D) was defined as proteins enriched in GEMIN5-eGFP IPs over eGFP IPs with p value < 0.01. STRING-based GO enrichment for GEMIN5 protein interactome is provided in Table S5.

RNA sequencing data analysis

We combined the human genome (version hg38) with SINV sequence as our reference genome. RNA-seq reads were then mapped to this reference genome using STAR (Dobin et al., 2013). Reads mapping to each transcript were counted with *featureCounts* in Subread software package (Liao et al., 2013). Only uniquely mapped reads are considered for counting. SINV infection is known to shut off transcription globally (Gorchakov et al., 2005), which may bias (underestimate) differential expression results if normalization is carried out assuming that overall RNA abundance remains unchanged. Therefore, we decided to normalize reach counts in each condition to the corresponding rRNA expression by dividing a factor proportional to the total rRNA read counts in 3 conditions

(0.899, 1 and 0.473 for Mock, 4 hpi and 18 hpi respectively). We confirmed by RT-qPCR that rRNA does not change in abundance in course of infection. The R package DESeq2 (Love et al., 2014) was used for differential gene expression analysis based on rRNA normalized read counts. As DESeq2 requires the reads counts to be un-normalized and in the form of integer values, rRNA normalized read counts were rounded to the closest integer to make the ''DESeqDataSet'' to start the differential analysis. We estimated the size factor of each sample separately in DESeq2, instead of pooling all the samples prior to estimating this parameter.

Differential RNA expression between infected (4 and 18 hpi) and uninfected cells was visualized in MA plots (Figures 3F and 3G) using DESeq2. To visualize the overall effect of experimental covariates and potential batch effects, a principal component plot of the samples was generated using the plotPCA function in DESeq2, based on the principal component analysis (PCA) of the variance stabilized expression of the top 500 genes with the highest expression variance among samples. As shown in Figure S3F, the variance explained by the first and second PC (on X and Y-axes) combined accounts for a high percentage (96%) of the total variance, and samples within the same condition clustered better between them than with the other two conditions. It is interesting to note that the first PC along accounts for 94% of the total variance, and it distinctly separates 18 hpi to the other samples (i.e., uninfected and 4 hpi), indicating that the cellular transcriptome is dramatically altered at 18 hpi.

Genes related to GO terms 'Response to virus' (GO:0009615) and 'Defense response to virus' (GO:0051607) were extracted from ''hsapiens_gene_ensembl'' dataset (GRCh37) from Bioconductor package biomaRt (Durinck et al., 2009) and plotted as a heatmap using the R package pheatmap (Kolde, 2015) (Figure S1E). This package was also used to make a heatmap for differentially expressed cellular RNAs, including those transcripts passing the following thresholds: i) log2 fold change > 3 or < −3 and ii) adjusted p value < 0.01 (Figure S3E).

Reads mapping to positive and negative strands of viral RNAs were separated using SAMtools *view* utility (Li et al., 2009). In Illumina reverse paired end sequencing, paired reads came from opposite strands. Therefore, reads with the second pair mapping to the positive strand, or with the first pair mapping to the negative strand, were both counted as mapping to the positive strand and vice versa. The total read counts mapping to each strand were compiled and counted using SAMtools *merge* and SAMtools *depth*, respectively.

Analysis of RNA synthesis, processing, and degradation

We used analysis of variance (ANOVA) to evaluate in what extent the changes in transcript levels are explained by the rate of RNA synthesis, processing and degradation. The measurement of the rate of these RNA processes for each individual RNA were obtained from (Mukherjee et al., 2017). We built a multiple linear regression using the rate of the above-mentioned RNA processes as 'predictors' or 'factors', and the transcriptome changes in SINV infected cells as the 'response variable'.

$$Ti = A0i + A1iDi + A2iPi + A3iSi + Ei$$

i indicates all the individual RNA molecules; Ti is the expression change for the molecule between the two conditions compared; A0i is the regression intercept; Di, Pi and Si are the rate of degradation, processing and synthesis, respectively; Ei is the 'error term' in the multiple linear regression.

After fitting the model, the total variance explained, or R-squared, is defined as the sum of squares (SS) contributed to the total SS by different factors, i.e., the three predictor variables and the error term, as indicated in the equation below:

$$SStotal = SSDegration + SSProcessing + SSSynthesis + SSerror$$

Therefore, the contribution of the three predictors to the alterations in the transcriptome can be measured by their proportion of SS. The partial SS for each predictor is obtained using the ''sequential sum of squares'' method implemented in ANOVA function in R (Key Resources Table). These data (mock compare to 4 hpi and mock compare to 18 hpi) are shown in Figure 5A. A more detailed description of ANOVA can be found in NIST/SEMATECH e-Handbook of Statistical Methods (https://www.itl.nist.gov/div898/handbook/eda/section3/eda355.htm).

iCLIP-seq data processing

To identify GEMIN5 binding sites on SINV RNAs, reads in the fastq files from sequencing were demultiplexed to separate the samples according to the sample barcodes. Molecular and sample barcodes as well as trailing adaptor sequences were trimmed off. Molecular barcode information was stored in the read name. Reads were then mapped to a combined human (GRCh38) and SINV genome (pT7-SVwt) sequence using STAR. Uniquely aligned reads were then extracted using SAMtools. Binding sites were determined as the 5′-most base of each uniquely mapped read. PCR duplicates were identified as reads with the same mapping position and molecular barcode and each unique fragment counted just once. The 5′-most base in sequenced reads corresponds to the base directly 3′ of the crosslinked base. The number of unique fragment counts per position gives a measure of GEMIN5 interaction strength with that position along the RNA.

Due to the sheer abundance of SINV RNA at 18 hpi, some background signal could be observed in GFP control. To account for this background, GFP signal was subtracted from GEMIN5 signal after correction to total SINV reads. Signal along SINV was then visualized individually per replicate (Figure S7) and as an average of all five replicates (Figure 7) as a coverage track and heatmap.

Because the binding sites are narrow (sharp) and hence difficult to see when plotting the full SINV region, the plot shows an average over a sliding window of 20 nt. Note that the negative signal from y axis (higher signal in GFP) is cut off to better highlight GEMIN5 enriched regions.

Significantly crosslinked sites were determined using iCount peaks (Key Resources Table). iCount peaks was run to generate a background distribution by randomly distributing the crosslinked sites a hundred times along the SINV genome and compare the actual observed distribution to this background to generate a false discovery rate. Since regions corresponding to genomic, subgenomic and 3′ end region have different overall abundance, they were indicated as individual gene segments in the calculation to account for potentially higher background. Sites meeting FDR cutoff of 0.01 within 5 nt of each other were then merged using iCount clusters to form binding sites. Binding sites were then given a 'strength score' calculated as counts within the binding site divided by its width, and visualized in a heatmap in five bins to differently highlight the strengths of binding at different sites (Figures 7 and S7). This process was done for the GEMIN5 replicates separately as well as for the library size normalized average of the five replicates. Figure 7D additionally shows a heatmap that indicates how many replicates support a genomic position as binding site when determined individually per replicate. ggplot2 was used to facilitate plotting the heatmaps.

To look at base composition around the start of the SINV sgRNA, the 5′-most base of unique fragments was extracted from aligned reads taking softclipping into account. Count per base relative to total count in the sgRNA region is show in Figure S7H to indicate relative binding site frequency and whether the sequenced base matches the genome.

Raw and processed iCLIP-seq data are available at GEO: GSE125182.

DATA AND SOFTWARE AVAILABILITY

The accession number for the mass spectrometry data reported in this paper is ProteomeXchange: PXD009789. The accession number for the RNA-seq and iCLIP data reported in this paper is GEO: GSE125182.

ARTÍCULO 5:

The initiation factors eIF2, eIF2A, eIF2D, eIF4A, and eIF4G are not involved in translation driven by Hepatitis C virus IRES in human cells

Uno de los objetivos principales de esta tesis es examinar la implicación de diferentes eIFs en la traducción viral. Una de las estrategias de los virus para evitar el requerimiento de diferentes eIFs es la presencia de elementos IRES en sus RNAs. Este es el caso de HCV, cuyo único mRNA posee un elemento IRES en su extremo 5'. Se han hecho muchos esfuerzos para averiguar el mecanismo preciso de iniciación de la traducción del mRNA de HCV. En este trabajo, se examina la participación de varios eIFs en este proceso. Para ello, se realizó un análisis comparativo con distintos mRNAs que expresan luciferasa como gen reportero bajo el control de diferentes IRES y secuencias */leader* con requerimientos conocidos de eIFs. Este estudio se llevó a cabo en las líneas celulares humanas Huh-7, derivada de células de hepatocarcinoma, y HAP1 wt y KO para eIF2A, eIF2D o doble KO para ambos (Horizon Discovery Group plc). Para analizar la participación de los diferentes eIFs, se emplearon: inhibidores conocidos para eIF2 y eIF4A, agentes que inducen el secuestro de eIF4G en SGs, y las líneas KO mencionadas. Nuestros resultados mostraron que ninguno de los inhibidores logró bloquear la síntesis de proteínas dirigida por el IRES de HCV. Por otra parte, también se estudió mediante inmunohistoquímica el efecto de varios compuestos en la salida de proteínas del núcleo al citoplasma y la formación de SGs, donde quedarían secuestrados factores que, en consecuencia, no podrían participar en la traducción del mRNA de HCV.

Finalmente, como varios estudios han sugerido que el eIF2 podría ser reemplazado por los factores eIF2A o eIF2D en condiciones de estrés (Terenin, Dmitriev et al. 2008, Dmitriev, Terenin et al. 2010, Skabkin, Skabkina et al. 2010, Kim, Park et al. 2011), se analizó la síntesis de proteínas dirigida por el IRES de HCV mediante la expresión del gen reportero luciferasa. Este ensayo se realizó en líneas celulares humanas KO para eIF2A, eIF2D o ambos factores en condiciones donde eIF2α estaba fosforilado. Nuestros resultados indicaron que ninguna de estas dos proteínas es requerida para la traducción del mRNA de HCV incluso cuando eIF2 está inactivo.

GONZALEZ-ALMELA, E., WILLIAMS, H., SANZ, M.A. & CARRASCO, L. 2018. The Initiation Factors eIF2, eIF2A, eIF2D, eIF4A, and eIF4G Are Not Involved in Translation Driven by Hepatitis C Virus IRES in Human Cells. *Front Microbiol*, 9: 207.

frontiers in Microbiology

ORIGINAL RESEARCH
published: 13 February 2018
doi: 10.3389/fmicb.2018.00207

The Initiation Factors eIF2, eIF2A, eIF2D, eIF4A, and eIF4G Are Not Involved in Translation Driven by Hepatitis C Virus IRES in Human Cells

*Esther González-Almela, Hugh Williams, Miguel A. Sanz and Luis Carrasco**

Centro de Biología Molecular Severo Ochoa (CSIC-UAM), Universidad Autónoma de Madrid, Madrid, Spain

Animal viruses have evolved a variety of strategies to ensure the efficient translation of their mRNAs. One such strategy is the use of internal ribosome entry site (IRES) elements, which circumvent the requirement for some eukaryotic initiation factors (eIFs). Much effort has been directed to unravel the precise mechanism of translation initiation by hepatitis C virus (HCV) mRNA. In the present study, we examined the involvement of several eIFs in HCV IRES-driven translation in human cells in a comparative analysis with mRNAs bearing the encephalomyocarditis virus or the Cricket paralysis virus IRES element. Consistent with previous findings, several inhibitors of eIF2 activity, including sodium arsenite, thapsigargin, tunicamycin, and salubrinal, had no inhibitory effect on the translation of an mRNA bearing the HCV IRES, and all induced the phosphorylation of eIF2α. In addition, hippuristanol and pateamine A, two known inhibitors of eIF4A, failed to block HCV IRES-directed translation. To test the release of nuclear proteins to the cytoplasm and to analyze the formation of stress granules, the location of the nuclear protein TIA1 was tested by immunocytochemistry. Both arsenite and pateamine A could efficiently induce the formation of stress granules containing TIA1 and eIF4G, whereas eIF3 and eIF2 failed to localize to these cytoplasmic bodies. The finding of eIF4A and eIF4G in stress granules suggests that they do not participate in mRNA translation. Human HAP1 cells depleted for eIF2A, eIF2D, or both factors, were able to synthesize luciferase from an mRNA bearing the HCV IRES even when eIF2α was phosphorylated. Overall, these results demonstrate that neither eIF2A nor eIF2D does not participate in the translation directed by HCV IRES. We conclude that eIF2, eIF4A, eIF2A, and eIF2D do not participate in the initiation of translation of HCV mRNA.

Keywords: regulation of protein synthesis, initiation factor of translation, inhibitors of eIF2, regulation of viral translation, eIF2 phosphorylation

OPEN ACCESS

Edited by:
Akihide Ryo,
Yokohama City University, Japan

Reviewed by:
Toru Okamoto,
Osaka University, Japan
Yoshihiro Shimizu,
RIKEN, Japan
Kyoko Tsukiyama-Kohara,
Kagoshima University, Japan

****Correspondence:***
Luis Carrasco
lcarrasco@cbm.csic.es

Specialty section:
This article was submitted to Virology, a section of the journal Frontiers in Microbiology

Received: *01 December 2017*
Accepted: *30 January 2018*
Published: *13 February 2018*

Citation:
González-Almela E, Williams H, Sanz MA and Carrasco L (2018) The Initiation Factors eIF2, eIF2A, eIF2D, eIF4A, and eIF4G Are Not Involved in Translation Driven by Hepatitis C Virus IRES in Human Cells. Front. Microbiol. 9:207. doi: 10.3389/fmicb.2018.00207

INTRODUCTION

Hepatitis C virus (HCV) is responsible for the vast majority of chronic viral hepatitis and induces hepatocarcinoma in humans (Hajarizadeh et al., 2013; Khullar and Firpi, 2015). HCV belongs to the *Flaviviridae* family and contains a 9.6 kb single-stranded RNA of positive polarity as its genome. Its genomic RNA is the only known viral mRNA and bears a single open reading frame (ORF)

encoding for a large polyprotein, which after proteolytic processing renders the mature viral proteins that participate in genome replication and in the assembly of new virus particles (Paul et al., 2014). Translation of HCV mRNA is promoted and regulated by an internal ribosome entry site (IRES) element that mediates the internal initiation of translation by supporting the interaction of components that participate in protein synthesis (Hellen and Pestova, 1999; Khawaja et al., 2015). Results from *in vitro* experiments initially suggested that the first step in the initiation of this viral mRNA involved the recruitment of initiation factors eIF3, eIF2, eIF5, GTP, initiator $tRNA_i^{Met}$ and a 40S ribosomal subunit by HCV IRES, yielding a 43S preinitiation complex (Pestova et al., 1998; Otto and Puglisi, 2004). Precise attachment of this complex at the initiation AUG codon forms a 48S complex in a process that does not involve eIF4F or the scanning of the 5′-UTR. The HCV mRNA has the ability to interact directly with the 40S ribosomal subunit, recruiting then eIF3 and the ternary complex. In this process, two modules of the IRES region, domains II and III, are necessary for the interaction with the small ribosomal subunit and eIF3 (Lukavsky, 2009; Khawaja et al., 2015; Yamamoto et al., 2015). Also, interaction of the HCV mRNA with preinitiation complexes bearing eIFs can take place, in a process that displaces eIF2, but requires eIF1A and eIF3 (Jaafar et al., 2016). Subsequently, the 60S ribosomal subunit interacts with this complex in a process mediated by eIF5B, which induces the release of eIF3 and leads to the formation of the 80S initiation complex, ready to start the elongation process. This mechanism of internal initiation is in sharp contrast to the canonical initiation of cellular capped mRNAs. In this latter instance, the initiation of protein synthesis begins with the recognition of the cap structure by the eIF4F complex, which contains eIF4E, the cap recognition protein, eIF4G, a scaffolding protein, and eIF4A, which exhibits helicase activity in an ATP-dependent manner (Topisirovic et al., 2011). Once eIF4F is bound to the cap structure at the 5′ end of cellular mRNAs, the small 40S ribosomal subunit bearing eIF3 and the ternary complex eIF2-Met-$tRNA_i^{Met}$-GTP interact with the mRNA. In addition, other factors such as eIF1, eIF1A, and eIF5 bind to the small ribosomal subunit forming the 48S complex. Then, this complex scans the 5′-UTR until the initiator AUG codon is encountered (Sonenberg and Hinnebusch, 2009; Hinnebusch et al., 2016). Joining of the 60S ribosomal subunit is promoted by eIF5B concomitant with the release of the eIFs in a GTP-dependent manner. Aside from the requirement of only a few eIFs for the translation of HCV mRNA, a number of IRES *trans*-acting factors, which modulate HCV mRNA translation have been reported. These factors include NSAP1, La protein, hnRNP L and D, Gemin5, LSm1-7, IMP-1 and PCBP2; although their exact mechanism of action in the translation of this viral mRNA remains largely unknown (Niepmann, 2013).

The participation of eIF2 in the initiation of HCV mRNA translation is controversial. In principle, two different mechanisms can be followed: translation of HCV mRNA takes place with eIF2 when this factor is active under normal conditions; yet, IRES-driven translation occurs after inactivation of this factor by phosphorylation under stress conditions. Initial studies using reconstituted translation systems indicated that eIF2 was necessary for the translation of this viral mRNA *in vitro* (Pestova et al., 1998; Hellen and Pestova, 1999). Moreover, analyses using mRNAs bearing HCV IRES in cell free systems revealed the presence of eIF2 in the initiation complexes (Otto and Puglisi, 2004). However, the interaction of this viral IRES with preinitiation complexes displaces eIF2 from them (Jaafar et al., 2016). That said, a novel class of inhibitors of the formation of the ternary complex had no effect on HCV IRES-driven translation, whereas these compounds potently interfered with canonical protein synthesis (Robert et al., 2006). In addition, stress conditions that promote the phosphorylation of eIF2α and block cellular protein synthesis did not compromise HCV mRNA translation (Terenin et al., 2008; Kim et al., 2011; Dabo and Meurs, 2012; Jaafar et al., 2016). In light of this, several candidates have been put forward to replace eIF2 for protein synthesis promoted by HCV IRES under stress conditions. For example, eIF5B can substitute for eIF2 *in vitro* in the delivery of Met-$tRNA_i^{Met}$ to small ribosomal subunits directed by HCV mRNA (Terenin et al., 2008). Under these conditions, the initiation of protein synthesis by HCV mRNA only requires two initiation factors: eIF3 and eIF5B. Another proposal suggested that eIF2D can substitute for eIF2 when this factor is inactivated (Dmitriev et al., 2010; Skabkin et al., 2010). However, the possibility that eIF5B or eIF2D participate in the initiation of HCV mRNA in intact cells under stress conditions was not analyzed, and only *in vitro* observations were reported. The involvement of eIF2A for the translation of HCV mRNA in place of eIF2 in intact cells and in cell free systems, has also been proposed (Kim et al., 2011). Accordingly, Huh-7 cells depleted for eIF2A cannot translate luciferase driven by the HCV IRES in a bicistronic mRNA when eIF2α is phosphorylated. In contrast to these findings, recent results have shown that depletion of eIF2A or eIF2D or both factors in Huh-7 cells have no effect for the translation of HCV mRNA (Jaafar et al., 2016). Under stress conditions, only eIF1A, eIF5B, and eIF3 should be necessary to direct the synthesis of proteins by this viral mRNA. It has been speculated that under conditions in which eIF2 is non-functional, the initiator Met-$tRNA_i^{Met}$ can bind directly to the ribosome following a mechanism that does not require the ternary complex, but is directed by HCV IRES (Jaafar et al., 2016).

Although eIF2A and eIF2D can form a complex with Met-$tRNA_i^{Met}$ and deliver it to 40S or 80S ribosomes, their involvement in translation remains obscure. Indeed, early results demonstrated that eIF2A can interact with Met-$tRNA_i^{Met}$ and deliver it to the ribosome (Merrick and Anderson, 1975). However, this binding was much less efficient than that observed using genuine eIF2 on artificial templates and eIF2A was unable to promote the binding of Met-$tRNA_i^{Met}$ to globin mRNA (Adams et al., 1975). Moreover, a complex between Met-$tRNA_i^{Met}$ and eIF2D is formed in a GTP-independent fashion, which can interact with the 40S ribosomal subunit to deliver the initiator to the P site of the ribosome (Dmitriev et al., 2010). eIF2D could displace deacylated tRNA and mRNA from recycled 40S ribosomal subunits, and was also able to interfere with the formation of the 48S initiation complex promoted

by eIF2 (Skabkin et al., 2010). Both eIF2A and eIF2D are 65 kDa proteins. Deletion of the yeast ortholog of eIF2A or eIF2D has no effect on cell viability (Zoll et al., 2002; Dmitriev et al., 2010). Consistent with these observations, human cells depleted for the genes encoding these two initiation factors are also viable and global protein synthesis is unaffected (Sanz et al., 2017). Results from mammalian cells have suggested that eIF2A is involved in the translation of specialized cellular mRNAs that initiate translation with non-AUG codons (Liang et al., 2014; Starck et al., 2016). Elegant studies have recently implicated eIF2A in cancer progression because it is involved in the initiation of translation of upstream ORFs (Sendoel et al., 2017). However, mice deleted for the eIF2A gene are completely normal, supporting the concept that eIF2A is not necessary for the translation of both normal and specialized cellular mRNAs (Golovko et al., 2016).

Here, we examined the involvement of several eIFs in HCV IRES-driven translation in human cells. Our findings indicate that knock out human cells for eIF2A, eIF2D, or both, are not only viable, but also synthesize proteins in a manner similar to that of wild-type cells. In addition, by investigating the potential involvement of these two proteins for the translation of HCV mRNA, we demonstrate that these factors are not required for translation of this viral mRNA, even when eIF2α is phosphorylated.

MATERIALS AND METHODS

Cell Lines

Huh-7 cells are a well differentiated hepatocyte-derived cellular carcinoma cell line established by Nakabayashi et al. (1982). Cells were cultured in Dulbecco's Modified Eagle's Medium (DMEM, Thermo Fisher Scientific, Waltham, MA, United States) supplemented with non-essential amino acids, 4 μM glutamine, 10% fetal calf serum, 50 U mL^{-1} penicillin and 50 U mL^{-1} streptomycin.

Wild-type (WT) HAP1 human near-haploid cells and knock-out HAP1 cells for eIF2A (cat# HZGHC002650c001), eIF2D (cat# HZGHC002652c005) or double knock-cells (cat# HZGHC005122c010) were purchased from Horizon Discovery Group plc (Cambridge, United Kingdom). The eIF2A knockout (KO) cell line (gi|977380191|ref|NM_032025.4|) has a 16 bp deletion in exon 4 resulting in a frameshift that generates a protein of 108 amino acids in place of the original protein of 585 amino acids. The eIF2D KO cell line (gi|56699484|ref|NM_006893.2|) has a 10 bp deletion in exon 3 resulting in a frameshift that generates a protein of 103 amino acids in place of the original protein of 584 amino acids. The double KO line has the same 16 bp deletion in exon 4 of the single eIF2A KO cell line and a 22 bp deletion in exon 3 of eIF2D that generates a protein of 99 amino acids in place of the 584 amino acid protein. Cells were cultured in Iscove's Modified Dulbecco's Medium (IMDM, Invitrogen, Carlsbad, CA, United States) supplemented with 10% fetal calf serum.

All cell lines were maintained at 37°C with 95% humidity and 5% CO_2.

Plasmids and Reporter Constructs

The pT7HCV33core-Luc vector was kindly donated by Dr. Takashi Shimoike (National Institute of Infectious Diseases, Musashimurayama, Tokyo). It contains nucleotides 1–374 of the HCV genome followed by the firefly luciferase gene and finally the 3′ UTR of HCV. The construct is transcribed from a T7 polymerase promoter that precedes these sequences (Shimoike et al., 2009). The gene segments from HCV comprise the 5′ UTR containing the IRES, followed by the first 33 nucleotides of the HCV Core protein encoding a sequence that has previously been shown to be crucial for the proper function of the IRES (Reynolds et al., 1995). HCV-Luc RNA was *in vitro* transcribed from pT7HCV33core-Luc.

The pTM1-Luc vector was derived from pTM1 (Moss et al., 1990), and was constructed as described (Sanz et al., 2010). It contains a modified form of the encephalomyocarditis virus (EMCV) IRES along with the firefly luciferase gene. EMCV-Luc RNA was *in vitro* transcribed from pTM1-Luc.

The pT7-RLuc-ΔEMCV-IGR-FLuc vector has been previously described (Redondo et al., 2011). It contains the T7 promoter followed by the *Renilla* luciferase gene and a deactivated form of the EMCV IRES; it also contains the intergenic region of cricket paralysis virus (CrPV) followed by the firefly luciferase gene. CrPV-Luc RNA was *in vitro* transcribed from pT7-RLuc-ΔEMCV-IGR-FLuc.

The β-globin construct contains the leader sequence from the human β-globin gene followed by the firefly luciferase gene. A Cap.βGlobin-Luc transcript was obtained by *in vitro* transcription using pKS-GL-FL as a template, as described by Castello et al. (2009). This plasmid was kindly provided by Dr. Matthias Hentze and Dr. Francesca Moretti (EMBL, Heidelberg, Germany).

The pFKi389LucNS3-3_dg_JFH vector, which was kindly donated by Dr. Ralph Bartenschlager (Department of Molecular Virology, University of Heidelberg, Heidelberg, Germany), was used to obtain rep HCV-Luc RNA by *in vitro* transcription. This plasmid contains the T7 promoter sequence fused to nucleotides 1–389 of the JFH-1 consensus sequence, followed by the firefly luciferase gene, the EMCV IRES, the NS3-to-NS5B coding sequence, the 3′ NTR of JFH-1, the hepatitis delta virus genomic ribozyme (dg), and the T7 terminator sequence (Schaller et al., 2007). All plasmids contain the ampicillin resistance gene for selection purposes.

In Vitro Transcription

Plasmids were linearized with the appropriate restriction enzymes (pT7HCV33core-Luc: BamHI, pT7-RLuc-ΔEMCV-IGR-FLuc: BamHI, pTM1-Luc: XhoI, pKS-GL-FL: HindIII; pFKi389LucNS3-3_dg_JFH: MluI). All restriction enzymes were purchased from New England Biolabs (Ipswich, MA, United States). Linearized plasmids were used as templates for *in vitro* RNA transcription using T7 or T3 RNA polymerases (New England Biolabs, Ipswich, MA, United States), the m7G(5′)ppp(5′)G cap analog (New England Biolabs) was used for Cap.βGlobin-Luc transcription. Mixtures were incubated for 2 h at 37°C. *In vitro*-synthesized RNAs were treated with recombinant DNase I (RNase-free) (Takara Bio USA Inc., Terra

Bella, CA, United States) for 30 min at 37°C. All transcripts were transfected using Lipofectamine 2000 reagent (Invitrogen, Carlsbad, CA, United States) following the manufacturer recommendations.

Inhibitors

Pateamine A [purified as described (Bordeleau et al., 2005)] and hippuristanol (Bordeleau et al., 2006b) were kindly provided by J. Pelletier (McGill University, Montreal, QC, Canada). Sodium arsenite was obtained from Riedel-de Haën (Hanover, Germany), and thapsigargin, tunicamycin, salubrinal, and cycloheximide were purchased from Sigma–Aldrich (St. Louis, MO, United States). Inhibitors are described in **Table 1**.

Luciferase Activity Assay

Cells were lysed in a buffer containing 0.5% Triton X-100, 25 mM glycylglycine pH 7.8, 1 mM dithiothreitol and complete EDTA-free protease inhibitor cocktail (Roche Molecular Systems Inc., Pleasanton, CA, United States) at the concentration indicated by the supplier. Luciferase activity was determined using the Luciferase Assay System (Promega, Madison, WI, United States) and a Sirius Luminometer (Titertek-Berthold, Pforzheim, Germany).

As a control, cycloheximide (CHX) was added to block translation, in order to determine the luciferase synthesized in the absence of compounds during the 1st hour of transfection.

Antibodies

Goat polyclonal anti-TIA-1 (C-20) (catalog number sc-17519), rabbit polyclonal anti-eIF2α (catalog number sc-11386), mouse monoclonal anti-eIF2α (catalog number sc-133132), goat polyclonal anti-eIF3 (catalog number sc-16376), mouse monoclonal anti-eIF4A (catalog number sc-14211), goat polyclonal anti-eIF1 (catalog number sc-390122) antibodies were purchased from Santa Cruz Biotechnology (Dallas, TX, United States). Rabbit monoclonal anti-eIF1A antibody (catalog number ab172623) was purchased from Abcam (Cambridge, United Kingdom). Rabbit polyclonal anti-eIF2D antibody (catalog number 12840-1-AP) was purchased from Proteintech Group, Inc. (Rosemont, IL, United States). Rabbit polyclonal anti-eIF2A antibody (catalog number A301-949A-M) was purchased from Bethyl Laboratories Inc. (Montgomery, TX, United States). Rabbit polyclonal anti-phospho-eIF2α (serine 51) antibody (catalog number 9721) was purchased from Cell Signaling Technology Inc. (Danvers, MA, United States). Rabbit polyclonal antibody anti-eIF4GI has been obtained as previously described (Aldabe and Carrasco, 1995).

Anti-rabbit immunoglobulin G antibody coupled to peroxidase was purchased from Amersham (catalog number NA934V) (GE Healthcare, Chicago, IL, United States). Specific antibodies conjugated to Alexa 488 or Alexa 555 (A-21202 and A-21432, respectively) were obtained from Invitrogen (Carlsbad, CA, United States).

TABLE 1 | eIF2 inhibitors utilized in this study and the mechanisms by which they increase eIF2α phosphorylation.

Inhibitor	Mechanism of action
Sodium arsenite	Induces phosphorylation of eIF2α by activating heme-regulated inhibitor kinase, a member of the eIF2α-specific kinase subfamily.
Thapsigargin	Triggers the release of calcium to the cytoplasm from the endoplasmic reticulum, activating PERK which in turn phosphorylates eIF2.
Tunicamycin	Inhibits protein glycosylation and leads to endoplasmic stress.
Salubrinal	Inhibits the PP1/GADD34 complex which is known to dephosphorylate eIF2α.

Immunocytochemistry and Confocal Microscopy

Fixation, permeabilization and confocal microscopy were performed as described by Madan et al. (2008) using the LSM 710 confocal laser scanning and multiphoton microscope coupled to an inverted microscope (Axio Observer, Zeiss, Oberkochen, Germany). Bound primary antibodies were detected by secondary antibodies coupled to Alexa 488 or Alexa 555 (Molecular Probes Inc., Eugene, OR, United States). Nuclei were stained with DAPI (4′-6-diamidino-2-phenylindole). All images were collected and analyzed using Zeiss ZEN 2010 software.

Western Blotting

Cells were collected in sample buffer, boiled for 5 min and processed by SDS-PAGE. After electrophoresis, proteins were transferred to nitrocellulose membranes. Specific rabbit polyclonal antibodies raised against phospho-eIF2α (Ser 51), total eIF2α, eIF2A, and eIF2D were used at 1:1000 dilution in TBS with 3% bovine serum albumin and 0.1% Tween 20. Anti-rabbit immunoglobulin G antibody coupled to peroxidase (Amersham GE Healthcare, Chicago, IL, United States) was used as secondary antibody at a 1:5000 dilution. Protein bands were visualized with the ECL detection system (Amersham, GE Healthcare).

Statistical Analysis

Data analysis was performed using Excel (Microsoft, Redmond, WA, United States) and GraphPad Prism 6 (GraphPad Software Inc., La Jolla, CA, United States) softwares. Data are shown as mean with standard error. Statistical validation was done using two-way analysis of variance (ANOVA) followed by a Bonferroni *post hoc* test or one-way ANOVA with Tukey's *post hoc* test. Statistical significance is shown as: $^{*}p < 0.05$, $^{**}p < 0.01$, $^{***}p < 0.001$.

RESULTS

HCV IRES-Driven Translation Is Refractory to Inhibitors That Induce the Phosphorylation of eIF2α in Human Hepatic Cells

We sought to investigate the behavior of HCV IRES regarding its dependence on several eIFs under appropriate physiological

conditions. To accomplish this, we used the Huh-7 human hepatoma cell line. We first tested a monocistronic mRNA encoding for luciferase, bearing the HCV IRES at the 5′ end and containing the 3′-UTR of this RNA (HCV-Luc). The presence of the 3′-UTR is important because it is involved in modulating translation of HCV mRNA (Ito et al., 1998; Bai et al., 2013; Shwetha et al., 2015). To reproduce conditions similar to those found during HCV infection, we also tested a replicon of HCV (rep HCV-Luc), which contains the firefly luciferase gene, the EMCV IRES, the NS3-to-NS5B coding sequence, the 3′ NTR of JFH-1 and the hepatitis delta virus genomic ribozyme (dg) (Schaller et al., 2007). As controls, we employed an mRNA bearing the CrPV intergenic region (IGR) (CrPV-Luc), which does not require eIFs to initiate protein synthesis (Jan and Sarnow, 2002; Fernandez et al., 2014). We also employed the IRES of EMCV (EMCV-Luc), which uses eIF2 and eIF4A for translation (Welnowska et al., 2011), and a capped mRNA containing the globin 5′-leader sequence (Cap.βGlo-Luc), which follows the canonical mechanism for its translation. All these mRNAs encode luciferase as a reporter gene (Supplementary Figure 1).

Initially, we explored the action of different concentrations of several compounds that induce the phosphorylation of eIF2α. Accordingly, Huh-7 cells were first transfected with HCV-Luc and EMCV-Luc mRNAs for 1 h and the following compunds were added to the culture medium for a further 2 h: sodium arsenite (ARS), thapsigargin (TG), tunicamycin (TM), and salubrinal (SAL). The first three compounds activate kinases that induce eIF2α phosphorylation, whereas SAL inhibits eIF2α dephosphorylation (Boyce et al., 2005; Sanz et al., 2009; Vaughn et al., 2014; Garcia-Moreno et al., 2015). As a control, cycloheximide (CHX) was added to block translation, in order to determine the luciferase synthesized in the absence of compounds during the 1st hour of transfection. The four compounds tested blocked luciferase synthesis directed by EMCV IRES in a concentration-dependent manner, albeit to different extents and with different inhibitory concentrations (**Figure 1A**). By contrast, the same compounds exerted a stimulatory effect on HCV-Luc mRNA translation. Among the compounds, ARS and TG were the most potent inhibitors/stimulators. Accordingly, 100 μM ARS almost entirely inhibited EMCV-Luc translation and stimulated HCV-Luc translation by ∼250%. A similar result was obtained with 2 μM TG. TM also stimulated luciferase production from HCV-Luc ∼200% at 10 μg mL^{-1}, but the same concentration inhibited EMCV-Luc translation by only 30%. Higher concentrations of this compound further decreased the translation of EMCV-Luc, whereas the translation of HCV-Luc was partially inhibited. Perhaps this inhibition is due to the toxicity of TM at these high concentrations. A moderate inhibition of luciferase activity from EMCV-Luc was observed with SAL up to 200 μM (∼40%), and activity was completely inhibited at 400 μM. Conversely, the activity of HCV-Luc was stimulated ∼150–175% or remained unaltered in relation to the control.

To assess whether the compounds induced the phosphorylation of eIF2α, we performed western blotting on cell extracts using specific antibodies. A robust increase in eIF2α phosphorylation in Huh-7 cells was found with the four agents assayed, with the most potent being ARS (**Figure 1B**). We next tested the activity of the two most potent inhibitors, ARS and TG, on four different mRNAs: HCV-Luc, EMCV-Luc, CrPV-Luc, and Cap.βGlo-Luc. Two concentrations of the inhibitors were added 1 h after transfection of the different mRNAs, and CHX was also added as a control as before. We found that protein synthesis directed by both EMCV-Luc and Cap.βGlo-Luc was effectively blocked by both compounds (**Figure 1C**). Notably, HCV-Luc was stimulated by ARS and TG ∼150%. A comparable response was also found with CrPV-Luc mRNA, albeit with a stronger stimulation, overall indicating a similar behavior of both mRNAs in the presence of these inhibitors as regards to their dependence on eIF2. This stimulation of HCV and CrPV IRESs is probably due to the inhibition of global cellular translation by these compounds, thus reducing cellular mRNA competition.

The translation driven by rep HCV-Luc mRNA in the presence of ARS was also tested. To do this, Huh-7 cells were transfected with rep HCV-Luc mRNA for 1 h, and subsequently different concentrations of ARS were added to the culture medium for a further 2 h. The luciferase synthesis directed by rep HCV-Luc was stimulated ∼158% by treatment with 50 μM ARS (**Figure 1D**), which is in good agreement with the results obtained with HCV-Luc, suggesting that HCV does not require eIF2 for its translation under replication conditions. Curiously, ARS concentrations above 200 μM were inhibitory for rep HCV translation. This result suggests that some differences exist between the translation of the HCV-Luc mRNA and the rep HCV, which bears most of the viral coding sequences.

Requirement of eIF4A for IRES-Driven Translation

Two natural compounds of marine origin, hippuristanol (Hipp) and pateamine A (Pat A), have been characterized as potent blockers of eIF4A activity (Bordeleau et al., 2006a; Low et al., 2007). eIF4A is the helicase subunit of the eIF4F complex, which additionally contains eIF4E and eIF4G (Topisirovic et al., 2011). Both inhibitors have been shown to exhibit a dual inhibitory effect on some viral mRNAs (Garcia-Moreno et al., 2013; Gonzalez-Almela et al., 2015). To analyze the action of Hipp and Pat A on luciferase synthesis driven by the HCV, EMCV and CrPV IRES elements, different concentrations of these compounds were added 1 h after transfection for a further 2 h. Consistent with previous works (Garcia-Moreno et al., 2013; Gonzalez-Almela et al., 2015), both Hipp and Pat A potently blocked EMCV IRES-dependent luciferase synthesis in human hepatic cells. By contrast, both compounds had no detrimental effect on translation driven by HCV or CrPV IRESs in these cells, and in fact strongly stimulated translation (**Figure 2**). These results are consistent with the concept that eIF4F does not participate in protein synthesis directed by HCV IRES (Hellen, 2009; Niepmann, 2013).

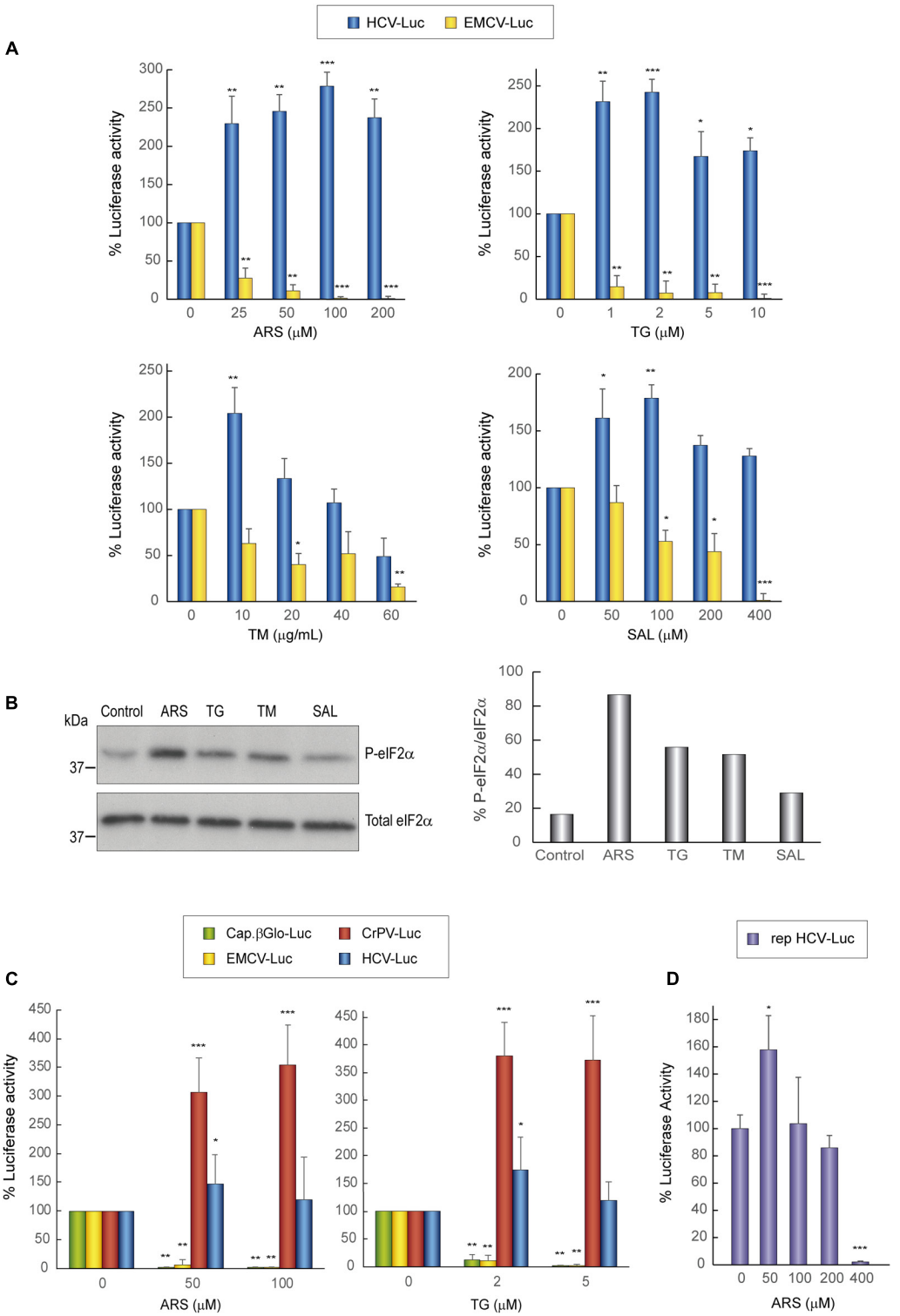

FIGURE 1 | Translation from the HCV IRES in Huh-7 cells is resistant to the action of eIF2 inhibitors. **(A)** Translation from the IRES of HCV or EMCV as measured by luciferase activity in response to eIF2 inhibitor treatment in Huh-7 cells. Cells were transfected with *in vitro* synthesized HCV-Luc or EMCV-Luc mRNAs for 1 h and then incubated with either cycloheximide CHX (5 μg mL^{-1}) or ARS, TG, SAL, or TM for a further 2 h. Percentage change is relative to that in the non-treated control (inhibitor concentration = 0). The readings from CHX treatments were subtracted from all as a baseline. Error bars represent the standard error of the mean, $n = 3$. **(B)** Inhibitor treatment induces eIF2 phosphorylation in Huh-7 cells. Cells were transfected with *in vitro* synthesized HCV-Luc RNA as above and then treated or not

(Continued)

FIGURE 1 | Continued
with ARS (100 μM), TG (5 μM), TM (40 μg mL^{-1}), or SAL (200 μM) for 2 h. Proteins were resolved by SDS-PAGE and blots were probed with antibodies against phospho-eIF2α and total eIF2α. Shown is a representative blot from three independent experiments. The phosphorylation of eIF2α induction rate was evaluated by normalizing the raw value of P-eIF2α to that of total eIF2α as shown in the bar graph. **(C)** Huh-7 cells were transfected with different *in vitro* transcribed reporter RNAs: HCV-Luc, EMCV-Luc, CrPV-Luc or Cap.βGlobin-Luc. After 1 h of transfection, cells were treated or not with ARS or TG, or with CHX, after which luciferase activity was measured. Bars represent the relative luciferase activity with non-treated control (inhibitor concentration = 0) set as 100%. The readings from CHX treatments were subtracted from all as a baseline. Error bars represent the standard error of the mean, $n = 3$. **(A,C)** Statistical significance of the differences between treated samples compared to control was calculated with two-way ANOVA and a Bonferroni *post hoc* test, and is shown as: $*p < 0.05$, $**p < 0.01$, $***p < 0.001$. **(D)** Huh-7 cells were transfected with *in vitro* synthesized rep HCV-Luc mRNA. After 1 h of transfection, cells were treated with different concentrations of ARS or CHX (5 μg mL^{-1}) for 2 h, after which luciferase activity was measured. Bars represent the relative luciferase activity with non-treated control (inhibitor concentration = 0) set as 100%. The readings from CHX treatments were subtracted as a baseline. Error bars represent the standard error of the mean, $n = 3$. Statistical significance of the differences between treated samples compared to control was calculated with one-way ANOVA and a Tukey's *post hoc* test, and is shown as: $*p < 0.05$, $***p < 0.001$.

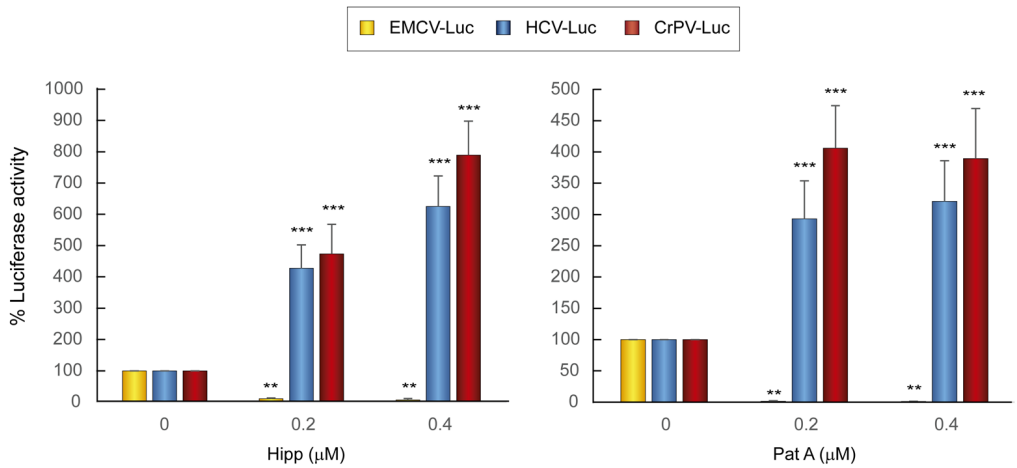

FIGURE 2 | Translation from the HCV IRES in Huh-7 cells is resistant to the action of eIF4A inhibitors. Huh-7 cells were transfected with reporter RNAs (HCV-Luc, EMCV-Luc, or CrPV-Luc) for 1 h and then treated with either Hipp (0.2 and 0.4 μM) or Pat A (0.2 and 0.4 μM) for 2 h, after which luciferase activity was measured. Bars represent the relative luciferase activity with non-treated control (inhibitor concentration = 0) set as 100%. The readings from CHX treatments were subtracted from all as a baseline. Error bars represent the standard error of the mean, $n = 3$. Statistical significance of the differences between treated samples compared to control was calculated with two-way ANOVA and a Bonferroni *post hoc* test, and is shown as: $**p < 0.01$, $***p < 0.001$.

Cellular Localization of eIFs Treated with Sodium Arsenite or Pateamine A

It is well established that ARS and Pat A induce the formation of cytoplasmic stress granules (SGs). The molecular mechanism of this induction is different for each compound: ARS induces eIF2α phosphorylation, whereas SG formation by Pat A occurs via a mechanism independent of this process (Dang et al., 2006; Linero et al., 2011). A number of components of the translation machinery, including preinitiation complexes containing 40S ribosomal subunits, are present in SGs (Kedersha and Anderson, 2009; Anderson et al., 2015; Penas et al., 2016). It was of note that HCV-Luc mRNA was efficiently translated even in the presumed presence of SGs (**Figures 1**, **2**). Curiously, HCV infection of Huh-7 cells leads to a dynamic oscillation in the formation of SGs (Ruggieri et al., 2012; Valadao et al., 2016).

To survey the action of ARS and Pat A on SG formation and to examine the localization of different eIFs, Huh-7 cells were transfected with HCV-Luc, incubated with ARS and Pat A for 2 h, and then processed for immunocytochemistry. We initially examined the localization of eIF4G together with TIA-1, eIF3 or eIF4A. As illustrated in **Figure 3A**, eIF4G (stained green) was mostly located in the cytoplasm in Huh-7 control cells, whereas TIA-1 (stained red) was predominantly nuclear. Transfection with HCV-Luc RNA led to the appearance of a few SGs in Huh-7 cells containing both eIF4G and TIA-1. Treatment of transfected cells with ARS or Pat A greatly increased the number and size of SGs containing TIA-1 and eIF4G (**Figure 3A**). eIF3 (stained red) commonly showed a granular and cytoplasmic location. Furthermore, transfection with HCV-Luc RNA led to the formation of some granules with concentrated eIF4G, presumably SGs, without co-localization of eIF3. However, ARS treatment robustly modified eIF3 distribution, which showed a more compacted perinuclear location without co-localization of eIF4G. This effect was not seen after Pat A treatment (**Figures 3A,B**). Moreover, whereas eIF4A (stained red) displayed a cytoplasmic location with a homogeneous dispersion in control cells, it was clearly present in small SGs coincident with eIF4G (stained green) in HCV-Luc transfected cells, which were larger after treatment with ARS or Pat A (**Figure 3A**). The finding that eIF4G is present in SGs suggests that it is not participating in the translation of HCV-Luc mRNA. This is also in agreement with the lack of inhibition when eIF4A is blocked by Hipp or

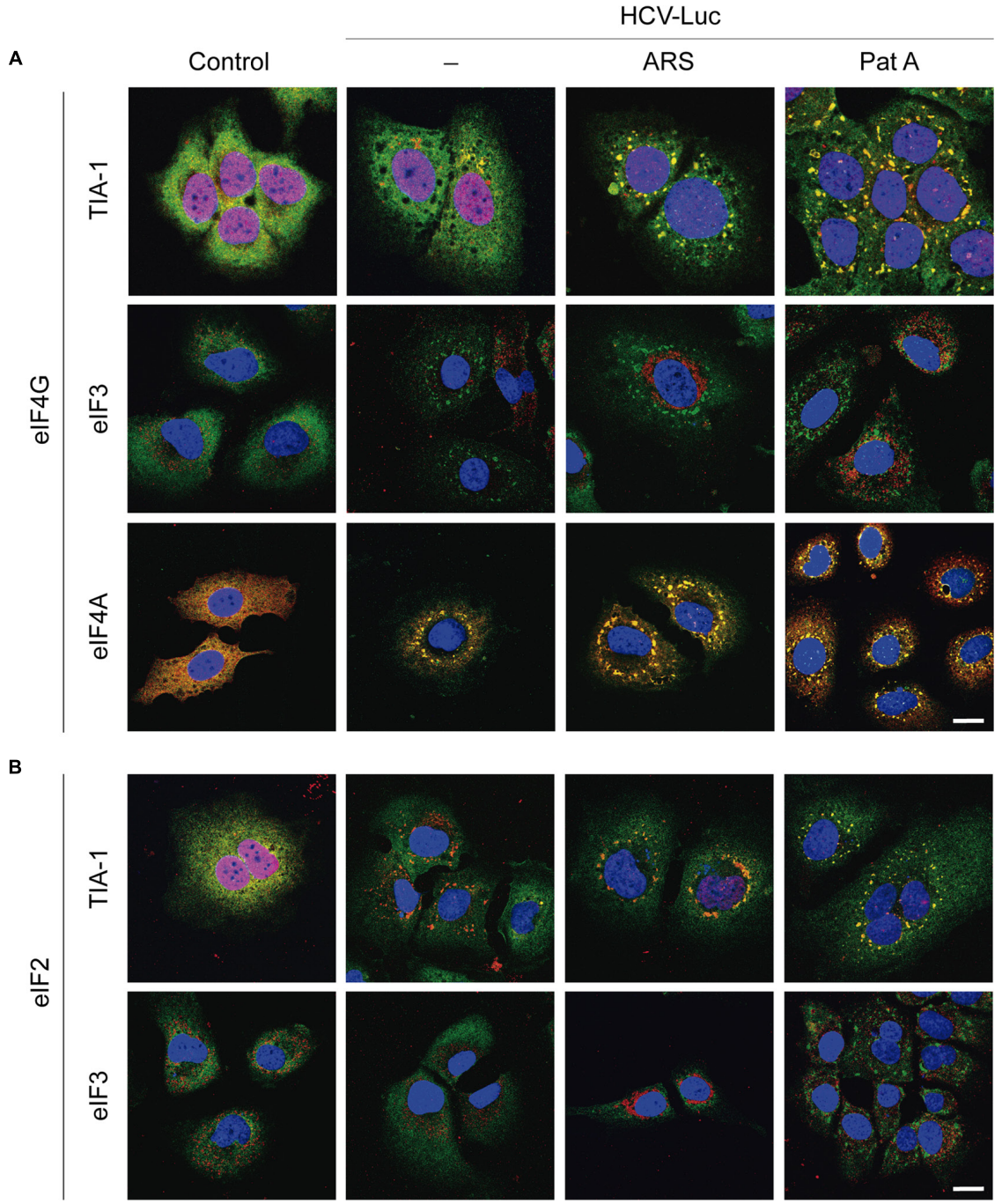

FIGURE 3 | Analysis of stress granule formation in Huh-7 cells transfected with *in vitro* synthesized HCV-Luc RNA and treated with sodium arsenite or pateamine A. Cells were seeded on microscope cover slips, transfected with HCV-Luc mRNA for 1 h and then treated with either ARS (200 μM) or Pat A (0.4 μM) for 2 h. Control cells underwent the transfection procedure without RNA. After treatments, cells were permeabilized for immunocytochemistry. **(A)** Shows staining with primary rabbit anti-eIF4G antibody (green) together with primary goat anti-TIA-1, goat anti-eIF3 or mouse anti-eIF4A antibodies (red). **(B)** Shows staining with primary rabbit anti-eIF2 antibody (green) together with primary goat anti-TIA-1 or goat anti-eIF3 antibodies (red). Anti-goat antibodies conjugated to Alexa 555 were used to detect TIA-1 or eIF3 (red), anti-mouse antibody conjugated to Alexa 555 was used to detect eIF4A (red), anti-rabbit antibodies conjugated to Alexa 448 were employed to detect eIF4G or eIF2 (green). DAPI was used to stain the nuclei (blue). Scale bar, 20 μm.

Pat A, suggesting that the eIF4F complex is not involved in HCV mRNA translation. We also considered it of interest to analyze other factors of the translation machinery (**Figure 3B**). eIF2 (stained green) had a dispersed cytoplasmic localization in control and transfected cells with or without ARS treatment, whereas in transfected cells treated with Pat A eIF2 appeared in

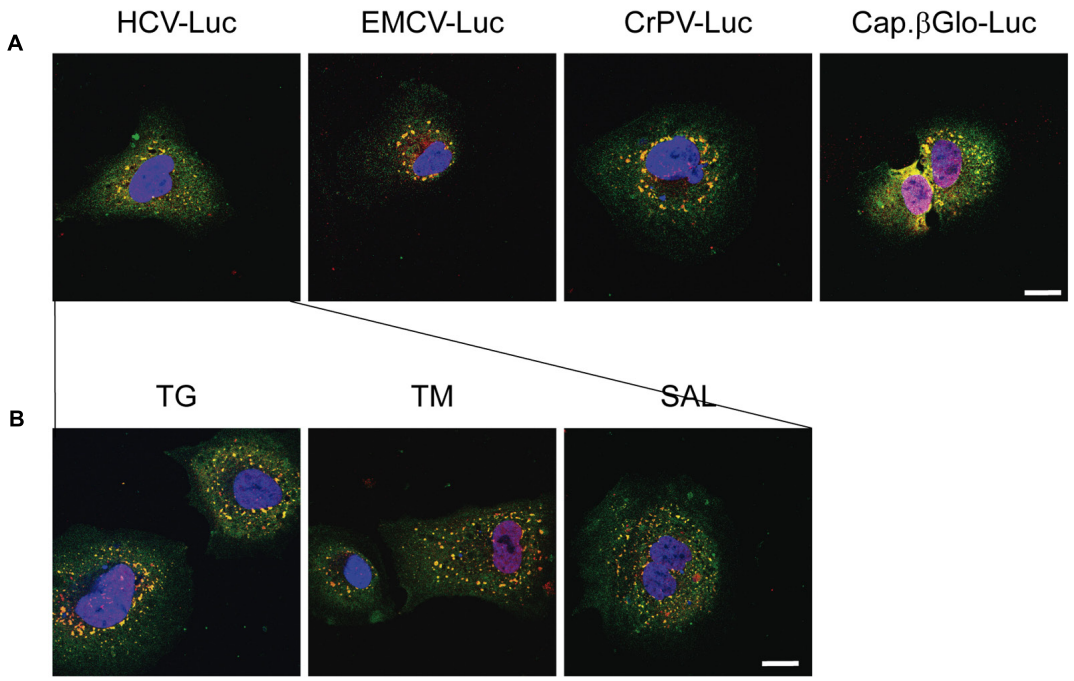

FIGURE 4 | Thapsigargin, tunicamycin or salubrinal treatment induces stress granule formation in transfected Huh-7 cells. **(A)** Cells were seeded on microscope cover slips and transfected with different reporter RNAs: HCV-Luc, EMCV-Luc, CrPV-Luc or Cap.βGlobin-Luc. After 1 h of transfection, cells were incubated in DMEM medium for 2 h. **(B)** Cells were seeded on microscope cover slips and transfected with HCV-Luc. After 1 h of transfection, cells were treated with various eIF2 inhibitors (TG, TM, or SAL) for 2 h. In both cases, after treatments cells were permeabilized for immunocytochemistry using primary goat anti-TIA-1 and rabbit anti-eIF4G antibodies. An anti-goat antibody conjugated to Alexa 555 was used to detect TIA-1 (red) and an anti-rabbit antibody conjugated to Alexa 448 was employed to detect eIF4G (green). DAPI was used to stain the nuclei (blue). Scale bar, 20 μm.

SGs coincident with TIA-1 (stained red) (**Figure 3B**). Curiously, Pat A not only blocked the action of eIF4A, but also induced the sequestration of eIF2 into SG granules. Finally, as shown in Supplementary Figure 2, no change in the localization pattern of eIF1A was found after RNA transfection with or without treatment with ARS or Pat A. Therefore, eIF1A is not sequestered into SGs. This is consistent with the idea that eIF1A may participate in the translation of HCV mRNA (Jaafar et al., 2016). In conclusion, eIF4G and eIF4A, which are located in SG, are not involved in HCV mRNA translation, whereas eIF3 and eIF1A, which are present in the cytosol, could be engage in the initiation of this translation. In the case of eIF2, it is located in SG after phosphorylation by Pat A, consistent with the concept that it does not participate in HCV IRES translation.

We next addressed whether transfection with other RNAs could also induce the formation of SGs. We transfected Huh-7 cells with HCV-Luc (as a control), EMCV-Luc, CrPV-Luc or Cap.βGlobin-Luc RNAs for 1 h followed by incubation in DMEM for 2 h before immunocytochemistry analysis. Interestingly, the transfection with these RNAs also induced the formation of a few small granules (**Figure 4A**). This represent an interesting aspect to take into consideration, since not only HCV-Luc RNA but also transfection with other RNAs may induce this response. Of interest, treatment with TG, TM or SAL also increased the formation of large quantities of SGs in cells transfected with HCV-Luc mRNA as shown by staining for eIF4G (green) and TIA-1 (red) (**Figure 4B**).

Translation of mRNA Bearing HCV IRES in Knock-out Human Cells Depleted for eIF2A, eIF2D, or Both Factors

Several studies have suggested that eIF2 can be replaced with other cellular proteins under stress conditions (Terenin et al., 2008; Dmitriev et al., 2010; Skabkin et al., 2010; Kim et al., 2011). Accordingly, the possibility that eIF2A or eIF2D participate in the initiation of translation of HCV mRNA when eIF2α is phosphorylated has been put forward. To test this idea, we made use of human cells knocked out for eIF2A (HAP1-eIF2A^{-}), or eIF2D (HAP1-eIF2D^{-}) or both (HAP1-eIF2A^{-}/2D^{-}). We have recently shown that these cells are viable, exhibit a normal morphology and have a similar synthesis of global proteins to that of parental control cells (Sanz et al., 2017).

First, we analyzed the activity of the different inhibitors that induce the phosphorylation of eIF2α in WT HAP1 cells transfected with different mRNAs. We followed a protocol similar to that used for Huh-7 cells and each compound was assayed at different concentrations. Consistent with the results for hepatoma cells, the compounds differentially affected

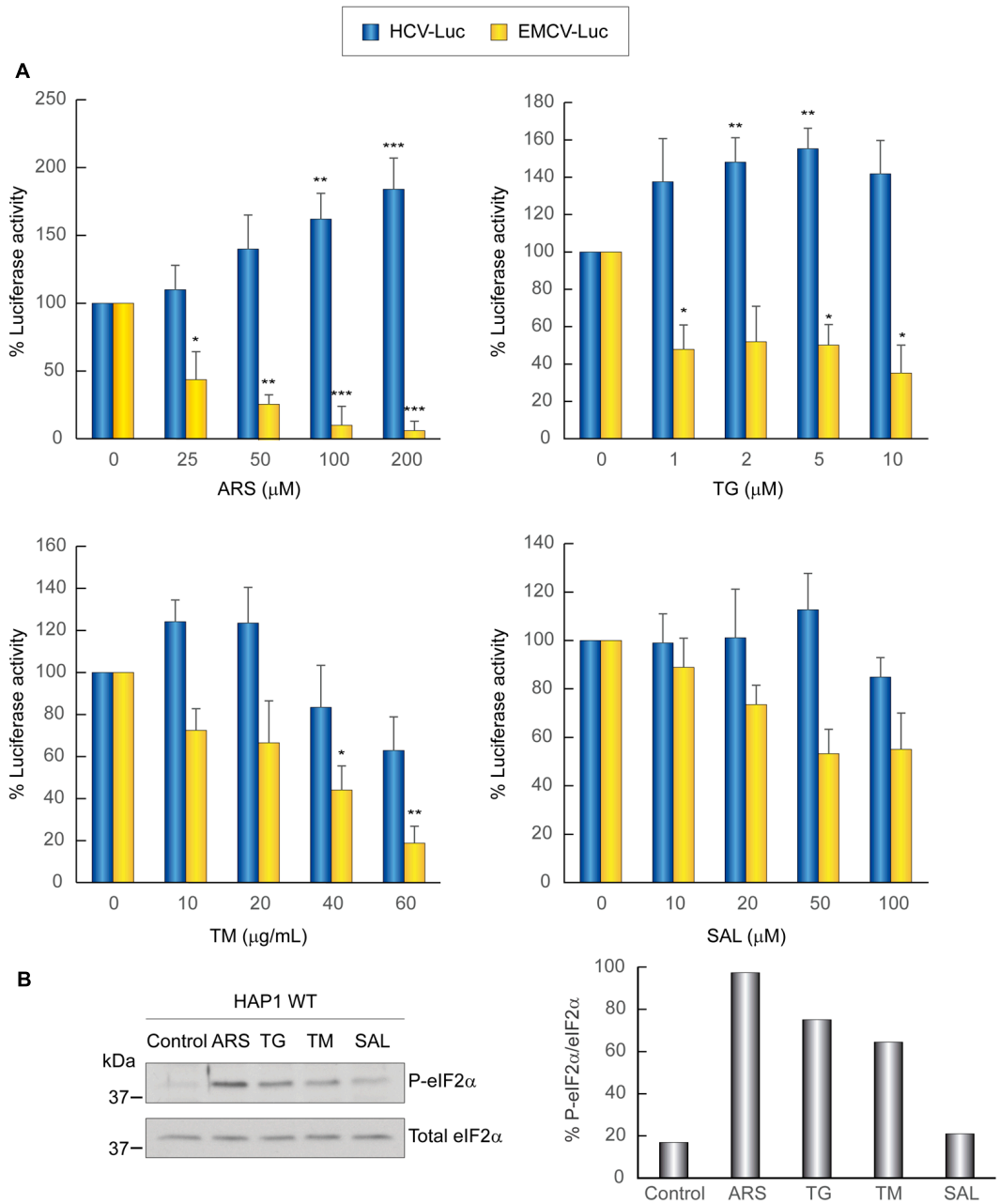

FIGURE 5 | Translation from the HCV IRES in HAP1 WT cells is resistant to the action of eIF2 inhibitors. **(A)** Translation from the IRES of HCV or EMCV as measured by luciferase activity in response to eIF2 inhibitor treatment in HAP1 WT cells. Cells were transfected with HCV-Luc or EMCV-Luc mRNAs for 1 h and then incubated with either CHX (5 μg mL^{-1}) or ARS, TG, TM, or SAL for a further 2 h. Percentage change is relative to non-treated control (inhibitor concentration = 0). The readings from CHX treatments were subtracted from all as a baseline. Error bars represent the standard error of the mean, $n = 3$. Statistical significance of the differences between treated samples compared to control was calculated with two-way ANOVA and a Bonferroni *post hoc* test, and is shown as: $^{*}p < 0.05$, $^{**}p < 0.01$, $^{***}p < 0.001$. **(B)** Inhibitor treatment induces eIF2α phosphorylation in HAP1 WT cells. Cells were transfected for 1 h and then treated or not with either ARS (200 μM), TG (5 μM), TM (40 μg mL^{-1}) or SAL (50 μM) for 2 h. Proteins were resolved using SDS-PAGE and then samples were probed with antibodies for phospho-eIF2α and total eIF2α. Shown is a representative blot from three independent experiments. The phosphorylation of eIF2α induction rate was evaluated by normalizing the raw value of P-eIF2α to that of total eIF2α as shown in the bar graph.

the translation directed by EMCV or HCV IRESs: whereas translation driven by EMCV IRES was inhibited, HCV IRES-dependent translation was stimulated by these compounds (**Figure 5A**). As stated earlier, this stimulation can be due to phosphorylation of eIF2α (**Figure 5B**), which blocks cellular translation, and also to the sequestration of many cellular mRNAs in SGs, impeding the competition for components of the translational machinery.

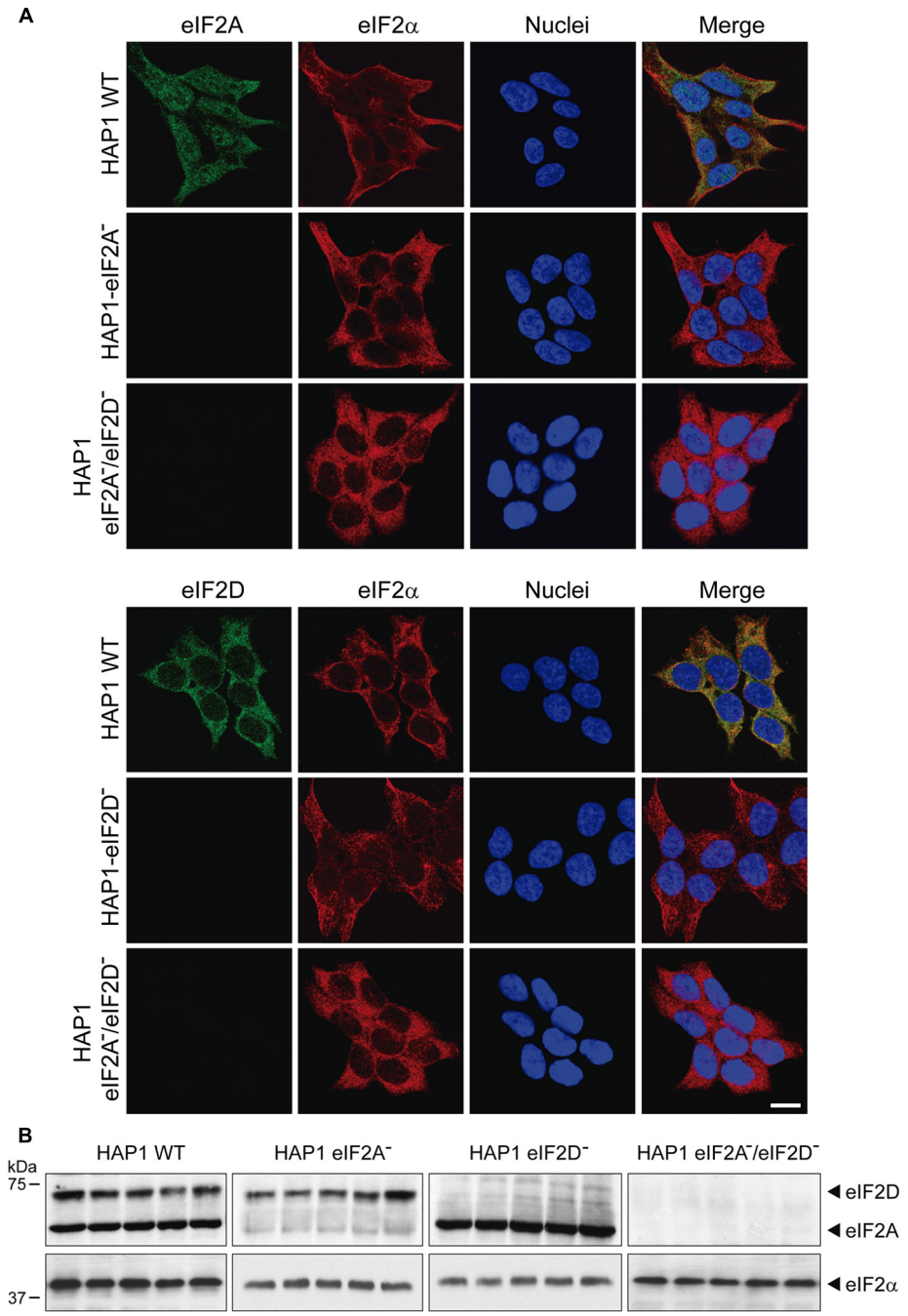

FIGURE 6 | Characterization of the different HAP1 cell lines by immunocytochemistry and western blotting. **(A)** HAP1 WT, HAP1-eIF2A^{-}, HAP1-eIF2D^{-}, and HAP1-eIF2A^{-}/eIF2D^{-} cells were seeded on microscope coverslips, fixed and stained with primary rabbit polyclonal anti-eIF2A or anti-eIF2D antibodies and a mouse monoclonal anti-eIF2α antibody. An anti-mouse antibody conjugated to Alexa 555 was used to detect eIF2α (red) and an anti-rabbit antibody conjugated to Alexa 488 was employed to detect eIF2A and eIF2D (green). DAPI was used to stain the nuclei (blue). Scale bar, 20 μm. **(B)** The presence of eIF2A or eIF2D in HAP1 WT, HAP1-eIF2A^{-}, HAP1-eIF2D^{-}, and HAP1-eIF2A^{-}/eIF2D^{-} cells was also determined by western blotting with rabbit polyclonal anti-eIF2A and anti-eIF2D antibodies. eIF2α was used as loading control for the four cell lines. Proteins were resolved by SDS-PAGE and samples were probed with antibodies to show the presence of these factors in the HAP1 cells lines. Shown is a representative blot from three independent experiments.

To study the participation of eIF2A and eIF2D in the translation of the mRNA reporter bearing HCV IRES, we employed the KO cell lines indicated above. We first validated the cell lines by immunohistochemistry and western blotting. The subcellular localization of eIF2A and eIF2D in HAP1 WT, single KO and double KO variants is shown in **Figure 6**. The expression

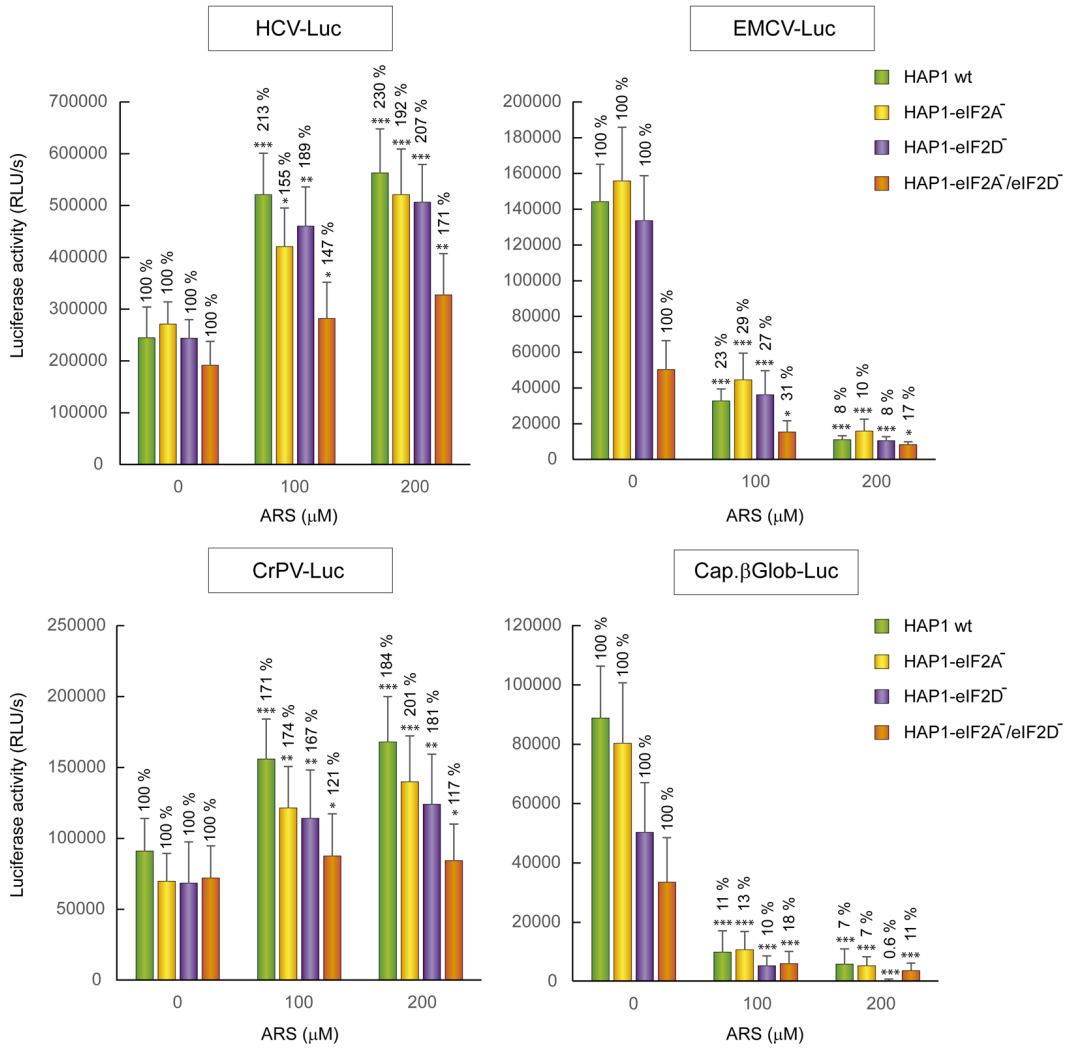

FIGURE 7 | Resistance of HCV IRES translation to the eIF2 inhibitor sodium arsenite is independent of eIF2A and eIF2D. HAP1 cell lines WT, HAP1-eIF2A$^-$, HAP1-eIF2D$^-$, and HAP1-eIF2A$^-$/eIF2D$^-$ were transfected with reporter RNAs (HCV-Luc, EMCV-Luc, CrPV-Luc or Cap.βGlobin-Luc) for 1 h and treated with ARS (200 μM) for 2 h. Bars represent the relative luciferase activity with non-treated control (inhibitor concentration = 0) set as 100%. The readings from CHX treatments were subtracted from all as a baseline. Error bars represent the standard error of the mean, $n = 3$. Statistical significance of the differences between ARS treated samples compared to control was calculated with two-way ANOVA and a Bonferroni *post hoc* test, and is shown as: $*p < 0.05$, $**p < 0.01$, $***p < 0.001$.

of eIF2A and eIF2D was examined by immunocytochemistry using specific antibodies. Double staining of HAP1 WT cells revealed that eIF2A was clearly expressed in the cytoplasm and a proportion was also found in the nucleus, whereas eIF2D was mainly cytoplasmic. As expected, eIF2A was not detected in HAP1-eIF2A$^-$ cells or HAP1 eIF2A$^-$/eIF2D$^-$ (**Figure 6A**). Similarly, eIF2D was not found in HAP1-eIF2D$^-$ cells or HAP1 eIF2A$^-$/eIF2D$^-$ (**Figure 6A**). Loss of eIF2A or eIF2D in the respective KO cell lines was verified by western blotting (**Figure 6B**).

The four cell lines, HAP1 WT, HAP1-eIF2A$^-$, HAP1-eIF2D$^-$, and HAP1-eIF2A$^-$/2D$^-$ were transfected with different mRNAs encoding luciferase and treated or not with ARS to induce eIF2α phosphorylation. Interestingly, the translation of the different mRNAs was similar in all four cell lines analyzed, both in the absence or presence of ARS (**Figure 7**). As expected, luciferase synthesis from both control mRNAs, EMCV-Luc and Cap.βGlo-Luc was strongly inhibited by ARS in all four cell lines. By contrast, luciferase translation from CrPV-Luc mRNA was stimulated by ARS treatment. Thus, HCV-Luc mRNA directed the synthesis of luciferase in all four cell lines, even when ARS was present and eIF2α was phosphorylated. This finding clearly demonstrates that neither eIF2A nor eIF2D are involved in HCV-Luc translation. Moreover, these two factors do not replace the activity of eIF2 in IRES-driven translation when it is inactivated. In the statistical analysis using two-way ANOVA, we have seen that there is no statistical interaction between any of the four HAP1 lines. That means that the effect of ARS is the same in the four cell lines, although there are differences between the levels of translation between them. The ARS increases in

the same way the expression of Luc in the four lines tested despite the absence of eIF2A and/or eIF2D. Therefore the level of translation of HCV-Luc does not seem to depend on the presence of these factors. In turn, we also see that there is a significant difference between control cells and treated with ARS, as indicated in **Figure 7**, therefore ARS effectively stimulates the translation of HCV-Luc in the four HAP1 lines in a similar degree. These findings are consistent with a recent report showing that depleting Huh-7 cells of eIF2A, eIF2D or both with siRNAs has no effect on luciferase synthesis promoted by HCV IRES (Jaafar et al., 2016).

DISCUSSION

Animal viruses employ a variety of mechanisms to translate their mRNAs (Firth and Brierley, 2012). The precise mechanisms of viral mRNA translation remain the subject of intense research. Some animal viruses utilize RNA components known as IRES elements to direct the translation machinery to an internal position at the 5′-UTR of the viral messenger (Hellen, 2009; Plank and Kieft, 2012). However, the mechanism of IRES-driven translation also can differ between the various animal viruses that use this strategy. In the case of HCV, the exact mode by which its mRNA initiates protein synthesis as regards to participating eIFs is controversial. One school of thought is that under normal cellular conditions, HCV mRNA initiates translation using the ternary Met-tRNA$_i^{Met}$-eIF2-GTP complex, whereas eIF2 is dispensable under stress conditions (Jaafar et al., 2016). Yet, the possibility exists that eIF2 never participates in the initiation of HCV mRNA in infected cells. Indeed, the interaction of HCV IRES with the preinitiation complexes displaces eIF2 (Jaafar et al., 2016), and it is conceivable that the IRES element itself is sufficient to initiate translation without eIF2, even when this factor is active. Studies *in vitro* and experiments in culture cells indicate that eIF2A can replace eIF2 in HCV IRES-directed translation (Kim et al., 2011). Moreover, other studies point to eIF2D as the responsible factor to initiate translation in place of eIF2 (Dmitriev et al., 2010; Skabkin et al., 2010), based mainly on *in vitro* observations. Our present findings in human cells clearly demonstrate that neither eIF2A nor eIF2D are involved in protein synthesis directed by HCV IRES, and are in accord with a recent result demonstrating that knockdown of eIF2A or eIF2D in hepatoma cells has little effect on HCV IRES-driven translation (Jaafar et al., 2016). Therefore, the results obtained using siRNAs by Jaafar et al. and our present findings with KO cell lines are complementary and both demonstrate that those factors do not participate in HCV translation. In addition, the possibility that eIF2A can be replaced by eIF2D, or vice versa, is not supported by the finding that in the double KO cell line HCV-Luc mRNA is efficiently translated even under stress conditions in the presence of ARS. Moreover, elegant studies directed to uncover the cellular genes necessary for HCV replication and growth failed to detect eIF2A or eIF2D (Marceau et al., 2016). Although that study only examined cellular genes dispensable for human HAP1 cells, it must be stressed that, as we have demonstrated, neither eIF2A nor eIF2D are necessary for the viability of this cell line (Sanz et al., 2017). Therefore, we can conclude that these genes do not participate in the translation of this viral mRNA, and they do not replace eIF2 even after the induction of cellular stress. The use of KO cell lines will be helpful in future studies to unravel the mode of initiation and the factors required to translate viral mRNAs. Indeed, we believe that *in vitro* experiments that suggest the requirement for some eIFs to translate a given mRNA should be followed by *in vivo* experiments in culture cells and in this respect KO cells will be useful tools. Remarkably, all eIFs could be dispensable in *in vitro* translation of HCV at high concentrations of magnesium ions (Lancaster et al., 2006). Thus, the modulation of *in vitro* conditions strongly affects the requirements for eIFs in the initiation of protein synthesis by HCV IRES.

There is more consensus about the lack of any involvement of the three factors that form part of the eIF4F complex for the initiation of protein synthesis directed by HCV mRNA (Niepmann, 2013). Since this viral messenger does not have a 5′ cap structure, it seems logical that eIF4E is not involved in its translation. Also, since there is no scanning mechanism during the initiation event, eIF4A (the helicase enzyme involved in scanning) does not participate in this process. There are currently two compounds (Hipp and Pat A) from marine origin that are selective inhibitors of eIF4A (Bordeleau et al., 2006a; Low et al., 2007). Both are very useful to test the involvement of this factor in the translation of any given mRNA. We show here that these two agents do not affect luciferase synthesis driven by HCV IRES in monocistronic mRNAs containing the HCV 3′-UTR in human hepatic cells. Our results are in good agreement with previous observations showing that these compounds do not block HCV IRES-dependent translation in dicistronic mRNAs (Bordeleau et al., 2006a; Low et al., 2007). This fact, together with the finding that eIF4G are localized in SGs after ARS treatment, is consistent with the idea that the eIF4F complex does not participate in the initiation of translation of HCV mRNA.

Possibly the most important issue to be clarified in the initiation of protein synthesis driven by HCV IRES is to determine whether eIF2 is employed or not under normal conditions. *In vitro* observations have demonstrated that the HCV IRES can directly interact with native 40S ribosomal subunits devoid of eIFs that, afterward, can recruit eIF3 and the ternary complex containing eIF2 (Ji et al., 2004; Otto and Puglisi, 2004). The interaction of the HCV IRES with 40S or 80S ribosomes leads to the remodeling of its structure, in such a way that domain II is bound to the tRNA exit site, whereas domain III positions with the initiation codon at the head of the small ribosomal subunit (Boehringer et al., 2005). Fluorescently labeled 40S ribosomal subunits in the ribosomal protein RPS25 irreversibly bind to HCV IRES, leading to conformational rearrangements of domain II that are stabilized by yet undefined cellular proteins (Fuchs et al., 2015). It is, however, unclear if under physiological conditions in intact cells HCV mRNA interacts with native 40S or more probably with preinitiation complexes that would contain several eIFs, including eIF3 and eIF1A (Jaafar et al., 2016). IRES binding to preinitiation complexes in intact cells can displace eIF2 by the interaction of domain II with the 40S subunit (Locker et al., 2007). In fact, the binding sites of domain II and the ternary complex

overlap in such a way that the interaction of both on the 40S would clash (Jaafar et al., 2016). It is feasible that domain II of HCV IRES functionally replaces the ternary complex, without the necessity for other cellular factors such as eIF2A or eIF2D even under normal cellular conditions. Indeed, domain II adopts an L-shaped structure and interacts with the 40S subunit in the head region of the E site, allowing the apical loop of domain II to reach deeply into the mRNA cleft near the coding RNA in the ribosomal P site (Spahn et al., 2001; Lukavsky et al., 2003). Therefore, the IRES may be able to replace the ternary complex and after the formation of the 80S ribosome, the P site could be occupied, leaving the A site free that could be positioned with the AUG initiation codon ready to start translation. This model is akin to that described for the functioning of CrPV IRES, with the exception that eIF3 is involved in HCV translation (Jan and Sarnow, 2002; Fernandez et al., 2014).

The exact functioning of eIF2A or eIF2D during cellular mRNA translation remains to be elucidated. The recent generation of an eIF2A knockout mouse clearly demonstrates that this factor is not required during embryogenesis, nor involved in the translation of tissue-specific mRNAs (Golovko et al., 2016). The recent finding that eIF2A participates in tumorigenesis makes the study of this factor particularly relevant (Sendoel et al., 2017). Nonetheless, eIF2A is likely required for additional functions besides its involvement in cancer progression. The use of the human KO cell lines employed in this work could help to improve our understanding of eIF2A and eIF2D in translation. As observed recently (Sanz et al., 2017), and in the present study, these two factors are not necessary for global translation of cellular mRNAs and for luciferase synthesis directed by HCV, EMCV, or CrPV IRESs. Future studies directed to analyze the behavior of specialized cellular mRNAs in these KO cell lines will help to ascertain the precise roles of eIF2A and eIF2D.

AUTHOR CONTRIBUTIONS

EG-A, HW, and MS performed the experiments. LC designed the experiments and wrote the manuscript. All authors listed have made a substantial, direct and intellectual contribution to the work, and approved it for publication.

FUNDING

This study was supported by a DGICYT (Dirección General de Investigación Científica y Técnica, Ministerio de Economía y Competitividad, Spain) grant SAF2015-66170-R (MINECO/FEDER) and by Ministerio de Educación, Cultura y Deporte grant FPU15/05709. Institutional grants from the Fundación Ramón Areces and Banco de Santander to the Centro de Biología Molecular "Severo Ochoa" (CSIC-UAM) are also acknowledged.

ACKNOWLEDGMENTS

We thank Dr. Takashi Shimoike (National Institute of Infectious Diseases, Musashimurayama, Tokyo) for kindly donating pT7HCV-Luc (Full name: pT7HCV33core-Luc). We also thank Dr. Ralph Bartenschlager (Department of Molecular Virology, University of Heidelberg, Heidelberg, Germany) for kindly donating pFKi389LucNS3-3_dg_JFH.

SUPPLEMENTARY MATERIAL

The Supplementary Material for this article can be found online at: https://www.frontiersin.org/articles/10.3389/fmicb.2018.00207/full#supplementary-material

REFERENCES

Adams, S. L., Safer, B., Anderson, W. F., and Merrick, W. C. (1975). Eukaryotic initiation complex formation. Evidence for two distinct pathways. *J. Biol. Chem.* 250, 9083–9089.

Aldabe, R., and Carrasco, L. (1995). Induction of membrane proliferation by poliovirus proteins 2C and 2BC. *Biochem. Biophys. Res. Commun.* 206, 64–76. doi: 10.1006/bbrc.1995.1010

Anderson, P., Kedersha, N., and Ivanov, P. (2015). Stress granules. P-bodies and cancer. *Biochim. Biophys. Acta* 1849, 861–870. doi: 10.1016/j.bbagrm.2014.11.009

Bai, Y., Zhou, K., and Doudna, J. A. (2013). Hepatitis C virus 3′UTR regulates viral translation through direct interactions with the host translation machinery. *Nucleic Acids Res.* 41, 7861–7874. doi: 10.1093/nar/gkt543

Boehringer, D., Thermann, R., Ostareck-Lederer, A., Lewis, J. D., and Stark, H. (2005). Structure of the hepatitis C virus IRES bound to the human 80S ribosome: remodeling of the HCV IRES. *Structure* 13, 1695–1706. doi: 10.1016/j.str.2005.08.008

Bordeleau, M. E., Cencic, R., Lindqvist, L., Oberer, M., Northcote, P., Wagner, G., et al. (2006a). RNA-mediated sequestration of the RNA helicase eIF4A by pateamine A inhibits translation initiation. *Chem. Biol.* 13, 1287–1295. doi: 10.1016/j.chembiol.2006.10.005

Bordeleau, M. E., Matthews, J., Wojnar, J. M., Lindqvist, L., Novac, O., Jankowsky, E., et al. (2005). Stimulation of mammalian translation initiation factor eIF4A activity by a small molecule inhibitor of eukaryotic translation. *Proc. Natl. Acad. Sci. U.S.A.* 102, 10460–10465. doi: 10.1073/pnas.0504249102

Bordeleau, M. E., Mori, A., Oberer, M., Lindqvist, L., Chard, L. S., Higa, T., et al. (2006b). Functional characterization of IRESes by an inhibitor of the RNA helicase eIF4A. *Nat. Chem. Biol.* 2, 213–220. doi: 10.1038/nchembio776

Boyce, M., Bryant, K. F., Jousse, C., Long, K., Harding, H. P., Scheuner, D., et al. (2005). A selective inhibitor of eIF2alpha dephosphorylation protects cells from ER stress. *Science* 307, 935–939. doi: 10.1126/science.1101902

Castello, A., Franco, D., Moral-Lopez, P., Berlanga, J. J., Alvarez, E., Wimmer, E., et al. (2009). HIV- 1 protease inhibits Cap- and poly(A)-dependent translation upon eIF4GI and PABP cleavage. *PLOS ONE* 4:e7997. doi: 10.1371/journal.pone.0007997

Dabo, S., and Meurs, E. F. (2012). DsRNA-dependent protein kinase PKR and its role in stress, signaling and HCV infection. *Viruses* 4, 2598–2635. doi: 10.3390/v4112598

Dang, Y., Kedersha, N., Low, W. K., Romo, D., Gorospe, M., Kaufman, R., et al. (2006). Eukaryotic initiation factor 2alpha-independent pathway of stress granule induction by the natural product pateamine A. *J. Biol. Chem.* 281, 32870–32878. doi: 10.1074/jbc.M606149200

Dmitriev, S. E., Terenin, I. M., Andreev, D. E., Ivanov, P. A., Dunaevsky, J. E., Merrick, W. C., et al. (2010). GTP-independent tRNA delivery to the ribosomal P-site by a novel eukaryotic translation factor. *J. Biol. Chem.* 285, 26779–26787. doi: 10.1074/jbc.M110.119693

Fernandez, I. S., Bai, X. C., Murshudov, G., Scheres, S. H., and Ramakrishnan, V. (2014). Initiation of translation by cricket paralysis virus IRES requires its translocation in the ribosome. *Cell* 157, 823–831. doi: 10.1016/j.cell.2014.04.015

Firth, A. E., and Brierley, I. (2012). Non-canonical translation in RNA viruses. *J. Gen. Virol.* 93(Pt 7), 1385–1409. doi: 10.1099/vir.0.042499-0

Fuchs, G., Petrov, A. N., Marceau, C. D., Popov, L. M., Chen, J., O'Leary, S. E., et al. (2015). Kinetic pathway of 40S ribosomal subunit recruitment to hepatitis C virus internal ribosome entry site. *Proc. Natl. Acad. Sci. U.S.A.* 112, 319–325. doi: 10.1073/pnas.1421328111

Garcia-Moreno, M., Sanz, M. A., and Carrasco, L. (2015). Initiation codon selection is accomplished by a scanning mechanism without crucial initiation factors in Sindbis virus subgenomic mRNA. *RNA* 21, 93–112. doi: 10.1261/rna.047084.114

Garcia-Moreno, M., Sanz, M. A., Pelletier, J., and Carrasco, L. (2013). Requirements for eIF4A and eIF2 during translation of Sindbis virus subgenomic mRNA in vertebrate and invertebrate host cells. *Cell Microbiol.* 15, 823–840. doi: 10.1111/cmi.12079

Golovko, A., Kojukhov, A., Guan, B. J., Morpurgo, B., Merrick, W. C., Mazumder, B., et al. (2016). The eIF2A knockout mouse. *Cell Cycle* 15, 3115–3120. doi: 10.1080/15384101.2016.1237324

Gonzalez-Almela, E., Sanz, M. A., Garcia-Moreno, M., Northcote, P., Pelletier, J., and Carrasco, L. (2015). Differential action of pateamine A on translation of genomic and subgenomic mRNAs from Sindbis virus. *Virology* 484, 41–50. doi: 10.1016/j.virol.2015.05.002

Hajarizadeh, B., Grebely, J., and Dore, G. J. (2013). Epidemiology and natural history of HCV infection. *Nat. Rev. Gastroenterol. Hepatol.* 10, 553–562. doi: 10.1038/nrgastro.2013.107

Hellen, C. U. (2009). IRES-induced conformational changes in the ribosome and the mechanism of translation initiation by internal ribosomal entry. *Biochim. Biophys. Acta* 1789, 558–570. doi: 10.1016/j.bbagrm.2009.06.001

Hellen, C. U., and Pestova, T. V. (1999). Translation of hepatitis C virus RNA. *J. Viral. Hepat.* 6, 79–87. doi: 10.1046/j.1365-2893.1999.00150.x

Hinnebusch, A. G., Ivanov, I. P., and Sonenberg, N. (2016). Translational control by 5′-untranslated regions of eukaryotic mRNAs. *Science* 352, 1413–1416. doi: 10.1126/science.aad9868

Ito, T., Tahara, S. M., and Lai, M. M. (1998). The 3′-untranslated region of hepatitis C virus RNA enhances translation from an internal ribosomal entry site. *J. Virol.* 72, 8789–8796.

Jaafar, Z. A., Oguro, A., Nakamura, Y., and Kieft, J. S. (2016). Translation initiation by the hepatitis C virus IRES requires eIF1A and ribosomal complex remodeling. *Elife* 5:e21198. doi: 10.7554/eLife.21198

Jan, E., and Sarnow, P. (2002). Factorless ribosome assembly on the internal ribosome entry site of cricket paralysis virus. *J. Mol. Biol.* 324, 889–902. doi: 10.1016/S0022-2836(02)01099-9

Ji, H., Fraser, C. S., Yu, Y., Leary, J., and Doudna, J. A. (2004). Coordinated assembly of human translation initiation complexes by the hepatitis C virus internal ribosome entry site RNA. *Proc. Natl. Acad. Sci. U.S.A.* 101, 16990–16995. doi: 10.1073/pnas.0407402101

Kedersha, N., and Anderson, P. (2009). Regulation of translation by stress granules and processing bodies. *Prog. Mol. Biol. Transl. Sci.* 90, 155–185. doi: 10.1016/S1877-1173(09)90004-7

Khawaja, A., Vopalensky, V., and Pospisek, M. (2015). Understanding the potential of hepatitis C virus internal ribosome entry site domains to modulate translation initiation via their structure and function. *Wiley Interdiscip. Rev. RNA* 6, 211–224. doi: 10.1002/wrna.1268

Khullar, V., and Firpi, R. J. (2015). Hepatitis C cirrhosis: new perspectives for diagnosis and treatment. *World J. Hepatol.* 7, 1843–1855. doi: 10.4254/wjh.v7.i14.1843

Kim, J. H., Park, S. M., Park, J. H., Keum, S. J., and Jang, S. K. (2011). EIF2A mediates translation of hepatitis C viral mRNA under stress conditions. *EMBO J.* 30, 2454–2464. doi: 10.1038/emboj.2011.146

Lancaster, A. M., Jan, E., and Sarnow, P. (2006). Initiation factor-independent translation mediated by the hepatitis C virus internal ribosome entry site. *RNA* 12, 894–902. doi: 10.1261/rna.2342306

Liang, H., He, S., Yang, J., Jia, X., Wang, P., Chen, X., et al. (2014). PTENalpha, a PTEN isoform translated through alternative initiation, regulates mitochondrial function and energy metabolism. *Cell Metab.* 19, 836–848. doi: 10.1016/j.cmet.2014.03.023

Linero, F. N., Thomas, M. G., Boccaccio, G. L., and Scolaro, L. A. (2011). Junin virus infection impairs stress-granule formation in Vero cells treated with arsenite via inhibition of eIF2alpha phosphorylation. *J. Gen. Virol.* 92(Pt 12), 2889–2899. doi: 10.1099/vir.0.033407-0

Locker, N., Easton, L. E., and Lukavsky, P. J. (2007). HCV and CSFV IRES domain II mediate eIF2 release during 80S ribosome assembly. *EMBO J.* 26, 795–805. doi: 10.1038/sj.emboj.7601549

Low, W. K., Dang, Y., Schneider-Poetsch, T., Shi, Z., Choi, N. S., Rzasa, R. M., et al. (2007). Isolation and identification of eukaryotic initiation factor 4A as a molecular target for the marine natural product Pateamine A. *Methods Enzymol.* 431, 303–324. doi: 10.1016/S0076-6879(07)31014-8

Lukavsky, P. J. (2009). Structure and function of HCV IRES domains. *Virus Res.* 139, 166–171. doi: 10.1016/j.virusres.2008.06.004

Lukavsky, P. J., Kim, I., Otto, G. A., and Puglisi, J. D. (2003). Structure of HCV IRES domain II determined by NMR. *Nat. Struct. Biol.* 10, 1033–1038. doi: 10.1038/nsb1004

Madan, V., Castello, A., and Carrasco, L. (2008). Viroporins from RNA viruses induce caspase-dependent apoptosis. *Cell. Microbiol.* 10, 437–451. doi: 10.1111/j.1462-5822.2007.01057.x

Marceau, C. D., Puschnik, A. S., Majzoub, K., Ooi, Y. S., Brewer, S. M., Fuchs, G., et al. (2016). Genetic dissection of Flaviviridae host factors through genome-scale CRISPR screens. *Nature* 535, 159–163. doi: 10.1038/nature18631

Merrick, W. C., and Anderson, W. F. (1975). Purification and characterization of homogeneous protein synthesis initiation factor M1 from rabbit reticulocytes. *J. Biol. Chem.* 250, 1197–1206.

Moss, B., Elroy-Stein, O., Mizukami, T., Alexander, W. A., and Fuerst, T. R. (1990). Product review. New mammalian expression vectors. *Nature* 348, 91–92. doi: 10.1038/348091a0

Nakabayashi, H., Taketa, K., Miyano, K., Yamane, T., and Sato, J. (1982). Growth of human hepatoma cells lines with differentiated functions in chemically defined medium. *Cancer Res.* 42, 3858–3863.

Niepmann, M. (2013). Hepatitis C virus RNA translation. *Curr. Top. Microbiol. Immunol.* 369, 143–166. doi: 10.1007/978-3-642-27340-7_6

Otto, G. A., and Puglisi, J. D. (2004). The pathway of HCV IRES-mediated translation initiation. *Cell* 119, 369–380. doi: 10.1016/j.cell.2004.09.038

Paul, D., Madan, V., and Bartenschlager, R. (2014). Hepatitis C virus RNA replication and assembly: living on the fat of the land. *Cell Host Microbe* 16, 569–579. doi: 10.1016/j.chom.2014.10.008

Penas, C., Mascarenas, J. L., and Vazquez, M. E. (2016). Coupling the folding of a beta-hairpin with chelation-enhanced luminescence of Tb(III) and Eu(III) ions for specific sensing of a viral RNA. *Chem. Sci.* 2016, 2674–2678. doi: 10.1039/C5SC04501K

Pestova, T. V., Shatsky, I. N., Fletcher, S. P., Jackson, R. J., and Hellen, C. U. (1998). A prokaryotic-like mode of cytoplasmic eukaryotic ribosome binding to the initiation codon during internal translation initiation of hepatitis C and classical swine fever virus RNAs. *Genes Dev.* 12, 67–83. doi: 10.1101/gad.12.1.67

Plank, T. D., and Kieft, J. S. (2012). The structures of nonprotein-coding RNAs that drive internal ribosome entry site function. *Wiley Interdiscip. Rev. RNA* 3, 195–212. doi: 10.1002/wrna.1105

Redondo, N., Sanz, M. A., Welnowska, E., and Carrasco, L. (2011). Translation without eIF2 promoted by poliovirus 2A protease. *PLOS ONE* 6:e25699. doi: 10.1371/journal.pone.0025699

Reynolds, J. E., Kaminski, A., Kettinen, H. J., Grace, K., Clarke, B. E., Carroll, A. R., et al. (1995). Unique features of internal initiation of hepatitis C virus RNA translation. *EMBO J.* 14, 6010–6020.

Robert, F., Kapp, L. D., Khan, S. N., Acker, M. G., Kolitz, S., Kazemi, S., et al. (2006). Initiation of protein synthesis by hepatitis C virus is refractory to reduced eIF2.GTP.Met-tRNA(i)(Met) ternary complex availability. *Mol. Biol. Cell* 17, 4632–4644. doi: 10.1091/mbc.E06-06-0478

Ruggieri, A., Dazert, E., Metz, P., Hofmann, S., Bergeest, J. P., Mazur, J., et al. (2012). Dynamic oscillation of translation and stress granule formation mark the cellular response to virus infection. *Cell Host Microbe* 12, 71–85. doi: 10.1016/j.chom.2012.05.013

Sanz, M. A., Castello, A., Ventoso, I., Berlanga, J. J., and Carrasco, L. (2009). Dual mechanism for the translation of subgenomic mRNA from Sindbis virus in infected and uninfected cells. *PLOS ONE* 4:e4772. doi: 10.1371/journal.pone.0004772

Sanz, M. A., Gonzalez Almela, E., and Carrasco, L. (2017). Translation of Sindbis subgenomic mRNA is independent of eIF2, eIF2A and eIF2D. *Sci. Rep.* 7:43876. doi: 10.1038/srep43876

Sanz, M. A., Welnowska, E., Redondo, N., and Carrasco, L. (2010). Translation driven by picornavirus IRES is hampered from Sindbis virus replicons: rescue by poliovirus 2A protease. *J. Mol. Biol.* 402, 101–117. doi: 10.1016/j.jmb.2010.07.014

Schaller, T., Appel, N., Koutsoudakis, G., Kallis, S., Lohmann, V., Pietschmann, T., et al. (2007). Analysis of hepatitis C virus superinfection exclusion by using novel fluorochrome gene-tagged viral genomes. *J. Virol.* 81, 4591–4603. doi: 10.1128/JVI.02144-06

Sendoel, A., Dunn, J. G., Rodriguez, E. H., Naik, S., Gomez, N. C., Hurwitz, B., et al. (2017). Translation from unconventional 5′ start sites drives tumour initiation. *Nature* 541, 494–499. doi: 10.1038/nature21036

Shimoike, T., McKenna, S. A., Lindhout, D. A., and Puglisi, J. D. (2009). Translational insensitivity to potent activation of PKR by HCV IRES RNA. *Antiviral Res.* 83, 228–237. doi: 10.1016/j.antiviral.2009.05.004

Shwetha, S., Kumar, A., Mullick, R., Vasudevan, D., Mukherjee, N., and Das, S. (2015). HuR displaces polypyrimidine tract binding protein to facilitate la binding to the 3′ untranslated region and enhances hepatitis C virus replication. *J. Virol.* 89, 11356–11371. doi: 10.1128/JVI.01714-15

Skabkin, M. A., Skabkina, O. V., Dhote, V., Komar, A. A., Hellen, C. U., and Pestova, T. V. (2010). Activities of Ligatin and MCT-1/DENR in eukaryotic translation initiation and ribosomal recycling. *Genes Dev.* 24, 1787–1801. doi: 10.1101/gad.1957510

Sonenberg, N., and Hinnebusch, A. G. (2009). Regulation of translation initiation in eukaryotes: mechanisms and biological targets. *Cell* 136, 731–745. doi: 10.1016/j.cell.2009.01.042

Spahn, C. M., Kieft, J. S., Grassucci, R. A., Penczek, P. A., Zhou, K., Doudna, J. A., et al. (2001). Hepatitis C virus IRES RNA-induced changes in the conformation of the 40s ribosomal subunit. *Science* 291, 1959–1962. doi: 10.1126/science.1058409

Starck, S. R., Tsai, J. C., Chen, K., Shodiya, M., Wang, L., Yahiro, K., et al. (2016). Translation from the 5' untranslated region shapes the integrated stress response. *Science* 351:aad3867. doi: 10.1126/science.aad3867

Terenin, I. M., Dmitriev, S. E., Andreev, D. E., and Shatsky, I. N. (2008). Eukaryotic translation initiation machinery can operate in a bacterial-like mode without eIF2. *Nat. Struct. Mol. Biol.* 15, 836–841. doi: 10.1038/nsmb.1445

Topisirovic, I., Svitkin, Y. V., Sonenberg, N., and Shatkin, A. J. (2011). Cap and cap-binding proteins in the control of gene expression. *Wiley Interdiscip. Rev. RNA* 2, 277–298. doi: 10.1002/wrna.52

Valadao, A. L., Aguiar, R. S., and de Arruda, L. B. (2016). Interplay between inflammation and cellular stress triggered by flaviviridae viruses. *Front. Microbiol.* 7:1233. doi: 10.3389/fmicb.2016.01233

Vaughn, L. S., Snee, B., and Patel, R. C. (2014). Inhibition of PKR protects against tunicamycin-induced apoptosis in neuroblastoma cells. *Gene* 536, 90–96. doi: 10.1016/j.gene.2013.11.074

Welnowska, E., Sanz, M. A., Redondo, N., and Carrasco, L. (2011). Translation of viral mRNA without active eIF2: the case of picornaviruses. *PLOS ONE* 6:e22230. doi: 10.1371/journal.pone.0022230

Yamamoto, H., Collier, M., Loerke, J., Ismer, J., Schmidt, A., Hilal, T., et al. (2015). Molecular architecture of the ribosome-bound hepatitis C virus internal ribosomal entry site RNA. *EMBO J.* 34, 3042–3058. doi: 10.15252/embj.201592469

Zoll, W. L., Horton, L. E., Komar, A. A., Hensold, J. O., and Merrick, W. C. (2002). Characterization of mammalian eIF2A and identification of the yeast homolog. *J. Biol. Chem.* 277, 37079–37087. doi: 10.1074/jbc.M207109200

Conflict of Interest Statement: The authors declare that the research was conducted in the absence of any commercial or financial relationships that could be construed as a potential conflict of interest.

DISCUSIÓN

DISCUSIÓN

1. FACTORES Y REQUERIMIENTOS ESTRUCTURALES IMPLICADOS EN LA TRADUCCIÓN DE LOS mRNAS DE SINV

Los virus emplean la maquinaria de traducción celular para sintetizar sus propias proteínas compitiendo con los mRNAs celulares (Bushell and Sarnow, 2002). En el caso del virus SINV, a tiempos tempranos de la infección, una pequeña cantidad de proteínas virales es suficiente para realizar la replicación de su genoma, por lo que la traducción viral puede coexistir con la traducción celular. Sin embargo, a tiempos tardíos, la síntesis de gran cantidad de proteínas estructurales virales requiere el uso exclusivo de la maquinaria de traducción de la célula. Los mRNAs de SINV (gRNA y sgRNA), al igual que los mRNAs celulares, presentan una estructura cap en su extremo 5'-UTR, y una cola poli(A) en el 3'-UTR. A pesar de estas semejanzas con los mRNAs celulares, resulta interesante que el sgRNA de SINV no sólo puede traducirse mediante el mecanismo canónico sino, también, de forma no canónica e independiente de varios eIFs cuando se encuentra en un contexto replicativo, en la fase tardía de la infección (Sanz et al., 2009). Trabajos anteriores han descrito que, en un contexto replicativo, la traducción del sgRNA de SINV no necesita eIF4G intacto, PABP o eIF2 activo (Ventoso et al., 2006, Castello et al., 2016, Castello et al., 2009). Esta adaptabilidad le ha permitido traducirse en ambientes celulares con diferente disponibilidad de eIFs y desarrollar su ciclo biológico entre invertebrados y vertebrados. Sin embargo, aún se desconoce el mecanismo exacto de iniciación de la traducción del sgRNA de SINV y, por tanto, qué factores celulares podrían participar en ella. En el caso de SINV, se han identificado varios elementos estructurales en los mRNAs virales que maximizan su traducción en diferentes tipos de células hospedadoras, lo que demuestra la gran plasticidad funcional que este virus ha desarrollado durante su evolución para adaptarse a diferentes especies (Ventoso, 2012, Ventoso et al., 2006, Garcia-Moreno et al., 2016).

Durante la fase tardía de la infección, SINV induce una profunda supresión de la síntesis de proteínas en células de mamífero, lo cual facilita que la maquinaria celular se dedique prioritariamente a la traducción del sgRNA (Griffin, 2007). Esta inhibición de la traducción celular no se observa en la misma medida en células de mosquito (Garcia-Moreno et al., 2013, Sanz et al., 2015). La coincidencia entre el *shut-off* de la síntesis de proteínas celulares con la prevalencia de la traducción viral demuestra que la traducción celular y viral emplean diferentes mecanismos. Dentro del ciclo de infección de SINV,

encontramos también diferencias entre la traducción del gRNA y del sgRNA. El gRNA se traduce inmediatamente tras la entrada en la célula empleando varios eIFs canónicos (Castello et al., 2006). Durante la fase tardía, la síntesis de proteínas no estructurales dirigida por el gRNA disminuye en favor de una muy eficiente traducción del sgRNA (Strauss and Strauss, 1994). Estas diferencias se ven reflejadas también en un distinto requerimiento de factores de traducción.

En este trabajo se ha continuado con el estudio desarrollado durante los últimos años en nuestro laboratorio sobre las peculiaridades de la traducción de los mRNAs virales, especialmente de los mRNAs de SINV, así como el análisis del requerimiento de diferentes eIFs para la iniciación de su traducción. En este sentido, la participación de la helicasa eIF4A en la traducción de los mRNAs de SINV fue estudiada mediante el inhibidor selectivo Pat A (Gonzalez-Almela et al., 2015). Esta molécula interacciona de manera específica con el eIF4A resultando en la desorganización del eIF4F, e impidiendo la iniciación por el mecanismo canónico de traducción (Bordeleau et al., 2006). Nuestros resultados concuerdan con trabajos anteriormente publicados (Bordeleau et al., 2005, Low et al., 2005), y muestran que el tratamiento con Pat A inhibe la síntesis de proteínas celulares. Además, se ha observado que, tras una hora de tratamiento con esta molécula, la traducción no se recupera, por lo que la inhibición mediada por Pat A es irreversible.

A tiempos tempranos de la infección, la Pat A bloquea la síntesis de las nsPs de SINV. Sin embargo, durante la fase tardía de la infección, la traducción del sgRNA de SINV no se ve inhibida por la acción de este inhibidor. Curiosamente, fuera del contexto de replicación viral, la síntesis de proteínas virales dirigida por el sgRNA sí se encuentra afectada negativamente por el efecto de este inhibidor. No obstante, no parece que la Pat A influya en otros pasos de la traducción como la elongación o la terminación, puesto que la traducción dirigida por el IRES de la región intergénica (IGR) del virus de la parálisis del grillo (CrPV) no sólo es resistente, sino que se ve estimulada por el tratamiento con Pat A. Estos resultados coinciden con los obtenidos en el estudio de otro inhibidor selectivo del eIF4A, el hippuristanol (Garcia-Moreno et al., 2013) y con los conseguidos mediante la técnica cRIC donde se muestra que la actividad de unión al RNA de eIF4A no se ve alterada por la infección por SINV (Garcia-Moreno et al., 2019). Estas observaciones refuerzan la hipótesis de que el sgRNA presenta un comportamiento dual respecto al requerimiento de eIF4A dependiendo de si se encuentra en un contexto replicativo o no. Empleando Pat A, se ha observado que este cambio drástico ocurre en torno a las 4 hpi. Desde este momento en adelante, la

traducción del sgRNA pasa a ser independiente de varios eIFs, incluyendo el complejo eIF4F. Dado que, fuera del contexto de replicación viral, el sgRNA no puede traducirse sin eIF4A, eIF4G o eIF2, pero, en condiciones de replicación, su traducción es independiente de estos factores (Castello et al., 2006, Garcia-Moreno et al., 2013, Sanz et al., 2009, Gonzalez-Almela et al., 2015), la estructura de este RNA no debe de ser el único determinante de su modo de traducción. Resulta interesante que la independencia del eIF2 también se ve condicionada a un contexto replicativo. En este caso, la estructura del sgRNA, en concreto del DSH, es esencial para la independencia del eIF2 en células de vertebrado (Garcia-Moreno et al., 2015, Garcia-Moreno et al., 2013, McInerney et al., 2005, Ventoso et al., 2006, Carrasco et al., 2018, Sanz et al., 2017, Sanz et al., 2019). Sin embargo, el DSH no confiere independencia del eIF4A (Garcia-Moreno et al., 2013), por lo que los requerimientos estructurales que pudieran intervenir en este aspecto aún no han sido descubiertos.

Muchos virus animales son capaces de traducir sus mRNAs tras la fosforilación de eIF2α (Clemens, 2005, Roberts et al., 2009, Dabo and Meurs, 2012). El mecanismo que permite la iniciación de la traducción cuando eIF2 está inactivo aún se desconoce. En el caso del sgRNA de SINV, el elemento DSH es requerido para iniciar la traducción cuando eIF2 no está disponible, aunque no se ha descrito aún el modo en el que esta estructura interviene en la iniciación (Sanz et al., 2009, McInerney et al., 2005, Ventoso et al., 2006). El sgRNA representa el primer ejemplo descrito de un mRNA viral capeado cuyo mecanismo de iniciación requiere de *scanning* y, pese a ello, no utiliza el eIF2 (Garcia-Moreno et al., 2015). Inicialmente, se describió que esta estructura *hairpin* de la región codificante del sgRNA podría actuar parando el avance del ribosoma y posicionando el AUG_i en el sitio P ribosómico (Frolov and Schlesinger, 1996). Sin embargo, esto no parece muy probable, ya que el DSH debería encontrarse a 14 nt *downstream* del codón de iniciación (Kozak, 1990). Más adelante, se observó que cuando eIF2α no se encontraba fosforilado, la traducción del sgRNA era independiente de la integridad del DSH (McInerney et al., 2005, Ventoso et al., 2006). Otra posibilidad es que el DSH actúe de forma parecida al IRES de la región IGR de CrPV. La estructura *pseudoknot* presente en la región 3' de este IRES asemeja a un tRNA e interacciona con el sitio A ribosómico (Fernandez et al., 2014, Muhs et al., 2015, Johnson et al., 2017, Murray et al., 2016). Tras esto, el IRES se posiciona en el sitio P mediante la acción del eEF2, dejando el sitio A libre para que el codón iniciador comience la traducción. De forma semejante al IRES de CrPV, el DSH de SINV podría interaccionar con el sitio P del ribosoma (Garcia-Moreno et al., 2015). Por otro lado, estudios basados en silenciamiento

génico apuntan a que el eIF2 podría ser reemplazado por otro factor celular, como el eIF2A (Ventoso et al., 2006) o el eIF2D, anteriormente identificado como ligatina (Skabkin et al., 2010). Sin embargo, esta posibilidad parece poco probable considerando que nuestros resultados muestran que el sgRNA se traduce eficientemente en células HAP1 que carecen de eIF2A, eIF2D, o ambos, incluso cuando el eIF2α está fosforilado. Por tanto, aunque el mecanismo preciso por el que el sgRNA de SINV es capaz de dirigir la síntesis de proteínas en ausencia de eIF2 activo aún se desconoce, hemos demostrado que el eIF2A y el eIF2D no son necesarios para este proceso.

El DSH también interviene en la señalización del codón de iniciación correcto en el sgRNA. Esta estructura es capaz de señalizar el codón iniciador incluso cuando se cambia el AUG_i por otros codones, aunque en estos casos, la traducción resulta menos eficiente (Sanz et al., 2009). Nuestros experimentos muestran que la sustitución de AUG_i por CUG (leucina) tiene un efecto moderado, manteniendo un 50-60% de la síntesis de C respecto a la forma wt. Destaca el hecho de que el DSH también permite la iniciación en otros codones alternativos como GCG o GUG. Resulta de interés que el codón CUC, aunque también codifique para leucina, fue muy ineficaz en traducción, por lo que el tipo de aminoácido codificado no parece ser relevante, aunque sí lo es la composición de nt del codón. Nuestros resultados apuntan a que eIF2, eIF2A y eIF2D no son necesarios para la iniciación en codones no-AUG. Como hemos observado, el nivel de producción de proteína C es similar entre las líneas HAP1 KO para eIF2A o eIF2D y la línea HAP1 wt cuando son transfectadas con rep C+luc (CUG). En cambio, la desestabilización del DSH tiene un gran efecto en la iniciación en codones no-AUG para el sgRNA. Como ocurre para rep C+luc DSH-destab (AUG), la desestabilización de la estructura del DSH promueve que la iniciación de la traducción no sólo ocurra en el primer AUG_i, sino también en el segundo y el tercer AUG que se encuentran en un marco de lectura correcto. Esto demuestra que el mantenimiento de la estructura genuina del DSH es importante para señalizar el codón de iniciación. Los resultados obtenidos con rep C+luc DSH-destab (CUG) señalan que la iniciación en CUG se ve anulada cuando el DSH está desestructurado. En este caso la poca proteína C sintetizada corresponde a una variante truncada que inicia en el tercer AUG. Este patrón fue similar entre las líneas HAP1, sin encontrarse diferencias significativas en ausencia de eIF2A o eIF2D. Por tanto, se puede concluir que la estructura del DSH es muy importante para la selección del codón de iniciación correcto y que eIF2A y eIF2D no participan en la iniciación. En contraste con trabajos anteriores, nuestros descubrimientos apuntan a que eIF2 no es sustituido por otro factor celular en la traducción del sgRNA de SINV en células

infectadas. Más bien, estos datos sugieren la posibilidad de que el DSH por sí mismo sea el responsable de asegurar la traducción en independencia del eIF2. Como hemos propuesto anteriormente, el DSH podría interaccionar directamente con la subunidad ribosómica 40S o con el ribosoma 80S en el sitio P, de forma parecida a como lo hace el IRES de la IGR de CrPV (Garcia-Moreno et al., 2015, Hellen, 2009, Fernandez et al., 2014). Por otra parte, parece ser que el DSH de SINV se une al 18S rRNA para comenzar la traducción en el codón iniciador correcto, como se ha sugerido también para el DSH del virus del Bosque Semliki (Toribio et al., 2016), aunque no parece que la helicasa eIF4A esté implicada en este proceso fuera de los ensayos *in vitro*. En esta línea, varios trabajos muestran una clara evidencia de que inhibidores específicos del eIF4A no afectan a la iniciación del sgRNA de SINV (Gonzalez-Almela et al., 2015, Garcia-Moreno et al., 2013). Estas observaciones apoyan la idea de que la adquisición de la estructura DSH durante la evolución de los alfavirus permitió la independencia del eIF2 para su traducción en vertebrados (McInerney et al., 2005, Ventoso et al., 2006, Garcia-Moreno et al., 2013, Ventoso, 2012) facilitando así la síntesis de una gran cantidad de proteínas estructurales en las condiciones de estrés celular provocadas por la infección.

Para todos los organismos vivos, incluyendo los virus, la selección del codón correcto de iniciación es muy importante para evitar la formación de polipéptidos aberrantes durante la síntesis de proteínas (Drummond and Wilke, 2009, Rozov et al., 2016). Mientras que la mayoría de los mRNAs celulares y virales inician la traducción en codones AUG (Haimov et al., 2015, Kearse and Wilusz, 2017), algunos mRNAs pueden iniciar la síntesis de proteínas en codones alternativos, particularmente en ORFs situadas *upstream* de la secuencia codificante (uORFs) (Starck et al., 2016, Kearse and Wilusz, 2017). En estos casos, la iniciación puede comenzar en codones CUG, GUG o AUU, entre otros (Peabody, 1989, Van Damme et al., 2014). Existe mucha controversia en la literatura sobre si para codones de iniciación no-AUG se incorpora el propio aminoácido que codifican o metionina (Starck et al., 2012, Liang et al., 2017, Sellier et al., 2017, Na et al., 2018). Se ha demostrado que, en células de mamífero, la leucina puede incorporarse como el primer aminoácido durante la traducción de ciertos mRNAs que presentan CUG en lugar de AUG como codón iniciador (Starck et al., 2012). Sin embargo, pocos trabajos han conseguido analizar la iniciación con aminoácidos distintos a metionina en codones no-AUG (Liang et al., 2017). Esto podría deberse a que la iniciación en estos codones es poco eficiente, lo que dificulta la obtención de polipéptidos suficientes para su estudio. En este sentido, el sistema viral empleado en nuestros trabajos permite obtener cantidades relativamente altas de proteína C y de sus variantes que inician en codones

similares a AUG, facilitando su análisis. Por ello, SINV es un modelo excepcional para estudiar la iniciación de la traducción en codones no-AUG. La hipótesis más extendida es que la metionina es incorporada en el sitio P ribosómico de forma errónea para codones no-AUG por el complejo ternario Met-tRNA$_i^{Met}$-eIF2-GTP (Peabody, 1989, Liang et al., 2017, Sellier et al., 2017). Otros trabajos han sugerido que cuando la iniciación ocurre con el Leu-tRNA, la proteína eIF2A reemplaza al eIF2 (Starck et al., 2012, Starck et al., 2016). Sin embargo, la depleción de eIF2A en células supone sólo una inhibición parcial de este evento de iniciación. Por tanto, el mecanismo exacto por el que la iniciación ocurre en codones no-AUG aún requiere más investigación. En este sentido, el uso de líneas celulares KO similares a las empleadas en nuestros trabajos será de gran utilidad para descubrir las proteínas implicadas en este proceso.

Uno de los mecanismos mejor estudiados de iniciación en codones no-AUG es el que se da en el segundo cistrón del RNA del virus CrPV. En este caso, el codón de iniciación empleado es GCU, que dirige la incorporación de alanina en el extremo amino-terminal de la proteína cuando el segundo cistrón es traducido. Ningún eIF participa en este evento de iniciación, y la unión del Ala-tRNA al sitio A ribosómico está mediada por el factor de elongación de la traducción eEF1A (Jan and Sarnow, 2002, Fernandez et al., 2014). Este aminoacil-tRNA es entonces translocado al sitio P por acción del eEF2 en un proceso dependiente de GTP (Murray et al., 2016). Como se ha señalado anteriormente, se ha avanzado en la idea de que existen algunas similitudes entre el mecanismo de iniciación dirigido por el IRES de CrPV y el del DSH de alfavirus (Garcia-Moreno et al., 2015, Sanz et al., 2017, Carrasco et al., 2018). En principio, varias posibilidades podrían valorarse para la iniciación de la traducción en codones no-AUG. Una de ellas es que se incorpore metionina cuando CUG, u otro codón no-AUG, esté presente. Alternativamente, es posible que se incorpore como primer aminoácido en el extremo amino-terminal el que se encuentra codificado por el codón no-AUG; en el caso de CUG, leucina. Nuestros resultados demuestran que ambas posibilidades pueden ocurrir, aunque para CUG, la leucina es preferencialmente incorporada en el extremo amino-terminal. Por tanto, el Met-tRNA y el Leu-tRNA pueden actuar como iniciadores para este codón CUG. No obstante, aún se desconoce qué isoforma del Met-tRNA participa en este proceso: el iniciador (Met-tRNA$_i^{Met}$) o la isoforma que interviene en la fase de elongación de la traducción (Met-tRNA$_e^{Met}$). Met-tRNA$_i^{Met}$ forma el complejo ternario con eIF2 y GTP, mientras que Met-tRNA$_e^{Met}$ interacciona con eEF1A y GTP. Los dos modelos son concebibles. Como se ha señalado anteriormente, el factor eIF2 es muy selectivo a la hora de formar el complejo ternario con el Met-tRNA$_i^{Met}$, pese a que

es capaz también de formarlo con otros aminoacil-tRNAs, aunque de forma muy ineficiente (Kolitz and Lorsch, 2010). No obstante, a pesar de que, tanto el Leu-tRNA como el Met-tRNA son capaces de formar un complejo ternario con eIF2, la inactivación del eIF2 tras su fosforilación en células infectadas por SINV impediría su participación en la traducción. El reemplazo del eIF2 por otros factores como el eIF2A o el eIF2D también puede descartarse, ya que la síntesis de la proteína C de SINV puede ocurrir en células KO para estos factores, incluso cuando AUG_i ha sido reemplazado por CUG. Aunque no podemos descartar que exista otro mecanismo que implique la participación de otro factor celular putativo capaz de interaccionar con algunos aminoacil-tRNAs y unirlos a los ribosomas (Schleich et al., 2017, Hellen, 2018). Por ejemplo, el heterodímero DENR-MCT1 puede interaccionar con el tRNA para acoplarlo al ribosoma durante la reiniciación de la traducción (Schleich et al., 2014, Lomakin et al., 2003, Ahmed et al., 2018). Por otra parte, existe la posibilidad de que pequeñas cantidades de eIF2 no fosforilado participen en la traducción del sgRNA, si hay fosfatasas en los *foci* donde ocurre la traducción del sgRNA. Sin embargo, creemos que estas hipótesis resultan poco probables porque eIF2 no colocaliza con los ribosomas en células infectadas por SINV (Sanz et al., 2009). Además, incluso pequeñas cantidades de eIF2 fosforilado son capaces de inhibir potentemente la traducción, ya que la fosforilación de su subunidad α bloquea el intercambio de GDP a GTP, impidiendo la reactivación de eIF2 (Donnelly et al., 2013).

Tanto el Leu-tRNA como el Met-tRNA interactúan con eEF1A, por lo que es también posible que el eEF1A, u otra proteína celular con la habilidad de interaccionar con los aminoacil-tRNAs, participe en este evento de iniciación. Resulta interesante que la actividad de unión al RNA de eEF1A se ve estimulada en células infectadas por SINV (Garcia-Moreno et al., 2019). En el caso de que se formen estos complejos ternarios aminoacil-tRNA-eEF1A-GTP, el aminoacil-tRNA debería unirse al sitio A en el ribosoma 80S, ya que los factores de elongación se acoplan al centro GTPasa localizado en la subunidad mayor ribosómica. Anteriormente, se ha sugerido que este sitio A debería estar en conformación abierta si el sitio P está ocupado por el elemento DSH (Garcia-Moreno et al., 2015, Carrasco et al., 2018). Nuestros resultados con bruceantina concuerdan con esta idea, ya que este inhibidor, que bloquea la iniciación en el sitio P ribosómico, no tiene efecto en la traducción del sgRNA C+luc (CUG) en RRL, y produce un bloqueo menor de la traducción viral respecto de la traducción celular en células BHK infectadas por SINV. Resulta de interés que el elemento DSH es capaz de interaccionar directamente con el 18S rRNA (Toribio et al., 2016), y de esta forma podría promover la

formación del ribosoma 80S posicionando correctamente el codón de iniciación (Carrasco et al., 2018). Además, el DSH exhibe similitudes estructurales con el dominio II del IRES de HCV (Carrasco et al., 2018). A su vez, este último es similar al IRES de CrPV (Pisareva et al., 2018). El parecido entre el DSH y el dominio II del IRES de HCV no es simplemente estructural, las secuencias del *loop* del DSH y del *loop* apical del dominio II presentan una alta semejanza: CUAGCCAUG en HCV y CUGCCAUG en SINV. Por tanto, es probable que exista también similitud en la función entre el DSH y el dominio II de HCV. El mecanismo de acción del dominio II implica su interacción con los sitios ribosómicos E y P para reemplazar el Met-tRNA$_i^{Met}$ (Spahn et al., 2001, Lukavsky et al., 2003, Locker et al., 2007). Incluso, se ha descrito que el dominio II podría ser capaz de desplazar el complejo ternario previamente cargado en el ribosoma (Jaafar et al., 2016). El hecho de que treonina o valina, entre otros, puedan ser encontrados en el extremo amino-terminal de la proteína C indicaría que otros aminoacil-tRNAs pueden participar en el evento de iniciación dependiendo del codón que se encuentre en el sitio A del ribosoma. Esto sería consistente con el modelo propuesto del funcionamiento del DSH.

El descubrimiento de que CUG puede reemplazar al AUG$_i$ en el sgRNA de SINV y que su traducción es dependiente de la integridad del DSH genera gran interés en analizar los requerimientos estructurales de este *hairpin* para participar en la señalización del codón de iniciación. Nuestras observaciones apoyan el modelo en el que el DSH interacciona con la subunidad ribosómica 40S y promueve el reclutamiento de la subunidad 60S para el ensamblaje del ribosoma 80S (Carrasco et al., 2018). Para que se dé esta interacción, la estructura, pero no la secuencia, de la región *stem* parece ser importante. Sin embargo, la secuencia del *loop* es crucial. Como muestran nuestros resultados, la mutación en los seis nucleótidos de este *loop* afecta negativamente a la iniciación en CUG, particularmente en células de insecto (Sanz et al., 2019). De hecho, esta variante del DSH demuestra que la función del *hairpin* no es detener el complejo de preiniciación en el codón correcto. Según el modelo de Kozak, la posición óptima para que un *hairpin* pare al ribosoma en el codón de iniciación es a 14 nt de este (Kozak, 1991, Kozak, 1990). Sin embargo, el cambio en la posición del DSH de 24 a 15 nt *downstream* del AUG$_i$ es altamente perjudicial para su actividad (Frolov and Schlesinger, 1996). Como hemos señalado anteriormente, la estructura del DSH es muy importante para la traducción del sgRNA en células de mamífero (Carrasco et al., 2018). Aunque, esta estructura puede sufrir algunas modificaciones muy leves y seguir manteniendo su función. Cabe destacar que el DSH no puede ser completamente reemplazado por otro *hairpin* nuevo, aunque presente una energía libre similar (Garcia-Moreno et al., 2015).

Estos descubrimientos sobre la relación entre estructura y función del DSH conducen a las siguientes conclusiones: la estructura del *stem* es importante pero no su secuencia; la secuencia del *loop* tiene un papel crucial en la función del DSH; y el DSH puede ser reemplazado en cierta medida por el dominio II del IRES de HCV sugiriendo una convergencia funcional entre ambas estructuras. A pesar de que los resultados expuestos permiten comprender mejor el funcionamiento del DSH de SINV, será necesario continuar la investigación para conocer mejor su actividad durante la iniciación de la traducción.

2. RESPUESTA DEL RBPOMA A LA INFECCIÓN POR SINV

Tras el estudio analítico de proteínas celulares específicas, previamente sugeridas como potenciales factores implicados en la traducción viral, se realizó un estudio exploratorio para determinar qué proteínas celulares interaccionan con los mRNAs virales de SINV. Como se ha podido observar, la infección por SINV induce profundos cambios fisiológicos en las células. Estos cambios alteran la dinámica del conjunto de las proteínas de unión a RNA (RBPs) celulares, el RBPoma. La detección de todas las proteínas de unión al RNA cuya actividad cambia durante el ciclo viral de SINV es esencial para determinar potenciales factores celulares que se unan a los mRNAs virales e intervengan en su traducción. Para identificar estas proteínas, se realizó un estudio exploratorio de las RBPs celulares y sus dinámicas durante la infección por SINV en las células de origen humano HEK293. Estas células son un buen modelo para estudiar las proteínas y factores implicados en el ciclo de SINV, ya que en ellas se puede observar la replicación viral, el *shut-off* de la síntesis de proteínas celulares, la alta producción de proteínas virales, la fosforilación de eIF2α, la formación de factorías de replicación, y la respuesta antiviral celular.

La infección por SINV induce cambios en el RBPoma activo. Se detectaron 247 RBPs que mostraban alteraciones en su actividad de unión al RNA bajo condiciones de infección; 133 de ellas veían su actividad de unión al RNA reducida, mientras que para las otras 114 era estimulada. Resulta muy interesante, que 181 del total de estas RBPs carecen de los dominios de unión al RNA clásicos. Este hecho parece resaltar la importancia del papel de RBPs no convencionales en el desarrollo de la infección viral. El reajuste del RBPoma durante la infección por SINV puede derivar de la pérdida masiva de RNA celular y la aparición de grandes cantidades de RNA viral. La inhibición de la

transcripción parece ser la principal responsable de la disminución de los RNAs celulares a las 4 hpi, mientras que, a las 18 hpi, la degradación del RNA representa más del 50% del cambio descrito. Pensamos que este fenómeno puede deberse a un efecto combinado de la reducción en la actividad transcripcional y la activación de la maquinaria de degradación 5'-3' del RNA, como es el caso de la exonucleasa XRN1, cuya actividad se encuentra estimulada a las 18 hpi (Mukherjee et al., 2017, Gorchakov et al., 2005). XRN1 está ampliamente considerada como un factor antiviral que degrada el RNA viral (Molleston and Cherry, 2017). Aunque en algunos casos, como en los flavivirus, XRN1 es esencial para la formación de los sfRNAs, que interfieren con la respuesta antiviral de la célula (Chapman et al., 2014, Pijlman et al., 2008, Manokaran et al., 2015). Nuestros resultados muestran la yuxtaposición de XRN1 con las factorías de replicación viral, sugiriendo que esta exonucleasa podría atacar al RNA viral. Pero sorprendentemente, las células KO para XRN1 son refractarias a la infección por SINV, y las KO parciales muestran un fenotipo intermedio. Estos datos sugieren que XRN1 es esencial para el desarrollo de la infección por SINV.

La remodelación del RBPoma dirigida por los cambios en la abundancia de los RNAs es compatible con el afinado mecanismo regulatorio que modula la actividad de las RBPs de forma individual. Por ejemplo, se conoce que la infección viral dispara una serie de vías de señalización que implican la activación de varias quinasas, E3 ubiquitin ligasas, isomerasas y chaperonas (Carrasco et al., 2018, Gack et al., 2007, Li et al., 2017). En nuestro estudio, se muestra que estas familias de proteínas están representadas entre las RBPs cuya actividad resultó estimulada en la infección, incluyendo SRPK1, TRIM25, TRIM56, PPIA y HSP90AB1. Por tanto, es plausible que el control post-traduccional también contribuya a la regulación de las RBPs en células infectadas por SINV. A su vez, hemos observado que la mayoría de las RBPs cuya actividad de unión al RNA se ve estimulada por la infección se acumulan en las factorías de replicación junto al RNA viral. Por otro lado, la interacción con proteínas virales podría regular la función de las RBPs (Fros et al., 2012). Uno de los casos más interesantes es el de GEMIN5. Nuestros datos muestran que GEMIN5 interactúa con varias proteínas virales, como nsP1, nsP2, nsP3 y C. Esta RBP está fuertemente estimulada por la infección con SINV y colocaliza con los RNAs de este virus en las factorías de replicación. Además, su sobreexpresión causa un moderado, pero significativo, retraso en la producción de proteínas virales. Estas observaciones coinciden con la descripción de GEMIN5 como un regulador de la traducción (Francisco-Velilla et al., 2018, Pineiro et al., 2013). Además, la interacción de GEMIN5 con la estructura cap, la 5'-UTR, y el DSH del sgRNA de SINV

apoyan el modelo en el que GEMIN5 reconoce el extremo 5' del gRNA y del sgRNA, y previene su traducción, interfiriendo con la función del ribosoma. Las implicaciones de las interacciones con elementos virales en la modulación de la función de GEMIN5 deberán estudiarse en futuras investigaciones.

Otro factor cuya actividad de unión al RNA se ve estimulada durante la infección por SINV es el eIF3, en concreto su subunidad eIF3D, que es capaz de unirse al cap (Lee et al., 2016) y podría sustituir al eIF4E. Lo mismo ocurre con la actividad de la helicasa DHX29, lo cual podría apuntar a su posible papel en la traducción de SINV sustituyendo al eIF4A (Skabkin et al., 2010).

Los cambios en el RBPoma son biológicamente importantes, ya que la perturbación de las RBPs afecta enormemente a la infección por SINV. Por tanto, las proteínas que, como se ha reportado, responden a la infección por SINV tienen una potencial función anti- o pro-viral, posicionando a las RBPs celulares como prometedoras dianas para terapias antivirales.

Algunas de las cuestiones más relevantes que se derivan de este trabajo son (1) si la composición de los ribosomas en células infectadas altera sus propiedades de traducción, (2) por qué la ausencia de la exonucleasa XRN1 convierte a la célula en refractaria para SINV, (3) qué dispara la degradación del RNA celular, y (4) por qué la transcripción inducida por la respuesta antiviral es resistente a la degradación.

3. REQUERIMIENTO DE FACTORES DE INICIACIÓN PARA LA TRADUCCIÓN DEL IRES DE HCV

En este trabajo doctoral también se han analizado los requerimientos de eIFs para la traducción de un mRNA viral que, en este caso, utiliza el elemento IRES en su iniciación. Este estudio se ha llevado a cabo para comparar este mecanismo de iniciación con el estudiado anteriormente en el sgRNA de SINV.

Los virus animales emplean una gran variedad de mecanismos para traducir sus mRNAs en condiciones de estrés, evitando la respuesta antiviral de las células (Firth and Brierley, 2012). HCV utiliza una estructura del RNA, conocida como elemento IRES, para dirigir la maquinaria de traducción a una posición interna en el 5'-UTR del mRNA viral (Hellen, 2009, Plank and Kieft, 2012). Numerosas investigaciones continúan analizando el mecanismo de la traducción dirigida por el IRES de HCV y su requerimiento de eIFs.

Algunos autores consideran que, en condiciones normales, el mRNA de HCV inicia su traducción usando el complejo ternario Met-tRNA$_i^{Met}$-eIF2-GTP, aunque eIF2 sea dispensable en condiciones de estrés (Jaafar et al., 2016). No obstante, existe la posibilidad de que eIF2 nunca participe en la iniciación del mRNA de HCV en células infectadas. De hecho, la interacción del IRES de HCV con los complejos de preiniciación parece desplazar el eIF2 fuera de estos complejos (Jaafar et al., 2016). Por lo tanto, es concebible que el elemento IRES sea suficiente para iniciar la traducción sin eIF2, incluso cuando este factor esté activo. Por otro lado, ensayos *in vitro* y experimentos en cultivos celulares apuntan a que el eIF2A puede reemplazar al eIF2 en la traducción dirigida por el IRES de HCV (Kim et al., 2011). Otros estudios *in vitro* señalan al eIF2D como sustituto del eIF2 en la traducción de HCV (Dmitriev et al., 2010, Skabkin et al., 2010). Nuestros resultados en células humanas demuestran que ni eIF2A ni eIF2D están implicados en la síntesis de proteínas dirigida por el IRES de HCV, y se corresponden con el estudio llevado a cabo por Jaafar et al. en células de hepatocarcinoma, donde el *knockdown* de eIF2A o eIF2D tiene muy poco efecto en la traducción dirigida por IRES de HCV (Jaafar et al., 2016). Los datos obtenidos con siRNAs aportan información complementaria a la generada a partir de las líneas HAP1 KO, y ambos coinciden en que estos factores no participan en la traducción del HCV. Además, la posibilidad de que eIF2A pueda estar reemplazado por eIF2D, o viceversa, fue descartada mediante ensayos realizados con la línea HAP1 doble KO. En esta línea celular, el mRNA HCV-Luc se traduce eficientemente en las condiciones de estrés producidas por el tratamiento con arsenito sódico. Por otra parte, estudios enfocados en identificar los genes necesarios para la replicación de HCV pero dispensables para el crecimiento celular no han señalado a eIF2A ni a eIF2D como candidatos (Marceau et al., 2016). Tanto eIF2A como eIF2D son genes dispensables para la viabilidad celular, según hemos demostrado (Sanz et al., 2017). Así pues, podemos concluir que estos genes no participan en la traducción del mRNA de HCV, y no reemplazan al eIF2, ni tan siquiera en condiciones de estrés celular.

El uso de líneas celulares KO será de gran utilidad en estudios futuros para descubrir el modo de iniciación y los factores requeridos para la traducción de los mRNAs virales. Curiosamente, a altas concentraciones de magnesio, la traducción *in vitro* del mRNA de HCV no requiere de ningún eIF (Lancaster et al., 2006). Por tanto, la modulación de las condiciones *in vitro* afecta enormemente a los requerimientos de eIFs en la iniciación de la síntesis de proteínas dirigida por el IRES de HCV. Por ello, consideramos que sería de gran relevancia científica que los experimentos *in vitro* que sugieren el requerimiento de ciertos eIFs para la traducción de un determinado mRNA

se pudieran contrastar con ensayos *in vivo* en cultivos celulares y, en este aspecto, las líneas KO serían herramientas de gran utilidad.

Existe un mayor consenso científico acerca de la independencia del complejo eIF4F, y sus tres factores, eIF4E, eIF4G y eIF4A, para la traducción del mRNA de HCV (Niepmann, 2013). Debido a que este mRNA viral no presenta una estructura cap en su extremo 5', resulta lógico que el eIF4E no esté implicado en su traducción. Además, como durante la iniciación no ocurre el mecanismo de *scanning*, tampoco resultaría necesaria la helicasa el eIF4A. En nuestro trabajo mostramos que el tratamiento con inhibidores selectivos de eIF4A no afecta a la síntesis de luciferasa dirigida por el IRES de HCV presente en un mRNA monocistrónico, que contiene la región 3'-UTR de HCV, transfectado en células humanas de origen hepático. Por lo tanto, nuestros resultados con hipp y Pat A demuestran que el eIF4A no participa en el proceso de iniciación. Esto está en concordancia con las observaciones previas que mostraban que estos inhibidores no bloquean la traducción dirigida por el IRES de HCV en mRNAs dicistrónicos (Bordeleau et al., 2006, Low et al., 2007). Estas observaciones, junto con el descubrimiento de que eIF4G se encuentra localizado en los SGs tras el tratamiento con arsenito sódico, son consistentes con la idea de que el complejo eIF4F no participa en la traducción del mRNA de HCV.

Posiblemente, el aspecto más importante para ser clarificado en la iniciación de la síntesis de proteínas dirigida por el IRES de HCV es determinar si el eIF2 está implicado en condiciones en las que no haya estrés celular. Experimentos *in vitro* han demostrado que el IRES de HCV puede interaccionar directamente con la subunidad 40S ribosómica sin eIFs, y que después, puede reclutar al eIF3 y al complejo ternario con eIF2 (Ji et al., 2004, Otto and Puglisi, 2004). La interacción del IRES de HCV con la subunidad 40S o el ribosoma 80S lleva a la remodelación de su estructura. De esta forma, el dominio II queda unido al sitio de salida del tRNA, mientras que el dominio III se posiciona con el codón de iniciación en la cabeza de la subunidad pequeña ribosómica (Boehringer et al., 2005). Se ha observado que subunidades ribosómicas 40S marcadas con fluorescencia en su proteína RPS25 se unen de manera irreversible al IRES de HCV, provocando reajustes conformacionales del dominio II, que se encuentra estabilizado por proteínas celulares aún por identificar (Fuchs et al., 2015). Sin embargo, se desconoce si, en condiciones fisiológicas sin estrés, el mRNA de HCV interactuaría con la subunidad 40S, o más probablemente con los complejos de preiniciación que podrían contener ya varios eIFs, como eIF3 y eIF1A (Jaafar et al., 2016). La unión del IRES a los complejos de preiniciación en células sin condiciones de estrés puede desplazar el eIF2

mediante la interacción del dominio II con la subunidad 40S (Locker et al., 2007). De hecho, los sitios de unión al dominio II y al complejo ternario solapan de tal forma que la interacción de los dos sobre la subunidad 40S interferiría entre sí (Jaafar et al., 2016). Es posible que el dominio II del IRES de HCV reemplace funcionalmente al complejo ternario sin la necesidad de otros factores celulares como el eIF2A o el eIF2D, incluso en condiciones fisiológicas sin estrés. De hecho, el dominio II adopta una estructura en forma de "L" e interacciona con la subunidad 40S en la región de la cabeza del sitio E, permitiendo que el *loop* apical del dominio II pueda penetrar profundamente en la hendidura del mRNA cerca de la región codificante en el sitio P del ribosoma (Spahn et al., 2001, Lukavsky et al., 2003). Por tanto, el IRES podría ser capaz de reemplazar el complejo ternario y, tras la formación del ribosoma 80S, el sitio P estaría ocupado, dejando el sitio A libre para que se posicione el AUG_i y comenzar la traducción. Este modelo es parecido al descrito para el funcionamiento del IRES de CrPV, con la excepción de que eIF3 sí está implicado en la traducción de HCV (Jan and Sarnow, 2002, Fernandez et al., 2014).

La función exacta del eIF2A o del eIF2D durante la traducción de los mRNAs celulares permanece desconocida. La generación de un ratón KO para eIF2 claramente demuestra que este factor no es requerido durante la embriogénesis, ni tampoco está implicado en la traducción de mRNAs específicos de tejido (Golovko et al., 2016). El reciente descubrimiento de que el eIF2A participa en la tumorogénesis hace que el estudio de este factor sea especialmente relevante (Sendoel et al., 2017). Sin embargo, eIF2A es probablemente requerido para otras funciones adicionales en la célula aparte de su implicación en la progresión del cáncer. El uso de líneas celulares humanas KO como las empleadas en nuestros trabajos, puede ayudar a mejorar nuestro entendimiento del eIF2A y del eIF2D en la traducción. Como se ha observado recientemente (Sanz et al., 2017, Gonzalez-Almela et al., 2018), estos dos factores no son necesarios para la traducción global de mRNAs celulares ni para la síntesis de luciferasa dirigida por los IRES de HCV, EMCV o CrPV. Futuros estudios dirigidos a analizar el comportamiento de mRNAs celulares especializados en estas líneas KO ayudarán a averiguar la función de eIF2A y eIF2D en células de mamífero.

CONCLUSIONS

CONCLUSIONS

1. Pateamine A strongly blocks the synthesis of SINV nsPs at early times post infection in an irreversible manner and therefore, SINV gRNA requires the eukaryotic initiation factor eIF4A for translation.
2. SINV sgRNA is resistant to pateamine A inhibition at late times of infection but it is sensitive to pateamine A in transfected cells or in cell-free systems, indicating that this viral mRNA exhibits a dual mechanism for translation. Consequently, the structure of sgRNA is not the only element involved in the independence from several eIFs.
3. The eukaryotic factors eIF2A and eIF2D are not required for SINV gRNA and sgRNA translation when eIF2α is phosphorylated. They are not necessary either for global translation of cellular mRNAs or for luciferase synthesis directed by EMCV or CrPV IRESs.
4. SINV sgRNA can initiate translation in non-AUG codons, such as CUG, in a mechanism dependent on the downstream stable hairpin (DSH) element but independent of eIF2, eIF2A or eIF2D.
5. The structure, but not the sequence, of the stem region of the SINV DSH, and the sequence of its loop play important roles in the function of this hairpin. DSH can be replaced to some extent by domain II of the HCV IRES.
6. SINV infection induces changes in the active RBPome: 247 RNA binding proteins (RBPs) display differential interaction with RNA, and 181 of these lack classical RNA binding domains. These alterations are mainly driven by the loss of cellular mRNAs and the emergence of viral RNA.
7. The RNA binding activity of the RBPs eIF3D, DHX29, PPIA, SRPK1, XRN1, TRIM25, TRIM56, GEMIN5 is stimulated upon SINV infection. These RBPs are located in close proximity to SINV replication factories. SINV fitness seems to benefit from the activity of IRE1α, tRNA-ligase complex (TRLC), HSP90AB1, PA2G4 and SRPK1, but TRIM25, TRIM56 and GEMIN5 hamper the infection. Interestingly, XRN1 is essential for SINV infection.
8. The initiation factors eIF2, eIF2A, eIF2D, eIF4A, and eIF4G are not involved in translation driven by HCV IRES in human cells.

BIBLIOGRAFÍA

BIBLIOGRAFÍA

ABAEVA, I. S., MARINTCHEV, A., PISAREVA, V. P., HELLEN, C. U. & PESTOVA, T. V. 2011. Bypassing of stems versus linear base-by-base inspection of mammalian mRNAs during ribosomal scanning. *EMBO J,* 30**,** 115-29.

ADAMS, S. L., SAFER, B., ANDERSON, W. F. & MERRICK, W. C. 1975. Eukaryotic initiation complex formation. Evidence for two distinct pathways. *J Biol Chem,* 250**,** 9083-9.

AHMED, Y. L., SCHLEICH, S., BOHLEN, J., MANDEL, N., SIMON, B., SINNING, I. & TELEMAN, A. A. 2018. DENR-MCTS1 heterodimerization and tRNA recruitment are required for translation reinitiation. *PLoS Biol,* 16**,** e2005160.

AHOLA, T., KUJALA, P., TUITTILA, M., BLOM, T., LAAKKONEN, P., HINKKANEN, A. & AUVINEN, P. 2000. Effects of palmitoylation of replicase protein nsP1 on alphavirus infection. *J Virol,* 74**,** 6725-33.

AHOLA, T., LAAKKONEN, P., VIHINEN, H. & KAARIAINEN, L. 1997. Critical residues of Semliki Forest virus RNA capping enzyme involved in methyltransferase and guanylyltransferase-like activities. *J Virol,* 71**,** 392-7.

AHOLA, T., LAMPIO, A., AUVINEN, P. & KAARIAINEN, L. 1999. Semliki Forest virus mRNA capping enzyme requires association with anionic membrane phospholipids for activity. *EMBO J,* 18**,** 3164-72.

AKHRYMUK, I., KULEMZIN, S. V. & FROLOVA, E. I. 2012. Evasion of the innate immune response: the Old World alphavirus nsP2 protein induces rapid degradation of Rpb1, a catalytic subunit of RNA polymerase II. *J Virol,* 86**,** 7180-91.

ASANO, K. & SACHS, M. S. 2007. Translation factor control of ribosome conformation during start codon selection. *Genes Dev,* 21**,** 1280-7.

ASANO, K., SHALEV, A., PHAN, L., NIELSEN, K., CLAYTON, J., VALASEK, L., DONAHUE, T. F. & HINNEBUSCH, A. G. 2001. Multiple roles for the C-terminal domain of eIF5 in translation initiation complex assembly and GTPase activation. *EMBO J,* 20**,** 2326-37.

BALVAY, L., SOTO RIFO, R., RICCI, E. P., DECIMO, D. & OHLMANN, T. 2009. Structural and functional diversity of viral IRESes. *Biochim Biophys Acta,* 1789**,** 542-57.

BARNHART, M. D., MOON, S. L., EMCH, A. W., WILUSZ, C. J. & WILUSZ, J. 2013. Changes in cellular mRNA stability, splicing, and polyadenylation through HuR protein sequestration by a cytoplasmic RNA virus. *Cell Rep,* 5**,** 909-17.

BELSHAM, G. J. 2009. Divergent picornavirus IRES elements. *Virus Res,* 139**,** 183-92.

BERGLUND, P., FINZI, D., BENNINK, J. R. & YEWDELL, J. W. 2007. Viral alteration of cellular translational machinery increases defective ribosomal products. *J Virol,* 81**,** 7220-9.

BESSE, F. & EPHRUSSI, A. 2008. Translational control of localized mRNAs: restricting protein synthesis in space and time. *Nat Rev Mol Cell Biol,* 9**,** 971-80.

BOEHRINGER, D., THERMANN, R., OSTARECK-LEDERER, A., LEWIS, J. D. & STARK, H. 2005. Structure of the hepatitis C virus IRES bound to the human 80S ribosome: remodeling of the HCV IRES. *Structure,* 13**,** 1695-706.

BORDELEAU, M. E., CENCIC, R., LINDQVIST, L., OBERER, M., NORTHCOTE, P., WAGNER, G. & PELLETIER, J. 2006. RNA-mediated sequestration of the RNA helicase eIF4A by Pateamine A inhibits translation initiation. *Chem Biol,* 13**,** 1287-95.

BORDELEAU, M. E., MATTHEWS, J., WOJNAR, J. M., LINDQVIST, L., NOVAC, O., JANKOWSKY, E., SONENBERG, N., NORTHCOTE, P., TEESDALE-SPITTLE, P. & PELLETIER, J. 2005. Stimulation of mammalian translation initiation factor eIF4A activity by a small molecule inhibitor of eukaryotic translation. *Proc Natl Acad Sci U S A,* 102**,** 10460-5.

BREAKWELL, L., DOSENOVIC, P., KARLSSON HEDESTAM, G. B., D'AMATO, M., LILJESTROM, P., FAZAKERLEY, J. & MCINERNEY, G. M. 2007. Semliki Forest virus nonstructural protein 2 is involved in suppression of the type I interferon response. *J Virol,* 81**,** 8677-84.

BROWN, D. T. & HERNANDEZ, R. 2012. Infection of cells by alphaviruses. *Adv Exp Med Biol,* 726**,** 181-99.

BUSHELL, M. & SARNOW, P. 2002. Hijacking the translation apparatus by RNA viruses. *J Cell Biol,* 158**,** 395-9.

CARRASCO, L. 1978. Membrane leakiness after viral infection and a new approach to the development of antiviral agents. *Nature,* 272**,** 694-9.

CARRASCO, L., SANZ, M. A. & GONZALEZ-ALMELA, E. 2018. The Regulation of Translation in Alphavirus-Infected Cells. *Viruses,* 10.

CARRASCO, L. G., R.; IRURZUN, A.; BARCO, A. 2002. Effects of viral replication on cellular membrane metabolism and function. *Molecular Biology of Picornaviruses.* Washington,

DC, USA: Wimmer, E., Semler, B.L., Eds.; ASM Press.

CASTELLO, A., FISCHER, B., EICHELBAUM, K., HOROS, R., BECKMANN, B. M., STREIN, C., DAVEY, N. E., HUMPHREYS, D. T., PREISS, T., STEINMETZ, L. M., KRIJGSVELD, J. & HENTZE, M. W. 2012. Insights into RNA biology from an atlas of mammalian mRNA-binding proteins. *Cell,* 149**,** 1393-406.

CASTELLO, A., FISCHER, B., FRESE, C. K., HOROS, R., ALLEAUME, A. M., FOEHR, S., CURK, T., KRIJGSVELD, J. & HENTZE, M. W. 2016. Comprehensive Identification of RNA-Binding Domains in Human Cells. *Mol Cell,* 63**,** 696-710.

CASTELLO, A., FRANCO, D., MORAL-LOPEZ, P., BERLANGA, J. J., ALVAREZ, E., WIMMER, E. & CARRASCO, L. 2009. HIV- 1 protease inhibits Cap- and poly(A)-dependent translation upon eIF4GI and PABP cleavage. *PLoS One,* 4**,** e7997.

CASTELLO, A., SANZ, M. A., MOLINA, S. & CARRASCO, L. 2006. Translation of Sindbis virus 26S mRNA does not require intact eukariotic initiation factor 4G. *J Mol Biol,* 355**,** 942-56.

CENCIC, R., GALICIA-VAZQUEZ, G. & PELLETIER, J. 2012. Inhibitors of translation targeting eukaryotic translation initiation factor 4A. *Methods Enzymol,* 511**,** 437-61.

CLEMENS, M. J. 2005. Translational control in virus-infected cells: models for cellular stress responses. *Semin Cell Dev Biol,* 16**,** 13-20.

CONTRERAS, A. & CARRASCO, L. 1979. Selective inhibition of protein synthesis in virus-infected mammalian cells. *J Virol,* 29**,** 114-22.

CRISTEA, I. M., ROZJABEK, H., MOLLOY, K. R., KARKI, S., WHITE, L. L., RICE, C. M., ROUT, M. P., CHAIT, B. T. & MACDONALD, M. R. 2010. Host factors associated with the Sindbis virus RNA-dependent RNA polymerase: role for G3BP1 and G3BP2 in virus replication. *J Virol,* 84, 6720-32.

CHAPMAN, E. G., COSTANTINO, D. A., RABE, J. L., MOON, S. L., WILUSZ, J., NIX, J. C. & KIEFT, J. S. 2014. The structural basis of pathogenic subgenomic flavivirus RNA (sfRNA) production. *Science,* 344, 307-10.

CHEN, L., WANG, M., ZHU, D., SUN, Z., MA, J., WANG, J., KONG, L., WANG, S., LIU, Z., WEI, L., HE, Y., WANG, J. & ZHANG, X. 2018. Implication for alphavirus host-cell entry and assembly indicated by a 3.5A resolution cryo-EM structure. *Nat Commun,* 9, 5326.

CHEUNG, Y. N., MAAG, D., MITCHELL, S. F., FEKETE, C. A., ALGIRE, M. A., TAKACS, J. E., SHIROKIKH, N., PESTOVA, T., LORSCH, J. R. & HINNEBUSCH, A. G. 2007. Dissociation of eIF1 from the 40S ribosomal subunit is a key step in start codon selection in vivo. *Genes Dev,* 21, 1217-30.

CHUNG, B. Y., FIRTH, A. E. & ATKINS, J. F. 2010. Frameshifting in alphaviruses: a diversity of 3' stimulatory structures. *J Mol Biol,* 397, 448-56.

DABO, S. & MEURS, E. F. 2012. dsRNA-dependent protein kinase PKR and its role in stress, signaling and HCV infection. *Viruses,* 4, 2598-635.

DE GROOT, R. J., HARDY, W. R., SHIRAKO, Y. & STRAUSS, J. H. 1990. Cleavage-site preferences of Sindbis virus polyproteins containing the non-structural proteinase. Evidence for temporal regulation of polyprotein processing in vivo. *EMBO J,* 9, 2631-8.

DERRY, M. C., YANAGIYA, A., MARTINEAU, Y. & SONENBERG, N. 2006. Regulation of poly(A)-binding protein through PABP-interacting proteins. *Cold Spring Harb Symp Quant Biol,* 71, 537-43.

DICKSON, A. M., ANDERSON, J. R., BARNHART, M. D., SOKOLOSKI, K. J., OKO, L., OPYRCHAL, M., GALANIS, E., WILUSZ, C. J., MORRISON, T. E. & WILUSZ, J. 2012. Dephosphorylation of HuR protein during alphavirus infection is associated with HuR relocalization to the cytoplasm. *J Biol Chem,* 287, 36229-38.

DMITRIEV, S. E., TERENIN, I. M., ANDREEV, D. E., IVANOV, P. A., DUNAEVSKY, J. E., MERRICK, W. C. & SHATSKY, I. N. 2010. GTP-independent tRNA delivery to the ribosomal P-site by a novel eukaryotic translation factor. *J Biol Chem,* 285, 26779-87.

DONNELLY, N., GORMAN, A. M., GUPTA, S. & SAMALI, A. 2013. The eIF2alpha kinases: their structures and functions. *Cell Mol Life Sci,* 70, 3493-511.

DRUMMOND, D. A. & WILKE, C. O. 2009. The evolutionary consequences of erroneous protein synthesis. *Nat Rev Genet,* 10, 715-24.

FATA, C. L., SAWICKI, S. G. & SAWICKI, D. L. 2002. Modification of Asn374 of nsP1 suppresses a Sindbis virus nsP4 minus-strand polymerase mutant. *J Virol,* 76, 8641-9.

FERNANDEZ, I. S., BAI, X. C., MURSHUDOV, G., SCHERES, S. H. & RAMAKRISHNAN, V. 2014. Initiation of translation by cricket paralysis virus IRES requires its translocation in the ribosome. *Cell,* 157, 823-31.

FIRTH, A. E. & BRIERLEY, I. 2012. Non-canonical translation in RNA viruses. *J Gen Virol,* 93, 1385-409.

FIRTH, A. E., CHUNG, B. Y., FLEETON, M. N. & ATKINS, J. F. 2008. Discovery of frameshifting in Alphavirus 6K resolves a 20-year enigma. *Virol J,* 5**,** 108.

FITZGERALD, K. D. & SEMLER, B. L. 2009. Bridging IRES elements in mRNAs to the eukaryotic translation apparatus. *Biochim Biophys Acta,* 1789**,** 518-28.

FORRESTER, N. L., PALACIOS, G., TESH, R. B., SAVJI, N., GUZMAN, H., SHERMAN, M., WEAVER, S. C. & LIPKIN, W. I. 2012. Genome-scale phylogeny of the alphavirus genus suggests a marine origin. *J Virol,* 86**,** 2729-38.

FRANCISCO-VELILLA, R., FERNANDEZ-CHAMORRO, J., DOTU, I. & MARTINEZ-SALAS, E. 2018. The landscape of the non-canonical RNA-binding site of Gemin5 unveils a feedback loop counteracting the negative effect on translation. *Nucleic Acids Res,* 46**,** 7339-7353.

FROLOV, I. & SCHLESINGER, S. 1994. Comparison of the effects of Sindbis virus and Sindbis virus replicons on host cell protein synthesis and cytopathogenicity in BHK cells. *J Virol,* 68**,** 1721-7.

FROLOV, I. & SCHLESINGER, S. 1996. Translation of Sindbis virus mRNA: analysis of sequences downstream of the initiating AUG codon that enhance translation. *J Virol,* 70**,** 1182-90.

FROS, J. J., DOMERADZKA, N. E., BAGGEN, J., GEERTSEMA, C., FLIPSE, J., VLAK, J. M. & PIJLMAN, G. P. 2012. Chikungunya virus nsP3 blocks stress granule assembly by recruitment of G3BP into cytoplasmic foci. *J Virol,* 86**,** 10873-9.

FROS, J. J. & PIJLMAN, G. P. 2016. Alphavirus Infection: Host Cell Shut-Off and Inhibition of Antiviral Responses. *Viruses,* 8.

FUCHS, G., PETROV, A. N., MARCEAU, C. D., POPOV, L. M., CHEN, J., O'LEARY, S. E., WANG, R., CARETTE, J. E., SARNOW, P. & PUGLISI, J. D. 2015. Kinetic pathway of 40S ribosomal subunit recruitment to hepatitis C virus internal ribosome entry site. *Proc Natl Acad Sci U S A,* 112**,** 319-25.

FULLER, S. D. 1987. The T = 4 envelope of Sindbis virus is organized by interactions with a complementary T = 3 capsid. *Cell,* 48**,** 923-934.

GACK, M. U., SHIN, Y. C., JOO, C. H., URANO, T., LIANG, C., SUN, L., TAKEUCHI, O., AKIRA, S., CHEN, Z., INOUE, S. & JUNG, J. U. 2007. TRIM25 RING-finger E3 ubiquitin ligase is essential for RIG-I-mediated antiviral activity. *Nature,* 446**,** 916-920.

GAEDIGK-NITSCHKO, K. & SCHLESINGER, M. J. 1990. The Sindbis virus 6K protein can be detected in virions and is acylated with fatty acids. *Virology,* 175**,** 274-81.

GALE, M., JR., TAN, S. L. & KATZE, M. G. 2000. Translational control of viral gene expression in eukaryotes. *Microbiol Mol Biol Rev,* 64**,** 239-80.

GARCIA-MORENO, M., NOERENBERG, M., NI, S., JARVELIN, A. I., GONZALEZ-ALMELA, E., LENZ, C. E., BACH-PAGES, M., COX, V., AVOLIO, R., DAVIS, T., HESTER, S., SOHIER, T. J. M., LI, B., HEIKEL, G., MICHLEWSKI, G., SANZ, M. A., CARRASCO, L., RICCI, E. P., PELECHANO, V., DAVIS, I., FISCHER, B., MOHAMMED, S. & CASTELLO, A. 2019. System-wide Profiling of RNA-Binding Proteins Uncovers Key Regulators of Virus Infection. *Mol Cell,* 74**,** 196-211.

GARCIA-MORENO, M., SANZ, M. A. & CARRASCO, L. 2015. Initiation codon selection is accomplished by a scanning mechanism without crucial initiation factors in Sindbis virus subgenomic mRNA. *RNA,* 21**,** 93-112.

GARCIA-MORENO, M., SANZ, M. A. & CARRASCO, L. 2016. A Viral mRNA Motif at the 3'-Untranslated Region that Confers Translatability in a Cell-Specific Manner. Implications for Virus Evolution. *Sci Rep,* 6**,** 19217.

GARCIA-MORENO, M., SANZ, M. A., PELLETIER, J. & CARRASCO, L. 2013. Requirements for eIF4A and eIF2 during translation of Sindbis virus subgenomic mRNA in vertebrate and invertebrate host cells. *Cell Microbiol,* 15**,** 823-40.

GARMASHOVA, N., GORCHAKOV, R., FROLOVA, E. & FROLOV, I. 2006. Sindbis virus nonstructural protein nsP2 is cytotoxic and inhibits cellular transcription. *J Virol,* 80**,** 5686-96.

GARNEAU, N. L., SOKOLOSKI, K. J., OPYRCHAL, M., NEFF, C. P., WILUSZ, C. J. & WILUSZ, J. 2008. The 3' untranslated region of sindbis virus represses deadenylation of viral transcripts in mosquito and Mammalian cells. *J Virol,* 82**,** 880-92.

GARRY, R. F. 1994. Sindbis virus-induced inhibition of protein synthesis is partially reversed by medium containing an elevated potassium concentration. *J Gen Virol,* 75 (Pt 2)**,** 411-5.

GARRY, R. F., BISHOP, J. M., PARKER, S., WESTBROOK, K., LEWIS, G. & WAITE, M. R. 1979. Na+ and K+ concentrations and the regulation of protein synthesis in Sindbis virus-infected chick cells. *Virology,* 96**,** 108-20.

GINGRAS, A. C., RAUGHT, B. & SONENBERG, N. 1999. eIF4 initiation factors: effectors of mRNA recruitment to ribosomes and regulators of translation. *Annu Rev Biochem,* 68**,** 913-63.

GOLOVKO, A., KOJUKHOV, A., GUAN, B. J., MORPURGO, B., MERRICK, W. C., MAZUMDER, B., HATZOGLOU, M. & KOMAR, A. A. 2016. The eIF2A knockout mouse. *Cell Cycle,* 15**,** 3115-3120.

GOMEZ DE CEDRON, M., EHSANI, N., MIKKOLA, M. L., GARCIA, J. A. & KAARIAINEN, L. 1999. RNA helicase activity of Semliki Forest virus replicase protein NSP2. *FEBS Lett,* 448**,** 19-22.

GONZALEZ-ALMELA, E., SANZ, M. A., GARCIA-MORENO, M., NORTHCOTE, P., PELLETIER, J. & CARRASCO, L. 2015. Differential action of pateamine A on translation of genomic and subgenomic mRNAs from Sindbis virus. *Virology,* 484**,** 41-50.

GONZALEZ-ALMELA, E., WILLIAMS, H., SANZ, M. A. & CARRASCO, L. 2018. The Initiation Factors eIF2, eIF2A, eIF2D, eIF4A, and eIF4G Are Not Involved in Translation Driven by Hepatitis C Virus IRES in Human Cells. *Front Microbiol,* 9**,** 207.

GORCHAKOV, R., FROLOVA, E. & FROLOV, I. 2005. Inhibition of transcription and translation in Sindbis virus-infected cells. *J Virol,* 79**,** 9397-409.

GORCHAKOV, R., FROLOVA, E., WILLIAMS, B. R., RICE, C. M. & FROLOV, I. 2004. PKR-dependent and -independent mechanisms are involved in translational shutoff during Sindbis virus infection. *J Virol,* 78**,** 8455-67.

GRIFFIN, D. E. 2007. Alphaviruses. *In:* FIELDS, F. V. (ed.) *Alphaviruses.* Philadelphia, PA, USA: B.N., Knipe, D.M., Howley, P.M., Eds.;Wolters Kluwer Health/Lippincott Williams & Wilkins.

GRITSUN, T. S. & GOULD, E. A. 2006. Direct repeats in the 3' untranslated regions of mosquito-borne flaviviruses: possible implications for virus transmission. *J Gen Virol,* 87**,** 3297-305.

HAASNOOT, J. & BERKHOUT, B. 2011. RNAi and cellular miRNAs in infections by mammalian viruses. *Methods Mol Biol,* 721**,** 23-41.

HAIMOV, O., SINVANI, H. & DIKSTEIN, R. 2015. Cap-dependent, scanning-free translation initiation mechanisms. *Biochim Biophys Acta,* 1849**,** 1313-8.

HAJARIZADEH, B., GREBELY, J. & DORE, G. J. 2013. Epidemiology and natural history of HCV infection. *Nat Rev Gastroenterol Hepatol,* 10**,** 553-62.

HARAK, C. & LOHMANN, V. 2015. Ultrastructure of the replication sites of positive-strand RNA viruses. *Virology*, 479-480, 418-33.

HARDY, R. W. 2006. The role of the 3' terminus of the Sindbis virus genome in minus-strand initiation site selection. *Virology,* 345**,** 520-31.

HELLEN, C. U. 2009. IRES-induced conformational changes in the ribosome and the mechanism of translation initiation by internal ribosomal entry. *Biochim Biophys Acta,* 1789**,** 558-70.

HELLEN, C. U. & PESTOVA, T. V. 1999. Translation of hepatitis C virus RNA. *J Viral Hepat,* 6**,** 79-87.

HELLEN, C. U. T. 2018. Translation Termination and Ribosome Recycling in Eukaryotes. *Cold Spring Harb Perspect Biol,* 10.

HELLSTROM, K., KALLIO, K., UTT, A., QUIRIN, T., JOKITALO, E., MERITS, A. & AHOLA, T. 2017. Partially Uncleaved Alphavirus Replicase Forms Spherule Structures in the Presence and Absence of RNA Template. *J Virol,* 91.

HERSHEY, J. W. 1989. Protein phosphorylation controls translation rates. *J Biol Chem,* 264**,** 20823-6.

HERTZ, M. I. & THOMPSON, S. R. 2011. Mechanism of translation initiation by Dicistroviridae IGR IRESs. *Virology,* 411**,** 355-61.

HINNEBUSCH, A. G. 2011. Molecular mechanism of scanning and start codon selection in eukaryotes. *Microbiol Mol Biol Rev,* 75**,** 434-67, first page of table of contents.

HINNEBUSCH, A. G. 2014. The scanning mechanism of eukaryotic translation initiation. *Annu Rev Biochem,* 83**,** 779-812.

HYDE, J. L., CHEN, R., TROBAUGH, D. W., DIAMOND, M. S., WEAVER, S. C., KLIMSTRA, W. B. & WILUSZ, J. 2015. The 5' and 3' ends of alphavirus RNAs--Non-coding is not non-functional. *Virus Res,* 206**,** 99-107.

JAAFAR, Z. A., OGURO, A., NAKAMURA, Y. & KIEFT, J. S. 2016. Translation initiation by the hepatitis C virus IRES requires eIF1A and ribosomal complex remodeling. *Elife,* 5.

JACKSON, R. J., HELLEN, C. U. & PESTOVA, T. V. 2010. The mechanism of eukaryotic translation initiation and principles of its regulation. *Nat Rev Mol Cell Biol,* 11**,** 113-27.

JAN, E., MOHR, I. & WALSH, D. 2016. A Cap-to-Tail Guide to mRNA Translation Strategies in Virus-Infected Cells. *Annu Rev Virol,* 3**,** 283-307.

JAN, E. & SARNOW, P. 2002. Factorless ribosome assembly on the internal ribosome entry site of cricket paralysis virus. *J Mol Biol,* 324**,** 889-902.

JANG, S. K. 2006. Internal initiation: IRES elements of picornaviruses and hepatitis c virus. *Virus Res,* 119**,** 2-15.

JI, H., FRASER, C. S., YU, Y., LEARY, J. & DOUDNA, J. A. 2004. Coordinated assembly of human translation initiation complexes by the hepatitis C virus internal ribosome entry site RNA. *Proc Natl Acad Sci U S A,* 101, 16990-5.

JOHNSON, A. G., GROSELY, R., PETROV, A. N. & PUGLISI, J. D. 2017. Dynamics of IRES-mediated translation. *Philos Trans R Soc Lond B Biol Sci,* 372.

JOSE, J., SNYDER, J. E. & KUHN, R. J. 2009. A structural and functional perspective of alphavirus replication and assembly. *Future Microbiol,* 4, 837-56.

KARPF, A. R., BLAKE, J. M. & BROWN, D. T. 1997. Characterization of the infection of Aedes albopictus cell clones by Sindbis virus. *Virus Res,* 50, 1-13.

KEARSE, M. G. & WILUSZ, J. E. 2017. Non-AUG translation: a new start for protein synthesis in eukaryotes. *Genes Dev,* 31, 1717-1731.

KHAWAJA, A., VOPALENSKY, V. & POSPISEK, M. 2015. Understanding the potential of hepatitis C virus internal ribosome entry site domains to modulate translation initiation via their structure and function. *Wiley Interdiscip Rev RNA,* 6, 211-24.

KHULLAR, V. & FIRPI, R. J. 2015. Hepatitis C cirrhosis: New perspectives for diagnosis and treatment. *World J Hepatol,* 7, 1843-55.

KIEFT, J. S. 2008. Viral IRES RNA structures and ribosome interactions. *Trends Biochem Sci,* 33, 274-83.

KIM, J. H., PARK, S. M., PARK, J. H., KEUM, S. J. & JANG, S. K. 2011. eIF2A mediates translation of hepatitis C viral mRNA under stress conditions. *EMBO J,* 30, 2454-64.

KNELLER, E. L., RAKOTONDRAFARA, A. M. & MILLER, W. A. 2006. Cap-independent translation of plant viral RNAs. *Virus Res,* 119, 63-75.

KOLITZ, S. E. & LORSCH, J. R. 2010. Eukaryotic initiator tRNA: finely tuned and ready for action. *FEBS Lett,* 584, 396-404.

KOMAR, A. A., MAZUMDER, B. & MERRICK, W. C. 2012. A new framework for understanding IRES-mediated translation. *Gene,* 502, 75-86.

KOROMILAS, A. E. 2015. Roles of the translation initiation factor eIF2alpha serine 51 phosphorylation in cancer formation and treatment. *Biochim Biophys Acta,* 1849, 871-80.

KOZAK, M. 1990. Downstream secondary structure facilitates recognition of initiator codons by eukaryotic ribosomes. *Proc Natl Acad Sci U S A,* 87, 8301-5.

KOZAK, M. 1991. Structural features in eukaryotic mRNAs that modulate the initiation of translation. *J Biol Chem,* 266, 19867-70.

KOZAK, M. 1999. Initiation of translation in prokaryotes and eukaryotes. *Gene,* 234, 187-208.

KRAFT, J. J., TREDER, K., PETERSON, M. S. & MILLER, W. A. 2013. Cation-dependent folding of 3' cap-independent translation elements facilitates interaction of a 17-nucleotide conserved sequence with eIF4G. *Nucleic Acids Res,* 41, 3398-413.

LAAKKONEN, P., AHOLA, T. & KAARIAINEN, L. 1996. The effects of palmitoylation on membrane association of Semliki forest virus RNA capping enzyme. *J Biol Chem,* 271, 28567-71.

LANCASTER, A. M., JAN, E. & SARNOW, P. 2006. Initiation factor-independent translation mediated by the hepatitis C virus internal ribosome entry site. *RNA,* 12, 894-902.

LARK, T., KECK, F. & NARAYANAN, A. 2017. Interactions of Alphavirus nsP3 Protein with Host Proteins. *Front Microbiol,* 8**,** 2652.

LASTARZA, M. W., LEMM, J. A. & RICE, C. M. 1994. Genetic analysis of the nsP3 region of Sindbis virus: evidence for roles in minus-strand and subgenomic RNA synthesis. *J Virol,* 68**,** 5781-91.

LEE, A. S., KRANZUSCH, P. J., DOUDNA, J. A. & CATE, J. H. 2016. eIF3d is an mRNA cap-binding protein that is required for specialized translation initiation. *Nature,* 536**,** 96-9.

LEE, K. M., CHEN, C. J. & SHIH, S. R. 2017. Regulation Mechanisms of Viral IRES-Driven Translation. *Trends Microbiol,* 25**,** 546-561.

LEMM, J. A., RUMENAPF, T., STRAUSS, E. G., STRAUSS, J. H. & RICE, C. M. 1994. Polypeptide requirements for assembly of functional Sindbis virus replication complexes: a model for the temporal regulation of minus- and plus-strand RNA synthesis. *EMBO J,* 13**,** 2925-34.

LEUNG, J. Y., NG, M. M. & CHU, J. J. 2011. Replication of alphaviruses: a review on the entry process of alphaviruses into cells. *Adv Virol,* 2011**,** 249640.

LI, G. & RICE, C. M. 1993. The signal for translational readthrough of a UGA codon in Sindbis virus RNA involves a single cytidine residue immediately downstream of the termination codon. *J Virol,* 67**,** 5062-7.

LI, M. M., LAU, Z., CHEUNG, P., AGUILAR, E. G., SCHNEIDER, W. M., BOZZACCO, L., MOLINA, H., BUEHLER, E., TAKAOKA, A., RICE, C. M., FELSENFELD, D. P. & MACDONALD, M. R. 2017. TRIM25 Enhances the Antiviral Action of Zinc-Finger Antiviral Protein (ZAP). *PLoS Pathog,* 13**,** e1006145.

LIANG, H., CHEN, X., YIN, Q., RUAN, D., ZHAO, X., ZHANG, C., MCNUTT, M. A. & YIN, Y. 2017. PTENbeta is an alternatively translated isoform of PTEN that regulates rDNA transcription. *Nat Commun,* 8**,** 14771.

LIANG, H., HE, S., YANG, J., JIA, X., WANG, P., CHEN, X., ZHANG, Z., ZOU, X., MCNUTT, M. A., SHEN, W. H. & YIN, Y. 2014. PTENalpha, a PTEN isoform translated through alternative initiation, regulates mitochondrial function and energy metabolism. *Cell Metab,* 19**,** 836-48.

LOCKER, N., EASTON, L. E. & LUKAVSKY, P. J. 2007. HCV and CSFV IRES domain II mediate eIF2 release during 80S ribosome assembly. *EMBO J,* 26**,** 795-805.

LOMAKIN, I. B., KOLUPAEVA, V. G., MARINTCHEV, A., WAGNER, G. & PESTOVA, T. V. 2003. Position of eukaryotic initiation factor eIF1 on the 40S ribosomal subunit determined by directed hydroxyl radical probing. *Genes Dev,* 17**,** 2786-97.

LOPEZ-LASTRA, M., RAMDOHR, P., LETELIER, A., VALLEJOS, M., VERA-OTAROLA, J. & VALIENTE-ECHEVERRIA, F. 2010. Translation initiation of viral mRNAs. *Rev Med Virol,* 20**,** 177-95.

LORSCH, J. R. & DEVER, T. E. 2010. Molecular view of 43 S complex formation and start site selection in eukaryotic translation initiation. *J Biol Chem,* 285**,** 21203-7.

LOW, W. K., DANG, Y., SCHNEIDER-POETSCH, T., SHI, Z., CHOI, N. S., MERRICK, W. C., ROMO, D. & LIU, J. O. 2005. Inhibition of eukaryotic translation initiation by the marine natural product pateamine A. *Mol Cell,* 20**,** 709-22.

LOW, W. K., DANG, Y., SCHNEIDER-POETSCH, T., SHI, Z., CHOI, N. S., RZASA, R. M., SHEA, H. A., LI, S., PARK, K., MA, G., ROMO, D. & LIU, J. O. 2007. Isolation and

identification of eukaryotic initiation factor 4A as a molecular target for the marine natural product Pateamine A. *Methods Enzymol,* 431, 303-24.

LOZANO, G. & MARTINEZ-SALAS, E. 2015. Structural insights into viral IRES-dependent translation mechanisms. *Curr Opin Virol,* 12, 113-20.

LUKAVSKY, P. J., KIM, I., OTTO, G. A. & PUGLISI, J. D. 2003. Structure of HCV IRES domain II determined by NMR. *Nat Struct Biol,* 10, 1033-8.

LULLA, A., LULLA, V. & MERITS, A. 2012. Macromolecular assembly-driven processing of the 2/3 cleavage site in the alphavirus replicase polyprotein. *J Virol,* 86, 553-65.

LUNA, R. E., ARTHANARI, H., HIRAISHI, H., NANDA, J., MARTIN-MARCOS, P., MARKUS, M. A., AKABAYOV, B., MILBRADT, A. G., LUNA, L. E., SEO, H. C., HYBERTS, S. G., FAHMY, A., REIBARKH, M., MILES, D., HAGNER, P. R., O'DAY, E. M., YI, T., MARINTCHEV, A., HINNEBUSCH, A. G., LORSCH, J. R., ASANO, K. & WAGNER, G. 2012. The C-terminal domain of eukaryotic initiation factor 5 promotes start codon recognition by its dynamic interplay with eIF1 and eIF2beta. *Cell Rep,* 1, 689-702.

MANOKARAN, G., FINOL, E., WANG, C., GUNARATNE, J., BAHL, J., ONG, E. Z., TAN, H. C., SESSIONS, O. M., WARD, A. M., GUBLER, D. J., HARRIS, E., GARCIA-BLANCO, M. A. & OOI, E. E. 2015. Dengue subgenomic RNA binds TRIM25 to inhibit interferon expression for epidemiological fitness. *Science,* 350, 217-21.

MARCEAU, C. D., PUSCHNIK, A. S., MAJZOUB, K., OOI, Y. S., BREWER, S. M., FUCHS, G., SWAMINATHAN, K., MATA, M. A., ELIAS, J. E., SARNOW, P. & CARETTE, J. E. 2016. Genetic dissection of Flaviviridae host factors through genome-scale CRISPR screens. *Nature,* 535, 159-63.

MARTIN, K. C. & EPHRUSSI, A. 2009. mRNA localization: gene expression in the spatial dimension. *Cell,* 136, 719-30.

MAYOR, S. & PAGANO, R. E. 2007. Pathways of clathrin-independent endocytosis. *Nat Rev Mol Cell Biol,* 8, 603-12.

MCINERNEY, G. M., KEDERSHA, N. L., KAUFMAN, R. J., ANDERSON, P. & LILJESTROM, P. 2005. Importance of eIF2alpha phosphorylation and stress granule assembly in alphavirus translation regulation. *Mol Biol Cell,* 16, 3753-63.

MELTON, J. V., EWART, G. D., WEIR, R. C., BOARD, P. G., LEE, E. & GAGE, P. W. 2002. Alphavirus 6K proteins form ion channels. *J Biol Chem,* 277, 46923-31.

MERRICK, W. C. & ANDERSON, W. F. 1975. Purification and characterization of homogeneous protein synthesis initiation factor M1 from rabbit reticulocytes. *J Biol Chem,* 250, 1197-206.

MI, S., DURBIN, R., HUANG, H. V., RICE, C. M. & STOLLAR, V. 1989. Association of the Sindbis virus RNA methyltransferase activity with the nonstructural protein nsP1. *Virology,* 170, 385-91.

MOLLESTON, J. M. & CHERRY, S. 2017. Attacked from All Sides: RNA Decay in Antiviral Defense. *Viruses,* 9.

MUDIGANTI, U., HERNANDEZ, R., FERREIRA, D. & BROWN, D. T. 2006. Sindbis virus infection of two model insect cell systems--a comparative study. *Virus Res,* 122, 28-34.

MUHS, M., HILAL, T., MIELKE, T., SKABKIN, M. A., SANBONMATSU, K. Y., PESTOVA, T. V. & SPAHN, C. M. 2015. Cryo-EM of ribosomal 80S complexes with termination factors reveals the translocated cricket paralysis virus IRES. *Mol Cell,* 57, 422-32.

MUKHERJEE, N., CALVIELLO, L., HIRSEKORN, A., DE PRETIS, S., PELIZZOLA, M. & OHLER, U. 2017. Integrative classification of human coding and noncoding genes through RNA metabolism profiles. *Nat Struct Mol Biol,* 24**,** 86-96.

MURRAY, J., SAVVA, C. G., SHIN, B. S., DEVER, T. E., RAMAKRISHNAN, V. & FERNANDEZ, I. S. 2016. Structural characterization of ribosome recruitment and translocation by type IV IRES. *Elife,* 5.

NA, C. H., BARBHUIYA, M. A., KIM, M. S., VERBRUGGEN, S., EACKER, S. M., PLETNIKOVA, O., TRONCOSO, J. C., HALUSHKA, M. K., MENSCHAERT, G., OVERALL, C. M. & PANDEY, A. 2018. Discovery of noncanonical translation initiation sites through mass spectrometric analysis of protein N termini. *Genome Res,* 28**,** 25-36.

NAKASHIMA, N. & UCHIUMI, T. 2009. Functional analysis of structural motifs in dicistroviruses. *Virus Res,* 139**,** 137-47.

NASAR, F., PALACIOS, G., GORCHAKOV, R. V., GUZMAN, H., DA ROSA, A. P., SAVJI, N., POPOV, V. L., SHERMAN, M. B., LIPKIN, W. I., TESH, R. B. & WEAVER, S. C. 2012. Eilat virus, a unique alphavirus with host range restricted to insects by RNA replication. *Proc Natl Acad Sci U S A,* 109**,** 14622-7.

NIEPMANN, M. 2013. Hepatitis C virus RNA translation. *Curr Top Microbiol Immunol,* 369**,** 143-66.

NIEVA, J. L., MADAN, V. & CARRASCO, L. 2012. Viroporins: structure and biological functions. *Nat Rev Microbiol,* 10**,** 563-74.

NOVELLA, I. S., PRESLOID, J. B., SMITH, S. D. & WILKE, C. O. 2011. Specific and nonspecific host adaptation during arboviral experimental evolution. *J Mol Microbiol Biotechnol,* 21**,** 71-81.

OTTO, G. A. & PUGLISI, J. D. 2004. The pathway of HCV IRES-mediated translation initiation. *Cell,* 119**,** 369-80.

OU, J. H., TRENT, D. W. & STRAUSS, J. H. 1982. The 3'-non-coding regions of alphavirus RNAs contain repeating sequences. *J Mol Biol,* 156**,** 719-30.

PAGER, C. T., WEHNER, K. A., FUCHS, G. & SARNOW, P. 2009. MicroRNA-mediated gene silencing. *Prog Mol Biol Transl Sci,* 90**,** 187-210.

PANAS, M. D., VARJAK, M., LULLA, A., ENG, K. E., MERITS, A., KARLSSON HEDESTAM, G. B. & MCINERNEY, G. M. 2012. Sequestration of G3BP coupled with efficient translation inhibits stress granules in Semliki Forest virus infection. *Mol Biol Cell,* 23**,** 4701-12.

PARSYAN, A., SVITKIN, Y., SHAHBAZIAN, D., GKOGKAS, C., LASKO, P., MERRICK, W. C. & SONENBERG, N. 2011. mRNA helicases: the tacticians of translational control. *Nat Rev Mol Cell Biol,* 12**,** 235-45.

PATEL, R. K., BURNHAM, A. J., GEBHART, N. N., SOKOLOSKI, K. J. & HARDY, R. W. 2013. Role for subgenomic mRNA in host translation inhibition during Sindbis virus infection of mammalian cells. *Virology,* 441**,** 171-81.

PAUL, D., MADAN, V. & BARTENSCHLAGER, R. 2014. Hepatitis C virus RNA replication and assembly: living on the fat of the land. *Cell Host Microbe,* 16**,** 569-79.

PEABODY, D. S. 1989. Translation initiation at non-AUG triplets in mammalian cells. *J Biol Chem,* 264**,** 5031-5.

PEARSON, C. E. 2011. Repeat associated non-ATG translation initiation: one DNA, two transcripts, seven reading frames, potentially nine toxic entities! *PLoS Genet,* 7**,** e1002018.

PERANEN, J., LAAKKONEN, P., HYVONEN, M. & KAARIAINEN, L. 1995. The alphavirus replicase protein nsP1 is membrane-associated and has affinity to endocytic organelles. *Virology,* 208**,** 610-20.

PEREZ, L. & CARRASCO, L. 1994. Involvement of the vacuolar H(+)-ATPase in animal virus entry. *J Gen Virol,* 75 (Pt 10)**,** 2595-606.

PEREZ, L., IRURZUN, A. & CARRASCO, L. 1994. Action of brefeldin A on translation in Semliki Forest virus-infected HeLa cells and cells doubly infected with poliovirus. *J Gen Virol,* 75 (Pt 9)**,** 2197-203.

PESTOVA, T. V. & KOLUPAEVA, V. G. 2002. The roles of individual eukaryotic translation initiation factors in ribosomal scanning and initiation codon selection. *Genes Dev,* 16**,** 2906-22.

PESTOVA, T. V., LOMAKIN, I. B., LEE, J. H., CHOI, S. K., DEVER, T. E. & HELLEN, C. U. 2000. The joining of ribosomal subunits in eukaryotes requires eIF5B. *Nature,* 403**,** 332-5.

PESTOVA, T. V., SHATSKY, I. N., FLETCHER, S. P., JACKSON, R. J. & HELLEN, C. U. 1998. A prokaryotic-like mode of cytoplasmic eukaryotic ribosome binding to the initiation codon during internal translation initiation of hepatitis C and classical swine fever virus RNAs. *Genes Dev,* 12**,** 67-83.

PFEFFER, M., KINNEY, R. M. & KAADEN, O. R. 1998. The alphavirus 3'-nontranslated region: size heterogeneity and arrangement of repeated sequence elements. *Virology,* 240**,** 100-8.

PIETILA, M. K., HELLSTROM, K. & AHOLA, T. 2017. Alphavirus polymerase and RNA replication. *Virus Res,* 234**,** 44-57.

PIJLMAN, G. P., FUNK, A., KONDRATIEVA, N., LEUNG, J., TORRES, S., VAN DER AA, L., LIU, W. J., PALMENBERG, A. C., SHI, P. Y., HALL, R. A. & KHROMYKH, A. A. 2008. A highly structured, nuclease-resistant, noncoding RNA produced by flaviviruses is required for pathogenicity. *Cell Host Microbe,* 4**,** 579-91.

PINEIRO, D., FERNANDEZ, N., RAMAJO, J. & MARTINEZ-SALAS, E. 2013. Gemin5 promotes IRES interaction and translation control through its C-terminal region. *Nucleic Acids Res,* 41**,** 1017-28.

PISAREVA, V. P., PISAREV, A. V. & FERNANDEZ, I. S. 2018. Dual tRNA mimicry in the Cricket Paralysis Virus IRES uncovers an unexpected similarity with the Hepatitis C Virus IRES. *Elife,* 7.

PISAREVA, V. P., PISAREV, A. V., KOMAR, A. A., HELLEN, C. U. & PESTOVA, T. V. 2008. Translation initiation on mammalian mRNAs with structured 5'UTRs requires DExH-box protein DHX29. *Cell,* 135**,** 1237-50.

PLANK, T. D. & KIEFT, J. S. 2012. The structures of nonprotein-coding RNAs that drive internal ribosome entry site function. *Wiley Interdiscip Rev RNA,* 3**,** 195-212.

PROUD, C. G. 2005. eIF2 and the control of cell physiology. *Semin Cell Dev Biol,* 16**,** 3-12.

RAMSEY, J. & MUKHOPADHYAY, S. 2017. Disentangling the Frames, the State of Research on the Alphavirus 6K and TF Proteins. *Viruses,* 9.

REDONDO, N., SANZ, M. A., WELNOWSKA, E. & CARRASCO, L. 2011. Translation without eIF2 promoted by poliovirus 2A protease. *PLoS One,* 6, e25699.

RIKKONEN, M., PERANEN, J. & KAARIAINEN, L. 1994. Nuclear targeting of Semliki Forest virus nsP2. *Arch Virol Suppl,* 9, 369-77.

ROBERTS, L. O., JOPLING, C. L., JACKSON, R. J. & WILLIS, A. E. 2009. Viral strategies to subvert the mammalian translation machinery. *Prog Mol Biol Transl Sci,* 90, 313-67.

ROZOV, A., DEMESHKINA, N., WESTHOF, E., YUSUPOV, M. & YUSUPOVA, G. 2016. New Structural Insights into Translational Miscoding. *Trends Biochem Sci,* 41, 798-814.

RUBACH, J. K., WASIK, B. R., RUPP, J. C., KUHN, R. J., HARDY, R. W. & SMITH, J. L. 2009. Characterization of purified Sindbis virus nsP4 RNA-dependent RNA polymerase activity in vitro. *Virology,* 384, 201-8.

RUPP, J. C., SOKOLOSKI, K. J., GEBHART, N. N. & HARDY, R. W. 2015. Alphavirus RNA synthesis and non-structural protein functions. *J Gen Virol,* 96, 2483-500.

RUSSO, A. T., WHITE, M. A. & WATOWICH, S. J. 2006. The crystal structure of the Venezuelan equine encephalitis alphavirus nsP2 protease. *Structure,* 14, 1449-58.

SALONEN, A., VASILJEVA, L., MERITS, A., MAGDEN, J., JOKITALO, E. & KAARIAINEN, L. 2003. Properly folded nonstructural polyprotein directs the semliki forest virus replication complex to the endosomal compartment. *J Virol,* 77, 1691-702.

SANZ, M. A. & CARRASCO, L. 2001. Sindbis virus variant with a deletion in the 6K gene shows defects in glycoprotein processing and trafficking: lack of complementation by a wild-type 6K gene in trans. *J Virol,* 75, 7778-84.

SANZ, M. A., CASTELLO, A. & CARRASCO, L. 2007. Viral translation is coupled to transcription in Sindbis virus-infected cells. *J Virol,* 81, 7061-8.

SANZ, M. A., CASTELLO, A., VENTOSO, I., BERLANGA, J. J. & CARRASCO, L. 2009. Dual mechanism for the translation of subgenomic mRNA from Sindbis virus in infected and uninfected cells. *PLoS One,* 4, e4772.

SANZ, M. A., GARCIA-MORENO, M. & CARRASCO, L. 2015. Inhibition of host protein synthesis by Sindbis virus: correlation with viral RNA replication and release of nuclear proteins to the cytoplasm. *Cell Microbiol,* 17, 520-41.

SANZ, M. A., GONZALEZ-ALMELA, E., GARCIA MORENO, M., MARINA, A. I. & CARRASCO, L. 2019. A Viral Rna Motif Involved in Signalling the Initiation of Translation on Non-Aug Codons. *RNA,* 25, 431-452.

SANZ, M. A., GONZALEZ ALMELA, E. & CARRASCO, L. 2017. Translation of Sindbis Subgenomic mRNA is Independent of eIF2, eIF2A and eIF2D. *Sci Rep,* 7, 43876.

SANZ, M. A., MADAN, V., CARRASCO, L. & NIEVA, J. L. 2003. Interfacial domains in Sindbis virus 6K protein. Detection and functional characterization. *J Biol Chem,* 278, 2051-7.

SANZ, M. A., PEREZ, L. & CARRASCO, L. 1994. Semliki Forest virus 6K protein modifies membrane permeability after inducible expression in Escherichia coli cells. *J Biol Chem,* 269, 12106-10.

SANZ, M. A., REDONDO, N., GARCIA-MORENO, M. & CARRASCO, L. 2013. Phosphorylation of eIF2alpha is responsible for the failure of the picornavirus internal ribosome entry site to direct translation from Sindbis virus replicons. *J Gen Virol,* 94, 796-806.

SANZ, M. M., V.; NIEVA, J.L.; CARRASCO, L 2005. The Alphavirus 6K Protein. *In:* FISHER, W., ED.; KLUWER ACADEMIC/PLENUM PLUBLISHERS (ed.) *Viral Membrane Proteins: Structure, Function, and Drug Design.* New York, NY, USA.

SARIOLA, M., SARASTE, J. & KUISMANEN, E. 1995. Communication of post-Golgi elements with early endocytic pathway: regulation of endoproteolytic cleavage of Semliki Forest virus p62 precursor. *J Cell Sci,* 108 (Pt 6), 2465-75.

SCHLEICH, S., ACEVEDO, J. M., CLEMM VON HOHENBERG, K. & TELEMAN, A. A. 2017. Identification of transcripts with short stuORFs as targets for DENR*MCTS1-dependent translation in human cells. *Sci Rep,* 7, 3722.

SCHLEICH, S., STRASSBURGER, K., JANIESCH, P. C., KOLEDACHKINA, T., MILLER, K. K., HANEKE, K., CHENG, Y. S., KUECHLER, K., STOECKLIN, G., DUNCAN, K. E. & TELEMAN, A. A. 2014. DENR-MCT-1 promotes translation re-initiation downstream of uORFs to control tissue growth. *Nature,* 512, 208-212.

SELLIER, C., BUIJSEN, R. A. M., HE, F., NATLA, S., JUNG, L., TROPEL, P., GAUCHEROT, A., JACOBS, H., MEZIANE, H., VINCENT, A., CHAMPY, M. F., SORG, T., PAVLOVIC, G., WATTENHOFER-DONZE, M., BIRLING, M. C., OULAD-ABDELGHANI, M., EBERLING, P., RUFFENACH, F., JOINT, M., ANHEIM, M., MARTINEZ-CERDENO, V., TASSONE, F., WILLEMSEN, R., HUKEMA, R. K., VIVILLE, S., MARTINAT, C., TODD, P. K. & CHARLET-BERGUERAND, N. 2017. Translation of Expanded CGG Repeats into FMRpolyG Is Pathogenic and May Contribute to Fragile X Tremor Ataxia Syndrome. *Neuron,* 93, 331-347.

SENDOEL, A., DUNN, J. G., RODRIGUEZ, E. H., NAIK, S., GOMEZ, N. C., HURWITZ, B., LEVORSE, J., DILL, B. D., SCHRAMEK, D., MOLINA, H., WEISSMAN, J. S. & FUCHS, E. 2017. Translation from unconventional 5' start sites drives tumour initiation. *Nature,* 541, 494-499.

SHATSKY, I. N., DMITRIEV, S. E., TERENIN, I. M. & ANDREEV, D. E. 2010. Cap- and IRES-independent scanning mechanism of translation initiation as an alternative to the concept of cellular IRESs. *Mol Cells,* 30, 285-93.

SHIN, G., YOST, S. A., MILLER, M. T., ELROD, E. J., GRAKOUI, A. & MARCOTRIGIANO, J. 2012. Structural and functional insights into alphavirus polyprotein processing and pathogenesis. *Proc Natl Acad Sci U S A,* 109, 16534-9.

SHIRAKO, Y., STRAUSS, E. G. & STRAUSS, J. H. 2000. Suppressor mutations that allow sindbis virus RNA polymerase to function with nonaromatic amino acids at the N-terminus: evidence for interaction between nsP1 and nsP4 in minus-strand RNA synthesis. *Virology,* 276, 148-60.

SHIRAKO, Y. & STRAUSS, J. H. 1994. Regulation of Sindbis virus RNA replication: uncleaved P123 and nsP4 function in minus-strand RNA synthesis, whereas cleaved products from P123 are required for efficient plus-strand RNA synthesis. *J Virol,* 68, 1874-85.

SIMON, A. E. & MILLER, W. A. 2013. 3' cap-independent translation enhancers of plant viruses. *Annu Rev Microbiol,* 67, 21-42.

SKABKIN, M. A., SKABKINA, O. V., DHOTE, V., KOMAR, A. A., HELLEN, C. U. & PESTOVA, T. V. 2010. Activities of Ligatin and MCT-1/DENR in eukaryotic translation initiation and ribosomal recycling. *Genes Dev,* 24, 1787-801.

SNYDER, J. E., KULCSAR, K. A., SCHULTZ, K. L., RILEY, C. P., NEARY, J. T., MARR, S., JOSE, J., GRIFFIN, D. E. & KUHN, R. J. 2013. Functional characterization of the alphavirus TF protein. *J Virol,* 87, 8511-23.

SOKOLOSKI, K. J., DICKSON, A. M., CHASKEY, E. L., GARNEAU, N. L., WILUSZ, C. J. & WILUSZ, J. 2010. Sindbis virus usurps the cellular HuR protein to stabilize its transcripts and promote productive infections in mammalian and mosquito cells. *Cell Host Microbe,* 8**,** 196-207.

SOKOLOSKI, K. J., HAIST, K. C., MORRISON, T. E., MUKHOPADHYAY, S. & HARDY, R. W. 2015. Noncapped Alphavirus Genomic RNAs and Their Role during Infection. *J Virol,* 89**,** 6080-92.

SOKOLOSKI, K. J., NEASE, L. M., MAY, N. A., GEBHART, N. N., JONES, C. E., MORRISON, T. E. & HARDY, R. W. 2017. Identification of Interactions between Sindbis Virus Capsid Protein and Cytoplasmic vRNA as Novel Virulence Determinants. *PLoS Pathog,* 13**,** e1006473.

SONENBERG, N. & HINNEBUSCH, A. G. 2009. Regulation of translation initiation in eukaryotes: mechanisms and biological targets. *Cell,* 136**,** 731-45.

SPAHN, C. M., KIEFT, J. S., GRASSUCCI, R. A., PENCZEK, P. A., ZHOU, K., DOUDNA, J. A. & FRANK, J. 2001. Hepatitis C virus IRES RNA-induced changes in the conformation of the 40s ribosomal subunit. *Science,* 291**,** 1959-62.

STARCK, S. R., JIANG, V., PAVON-ETERNOD, M., PRASAD, S., MCCARTHY, B., PAN, T. & SHASTRI, N. 2012. Leucine-tRNA initiates at CUG start codons for protein synthesis and presentation by MHC class I. *Science,* 336**,** 1719-23.

STARCK, S. R., TSAI, J. C., CHEN, K., SHODIYA, M., WANG, L., YAHIRO, K., MARTINS-GREEN, M., SHASTRI, N. & WALTER, P. 2016. Translation from the 5' untranslated region shapes the integrated stress response. *Science,* 351**,** aad3867.

STRAUSS, J. H. & STRAUSS, E. G. 1994. The alphaviruses: gene expression, replication, and evolution. *Microbiol Rev,* 58**,** 491-562.

SUZME, R., TSENG, J. C., LEVIN, B., IBRAHIM, S., MERUELO, D. & PELLICER, A. 2012. Sindbis viral vectors target hematopoietic malignant cells. *Cancer Gene Ther,* 19**,** 757-66.

TASSETTO, M., KUNITOMI, M. & ANDINO, R. 2017. Circulating Immune Cells Mediate a Systemic RNAi-Based Adaptive Antiviral Response in Drosophila. *Cell,* 169**,** 314-325 e13.

TERENIN, I. M., DMITRIEV, S. E., ANDREEV, D. E. & SHATSKY, I. N. 2008. Eukaryotic translation initiation machinery can operate in a bacterial-like mode without eIF2. *Nat Struct Mol Biol,* 15**,** 836-41.

THOMAS, M. G., LOSCHI, M., DESBATS, M. A. & BOCCACCIO, G. L. 2011. RNA granules: the good, the bad and the ugly. *Cell Signal,* 23**,** 324-34.

TORIBIO, R., DIAZ-LOPEZ, I., BOSKOVIC, J. & VENTOSO, I. 2016. An RNA trapping mechanism in Alphavirus mRNA promotes ribosome stalling and translation initiation. *Nucleic Acids Res,* 44**,** 4368-80.

VAIDYA, A. T., LOMAKIN, I. B., JOSEPH, N. N., DMITRIEV, S. E. & STEITZ, T. A. 2017. Crystal Structure of the C-terminal Domain of Human eIF2D and Its Implications on Eukaryotic Translation Initiation. *J Mol Biol,* 429**,** 2765-2771.

VAN DAMME, P., GAWRON, D., VAN CRIEKINGE, W. & MENSCHAERT, G. 2014. N-terminal proteomics and ribosome profiling provide a comprehensive view of the alternative translation initiation landscape in mice and men. *Mol Cell Proteomics,* 13**,** 1245-61.

VANCINI, R., WANG, G., FERREIRA, D., HERNANDEZ, R. & BROWN, D. T. 2013. Alphavirus genome delivery occurs directly at the plasma membrane in a time- and temperature-dependent process. *J Virol,* 87**,** 4352-9.

VARJAK, M., SAUL, S., ARIKE, L., LULLA, A., PEIL, L. & MERITS, A. 2013. Magnetic fractionation and proteomic dissection of cellular organelles occupied by the late replication complexes of Semliki Forest virus. *J Virol,* 87**,** 10295-312.

VENTOSO, I. 2012. Adaptive changes in alphavirus mRNA translation allowed colonization of vertebrate hosts. *J Virol,* 86**,** 9484-94.

VENTOSO, I., SANZ, M. A., MOLINA, S., BERLANGA, J. J., CARRASCO, L. & ESTEBAN, M. 2006. Translational resistance of late alphavirus mRNA to eIF2alpha phosphorylation: a strategy to overcome the antiviral effect of protein kinase PKR. *Genes Dev,* 20**,** 87-100.

WEAVER, S. C., WINEGAR, R., MANGER, I. D. & FORRESTER, N. L. 2012. Alphaviruses: population genetics and determinants of emergence. *Antiviral Res,* 94**,** 242-57.

WELLS, S. E., HILLNER, P. E., VALE, R. D. & SACHS, A. B. 1998. Circularization of mRNA by eukaryotic translation initiation factors. *Mol Cell,* 2**,** 135-40.

WETHMAR, K., SMINK, J. J. & LEUTZ, A. 2010. Upstream open reading frames: molecular switches in (patho)physiology. *Bioessays,* 32**,** 885-93.

YAMAMOTO, H., UNBEHAUN, A. & SPAHN, C. M. T. 2017. Ribosomal Chamber Music: Toward an Understanding of IRES Mechanisms. *Trends Biochem Sci,* 42**,** 655-668.

YAMAMOTO, Y., SINGH, C. R., MARINTCHEV, A., HALL, N. S., HANNIG, E. M., WAGNER, G. & ASANO, K. 2005. The eukaryotic initiation factor (eIF) 5 HEAT domain mediates multifactor assembly and scanning with distinct interfaces to eIF1, eIF2, eIF3, and eIF4G. *Proc Natl Acad Sci U S A,* 102**,** 16164-9.

YUEH, A. & SCHNEIDER, R. J. 1996. Selective translation initiation by ribosome jumping in adenovirus-infected and heat-shocked cells. *Genes Dev,* 10**,** 1557-67.

YUEH, A. & SCHNEIDER, R. J. 2000. Translation by ribosome shunting on adenovirus and hsp70 mRNAs facilitated by complementarity to 18S rRNA. *Genes Dev,* 14**,** 414-21.

ZOLL, W. L., HORTON, L. E., KOMAR, A. A., HENSOLD, J. O. & MERRICK, W. C. 2002. Characterization of mammalian eIF2A and identification of the yeast homolog. *J Biol Chem,* 277**,** 37079-87.

ZU, T., GIBBENS, B., DOTY, N. S., GOMES-PEREIRA, M., HUGUET, A., STONE, M. D., MARGOLIS, J., PETERSON, M., MARKOWSKI, T. W., INGRAM, M. A., NAN, Z., FORSTER, C., LOW, W. C., SCHOSER, B., SOMIA, N. V., CLARK, H. B., SCHMECHEL, S., BITTERMAN, P. B., GOURDON, G., SWANSON, M. S., MOSELEY, M. & RANUM, L. P. 2011. Non-ATG-initiated translation directed by microsatellite expansions. *Proc Natl Acad Sci U S A,* 108**,** 260-5.

ANEXO

ANEXO

Publicaciones científicas no incluidas

Durante el Desarrollo de esta tesis se publicó también una revisión sobre alfavirus:

CARRASCO, L., SANZ, M. A. & **GONZALEZ-ALMELA, E**. 2018. The Regulation of Translation in Alphavirus-Infected Cells. *Viruses*, 10, 70-98.

viruses

MDPI

Review

The Regulation of Translation in Alphavirus-Infected Cells

Luis Carrasco *, Miguel Angel Sanz and Esther González-Almela

Centro de Biología Molecular Severo Ochoa (CSIC-UAM), Universidad Autónoma de Madrid c/Nicolás Cabrera, 1., Cantoblanco, 28049 Madrid, Spain; masanz@cbm.csic.es (M.A.S.); emgonzalez@cbm.csic.es (E.G.-A.)

* Correspondence: lcarrasco@cbm.csic.es; Tel.: +34-914-978-450

Received: 15 January 2018; Accepted: 6 February 2018; Published: 8 February 2018

Abstract: Sindbis virus (SINV) contains an RNA genome of positive polarity with two open reading frames (ORFs). The first ORF is translated from the genomic RNA (gRNA), rendering the viral non-structural proteins, whereas the second ORF is translated from a subgenomic mRNA (sgRNA), which directs the synthesis of viral structural proteins. SINV infection strongly inhibits host cell translation through a variety of different mechanisms, including the phosphorylation of the eukaryotic initiation factor eIF2α and the redistribution of cellular proteins from the nucleus to the cytoplasm. A number of motifs have been identified in SINV sgRNA, including a hairpin downstream of the AUG initiation codon, which is involved in the translatability of the viral sgRNA when eIF2 is inactivated. Moreover, a 3′-UTR motif containing three stem-loop structures is involved in the enhancement of translation in insect cells, but not in mammalian cells. Accordingly, SINV sgRNA has evolved several structures to efficiently compete for the cellular translational machinery. Mechanistically, sgRNA translation involves scanning of the 5′-UTR following a non-canonical mode and without the requirement for several initiation factors. Indeed, sgRNA-directed polypeptide synthesis occurs even after eIF4G cleavage or inactivation of eIF4A by selective inhibitors. Remarkably, eIF2α phosphorylation does not hamper sgRNA translation during the late phase of SINV infection. SINV sgRNA thus constitutes a unique model of a capped viral mRNA that is efficiently translated in the absence of several canonical initiation factors. The present review will mainly focus in the non-canonical mechanism of translation of SINV sgRNA.

Keywords: regulation of translation; alphaviruses; initiation factors; RNA structure; IRES

1. Introduction

Sindbis virus (SINV) belongs to the alphavirus genus in the *Togaviridae* family and contains a positive-strand RNA genome [1]. The alphavirus genus comprises ~30 virus species that are transmitted by arthropods, typically mosquitoes, to a range of vertebrate hosts [2]. Exceptions to this rule are the aquatic viruses salmonid alphavirus and Southern elephant seal virus, which are not transmitted by mosquitoes. In addition, Eilat virus can replicate only in insects [3]. Alphaviruses and their genetic variants have a very broad geographical distribution, indicating an ancient origin and evolution [4,5]. Alphaviruses can be subdivided into two groups according to their geographical origin—Old World viruses and New World viruses. Examples of Old World alphaviruses include Semliki Forest Virus (SFV), Chikungunya virus (CHIKV), Ross River virus (RRV) and O'nyong'nyong virus (ONNV), whereas New World alphaviruses are represented by SINV, Venezuelan, Western and Eastern equine encephalitis viruses (VEEV, WEEV and EEEV) [2]. In mammals, alphaviruses typically cause an acute infection, leading to a variety of symptoms and illnesses that are dependent on the virus and host [1], including encephalitis, polyarthritis, myalgia, athritis and rash. By contrast, insects survive the acute phase of infection and become persistently infected for life without apparent

pathological consequences [6,7]. Although, some mosquito cells infected with SINV can die in culture in a cell clone specific manner [6]. SINV and SFV have been widely used in the laboratory as model systems to study protein synthesis, transcription and replication at the molecular level, and to understand viral pathogenesis and the interaction of these viruses with their hosts. In this regard, fundamental aspects of translation regulation in virus-infected cells have been uncovered using SINV and SFV. Moreover, the mechanisms of protein synthesis directed by SINV mRNAs are helping to shed light on the structure-function relationship of viral mRNAs. From a practical viewpoint, SINV has been employed in fields as diverse as cancer therapy and has aided in the understanding of the adaptive antiviral response [8,9]. In the current review, we will summarize what is known about the mechanisms of translation of SINV mRNAs, with a focus on the initiation events of non-canonical translation of subgenomic mRNA (sgRNA).

2. Overview of the Sindbis Virus Life Cycle

The SINV virion is approximately 70 nm in diameter and has a single-strand 11.7 kb RNA genome contained within an icosahedral-structured nucleocapsid made up of 240 copies of capsid protein [10,11]. This is enveloped by a host-derived lipid bilayer membrane into which are embedded viral-encoded glycoproteins E1 and E2. SINV replication occurs in the cytoplasm of infected cells and begins by the recognition of receptors at the cell surface. These receptors include the laminin receptor in mammalian cells, the C-type lectins DC-SIGN and L-SIGN in dendritic cells and the metal ion transporter NRAMP (Natural Resistance-Associated Macrophage Protein), expressed both in mammalian and insect hosts [12–14]. After entry, virus particles can follow different pathways to reach the cytoplasm, the most relevant of which is the endocytosis mediated by clathrin. Following endocytosis, virions are delivered into acidic endosomes from which, after fusion of the virus and endosome membranes, the positive-sense RNA genome is delivered into the cytoplasm [15–17]. Virions can also enter cells by directly penetrating the plasma membrane [18]. Efficient infection requires that the genome maintains interactions with the capsid protein after genome delivery to the cytoplasm [19]. The arrival of the SINV genome RNA to the cytoplasm can specifically activate the protein kinase general control nonderepressible-2 (GCN2), triggering an early antiviral response [20]. The SINV genome contains two open reading frames (ORFs) that are expressed from two different mRNAs that are translated at different times during the infection process—-the genomic RNA (gRNA) and the sgRNA (Figure 1). The gRNA comprises the proximal two-thirds of the genome at the 5′ end, and serves as mRNA for the synthesis of non-structural proteins (nsPs), whereas the more distal one-third sgRNA encodes for structural proteins (Figure 1). The gRNA is translated promptly after virus entry and genome delivery, whereas the sgRNA is translated at late phases of infection [21]. Both gRNA and sgRNA are capped at their 5′ ends and contain a poly(A) tail at the 3′ end. Interestingly, a portion of gRNAs do not contain a cap structure at their 5′ end [22]. The first event in SINV replication is the translation of the imput gRNA to produce nsP1–4, which participate in genome replication and transcription [11]. These nsPs are synthesized from a single AUG initiation codon initially producing two precursor polyproteins (P123 and P1234), which are then post-translationally processed through proteolytic cleavage by nsP2 [23–26] (Figure 1). After initiation at the first AUG initiation codon in gRNA, the majority of ribosomes (90–95%) translate this template until a stop codon (UGA) is encountered, producing the first of the two precursor polyproteins, P123 [27]. In a small proportion of cases, however, there is read-through of this stop codon, which can be suppressed by several aminoacyl-tRNAs, generating the second precursor polyprotein, P1234. The precise function of the individual nsPs has been the subject of intensive research [24–26,28]. nsP1 is a palmitoylated protein that comprises an abundant component of the replicative complex and can interact with membranes. It functions in the initiation and elongation of the minus-strand RNA synthesis via its interaction with nsP4 [29,30]. The N-terminal moiety of nsP1 exhibits methyltransferase and guanylyltransferase activities, which are involved in capping the viral positive-strand RNAs [31–33]. Its association with cellular membranes is promoted by an amphipatic helix located in the middle region of nsP1 [33],

which serves to anchor viral replicative complexes to membranes [34]. In addition, nsP1 can exhibit its activity either as a mature protein or in the form of the precursors P123 or P1234. nsP2 also contains several domains—an amino-terminal RNA helicase domain, a central protease region that catalyzes all cleavage reactions between the non-structural proteins, and an inactive RNA methyltransferase-like moiety [35,36]. nsP2 also functions in the obstruction of host cellular macromolecular synthesis, such as transcription and translation, and can accordingly antagonize cellular antiviral responses triggered by alphavirus infection [37,38]. Indeed, a fraction of nsP2 localizes to the nucleus and blocks cellular RNA export to the cytoplasm [38,39]. Moreover, nsP2 induces degradation of Rpb1, a catalytic subunit of the RNA polymerase II polymerization complex, mediated by its ubiquitination [40]. nsP3 is also organized into three domains—an amino-terminal macro or X domain [41], a central alphavirus-specific region, and a carboxyl region with a hypervariable sequence containing several phosphorylation sites [42]. nsP3 residues located after the macro domain participate in the positioning of the P23 cleavage site [43]. nsP3 interferes with the formation of host cellular stress granules (SGs), which are involved in innate antiviral mechanisms, through the interaction of its carboxy-terminal domain with Ras-GTPase activating protein (GAP)-binding protein (G3BP) [44,45]. Finally, nsP4 is an RNA-dependent RNA polymerase involved in the synthesis of the different viral RNAs—namely, gRNA, sgRNA and minus-strand RNA complementary to the genome [46,47]. Preferential synthesis of the negative strand of viral RNA is accomplished by P123 + nsP4 complex, whereas nsP1 + P23 + nsP4 complex synthesize both positive and negative sense strands [48,49]. Fully mature nsPs are produced after the final cleavage event of P23, which switches the RNA template for synthesis of positive sense genomic and subgenomic RNAs.

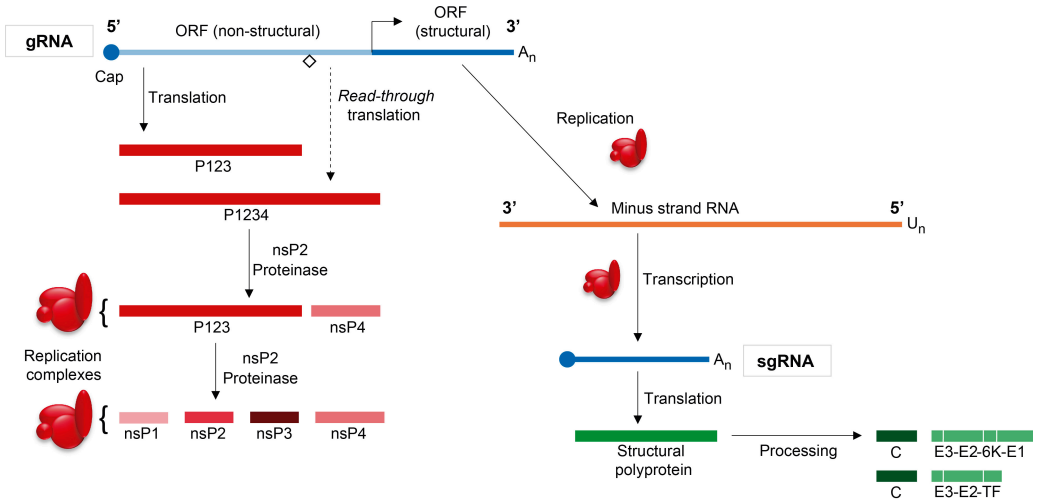

Figure 1. Schematic representation of the synthesis of SINV non-structural and structural proteins. SINV has two different mRNAs that are translated at different times during infection. SINV genomic RNA (gRNA) codes both for non-structural proteins (nsPs) and structural proteins. The first two thirds of the SINV genome is translated to nsP1–nsP4, which are required for transcription and replication of SINV RNA; the remaining one-third of the genome codes for the viral structural proteins. This subgenomic mRNA (sgRNA) is transcribed from an internal promoter in the minus strand RNA derived from the replication of the gRNA, and is translated to a polyprotein that will be processed to C (capsid)-E3-E2-6K-E1. ORF: open reading frame.

Overall, SINV gRNA participates in three different functions: (1) As an mRNA to direct the synthesis of early viral nsPs; (2) as a template for the synthesis of the negative-strand RNA; and (3) by interacting with the capsid protein, it helps forming nucleocapsids during the assembly process to produce new virus particles. Furthermore, the negative-strand RNA serves as template to synthesize the two different viral mRNAs by the viral replicative machinery [49,50]. In SFV, genomic and negative-

strand synthesis takes place within structures referred to as spherules, which are bulb-shaped invaginations of the membrane of virus–modified endosomes known as type I cytopathic vacuoles (CPV-1), which are induced after infection [34,51]. These spherules contain the replicative complexes and their size depends on the length of the replicated RNA [52,53]. Thus, the synthesis of viral RNAs in cytoplasmic RNA viruses takes place in close association with the cellular membranes [54,55]. The synthesis of cleavage intermediates of the alphavirus replicase can lead to membrane invaginations in the absence of viral replication. Thus, the formation of membranous spherules can occur in the absence of viral RNA synthesis [56]. Therefore, partially cleaved replicase proteins can participate in the assembly of replication complexes, membrane deformation, and in different stages of viral RNA synthesis. Analysis of the proteome of these replicative complexes has led to the identification of a number of cellular proteins that can up- or down-regulate their activity on RNA synthesis [57]. A number of host cellular factors can interact with nsPs, as has been shown for nsP2 and nsP3, and can modulate SINV RNA replication [58]. The recognition of an internal promoter in the negative strand RNA that is complementary to the gmRNA is necessary to initiate synthesis of sgRNA. This sgRNA is the most abundant SINV mRNA during the late phase of infection and directs the synthesis of five structural proteins initially as a polyprotein, C-E3-E2-6K-E1. Translation of this sgRNA is coincident with the dramatic inhibition of cellular mRNA translation.

The first protein to be synthesized during sgRNA translation is the capsid (C) protein, which is autocatalytically cleaved off the nascent chain upon translation of the polyprotein on the polysomes [11] (Figure 2). The C protein then binds to gRNA to form nucleocapsids in the cytoplasm. The amino-terminus of the E3 glycoprotein contains the signal peptide, which interacts with membranes of the endoplasmic reticulum (ER), and the polyprotein is translocated to the lumen. Here, it is cleaved by host cellular proteases, including furin and signalase, to render E3, E2, 6K and E1 proteins [59]. Some years ago, a heptanucleotide slip site (UUUUUUA) was discovered within the gene encoding 6K that, in about 10% of cases, results in the ribosome shifting to the −1 reading frame, rendering a novel transframe form (TF) of 6K and the E1 protein is not translated on these ocassions [60,61]. E2 and E1 interact with one and other to form dimers that migrate to the plasma membrane, leaving their carboxy-termini at the cytoplasmic face of the membrane. Nucleocapsids containing one copy of the genome interact with the cytoplasmic tails of viral glycoproteins to promote the budding of new virus particles [62]. At only 55 amino acids in size, the SINV 6K protein belongs to the viroporin family of proteins and is palmitoylated, helping it to target membranes [63–67]. The 6K protein is also involved in the transport of viral glycoproteins through the vesicular system to the plasma membrane [68,69]. As occurs with most viroporins, virus budding is promoted by 6K, but it is largely excluded from virions and is only detected in low amounts in mature virus particles [66,70]. By contrast, the transframe protein is apparently preferentially incorporated into released virions [71].

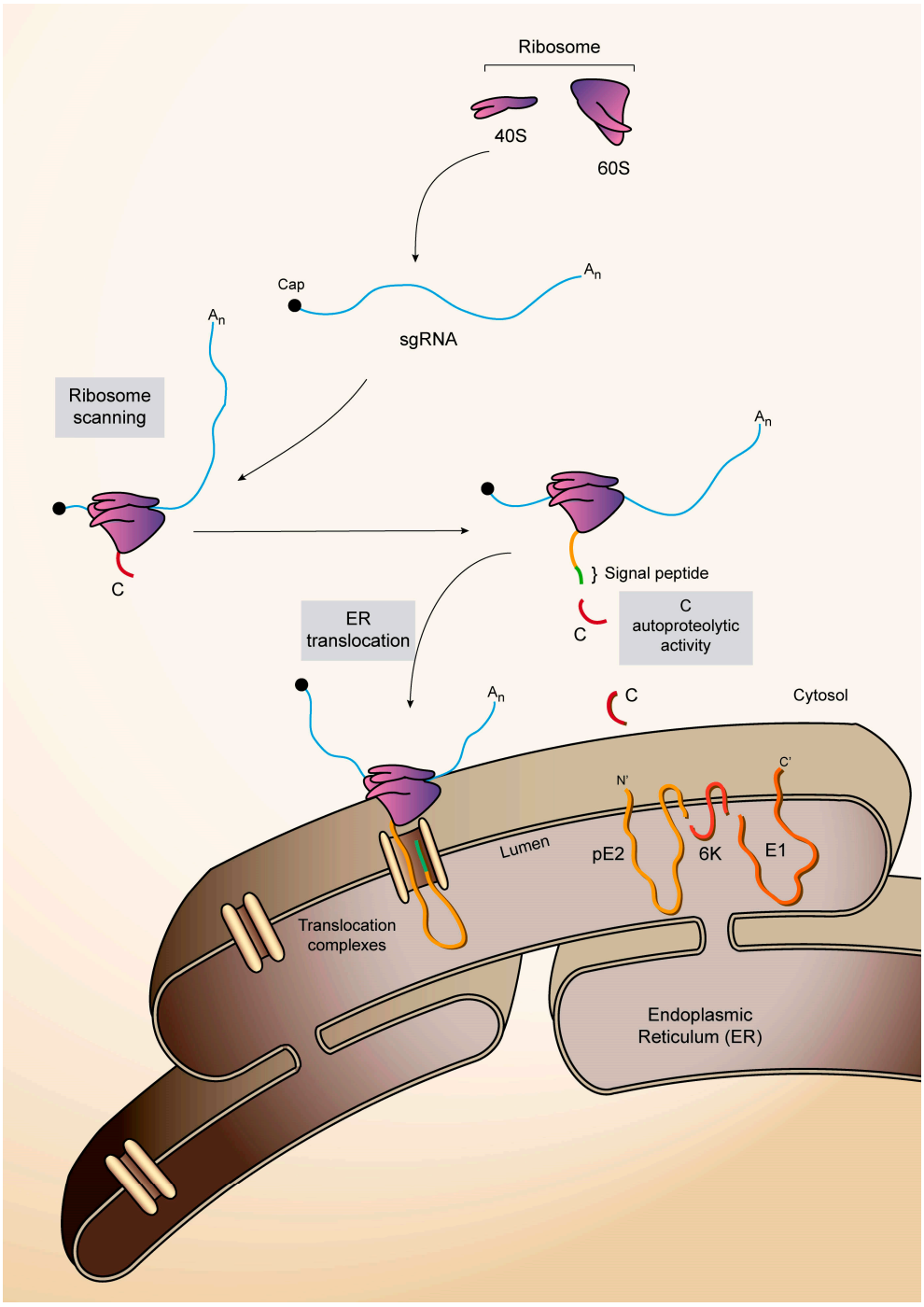

Figure 2. Schematic representation of SINV sgRNA translation to render structural proteins C (capsid)-E3-E2-6K-E1. The sgRNA coding sequence is flanked by two untranslated regions (UTRs): 5′-UTR, which contains a cap structure at its 5′ end, and 3′-UTR, which ends in a poly-(A) tail. The structural proteins are initially synthesized as a polyprotein. Ribosomes scan the capped sgRNA up to the first AUG and translation begins. First, C is synthesized and released from the polyprotein by autoproteolysis. The new N-terminus of the nascent polyprotein chain has a signal peptide for translocation to the endoplasmic reticulum (ER). Translation of the sgRNA continues, associated with the ER membranes, giving rise to the synthesis of the three glycoproteins E3, E2 and E1 and the viroporin 6K. The pE2 glycoprotein is synthesized across the ER membrane, where a carbohydrate attachment site may be responsible for the retention of the signal sequence in E2. The translocation of the glycoproteins across the ER membrane is regulated by various signal sequences. The glycoproteins and 6K are processed and cleaved by cellular proteases of the host vesicular system. Once the pE2–E1 heterodimer complex reaches the trans-Golgi, pE2 is cleaved by furin to form E3 and E2. The cleavage of pE2 is required to generate infectious particles.

3. Inhibition of Host Translation by SINV Infection

Most cytolytic animal viruses induce a profound suppression of cellular protein synthesis in infected cells, particularly during the late phase of infection [72]. This inhibition would thus clearly interfere with the innate immune system and hence with the antiviral response [73]. This is the case for SINV, which blocks cellular translation in order to get the protein synthesizing machinery preferentially dedicated to translate the sgRNA, usually in a short time after infection (in BHK cells it occurs approximately 3 h after virus entry) but this process is dependent on cell line. A strong inhibition of host protein synthesis is found in vertebrate cells, but curiously, it is not observed when SINV infects mosquitos [74,75]. Therefore, it is likely that cellular and viral mRNAs are translated by different mechanisms. Although it is believed that gRNA is translated by a mechanism similar to that used for host mRNAs, we are still largely ignorant of the precise eukaryotic initiation factors (eIFs) necessary to initiate translation of SINV gRNA. In principle, both cellular and gRNA translation is down regulated at late phases of infection, when sgRNA directs the synthesis of structural proteins very efficiently [11]. The vast majority of cellular mRNAs contain a blocked cap structure at their 5′ end and are translated by the canonical cap-dependent scanning mechanism. This involves recognition of the cap by the heterotrimeric factor eIF4F, followed by the interaction of the preinitiation 43S complex with the mRNA [76]. The eIF4F complex is composed of the cap-binding factor eIF4E, the helicase and ATPase enzyme eIF4A, and the scaffolding protein eIF4G [77]. Unwinding of the secondary structure present in the mRNA leader sequence is accomplished by the preinitiation complex together with eIF4AI or eIF4AII, which are functionally interchangeable isoforms with 90% similarity [78]. After RNA unwinding, the 40S ribosomal subunit containing several eIFs linearly scans the leader sequence until an AUG codon is encountered in a good context [79]. Initiation of translation can also occur by other mechanisms independent of cap recognition, such as internal initiation. In this case, initiation takes place at an internal sequence located at the 5′ untranslated region (5′-UTR) of the mRNA, known as the internal ribosome entry site (IRES) [80,81]. Yet another mechanism of translation has been observed with SINV sgRNA, which contains a cap structure and is translated by a scanning mechanism of its rather short leader sequence without the participation of crucial eIFs such as eIF2 or eIF4A [82].

3.1. Mechanisms of Inhibition of Cellular Protein Synthesis by SINV Infection

Distinct mechanisms have been suggested to account for the abrogation of cellular protein synthesis by alphaviruses: (1) The phosphorylation of the α-subunit of eIF2; (2) Competition of viral mRNAs for the host translational machinery; and (3) Modifications of the cytoplasmic ionic environment. eIF2 plays a central role in mRNA translation and binds Met-tRNA$_i^{Met}$ and GTP to form a ternary complex that interacts with the AUG initiation codon and delivers the initiator Met-tRNA$_i^{Met}$ to the P site of the 40S ribosomal subunit. This event triggers GTP hydrolysis and eIF2-GDP is released to the cytoplasm to be recycled to eIF2-GTP by eIF2B. Phosphorylation of the α-subunit of eIF2 at serine 51 renders this factor inactive because it forms a stable complex with eIF2B and no recycling between GDP and GTP takes place [83,84]. Since the amount of eIF2B is about 10–20-fold less than eIF2, even a low percentage of eIF2α phosphorylation is sufficient to block the initiation of translation. eIF2 plays an important role in sensing metabolic status and cellular stress and, consequently, its activity is highly regulated by four known protein kinases that respond to distinct stress stimuli—protein kinase R (PKR) is activated by double-stranded RNA (dsRNA), PKR-like ER kinase (PERK) senses unfolded proteins in the ER, and GCN2 and heme-regulated inhibitor (HRI) are activated by nutrient starvation and heme deficiency, respectively [85].

SINV infection induces the phosphorylation of eIF2α in mammalian cells, which leads to an inhibition of host mRNA translation [86–89]. This is due to the activation of PKR by the synthesis of viral dsRNA in the cytoplasm [90]. Nevertheless, SINV infection of cells deficient in PKR, such as PKR$^{-/-}$ murine embryonic fibroblasts (MEFs), also produce this blockade despite the fact that no increased eIF2α phosphorylation is observed [87,90]. Moreover, SFV infection can reduce the levels of phosphorylated eIF4E, the cap binding protein of the eIF4F complex; however, the significance of

this finding is not clear [91]. It is possible that the lack of functionality of the eIF4F complex during infection leads to eIF4E inactivation.

The possibility that the translational efficiency and the quantity of sgRNA play a role in the inhibition of host protein synthesis has also been proposed [92]. Under this scenario, sgRNA would compete with cellular mRNAs for the translational machinery, which is logical since sgRNA is abundantly transcribed at late phases of infection and it is also efficiently engaged in translation [11]. However, SINV replicons encoding only for nsPs and lacking the coding sequences for sgRNA still induce a profound inhibition of cellular protein synthesis comparable to that observed in cells infected with wild-type virus [93,94]. Thus, in the absence of the synthesis of structural proteins directed by sgRNA, there remains a drastic suppression of host translation, pointing to the idea that competition is not necessary for this process. It is possible that the presence of abundant SINV mRNA sequences can interfere with host macromolecular synthesis, without participating directly in translation (see below). This type of competition may reflect the interaction with some cellular proteins by specific sequences of SINV mRNA, even in the absence of sgRNA translation. The imbalance of ionic concentrations in the cytoplasm of infected cells has been also implicated in the shut-off of host translation by several viruses, including SINV [95,96]. Indeed, at late stages of SINV or SFV infection, the ionic content of the cytoplasm is dramatically altered and plasma membrane permeability is increased [97,98]. This modification of the membrane is carried out by the 6K protein, which forms ion channels [66]. Yet, replicons that encode only for the capsid protein or for any structural protein fail to modify membrane permeability but still arrest cellular mRNA translation [88,94]. Overall, these observations suggest that SINV employs additional mechanisms to obstruct cellular protein synthesis.

3.2. Involvement of nsP2 in Host Translation Shut-Off

Because alphavirus replicons encoding solely nsPs obstruct cellular translation to a degree similar to that observed with wild-type virus, it was speculated that the synthesis of one of the nsPs was responsible for this inhibition [93]. Indeed, analysis of a number of alphavirus nsP variants pointed to nsP2 as being chiefly responsible for the inhibition of cellular macromolecular synthesis upon viral infection [37,90,99]. Accordingly, SINV with a single nsP2 point mutation at proline 726 presented defects in host translational shut-off [100]. Overall, these observations are consistent with the concept that nsPs are necessary to trigger the shut-off of host protein synthesis. However, mutations in the 5′-UTR sequence of SINV sgRNA leading to higher than wild-type levels of nsP2 were found to prevent the inhibition of host protein synthesis [92]. To reconcile these conflicting findings, we examined the inhibition of cellular mRNA translation mediated by individual nsPs and also by nsP1–4 [75]. We found that individual expression of nsP1, nsP2 and nsP3, or nsP1–4 had little effect on cellular protein synthesis. Of note, when nsP1–4 is expressed, not only are mature nsPs synthesized, but also their precursors, which is more akin to the situation observed in SINV-infected cells. As a control for these experiments, we expressed poliovirus (PV) $2A^{pro}$, which induces a profound arrest of cellular mRNA translation upon cleavage of eIF4G [101]. This result is in clear contrast to that found with SINV nsPs. Thus, the sole expression of nsPs is not sufficient to block cellular protein synthesis, and instead the strong replication of viral RNAs in the cytoplasm may be responsible for triggering this inhibition. In support of this concept, cellular shut-off does not occur in presence of inhibitors that reduce viral RNA replication [75]. Thus, treatment of SINV-infected baby hamster kidney (BHK) cells with two nucleoside analogs, 6-aza-uridine or ribavirin, prevents the inhibition of cellular protein synthesis even though sgRNA translation is still apparent. This prevention is not due to the inhibition of eIF2α phosphorylation, as it is also observed in $PKR^{-}/^{-}$ MEFs, which do not phosphorylate eIF2α after SINV infection.

3.3. Redistribution of Cellular Proteins between the Nucleus and Cytoplasm. A Proposal for the Mechanism of Cellular Translation Shut-Off

Several animal viruses provoke the relocalization of nuclear proteins to the cytoplasm as part of the cellular response to viral infection, leading to the formation of SGs [73,102]. Because a number of components that participate in protein synthesis are recruited to SGs, some viruses have evolved mechanisms to disrupt the formation of these inclusion bodies. Accordingly, SINV blocks SG formation by the interaction and complex formation of nsP3 with Ras-GTPase-activating protein SH3 domain-binding protein-1 (G3BP) [44,45]. Many of the nuclear proteins that are relocated to the cytoplasm after SINV or SFV infection are RNA-binding proteins (RBPs) and could directly interact with viral mRNAs, as has been found for T-cell restricted intracellular antigen-1 (TIA-1), heterogeneous nuclear ribonucleoprotein (hnRNP) A1, hnRNP K, hnRNP I, hnRNP M, polypyrimidine tract binding protein (PTB) or the ELAV RNA-binding protein HuR [75,86,103–106]. Indeed, HuR strongly interacts with the 3′-UTR of SINV and SFV mRNAs and participates in the regulation of their translation, transcription and replication [107]. Interestingly, sequences located at the 3′-UTR of SINV mRNAs are high-affinity binding sites for HuR, functioning with a "sponge"-like activity [108]. This sequestration of HuR on the cytoplasmic sgRNA has profound consequences for several cellular functions on host mRNAs, such as mRNA splicing, stability and decay.

As mentioned earlier, one plausible hypothesis to explain the shut-off of host translation is that viral RNA replication leads to high levels of viral sequences in the cytoplasm, that in turn induce the redistribution of nuclear proteins and the subsequent inhibition of protein synthesis. We found that the exit of nuclear proteins, including TIA-1 and PTB, is clearly detected in SINV-infected cells, but not upon the individual expression of nsPs or when viral RNA replication is reduced [75]. Moreover, the infection of BHK cells with the nsP2 P726G point mutation SINV variant, which exhibits defects in the shut-off of host protein synthesis, revealed that both viral RNA replication and the release of nuclear proteins to the cytoplasm are greatly inhibited. Thus, robust viral RNA replication must occur for the inhibition of cellular protein synthesis to proceed. Although this inhibition can take place via redundant mechanisms, such as redistribution of nuclear proteins, modification of eIFs, ionic imbalance or mRNA competition, it is probable that one of the most important factors to explain this event is the re-localization of nuclear proteins. In this regard, it is important to consider that a single viral protein that profoundly inhibits cellular translation, PV $2A^{pro}$, substantially modifies the shuttling of proteins between nucleus and cytoplasm. This viral protease not only cleaves eIF4G, but also several nuclear pore proteins (nuPs), disrupting the trafficking of proteins between nucleus and cytoplasm [109–113]. Based on this evidence, we propose that SINV replication leads to high levels of viral mRNAs in the cytoplasm that in turn modify the location of cellular proteins, triggering the blockade of host protein synthesis [75,92,108]. This can be accomplished either by the release of proteins that interact with cellular mRNAs or by sequestering components necessary for cellular translation on viral mRNAs due to their "sponge"-like activity [108]. Future characterization of the precise proteins that interact with viral and cellular mRNAs at late stages of infection in SINV infected cells should shed more light on this inhibition.

4. Structure of SINV sgRNA

A number of elements have been identified in sgRNA that make it particularly efficient for translation during infection (Figure 3). The SINV sgRNA is 4105 nucleotides (nt) in length without the poly(A) tail, and devotes the bulk of its sequence (3738 nt) to encode the structural polyprotein C-E3-E2-6K-E1. The coding sequence is flanked by two UTRs [114]. The 5′-UTR (49 nt) represents the leader sequence and contains a cap structure at its 5′ end. The 3′-UTR (323 nt) is organized in three different domains. In addition to the aforementioned 5′-and 3′-UTR, a hairpin (stem-loop) structure is present in the coding sequence at 77–139 nt from the 5′ end, which also participates in the translation of SINV sgRNA in infected cells.

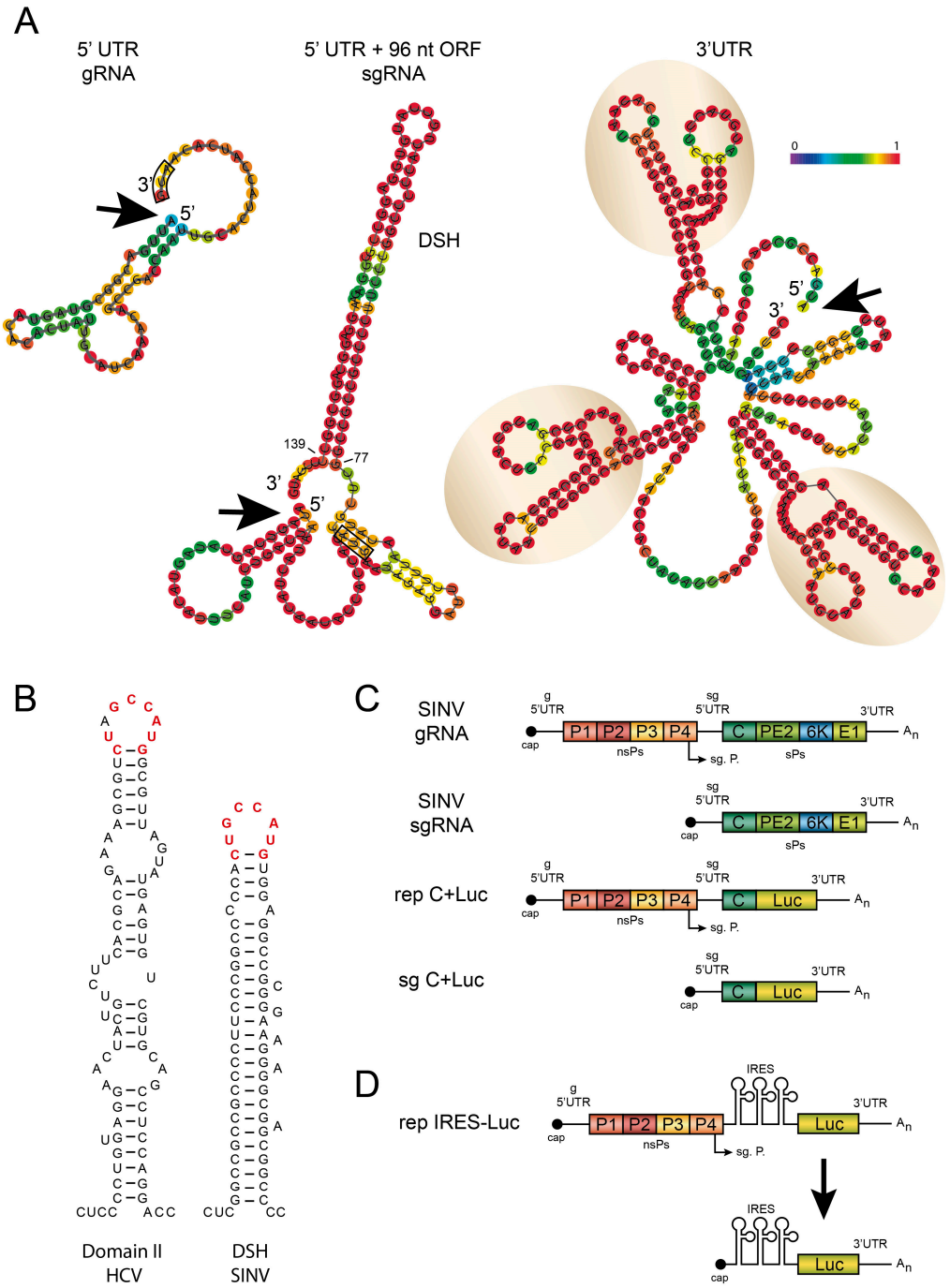

Figure 3. Some structural features of SINV mRNAs. (**A**) Secondary structure of the 5′-UTR and 3′-UTR regions of SINV gRNA and sgRNA. The 5′-UTR + 96 nt ORF of sgRNA include the downstream stable hairpin (DSH) from 77 to 139 nt. 5′-UTR gRNA has a free energy of the thermodynamic ensemble is −7.77 kcal/mol. 5′-UTR + 96 nt ORF sgRNA has a free energy of the thermodynamic ensemble is −60.31 kcal/mol. 3′-UTR has a free energy of the thermodynamic ensemble is −90.54 kcal/mol. These structures were obtained by The Vienna RNA Website. Nucleic Acids Res. 2008 (website tool: http://rna.tbi.univie.ac.at/cgi-bin/RNAWebSuite/RNAfold.cgi) and are colored by base-pairing probability. AUG start codons are shown surrounded by black boxes. Black arrows indicate the 5′ end of each RNA secondary structure. The three stem-loops at the 3′-UTR structure are highlighted within circles; (**B**) secondary structure of HCV Domain II and SINV DSH where similarity of the loops is marked in red; (**C**) schematic representation of SINV gRNA, sgRNA and the constructions encoding luciferase: (replicon) rep C+Luc and sgRNA C+Luc; (**D**) schematic representation of SINV construct containing the leader sequence of sgRNA replaced by an IRES element followed by the luciferase gene and the sgRNA synthesized from it. IRES: internal ribosome entry site.

4.1. The 5′-UTR of SINV sgRNA

Although the 5′-UTR leader sequence is rather short, it contains several motifs that are significantly implicated in different replicative functions, including transcription, translational shut-off, and viral pathogenesis (Figure 3A). The leader sequence contains a type 0 cap structure (N7mGppp) at its 5′-end, promoting RNA stability [114]. This leader sequence confers eIF4F complex-independence and is implicated in the inhibition of host translation [92,115]. Sequences in the negative-strand RNA complementary to the first 1–10 nt of the leader sequence are involved in promoter recognition and in the efficient transcription of sgRNA [114]. A SINV variant bearing a deletion of nucleotides 11–20 was found to be deficient for sgRNA transcription and failed to efficiently shut-off host cell translation, although it synthesized high levels of nsP2 [92]. By contrast, a revertant virus bearing a duplication of the promoter sequences was found to produce wild-type levels of sgRNA, and efficiently inhibited host translation. Accordingly, it has been postulated that this 11–20 nt region is necessary to interact with a cellular factor, which enhances viral translation and competes with cellular mRNAs [92].

The mechanism of the initiation of sgRNA translation and the selection of the AUG initiation codon have been studied in depth. Accordingly, sgRNA is translated via a scanning mechanism as the presence of a hairpin structure before the initiation codon hampers protein synthesis directed by this mRNA [82]. For this scanning process to occur, recognition of the cap structure by eIF4E is likely not necessary because cleavage of eIF4G by PV $2A^{pro}$ or human immunodeficiency virus (HIV) protease does not impede sgRNA translation in SINV-infected cells [88,115]. Moreover, this scanning on sgRNA takes place by a unique mechanism because it does not require some crucial initiation factors such as eIF2 and eIF4A [82].

4.2. The Hairpin Structure in the Coding Region of sgRNA

Early studies identified sequences in the coding region of the SINV capsid protein that enhanced the translation of sgRNAs [116,117]. Prediction of a stem-loop structure in these sequences indicated the presence of a hairpin located 27 nt downstream of the AUG initiation codon, at position +1, the first adenosine of AUG. This downstream hairpin structure, previously termed the downstream loop (DLP) by us [87], is not a true enhancer of protein synthesis, but instead is involved in conferring eIF2-independent translation of sgRNA in infected mammalian cells [86,87]. A second important function of this DLP, better known as the downstream stable hairpin (DSH), is to signal the precise codon at which translation begins [88,117]. Thus, whereas disorganization of the DSH does not diminish translation in PKR-deficient MEFs, translation is obstructed when eIF2α is phosphorylated [86,87]. The DSH has been proposed to be responsible for adaptation to certain vertebrate hosts since no orthologue of the *PKR* gene has been found in insect cells [118]. A hypothesis has been put forward that the acquisition of the DSH structure has allowed the colonization of vertebrate hosts and the consequent geographic expansion of some alphaviruses worldwide [107].

An intriguing observation is that SINV sgRNA translation can occur even when the AUG codon is replaced by other codons [88]. For instance, the substitution of AUG by CUG, which encodes leucine, is particularly efficient as shown by the abundant amounts of structural proteins synthesized by this variant [119]. However, this phenomenon is not observed after disorganization of the DSH and a SINV variant sgRNA bearing CUG instead of AUG is practically unable to participate in translation if the DSH is disorganized [119]. Moreover, a loss of fidelity of sgRNA bearing genuine AUG is observed when the DSH is disorganized, leading to leaky scanning; in this scenario, the AUG initiation codon is not recognized in many initiation events and ribosomes pass through to select other downstream alternative AUGs [88,117]. The DSH therefore plays an important role in the selection of the start codon on sgRNA.

Much effort has been made to better understand the functioning of the DSH during the process of sgRNA translation. Based on the Kozak model, it was speculated that this hairpin stalled ribosomes leaving the AUG_i at the P site [117], thereby serving to mechanically stop the preinitiation complex in such a way that initiation at the AUG could be facilitated. This hypothesis, however, is unlikely

because it is known that for a hairpin to facilitate initiation, it must be located 14 nt downstream of the AUG [79]. Placement of the DSH motif 9 nt closer to the AUG, which is an optimal position according to Kozak's model at 15 nt from the AUG, strongly reduces translation. Moreover, we found that replacement of the DSH with a hairpin with a similar free energy does not confer translatability to sgRNA when eIF2 is phosphorylated [82]. In contrast to this "mechanical" model, we have proposed a "functional" action of DSH. Thus, its precise function would involve its active interaction with ribosomes, probably at the P site, in such a way to signal the correct codon and replace the activity of eIF2 [82]. It is also of interest to note that SFV sgRNA contains sequences that could interact with the 18S rRNA [120]. In conclusion, it is possible that the binding of DSH to ribosomes not only relieves the necessity for eIF2, but also signals the correct codon to initiate translation.

4.3. The 3′-UTR of SINV sgRNA

The SINV 3′-UTR is rather long (323 nt) and can be divided into three distinct regions (Figure 3A). A conserved 19 nt sequence can be found close to the poly(A) tail that, together with at least 11 nt of this tail, forms part of the promoter to synthesize minus-strand RNA [121,122]. An AU-rich sequence of about 60 nt is found before this conserved region, which interacts with the host protein HuR and is involved in mRNA stabilization during alphavirus infection [104,107,108]. Finally, there are three repeated stem-loop structures that are present not only in alphaviruses, but also in other arthropod-borne viruses (e.g., arboviruses) [122–124]. These elements, as well as the AU-rich domain, may contribute to the repression of deadenylation of viral mRNAs [125]. Deletion of most of the 3′-UTR whilst retaining the 19 nt conserved sequence decreases the efficiency of SINV replication in mosquito cells relative to chicken cells [126]. Moreover, mutagenesis of this region has different effects on viral replication in mice and in cultured murine cells [127], which are not only species-dependent, but are also dependent on the tissue analyzed. The alphavirus 3′-UTR thus has an important role in viral replication and adaptation to new hosts in mosquitos and mammalian cells. Indeed, adaptation to mosquitoes, rather than mammalian hosts, is a major evolutionary force on the CHIKV 3′-UTR. Deletions in the repeated stem-loop sequences result in the poor replication of the Asian lineages in mosquito vectors [128]. Overall, these findings indicate that this motif and the 3′-UTR play a significant part in the adaptation and evolution of CHIKV. We recently examined the role of the repeated stem-loop structure at the 3′-UTR of SINV mRNAs during the virus life cycle in mammalian and insect cells [129]. Notably, mutation of the three stem-loops had little effect on the translation of gRNA and sgRNA in mammalian cells; however, protein synthesis directed by these two mRNAs lacking this motif was profoundly suppressed in mosquito cells. Interestingly, the addition of the SINV repeated sequence elements to the short 3′-UTR of sleeping disease virus (SDV), an alphavirus that does not have an insect vector [130–133], potently increased its replication and translation in insect cells [129]. To our knowledge, this motif constitutes the first example of an element from an animal virus that confers translatability to mRNAs in a cell-specific manner and, accordingly, it could be described as a translation enhancer "cell-specific" element. These observations explain, at a molecular level, the acquisition of the repeated regions along alphavirus evolution. Indeed, it is thought that an alphavirus ancestor initially infected marine organisms and did not have an invertebrate vector [2]. Subsequently, the marine alphavirus ancestor adapted along evolution to infect invertebrate hosts by acquiring these repeated sequences at the 3′-UTR.

Another intriguing aspect of the three repeated stem-loops at the 3′-UTR is that any one of them could theoretically interact by base-pairing with a stem-loop close to the cap structure at the 5′-end (Figure 3A). It could be speculated that this base pairing is involved in sgRNA circularization to facilitate translation. However, mutations of the loop at the 5′-UTR or disorganization of the stem-loop have little effect on protein synthesis directed by sgRNA [129]. Thus, this interaction is perhaps important for virus replication at the organismal level.

The 3′-UTR can also participate in the regulation of viral replication by its interaction with microRNAs (miRNAs), which regulate cellular protein synthesis through inhibition and/or

degradation of mRNAs. The expression of miRNAs is cell specific and is regulated at the transcriptional level; therefore, the miRNAs present in a given tissue can also modulate viral replication [134–136]. One interesting example of this regulation of alphavirus replication is provided by the infection of hematopoietic cells by EEEV. The hematopoietic-specific miRNA, miR-142-3p, binds to specific sites at the 3′-UTR of the EEEV genome, blocking translation [137,138]. This inhibition in murine myeloid cells minimizes induction of type I interferon and other innate immune effectors, allowing EEEV to replicate almost undetected by host defense responses, which exacerbates disease in animal models. Removal of the miR-142-3p binding sites from viral gRNA rescues viral translation and replication in myeloid cells, resulting in enhanced systemic type I interferon production, prodromal signs of disease, and attenuation of the virus [137]. The potential role that endogenous miRNAs can play in the regulation of SINV replication is, however, not well understood. Indeed, human cell lines lacking a functional Dicer enzyme, and therefore unable to produce miRNAs or siRNAs, showed no enhancement in the replication of a variety of viruses including SINV [139], whereas deletion of the miRNA processing enzyme Drosha in mammalian cells led to higher viral replication [140]. Since the miRNA machinery naturally exerts an antiviral response in mammalian cells [141], the SINV-induced translocation of Drosha into the cytoplasm may represent a broad antiviral response.

5. Mechanism of SINV sgRNA Translation

Perhaps the most relevant aspect of sgRNA translation is that it can take place in the absence of several eIFs. The misleading concept that sgRNA translation can occur with "reduced levels" of eIFs suggested that this mRNA is translated using the eIFs necessary to translate cellular mRNAs, albeit at lower concentrations. In contrast to this notion, overwhelming evidence has shown that SINV sgRNA can be translated in the absence of active eIF4F, after efficient cleavage of eIF4G, or in presence of compounds that powerfully block the activity of eIF4A or eIF2. We recently showed in human cells that eIF2A and eIF2D do not participate in the initiation of protein synthesis directed by sgRNA [119]. Accordingly, SINV sgRNA has evolved novel sequences and structures for efficient translation during infection. It is fascinating that the evolution of these structures accommodates two different hosts—insects and vertebrates [129]; the final outcome being the generation of a viral mRNA that has eliminated the requirements for several eIFs.

A very interesting aspect of sgRNA translation is that it is tightly coupled to its transcription in infected cells [94]. Thus, transfection of sgRNA into cells at late stages of infection does not result in its translation, since only the sgRNA synthesized during viral transcription is recognized by the translational machinery. It is still not well understood why the transfected sgRNA, which contains all the elements for efficient translation, is excluded from the protein-synthesizing machinery. Ostensibly, only the newly-manufactured sgRNA at the viral replicative foci is engaged with ribosomes to direct protein synthesis.

5.1. Protein Synthesis Directed by sgRNA without an Intact eIF4F Complex

Early work with cultured cells doubly infected with PV and SFV indicated that the synthesis of structural proteins from alphaviruses was resistant, at least in part, to PV infection [54,142]. To examine this in more detail, we constructed SINV strains bearing the PV $2A^{pro}$ or the HIV *PR* gene under a second internal promotor. Infection of mammalian cells with these recombinant SINV strains led to the expression of PV $2A^{pro}$ or HIV PR and the consequent cleavage of eIF4G [115]. Under these conditions, no intact eIF4G was detected, but abundant synthesis of SINV structural proteins took place. Moreover, HIV PR not only cleaves eIF4G, but also poly (A)-binding protein (PABP) [143], suggesting that initiation on sgRNA does not require eIF4G or PABP. Overall, these results establish that an intact eIF4F complex is not necessary to initiate sgRNA translation, which begs the question of why this messenger contains a cap structure at its 5′ end but does not work as an IRES. A likely possibility is that other proteins or factors replace the recognition of the cap by eIF4E in the eIF4F complex. Indeed, this factor could be eIF3D, since it has been shown that it can participate in cap

recognition on some specialized mRNAs without the requirement for eIF4E [144]. Moreover, eIF3 is necessary for initiation in vitro on sgRNA in reconstituted systems [145].

Aside from the non-requirement of eIF4G, potent inhibition of eIF4A by selective inhibitors does not affect protein synthesis directed by sgRNA, reinforcing the concept that the eIF4F complex is not involved in the synthesis of SINV late proteins. In this regard, a number of new translation inhibitors have been discovered through high-throughput screening methods [146]. One such molecule is pateamine A (Pat A), a natural marine compound synthesized by the sponge *Mycale* sp. [147,148] (Figure 4). Pat A targets eIF4A and enhances its helicase and ATPase activities in vitro, leading to the disruption of its interaction with eIF4G and promoting the formation of a stable complex between eIF4A and eIF4B [149,150]. Thus, translation of capped mRNAs that require eIF4F is blocked. However, hepatitis C virus (HCV) mRNA is not inhibited by Pat A, although other mRNAs bearing picornavirus IRES elements are blocked by this compound [149,150]. Additionally, Pat A induces the formation of SGs by a pathway independent of eIF2α phosphorylation [151]. Protein synthesis directed by sgRNA is resistant to Pat A inhibition, whereas gRNA translation is blocked [152]. Interestingly, the resistance of sgRNA to Pat A is observed only in SINV-infected cells, and not when this mRNA is translated out of the virus replicative context. To our knowledge, this represents the first example of a capped mRNA that is resistant to Pat A.

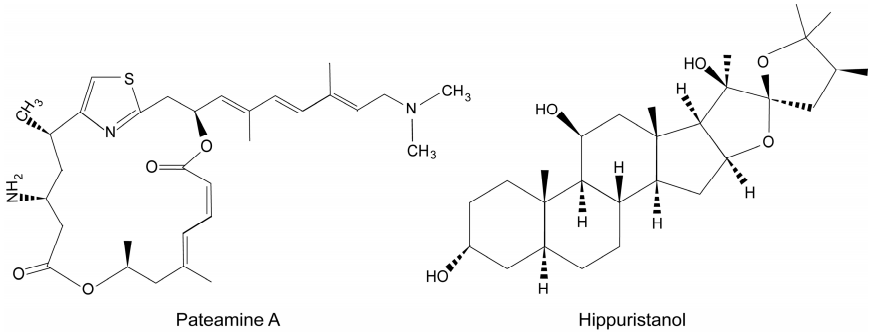

Figure 4. Chemical structure of pateamine A and hippuristanol.

A second potent and selective inhibitor of eIF4A is hippuristanol (hipp) [149,153] (Figure 4), a marine natural product isolated from the gorgonian coral *Isis hippuris* [146]. Hipp binds to the C-terminal domain of eIF4A, acting as an allosteric inhibitor of RNA interaction. This compound blocks translation of cellular mRNAs but not HCV IRES-driven translation. Notably, protein synthesis directed by sgRNA is not inhibited by hipp in SV-infected cells [74]; however, eIF4A is required to translate this mRNA in transfected cells or in cell-free systems. Perhaps, the modifications of the cytoplasm in the infected cells may create an environment that modifies the requirements for eIFs in the translation of sgRNA.

5.2. Translation without eIF2

As mentioned earlier, SINV infection induces the phosphorylation of eIF2α leading to its inactivation via activation of PKR by dsRNA. Several inhibitors such as sodium arsenite, dithiotreitol or thapsigargin can further increase this phosphorylation in SINV-infected cells, from about 80% in untreated cells to virtually 100% eIF2α phosphorylation in treated cells [88]. This finding demonstrated that sgRNA translation did not occur at reduced levels of active eIF2, but rather took place when practically all eIF2 was inactivated. As discussed previously, the hairpin located between 27 and 89 nt downstream from the AUG initiation codon is crucial to translate this mRNA when eIF2α is inactivated [74,86,87,89]. It could be speculated that although the majority of eIF2α is phosphorylated in SINV-infected cells, a small portion of active eIF2 remains in close proximity to the translation machinery at sgRNAs. We evaluated this possibility by generating specific variant SINV sgRNAs

containing two in-frame AUG start codons [82] (Figure 5). Curiously, initiation on this artificial sgRNA took place at both AUGs, but each of them was preferentially selected depending on the activity of eIF2. Thus, after eIF2α phosphorylation, translation on one AUG was reduced, while the initiation codon closest to DSH was resistant to this inhibition. This result shows that on a single mRNA, one AUG requires active eIF2 whereas the second one, which is at a short distance to the first AUG, initiates translation in an eIF2-independent manner.

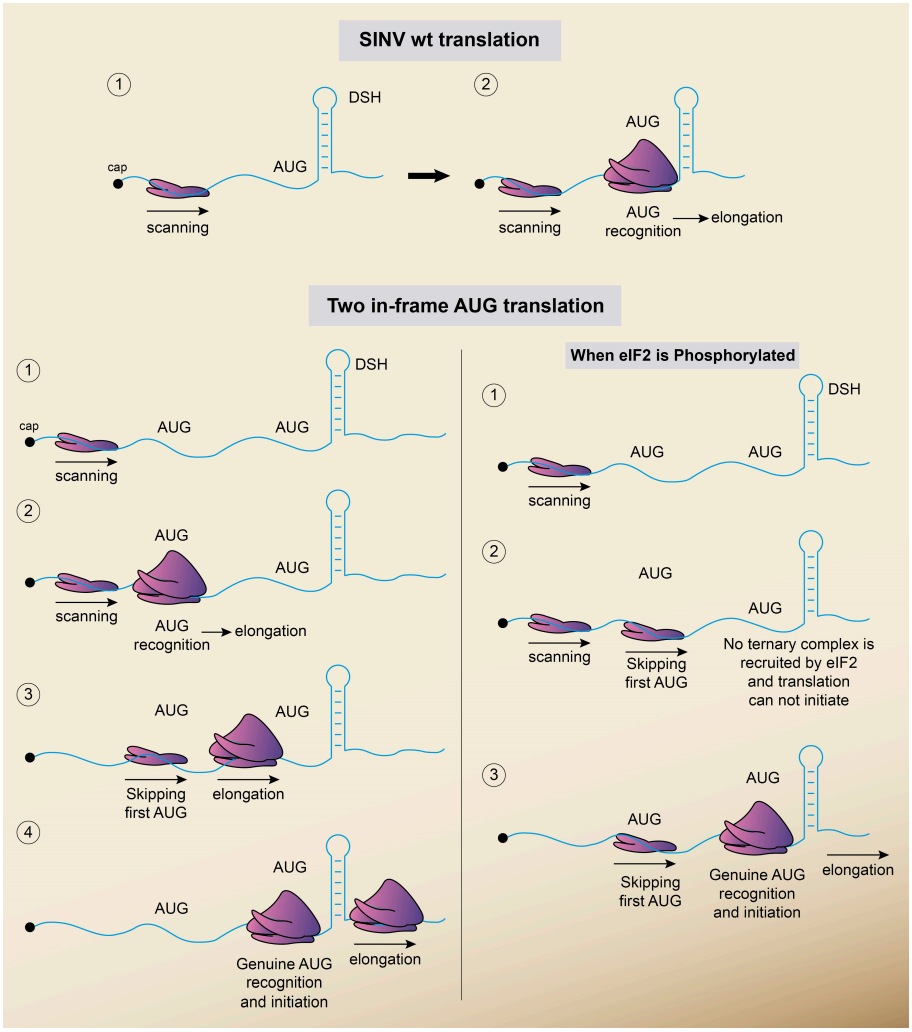

Figure 5. Schematic representation of the model for the initiation of translation on SINV sgRNA. (Upper panel) In the model of the scanning mechanism followed by WT SINV sgRNA to initiate translation, the 40S ribosomal subunit attaches initially at the 5′ cap structure. Then, the 5′ UTR is scanned base-by-base in a 5′–3′ direction until the initiation codon (AUG) is recognized. (Lower panel) Model for translation initiation on SINV sgRNA bearing two alternative start codons (AUG). Under no stress conditions (left part), the preinitiation complex containing the 40S ribosomal subunit interacts with the cap structure and scans the leader sequence of sgRNA until the first AUG is encountered. Then, the 80S initiation complex can be formed and elongation ensues. Another preinitiation complexes can start scanning from the cap structure and, in some cases, skip the first AUG start codon and reach the second AUG (genuine AUG), initiating the synthesis of authentic C protein from this start codon. When eIF2 is phosphorylated (right part), the lack of functional eIF2 prevents the initiation in the first AUG, nevertheless the genuine AUG, which is in proximity with DSH, manages to initiate the translation independently of the eIF2.

We have previously proposed that the function of eIF2 in SINV-infected cells can be replaced by other cellular factors, such as eIF2A [87]. eIF2A was described several years ago, but its precise activity in mammalian cells remains unclear and deletion of the yeast orthologue has no effect on cell viability [154]. Early results demonstrated that eIF2A can interact with Met-tRNA$_i^{Met}$ to bind it to the ribosome [155]; however, this binding was much less efficient than that observed using genuine eIF2 on artificial templates. Moreover, eIF2A was unable to promote the binding of Met-tRNA$_i^{Met}$ to globin mRNA [156]. Recent findings suggest that eIF2A is involved in the translation of some specialized cellular mRNAs that initiate translation with non-AUG codons [157,158]. Of interest, eIF2A has been implicated in cancer progression because it is involved in the initiation of translation of unconventional upstream ORFs [159]. Surprisingly, the development of mice with deletion for the *eIF2A* gene is completely normal, indicating that *eIF2A* is not required for the translation of both normal and specialized cellular mRNAs [160]. Another possibility is that *eIF2D* initiates sgRNA translation in place of eIF2 [145]. eIF2D was initially purified from rabbit reticulocyte lysates as an activity that could displace deacylated tRNA and mRNA from recycled 40S ribosomal subunits. In addition, eIF2D could interfere with the formation of the 48S initiation complex promoted by eIF2 [145]. A complex between Met-tRNA$_i^{Met}$ and eIF2D is formed in a GTP-independent fashion, and can interact with the 40S ribosomal subunit to deliver the initiator to the ribosomal P site [161]. However, as with eIF2A, the precise function of eIF2D in mammalian cells remains enigmatic.

To test the potential role of eIF2A and eIF2D in translation, we used human wild-type haploid HAP1 cell lines or equivalent cells knocked-out for eIF2A, eIF2D or both by CRISPR/Cas9 genome engineering. Cellular morphology, global protein synthesis and SINV infection was comparable between all four cell lines [119]. Moreover, synthesis of viral proteins at late stages of infection also was similar despite the fact that eIF2α became phosphorylated [119]. These findings show that eIF2A and eIF2D are not required for the translation of sgRNA when eIF2α is phosphorylated. Moreover, silencing of eIF2A or eIF2D by transfection of the corresponding siRNAs in HAP1 WT, HAP1-eIF2A$^-$ and HAP1-eIF2D$^-$ cells had little effect on the synthesis of viral proteins late in infection. Elegant studies employing CRISPR/Cas9 technology in HAP cells has provided an extensive analysis of the human proteins that are involved in the replication of HCV, and are dispensable for cell viability [162]. Curiously, some of these proteins are not required for SINV replication. These results provide an interesting approach to develop antiviral compounds against human viruses.

Our observations support the novel proposal that eIF2 is not replaced by a cellular protein during the translation of SINV sgRNA. Instead, this viral mRNA has evolved a specialized structure that confers independence for eIF2. In this regard, it is possible that the DSH functions in a way similar to that of domain II of HCV IRES, because there are also great similarities between these elements, including the sequence present at the loop (Figure 3B). Thus, domain II from HCV IRES can directly interact with preinitiation complexes and 80S ribosomes and displace the bound eIF2, substituting the requirement for this factor [163,164]. It can be hypothesized that some viral mRNAs can acquire elements to maximize the translation process under infection conditions. The consequences for the virus life cycle are that significant amounts of structural proteins can be produced upon the translation of sgRNA even under stress conditions that appear after viral infection.

5.3. Mechanism of sgRNA Translation. Comparison with Cellular mRNAs

Work carried out in the past few years has provided a more detailed picture on the mechanism by which sgRNA initiates translation. To compare this initiation mechanism with the canonical cap-dependent scanning mechanism that takes place on cellular mRNAs, we will briefly summarize the molecular events that initiate translation on cellular mRNAs. Cap recognition involves the interaction of eIF4E with the methylated structure m7GpppN located at the 5′ end of eukaryotic cellular mRNAs [77]. Binding of eIF3 to the eIF4G middle domain promotes the interaction of the preinitiation complex 43S at the 5′ end of mRNAs [165]. Thus, there is an interaction of the ribosomal subunit 40S, containing several eIFs such as eIF1, eIF1A, eIF3, and eIF2 in the form of

ternary complex [166,167]. It has been proposed that the 40S ribosomal subunit bound to these eIFs is in an "open" conformation, that is, competent for scanning, which involves linear base-by-base inspection of the 5′-UTR [79,166,168,169]. This scanning takes place until an AUG initiation codon is found in a suitable sequence context [79,170]. The secondary structure of the 5′-UTR is melted during the scanning process, in part by the helicase activity of eIF4A, although stable hairpins cannot be melted by small ribosomal subunits and eIF4A [78]. After positioning of the preinitiation complex at the AUG initiation codon, base-pairing takes place with the anticodon present in the initiator tRNA Met-tRNA$_i^{Met}$. Subsequently, the eIF5 carboxy moiety promotes the dissociation of eIF1, together with inorganic phosphate derived from the GTP hydrolysis of the ternary complex [171,172]. In addition, the eIF1A carboxy terminus moves closer to the eIF5 amino terminus [173]. This movement is coupled to eIF1 exit, which leaves the P site free and allows tighter binding of the initiator tRNA at this site. Concomitant with this rearrangement, eIF5B-GTP can now interact with the 40S subunit. In this manner, eIF5 together with eIF2-GDP are released from the small ribosomal subunit, which is now in the "closed" conformation and is committed to continue mRNA translation [172,173]. This interaction of eIF5B-GTP stimulates the joining of the 60S subunit to form an 80S initiation complex. The initiation phase ends with the Met-tRNA$_i^{Met}$ accommodated in the P site of the 80S, leaving free the A site. The interaction of the ternary complex aminoacyl-tRNA-eEF1-GTP to this site starts the elongation phase.

In common with cellular mRNAs, the initiation of SINV sgRNA translation also takes place following the scanning mechanism [74,82]. The first event in this initiation could be the interaction of eIF3, by means of its subunit eIF3D, to the cap structure at the 5′-end, without the participation of eIF4E and the entire eIF4F complex [115,144,152]. After the interaction of eIF3 with the cap structure, the 40S ribosomal subunit can bind to the mRNA. Although exactly which eIFs bind to this 40S ribosomal subunit remain unclear, the ternary complex containing active eIF2 is definitely not required for this interaction, nor for the subsequent scanning of the leader sequence [129]. Once the 40S in the "open" conformation (with some still undefined eIFs) reaches the AUG initiation codon, it can stop to interact with the stable hairpin loop that could bind to the ribosomal P site, inducing the "close" conformation. This event would promote the joining of the 60S subunit to build-up the 80S ribosome competent to translate this viral messenger. How the Met-tRNA is delivered to the ribosome in order to establish the codon-anticodon based pairing remains unknown. The finding that other codons can replace AUG to initiate translation of sgRNA, albeit with lower efficiency, makes it possible that aminoacyl-tRNAs different from Met-tRNA can participate in this process [88,119]. Since active eIF2 is not required for this initiation event, perhaps other cellular factors, including elongation factor eEF1, are responsible for this event following a mechanism akin to that reported for cricket paralysis virus (CrPV) [174,175]. The similarities in the structure between the DSH and domain II of HCV IRES points to the possibility that their functioning is also similar (Figure 3B) [163,164], since translation of HCV is independent of active eIF2. Once the 80S ribosome has been built-up, it can initiate the elongation phase to synthesize the polyprotein that contains the SINV structural proteins. A puzzling aspect of sgRNA translation is that the 80S has to pass through the DSH, melting its structure. Clearly the DSH cannot be functional during the translation of this hairpin because it would remain disorganized. After the ribosome passes, the hairpin must reorganize to become functional on the 40S ribosomal subunit that is paused at the start position. Therefore, the DSH is melted and reorganized each time that the ribosome translates this sequence of the capsid protein. The obvious question that arises is why the DSH is located at the coding region and not at the leader sequence. A possible reason could be that since the mRNA is capped, the 40S ribosomal subunit could not melt this structure and necessarily should be placed after the initiation codon at an optimal distance to exert its function. It must be considered that the preinitiation complexes containing the small ribosome subunit are unable to melt the DSH hairpin, and only 80S ribosomes have the potential to pass through this stem-loop.

6. Translation of SINV sgRNA Bearing IRES Elements

The singular translation system represented by SINV-infected cells provides a good model to analyze the requirements of some specialized mRNAs to direct protein synthesis. This is because high amounts of sgRNA are present at late stages of infection and this is the only mRNA efficiently translated after the abrogation of cellular protein synthesis. Against this background, the translatability of sgRNAs bearing different IRES elements has been studied in mammalian cells using SINV replicons, and a number of surprising results, some of them remaining unresolved, have been reported during IRES-driven translation in SINV-replicating cells [89,176].

6.1. The Variety of Internal Ribosome Entry Site Elements

There is a great variety of IRES elements with regards to their structure and functioning, and several have been analyzed in cellular and viral mRNAs [177–179]. In the case of animal viruses, four major groups are known to contain mRNAs bearing IRES elements: picornaviruses, flaviviruses, pestiviruses and retroviruses [178,180–183]. Picornavirus IRES elements can be classified into at least two groups—IRES type I is typical of entero/rhinoviruses, with PV considered as the prototype, whereas type II IRESs are present in cardio/aphtoviruses, with encephalomyocarditis virus (EMCV) as the prototype [181,184,185]. IRES elements contain a rich secondary structure with several stem-loops, which are crucial for their activity. Most IRES elements bear a tRNA-like motif that is involved in binding to ribosomes [186–188]. The requirement for eIFs varies according to the IRES under study. Thus, picornavirus IRESs do not require eIF4E and can be translated when eIF4G is cleaved by some picornavirus proteases, such as PV $2A^{pro}$ or foot-and-mouth disease virus (FMDV) leader $(L)^{pro}$ [81,189,190]. Notably, HCV mRNA can be translated without the eIF4F complex and even in the absence of eIF2 [187]. Perhaps most strikingly, the intergenic region (IGR) of CrPV mRNA directs protein synthesis in the absence of all known initiation factors [182]. In addition to eIFs, a number of cellular proteins known as IRES trans-activating factors (ITAFs) have the ability to interact directly with IRESs and modulate their activity [183,191,192].

6.2. IRES-Driven Translation in Alphavirus Replicons

In the early days of research on alphavirus translation, it was discovered that gRNA only directed the translation of the first ORF, whereas those proteins encoded by the second cistron were synthesized from a second mRNA (sgRNA) [193]. The implication was that only the AUG initiation codon nearest to the cap structure was functional, and not the internal AUG present in sgRNA. Therefore, the leader sequence of sgRNA was thought to have no IRES activity. Indeed, transfection of uncapped gRNA in mammalian cells failed to direct the translation of a reporter gene located in the second cistron [176]. It is appreciated that mRNAs containing IRES elements are very efficiently translated, both in cultured cells and in in vitro systems, and for this reason a number of viral vectors have been developed bearing IRES elements to provide robust gene expression. In this regard, alphavirus vectors are potentially useful tools to express heterologous genes and for the design of vaccines [194–196]. However, the use of IRES elements in alphavirus vectors results in poor gene expression [176,197]. Indeed, IRES elements belonging to picornaviruses HCV and CrPV perform poorly in SINV replicating cells [89,176]. SINV constructs containing the leader sequence of sgRNA replaced by an IRES element followed by the luciferase gene are able to synthesize luciferase protein when uncapped gRNA is transfected into mammalian cells, demonstrating that internal initiation on gRNA occurs early after transfection (Figure 3D). Notably, the translation is inhibited in the late phase of SINV replication. Co-expression of different PV non-structural genes has revealed that PV $2A^{pro}$ can increase translation of sgRNAs containing the PV or EMCV IRESs, but not of those from HCV or CrPV. The L^{pro} protease from FMDV also rescues translation, whereas a PV $2A^{pro}$ variant deficient in eIF4G cleavage does not increase picornavirus IRES-driven translation in SINV replicons. Overall, these findings suggest that the replicative foci of SINV-infected cells, where sgRNA translation takes place, are deficient in

components necessary to translate IRES-containing mRNAs. In the case of picornavirus IRES elements, cleavage of eIF4GI by PV $2A^{pro}$ or FMDV L^{pro} rescues this inhibition. The fact that translation of picornavirus IRESs requires functional eIF2 at early stages of infection, but not later [198], suggested that the lack of picornavirus IRES-driven translation in SINV-replicating cells was due to the phosphorylation of eIF2. Indeed, PV IRES-driven translation can take place from SINV replicons if eIF2α remains unphosphorylated in $PKR^{-}/^{-}$ MEFS [89]. It was therefore concluded that these viral proteases conferred eIF2-independent translation to picornavirus IRESs [89,189,190,199]. Thus far, no explanation has been proposed for the failure of HCV or IGR CrPV IRES elements to direct protein synthesis in SINV replicating cells. In the case of HCV IRES, it is independent of both the eIF4F complex and eIF2, a situation similar to that described for sgRNA translation [200]. Even more intriguing is the fact that IGR CrPV IRES, which does not require any eIF [175,201], is inactive in the context of SINV replicons [176]. Perhaps these IRES elements require an ITAF that is not present in the replicating foci of SINV-infected cells. Alternatively, it is possible that the redistribution of nuclear proteins to the cytoplasm is inhibitory for the translation of these IRES elements. This latter possibility is more likely given that all the viral IRES elements are functional on uncapped gRNA early after transfection.

7. Concluding Remarks and Future Perspectives

The study of the regulation of protein synthesis in SINV-infected mammalian and insect cells has broadened our understanding of the basic translation mechanisms of viral mRNAs. In this regard, several elements have been identified in SINV mRNAs that maximize their translatability in different host cells. These viral messengers have thus exhibited functional plasticity during evolution to adapt to different species and environments. Most probably, alphaviruses first appeared in marine vertebrates [2] and expanded their host range by acquiring the ability to infect insects, which became effective vectors for viral transmission to terrestrial vertebrates. In the adaptation to insects, alphaviruses recruited a motif at their 3′-UTR, which is necessary for the powerful translation of their mRNAs in this host. However, the precise functioning of this motif as regards to its interaction with cellular factors remains enigmatic. Although we now comprehend the functioning of DSH and the leader sequence of these mRNAs, additional efforts are needed to better understand their activity during the initiation of translation. In particular, further work is necessary to address the mechanism of translation of SINV gRNA, to discern if it follows the canonical pathway exhibited by cellular mRNAs, and also the explicit eIFs involved in the initiation of protein synthesis. Finally, the abrogation of host protein synthesis after infection of vertebrate cells by SINV would appear to be due to the redistribution of nuclear proteins to the cytoplasm. However, we do not know which RNA-binding proteins interact with viral and cellular mRNAs at late stages of infection. Comprehensive proteomic analysis will be essential to identify which cellular (or viral) proteins interact with mRNAs and may shed more light on the control of host cell translational machinery by SINV. If translational shut-off is indeed due to the accumulation of nuclear proteins in the cytoplasm of infected cells, several questions will need to be addressed: (1) Which nuclear proteins are able to interact with cellular mRNAs and, from those, which ones are responsible for the inhibition of protein synthesis? (2) Why is this blockade selective for host cell translation? (3) Is the presence of viral RNA sequences responsible for the relocalization of nuclear proteins to the cytoplasm following the "sponge-like" mechanism and consequently for the inhibition of host translation? Future work using the SINV infection model will answer some of these questions.

Acknowledgments: We thank Manuel García Moreno (Department of Biochemistry, University of Oxford, UK) for critical reading of this manuscript and his suggestions. This study was supported by a DGICYT (Dirección General de Investigación Científica y Técnica, Ministerio de Economía y Competitividad, Spain) grant (SAF2015-66170-R (MINECO/FEDER)) to LC. EGA is the holder of an FPU (Formación de Personal Universitario) Fellowship (FPU15/05709). Institutional grants from the Fundación Ramón Areces and Banco de Santander to the Centro de Biología Molecular "Severo Ochoa" (CSIC-UAM) are also acknowledged.

Author Contributions: Luis Carrasco, Miguel Angel Sanz and Esther González-Almela wrote the manuscript.

Conflicts of Interest: The authors declare no conflict of interest.

References

1. Griffin, D.E. Alphaviruses. In *Fields Virology*; Fields, B.N., Knipe, D.M., Howley, P.M., Eds.; Wolters Kluwer Health/Lippincott Williams & Wilkins: Philadelphia, PA, USA, 2007; pp. 1023–1068.
2. Forrester, N.L.; Palacios, G.; Tesh, R.B.; Savji, N.; Guzman, H.; Sherman, M.; Weaver, S.C.; Lipkin, W.I. Genome-scale phylogeny of the alphavirus genus suggests a marine origin. *J. Virol.* **2012**, *86*, 2729–2738. [CrossRef] [PubMed]
3. Nasar, F.; Palacios, G.; Gorchakov, R.V.; Guzman, H.; da Rosa, A.P.; Savji, N.; Popov, V.L.; Sherman, M.B.; Lipkin, W.I.; Tesh, R.B.; et al. Eilat virus, a unique alphavirus with host range restricted to insects by RNA replication. *Proc. Natl. Acad. Sci. USA* **2012**, *109*, 14622–14627. [CrossRef] [PubMed]
4. Novella, I.S.; Presloid, J.B.; Smith, S.D.; Wilke, C.O. Specific and nonspecific host adaptation during arboviral experimental evolution. *J. Mol. Microbiol. Biotechnol.* **2011**, *21*, 71–81. [CrossRef] [PubMed]
5. Weaver, S.C.; Winegar, R.; Manger, I.D.; Forrester, N.L. Alphaviruses: Population genetics and determinants of emergence. *Antivir. Res.* **2012**, *94*, 242–257. [CrossRef] [PubMed]
6. Karpf, A.R.; Blake, J.M.; Brown, D.T. Characterization of the infection of *Aedes albopictus* cell clones by Sindbis virus. *Virus Res.* **1997**, *50*, 1–13. [CrossRef]
7. Mudiganti, U.; Hernandez, R.; Ferreira, D.; Brown, D.T. Sindbis virus infection of two model insect cell systems—A comparative study. *Virus Res.* **2006**, *122*, 28–34. [CrossRef] [PubMed]
8. Suzme, R.; Tseng, J.C.; Levin, B.; Ibrahim, S.; Meruelo, D.; Pellicer, A. Sindbis viral vectors target hematopoietic malignant cells. *Cancer Gene Ther.* **2012**, *19*, 757–766. [CrossRef] [PubMed]
9. Tassetto, M.; Kunitomi, M.; Andino, R. Circulating Immune Cells Mediate a Systemic RNAi-Based Adaptive Antiviral Response in Drosophila. *Cell* **2017**, *169*, 314–325. [CrossRef] [PubMed]
10. Fuller, S.D. The T = 4 envelope of Sindbis virus is organized by interactions with a complementary T = 3 capsid. *Cell* **1987**, *48*, 923–934. [CrossRef]
11. Strauss, J.H.; Strauss, E.G. The alphaviruses: Gene expression, replication, and evolution. *Microbiol. Rev.* **1994**, *58*, 491–562. [PubMed]
12. Wang, K.S.; Kuhn, R.J.; Strauss, E.G.; Ou, S.; Strauss, J.H. High-affinity laminin receptor is a receptor for Sindbis virus in mammalian cells. *J. Virol.* **1992**, *66*, 4992–5001. [PubMed]
13. Klimstra, W.B.; Nangle, E.M.; Smith, M.S.; Yurochko, A.D.; Ryman, K.D. DC-SIGN and L-SIGN can act as attachment receptors for alphaviruses and distinguish between mosquito cell- and mammalian cell-derived viruses. *J. Virol.* **2003**, *77*, 12022–12032. [CrossRef] [PubMed]
14. Rose, P.P.; Hanna, S.L.; Spiridigliozzi, A.; Wannissorn, N.; Beiting, D.P.; Ross, S.R.; Hardy, R.W.; Bambina, S.A.; Heise, M.T.; Cherry, S. Natural resistance-associated macrophage protein is a cellular receptor for sindbis virus in both insect and mammalian hosts. *Cell Host Microbe* **2011**, *10*, 97–104. [CrossRef] [PubMed]
15. Perez, L.; Carrasco, L. Involvement of the vacuolar H^+-ATPase in animal virus entry. *J. Gen. Virol.* **1994**, *75 Pt 10*, 2595–2606. [CrossRef] [PubMed]
16. Mayor, S.; Pagano, R.E. Pathways of clathrin-independent endocytosis. *Nat. Rev. Mol. Cell Biol.* **2007**, *8*, 603–612. [CrossRef] [PubMed]
17. Leung, J.Y.; Ng, M.M.; Chu, J.J. Replication of alphaviruses: A review on the entry process of alphaviruses into cells. *Adv. Virol.* **2011**, *2011*, 249640. [CrossRef] [PubMed]
18. Vancini, R.; Wang, G.; Ferreira, D.; Hernandez, R.; Brown, D.T. Alphavirus genome delivery occurs directly at the plasma membrane in a time- and temperature-dependent process. *J. Virol.* **2013**, *87*, 4352–4359. [CrossRef] [PubMed]
19. Sokoloski, K.J.; Nease, L.M.; May, N.A.; Gebhart, N.N.; Jones, C.E.; Morrison, T.E.; Hardy, R.W. Identification of Interactions between Sindbis Virus Capsid Protein and Cytoplasmic vRNA as Novel Virulence Determinants. *PLoS Pathog.* **2017**, *13*, e1006473. [CrossRef] [PubMed]
20. Berlanga, J.J.; Ventoso, I.; Harding, H.P.; Deng, J.; Ron, D.; Sonenberg, N.; Carrasco, L.; de Haro, C. Antiviral effect of the mammalian translation initiation factor 2α kinase GCN2 against RNA viruses. *EMBO J.* **2006**, *25*, 1730–1740. [CrossRef] [PubMed]
21. Shin, G.; Yost, S.A.; Miller, M.T.; Elrod, E.J.; Grakoui, A.; Marcotrigiano, J. Structural and functional insights into alphavirus polyprotein processing and pathogenesis. *Proc. Natl. Acad. Sci. USA* **2012**, *109*, 16534–16539. [CrossRef] [PubMed]

22. Sokoloski, K.J.; Haist, K.C.; Morrison, T.E.; Mukhopadhyay, S.; Hardy, R.W. Noncapped Alphavirus Genomic RNAs and Their Role during Infection. *J. Virol.* **2015**, *89*, 6080–6092. [CrossRef] [PubMed]
23. De Groot, R.J.; Hardy, W.R.; Shirako, Y.; Strauss, J.H. Cleavage-site preferences of Sindbis virus polyproteins containing the non-structural proteinase. Evidence for temporal regulation of polyprotein processing in vivo. *EMBO J.* **1990**, *9*, 2631–2638. [PubMed]
24. Laakkonen, P.; Ahola, T.; Kaariainen, L. The effects of palmitoylation on membrane association of Semliki forest virus RNA capping enzyme. *J. Biol. Chem.* **1996**, *271*, 28567–28571. [CrossRef] [PubMed]
25. Ahola, T.; Lampio, A.; Auvinen, P.; Kaariainen, L. Semliki Forest virus mRNA capping enzyme requires association with anionic membrane phospholipids for activity. *EMBO J.* **1999**, *18*, 3164–3172. [CrossRef] [PubMed]
26. Ahola, T.; Kujala, P.; Tuittila, M.; Blom, T.; Laakkonen, P.; Hinkkanen, A.; Auvinen, P. Effects of palmitoylation of replicase protein nsP1 on alphavirus infection. *J. Virol.* **2000**, *74*, 6725–6733. [CrossRef] [PubMed]
27. Li, G.; Rice, C.M. The signal for translational readthrough of a UGA codon in Sindbis virus RNA involves a single cytidine residue immediately downstream of the termination codon. *J. Virol.* **1993**, *67*, 5062–5067. [PubMed]
28. Rupp, J.C.; Sokoloski, K.J.; Gebhart, N.N.; Hardy, R.W. Alphavirus RNA synthesis and non-structural protein functions. *J. Gen. Virol.* **2015**, *96*, 2483–2500. [CrossRef] [PubMed]
29. Shirako, Y.; Strauss, E.G.; Strauss, J.H. Suppressor mutations that allow sindbis virus RNA polymerase to function with nonaromatic amino acids at the N-terminus: Evidence for interaction between nsP1 and nsP4 in minus-strand RNA synthesis. *Virology* **2000**, *276*, 148–160. [CrossRef] [PubMed]
30. Fata, C.L.; Sawicki, S.G.; Sawicki, D.L. Modification of Asn374 of nsP1 suppresses a Sindbis virus nsP4 minus-strand polymerase mutant. *J. Virol.* **2002**, *76*, 8641–8649. [CrossRef] [PubMed]
31. Mi, S.; Durbin, R.; Huang, H.V.; Rice, C.M.; Stollar, V. Association of the Sindbis virus RNA methyltransferase activity with the nonstructural protein nsP1. *Virology* **1989**, *170*, 385–391. [CrossRef]
32. Ahola, T.; Laakkonen, P.; Vihinen, H.; Kaariainen, L. Critical residues of Semliki Forest virus RNA capping enzyme involved in methyltransferase and guanylyltransferase-like activities. *J. Virol.* **1997**, *71*, 392–397. [PubMed]
33. Peranen, J.; Laakkonen, P.; Hyvonen, M.; Kaariainen, L. The alphavirus replicase protein nsP1 is membrane-associated and has affinity to endocytic organelles. *Virology* **1995**, *208*, 610–620. [CrossRef] [PubMed]
34. Salonen, A.; Vasiljeva, L.; Merits, A.; Magden, J.; Jokitalo, E.; Kaariainen, L. Properly folded nonstructural polyprotein directs the Semliki Forest virus replication complex to the endosomal compartment. *J. Virol.* **2003**, *77*, 1691–1702. [CrossRef] [PubMed]
35. Russo, A.T.; White, M.A.; Watowich, S.J. The crystal structure of the Venezuelan equine encephalitis alphavirus nsP2 protease. *Structure* **2006**, *14*, 1449–1458. [CrossRef] [PubMed]
36. Gomez de Cedron, M.; Ehsani, N.; Mikkola, M.L.; Garcia, J.A.; Kaariainen, L. RNA helicase activity of Semliki Forest virus replicase protein NSP2. *FEBS Lett.* **1999**, *448*, 19–22. [CrossRef]
37. Garmashova, N.; Gorchakov, R.; Frolova, E.; Frolov, I. Sindbis virus nonstructural protein nsP2 is cytotoxic and inhibits cellular transcription. *J. Virol.* **2006**, *80*, 5686–5696. [CrossRef] [PubMed]
38. Breakwell, L.; Dosenovic, P.; Karlsson Hedestam, G.B.; D'Amato, M.; Liljestrom, P.; Fazakerley, J.; McInerney, G.M. Semliki Forest virus nonstructural protein 2 is involved in suppression of the type I interferon response. *J. Virol.* **2007**, *81*, 8677–8684. [CrossRef] [PubMed]
39. Rikkonen, M.; Peranen, J.; Kaariainen, L. Nuclear targeting of Semliki Forest virus nsP2. *Arch. Virol. Suppl.* **1994**, *9*, 369–377. [PubMed]
40. Akhrymuk, I.; Kulemzin, S.V.; Frolova, E.I. Evasion of the innate immune response: The Old World alphavirus nsP2 protein induces rapid degradation of Rpb1, a catalytic subunit of RNA polymerase II. *J. Virol.* **2012**, *86*, 7180–7191. [CrossRef] [PubMed]
41. Koonin, E.V.; Gorbalenya, A.E.; Purdy, M.A.; Rozanov, M.N.; Reyes, G.R.; Bradley, D.W. Computer-assisted assignment of functional domains in the nonstructural polyprotein of hepatitis E virus: Delineation of an additional group of positive-strand RNA plant and animal viruses. *Proc. Natl. Acad. Sci. USA* **1992**, *89*, 8259–8263. [CrossRef] [PubMed]
42. Vihinen, H.; Ahola, T.; Tuittila, M.; Merits, A.; Kaariainen, L. Elimination of phosphorylation sites of Semliki Forest virus replicase protein nsP3. *J. Biol. Chem.* **2001**, *276*, 5745–5752. [CrossRef] [PubMed]

43. Lulla, A.; Lulla, V.; Merits, A. Macromolecular assembly-driven processing of the 2/3 cleavage site in the alphavirus replicase polyprotein. *J. Virol.* **2012**, *86*, 553–565. [CrossRef] [PubMed]
44. Panas, M.D.; Varjak, M.; Lulla, A.; Eng, K.E.; Merits, A.; Karlsson Hedestam, G.B.; McInerney, G.M. Sequestration of G3BP coupled with efficient translation inhibits stress granules in Semliki Forest virus infection. *Mol. Biol. Cell* **2012**, *23*, 4701–4712. [CrossRef] [PubMed]
45. Fros, J.J.; Domeradzka, N.E.; Baggen, J.; Geertsema, C.; Flipse, J.; Vlak, J.M.; Pijlman, G.P. Chikungunya virus nsP3 blocks stress granule assembly by recruitment of G3BP into cytoplasmic foci. *J. Virol.* **2012**, *86*, 10873–10879. [CrossRef] [PubMed]
46. Rubach, J.K.; Wasik, B.R.; Rupp, J.C.; Kuhn, R.J.; Hardy, R.W.; Smith, J.L. Characterization of purified Sindbis virus nsP4 RNA-dependent RNA polymerase activity in vitro. *Virology* **2009**, *384*, 201–208. [CrossRef] [PubMed]
47. Pietila, M.K.; Hellstrom, K.; Ahola, T. Alphavirus polymerase and RNA replication. *Virus Res.* **2017**, *234*, 44–57. [CrossRef] [PubMed]
48. Shirako, Y.; Strauss, J.H. Regulation of Sindbis virus RNA replication: Uncleaved P123 and nsP4 function in minus-strand RNA synthesis, whereas cleaved products from P123 are required for efficient plus-strand RNA synthesis. *J. Virol.* **1994**, *68*, 1874–1885. [PubMed]
49. Lemm, J.A.; Rumenapf, T.; Strauss, E.G.; Strauss, J.H.; Rice, C.M. Polypeptide requirements for assembly of functional Sindbis virus replication complexes: A model for the temporal regulation of minus- and plus-strand RNA synthesis. *EMBO J.* **1994**, *13*, 2925–2934. [PubMed]
50. LaStarza, M.W.; Lemm, J.A.; Rice, C.M. Genetic analysis of the nsP3 region of Sindbis virus: Evidence for roles in minus-strand and subgenomic RNA synthesis. *J. Virol.* **1994**, *68*, 5781–5791. [PubMed]
51. Kujala, P.; Ikaheimonen, A.; Ehsani, N.; Vihinen, H.; Auvinen, P.; Kaariainen, L. Biogenesis of the Semliki Forest virus RNA replication complex. *J. Virol.* **2001**, *75*, 3873–3884. [CrossRef] [PubMed]
52. Kallio, K.; Hellstrom, K.; Balistreri, G.; Spuul, P.; Jokitalo, E.; Ahola, T. Template RNA length determines the size of replication complex spherules for Semliki Forest virus. *J. Virol.* **2013**, *87*, 9125–9134. [CrossRef] [PubMed]
53. Kallio, K.; Hellstrom, K.; Jokitalo, E.; Ahola, T. RNA Replication and Membrane Modification Require the Same Functions of Alphavirus Nonstructural Proteins. *J. Virol.* **2015**, *90*, 1687–1692. [CrossRef] [PubMed]
54. Perez, L.; Irurzun, A.; Carrasco, L. Action of brefeldin A on translation in Semliki Forest virus-infected HeLa cells and cells doubly infected with poliovirus. *J. Gen. Virol.* **1994**, *75*, 2197–2203. [CrossRef] [PubMed]
55. Carrasco, L.; Guinea, R.; Irurzun, A.; Barco, A. Effects of viral replication on cellular membrane metabolism and function. In *Molecular Biology of Picornaviruses*; Wimmer, E., Semler, B.L., Eds.; ASM Press: Washington, DC, USA, 2002; pp. 337–354.
56. Hellstrom, K.; Kallio, K.; Utt, A.; Quirin, T.; Jokitalo, E.; Merits, A.; Ahola, T. Partially Uncleaved Alphavirus Replicase Forms Spherule Structures in the Presence and Absence of RNA Template. *J. Virol.* **2017**, *91*. [CrossRef] [PubMed]
57. Varjak, M.; Saul, S.; Arike, L.; Lulla, A.; Peil, L.; Merits, A. Magnetic fractionation and proteomic dissection of cellular organelles occupied by the late replication complexes of Semliki Forest virus. *J. Virol.* **2013**, *87*, 10295–10312. [CrossRef] [PubMed]
58. Cristea, I.M.; Rozjabek, H.; Molloy, K.R.; Karki, S.; White, L.L.; Rice, C.M.; Rout, M.P.; Chait, B.T.; MacDonald, M.R. Host factors associated with the Sindbis virus RNA-dependent RNA polymerase: Role for G3BP1 and G3BP2 in virus replication. *J. Virol.* **2010**, *84*, 6720–6732. [CrossRef] [PubMed]
59. Sariola, M.; Saraste, J.; Kuismanen, E. Communication of post-Golgi elements with early endocytic pathway: Regulation of endoproteolytic cleavage of Semliki Forest virus p62 precursor. *J. Cell Sci.* **1995**, *108 Pt 6*, 2465–2475. [PubMed]
60. Firth, A.E.; Chung, B.Y.; Fleeton, M.N.; Atkins, J.F. Discovery of frameshifting in Alphavirus 6K resolves a 20-year enigma. *Virol. J.* **2008**, *5*, 108. [CrossRef] [PubMed]
61. Chung, B.Y.; Firth, A.E.; Atkins, J.F. Frameshifting in alphaviruses: A diversity of 3′ stimulatory structures. *J. Mol. Biol.* **2010**, *397*, 448–456. [CrossRef] [PubMed]
62. Jose, J.; Snyder, J.E.; Kuhn, R.J. A structural and functional perspective of alphavirus replication and assembly. *Future Microbiol.* **2009**, *4*, 837–856. [CrossRef] [PubMed]
63. Gaedigk-Nitschko, K.; Schlesinger, M.J. The Sindbis virus 6K protein can be detected in virions and is acylated with fatty acids. *Virology* **1990**, *175*, 274–281. [CrossRef]

64. Sanz, M.A.; Perez, L.; Carrasco, L. Semliki Forest virus 6K protein modifies membrane permeability after inducible expression in Escherichia coli cells. *J. Biol. Chem.* **1994**, *269*, 12106–12110. [PubMed]
65. Sanz, M.A.; Madan, V.; Carrasco, L.; Nieva, J.L. Interfacial domains in Sindbis virus 6K protein. Detection and functional characterization. *J. Biol. Chem.* **2003**, *278*, 2051–2057. [CrossRef] [PubMed]
66. Nieva, J.L.; Madan, V.; Carrasco, L. Viroporins: Structure and biological functions. *Nat. Rev. Microbiol.* **2012**, *10*, 563–574. [CrossRef] [PubMed]
67. Ramsey, J.; Mukhopadhyay, S. Disentangling the Frames, the State of Research on the Alphavirus 6K and TF Proteins. *Viruses* **2017**, *9*, 228. [CrossRef] [PubMed]
68. Sanz, M.A.; Carrasco, L. Sindbis virus variant with a deletion in the 6K gene shows defects in glycoprotein processing and trafficking: Lack of complementation by a wild-type 6K gene in trans. *J. Virol.* **2001**, *75*, 7778–7784. [CrossRef] [PubMed]
69. Sanz, M.; Madan, V.; Nieva, J.L.; Carrasco, L. The Alphavirus 6K Protein. In *Viral Membrane Proteins: Structure, Function, and Drug Design*; Fisher, W., Ed.; Kluwer Academic/Plenum Plublishers: New York, NY, USA, 2005; pp. 233–244.
70. Melton, J.V.; Ewart, G.D.; Weir, R.C.; Board, P.G.; Lee, E.; Gage, P.W. Alphavirus 6K proteins form ion channels. *J. Biol. Chem.* **2002**, *277*, 46923–46931. [CrossRef] [PubMed]
71. Snyder, J.E.; Kulcsar, K.A.; Schultz, K.L.; Riley, C.P.; Neary, J.T.; Marr, S.; Jose, J.; Griffin, D.E.; Kuhn, R.J. Functional characterization of the alphavirus TF protein. *J. Virol.* **2013**, *87*, 8511–8523. [CrossRef] [PubMed]
72. Bushell, M.; Sarnow, P. Hijacking the translation apparatus by RNA viruses. *J. Cell Biol.* **2002**, *158*, 395–399. [CrossRef] [PubMed]
73. Fros, J.J.; Pijlman, G.P. Alphavirus Infection: Host Cell Shut-Off and Inhibition of Antiviral Responses. *Viruses* **2016**, *8*, 166. [CrossRef] [PubMed]
74. Garcia-Moreno, M.; Sanz, M.A.; Pelletier, J.; Carrasco, L. Requirements for eIF4A and eIF2 during translation of Sindbis virus subgenomic mRNA in vertebrate and invertebrate host cells. *Cell. Microbiol.* **2013**, *15*, 823–840. [CrossRef] [PubMed]
75. Sanz, M.A.; Garcia-Moreno, M.; Carrasco, L. Inhibition of host protein synthesis by Sindbis virus: Correlation with viral RNA replication and release of nuclear proteins to the cytoplasm. *Cell. Microbiol.* **2015**, *17*, 520–541. [CrossRef] [PubMed]
76. Sonenberg, N.; Hinnebusch, A.G. Regulation of translation initiation in eukaryotes: Mechanisms and biological targets. *Cell* **2009**, *136*, 731–745. [CrossRef] [PubMed]
77. Gingras, A.C.; Raught, B.; Sonenberg, N. eIF4 initiation factors: Effectors of mRNA recruitment to ribosomes and regulators of translation. *Annu. Rev. Biochem.* **1999**, *68*, 913–963. [CrossRef] [PubMed]
78. Parsyan, A.; Svitkin, Y.; Shahbazian, D.; Gkogkas, C.; Lasko, P.; Merrick, W.C.; Sonenberg, N. mRNA helicases: The tacticians of translational control. *Nat. Rev. Mol. Cell Biol.* **2011**, *12*, 235–245. [CrossRef] [PubMed]
79. Kozak, M. Structural features in eukaryotic mRNAs that modulate the initiation of translation. *J. Biol. Chem.* **1991**, *266*, 19867–19870. [PubMed]
80. Komar, A.A.; Mazumder, B.; Merrick, W.C. A new framework for understanding IRES-mediated translation. *Gene* **2012**, *502*, 75–86. [CrossRef] [PubMed]
81. Niepmann, M. Internal translation initiation of picornaviruses and hepatitis C virus. *Biochim. Biophys. Acta* **2009**, *1789*, 529–541. [CrossRef] [PubMed]
82. Garcia-Moreno, M.; Sanz, M.A.; Carrasco, L. Initiation codon selection is accomplished by a scanning mechanism without crucial initiation factors in Sindbis virus subgenomic mRNA. *RNA* **2015**, *21*, 93–112. [CrossRef] [PubMed]
83. Proud, C.G. eIF2 and the control of cell physiology. *Semin. Cell Dev. Biol.* **2005**, *16*, 3–12. [CrossRef] [PubMed]
84. Donnelly, N.; Gorman, A.M.; Gupta, S.; Samali, A. The eIF2α kinases: Their structures and functions. *Cell. Mol. Life Sci.* **2013**, *70*, 3493–3511. [CrossRef] [PubMed]
85. Koromilas, A.E. Roles of the translation initiation factor eIF2α serine 51 phosphorylation in cancer formation and treatment. *Biochim. Biophys. Acta* **2015**, *1849*, 871–880. [CrossRef] [PubMed]
86. McInerney, G.M.; Kedersha, N.L.; Kaufman, R.J.; Anderson, P.; Liljestrom, P. Importance of eIF2α phosphorylation and stress granule assembly in alphavirus translation regulation. *Mol. Biol. Cell* **2005**, *16*, 3753–3763. [CrossRef] [PubMed]

87. Ventoso, I.; Sanz, M.A.; Molina, S.; Berlanga, J.J.; Carrasco, L.; Esteban, M. Translational resistance of late alphavirus mRNA to eIF2α phosphorylation: A strategy to overcome the antiviral effect of protein kinase PKR. *Genes Dev.* **2006**, *20*, 87–100. [CrossRef] [PubMed]
88. Sanz, M.A.; Castello, A.; Ventoso, I.; Berlanga, J.J.; Carrasco, L. Dual mechanism for the translation of subgenomic mRNA from Sindbis virus in infected and uninfected cells. *PLoS ONE* **2009**, *4*, e4772. [CrossRef] [PubMed]
89. Sanz, M.A.; Redondo, N.; Garcia-Moreno, M.; Carrasco, L. Phosphorylation of eIF2α is responsible for the failure of the picornavirus internal ribosome entry site to direct translation from Sindbis virus replicons. *J. Gen. Virol.* **2013**, *94*, 796–806. [CrossRef] [PubMed]
90. Gorchakov, R.; Frolova, E.; Williams, B.R.; Rice, C.M.; Frolov, I. PKR-dependent and -independent mechanisms are involved in translational shutoff during Sindbis virus infection. *J. Virol.* **2004**, *78*, 8455–8467. [CrossRef] [PubMed]
91. Berglund, P.; Finzi, D.; Bennink, J.R.; Yewdell, J.W. Viral alteration of cellular translational machinery increases defective ribosomal products. *J. Virol.* **2007**, *81*, 7220–7229. [CrossRef] [PubMed]
92. Patel, R.K.; Burnham, A.J.; Gebhart, N.N.; Sokoloski, K.J.; Hardy, R.W. Role for subgenomic mRNA in host translation inhibition during Sindbis virus infection of mammalian cells. *Virology* **2013**, *441*, 171–181. [CrossRef] [PubMed]
93. Frolov, I.; Schlesinger, S. Comparison of the effects of Sindbis virus and Sindbis virus replicons on host cell protein synthesis and cytopathogenicity in BHK cells. *J. Virol.* **1994**, *68*, 1721–1727. [PubMed]
94. Sanz, M.A.; Castello, A.; Carrasco, L. Viral translation is coupled to transcription in Sindbis virus-infected cells. *J. Virol.* **2007**, *81*, 7061–7068. [CrossRef] [PubMed]
95. Garry, R.F. Sindbis virus-induced inhibition of protein synthesis is partially reversed by medium containing an elevated potassium concentration. *J. Gen. Virol.* **1994**, *75*, 411–415. [CrossRef] [PubMed]
96. Garry, R.F.; Bishop, J.M.; Parker, S.; Westbrook, K.; Lewis, G.; Waite, M.R. Na^+ and K^+ concentrations and the regulation of protein synthesis in Sindbis virus-infected chick cells. *Virology* **1979**, *96*, 108–120. [CrossRef]
97. Carrasco, L. Membrane leakiness after viral infection and a new approach to the development of antiviral agents. *Nature* **1978**, *272*, 694–699. [CrossRef] [PubMed]
98. Contreras, A.; Carrasco, L. Selective inhibition of protein synthesis in virus-infected mammalian cells. *J. Virol.* **1979**, *29*, 114–122. [PubMed]
99. Frolov, I.; Garmashova, N.; Atasheva, S.; Frolova, E.I. Random Insertion Mutagenesis of Sindbis Virus Nonstructural Protein 2 and Selection of Variants Incapable of Downregulating Cellular Transcription. *J. Virol.* **2009**, *83*, 9031–9044. [CrossRef] [PubMed]
100. Frolov, I.; Agapov, E.; Hoffman, T.A., Jr.; Pragai, B.M.; Lippa, M.; Schlesinger, S.; Rice, C.M. Selection of RNA replicons capable of persistent noncytopathic replication in mammalian cells. *J. Virol.* **1999**, *73*, 3854–3865. [PubMed]
101. Castello, A.; Alvarez, E.; Carrasco, L. The multifaceted poliovirus 2A protease: Regulation of gene expression by picornavirus proteases. *J. Biomed. Biotechnol.* **2011**, *2011*, 369648. [CrossRef] [PubMed]
102. McCormick, C.; Khaperskyy, D.A. Translation inhibition and stress granules in the antiviral immune response. *Nat. Rev. Immunol.* **2017**, *17*, 647–660. [CrossRef] [PubMed]
103. Gui, H.; Lu, C.W.; Adams, S.; Stollar, V.; Li, M.L. hnRNP A1 interacts with the genomic and subgenomic RNA promoters of Sindbis virus and is required for the synthesis of G and SG RNA. *J. Biomed. Sci.* **2010**, *17*, 59. [CrossRef] [PubMed]
104. Dickson, A.M.; Anderson, J.R.; Barnhart, M.D.; Sokoloski, K.J.; Oko, L.; Opyrchal, M.; Galanis, E.; Wilusz, C.J.; Morrison, T.E.; Wilusz, J. Dephosphorylation of HuR protein during alphavirus infection is associated with HuR relocalization to the cytoplasm. *J. Biol. Chem.* **2012**, *287*, 36229–36238. [CrossRef] [PubMed]
105. Burnham, A.J.; Gong, L.; Hardy, R.W. Heterogeneous nuclear ribonuclear protein K interacts with Sindbis virus nonstructural proteins and viral subgenomic mRNA. *Virology* **2007**, *367*, 212–221. [CrossRef] [PubMed]
106. LaPointe, A.T.; Gebhart, N.N.; Meller, M.E.; Hardy, R.W.; Sokoloski, K.J. The Identification and Characterization of Sindbis Virus RNA: Host Protein Interactions. *J. Virol.* **2018**. [CrossRef] [PubMed]
107. Sokoloski, K.J.; Dickson, A.M.; Chaskey, E.L.; Garneau, N.L.; Wilusz, C.J.; Wilusz, J. Sindbis virus usurps the cellular HuR protein to stabilize its transcripts and promote productive infections in mammalian and mosquito cells. *Cell Host Microbe* **2010**, *8*, 196–207. [CrossRef] [PubMed]

108. Barnhart, M.D.; Moon, S.L.; Emch, A.W.; Wilusz, C.J.; Wilusz, J. Changes in cellular mRNA stability, splicing, and polyadenylation through HuR protein sequestration by a cytoplasmic RNA virus. *Cell Rep.* **2013**, *5*, 909–917. [CrossRef] [PubMed]
109. Castello, A.; Izquierdo, J.M.; Welnowska, E.; Carrasco, L. RNA nuclear export is blocked by poliovirus 2A protease and is concomitant with nucleoporin cleavage. *J. Cell Sci.* **2009**, *122*, 3799–3809. [CrossRef] [PubMed]
110. Park, N.; Katikaneni, P.; Skern, T.; Gustin, K.E. Differential targeting of nuclear pore complex proteins in poliovirus-infected cells. *J. Virol.* **2008**, *82*, 1647–1655. [CrossRef] [PubMed]
111. Park, N.; Skern, T.; Gustin, K.E. Specific cleavage of the nuclear pore complex protein Nup62 by a viral protease. *J. Biol. Chem.* **2010**, *285*, 28796–28805. [CrossRef] [PubMed]
112. Alvarez, E.; Castello, A.; Carrasco, L.; Izquierdo, J.M. Poliovirus 2A protease triggers a selective nucleo-cytoplasmic redistribution of splicing factors to regulate alternative pre-mRNA splicing. *PLoS ONE* **2013**, *8*, e73723.
113. Alvarez, E.; Castello, A.; Carrasco, L.; Izquierdo, J.M. Alternative splicing, a new target to block cellular gene expression by poliovirus 2A protease. *Biochem. Biophys. Res. Commun.* **2011**, *414*, 142–147. [CrossRef] [PubMed]
114. Hyde, J.L.; Chen, R.; Trobaugh, D.W.; Diamond, M.S.; Weaver, S.C.; Klimstra, W.B.; Wilusz, J. The 5′ and 3′ ends of alphavirus RNAs—Non-coding is not non-functional. *Virus Res.* **2015**, *206*, 99–107. [CrossRef] [PubMed]
115. Castello, A.; Sanz, M.A.; Molina, S.; Carrasco, L. Translation of Sindbis virus 26S mRNA does not require intact eukariotic initiation factor 4G. *J. Mol. Biol.* **2006**, *355*, 942–956. [CrossRef] [PubMed]
116. Frolov, I.; Schlesinger, S. Translation of Sindbis virus mRNA: Effects of sequences downstream of the initiating codon. *J. Virol.* **1994**, *68*, 8111–8117. [PubMed]
117. Frolov, I.; Schlesinger, S. Translation of Sindbis virus mRNA: Analysis of sequences downstream of the initiating AUG codon that enhance translation. *J. Virol.* **1996**, *70*, 1182–1190. [PubMed]
118. Ventoso, I. Adaptive changes in alphavirus mRNA translation allowed colonization of vertebrate hosts. *J. Virol.* **2012**, *86*, 9484–9494. [CrossRef] [PubMed]
119. Sanz, M.A.; Gonzalez Almela, E.; Carrasco, L. Translation of Sindbis Subgenomic mRNA is Independent of eIF2, eIF2A and eIF2D. *Sci. Rep.* **2017**, *7*, 43876. [CrossRef] [PubMed]
120. Toribio, R.; Diaz-Lopez, I.; Boskovic, J.; Ventoso, I. An RNA trapping mechanism in Alphavirus mRNA promotes ribosome stalling and translation initiation. *Nucleic Acids Res.* **2016**, *44*, 4368–4380. [CrossRef] [PubMed]
121. Hardy, R.W. The role of the 3′ terminus of the Sindbis virus genome in minus-strand initiation site selection. *Virology* **2006**, *345*, 520–531. [CrossRef] [PubMed]
122. Ou, J.H.; Trent, D.W.; Strauss, J.H. The 3′-non-coding regions of alphavirus RNAs contain repeating sequences. *J. Mol. Biol.* **1982**, *156*, 719–730. [CrossRef]
123. Pfeffer, M.; Kinney, R.M.; Kaaden, O.R. The alphavirus 3′-nontranslated region: Size heterogeneity and arrangement of repeated sequence elements. *Virology* **1998**, *240*, 100–108. [CrossRef] [PubMed]
124. Gritsun, T.S.; Gould, E.A. Direct repeats in the 3′ untranslated regions of mosquito-borne flaviviruses: Possible implications for virus transmission. *J. Gen. Virol.* **2006**, *87*, 3297–3305. [CrossRef] [PubMed]
125. Garneau, N.L.; Sokoloski, K.J.; Opyrchal, M.; Neff, C.P.; Wilusz, C.J.; Wilusz, J. The 3′ untranslated region of sindbis virus represses deadenylation of viral transcripts in mosquito and Mammalian cells. *J. Virol.* **2008**, *82*, 880–892. [CrossRef] [PubMed]
126. Kuhn, R.J.; Hong, Z.; Strauss, J.H. Mutagenesis of the 3′ nontranslated region of Sindbis virus RNA. *J. Virol.* **1990**, *64*, 1465–1476. [PubMed]
127. Kuhn, R.J.; Griffin, D.E.; Zhang, H.; Niesters, H.G.; Strauss, J.H. Attenuation of Sindbis virus neurovirulence by using defined mutations in nontranslated regions of the genome RNA. *J. Virol.* **1992**, *66*, 7121–7127. [PubMed]
128. Chen, R.; Wang, E.; Tsetsarkin, K.A.; Weaver, S.C. Chikungunya virus 3′ untranslated region: Adaptation to mosquitoes and a population bottleneck as major evolutionary forces. *PLoS Pathog.* **2013**, *9*, e1003591. [CrossRef] [PubMed]
129. Garcia-Moreno, M.; Sanz, M.A.; Carrasco, L. A Viral mRNA Motif at the 3′-Untranslated Region that Confers Translatability in a Cell-Specific Manner. Implications for Virus Evolution. *Sci. Rep.* **2016**, *6*, 19217. [CrossRef] [PubMed]

130. Karlsen, M.; Villoing, S.; Rimstad, E.; Nylund, A. Characterization of untranslated regions of the salmonid alphavirus 3 (SAV3) genome and construction of a SAV3 based replicon. *Virol. J.* **2009**, *6*, 173. [CrossRef] [PubMed]
131. McLoughlin, M.F.; Graham, D.A. Alphavirus infections in salmonids—A review. *J. Fish Dis.* **2007**, *30*, 511–531. [CrossRef] [PubMed]
132. Moriette, C.; Leberre, M.; Lamoureux, A.; Lai, T.L.; Bremont, M. Recovery of a recombinant salmonid alphavirus fully attenuated and protective for rainbow trout. *J. Virol.* **2006**, *80*, 4088–4098. [CrossRef] [PubMed]
133. Weston, J.; Villoing, S.; Bremont, M.; Castric, J.; Pfeffer, M.; Jewhurst, V.; McLoughlin, M.; Rodseth, O.; Christie, K.E.; Koumans, J.; et al. Comparison of two aquatic alphaviruses, salmon pancreas disease virus and sleeping disease virus, by using genome sequence analysis, monoclonal reactivity, and cross-infection. *J. Virol.* **2002**, *76*, 6155–6163. [CrossRef] [PubMed]
134. Landgraf, P.; Rusu, M.; Sheridan, R.; Sewer, A.; Iovino, N.; Aravin, A.; Pfeffer, S.; Rice, A.; Kamphorst, A.O.; Landthaler, M.; et al. A mammalian microRNA expression atlas based on small RNA library sequencing. *Cell* **2007**, *129*, 1401–1414. [CrossRef] [PubMed]
135. Guo, Y.E.; Steitz, J.A. Virus meets host microRNA: The destroyer, the booster, the hijacker. *Mol. Cell. Biol.* **2014**, *34*, 3780–3787. [CrossRef] [PubMed]
136. Trobaugh, D.W.; Klimstra, W.B. MicroRNA Regulation of RNA Virus Replication and Pathogenesis. *Trends Mol. Med.* **2017**, *23*, 80–93. [CrossRef] [PubMed]
137. Trobaugh, D.W.; Gardner, C.L.; Sun, C.; Haddow, A.D.; Wang, E.; Chapnik, E.; Mildner, A.; Weaver, S.C.; Ryman, K.D.; Klimstra, W.B. RNA viruses can hijack vertebrate microRNAs to suppress innate immunity. *Nature* **2014**, *506*, 245–248. [CrossRef] [PubMed]
138. Trobaugh, D.W.; Klimstra, W.B. Alphaviruses suppress host immunity by preventing myeloid cell replication and antagonizing innate immune responses. *Curr. Opin. Virol.* **2017**, *23*, 30–34. [CrossRef] [PubMed]
139. Bogerd, H.P.; Skalsky, R.L.; Kennedy, E.M.; Furuse, Y.; Whisnant, A.W.; Flores, O.; Schultz, K.L.; Putnam, N.; Barrows, N.J.; Sherry, B.; et al. Replication of many human viruses is refractory to inhibition by endogenous cellular microRNAs. *J. Virol.* **2014**, *88*, 8065–8076. [CrossRef] [PubMed]
140. Shapiro, J.S.; Schmid, S.; Aguado, L.C.; Sabin, L.R.; Yasunaga, A.; Shim, J.V.; Sachs, D.; Cherry, S.; tenOever, B.R. Drosha as an interferon-independent antiviral factor. *Proc. Natl. Acad. Sci. USA* **2014**, *111*, 7108–7113. [CrossRef] [PubMed]
141. Li, Y.; Lu, J.; Han, Y.; Fan, X.; Ding, S.W. RNA interference functions as an antiviral immunity mechanism in mammals. *Science* **2013**, *342*, 231–234. [CrossRef] [PubMed]
142. Alonso, M.A.; Carrasco, L. Translation of capped viral mRNAs in poliovirus-infected HeLa cells. *EMBO J.* **1982**, *1*, 913–917. [PubMed]
143. Castello, A.; Franco, D.; Moral-Lopez, P.; Berlanga, J.J.; Alvarez, E.; Wimmer, E.; Carrasco, L. HIV-1 protease inhibits Cap- and poly(A)-dependent translation upon eIF4GI and PABP cleavage. *PLoS ONE* **2009**, *4*, e7997. [CrossRef] [PubMed]
144. Lee, A.S.; Kranzusch, P.J.; Doudna, J.A.; Cate, J.H. eIF3d is an mRNA cap-binding protein that is required for specialized translation initiation. *Nature* **2016**, *536*, 96–99. [CrossRef] [PubMed]
145. Skabkin, M.A.; Skabkina, O.V.; Dhote, V.; Komar, A.A.; Hellen, C.U.; Pestova, T.V. Activities of Ligatin and MCT-1/DENR in eukaryotic translation initiation and ribosomal recycling. *Genes Dev.* **2010**, *24*, 1787–1801. [CrossRef] [PubMed]
146. Cencic, R.; Galicia-Vazquez, G.; Pelletier, J. Inhibitors of translation targeting eukaryotic translation initiation factor 4A. *Methods Enzymol.* **2012**, *511*, 437–461. [PubMed]
147. Hood, K.A.; West, L.M.; Northcote, P.T.; Berridge, M.V.; Miller, J.H. Induction of apoptosis by the marine sponge (Mycale) metabolites, mycalamide A and pateamine. *Apoptosis* **2001**, *6*, 207–219. [CrossRef] [PubMed]
148. Low, W.K.; Dang, Y.; Schneider-Poetsch, T.; Shi, Z.; Choi, N.S.; Rzasa, R.M.; Shea, H.A.; Li, S.; Park, K.; Ma, G.; et al. Isolation and identification of eukaryotic initiation factor 4A as a molecular target for the marine natural product Pateamine A. *Methods Enzymol.* **2007**, *431*, 303–324. [PubMed]
149. Bordeleau, M.E.; Mori, A.; Oberer, M.; Lindqvist, L.; Chard, L.S.; Higa, T.; Belsham, G.J.; Wagner, G.; Tanaka, J.; Pelletier, J. Functional characterization of IRESes by an inhibitor of the RNA helicase eIF4A. *Nat. Chem. Biol.* **2006**, *2*, 213–220. [CrossRef] [PubMed]

150. Low, W.K.; Dang, Y.; Schneider-Poetsch, T.; Shi, Z.; Choi, N.S.; Merrick, W.C.; Romo, D.; Liu, J.O. Inhibition of eukaryotic translation initiation by the marine natural product pateamine A. *Mol. Cell* **2005**, *20*, 709–722. [CrossRef] [PubMed]
151. Dang, Y.; Kedersha, N.; Low, W.K.; Romo, D.; Gorospe, M.; Kaufman, R.; Anderson, P.; Liu, J.O. Eukaryotic initiation factor 2α-independent pathway of stress granule induction by the natural product pateamine A. *J. Biol. Chem.* **2006**, *281*, 32870–32878. [CrossRef] [PubMed]
152. Gonzalez-Almela, E.; Sanz, M.A.; Garcia-Moreno, M.; Northcote, P.; Pelletier, J.; Carrasco, L. Differential action of pateamine A on translation of genomic and subgenomic mRNAs from Sindbis virus. *Virology* **2015**, *484*, 41–50. [CrossRef] [PubMed]
153. Lindqvist, L.; Oberer, M.; Reibarkh, M.; Cencic, R.; Bordeleau, M.E.; Vogt, E.; Marintchev, A.; Tanaka, J.; Fagotto, F.; Altmann, M.; et al. Selective pharmacological targeting of a DEAD box RNA helicase. *PLoS ONE* **2008**, *3*, e1583. [CrossRef] [PubMed]
154. Zoll, W.L.; Horton, L.E.; Komar, A.A.; Hensold, J.O.; Merrick, W.C. Characterization of mammalian eIF2A and identification of the yeast homolog. *J. Biol. Chem.* **2002**, *277*, 37079–37087. [CrossRef] [PubMed]
155. Merrick, W.C.; Kemper, W.M.; Kantor, J.A.; Anderson, W.F. Purification and properties of rabbit reticulocyte protein synthesis elongation factor 2. *J. Biol. Chem.* **1975**, *250*, 2620–2625. [PubMed]
156. Adams, S.L.; Safer, B.; Anderson, W.F.; Merrick, W.C. Eukaryotic initiation complex formation. Evidence for two distinct pathways. *J. Biol. Chem.* **1975**, *250*, 9083–9089. [PubMed]
157. Liang, H.; He, S.; Yang, J.; Jia, X.; Wang, P.; Chen, X.; Zhang, Z.; Zou, X.; McNutt, M.A.; Shen, W.H.; et al. PTENα, a PTEN isoform translated through alternative initiation, regulates mitochondrial function and energy metabolism. *Cell Metab.* **2014**, *19*, 836–848. [CrossRef] [PubMed]
158. Starck, S.R.; Tsai, J.C.; Chen, K.; Shodiya, M.; Wang, L.; Yahiro, K.; Martins-Green, M.; Shastri, N.; Walter, P. Translation from the 5′ untranslated region shapes the integrated stress response. *Science* **2016**, *351*. [CrossRef] [PubMed]
159. Sendoel, A.; Dunn, J.G.; Rodriguez, E.H.; Naik, S.; Gomez, N.C.; Hurwitz, B.; Levorse, J.; Dill, B.D.; Schramek, D.; Molina, H.; et al. Translation from unconventional 5′ start sites drives tumour initiation. *Nature* **2017**, *541*, 494–499. [CrossRef] [PubMed]
160. Golovko, A.; Kojukhov, A.; Guan, B.J.; Morpurgo, B.; Merrick, W.C.; Mazumder, B.; Hatzoglou, M.; Komar, A.A. The eIF2A knockout mouse. *Cell Cycle* **2016**, *15*, 3115–3120. [CrossRef] [PubMed]
161. Dmitriev, S.E.; Terenin, I.M.; Andreev, D.E.; Ivanov, P.A.; Dunaevsky, J.E.; Merrick, W.C.; Shatsky, I.N. GTP-independent tRNA delivery to the ribosomal P-site by a novel eukaryotic translation factor. *J. Biol. Chem.* **2010**, *285*, 26779–26787. [CrossRef] [PubMed]
162. Marceau, C.D.; Puschnik, A.S.; Majzoub, K.; Ooi, Y.S.; Brewer, S.M.; Fuchs, G.; Swaminathan, K.; Mata, M.A.; Elias, J.E.; Sarnow, P.; et al. Genetic dissection of Flaviviridae host factors through genome-scale CRISPR screens. *Nature* **2016**, *535*, 159–163. [CrossRef] [PubMed]
163. Boehringer, D.; Thermann, R.; Ostareck-Lederer, A.; Lewis, J.D.; Stark, H. Structure of the hepatitis C virus IRES bound to the human 80S ribosome: Remodeling of the HCV IRES. *Structure* **2005**, *13*, 1695–1706. [CrossRef] [PubMed]
164. Locker, N.; Easton, L.E.; Lukavsky, P.J. HCV and CSFV IRES domain II mediate eIF2 release during 80S ribosome assembly. *EMBO J.* **2007**, *26*, 795–805. [CrossRef] [PubMed]
165. Lorsch, J.R.; Dever, T.E. Molecular view of 43 S complex formation and start site selection in eukaryotic translation initiation. *J. Biol. Chem.* **2010**, *285*, 21203–21207. [CrossRef] [PubMed]
166. Hinnebusch, A.G. Molecular mechanism of scanning and start codon selection in eukaryotes. *Microbiol. Mol. Biol. Rev.* **2011**, *75*, 434–467. [CrossRef] [PubMed]
167. Valasek, L.S. 'Ribozoomin'—Translation initiation from the perspective of the ribosome-bound eukaryotic initiation factors (eIFs). *Curr. Protein Pept. Sci.* **2012**, *13*, 305–330. [CrossRef] [PubMed]
168. Pestova, T.V.; Kolupaeva, V.G. The roles of individual eukaryotic translation initiation factors in ribosomal scanning and initiation codon selection. *Genes Dev.* **2002**, *16*, 2906–2922. [CrossRef] [PubMed]
169. Asano, K. Why is start codon selection so precise in eukaryotes? *Translation* **2014**, *2*, e28387. [CrossRef] [PubMed]
170. Kozak, M. Initiation of translation in prokaryotes and eukaryotes. *Gene* **1999**, *234*, 187–208. [CrossRef]

171. Cheung, Y.N.; Maag, D.; Mitchell, S.F.; Fekete, C.A.; Algire, M.A.; Takacs, J.E.; Shirokikh, N.; Pestova, T.; Lorsch, J.R.; Hinnebusch, A.G. Dissociation of eIF1 from the 40S ribosomal subunit is a key step in start codon selection in vivo. *Genes Dev.* **2007**, *21*, 1217–1230. [CrossRef] [PubMed]
172. Luna, R.E.; Arthanari, H.; Hiraishi, H.; Nanda, J.; Martin-Marcos, P.; Markus, M.A.; Akabayov, B.; Milbradt, A.G.; Luna, L.E.; Seo, H.C.; et al. The C-terminal domain of eukaryotic initiation factor 5 promotes start codon recognition by its dynamic interplay with eIF1 and eIF2β. *Cell Rep.* **2012**, *1*, 689–702. [CrossRef] [PubMed]
173. Nanda, J.S.; Saini, A.K.; Munoz, A.M.; Hinnebusch, A.G.; Lorsch, J.R. Coordinated movements of eukaryotic translation initiation factors eIF1, eIF1A, and eIF5 trigger phosphate release from eIF2 in response to start codon recognition by the ribosomal preinitiation complex. *J. Biol. Chem.* **2013**, *288*, 5316–5329. [CrossRef] [PubMed]
174. Fernandez, I.S.; Bai, X.C.; Murshudov, G.; Scheres, S.H.; Ramakrishnan, V. Initiation of translation by cricket paralysis virus IRES requires its translocation in the ribosome. *Cell* **2014**, *157*, 823–831. [CrossRef] [PubMed]
175. Murray, J.; Savva, C.G.; Shin, B.S.; Dever, T.E.; Ramakrishnan, V.; Fernandez, I.S. Structural characterization of ribosome recruitment and translocation by type IV IRES. *eLife* **2016**, *5*, e13567. [CrossRef] [PubMed]
176. Sanz, M.A.; Welnowska, E.; Redondo, N.; Carrasco, L. Translation driven by picornavirus IRES is hampered from Sindbis virus replicons: Rescue by poliovirus 2A protease. *J. Mol. Biol.* **2010**, *402*, 101–117. [CrossRef] [PubMed]
177. Kieft, J.S. Viral IRES RNA structures and ribosome interactions. *Trends Biochem. Sci.* **2008**, *33*, 274–283. [CrossRef] [PubMed]
178. Balvay, L.; Soto Rifo, R.; Ricci, E.P.; Decimo, D.; Ohlmann, T. Structural and functional diversity of viral IRESes. *Biochim. Biophys. Acta* **2009**, *1789*, 542–557. [CrossRef] [PubMed]
179. Lozano, G.; Martinez-Salas, E. Structural insights into viral IRES-dependent translation mechanisms. *Curr. Opin. Virol.* **2015**, *12*, 113–120. [CrossRef] [PubMed]
180. Khawaja, A.; Vopalensky, V.; Pospisek, M. Understanding the potential of hepatitis C virus internal ribosome entry site domains to modulate translation initiation via their structure and function. *Wiley Interdiscip. Rev. RNA* **2015**, *6*, 211–224. [CrossRef] [PubMed]
181. Jang, S.K. Internal initiation: IRES elements of picornaviruses and hepatitis c virus. *Virus Res.* **2006**, *119*, 2–15. [CrossRef] [PubMed]
182. Nakashima, N.; Uchiumi, T. Functional analysis of structural motifs in dicistroviruses. *Virus Res.* **2009**, *139*, 137–147. [CrossRef] [PubMed]
183. Lee, K.M.; Chen, C.J.; Shih, S.R. Regulation Mechanisms of Viral IRES-Driven Translation. *Trends Microbiol.* **2017**, *25*, 546–561. [CrossRef] [PubMed]
184. Belsham, G.J. Divergent picornavirus IRES elements. *Virus Res.* **2009**, *139*, 183–192. [CrossRef] [PubMed]
185. Martinez-Salas, E.; Francisco-Velilla, R.; Fernandez-Chamorro, J.; Lozano, G.; Diaz-Toledano, R. Picornavirus IRES elements: RNA structure and host protein interactions. *Virus Res.* **2015**, *206*, 62–73. [CrossRef] [PubMed]
186. Filbin, M.E.; Kieft, J.S. Toward a structural understanding of IRES RNA function. *Curr. Opin. Struct. Biol.* **2009**, *19*, 267–276. [CrossRef] [PubMed]
187. Lukavsky, P.J. Structure and function of HCV IRES domains. *Virus Res.* **2009**, *139*, 166–171. [CrossRef] [PubMed]
188. Butcher, S.E.; Jan, E. tRNA-mimicry in IRES-mediated translation and recoding. *RNA Biol.* **2016**, *13*, 1068–1074. [CrossRef] [PubMed]
189. Redondo, N.; Sanz, M.A.; Welnowska, E.; Carrasco, L. Translation without eIF2 promoted by poliovirus 2A protease. *PLoS ONE* **2011**, *6*, e25699. [CrossRef] [PubMed]
190. Redondo, N.; Sanz, M.A.; Steinberger, J.; Skern, T.; Kusov, Y.; Carrasco, L. Translation directed by hepatitis A virus IRES in the absence of active eIF4F complex and eIF2. *PLoS ONE* **2012**, *7*, e52065. [CrossRef] [PubMed]
191. Martinez-Salas, E.; Lozano, G.; Fernandez-Chamorro, J.; Francisco-Velilla, R.; Galan, A.; Diaz, R. RNA-binding proteins impacting on internal initiation of translation. *Int. J. Mol. Sci.* **2013**, *14*, 21705–21726. [CrossRef] [PubMed]
192. Johnson, A.G.; Grosely, R.; Petrov, A.N.; Puglisi, J.D. Dynamics of IRES-mediated translation. *Philos. Trans. R. Soc. Lond. B Biol. Sci.* **2017**, *372*. [CrossRef] [PubMed]

193. Smith, A.E.; Carrasco, L. Eukaryotic viral protein synthesis. In *ATP International Review of Science, Biochemistry Series II, Synthesis of Amino Acids and Proteins*; Arnstein, H.V.R., Ed.; Butterworths: London, UK, 1978; Volume 18, pp. 261–311.
194. Kamrud, K.I.; Custer, M.; Dudek, J.M.; Owens, G.; Alterson, K.D.; Lee, J.S.; Groebner, J.L.; Smith, J.F. Alphavirus replicon approach to promoterless analysis of IRES elements. *Virology* **2007**, *360*, 376–387. [CrossRef] [PubMed]
195. Plante, K.; Wang, E.; Partidos, C.D.; Weger, J.; Gorchakov, R.; Tsetsarkin, K.; Borland, E.M.; Powers, A.M.; Seymour, R.; Stinchcomb, D.T.; et al. Novel chikungunya vaccine candidate with an IRES-based attenuation and host range alteration mechanism. *PLoS Pathog.* **2011**, *7*, e1002142. [CrossRef] [PubMed]
196. Erasmus, J.H.; Rossi, S.L.; Weaver, S.C. Development of Vaccines for Chikungunya Fever. *J. Infect. Dis.* **2016**, *214*, S488–S496. [CrossRef] [PubMed]
197. Rausalu, K.; Iofik, A.; Ulper, L.; Karo-Astover, L.; Lulla, V.; Merits, A. Properties and use of novel replication-competent vectors based on Semliki Forest virus. *Virol. J.* **2009**, *6*, 33. [CrossRef] [PubMed]
198. Welnowska, E.; Sanz, M.A.; Redondo, N.; Carrasco, L. Translation of viral mRNA without active eIF2: The case of picornaviruses. *PLoS ONE* **2011**, *6*, e22230. [CrossRef] [PubMed]
199. Moral-Lopez, P.; Alvarez, E.; Redondo, N.; Skern, T.; Carrasco, L. L protease from foot and mouth disease virus confers eIF2-independent translation for mRNAs bearing picornavirus IRES. *FEBS Lett.* **2014**, *588*, 4053–4059. [CrossRef] [PubMed]
200. Niepmann, M. Hepatitis C virus RNA translation. *Curr. Top. Microbiol. Immunol.* **2013**, *369*, 143–166. [PubMed]
201. Hellen, C.U. IRES-induced conformational changes in the ribosome and the mechanism of translation initiation by internal ribosomal entry. *Biochim. Biophys. Acta* **2009**, *1789*, 558–570. [CrossRef] [PubMed]